Application of zircon to magmatic investigations:
I. Exploring effects of magmatic-tectonic interplay on silicic magma genesis in Iceland;
II. Elucidating copper mineralization trends in a Mid-Jurassic magmatic system, Yerington, NV, USA

By

Tenley Jill Banik

Dissertation

Submitted to the Faculty of the

Graduate School of Vanderbilt University

in partial fulfillment of the requirements

for the degree of

DOCTOR OF PHILOSOPHY

in

Environmental Engineering

August, 2015

Nashville, Tennessee

Approved:

Calvin F. Miller, Ph.D
John C. Ayers, Ph.D
Janey Camp, Ph.D
James H. Clarke, Ph.D
Guilherme A.R. Gualda, Ph.D

ACKNOWLEDGEMENTS

This research would have been impossible without financial support from National Science Foundation Grant EAR-1220523, the U.S. Fulbright Fellowship program, the American-Scandinavian Foundation, Geological Society of America (GSA) and GSA-Southeastern Graduate Research Awards, a Vanderbilt University Dissertation Enhancement Award, and the Kenan Endowed Chair Research Fund. Thank you for supporting me and my research.

Thank you to collaborators far and wide—you have been instrumental in my professional development and the completion of this work. Matthew Coble, Christopher Fisher, and Ming-Chang Liu deserve recognition for continually providing insight and direction. I am indebted to Ármann Höskuldsson for introducing me to and helping me navigate Icelandic geology. I gratefully acknowledge additional support and cooperation from Roland Mundil, Yu Lin, Singatse Peak Services LLC, Kristján Jónasson, Brennan Jordan, Jeff Vervoort, Diane Wilford, and Charles Knaack.

I thank my advisory committee at Vanderbilt for their guidance. My advisor, Calvin Miller, deserves more thanks than I can bestow for encouraging my return to Vanderbilt, sparking my interest in magmatic processes in Iceland and Nevada, and generally putting up with me for many years. Calvin—þakka þér innilega fyrir allt.

Thanks to David Furbish and Lily Claiborne at Vanderbilt for giving me excellent advice and Aaron Covey for allowing me to bother him way too often. I appreciate the opportunity to grow as a scientist during meetings with the MESSY research group. I would have been adrift without support, discussions, and laughs during field and lab work from Tamara Carley and Abe Padilla—thanks for accepting me into Team Iceland! I can never thank my West Coast parents, Charlie Bacon and Cynthia Dusel-Bacon, enough for providing me with continuous encouragement and mentorship.

Finally, thank you to my loved ones near and far for supporting me on a seemingly endless graduate school journey. I never could have successfully found my path and completed the journey while maintaining positive thoughts for the future without your unwavering encouragement, understanding, and patience.

TABLE OF CONTENTS

Page

LIST OF TABLES

LIST OF FIGURES

LIST OF ICELANDIC PRONUNCIATIONS

Icelandic, not unsurprisingly, differs from English in many ways—the most obvious of these being the presence of letters not in the English alphabet. These letters are:

Letter	English Equivalent
Á, á	"ow"
Đ, đ	"th" as in "them"
É, é	"ee-yeh"
Í, í	"ee"
Ó, ó	"oh"
Ú, ú	"oo"
Ý, ý	"ee-yeh"
Þ, þ	"th" as in "thorn"
Æ, æ	"eye"
Ö, ö	"uh" as in "sun" or "e" as in "jerk"

Several letter combinations in Icelandic are pronounced in a way that is not intuitive for English speakers. The ones most commonly used in this dissertation are:

Combination	English Equivalent
fn	"pn"
ll	"tl"
vowel-g-i	g is silent
ei	"ay" as in "hay"

Finally, the most troublesome names mentioned in this dissertation for non-Icelandic speakers and their phonetic pronunciations are detailed below:

Name	Phonetic Pronunciation
Hafnarfjall	HAP-nar-fyatl
Skarðsheiði	SKARTHS-hey-thee
Snæfellsnes	SNEYE-fetls-nes
Skagi	SKA-ee
Króksfjörður	KROHKS-fyer-ther
Hrafnfjörður	HRAP-fyer-ther
Árnes	OUR-nes

CHAPTER 1

Introduction, Motivation, and Conclusions

1. Introduction and Motivation

Silicic magmas (>65 wt% SiO_2) comprise dominant volumes of continental crust on Earth and may attain far more mineralogical, geochemical, and isotopic complexity than their basaltic counterparts. This complexity leads to myriad magmatic products, including (but not limited to) explosive volcanism, batholiths, intra-crustal hybridization, and economic ore deposits, but also challenges us to be innovative and combine multiple lines of evidence to decipher petrogenetic processes associated with silicic magmatism. Timing and duration of magmatism, involvement of fluid or assimilation of material, and geodynamic context are all important when assessing the processes by which silicic magmas are produced, erupted, or emplaced. My research relies heavily on *in situ* analyses of zircon, in combination with whole rock elemental and isotopic data, to investigate the causes and effects of silicic magmatism in two very different contexts: first, I show how *in situ* zircon U-Pb geochronology, trace element, and oxygen isotope analyses aid in identifying controls on the duration of porphyry copper deposit formation at the Yerington Mine, Nevada. I also present an application of an old methodology to a new analytical problem and demonstrate that chemical abrasion of low-U zircon does not affect subsequent analyses. Second, I use *in situ* zircon U-Pb geochronology, trace element, and oxygen and hafnium isotope analyses in addition to whole rock elemental and isotopic data to evaluate the petrogenesis of multiple extinct understudied silicic magmatic systems in Iceland and the role tectonism plays on their formation and longevity, Questions that motivated this research are:

1. Can *in situ* trace element data, particularly in the form of Ce and Eu anomalies, in Yerington zircon be used to infer bulk copper content, as suggested by other authors (Ballard et al., 2002; Liang et al., 2006), or elucidate any controls on ore-forming processes?
2. What are the timescales associated with petrogenesis of silicic magmatic systems in Iceland and what role does rift relocation play (if any) in their formation or longevity?
3. How does silicic magma petrogenesis in Iceland vary within and between magmatic systems? What controls any differences? An ongoing debate over the dominant mechanism(s) by which Icelandic silicic magmas are formed invokes partial melting and fractional crystallization as the two endmember processes likely to be responsible—is the reality somewhere in the middle?

1.1. Why zircon?

Zircon ($ZrSiO_4$) has a long and well-documented tenure as a premier recorder of magmatic processes. Zircon is a common accessory mineral in felsic igneous rocks (and their metamorphic counterparts and detritus) regardless of tectonic setting. The seemingly simple chemical composition of zircon hides a wealth of trace elemental stowaways—U and Hf commonly substitute for Zr and rare earth (REE) and similar elements (Y, Sc) may participate in coupled substitutions with Ta, Nb, and less commonly P (among others) for Zr and Si (e.g. Hoskin and Schaltegger, 2003). Ti also substitutes for Si and Zr to a much lesser extent. These frequent substitutions lead to a chemical complexity that may be harnessed to shed light on a multitude of processes, from crystallization temperatures (Ferry and Watson, 2007; Watson and Harrison, 2005) to oxidation states of parent magmas (e.g. Ballard et al., 2002; Hoskin and Schaltegger, 2003; Trail et al., 2012) and growth timescales (e.g. Claiborne et al., 2010, 2006; Walker et al., 2007; and many others). The research presented in this dissertation takes advantage of these techniques, and others, to investigate a variety of magmatic processes.

Zircon readily incorporates significant quantities of U into the Zr^{4+} octahedral site while Pb, the radiogenic daughter product of U, is excluded during crystallization due to lack of an appropriate structural site. Consequently, zircon has functionally no initial Pb, which—combined with its propensity for U incorporation—makes it an excellent tool for application of U decay-based geochronology. Similarly, zircon strongly partitions Hf, the radiogenic daughter product of Lu decay, over its parent, resulting in decay system that may be utilized to track ages of fractionation events (e.g. Kinney and Maas, 2003). REE display varying degrees of compatibility in zircon—heavy REE (HREE) have ionic radii that more closely match that of Zr^{4+} than those of the light REE (LREE), rendering LREE incompatible and HREE highly compatible (Colombini et al., 2011). The notable exceptions to this trend are Ce and Eu, which are both capable of having valence states other than the 3+ characteristic of the REEs; Ce may also occur as Ce^{4+}, while Eu may be divalent as well as trivalent. In addition, Ce^{4+} has an ionic radius similar to Zr^{4+} and commonly substitutes for it, leading to a higher-than-expected compatibility and a positive Ce anomaly. Conversely, Eu^{2+} is even more incompatible in zircon than Eu^{3+}, which leads to a negative Eu anomaly. Grimes et al. 2007 demonstrated the utility of using REE in zircon to determine provenance, while other *in situ* trace element comparisons are known to track fractionation (Hf, Th/U, and Eu/Eu*; e.g. Claiborne et al., 2006; du Bray et al., 2010; Fohey-Breting et al., 2010) and oxidation state (Ce anomaly; e.g. Ballard et al. 2002), among other things.

Zircon's usefulness as both a geochronometer and a repository for information regarding magmatic processes is due not only to its incorporation of trace elements, but also to its refractory nature. The crystal structure of zircon renders it mechanically durable, relatively insoluble in melts and hydrous fluids, highly resistant to alteration, and results in extremely low diffusivities of most elements (e.g. Finch and Hanchar, 2003); therefore, in systems where hydrothermal or other potentially destructive processes operate, zircon remains a viable recorder of magmatic processes. The Iceland and Nevada study sites that discussed in this dissertation were influenced by

hydrothermal processes; therefore, using zircon to address the magmatic processes at work in each location is essential.

1.2. Background and Motivation for Yerington, NV Research

Yerington, NV is well known as a center for porphyry Cu and skarn deposits resulting from Jurassic arc magmatism (e.g. Dilles and Wright, 1988; Dilles et al., 2000; Proffett and Dilles, 1984). Three intrusive bodies comprise the greater Yerington batholith, the youngest of which—the Luhr Hill granite—hosts granitic mineralized porphyry dikes mined in the Yerington Pit, an open pit mine, that are the subject of this work. Previous studies on other large porphyry copper deposits (Ballard et al., 2002; Liang et al., 2006) indicate that Ce and Eu anomalies in zircon correlate with oxidation, which is correlated with Cu content. Therefore, there may be potential economic significance to screening target mineral exploration via zircon analyses. This portion of my dissertation—which is motivated by my previous work in the Yerington Pit system and my desire to remain involved in the economic geology realm—investigates the controls on petrogenesis of ore-bearing dikes exposed in the Yerington Pit porphyry Cu system through the use of U-Pb dating, trace element concentrations, and oxygen isotope analyses. This research also serves as an example in method development and illustrates the futility of chemical abrasion of low-U zircon prior to analysis to improve reproducibility of SHRIMP-RG U-Pb age analyses and its lack of effect on trace element and oxygen isotope analyses.

1.3. Background and Motivation for Iceland Research

Iceland is the only place in the world where silicic rocks are found in relative abundance (~10-15% of exposed rocks; e.g. Jónasson, 2007; Thorarinsson, 1967; Walker, 1966); and many others) in an ocean island setting, which is usually considered the domain of low-silica basaltic magmatism. Iceland is also the only place on Earth where an active mid-ocean ridge and a major

mantle plume coincide to produce a plateau and island of appreciable size, resulting in a proto-continent in a geologically unique environment with a dynamic history.

Iceland geologic history starts with a mantle plume and the opening of the North Atlantic around 60 Ma (e.g. Bjarnason, 2008; Lawver and Müller, 1994)). The Mid-Atlantic ridge (MAR) separating the North American and Eurasian plates was initially decoupled from the plume, but because the MAR axis moves northwest at ~1–3 cm/yr, the resulting surface expression of the Iceland plume moved first under the MAR axis and then progressively east of it (Lawver and Müller 1994). The MAR and plume became coupled roughly 25 Mya, which led to abnormally high rates of magma production and constructed the anomalously thick Icelandic crust (e.g. Bjarnason 2008; Brandsdóttir and Menke, 2008). As a result of MAR/plume coupling and northwestern drift of the ridge axis, the MAR around Iceland—exposed on land as a series of rift zones—deviates progressively east of the main MAR axis to remain coupled with the plume. The plume periodically recaptures the rift through a rift relocation, or "rift jump", which effectively moves the rift eastward (Harðarson et al., 2008). Rift jumps have occurred several times throughout Iceland's approximately 20 Myr history.

Silicic magmas in Iceland are thus generated within a complicated and dynamic tectonic framework. Central volcanoes are the only places in Iceland with abundant silicic volcanic rocks (Walker 1966) and are generally formed during periods of active rifting. While these observations are well-documented, investigation into the petrogenetic impact of rift relocation on silicic magma production in Iceland is generally lacking, and zircon-based studies of silicic systems with an eye toward rift relocation and volcano-scale petrogenetic variation were non-existent prior to this study. In addition, the scarcity of zircon-based studies investigating petrogenesis from Iceland, and particularly western Iceland—considering the high magnitude of geochemical investigation overall—presents an excellent opportunity to evaluate arguments in a long-standing and ongoing

debate about the mechanisms responsible for silicic magmatism in Iceland by accessing the magmatic record preserved in zircon and likely nowhere else.

2. Conclusions

Detailed conclusions are presented at the end of each chapter. Findings presented include:

1. The Yerington porphyry copper system experienced a late-stage event involving addition of hydrothermally altered, low-$\delta^{18}O$ material that effectively reduced conditions and halted ore-forming processes.
2. Thermal annealing and chemical abrasion treatment of zircon with low U concentration does not improve reproducibility in SHRIMP-RG U-Pb geochronology analysis, nor does it affect trace element concentrations or oxygen isotope values.
3. Duration and timing of Icelandic silicic magmatic systems is strongly tied to tectonic processes, particularly the spreading rate.
4. Involvement of hydrothermally altered, low-$\delta^{18}O$ material prior to zircon crystallization in silicic systems in Iceland is ubiquitous.
5. A combination of partial melting of Icelandic crust and fractional crystallization of those melts and/or fresh mantle melts produce the vast majority of silicic units studied; magmas produced via pure partial melting or fractional crystallization through are rare.
6. Two volcanoes examined in this study—Hrafnfjörður and Árnes—had no prior published data of any kind. Króksfjörður and Hafnarfjall-Skarðsheiði are better-studied with extensive whole-rock elemental datasets, but none of these volcanoes previously had geochronology-based ages or zircon work of any kind and lacked whole-rock isotopic analysis to further evaluate their petrogenesis.
7. Intra-volcano geochemical and isotopic variation in zircon and whole rock indicates open-system processes but also incremental construction of magmatic systems.

CHAPTER 2

In situ laser Raman, U-Pb, trace element, and oxygen analyses of zircon interpret controls on Cu mineralization in mid-Jurassic magmatism, Yerington, NV, USA

Abstract

Porphyry copper systems provide the majority of global copper resources and are generally formed from highly-oxidized magmas. Previous studies on Cu deposits in the Chuquicamata-El Abra porphyry copper belt of northern Chile and the Yulong copper belt, Tibet, have indicated that the magnitudes of Ce and Eu anomalies in zircon crystallizing in equilibrium with ore-forming Cu porphyry systems can be a proxy for increased ore content. Here we show that this is association is not always universally evident based on new *in situ* zircon analyses of a suite of cogenetic host rocks and ore-bearing porphyry dikes units from the Yerington Pit copper mine, western Nevada, USA. We present *in* situ SHRIMP-RG U-Pb ages from zircons that were chemically abraded and thermally annealed in order to minimize analyses of domains that have undergone Pb-loss or analytical artifacts that can occur from measurements of metamict portions of grains (i.e. non-crystalline zircon). We also measured trace element concentrations in zircon and oxygen isotope ratios by SIMS from the porphyry dike units and the host pluton to construct an enhanced geochemical picture of the Yerington Pit porphyry system. We find no statistically significant difference in analytical results from chemically abraded and untreated zircons. Based on calculated magmatic oxidation conditions (via Ce and Eu anomalies), model zircon crystallization temperatures, and $\delta^{18}O$ in zircon, we conclude that the Yerington system experienced increasing oxidation conditions a late-stage oxygen depletion event that is attributed to incorporation of hydrothermal fluid or material altered by such a fluid.

1. Introduction

Zircon ($ZrSiO_4$) is a common accessory mineral in silicic igneous rocks regardless of tectonic setting. Zircon exhibits physical and chemical resistance to external alteration processes and internal diffusion at magmatic temperatures. In addition, the relatively large ionic radius of Zr^{4+} allows for incorporation of U^{4+} and Th^{4+} and exclusion of Pb^{2+}, rendering it an ideal recorder of magmatic processes. Of particular interest to economic geology is the utility of Ce^4/Ce^{3+} and Eu^3/Eu^{2+} anomalies in zircon as proxies for oxidation state, for which several studies have demonstrated a positive correlation with Cu content in some ore-bearing magmas (e.g. Ballard et al., 2002; Dilles et al., 2015; Liang et al., 2006; Trail et al., 2012).

The Yerington porphyry copper mine in Yerington, NV, USA is an ideal location to investigate the utility of Ce and Eu anomalies in zircon and its correlation (or lack thereof) with ore-bearing rocks. Yerington is well known as a center for porphyry Cu deposits resulting from Jurassic arc magmatism (e.g. Dilles and Wright, 1988; Proffett and Dilles, 1984). The porphyry system exposed in the Yerington mine consists of three magmatic units that source or host several Cu-rich porphyry dike units. Previous work (Dilles and Wright, 1988) involved obtaining U-Pb TIMS zircon ages from plutonic and volcanic units from the Singatse and Buckskin Ranges, west of the Yerington mine, and showed that the ore-bearing porphyry dikes were emplaced over a roughly 1 Myr time span. However, no geochronologic crystallization ages for each dike and source unit are known.

This study integrates *in situ* analyses of zircon to establish geochronologic constraints on timing of mineralized porphyry dike crystallization at the Yerington mine with zircon trace element geochemistry, which preserves a prolonged record of magmatic compositional evolution that we use to investigate controls on Cu content of these ore-bearing units. Because zircon associated with mineralization can often have high-U and/or metamict zircon, we investigate whether thermal annealing and chemical abrasion (TA/CA) treatment of zircons prior to SHRIMP-RG analysis improved the reproducibility of U-Pb age populations and/or affects zircon trace element and

oxygen isotope compositions. In addition, we consider the efficacy of laser Raman spectroscopy to pre-select analytical spots that avoid metamict zones.

2. Background and Motivation

2.1. Geologic background

The Yerington batholith was emplaced during Jurassic arc magmatism and subsequently faulted and rotated up to 90° via Cenozoic extension (Proffett, 1977), exposing a rough cross-section through the paleomagmatic porphyry copper system and associated hydrothermal regime (Fig. 1). Three units comprise the Yerington batholith, the youngest and smallest of which—the Luhr Hill porphyritic granite (sub-units Jgd, Jpqm, and Jbqm)—hosts the ore-bearing porphyry dikes that are exposed in the Yerington mine (Dilles and Wright, 1988). Dilles and Wright (1988) report U-Pb TIMS ages for zircons from a sub-unit of the Luhr Hill granite and one of the porphyry dikes several km from the Yerington Pit of 169.4 ± 0.4 Ma and 168.5 ± 0.3 Ma, respectively (2σ errors). The porphyry dikes emanated from the top of the cupola-like host magma body, aided by fluid overpressure or tectonic fracturing, and were accompanied by magmatic-hydrothermal fluids that ultimately deposited economic amounts of bornite and chalcopyrite into and around the individual dike units (Fig. 1; Dilles et al., 2000; Proffett, 2009). Exposed within the Yerington mine are at least 6 granite porphyries, designated Jqmp1, N, 1.5, 2, 2.5, and 3, that decrease in age and Cu-ore content with increasing designation (i.e.—Jqmp1 is the oldest and most mineralized dike, while Jqmp3 is the youngest and least mineralized) (Dilles et al. 2000; Proffett 1977, 2009; Proffett pers. comm.).

Porphyries and host units have similar mineralogical and textural characteristics, including less than 20% quartz (mostly in the groundmass), 5-10% hornblende and biotite, plagioclase>potassium feldspar (occasionally as megacrysts), and trace amounts of zircon, apatite, sphene and Fe-Ti oxides in the groundmass (Proffett, pers. comm.). All porphyry dike units exhibit

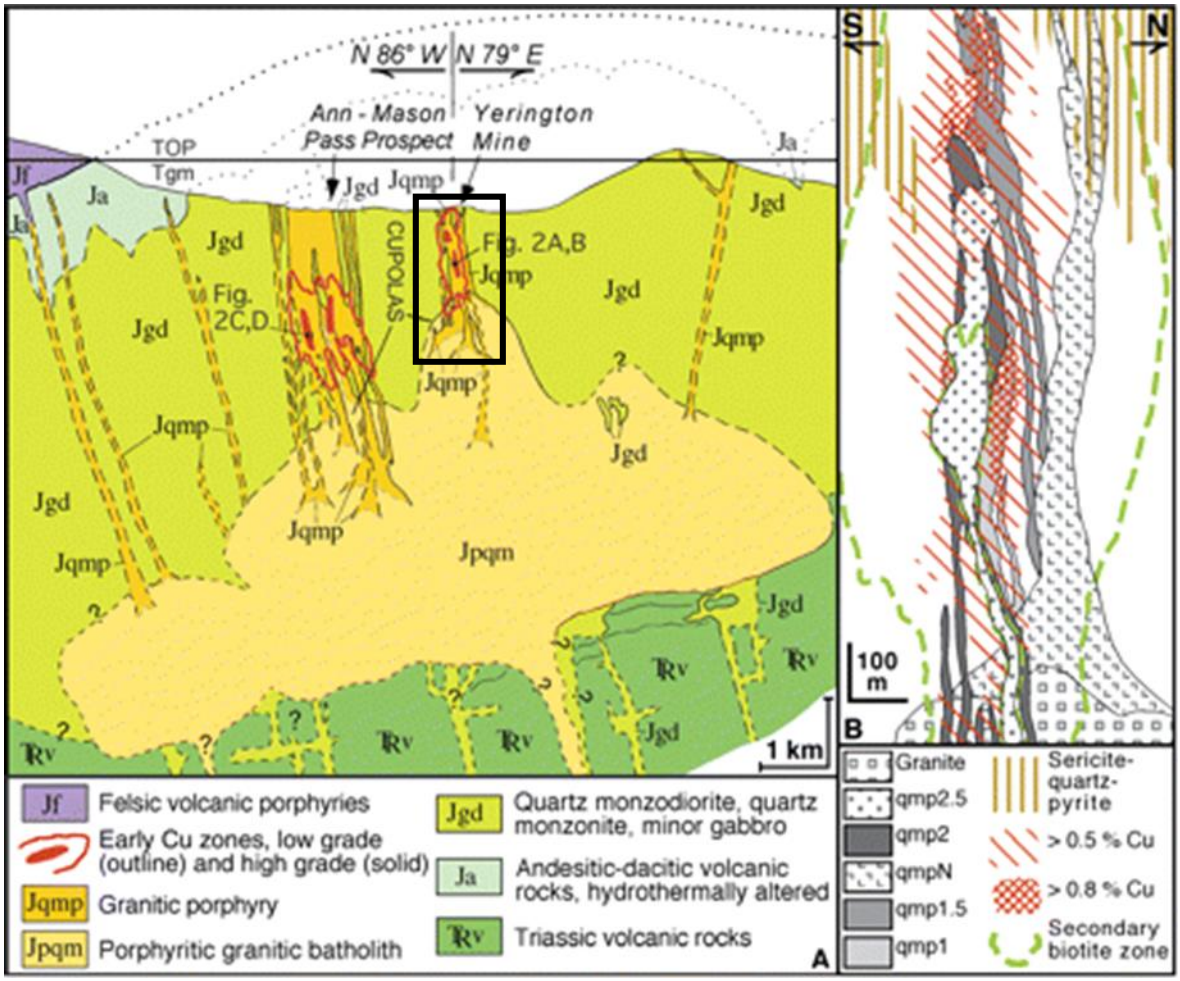

Figure 1. A: Pre-tilt paleogeologic cross section through Yerington district, Nevada, showing Mesozoic geology based on detailed geologic mapping (Proffett and Dilles, 1984, and unpublished data). B: Pretilt section through Yerington Mine from boxed area in (A). Legend lists porphyries (e.g., qmp1) by age, oldest at bottom, based on crosscutting relationships. Granite (Jpqm in A), similar to porphyries except for coarser grain size, is underlying magmatic source of porphyries and fluids. From Proffett 2009.

varying degrees of alteration, with stronger secondary mineralization in the early porphyry dike units (Jqmp1, N, 1.5) linked to early potassic alteration and minor albitization. Sericitic alteration has overprinted all porphyry units, with the youngest porphyries (Jqmp2.5 to 3) the most strongly affected. For a comprehensive summary of porphyry dikes and host unit physical characteristics, see Appendix A.

2.2. Ce and Eu anomalies in zircon and oxidation states in magmas

Ce and Eu are both capable of having multiple valence states: Ce can occur as Ce^{3+} and Ce^{4+}, while Eu may be divalent as well as trivalent. In addition, Ce^{4+} has an ionic radius similar to Zr^{4+} and commonly substitutes for it in zircon, leading to an enhanced compatibility and a positive Ce anomaly, whereby concentrations of Ce are much higher than its neighbors La and Pr. Conversely, Eu^{2+} is more incompatible in zircon than Eu^{3+}, which leads to a negative Eu anomaly as compared with concentrations of Sm and Gd. Oxygen fugacity of the parent magma and temperature of crystallization are the main controls on the Ce^{4+}/Ce^{3+} ratio in zircon (e.g. Ballard et al., 2002; Trail et al., 2012). Eu^{3+}/Eu^{2+} ratios are also controlled by these factors, but to a lesser extent because the Eu anomaly is influenced so heavily by feldspar fractionation, measuring the effect of fO_2 is challenging. Oxygen fugacity also controls the oxidation state of sulfur in a melt: at low oxygen fugacity, sulfur in the magma exists mainly as S^{2-}, whereas at high oxygen fugacity, it exists mainly as SO or SO_2 (e.g. Liang et al., 2006). The transition of S^{2-} to SO or SO_2 may prevent the formation of an immiscible sulfide melt phase that scavenges Cu from a fractionating melt (Sun et al., 2004). Copper in magma with high oxygen fugacity should then become enriched during differentiation and is expected to partition into a magmatic–hydrothermal fluid (e.g. Ballard et al., 2002; Cline and Bodnar, 1991; Pasteris, 1996; Sun et al., 2004; Urich et al., 1999). This is supported by several studies (e.g. Ballard et al. 2002; Liang et al. 2006) that report a positive correlation between Cu concentration in rocks

that contain zircons which show larger positive Ce anomalies and negative Eu anomalies closer to 1 when compared to barren or less-mineralized rocks.

Application of Ce and Eu anomalies to unraveling magmatic conditions is not straightforward. Accurate calculation of the Ce anomaly (Ce/Ce*) or the Ce^{4+}/Ce^{3+} ratio in zircon is notoriously problematic (e.g. Ballard et al., 2002; Dilles et al., 2015; Trail et al., 2015, and references therein) due to low concentrations of La or $Pr_{(calc)}$ that may be artificially elevated by incorporation of nanometer-scale inclusions of melt, apatite, monazite, and other LREE-philic minerals. Calculation of Ce/Ce* by projecting back from more-abundant Sm and Nd is more reliable (Ballard et al., 2002) but also requires making assumptions about overall REE abundances and assuming whole-rock Ce is equivalent to melt Ce during zircon crystallization, the pitfalls of which have been documented by numerous studies (e.g. Dilles et al., 2015; Wang et al., 2013). Similar calculations in this vein using glass contents were more promising (Colombini et al., 2011) but require the presence of fresh glass—an impossibility in porphyry copper rocks. Recently, Trail et al. (2012) derived an experimentally based protocol describing the correlative relationship between Ce/Ce* and oxygen fugacity, but application of this model tends to yield anomalous results that have debatable application for real magmatic systems (e.g. Wang et al. 2013; Dilles et al. 2015), and was subsequently downplayed by Trail et al. (2015).

2.3. *TA/CA treatment prior to in situ zircon geochronology via SHRIMP-RG*

Zircon readily incorporates significant quantities of U into its crystal structure while Pb is excluded during crystallization due to lack of an appropriate structural site. Consequently, zircon has functionally no initial Pb, which—combined with its propensity for U incorporation—makes it an excellent tool for application of U-Pb geochronology. However, the presence of radioactive elements (U, Th) in zircon poses potential analytical problems due to the accumulated radiation damage that increases the number of crystal defects may inflict on zircon's crystal structure, which

has been shown to yield metamict or other structurally unsound areas, induce Pb-loss, and affect isotope and trace element ratios, all of which may yield anomalous *in situ* data and high analytical errors (e.g. Wang et al., 2014, and references therein).

Removal of metamict and damaged portions of zircon grains via thermal annealing and chemical abrasion (TA/CA) prior to analysis has been standard procedure for high-precision TIMS U–Pb geochronology for over a decade (Mattinson, 2005). Grains treated in this manner yield more accurate and precise ages and greater concordance than untreated grains. Chemical abrasion attacks portions of zircon that have highly damaged crystal structures or are metamict and are no longer crystalline zircon because they are no longer chemically robust and can be easily dissolved and physically removed. Recently, the TA/CA treatment has been performed on zircons analyzed via *in situ* methods, including both LA-ICPMS and SHRIMP. Kryza et al. (2012) report SHRIMP-II results showing the TA/CA treated portion of a zircon population yielded an ~5% older age than the untreated portion, in addition to showing less scatter, which they attribute to removal of metamict zones susceptible to Pb-loss from the treated samples. In this study, the treated and analyzed zircons had initially high U (600-20,000 ppm) that was reduced to 175-1377 ppm post-treatment. Similarly, von Quadt et al. (2014) found that TA/CA treated zircons yield less data scatter and ~4-6% older ages than non-treated grains. However, no studies have heretofore reported an in-depth analysis of the effects of TA/CA treatment on trace element concentrations or $\delta^{18}O$ in zircon.

Trace elements and $\delta^{18}O$ in zircon are commonly used to investigate compositional variation and petrogenesis, and are underutilized tools for evaluating radiation damage in zircon. Since arguably the greatest strengths of *in situ* methods are high spatial resolution and the ability to target small-scale variations in individual mineral grains, and that trace elements are a key component in assessing this variability, establishing any affect that TA/CA treatment has on grains

intended for *in situ* U–Pb geochronology that will also be analyzed for trace elements and oxygen isotopes is critical to evaluating the overall usefulness of CA/TA treatment of zircon.

3. Methods

We collected 4 samples from ore-bearing Yerington porphyry dikes (from units Jqmp1, 1.5, 2, and 3) and 3 host units (Jbqm, Jpqm, and Jgd) from historic drill core increments (Table 1). Historical and modern drill logs and assay data provided guidance while sampling and were used in the calculation of overall sample Cu grade. Thin sections of each sample were characterized at Vanderbilt University (VU) via petrographic microscope and a Tescan Vega 3 LM scanning electron microscope (SEM) with EDS capabilities. Zircon was extracted from the samples using standard crushing, sieving, and density separation techniques, followed by hand picking. About half of each sample underwent the TA/CA process (see Section 3.1). TA/CA treated and untreated zircon grains from each sample, along with treated and untreated standards Temora-2, Plesovisce, and Mt. Dromedary and untreated R33 and MADDER (in house standard; Barth and Wooden, 2010), were mounted in a single epoxy mount and polished to roughly midsection.

3.1. Thermal annealing and chemical abrasion

A subset of zircons from each sample underwent thermal annealing and chemical abrasion at Berkeley Geochronology Center following a procedure similar to that of Mundil et al. (2004). Crystals were annealed at 850°C in uncovered quartz crucibles for 46 h, then rinsed in ethanol (EtOH) and transferred via pipette to Teflon microcapsules. Once the EtOH evaporated, capsules received 25 μL each of concentrated HNO_3 and HF and were placed inside pressurized bombs with 30 mL concentrated HF for 10 h at 220°C. After cooling, each capsule received 25 μL concentrated HNO_3 and was placed on a hot plate for 2 h to resuspend any precipitate. The liquid portion was decanted and the treated zircons were rinsed in 100 μL EtOH and dried before mounting.

Sample	Drill Hole	Depth (ft)	Description	Cu%	Sample wtd. Cu%
Jqmp1	L+100-16	65.5	1 piece, ~5 cm	0.67	
		68	1 piece, ~7 cm	0.67	
		69.4	1 piece, ~7 cm	1.38	0.839
		70	1 piece, ~7 cm	1.38	
	M+16/M-16	41-41.7	~20 cm rubble	0.58	
		49-49.8	~22 cm rubble	0.57	
Jqmp1.5	Q+100-24	176.5-178	~45 cm rubble	0.35	
		188	1 piece, ~9 cm	0.35	0.314
		189	1 piece, ~5 cm	0.09	
Jqmp2	L+100-16	48	1 piece, ~6 cm	0.37	
		53	1 piece, ~12 cm	0.81	0.701
		55.5	1 piece, ~10 cm	0.81	
		57	1 piece, ~10 cm	0.66	
Jqmp3	P+100-25	88	1 piece, ~7 cm	0.06	
		98	1 piece, ~15 cm	0.06	0.060
		101	1 piece, ~15 cm	0.06	
Jbqm	K+100-13	136-139	~90 cm rubble	1.24	1.240
Jpqm	A+100-5S	246	1 piece, ~9 cm	0.09	
		251	1 piece, ~15 cm	0.06	0.071
		254.5	2 pieces, 7 cm	0.07	
Jgd	O-18	214-214	~60 cm rubble	0.14	
		222	1 piece, ~11 cm	0.16	0.143
		224-226	~60 cm rubble	0.14	

Table 1. Summary of Yerington Pit samples from historic core.

3.2. Laser Raman spectroscopy

Laser Raman spectroscopy analyses were performed on polished and imaged zircons at the Stanford University Extreme Environments Laboratory using a Renishaw inVIA confocal laser microRaman spectrometer equipped with a CCD detector. Measurements were conducted at 23°C with 10 mW operating power and 514 nm light from the Ar^+ laser with a ~5 μm spot diameter. The spectral frequency resolution of the Raman spectrometer was 1–2 cm^{-1} and the measurement range was 100–1500 cm^{-1} using a static scan centered at 520 cm^{-1}, acquisition time of 5 s, and grating of 1800 grooves/mm. Spectra were collected using WIRE2 software. Amplitudes (Raman intensities) and detected full width half maximum (FWHM) for different peaks were obtained using OriginLab software (v. 9.0). FWHM corrections were applied using the approach of Irmer (1985) and Wang et al. (2014). Particular attention was paid to the B_{1g} (υ_3 [SiO4]), E_g (I [Si-Zr]), B_{1g} (υ_3 [SiO4]) bands, which have peaks at ~1005 cm^{-1}, ~435 cm^{-1}, and ~355 cm^{-1}, respectively. Complete laser Raman spectral analysis results are in Appendix B. Spectra were assessed for potential SHRIMP-RG analysis on the basis of presence of additional peaks and low peak intensity, which is a characteristic of metamict zircon (eg. Nasdala et al., 1998, 1995), and grains with a high potential for metamictization were noted (Fig. 2).

3.3. SHRIMP-RG analysis

After laser Raman analysis, the epoxy mount was cleaned and gold-coated. Zircon U–Pb dating combined with trace element analysis (Ti, Fe, Y, REE, U, and Th) were performed on the Stanford/USGS SHRIMP-RG at Stanford University using a O_2^- beam ~25 x 25 μm analytical spot. The complete U-Pb dataset is given in Appendix E. Analyses of Temora-2 zircon standard ($^{206}Pb/^{238}U$ age = 416.8 Ma; Black et al., 2004), both treated and untreated, were performed after every 4 unknown analyses. Treated and untreated grains of Mt. Dromedary zircon ($^{206}Pb/^{238}U$ age = 99.12 Ma; Schoene et al., 2006) were analyzed as a secondary standard interspersed within

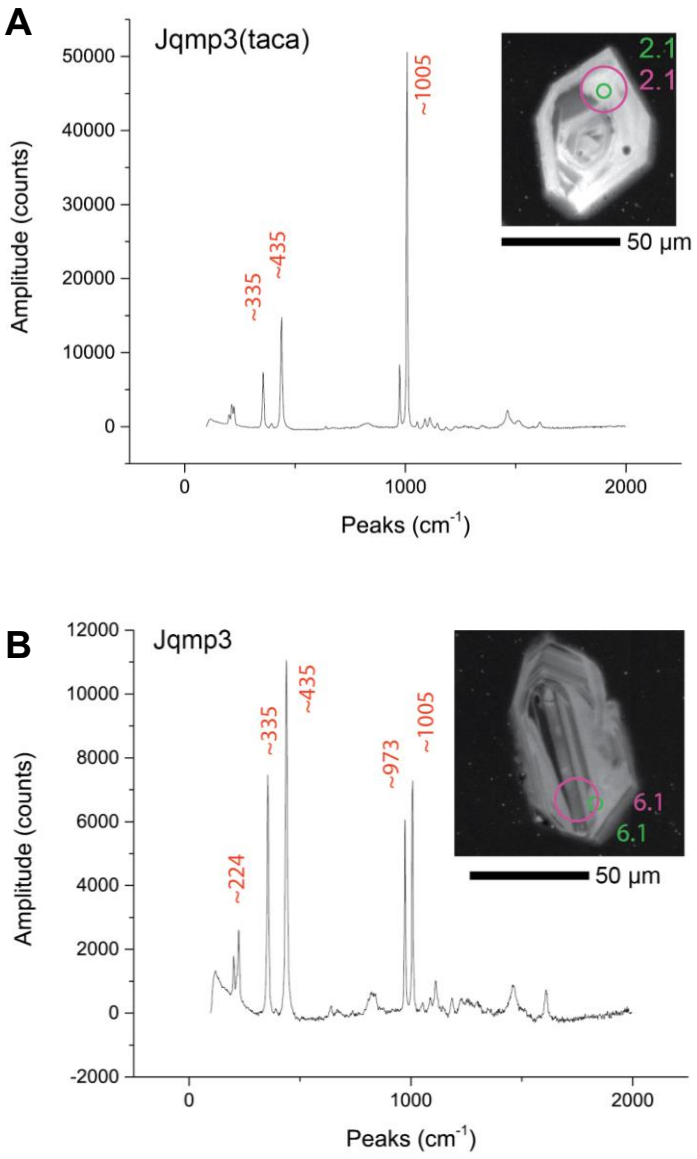

Figure 2. A) An example of a non-metamict Raman spectrum from analysis Jqmp3cata_2.1, a thermally annealed and chemically abraded zircon from sample Jqmp3. Raman analytical spot (small green circle) analysis guided combined U-Pb + TE spot (large purple circle) choice. Peaks of structurally intact zircons occur at ~335, ~435, and~1005 cm^{-1}, which correspond to SiO_4, SiO_4, and Zr-Si bands. B) An example of a metamict Raman spectrum from analysis Jqmp3_6.1, an untreated zircon from sample Jqmp3. Note the additional peaks at ~224 and ~973 cm^{-1} and lower intensity of the ~1005 cm^{-1} peak, indicating degradation in the zircon crystal structure. Images are cathodoluminesence.

unknown analyses. Trace element concentrations were standardized using MADDER (3435 ppm U; Barth & Wooden, 2010). Data were reduced using Squid 2.51 (Ludwig, 2009) and Isoplot 3.76 software (Ludwig, 2012). The measured $^{206}Pb/^{238}U$ was corrected for common Pb using ^{207}Pb using a model Pb composition from Stacey and Kramers (1975). Results are summarized in Table 2 and shown in Figs. 3 and 4. Calculation of Ce* involved using logarithmic regression using the chondrite-normalized values of Nd and Sm.

3.4. CAMECA ims1270 analysis: Oxygen isotopes

Zircons were re-imaged on the VU SEM after SHRIMP-RG analysis and the mount was lightly polished to remove existing analytical spots. After cleaning and gold-coating, oxygen isotope ratios were measured on the CAMECA ims1270 microprobe at UCLA. Operating conditions include a Cs^+ beam ~25 x 15 μm and sputter depth of ~1 μm. Additional operating conditions are listed in Table S4. Instrumental mass fractionation was determined using analyses of R33 standard zircons (5.55‰; Black et al. 2004). One-sigma external reproducibility in R33 was 0.325. Data reduction was performed with *Isotope* software. Oxygen data are reported as $\delta^{18}O$ per mil (‰) values with 2σ total error, calculated relative to Vienna Mean Standard Ocean Water (VSMOW; Baertschi, 1976). Grains were imaged by BSE and SE on the VU SEM after analysis to verify analytical pit locations and 34 (out of a total of 124) analyses that intersected significant cracks or inclusions or were partially off the grain were discarded. Results are listed in Table 2 and the complete dataset is available in Appendix D.

4. Results

4.1. Petrography

Results of thin section examination of the Yerington rocks sampled in this study generally reinforce previous findings (Dilles, 1987). A detailed summary of petrography is provided in

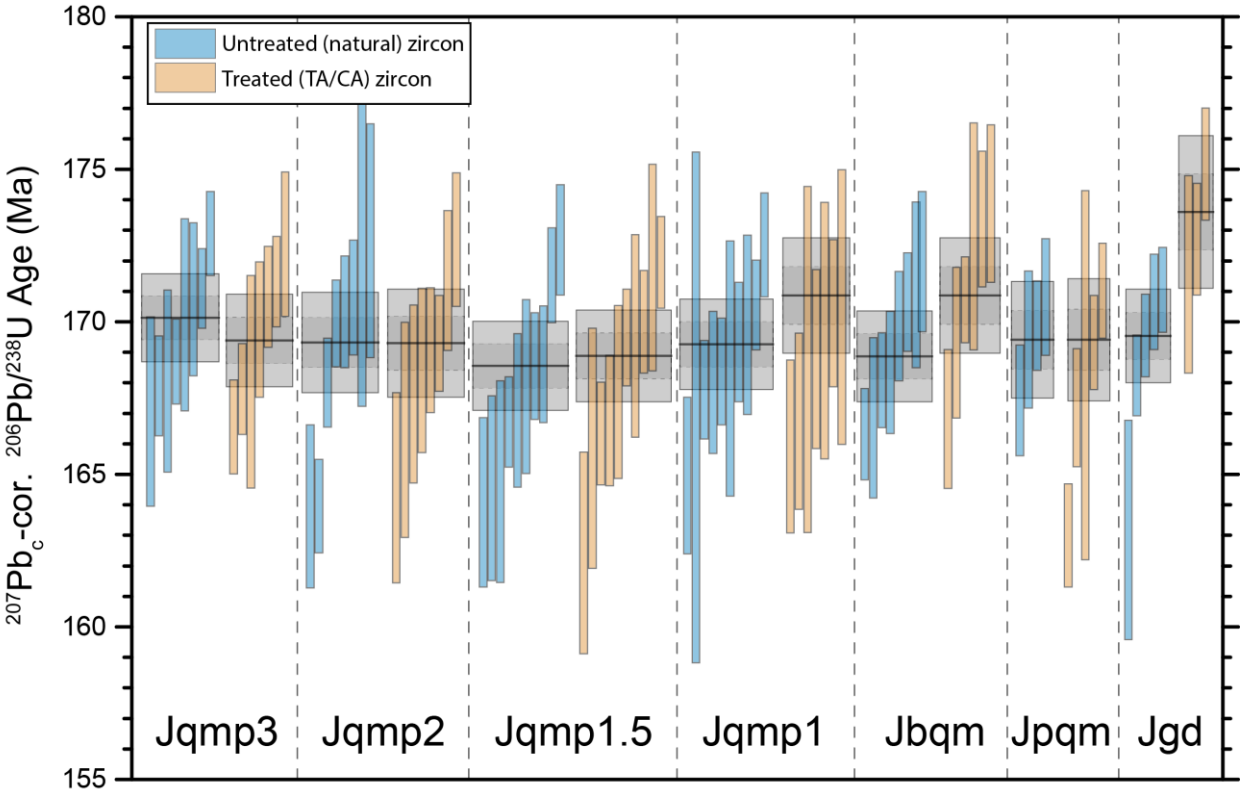

Figure 3. *In situ* zircon U-Pb analyses per Yerington sample. Grey boxes denote 1σ (small box) and 2σ (large box) errors. Weighted mean sample ages are horizontal black bars.

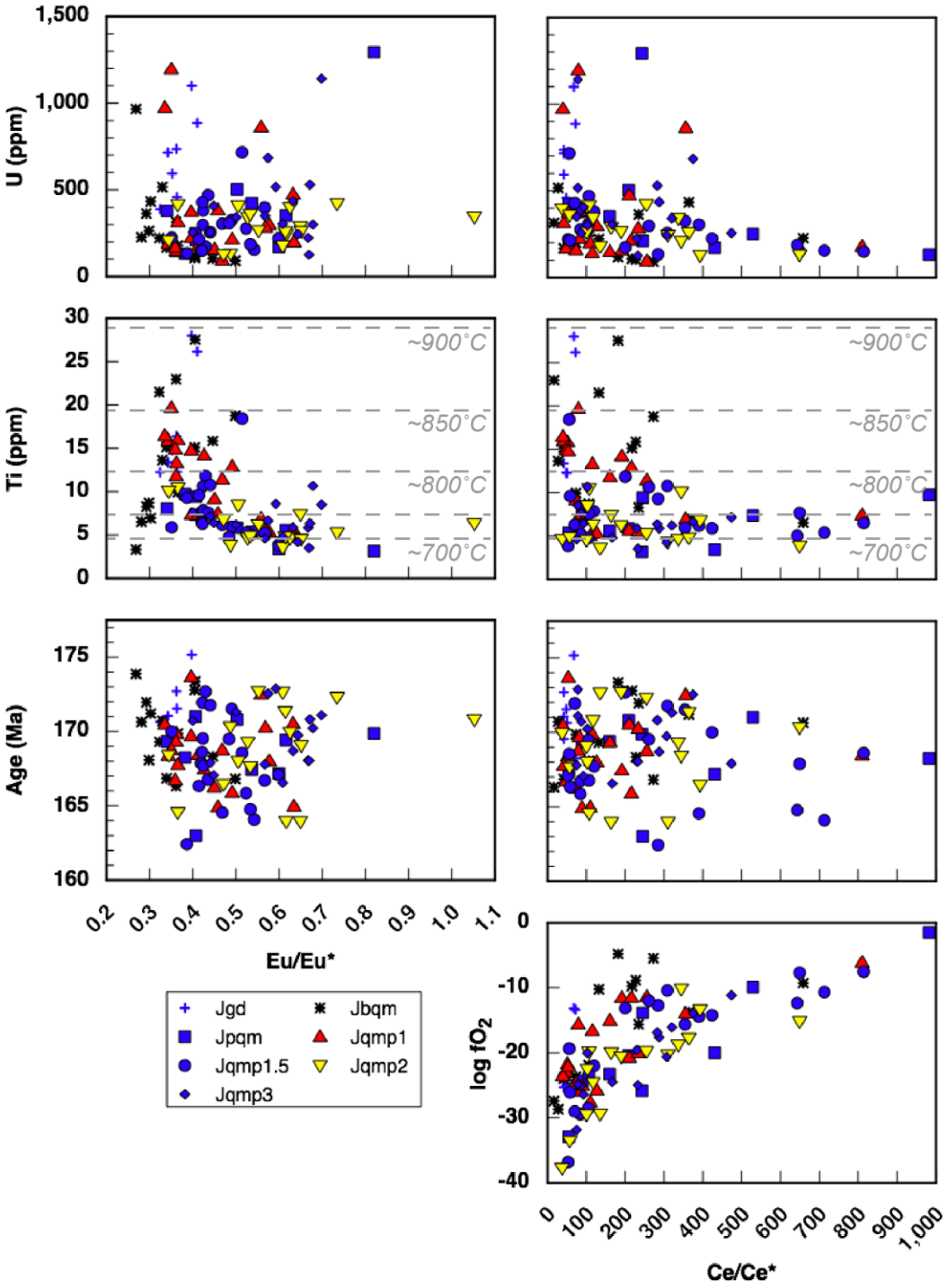

Figure 4. *In situ* zircon trace element and U-Pb age analyses and relevant calculated values for Yerington samples. Colors indicate bulk rock Cu%: <0.25% (blue); 0.25% < yellow < 0.75%; 0.75% < red < 1%; >1% (black). Approximate Ti-in-zircon crystallization temperatures calculated using $aSiO_2$=1 and $aTiO_2$=0.7 using the method of Ferry and Watson (2007). Log fO_2 calculated using the method of Trail et al. (2012).

Table 2. Summary of Yerington zircon analytical results

	Laser Raman		^{207}Pb corr. Age		Trace elements (ppm)																		Oxygen isotopes	
	Amplitude (cts)	FWHM (cm^{-1})	^{206}Pb/^{238}U (Ma)	1σ	Th	U	Y	La	Ce	Nd	Sm	Eu	Gd	Dy	Er	Yb	Hf	Eu/Eu*	Ce/Ce*	Ti	Fe	Xtal T[1] (°C)	δ^{18}O (‰)	2σ SE
Jqmp1																								
qmp1_1.1	34207	6.4	168	4	90	179	350	0.01	22.62	0.27	1.13	0.43	8.7	31.8	63.1	126	10682	0.41	812	7.4	0.3	751		
qmp1_3.1	15761	6.6	165	3	98	199	338	0.01	17.22	0.65	1.18	0.65	8.2	28.7	60.5	145	9419	0.63	110	5.0	0.2	716	5.6	0.7
qmp1_4.1	19002	6.5	168	2	174	299	380	0.01	22.38	0.71	1.23	0.63	9.1	31.1	68.3	177	9807	0.58	127	5.3	0.2	721		
qmp1_5.1	41566	5.9	170	3	98	142	504	0.02	17.95	0.88	2.16	0.68	15.0	51.2	86.1	167	10036	0.36	116	13.3	0.2	810	6.0	0.7
qmp1_6.1	40292	5.7	169	2	93	149	480	0.01	17.73	0.73	2.09	0.67	15.5	48.1	83.0	160	10943	0.36	161	11.8	0.2	798	5.8	0.7
qmp1_7																							4.6	0.7
qmp1_8																							5.9	0.7
qmp1_10.1	45261	6.7	173	2	631	863	589	0.02	48.34	0.79	2.02	1.02	15.4	51.4	103.9	237	10329	0.56	357	6.9	1.0	745		
qmp1_13.1	16284	6.5	171	1	303	475	411	0.20	26.88	0.54	0.99	0.59	8.3	32.1	69.5	175	9321	0.63	211	5.6	105.2	726		
qmp1_14.1	29273	6.2	168	2	147	190	649	0.02	18.97	1.56	2.85	0.89	21.8	67.3	111.4	212	9457	0.34	52	15.9	0.8	829	5.6	0.7
qmp1_15.1	24160	5.8	168	2	291	315	925	0.05	28.28	2.93	5.53	1.67	35.2	100.7	153.0	274	9544	0.37	42	16.0	0.9	830	5.9	0.6
qmp1_16																							5.7	0.7
qmp1_17																							5.6	0.7
qmp1_19.1	31547	5.9	167	8	95	157	369	0.07	15.55	0.47	1.16	0.47	9.6	34.2	64.3	138	10072	0.43	192	14.2	23.2	817	5.3	0.7
qmp1_20																							5.3	0.7
qmp1_24																							5.2	0.7
qmp1_28																							5.8	0.7
qmp1_29																							5.4	0.7
qmp1_30																							5.8	0.6
Jqmp1 (TA/CA)																								
qmp1cata_1.1	42003	5.5	166	3	120	216	406	0.05	20.73	0.53	1.27	0.61	11.2	38.6	70.8	145	8940	0.49	216	12.9	0.2	807		
qmp1cata_3.1	27353	5.9	170	2	129	284	280	0.01	19.31	0.36	0.67	0.35	5.4	21.7	49.5	130	10142	0.57	234	5.5	0.3	724	5.4	0.7
qmp1cata_4.1	16361	6.3																						
qmp1cata_5.1	27308	6.0																						
qmp1cata_6.1	3082	19.1	169	3	1943	1197	2547	0.11	79.98	4.99	10.75	3.34	78.8	258.8	422.8	752	9360	0.35	80	19.7	0.5	853		
qmp1cata_7.1	31003	5.9			430	375	1207	1.92	52.95	4.40	8.53	2.72	51.4	126.9	191.9	322	5542	0.40	54	14.8	3.0	821		
qmp1cata_8.1	21080	5.7			285	384	937	0.27	43.10	2.27	4.65	1.80	30.6	92.9	152.6	305	10045	0.46	89	7.5	3.4	752		
qmp1cata_9.1	11281	5.7			95	158	558	0.01	18.27	1.22	2.60	0.99	17.3	54.8	95.3	191	9817	0.45	74	9.1	0.2	772		
qmp1cata_10.1	44515	5.5	170	4	121	224	352	1.58	41.03	1.26	1.38	0.45	8.8	30.1	58.4	124	10480	0.40	83	7.4	4.4	751		
qmp1cata_12.1	8974	5.6	167	3	138	168	676	0.02	21.81	2.01	3.88	1.13	23.8	69.6	112.5	205	9500	0.36	48	14.9	0.3	822		
qmp1cata_13.1	14971	8.0	170	4	965	974	3152	0.05	46.06	4.43	7.36	2.59	75.3	301.5	549.6	1006	9806	0.33	40	16.5	1.2	833	5.5	0.7
qmp1cata_14.1	25244	6.0	169	6	46	94	281	0.04	12.61	0.34	1.01	0.40	6.9	25.8	49.0	103	10058	0.47	256	11.4	0.3	794	5.9	0.6
Jqmp1.5																								
qmp1.5_1.1	36134	5.8	173	2	79	173	413	0.01	16.41	0.50	1.33	0.51	9.7	37.3	71.5	155	9762	0.43	200	11.8	0.2	798		
qmp1.5_2.1	49247	6.0	164	3	61	155	232	0.04	16.21	0.17	0.57	0.30	5.0	20.1	42.4	95	10969	0.54	714	5.4	0.2	722	6.0	0.7
qmp1.5_3																							5.0	0.7
qmp1.5_4.2	46932	6.0	168	3	65	151	276	0.00	17.78	0.23	0.81	0.32	6.8	25.1	49.5	110	10470	0.42	650	7.6	0.3	754	5.8	0.7
qmp1.5_5																							4.8	0.7
qmp1.5_6.1	25758	6.2	165	3	73	187	224	0.01	15.63	0.18	0.60	0.28	4.4	16.9	39.6	98	11140	0.53	644	5.0	0.3	716	5.7	0.7
qmp1.5_8.1	49393	5.8	169	2	64	149	292	0.04	18.99	0.21	0.83	0.34	7.1	23.2	52.5	117	10829	0.42	816	6.5	0.4	739		
qmp1.5_9.1	41237	7.3	169	2	836	717	2333	0.11	79.67	6.84	14.26	6.08	91.3	258.1	378.4	645	8532	0.51	56	18.4	0.2	846		
qmp1.5_10.1	44848	5.8	167	3	110	220	285	0.02	14.33	0.88	1.24	0.62	8.1	25.1	51.8	125	10667	0.60	53	3.8	0.3	693	5.3	0.7
qmp1.5_11																							5.8	0.7
qmp1.5_12																							5.6	0.7
qmp1.5_24.1	34869	5.8	172	2	150	326	469	0.01	25.52	0.44	1.15	0.54	9.8	39.5	82.3	193	10389	0.49	355	6.0	0.3	731	5.5	0.7
qmp1.5_25.1	19082	6.3	167	1	263	397	530	0.03	27.54	1.42	2.70	1.21	15.8	48.4	91.4	206	10598	0.57	85	5.2	0.3	719		
qmp1.5_26.1	45383	5.8	165	3	145	305	441	0.01	31.46	0.49	1.30	0.55	9.9	36.3	78.3	182	10449	0.47	391	6.2	0.3	734	5.8	0.7
qmp1.5_28																							5.1	0.7
Jqmp1.5 (TA/CA)																								
qmp1.5cata_1.1																							3.4	0.6
qmp1.5cata_2.1	10426	5.8	170	2	103	225	268	0.01	19.98	0.30	0.81	0.27	6.8	24.1	48.7	102	11633	0.35	424	5.9	0.4	730		
qmp1.5cata_3.1	33145	5.7																					4.8	0.7
qmp1.5cata_3.2	46451	5.4	169	2	172	308	622	0.02	26.47	1.28	2.86	1.19	19.6	58.5	107.9	223	11243	0.48	106	4.8	0.3	711		
qmp1.5cata-4.1	21782	5.7	166	4	150	278	386	0.01	12.96	0.77	1.68	0.76	11.7	34.9	64.6	133	9781	0.52	85	5.3	0.4	720		
qmp1.5cata-5.1	47309	5.5	172	2	285	429	866	0.01	31.20	2.14	4.51	1.61	29.9	86.5	141.4	274	10175	0.42	71	6.3	0.2	736		
qmp1.5cata-6.1	66492	5.5	170	3	167	298	516	0.02	27.96	0.68	1.86	0.66	12.2	47.3	90.1	192	10245	0.42	262	10.6	0.4	787		
qmp1.5cata-7.1	31127	5.4	172	3	144	257	479	0.01	26.33	0.58	1.71	0.64	11.4	42.2	85.4	175	9608	0.44	309	10.8	0.2	788		
qmp1.5cata-8.1	19989	5.5	166	2	146	214	711	0.03	22.25	1.70	3.30	1.17	22.5	71.0	121.6	233	9992	0.41	58	9.6	0.3	776		
qmp1.5cata_10.1	20329	5.8	162	3	67	134	290	0.09	17.04	0.35	0.90	0.33	7.7	27.8	50.0	107	9364	0.39	285	9.3	1.3	773		
qmp1.5cata_12.1	40640	5.2	168	3	278	381	947	0.09	39.37	1.77	4.17	1.53	29.2	91.4	160.2	298	8633	0.42	120	7.8	0.8	757		
qmp1.5cata_15.1	21279	5.3	167	2	385	469	1193	0.06	48.53	2.29	5.00	2.01	39.6	115.8	196.4	355	9704	0.44	107	7.6	2.0	753		
Jqmp2																								
qmp2_1.1	34630	6.0	164	2	106	244	221	0.02	14.93	0.24	0.53	0.31	4.6	16.6	39.1	103	10660	0.62	311	4.3	5.4	702		

[1]Ti-in-zircon crystallization temperature calculated as described in Ferry and Watson (2007), using *a* TiO_2=0.7 and *a* SiO_2=1.

Table 2 cont. Summary of Yerington zircon analytical results

	Laser Raman		^{207}Pb corr. Age		Trace elements (ppm)																		Oxygen isotopes	
	Amplitude (cts)	FWHM (cm^{-1})	^{206}Pb/^{238}U (Ma)	1σ	Th	U	Y	La	Ce	Nd	Sm	Eu	Gd	Dy	Er	Yb	Hf	Eu/Eu*	Ce/Ce*	Ti	Fe	Xtal T[1] (°C)	δ^{18}O (‰)	2σ SE
qmp2_2.1	29639	6.0	171	2	204	344	312	0.04	23.19	0.64	0.89	0.86	6.9	26.1	56.8	127	10617	1.05	118	6.3	2.0	736		
qmp2_3.1	37981	5.5	170	2	49	131	158	0.00	12.35	0.14	0.46	0.20	3.6	12.4	27.9	67	11119	0.49	650	3.8	0.2	692		
qmp2_4.1	25154	6.0	173	4	86	179	224	0.01	10.45	0.42	0.97	0.50	6.3	18.7	37.6	94	10896	0.61	136	3.6	0.2	687		
qmp2_5.1	20884	5.7	172	5	269	421	328	0.01	28.63	0.48	0.90	0.61	7.0	24.6	58.7	152	10382	0.73	255	5.3	0.3	720	5.3	0.7
qmp2_6.1	42429	6.1	170	1	252	398	653	0.02	22.77	2.17	3.39	1.74	21.4	61.7	109.3	241	10101	0.62	38	4.6	0.2	708	5.3	0.7
qmp2_7.1	11732	6.3	164	3	137	290	311	0.07	19.58	0.47	0.82	0.47	6.0	25.7	57.0	149	10715	0.65	164	7.4	6.1	751	5.4	0.7
qmp2_8.1																							5.2	0.7
qmp2_9.1	48734	5.6	168	1	247	408	667	0.02	28.18	1.29	2.64	1.17	18.9	64.6	115.6	236	10438	0.51	103	8.5	0.2	764		
qmp2_10.1																							5.2	0.7
qmp2_12																							5.0	0.7
qmp2_14																							5.6	0.7
qmp2_15																							5.1	0.7
qmp2_18																							5.1	0.7
qmp2_19																							5.7	0.7
Jqmp2 (TA/CA)																								
qmp2cata_1.1	29553	5.4	169	2	174	341	231	0.02	20.83	0.34	0.81	0.39	6.1	18.9	39.7	95	10292	0.53	338	4.6	0.3	709		
qmp2cata_2.1	59662	5.3	165	3	255	415	712	0.01	29.80	1.39	3.03	0.97	21.7	68.9	120.9	238	10560	0.37	107	10.5	0.2	785	4.1	0.7
qmp2cata_3.1	12902	5.9	171	2	121	259	293	0.01	18.28	0.29	0.72	0.42	6.2	23.9	52.3	131	10413	0.61	365	4.8	0.2	712		
qmp2cata_4.1	46228	5.2	173	2	156	265	557	0.00	36.59	0.89	1.77	0.92	14.6	49.4	95.8	210	9634	0.55	190	6.2	0.2	735		
qmp2cata_5.1	41850	5.5	168	3	234	360	668	0.02	25.17	1.84	3.36	1.50	21.9	61.7	108.6	222	9695	0.53	57	4.9	0.2	713	4.2	0.7
qmp2cata_6.1	42205	5.6	168	3	105	209	328	0.21	20.84	0.35	0.90	0.30	8.0	29.7	56.4	120	10117	0.34	345	10.1	0.4	781		
qmp2cata_8.1	36180	5.6	169	2	136	262	271	0.01	15.79	0.61	1.03	0.57	6.9	21.9	45.8	113	10320	0.65	101	4.5	0.3	707		
qmp2cata_9.1																							4.8	0.6
qmp2cata_10.1	37266	5.3	166	4	49	128	247	0.01	11.82	0.23	0.75	0.32	5.7	22.2	44.6	108	10370	0.47	394	6.8	0.1	743	4.8	0.7
qmp2cata_16		5.5																					4.8	0.7
Jqmp3																								
qmp3_5.1	15240	5.6	168	3	98	224	568	0.11	28.11	0.68	1.66	1.04	13.6	45.7	97.5	221	9292	0.67	230	5.9	0.4	729		
qmp3_6.1	10893	5.8	170	3	159	301	1238	0.06	34.53	2.33	7.05	4.45	56.8	141.1	160.4	226	10150	0.68	103	10.7	11.7	787	5.0	0.7
qmp3_7.1	11718	9.4	171	1	1137	1142	1646	0.10	84.78	4.41	7.81	4.44	48.2	154.7	277.1	569	8129	0.70	78	8.5	0.4	765		
qmp3_8.1	13093	6.2	169	1	272	435	375	0.02	27.36	0.50	1.12	0.65	8.7	30.4	66.6	160	10049	0.63	288	5.9	0.6	730		
qmp3_12																							4.4	0.7
qmp3_16																							5.0	0.7
qmp3_17.1	36075	6.6	168	2	119	256	465	0.05	26.72	0.40	1.20	0.52	10.9	40.9	81.1	176	10429	0.44	475	7.1	1.1	748		
qmp3_18.1	29040	6.5	171	3	168	256	696	0.01	28.88	1.49	2.92	1.04	21.6	67.2	121.4	238	10060	0.40	87	7.6	0.2	754		
qmp3_19.1	49568	5.6	167	3	280	407	986	0.02	40.88	2.09	4.32	1.64	28.7	97.2	176.7	347	10398	0.45	93	6.4	0.2	738	5.1	0.7
qmp3_20.1	49312	5.9	173	1	410	517	1044	0.07	61.17	3.17	5.56	2.60	32.2	98.0	181.2	372	8152	0.59	78	8.6	0.7	766		
Jqmp3 (TA/CA)																								
qmp3cata_1.1	17582	6.1	171	1	160	342	326	0.01	22.79	0.38	0.87	0.41	7.1	27.0	58.8	140	10657	0.50	321	6.2	0.5	735		
qmp3cata_2.1	53575	5.6	171	2	462	530	346	0.01	35.68	0.62	1.31	0.79	9.8	31.3	58.9	125	9887	0.67	283	6.4	0.4	737	4.7	0.7
qmp3cata_3.1	22634	5.4	173	2	575	684	530	0.01	45.87	0.74	1.94	0.98	13.9	48.4	93.2	209	10247	0.57	375	6.7	0.2	741		
qmp3cata_4.1	7343	5.5	168	3	44	126	165	0.01	10.96	0.25	0.56	0.31	3.5	13.6	29.6	72	10651	0.67	233	3.5	0.3	685		
qmp3cata_6.1	3878	6.1	168	1	212	350	493	0.02	21.53	1.22	2.26	1.08	15.0	47.1	84.2	188	9827	0.57	75	4.6	0.4	708	4.3	0.7
qmp3cata_7.1	46867	5.1	167	2	149	305	417	0.14	22.08	0.63	1.30	0.71	9.7	35.4	72.9	171	9823	0.61	167	4.8	0.5	712		
qmp3cata_10.1	50672	5.3	170	2	108	245	255	0.02	14.41	0.29	0.77	0.42	5.1	19.2	46.1	129	9732	0.64	307	4.2	0.7	700		
Jbqm																								
bqm_1.1	48644	5.8	167	3	120	168	678	0.01	19.82	2.36	5.09	1.26	25.3	72.8	108.1	197	9796	0.34	42	15.2	0.1	824	5.7	0.6
bqm_2.1	65238	5.7	170	2	107	178	577	0.01	19.17	1.31	2.88	0.93	20.7	62.9	98.1	193	11432	0.37	74	9.9	0.2	780	5.9	0.7
bqm_3.1	40608	6.7	168	2	64	104	353	0.01	13.27	0.42	1.33	0.55	10.5	37.0	58.7	112	10130	0.45	228	15.9	0.2	829		
bqm_4.1	38612	7.0	166	1	241	315	1043	0.09	25.16	4.56	6.01	1.68	33.6	96.7	178.0	321	8905	0.36	17	23.0	0.1	871		
bqm_5.1																							5.3	0.7
bqm_6.1	57445	5.6	168	2	183	263	884	0.01	32.60	1.74	4.29	1.12	30.4	93.8	146.9	267	11374	0.30	107	8.7	39.7	767	5.5	0.7
bqm_7.1	43454	6.4	171	3	119	434	208	0.40	18.30	0.20	0.36	0.11	3.3	16.5	39.5	102	14219	0.30	365	7.0	4.7	745	5.6	0.7
bqm_8.1	63554	6.0	171	2	67	227	199	0.01	17.62	0.17	0.48	0.13	3.8	18.5	36.1	77	12666	0.28	660	6.5	0.6	739		
bqm_9.1	41465	5.9	172	2	219	364	731	0.01	25.42	0.77	2.39	0.67	20.3	73.1	127.6	245	12764	0.29	235	8.3	0.2	762	5.3	0.7
bqm_10																							5.2	0.7
bqm_11																							5.7	0.7
bqm_12																							4.9	0.7
bqm_13		6.1																					5.6	0.7
Jbqm (TA/CA)																								
bqmcata_1.1	58117	5.8	229	3	87	313	796	0.00	10.56	0.33	1.01	0.33	12.4	60.7	155.1	369	9846	0.28	226	18.8	0.2	848		
bqmcata_2.1																							4.9	0.7
bqmcata_9.1	15551	5.9	231	4	66	210	588	0.01	9.90	0.31	0.90	0.27	9.7	51.4	112.8	237	9522	0.27	219	9.0	0.5	770		
bqmcata_10.1	24091	6.8	174	3	70	967	86	0.01	13.47	0.04	0.16	0.04	1.3	6.0	16.0	51	15267	0.27	3313	3.3	2.5	680		

[1]Ti-in-zircon crystallization temperature calculated as described in Ferry and Watson (2007), using *a* TiO_2=0.7 and *a* SiO_2=1.

Table 2 cont. Summary of Yerington zircon analytical results

	Laser Raman		^{207}Pb corr. Age		Trace elements (ppm)																		Oxygen isotopes	
	Amplitude (cts)	FWHM (cm^{-1})	^{206}Pb/^{238}U (Ma)	1σ	Th	U	Y	La	Ce	Nd	Sm	Eu	Gd	Dy	Er	Yb	Hf	Eu/Eu*	Ce/Ce*	Ti	Fe	Xtal T[1] (°C)	δ^{18}O (‰)	2σ SE
bqmcata_11.1	36348	5.4	167	2	51	92	320	0.01	14.96	0.40	1.26	0.56	9.2	32.1	52.7	108	9678	0.50	273	18.8	0.2	848	5.7	0.7
bqmcata_12.1	20578	5.7	169	2	113	222	329	0.00	16.29	0.63	1.40	0.39	9.9	32.7	55.5	110	10835	0.32	133	21.5	0.6	863	5.2	0.7
bqmcata_13.1	17050	6.6	171	1	383	516	1070	0.04	27.92	3.46	5.17	1.31	28.3	99.7	187.1	341	10195	0.33	28	13.6	0.2	813	5.0	0.7
bqmcata_14.1	34001	5.2	173	4	55	108	293	0.01	14.22	0.39	1.00	0.36	7.2	29.3	50.8	103	9836	0.40	218	15.1	0.2	824	5.5	0.7
bqmcata_15.1	63856	5.6	173	2	66	118	298	0.36	18.26	0.50	1.09	0.41	8.6	30.0	52.4	101	10434	0.41	182	27.5	30.1	893		
Jpqm																								
pqm_2.1	19353	5.7	169	2	171	353	364	0.02	20.26	0.62	1.34	0.66	8.0	28.1	63.5	162	10174	0.62	160	5.6	0.6	725		
pqm_5.1	5276	6.6	170	1	390	1293	316	0.02	18.19	0.29	0.50	0.38	3.9	18.3	57.7	200	10640	0.82	244	3.1	0.8	676		
pqm_6.1	18484	6.3	167	2	262	423	720	0.03	28.13	1.98	3.32	1.44	20.2	66.2	124.2	279	10117	0.54	55	5.4	1.1	721	5.7	0.7
pqm_7																							4.9	0.7
pqm_8																							4.8	0.7
pqm_9.1	14750	6.7	171	2	312	503	545	0.03	30.47	0.73	1.60	0.70	11.1	41.7	97.9	259	10004	0.50	210	5.8	3.0	729		
pqm_10.1	13756	7.9	452	7	81	138	951	0.16	11.49	0.94	2.21	0.92	20.2	87.9	175.8	347	7842	0.42	66	19.9	35.3	855	6.0	0.7
pqm_11																							5.5	0.7
pqm_12																							5.0	0.7
pqm_13																							5.3	0.7
pqm_14		6.3																					5.5	0.7
Jpqm (TA/CA)																								
pqmcata_1.1	868	3.6	171	2	115	250	318	0.01	23.42	0.30	0.86	0.35	7.8	29.0	57.5	118	10671	0.41	530	7.4	0.2	751		
pqmcata_2.1	8678	5.7	168	6	45	132	196	0.00	14.20	0.15	0.63	0.20	4.0	16.1	35.1	80	10982	0.38	984	9.7	0.7	778	5.2	0.6
pqmcata_3.1	9953	5.5	163	2	107	212	494	0.15	24.16	0.55	1.35	0.52	11.1	42.9	88.4	188	9637	0.41	245	9.4	0.5	775		
pqmcata_6.1	19105	4.9	167	2	71	171	184	0.01	10.73	0.18	0.57	0.30	4.2	14.7	32.3	85	10832	0.60	431	3.4	0.3	682		
pqmcata_8.1	16556	5.5	169	2	219	379	464	0.02	22.29	1.07	1.97	0.58	13.5	45.5	79.8	166	10446	0.34	89	8.0	0.5	759		
Jgd																								
gd_1.1	19662	6.5	168	1	1450	886	2589	0.09	90.33	5.89	11.98	4.54	94.3	277.8	431.8	748	8526	0.41	72	26.2	0.2	887	5.9	0.7
gd_2.1	935	6.8	163	4	88	230	359	0.05	16.03	0.32	1.04	0.28	7.5	31.5	65.3	150	12280	0.30	387	28.7	70.0	898		
gd_3.1	6952	6.4	171	2	351	389	1155	0.02	29.31	2.80	5.86	1.60	38.5	120.3	197.1	367	10589	0.32	51	12.2	1.1	801		
gd_4.1	11467	7.0	171	1	709	716	1822	0.06	38.34	3.99	7.57	2.17	49.4	180.0	309.2	564	10351	0.34	42	13.4	2.4	811		
gd_5.1	3943	7.4	170	1	547	594	1838	0.26	43.71	4.24	7.55	2.35	54.7	181.1	306.8	569	10121	0.35	42	14.8	8.6	821		
gd_15																							5.6	0.7
Jgd (TA/CA)																								
gdcata_2.1	19468	5.9	172	3	227	459	997	0.02	25.97	2.38	4.60	1.45	32.2	99.5	167.7	313	11261	0.36	49	12.3	0.9	802		
gdcata_3.1	13243	7.7	104	1	1466	2189	1690	0.06	9.92	2.78	4.61	0.78	33.6	148.5	300.4	622	10135	0.19	14	9.8	0.7	779		
gdcata_4.1	22383	7.9	101	1	1717	1702	1137	0.04	13.79	1.68	3.29	0.67	26.0	97.7	201.5	421	8632	0.22	37	14.1	0.6	816	6.2	0.7
gdcata_6																							5.1	0.7
gdcata_7.1	4077	6.7	173	2	875	737	2386	0.08	52.85	5.37	10.00	3.38	81.1	246.8	389.5	688	9464	0.36	42	16.4	0.2	833		
gdcata_11.1	3910	7.5	175	2	1860	1100	4191	0.11	100.16	8.54	21.45	7.73	164.4	464.0	673.3	1129	8862	0.40	68	28.0	0.2	895		
Mt. Dromedary																								
MtD_27.2	8946	10.0	103	2	1375	1535	2214	0.09	8.61	2.73	5.84	1.72	62.7	213.2	382.8	724	8019	0.27	16	15.4	0.2	826	6.5	0.7
MtD_28.1	39378	6.4	97.1	1	125	360	435	0.01	4.13	0.56	1.22	0.31	9.3	34.7	80.3	193	8101	0.28	37	15.3	0.3	825	6.8	0.7
MtD_29.1	27370	6.7	101	1	372	505	1061	0.07	6.71	2.75	4.59	1.15	33.8	104.6	181.3	356	8019	0.28	9	17.2	0.3	838	6.5	0.7
MtD_31.2	52781	6.9	95.9	1	224	348	729	0.02	5.47	1.77	3.43	0.75	22.3	74.6	126.0	246	8677	0.26	14	12.2	0.9	801	7.0	0.7
Mt. Drom. (TA/CA)																								
MtDC_24.1	6037	6.8	100	1	68	184	229	0.00	3.19	0.20	0.58	0.13	4.4	20.3	42.3	102	9257	0.25	107	9.3	0.1	773		
MtDC_25.1	32636	6.1	99.2	2	112	358	297	0.00	4.23	0.20	0.68	0.15	5.2	24.7	55.6	135	10571	0.24	169	8.2	0.3	761	6.5	0.7
MtDC_26.2	44230	6.3	100	2	279	442	707	0.02	4.59	1.34	3.03	0.71	20.5	70.5	119.9	236	8904	0.28	18	11.4	0.3	794	6.4	0.7
MtDC_27.1	40306	6.7	100	1	254	653	459	0.01	6.07	0.40	1.16	0.22	9.6	37.8	82.9	200	10044	0.20	104	9.3	0.4	773	6.3	0.7

[1]Ti-in-zircon crystallization temperature calculated as described in Ferry and Watson (2007), using $a\ TiO_2$=0.7 and $a\ SiO_2$=1.

Appendix C. Optical petrography of the porphyry dike units reveals porphyritic textures dominated by feldspar phenocrysts (~25%; plagioclase≈potassium feldspar) in a fine- to medium-grained roughly equigranular groundmass of plagioclase, quartz, potassium feldspar, hornblende, and biotite. As previously mentioned, zircon, apatite, sphene, and Cu-sulfides are present in trace amounts. Especially notable in the earlier porphyry dikes (Jqmp1, 1.5) is the presence of abundant quartz veins up to 1 cm wide that host Cu sulfides and which decrease in abundance in later dike units. Abundance of alteration minerals such as chlorite, biotite, and epidote increases in the younger dike units, as does the magnitude of the sericitic overprint that all the porphyry dikes possess.

4.2. Laser Raman spectroscopy

The laser Raman spectroscopy results indicate a wide range of crystal structure variation. Of 118 TA/CA treated and untreated zircon grains analyzed by laser Raman that also underwent U–Pb age, trace element, and $\delta^{18}O$ analysis, 25 grains were specifically chosen for analysis because their Raman spectra had lower intensities or additional peaks than ideal crystalline zircon spectra, indicating a potentially metamict area in the grain. However, U–Pb and trace element data from 18 of those 25 grains were statistically indistinguishable from grains with spectra indicating crystalline structures and therefore were included in the overall data set, while 3 grains yielded data of questionable quality and data from 4 grains were not included (Appendix B).

4.3. U–Pb zircon geochronology

^{207}Pb-corrected $^{206}Pb/^{238}U$ ages of Yerington zircons are Jurassic in age, ranging from ~168 Ma to ~174 Ma, which agrees with previous work (Dilles and Wright, 1988). There is no statistically significant difference between ages from grains that underwent TA/CA treatment and untreated grains from the same sample (Tables 2 and 3; Fig. 3). Host rock units (Jgd, Jbqm, Jpqm)

have, with one exception, slightly older weighted mean ages (including treated and untreated grains) than porphyry dike units (170.0 ± 1.4 Ma (n=7; MSWD=1.44); 169.6 ± 1.3 Ma (n=14; MSWD=1.35); and 169.4 ± 1.5 Ma (n=8; MSWD=0.61), respectively. All errors are 2σ. Ages of porphyry dike units (Jqmp1: 169.0 ± 1.2 Ma (n=20; MSWD=1.50); Jqmp1.5: 168.7 ± 1.1 Ma (n=20; MSWD=1.58); and Jqmp2: 168.7 ± 1.2 Ma (n=16; MSWD=1.63)) conform to age trends established through field relations. The exception is the Jqmp3 porphyry dike unit, which yields a $^{206}Pb/^{238}U$ age of 169.8 ± 1.1 Ma (n=15; MSWD=1.33). This age is older, but within 2σ uncertainty, than the other porphyry dike units, despite field relationships that suggest it was the youngest porphyry dike to be emplaced.

Treated and untreated secondary standards Mt. Dromedary and Temora-2 vary in age and uncertainty for each standard. Treated Mt. Dromedary grains have a weighted mean age of 100.0 ± 1.7 Ma (n=4; MSWD=0.08) while untreated Mt. Dromedary yields a weighted mean age of 98.4 ± 4.9 Ma (n=4; MSWD=5.22), compared to the published TIMS age of 99.12± 0.14 Ma (Schoene et al., 2006). Combined the weighted mean age is 99.1 ± 2.0 Ma (n=8; MSWD=2.61). Temora-2 untreated and treated grains have a weighted mean age of 417.6 ± 2.3 Ma (n=14; MSWD=1.3) and 420.04 ± 2.2 Ma (n=21; MSWD=1.6), respectively. The combined weighted mean age is 419.0 ± 1.6 Ma (n=35; MSWD=1.3), which is older than the published age of 416.8 Ma± 0.33 (Black et al., 2004).

4.4. Trace element analyses

Results are listed in Table 2. The overwhelming majority (>90%) of analyzed Yerington zircons have low to moderate U (<500 ppm), and 6 grains were over 1000 ppm U (and 3 of those are from sample Jgd) (Fig. 4). Th/U ratios are dominantly between 0.25 and 0.75, with <20% of analyses >0.75 and only 1 analysis <0.25. REE values vary over 2 orders of magnitude between samples (Fig. 5). Intra-sample REE variability is ~1 order of magnitude, which is typical of zircon populations. Sample Jgd has the highest overall concentration of REE, while Jqmp2 has the lowest.

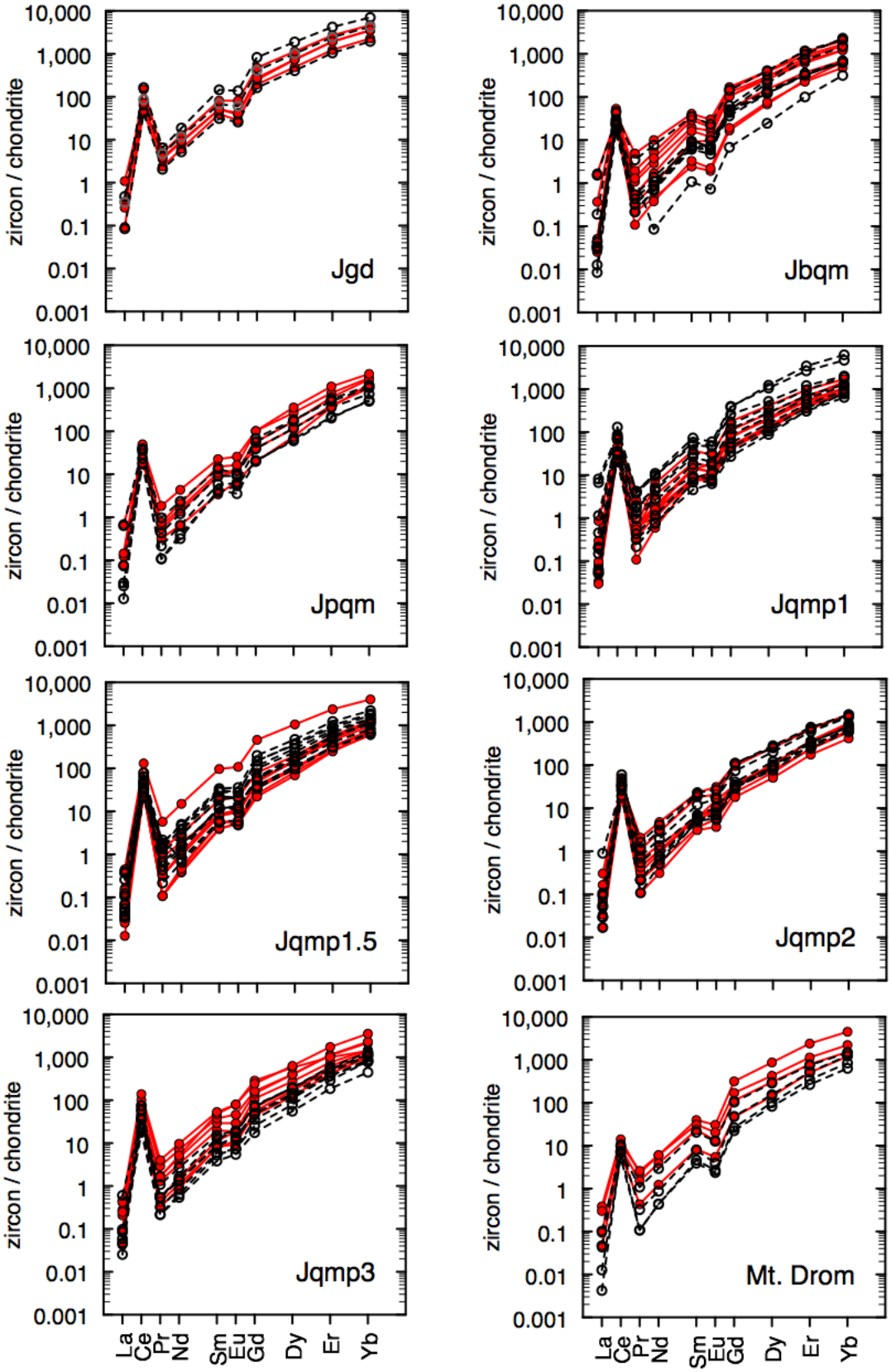
zircon / chondrite
10,000
1,000
100
10
1
0.1
0.01
0.001
Jgd
Jbqm
Jpqm
Jqmp1
Jqmp1.5
Jqmp2
Jqmp3
Mt. Drom
La
Ce
Pr
Nd
Sm
Eu
Gd
Dy
Er
Yb

Fig. 5 (previous page). Chondrite-normalized zircon REE patterns for treated (red solid line) and untreated (black dashed line) Yerington samples and secondary standard Mt. Dromedary. Normalized to C1 chondrite of McDonough and Sun (1995).

There are no systematic variations in REE concentrations between host units and porphyry dike unites. Ce/Ce* values are mostly <400 (225 mean; 160 median), with ~15 analyses >400. Only 1 grain had a Ce/Ce* value >1000, but also had unrealistically high Sm/Nd and is therefore not considered for further interpretation. Eu/Eu* ratios range from 0.19 to 1.05 with a median of 0.42 and mean of 0.44. Twenty grains (8 each in late porphyry samples Jqmp2 and Jqmp3) have Eu/Eu*≥0.60. There is a subtle relationship between Eu/Eu* and Ce/Ce* and time (based on age results presented in this study and field relationships) that indicates a shift toward more oxidizing conditions in the system (Figs. 4, 6)—older host units have lower Eu/Eu* than the younger porphyry dikes. Increasing oxidation during system development is a hallmark of porphyry Cu systems (e.g. Dilles et al., 2015, 2000; and many others). Ti concentrations range from 3.1 to 28.7 ppm with a mean value of 9.8 ppm and median of 8.0 ppm. Host units Jgd and Jbqm have higher average values (17.6 and 13.1 ppm Ti, respectively) than the porphyry dike units. Host unit Jpqm has Ti (<10 ppm) more similar to the porphyry dike units than to the other host units. These data are in good agreement with values reported by Dilles et al. (2015) for two Yerington batholith units.

4.5. Oxygen isotope analyses

Host units Jgd, Jbqm, and Jpqm have mean $\delta^{18}O$ values of 5.7±0.7‰, 5.4 ± 0.7‰, and 5.3 ± 0.7‰, respectively (all reported at 2σ total error), and are higher and more uniform than the range of $\delta^{18}O$ for dikes (4.8‰ to 5.6‰, sample means). The porphyry dike units display a decrease in $\delta^{18}O$ through time (Fig. 6); Jqmp1, the earliest-emplaced dike, has a mean value of 5.6±0.7‰ (analyses range from 5.2‰ to 6.0‰, with one outlier at 4.6‰), while Jqmp3, the latest dike, averages 4.8±0.7‰ with individual analyses ranging from 4.3‰ to 5.1‰. Jqmp1.5 and Jqmp2 average 5.3±0.7 ‰ and 5.0±0.7‰, respectively. The oxygen isotopes for TA/CA treated grains from these two samples have higher uncertainty and are depleted relative to untreated grains from

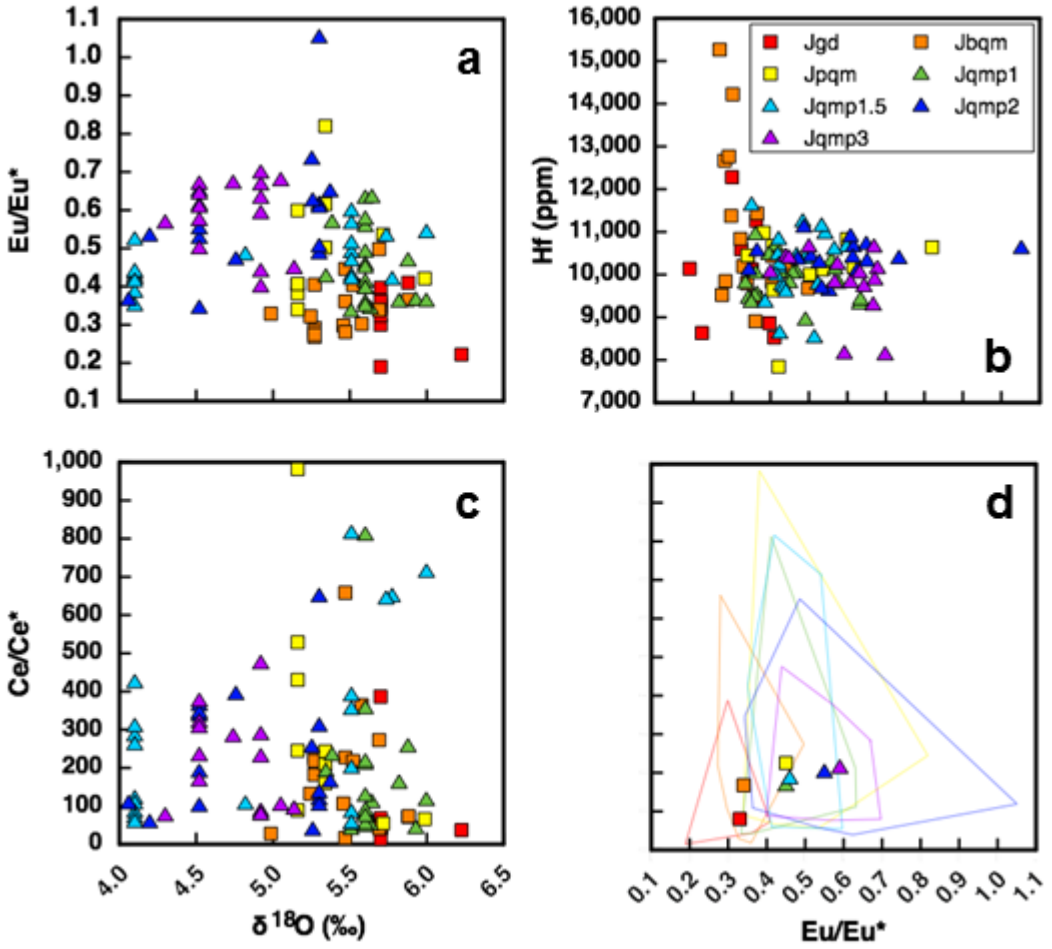

Fig. 6. Eu/Eu* (a) and Ce/Ce* (c) vs. $\delta^{18}O$ for Yerington zircons. b) *In situ* Hf vs. Eu/Eu* for Yerington zircons. d) Sample average Ce vs. Eu anomalies, minus outliers. Outlined fields correspond to range of individual analyses. Colors correspond to symbols. Color trend is oldest (Jgd) in red to youngest (Jqmp3) in purple.

the same samples. All other samples with treated and untreated grains yielded $\delta^{18}O$ values that were very similar. This discrepancy will be explored more in Section 5.

5. Discussion

5.1. Effect of TA/CA treatment on zircon analytical results

For secondary zircon standard Mt. Dromedary, 4 untreated zircon analyses ranged from 96 ± 1.2 to 103 ± 1.9 Ma (1σ), with the oldest two analyses having the highest U concentration (1535 and ~500 ppm U). Although the number of analyses is small, the weighted average age is 98.4 ± 4.9 Ma (2σ; MSWD=5.22). Mt. Dromedary zircon that had undergone TA/CA treatment yielded more reproducible results, and the weighted average of 4 treated grains is 100 ± 1.7 Ma (2σ; MSWD=0.08) with U concentrations ranging from 200-700 ppm and are concordant. Both ages are calculated using untreated Temora-2 as the age primary standard and agree with the published age of 98.8 ± 0.6 reported by White and Ireland (2012) at the 2σ level. Reducing the data using treated Temora-2 changes the calculated weighted mean age for Mt. Dromedary by 1.1 Ma (2σ), which could be statistically important if more grains were analyzed and the weighted average were more precise. Due to the small number of analyses, statistical significance is low.

Variations in age between untreated and treated grains from the Yerington samples are not resolvable at the 2σ level (Table 3). It should be noted that on average, the treated subsets have slightly larger 2σ errors (0-0.6 Ma) than their untreated counterparts, but not enough to be statistically significant at the 2σ level. Mt Dromedary is the only exception to this with the untreated 2σ error 3.2 Myr higher than the treated grains' error.

One potential reason for the lack of improved age precision for Yerington zircon that underwent TA/CA treatment compared to the untreated aliquot of each sample could be the overall low U content of the Yerington zircons. Since the majority of analyzed Yerington and Mt. Dromedary zircon grains have U<500 ppm, the likelihood of radiation damage in the zircon crystal

Sample	Description	Age (Ma)	2σ	$\delta^{18}O$ (‰)	2σ	Ce/Ce*	Eu/Eu*	Ti (ppm)	FWHM (cm^{-1})
Jgd	Untreated	169.6	1.5	5.7	0.5	119	0.35	19.1	6.82
Jgd	Treated	173.6	2.1	5.7	1.4	42	0.29	16.0	7.12
Jgd	Combined	170.0	1.4	5.7	0.8	80	0.33	17.6	6.97
Jbqm	Untreated	168.9	1.5	5.5	0.6	152	0.34	11.8	6.14
Jbqm	Treated	170.9	1.9	5.3	0.7	179	0.35	12.5	5.87
Jbqm	Combined	169.6	1.3	5.4	0.6	167	0.34	12.1	6.00
Jpqm	Untreated	169.4	1.9	5.3	0.8	146	0.58	8.0	6.32
Jpqm	Treated	169.4	2.0	5.2	----	455	0.43	7.6	5.03
Jpqm	Combined	169.4	1.5	5.3	0.8	301	0.50	7.8	5.83
Jqmp1	Untreated	169.3	1.4	5.6	0.7	152	0.47	10.2	6.23
Jqmp1	Treated	167.0	1.9	5.6	0.5	117	0.43	12.0	6.01
Jqmp1	Combined	169.0	1.2	5.6	0.7	134	0.45	11.1	6.11
Jqmp1.5	Untreated	168.6	1.5	5.5	0.8	396	0.50	7.6	6.09
Jqmp1.5	Treated	168.9	1.5	4.1	2.0	183	0.43	7.8	5.53
Jqmp1.5	Combined	168.7	1.1	5.3	1.4	289	0.46	7.7	5.80
Jqmp2	Untreated	169.8	1.7	5.3	0.4	160	0.60	5.5	5.90
Jqmp2	Treated	169.3	1.8	4.5	0.7	237	0.51	6.5	5.47
Jqmp2	Combined	169.6	1.3	5.0	0.9	201	0.55	6.0	5.68
Jqmp3	Untreated	170.1	1.4	4.9	0.6	137	0.57	7.6	6.45
Jqmp3	Treated	169.4	1.5	4.5	0.6	251	0.60	5.2	5.60
Jqmp3	Combined	169.8	1.1	4.8	0.7	194	0.59	6.5	6.05
Mt. Dromedary	Untreated	98.0	4.7	6.7	0.5	19	0.27	15.0	7.20
Mt. Dromedary	Treated	100.0	1.6	6.4	0.2	99	0.24	9.5	6.37
Mt. Dromedary	Combined	98.7	2.0	6.6	0.5	59	0.26	12.3	6.65

Table 3. Summary of analyses of TA/CA treated and untreated Yerington zircon.

lattice due to U decay is considerably lower than in high-U grains. Therefore, with relatively few potentially metamict areas removed during TA/CA treatment as compared to the untreated grains, little age discrepancy exists between treated and untreated grains. Alternatively, the non-resolvable age difference between treated and untreated grains may result from our preselection of analytical spots via the laser Raman analyses. By performing the laser Raman analyses prior to further analysis, we identified potentially metamict areas and mostly avoided them, thereby biasing our analyses toward areas that were crystalline zircon and less affected during the TA/CA treatment. In that case, we would expect similar results from treated and untreated grains. However, our laser Raman analyses did not reveal a noticeably higher propensity for potential metamictization in either the untreated grains or the treated ones, indicating that perhaps there was little overall structural damage in the Yerington samples.

Comparison of trace element analyses of treated and untreated Yerington zircons also reveals little variation that can be attributed to the TA/CA treatment. Th/U and Ti and Hf concentrations vary between treated and untreated grains in each sample, but not systematically or in amounts that significantly deviate from the normal range of elemental variation in the Yerington batholith (Dilles et al., 2015). Zircon REE patterns are similarly within the range of normal system variation (Dilles et al., 2015) (Fig. 5). Samples Jqmp2, Jqmp3, and Mt. Dromedary show slight differences in REE patterns between treated and untreated grains—the REE values for TA/CA treated Jqmp2 zircon are more enriched than their untreated counterparts, but still overlap the untreated patterns. Jqmp3 and Mt. Dromedary display treated and untreated REE patterns that overlap by ~50%, but the treated grains' values are uniformly lower than those of their untreated counterparts.

In situ oxygen isotope analyses reveal slight differences but fairly good agreement within error between treated and untreated zircons in Yerington samples. Differences in $\delta^{18}O$ between treated and untreated sample subsets vary from <0.2‰ (all host rock samples and Jqmp1) to 1.4‰

(Jqmp1.5), with treated grains always having lower—but not statistically significant—$\delta^{18}O$ values than the untreated grains. The only sample that has a statistically significant difference in $\delta^{18}O$ between treated and untreated grains at the 1σ level is Jqmp2 (4.5±0.7 vs. 5.3±0.7).

Metamictization has been shown to lower $\delta^{18}O$ in zircon (e.g. Valley, 2003; Valley et al., 1994) and incomplete removal of these areas during the TA/CA process may have resulted in the lower measured Jqmp2 treated zircon $\delta^{18}O$ values, especially if zircons from that sample had a higher degree of radiation damage. However, neither the treated nor untreated subsets of Jqmp2 have higher U than the other Yerington units so the likelihood of higher amounts of radiation damage in Jqmp2 leading to lower $\delta^{18}O$ values for untreated grains seems very low. Post-analysis imaging reveals no obvious cracks that could have affected $\delta^{18}O$ analysis in either of the Jqmp2 zircon subsets more than the other samples, and micron-scale inclusions are unlikely to cause a significant deviation from the pure zircon $\delta^{18}O$ value. Post-analysis re-imaging indicates that untreated Jqmp2 grains are functionally free of visible surface impurities, such as inclusions, but treated grains appear to have more. While this can be said of all the Yerington samples, Jqmp2 has a larger proportion of inclusions, which may be an artifact of the TA/CA process.

In summary, with the exception of one sample, there is no statistically significant difference in U–Pb age, trace element composition, or $\delta^{18}O$ between TA/CA treated and untreated zircon from the same sample that can be attributed to the TA/CA process. Therefore, all data interpretation henceforth is the combination of all treated and untreated analyses for a given sample.

5.2. Assessing utility of laser Raman-based pre-selection of analytical spots

Twenty-five grains had laser Raman spectra indicative of zircon that was not perfectly crystalline. Normally we would have avoided these grains, but we purposely analyzed them for U–Pb ages and trace elements to see if what we interpret as metamict or highly damaged—based on extra laser Raman spectral peaks, apparent physical abnormalities, and high U concentrations—

yielded larger errors, discordance, or difference in age relative to what we interpret to be non-metamict, intact grains. Fourteen of those grains were also analyzed for oxygen isotope compositions. The results of those analyses are highly variable. Eighteen of the 25 U–Pb age analyses showed no analytical reason to discard the data despite their Raman spectra having additional bonding peaks—UO/U values did obviously vary from the other grains, nor were common Pb corrections higher than for other grains. Four $\delta^{18}O$ analyses with extra spectral peaks also yielded data with no discernable difference than those from normal-spectra grains. Seven of the 18 analyses that were also analyzed for $\delta^{18}O$ yielded anomalous values with large errors. However, this is most likely due to the presence of inclusions, cracks, or intersection of epoxy during the analysis. Three grains that had Raman spectra with extra spectral peaks indicative of unsound structural quality were characterized by high middle to heavy REE values, but were included in the dataset after comparison to other samples indicated that, though high, the values were not unreasonable. One of these grains was analyzed for $\delta^{18}O$ and the value, error, and counting statistics were comparable to normal-spectra grain data. U–Pb/TE analyses from four grains with Raman spectra with highly erratic peak locations and counts were not included in the data set due to spurious ages, potential involvement of inclusions, or odd trace element results. Two grains were analyzed for oxygen isotopes—1 was acceptable and 1 was not. These results seem to indicate that, contrary to the findings of Wang et al. (2014), laser Raman spectroscopy prior to further *in situ* analysis may not be a reliable way to effectively discriminate zircons with metamict zones from those that remain structurally intact. This may be because the laser Raman analytical spot is 5 μm wide with a penetration depth of <1 μm (at 514 nm wavelength), while the analytical spots for combined U–Pb/TE and oxygen isotopes have diameters of at least 25 μm and penetrate several microns into the grain. Though we took care to overlap the laser Raman spot completely with the U–Pb/TE spot, a considerable amount of material not analyzed via laser Raman was included in the U–Pb/TE analysis. By quantifying such a small area of the grain via laser Raman and

extrapolating that result to a much larger analytical volume that will be analyzed for geochemical data, the margin for error in either direction is sufficiently large to render the laser Raman analyses incapable of "predicting" if the subsequent geochemical analyses will be of metamict areas or not. A potential solution to this issue in the future would be to analyze a larger portion of each grain via laser Raman prior to further geochemical analysis, although this would not reveal sub-surface metamictization without using a larger laser beam wavelength.

5.3. Geochemical implications for Yerington

Yerington has the distinction of being a well-studied magmatic system, but this study differs from previous Yerington research in that we present a suite of *in situ* age, trace element, and oxygen isotope data for the rocks exposed in the Yerington Pit to investigate the processes active in producing a range of geochemical variation in units of varying economic importance, and specifically any correlation between Eu and Ce anomalies and bulk Cu content. Our results show that there is no obvious correlation between Eu/Eu* and Ce/Ce* in zircon with whole-rock Cu concentrations for individual units (Tables 1 and 2; Fig. 4), contrary to the findings of other authors (e.g. Ballard et al., 2002; Liang et al., 2006).

One possible explanation for this difference may be that the zircon Ce and Eu anomalies may not be reliable indicators of the oxidation processes occurring in a magma that influence Cu fractionation. The evolution of a porphyry magmatic system to produce conditions suitable for Cu to concentrate and produce economic deposits is a multi-phase, multi-step process (e.g. Dilles et al. 2015 and references therein). When coupled with the uncertainties that arise from difficulties in and various methods for calculating Ce/Ce* in zircon, any subtleties in Ce/Ce* indicative of ore-forming processes may be muted or lost. As a consequence, it is unclear just how much of a Ce/Ce* variation in zircon is leveraged by petrogenetic processes in ore-forming systems and therefore evaluation of the effectiveness of the Ce anomaly is challenging at present. While the Eu anomaly

calculation in zircon is straightforward, the compatibility of Eu^{2+} in feldspars potentially overwhelms Eu's effective use as an oxidation indicator in feldspar-bearing systems. In this study, the zircon Ce and Eu anomalies appear to be recording changes in oxidation in the parent magma through time (Fig. 6), which bolsters the credibility of that indicators, but caution must still be used when extrapolating to other systems. We found no discernable link between zircon Ce/Ce* or Eu/Eu* and whole rock Cu content at Yerington.

It is possible that the lack of correlation between Ce and Eu anomalies and bulk Cu content results from zircons crystallizing in a porphyry Cu system that may not be recording the portion of the magma's evolution that is directly relevant to ore formation. If zircons were sequestered during part of their crystallization history in, say, a crystal-rich mush with little available melt, they could be largely insulated from the larger-scale geochemical changes occurring in the system. Multiple studies have provided evidence that zircons may be sequestered in melt-poor mushes before being rejuvenated and transported to other areas of a magma body or erupted (e.g. Schmitt et al., 2010; and many others), thereby depositing them in what in many ways is a foreign magmatic environment. Given the timescales and uncertainties in our measurements, zircon crystallizing over 100s of kyr prior to remobilization would be unresolvable.

Another consideration is whether it is reasonable to correlate data from zircons that may have been crystallized over a wide spatial, temporal, and chemical range with bulk Cu% from an incredibly spatially restricted area which the zircons wound up in. It seems unreasonable to assume that the amount of Cu mineralization in a meter-long section of rock core is truly a good indicator for the amount of Cu in that unit as a whole, and the zircons found in that meter section are also good indicators of that magma's evolutionary path. When the average Cu% of the entire unit exposed in the Yerington pit is considered, there is no correlation between Ce and Eu anomalies and Cu content.

The magnitude of the negative Eu and positive Ce anomalies in Yerington zircons indicate development of a more oxidizing environment over the system's lifetime. Ti-in-zircon thermometry also suggests a decrease in zircon crystallization temperature through time that correlates to a decrease in *in situ* Ti concentrations (Ferry and Watson, 2007) (Fig. 4). In addition, $\delta^{18}O$ values decrease with time (Fig. 6), which is generally in accordance with field evidence and historical records of decreasing Cu content and increasing amount of hydrothermally induced alteration in the Yerington porphyry dike units. Incorporation of low $\delta^{18}O$ meteoric water—or rocks altered by such water at high temperature—into magmatic systems is the only way to obtain $\delta^{18}O$ values lower than the mantle melt-equilibrated value (5.3±0.3‰; Valley 2003) in magmatic zircons. Zircons from the host units (Jgd, Jbqm, and Jpqm) and the earlier porphyry dike units (Jqmp1 and Jqmp1.5) display normal $\delta^{18}O$ of ~5.5-6.0‰, but the two youngest units (Jqmp2 and Jqmp3) have depleted oxygen signatures down to 4.0‰, suggesting late-stage assimilation of hydrothermally altered material. However, because whole-rock Cu concentration isn't significantly higher in Jqmp2 and Jqmp3, assimilation doesn't appear to be a significant source for Cu-rich material.

Yerington zircon Eu and Ce anomalies record a similar shift toward slightly more oxidizing conditions coincident with the drop in $\delta^{18}O$ and zircon crystallization temperature in the youngest and least-mineralized (overall) units (Figs. 4,6). Our in situ U–Pb ages are statistically irresolvable at a 2σ level to determine timescales of crystallization between the host and dike units, but field relations are well established and allow us to summarize these findings as being indicative of late-stage addition of lower-$\delta^{18}O$ material to an environment capable of reverting to more-oxidizing conditions. Dilles et al. (2015) state that Fe/S in magmas correlates negatively with fO_2. Late SO_2 degassing, which is a primary driver of Cu ore formation in porphyry systems, involves a decrease in Fe/S and an increase in fO_2. Dilles et al. (2015) also report a greater range of but general increase in Eu/Eu* with increasing Hf in zircon from mineralized Yerington samples—a trend not observed in this study when zircons from a suite of host rocks and porphyry dikes is considered

(Fig. 6). Perhaps the simplest explanation for the simultaneous decrease in $\delta^{18}O$ and increase in Ce/Ce* and Eu/Eu* is incorporation of more isotopically light, hydrothermally influenced material in latest, most oxidized stages of mineralization which effectively dropped the temperature and facilitated cessation of ore-bearing-fluid production.

6. Conclusions

TA/CA treatment of relatively low-U Jurassic-age zircons prior to analysis does not yield resolvable differences in U–Pb age, TE content, or $\delta^{18}O$ as compared to untreated grains. Lack of statistically different results from treated and untreated aliquots is likely due to low U content, as this methodology has shown to be useful for improving reproducibility in high-U, radiation-damaged zircon samples;

- New *in situ* U-Pb zircon ages support Dilles and Wright (1988)'s earlier zircon U-Pb TIMS ages that suggest porphyry dike emplacement between 168.5-169.5 Ma;
- New *in situ* data suggests subtle differences in crystallization temperatures of zircons from host magmas and porphyry dike units and an overall trend toward increased participation of hydrothermally altered material in petrogenesis and corresponding increase in oxidation over the source magma(s') lifetime;
- Eu and Ce anomalies in zircon are not useful indicators of whole rock Cu mineralization at Yerington.

CHAPTER 3

Zircon and whole rock compositions reveal magmatic-tectonic control on the generation of silicic magmas at Hafnarfjall-Skarðsheiði volcano, Iceland

Abstract

Iceland is the only place on Earth where a mid-ocean ridge and a major mantle plume coincide to produce a volcanic plateau with active subaerial volcanism. The Hafnarfjall-Skarðsheiði (H-S) central volcano, located in a rift transition zone and active from ca. 6 to 3.5 Ma, provides a snapshot into silicic magma generation that occurred relatively early during a rift cycle. H-S is a large volcanic center with relatively abundant (~16%) silicic volcanics, but their petrogenesis remains enigmatic. Here we present *in situ* zircon and whole rock data from the dominant silicic units erupted throughout H-S's lifetime. Our dataset combines *in situ* zircon U-Pb ages with oxygen and hafnium isotope compositions for the H-S volcano and is complimented by major and trace element and Pb, Nd, and Hf whole rock isotope data. Zircon U-Pb ages and field relationships indicate a protracted residence time for many of the silicic magmas. Relatively depleted whole rock εHf (11.9-13.3) and εNd (7.2-7.6) for Hafnarfjall-Skarðsheiði silicic rocks are consistent with an on-rift environment in which partial melting is expected to dominate petrogenesis. In contrast, our whole rock isotopic data from basalt and rhyolite units indicate that the same mantle-derived source is dominantly responsible for the geochemical characteristics observed in both, which is consistent with a model of fraction crystallization of mantle melts with subordinate contributions of partially melted altered crust to explain the low $\delta^{18}O_{zrc}$ values observed. Zircon REE compositions, model Ti-in-zircon crystallization temperatures, and slight differences between whole rock and zircon εHf suggest the pre-eruptive silicic magmas were isolated melts for some or most of their evolution. We ultimately invoke a petrogenetic model where the timescales of rift drift explain the

long-lived, episodic silicic magmatism produced during rift propagation at Hafnarfjall-Skarðsheiði volcano, Iceland.

1. Introduction

Iceland is a unique geologic environment where an active mid-ocean ridge and a major mantle plume coincide to produce an island plateau of appreciable size where silicic ($SiO_2 \geq 65$ wt%) rocks are found in relative abundance (~10% of exposed rocks; e.g. Jónasson, 2007; Thorarinsson, 1967; Walker, 1966; and many others), which is noteworthy at an ocean island because they are often thought of as producing only basaltic magmas. Current models for silicic magma petrogenesis in Iceland range from pure partial melting of hydrothermally altered crust (e.g. Bindeman et al., 2012; Gunnarsson et al., 1998; Jónasson, 1994; Marsh et al., 1991; Óskarsson et al., 1982; Sigmarsson et al., 1991; and many others) to pure fractional crystallization (e.g. Carmichael, 1964; Furman et al., 1992; Macdonald et al., 1987; Nicholson et al., 1991; Prestvik et al., 2001; and many other), and numerous models that invoke both processes (e.g. Sigmarsson et al., 1992). These studies are lacking in that they do not consider the greater tectonic environment in which silicic magmas are produced. Given the unique geodynamic setting in which Icelandic rhyolites are generated, effects of tectonism should be taken into account when addressing processes and timescales associated with their petrogenesis. This paper applies zircon and whole rock geochemistry to investigate the development of silicic magmas at the Hafnarfjall-Skarðsheiði central volcano and evaluates the contributions from rift relocation, rift spreading, and magmatism. The results presented here constitute the first comprehensive zircon-based, whole rock-supported study of silicic petrogenesis at a central volcano conducted both at Hafnarfjall-Skarðsheiði and in western Iceland in general.

2. Geologic setting and sampling of Hafnarfjall-Skarðsheiði

2.1. Geologic setting

Hafnarfjall-Skarðsheiði (H-S) is an eroded central volcano in western Iceland (Fig. 1a). It in the active Western Volcanic Zone (WVZ) and erupted between ~6 and 4 Ma, early in the Reykjanes rift's active history (e.g. Franzson, 1978; Harðarson et al., 2008). H-S is a well-preserved example of a multi-caldera central volcano complex constructed of numerous basaltic sheets and approximately 10 silicic units—overwhelmingly volcanic with one granophyric unit—erupted throughout the volcano's lifetime (Tables 1 and 4), accounting for ~20% of the succession (Franzson, 1978). Prior regional field reconnaissance, mapping, and sampling by Franzson (1972, 1978; the reader is referred to these studies for a detailed description of the study area) reveals tholeiitic basalts at the base of the succession that lie unconformably on olivine tholeiite and porphyritic tholeiite basalts that predate the H-S central volcano by several million years (up to ~10-13 Ma). Silicic magmas first appeared in the early stages of central volcano-forming activity (Table 1) and erupted intermittently before and after an early caldera collapse. The focus of eruptive activity then shifted southwest, resulting in a series of flood basalts that pre-dated the main Hafnarfjall caldera. Franzson (1978) described a large collapse event at ca. 4.6 Ma which resulted in a ~7.5×5 km caldera in Hafnarfjall, which has been suggested to be the result of intrusion of a basalt sheet deflecting into a subvertical ring fault that led to vertical displacement of over 200 m (Browning and Gudmundsson, 2015). However, neither extensive silicic lavas from that area and time period nor ignimbrite deposits typically associated with caldera formation are reported. Regardless, the Hafnarfjall caldera formation led to the eruption of several silicic domes around the eastern margin of the caldera and extensive basaltic and andesitic activity within the central portion of the caldera. After the Hafnarfjall caldera-forming event, the focus of volcanic activity shifted east, producing an extensive series of silicic and intermediate flows, domes, and ignimbrites in Skarðsheidi. The final magmatic activity at H-S consisted of dominantly basalt and

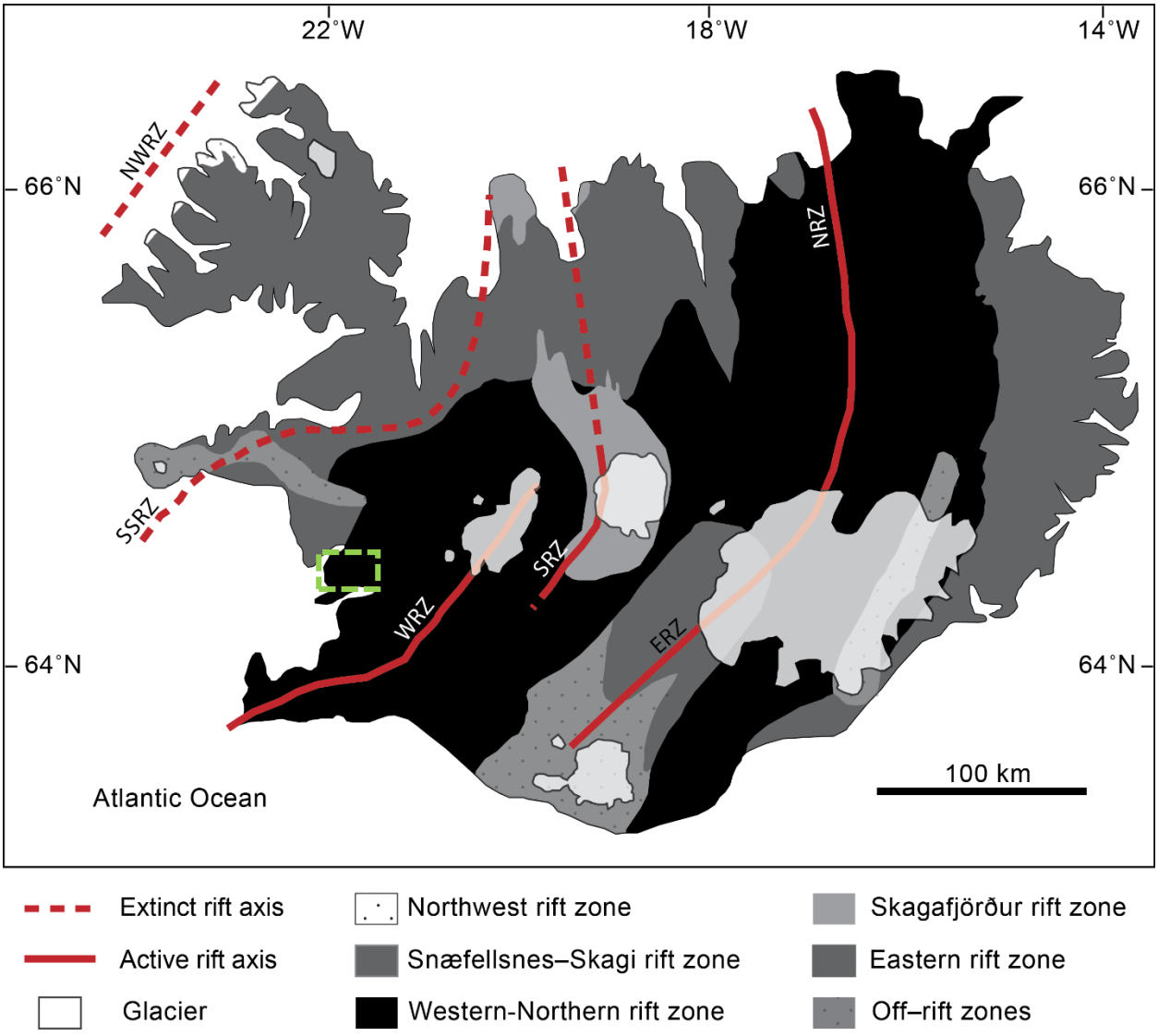

Fig. 1a: Geologic map of Iceland showing active and extinct rift axes and the rocks sourced from each. Location of Hafnarfjall-Skarðsheiði volcano is in the green dashed box on west coast and is shown in detail in Fig. 1b. Modified from Harðarson et al. (2008).

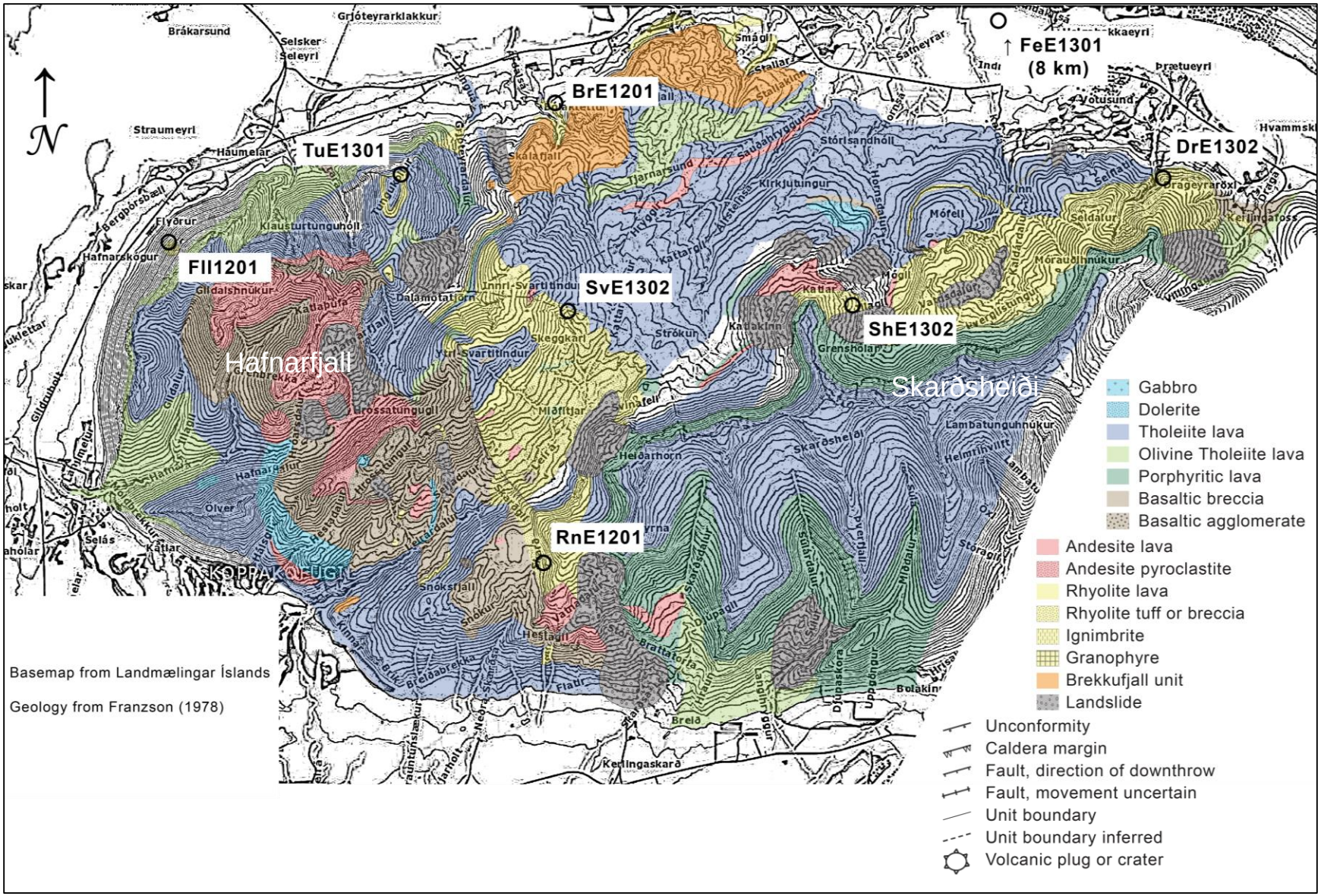

Fig. 1b) Geologic map of Hafnarfjall-Skarðsheiði central volcano. Labeled open circles denote sample names and locations.

Table 1. Eruptive history of Hafnarfjall-Skarðsheiði. Ages are estimates and not based on this study. From Franzson (1978).

Age (Ma)	Phase	Description	Unit	SubUnit	Samples
	Heiðarhorn Phase	Heiðarhorn tholeiite series			
		Heiðarhorn porphyritic series			
		Reinir compound lava shields			
			Demise of central volcano		
3.9±0.6		*Flyðrur granophrye*	iii. Skarðsdalur andesite		
4.1-4.0		*Skessuhorn gabbro*	ii. Snókur Basin pitchstone andesite		
↑		**Differentiated extrusives**	i. South Rauðihnúkur andesite		
4.25-4.05		**Basalt Succession**			
	Skarðsheiði Phase	*Hrossatungur gabbro + diabase plug*	Late: Drageyraröxl lava + ignimbrite		DrE1301/02
		Skarðsheiði tholeiite series	Selardalur rhyolite dome		*HrI1201/02, 1301
			Middle: Mófell andesite + rhyolite		KaE1301/02
			Hormsdalur		ShE1302
	Hafnarfjall Phase	**Hafnarfjall Caldera**	vi. Upper agglomerate		HrI1203
			v. Upper basalt		SnE1301
			iv. Andesite (pitchstone ignimbrite?)		HrE1204
			iii. Lower agglomerate		
			ii. Basalt hyaloclastite		
			i. Lower basalt		
↑		**Rauðihnúkur rhyolite dome (+ west Snókur rhyolite)**			RnE1201/02
4.4?		*Tungukollur granophyre?*	ii. Svartitindur + caldera margin		*TuE1201/02; SvE1301
4.5?			i. Hestfjall		
4.6?		**Rauðihnúkafjall rhyolite dome (+ Leirádalur)**			SvE1201/1302
			Hafnarfjall Caldera Collapse		
		Tholeiites	ii. Southern flank (Leirádalur)		
			i. Central		
↑		**Leirádalur flood basalt succession**	ii. Leirádalur compound series		
			i. Porphyritic series		
		Tungukollur tholeiite + rhyolite			TuE1301
5.2-5.0			*Brekkufjall Caldera Collapse*		
	Brekkufjall Phase	**Brekkufjall Acid Series**	ii. Brekkufjall Caldera Series	6. Sediments	
				5. Upper rhyolite group	SkE1201
				4. Composite unit	BrE1203
				3. Andesite group	BrE1202
				2. Brekkufjall ashöflow group	BrE1201
				1. Lower rhyolite group	BrE1204/05
			i. Flank series		
		Hvanneyri Tholeiite Series			
3 m.y. pre-CV		**Hafnarfjall Olivine Tholeiite Series + Hvítá Acid Rocks**			ÖlE1301; FeE1301
		Hafnarskógur Porphyritic Series			

andesite flows and several shallow intrusions, including the only silicic intrusion in the complex—the 3.9 Ma (whole rock, K-Ar age; 0.6 Myr error) Flyðrur granophyre (Moorbath et al., 1968). The demise of the central volcano occurred roughly at this time, but basaltic lavas continued to erupt intermittently around the southeastern margin of the volcano (Franzson, 1978).

Field relationships such as unconformities in sedimentary sequences (e.g. Sæmundsson, 1974) and synclinal structures in the basalt succession (e.g. Jóhannesson, 1980; Oskarsson et al., 1985; Sæmundsson, 1967; Vink, 1984), along with paleomagnetic and geochemical data, have been invoked to identify at least 2 formerly active segments of the main rift axis prior to the initiation of the currently active Reykjanes (Western) and North rift zones (WRZ and NRZ, respectively; Fig. 1a) (e.g. Harðarson et al., 2008). These rift zones also demarcate the main volcanic zones (VZ) on Iceland. The Snæfellsnes-Skagi rift zone (SSRZ) became extinct between 6.7 and 5.5 Ma at which time the main rift activity in the southwest of Iceland transferred to the WRZ. Snæfellsnes rocks from 6.7 Ma have Nd isotope compositions indicative of production in an on-rift setting, while rocks from 5.5 Ma have Nd isotope compositions consistent with production in an off-rift setting (Martin and Sigmarsson, 2010; Martin et al., 2011). Hafnarfjall-Skarðsheiði began forming nearly contemporaneously with the timing of SSRZ-to-WRZ rift relocation, and therefore presents an ideal location to study the timescales and processes—particularly with regard to tectonics—associated with silicic petrogenesis as it is one of the few areas with appreciable silicic material erupted soon after its parent rift relocated. Franzson (1978) largely focused on the petrogenesis of the volumetrically dominant basaltic units in the H-S volcanic complex and the regional tectonics, but speculated that the silicic rocks formed predominantly by partial melting of the lower crust without undertaking further investigation into silicic magma genesis and rift relocation. Here we present a geochemical model compiled largely from *in situ* zircon geochemical data to describe and explain the interplay between tectonics and silicic petrogenesis and the timing associated with silicic magma production after rift relocation.

2.2. Samples studied

Samples were collected from 7 silicic units within H-S (6 volcanic and 1 intrusive), as well as one related silicic unit several km north of the central volcano and two mafic samples—a tholeiitic basalt from the Hafnarfjall phase and a late-stage gabbro cumulate (Figure 1b, Table 2). We sampled every locatable silicic unit known at Hafnarfjall-Skarðsheiði in order to document the longevity and geochemical characteristics of the entire silicic magmatic system. The majority of the units in the central volcano are altered to varying degrees, which can compromise whole rock major and fluid-mobile trace element concentrations. Zircon is resistant to chemical weathering (Hoskin and Schaltegger, 2003; Valley, 2003; and many others) compared to whole rock and glass samples and therefore should provide a more robust measure of original melt composition from which zircon crystallized.

3. Analytical techniques

3.1. Whole rock analyses

Major element whole rock compositions were determined using X-ray florescence (XRF) at the Geoanalytical Lab at Washington State University (WSU) using the methods of Johnson et al. (1999). Whole rock trace-element abundances were determined using both XRF and ICP-MS via standard techniques at WSU. Absolute precision for XRF analyses is better than 1% (2σ) for major elements and within 2 ppm (2σ) for trace elements. Relative precision for ICP-MS analyses is typically better than 5% for the REEs and 10% for the remaining trace elements. Whole rock Nd, Hf, and Pb isotope compositions were measured at the Radiogenic Isotope and Geochronology Laboratory (RIGL) at Washington State University using the procedure outlined in McDowell et al. (2015). Isotopic compositions were measured on a Thermo-Finnigan Neptune MC-ICP-MS. Whole rock Hf isotope analyses were corrected for mass fractionation using $^{179}Hf/^{177}Hf = 0.7325$ and normalized using Hf standard JMC475 ($^{176}Hf/^{177}Hf = 0.282160$). Our measured JMC475 $^{176}Hf/^{177}Hf$

Table 2. Sample locations and descriptions.

Sample name	Latitude*	Longitude*	Elevation (m)	Rock type	Description	Zircon?
BrE1201	N64°31.321'	W21°47.377'	68	Rhyolite	Brekkufjall rhyolite, highly altered	✓
DrE1302	N64°30.987'	W21°34.726'	260	Rhyolite	Drageyraröxl ignimbrite; flow-banded and moderately altered	✓
FeE1301	N64°35.244'	W21°45.383'	20	Rhyolite	Ferjubakki rhyolite, not in central volcano	✓
FlI1201	N64°29.988'	W21°55.057'	90	Granophyre	Flyðrur granophyre	✓
HrI1202	N64°27.174'	W21°52.057'	388	Gabbro	Hrossatungar gabbro, slight alteration	✓
ÖlE1301	N64°27.646'	W21°56.104'	105	Basalt	Ölver tholeiite	
RnE1201	N64°27.276'	W21°47.154'	556	Rhyolite	Rauðihnúkur rhyolite; moderate alteration	✓
ShE1302	N64°29.702'	W21°40.592'	377	Rhyolite	Skessuhorn rhyolite	✓
SvE1302	N64°29.526'	W21°47.224'	541	Rhyolite	Svartitindur rhyolite; highly altered (QSP)	✓
TuE1301	N64°30.686'	W21°50.674'	628	Rhyolite	Tungukollur rhyolite; highly altered	✓

*All coordinates are WGS84

value was 0.282132 ± 0.000007 (2σ SD), which resulted in a correction factor of 1.000093. Nd isotope analyses were corrected for mass fractionation using $^{146}Nd/^{144}Nd = 0.7219$ and normalized using a correction factor of 1.000052 based on measurements of La Jolla Nd standard ($^{143}Nd/^{144}Nd = 0.511858$ (Vervoort et al., 2011)); our value was 0.511831 ± 0.000014 (2σ SD)). We corrected for mass bias in the Pb analyses using $^{205}Tl/^{203}Tl = 2.388$ and normalized the mass bias corrected values for standard NBS 981 using $^{206}Pb/^{204}Pb = 16.9405$, $^{207}Pb/^{204}Pb = 15.4963$, $^{208}Pb/^{204}Pb = 36.7219$ (Galer and Abouchami, 1998). Our measured NBS 981 values, with 2σ SD, were: $^{206}Pb/^{204}Pb = 16.9361 \pm 0.0010$, $^{207}Pb/^{204}Pb = 15.4924 \pm 0.0008$, and $^{208}Pb/^{204}Pb = 36.7016 \pm 0.0018$.

3.2. In situ zircon analyses

Zircons were separated from 9 H-S rock samples using standard crushing, sieving, and magmatic and density separation techniques, followed by hand-picking. Zircon grains were mounted in epoxy, polished, and imaged using the Vanderbilt University EES Tescan Vega 3 LM variable pressure scanning electron microscope (SEM) using cathodoluminescence (CL) prior to obtaining any *in situ* zircon analyses.

Following the methods of Trail et al. (2007), we carried out a total of 153 O isotope analyses at the University of California–Los Angeles National Science Foundation CAMECA ims-1270 secondary ion mass spectrometer (SIMS). Standard operating conditions for the ims-1270 include a Cs^+ primary ion beam with an analytical spot size of ~20-25 μm and analytical pit depth of ~1 μm. Measured ratios were corrected for mass discrimination using primary zircon standard R33 ($\delta^{18}O = +5.55 \pm 0.04$ ‰; Valley, 2003) and all data are reported as $\delta^{18}O$ calculated relative to VSMOW of Baertschi (1976). Cited precisions are 2σ total errors calculated from 1σ analytical error for each analysis and 1σ reproducibility error from all corrected R33 standard analyses. External 1σ reproducibility for R33 analyses ranged from 0.29 to 0.42 (Appendix D).

In situ ages and trace element compositions were obtained at the jointly operated U.S. Geological Survey-Stanford University sensitive high-resolution ion microprobe-reverse geometry (SHRIMP-RG) facility. Zircon mounts were re-imaged via CL and lightly polished to remove prior analytical pits before analysis. Operating procedure includes a $^{16}O_{2-}$ primary ion beam focused to a ~25x17 μm diameter analytical spot for U-Pb age determination and a ~12x12 μm diameter trace element analytical spot. Three samples (FeE1301, ShE1302, and SvE1302) were analyzed using a routine that combined U–Pb age and trace element composition within a single analysis using a ~25x25 μm analytical spot. Analyses were calibrated using zircon standard R33 (age=419 Ma; Valley, 2003) and internal zircon trace element standard MADDER (3435 ppm U; Barth and Wooden, 2010). Data were reduced using Squid 2.51 (Ludwig, 2009) and Isoplot 3.76 software (Ludwig, 2012). The measured $^{206}Pb/^{238}U$ was corrected for common Pb using ^{207}Pb. The common Pb correction was based on a model Pb composition from Stacey and Kramers (1975). We also corrected for ^{230}Th disequilibrium, although the magnitude of the correction was ~100 kyr or less.

After U-Pb and trace element analysis, zircon mounts were re-re-imaged via CL and Lu-Hf isotope composition was measured on a subset of the same grains using LA-MC-ICP-MS at RIGL. Fifty-eight total grains from 5 samples (BrE1021, TuE1301, RnE1201, DrE1302, and FlI1201) were analyzed for Hf. Analyses utilized a ThermoFinnigan Neptune MC-ICP-MS coupled to a New Wave 213 nm Nd-YAG laser with a spot size of 40 μm. We follow the instrument configuration, operating parameters, and data reduction methods outlined by Fisher et al. (2014), with the exception that U-Pb ages were not simultaneously determined. We use Mud Tank ($^{176}Hf/^{177}Hf$ = 0.282507 ± 6, Woodhead and Hergt (2005)) to normalize all samples and quality control reference zircons at the RIGL. Analyses of quality control zircons ("secondary standards") were interspersed with unknowns. Given the narrow range of Hf isotope composition present in Icelandic rocks, and large range of (Lu+Yb)/Hf present in H-S zircon samples combined with the importance of highly accurate correction for the isobaric interference of ^{176}Yb and ^{176}Lu on ^{176}Hf, quality control zircons

used in this study covered the range of (Lu+Yb)/Hf of the samples studied. Analyses of GJ-1 (S-MC-ICPMS $^{176}Hf/^{177}Hf$ = 0.282000 ± 23, Morel et al. (2008)) and MUNZirc 4 yield LA-MC-ICPMS $^{176}Hf/^{177}Hf$ of 0.282002 ± 32 (2SD; n=15) and 0.282131 ± 18 (2SD; n=13; $^{176}Yb/^{176}Hf$ ~0.08 to 0.26), respectively. Analyses of quality control zircons agree well with published S-MC-ICPMS determination of the isotope composition of purified Hf from these zircons. Present day ε_{Hf} values were calculated using the CHUR parameters reported by Bouvier et al. (2008) . Laser Lu-Hf isotopic data are reported with 2σ uncertainty in Table 4 and Appendix G.

4. Results

4.1. Major and trace elements

Major and trace element compositions of silicic and basaltic units sampled at H-S are listed in Table 3, together with whole rock Nd, Hf, and Pb isotope ratios. SiO_2 ranges from 64 to 77 wt% in H-S rhyolites. It should be noted that all the rhyolites sampled are altered to varying degrees, and therefore some aspects of the major and trace element geochemistry—such as Si, alkalis, and fluid-mobile trace elements—may be suspect. The most strongly altered samples are BrE1201 and SvE1302, as seen in Fig. 2. When compared to other H-S silicic samples from this study and fresh whole rock analyses reported by Franzson (1978), it appears that BrE1201 has lost Si and gained Ca (due to secondary calcite), while SvE1302 has lost Na and Ca and potentially gained Si. These findings fall within established element mobility trends for H-S established by Franzson et al. (2008). In addition, field observations of the SvE unit revealed complete quartz-sericite-pyrite alteration, which is a hallmark assemblage resulting from strong hydrothermal alteration and accounts for both the increased Si and very low Na and Ca. H-S silicic rocks straddle the metaluminous/peraluminous boundary (Fig. 2), which is not unusual for silicic rocks in Iceland (Martin and Sigmarsson, 2010). When normalized to primitive mantle (Sun and McDonough, 1989) and plotted on a multi-element diagram, (Fig. 3a), silicic samples display trace element patterns

Table 3. Whole rock major and trace element and isotope compositions

	Sample name and description				
	BrE1201 Rhyolite	RnE1201 Rhyolite	TuE1301 Rhyolite	DrE1302 Rhyolite	FlI1201 Granophyre
SiO2	63.54	70.31	77.23	73.91	73.01
TiO2	0.17	0.30	0.20	0.27	0.38
Al2O3	11.31	12.41	11.52	12.23	12.47
FeO*	1.41	3.10	2.18	2.71	4.35
MnO	0.21	0.10	0.02	0.05	0.14
MgO	0.19	0.05	0.09	0.21	0.17
CaO	8.25	1.35	0.25	0.28	1.50
Na2O	3.97	4.49	4.24	4.51	4.95
K2O	2.95	2.18	2.46	3.50	2.65
P2O5	0.02	0.02	0.02	0.03	0.04
LOI (%)	7.36	4.45	1.35	1.09	0.43
Total	99.36	98.77	99.55	98.79	100.09
Ni	2	2	1	3	1
Cr	3	2	3	3	BD
V	2	3	14	21	4
Ga	21	29	26	30	26
Cu	8	3	21	6	5
Zn	159	177	103	206	167
La	27.05	83.72	169.65	90.24	80.51
Ce	57.47	180.17	263.15	170.03	177.24
Pr	8.98	22.77	40.02	23.05	23.02
Nd	35.68	91.03	140.17	89.10	94.78
Sm	8.95	21.59	32.03	19.54	22.52
Eu	2.32	4.39	8.18	3.63	4.67
Gd	8.60	21.37	27.77	17.73	22.56
Tb	1.81	3.82	4.43	3.11	4.04
Dy	12.66	23.78	21.72	18.86	25.35
Ho	2.87	4.91	3.52	3.77	5.21
Er	8.82	13.41	8.43	10.10	14.47
Tm	1.45	1.98	1.17	1.50	2.13
Yb	9.38	11.95	6.80	9.06	12.92
Lu	1.45	1.81	0.98	1.35	2.00
Ba	489	663	529	636	521
Th	10.75	9.45	9.62	12.61	8.88
Nb	75.83	99.26	93.01	133.23	90.51
Y	78.15	123.11	72.95	89.72	130.95
Hf	12.63	20.46	14.95	18.40	22.02
Ta	5.43	6.49	6.67	8.70	5.84
U	2.16	2.79	2.70	3.57	2.62
Pb	6.23	7.03	7.86	7.98	5.02
Rb	68.3	67.5	46.2	71.6	51.6
Cs	0.43	1.00	0.10	0.28	0.15
Sr	71	131	75	64	101
Sc	3.4	2.2	0.7	1.7	6.5
Zr	415	765	452	585	850
$^{143}Nd/^{144}Nd$	0.513015	0.513010	0.513010	0.513012	0.513030
εNd	7.4	7.2	7.2	7.3	7.6
$^{176}Hf/^{177}Hf$	0.283162	0.283120	0.283148	0.283109	0.283137
εHf	13.3	11.9	12.8	11.4	12.4
$^{206}Pb/^{204}Pb$	18.9724	18.9680	19.0369	19.1136	18.9466
$^{207}Pb/^{204}Pb$	15.5238	15.5140	15.5271	15.5232	15.5134
$^{208}Pb/^{204}Pb$	38.5641	38.5462	38.6236	38.6783	38.5207
Zircon Sat (°C)	857	946	909	921	939

Table 3. Whole rock major and trace element and isotope compositions

	Sample name and description				
	HrI1202	ShE1302	SvE1302	FeE1301	ÖlE1301
	Gabbro	Rhyolite	Rhyolite	Rhyolite	Basalt
SiO2	43.19	73.68	76.94	75.50	49.33
TiO2	3.91	0.19	0.23	0.16	1.93
Al2O3	12.13	12.62	12.30	11.97	15.19
FeO*	17.95	3.01	2.54	2.72	10.46
MnO	0.24	0.03	0.00	0.06	0.19
MgO	6.86	0.10	0.20	0.07	6.18
CaO	12.31	0.42	0.05	1.09	11.34
Na2O	2.04	4.78	0.09	5.04	2.48
K2O	0.16	3.21	3.22	3.13	0.55
P2O5	0.08	0.03	0.01	0.01	0.26
LOI (%)	0.28	0.97	3.71	0.19	2.03
Total	99.13	99.05	99.28	99.94	99.93
Ni	68	2	BD	1	62
Cr	15	2	2	3	100
V	906	12	1		275
Ga	22	33	30	25	18
Cu	372	5	5	3	105
Zn	139	161	135	68	95
La	5.73	114.39	26.04	71.73	18.40
Ce	14.07	205.11	42.76	158.10	41.74
Pr	2.16	29.29	5.60	19.92	5.66
Nd	10.47	115.20	21.21	79.22	25.03
Sm	3.20	24.93	5.88	19.03	6.35
Eu	1.30	4.65	1.74	2.90	2.03
Gd	3.72	21.79	7.78	18.72	6.64
Tb	0.65	3.59	1.82	3.43	1.10
Dy	3.95	20.71	13.70	21.71	6.66
Ho	0.78	3.81	3.20	4.48	1.33
Er	1.99	9.73	10.00	12.57	3.57
Tm	0.28	1.41	1.68	1.91	0.49
Yb	1.63	8.51	10.98	12.18	2.96
Lu	0.24	1.25	1.72	1.85	0.45
Ba	42	650	409	528	132
Th	0.46	11.63	12.87	12.00	1.75
Nb	10.43	119.69	114.00	96.47	22.10
Y	18.40	78.26	73.71	113.71	32.74
Hf	2.27	17.81	18.79	15.91	4.79
Ta	0.68	8.47	7.72	6.65	1.47
U	0.14	2.46	3.28	3.11	0.53
Pb	0.57	7.43	8.79	3.27	1.56
Rb	2.5	66.6	75.8	63.5	6.1
Cs	0.02	0.12	0.52	0.23	0.01
Sr	225	73	11	66	304
Sc	53.8	0.8	1.4	3.9	37.8
Zr	79	507	595	510	186
$^{143}Nd/^{144}Nd$					0.513028
εNd					7.6
$^{176}Hf/^{177}Hf$					0.283120
εHf					11.9
$^{206}Pb/^{204}Pb$					19.0402
$^{207}Pb/^{204}Pb$					15.5244
$^{208}Pb/^{204}Pb$					38.6081
Zircon Sat (°C)	--	902	892	881	--

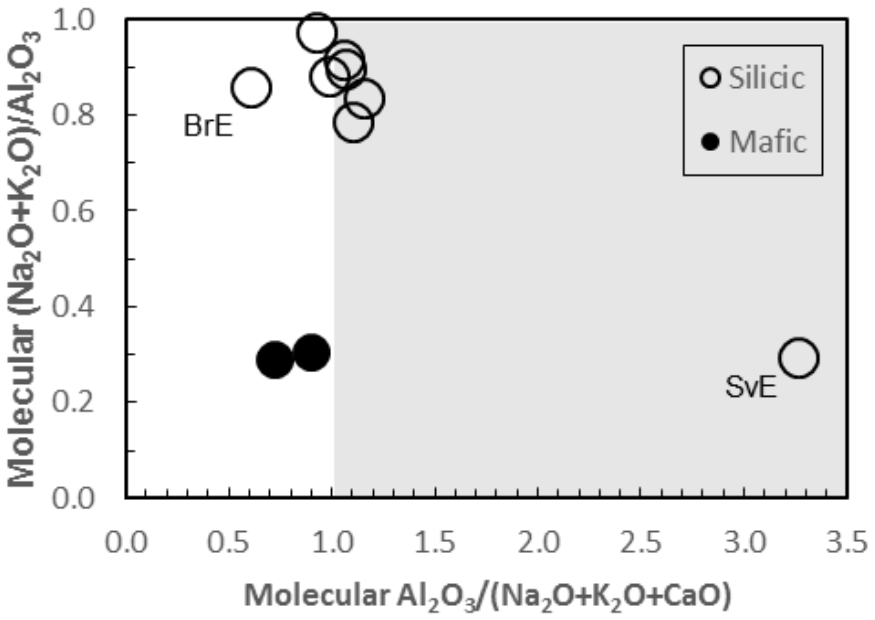

Fig. 2: Diagram showing metaluminous (white field) and peraluminous (grey field) compositions of Hafnarfjall-Skarðsheiði rocks. Note that samples SvE1302 and BrE1201 are highly altered—SvE has lost Na, BrE is enriched in Ca—and therefore not representative of magmatic variation.

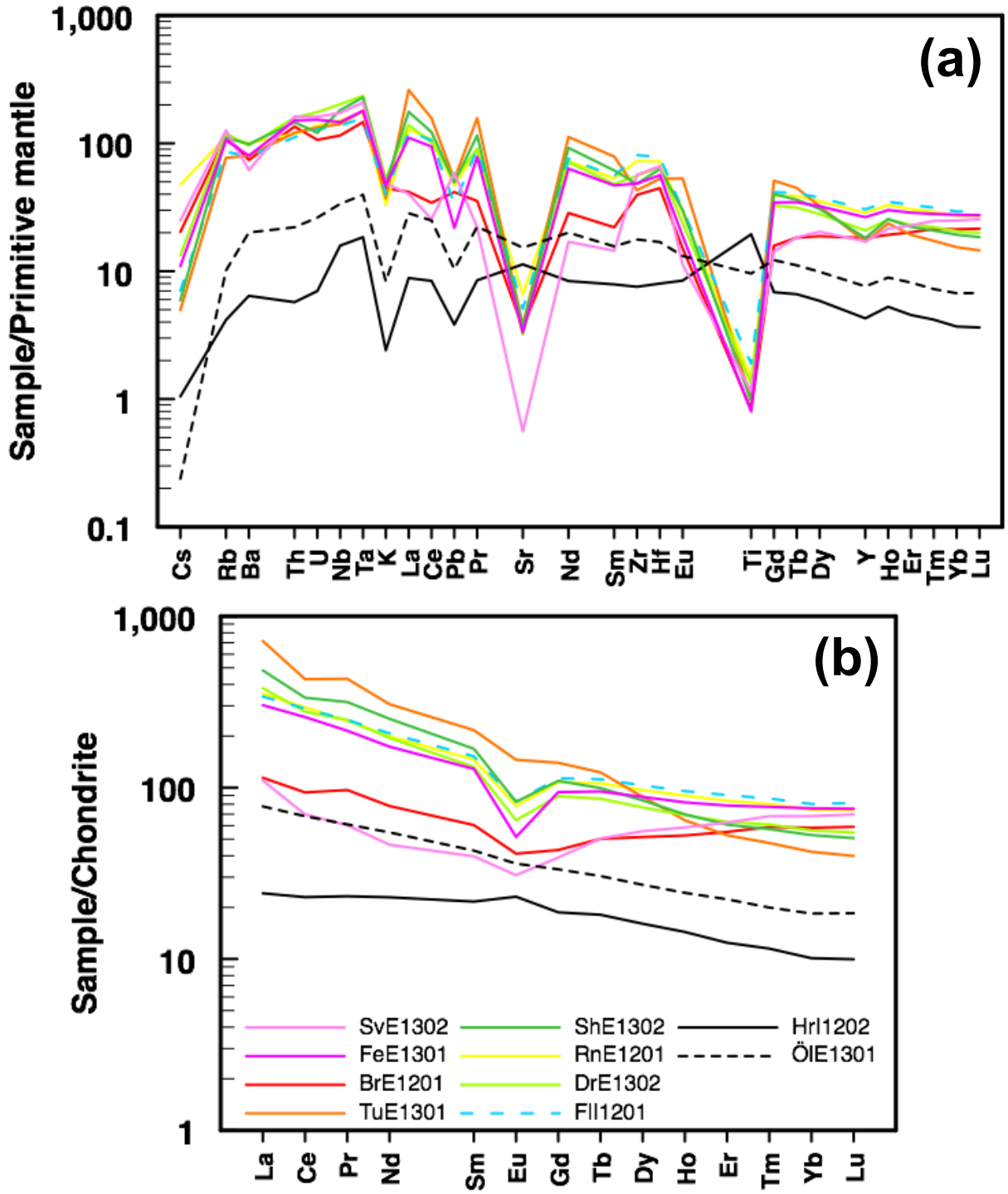

Fig. 3 a) Primitive mantle-normalized (Sun & McDonough, 1989) whole rock multi-element diagram. Legend as in 3b. All silicic samples show higher concentrations of all elements except Sr and Ti. b) Chrondrite-normalized (McDonough & Sun, 1995) whole rock REE diagram. Mafic samples display a typical LREE-enriched OIB signature. Silicic samples SvE1302 and BrE1201 are highly altered, resulting in anomalous REE patterns depleted in LREE and MREE. Sample TuE1301 has a steeper REE pattern than the other silicic samples and almost no Eu anomaly and slight negative Ce anomaly. Remaining silicic samples show a significant negative Eu anomaly.

with K, Pb, Sr, and Ti depletions and enrichment in incompatible elements in all but the most incompatible elements (Cs, Rb, Ba, Th, Nb, Ta). Samples BrE1201 and SvE1302, which underwent post-emplacement alteration as noted above, also show anomalous trace element patterns that are likely not indicative of actual magmatic values. Mafic samples also show an enrichment in incompatible elements proportional to the degree of incompatibility, indicating likely involvement of a depleted mantle source in their production. This trend is especially evident in chondrite-normalized (McDonough and Sun, 1995) rare earth element (REE) patterns (Fig. 3b), where basalt sample ÖlE1301 shows LREE enrichment compared to HREE. ÖlE1301 also has similar elemental chemistry values to basalts erupted from the currently propagating Eastern rift zone (Sigmarsson et al., 2008). The gabbro sample HrI1202 shows a similar, but more depleted pattern marked by a slight positive Eu anomaly, indicating likely plagioclase accumulation. Th/U are 3.21 and 3.29 for mafic samples and range from 3.38 to 4.97 for silicic samples, and the silicic units further define two subgroups of narrower range (3.38-3.93 (n=6); 4.73-4.97 (n=2)). Such comparatively high Th/U ratios for samples BrE1201 and ShE1302 may be the result of open-system behavior and leaching of U, a fluid-mobile element, during post-emplacement hydrothermal alteration. Overall, the ubiquity of hydrothermal alteration processes in the Hafnarfjall-Skarðsheiði central volcano complicates use of major and trace element data to infer petrogenetic processes. We therefore focused on data sources that are likely to reflect original magmatic geochemical compositions—particularly whole rock Pb, Nd, and Hf and *in situ* zircon analyses—to explore the differentiation mechanisms behind silicic magma production at H-S.

4.2. Whole rock Nd, Hf, and Pb isotopes

Neodymium, hafnium, and lead isotopic ratios for 5 silicic and 1 basaltic whole rock samples are within established ranges for Icelandic rocks (Figs. 4,5; Table 3; Appendix H) (e.g. Peate et al., 2010; Willbold et al., 2009). The $^{143}Nd/^{144}Nd$ compositions for H-S rocks fall in a restricted range

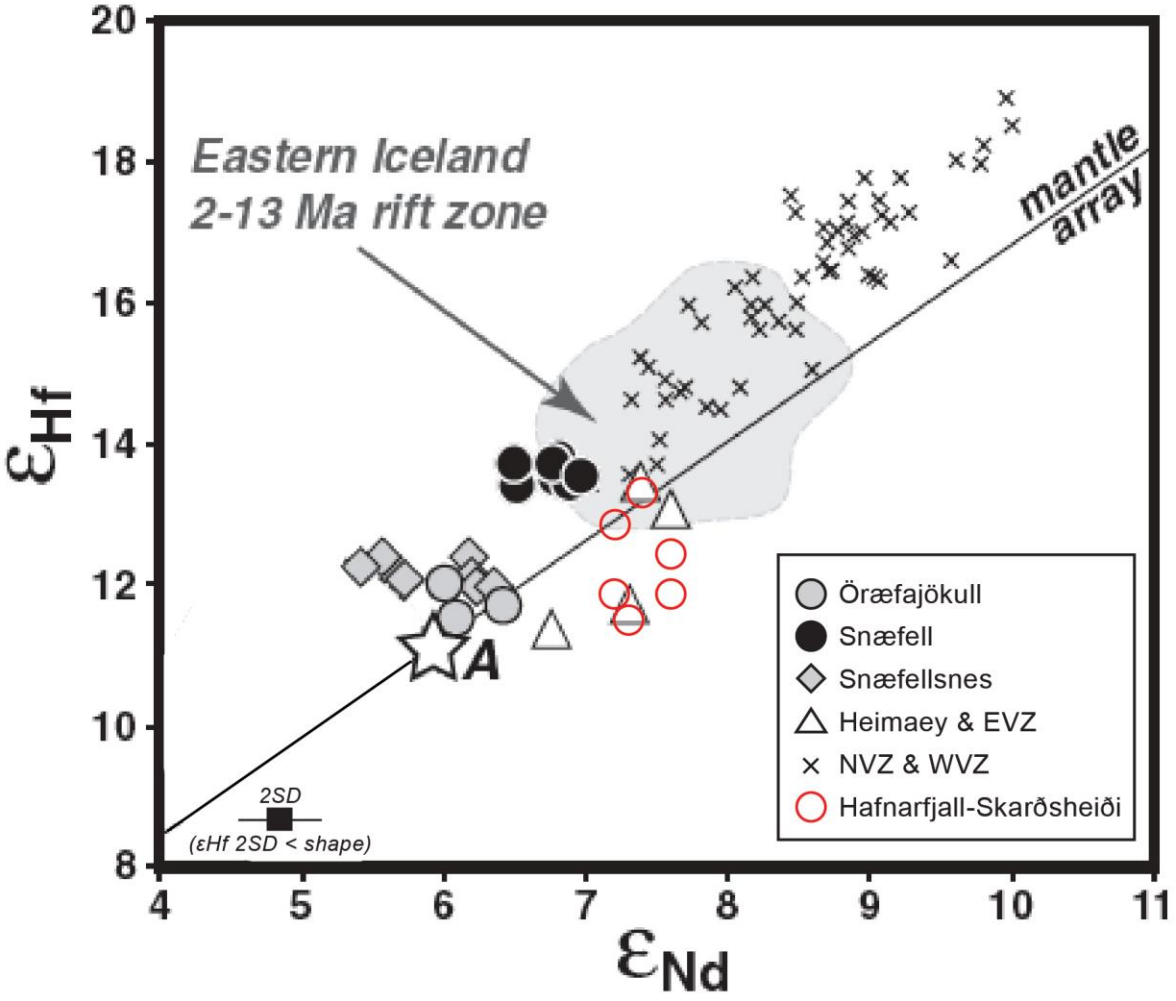

Fig. 4. Whole rock εHf vs. εNd data from H-S plotted against the Iceland array of Peate et al. (2010). Note the overlap with the sparse Heimaey/EVZ samples from a propagating rift. Modified from Peate et al. (2010).

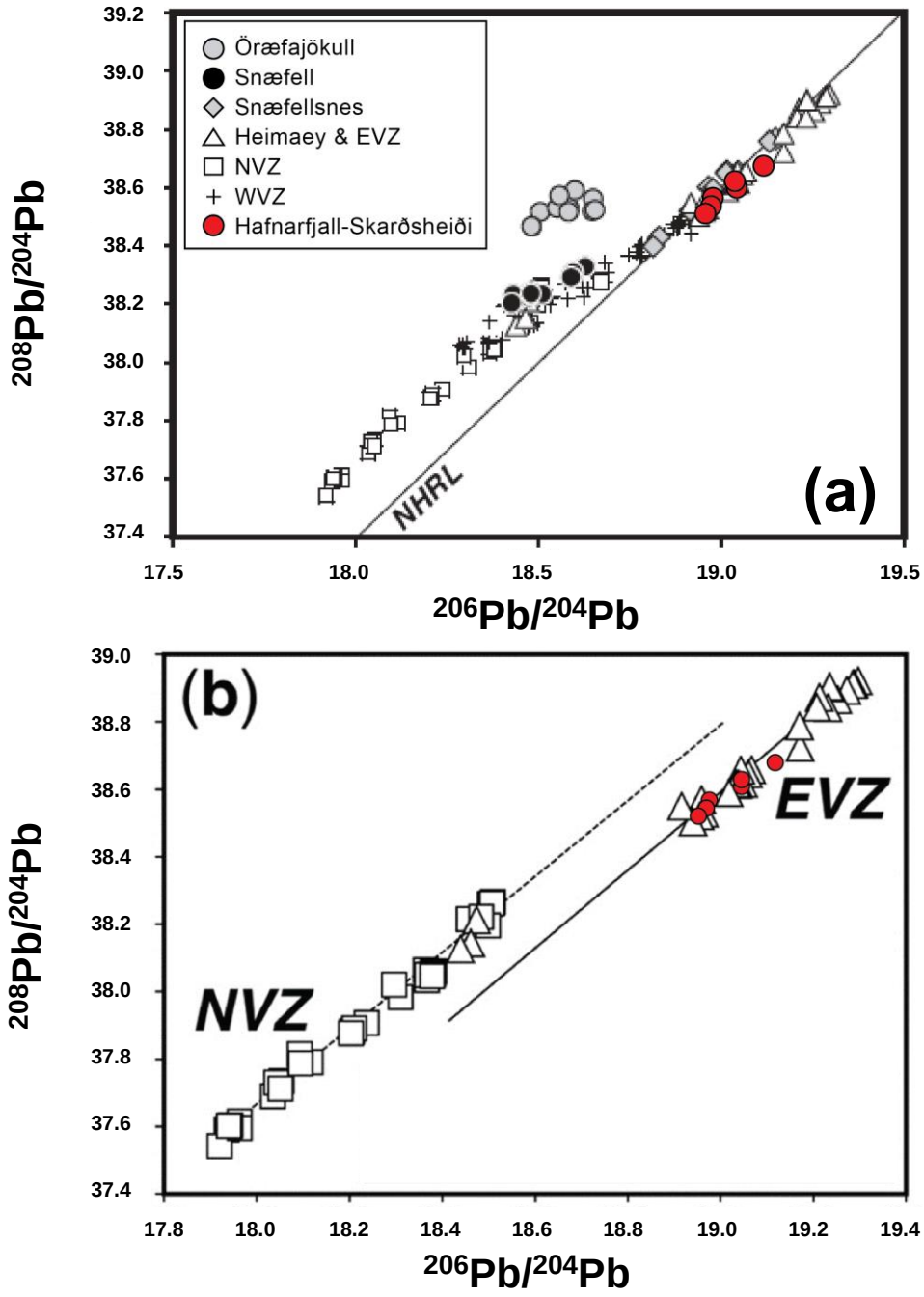

Fig. 5. a) Whole rock $^{208}Pb/^{204}Pb$ vs. $^{206}Pb/^{204}Pb$ for Icelandic volcanic regions. H-S plots in an overlapping space with modern Heimaey/EVZ and Snæfellsnes. b) Whole rock $^{208}Pb/^{204}Pb$ vs. $^{206}Pb/^{204}Pb$ data from H-S rocks plots with those for a modern propagating rift. Modified from Peate et al. (2010).

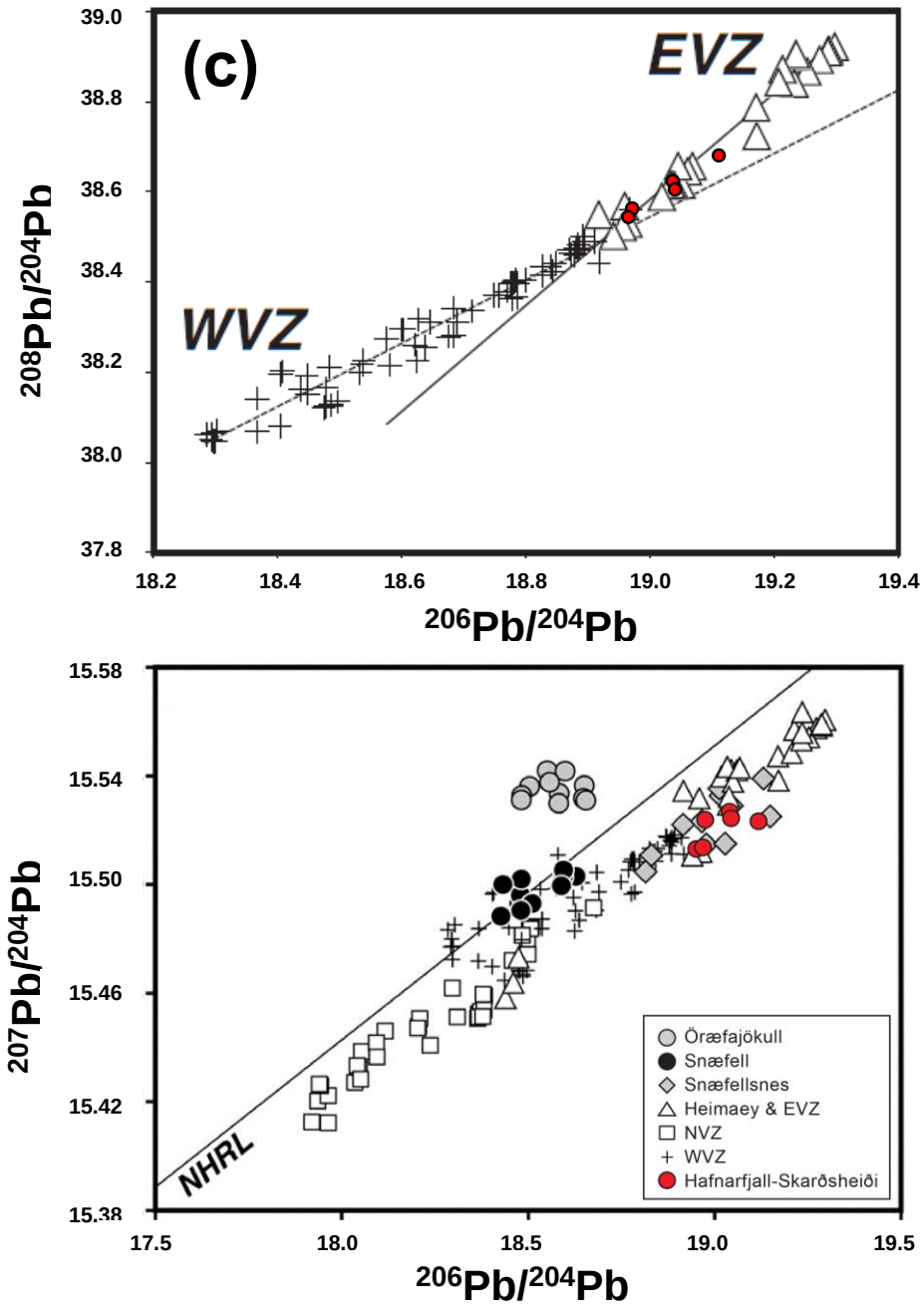

Fig. 5. c) Whole rock $^{208}Pb/^{204}Pb$ vs. $^{206}Pb/^{204}Pb$ for Icelandic rift zones. H-S plots in an overlapping space with modern EVZ rocks. Symbols as in (d). d) Whole rock $^{207}Pb/^{204}Pb$ vs. $^{206}Pb/^{204}Pb$ for modern Iceland rift zones. The NVZ is an established rift while the EVZ is a propagating rift. H-S samples clearly overlap with those from the EVZ. Modified from Peate et al. (2010).

(0.513010-0.513030; ε_{Nd} is +7.2 to +7.6), with no clear distinction between the silicic samples and basalt. These high values indicate all H-S samples were produced in an "on-rift" setting as defined by Martin and Sigmarsson (2010), who identified rocks with $^{143}Nd/^{144}Nd>0.51296$ as being generated in rift zone settings. Hf-isotope ratios show no correlation with chemical composition. $^{176}Hf/^{177}Hf$ compositions range from 0.283109-0.283162 (ε_{Hf} is +11.4 to +13.3 (2SD <0.1)) and show no correlation with major element composition. H-S samples plot on or slightly below the $\varepsilon_{Hf}/\varepsilon_{Nd}$ Icelandic mantle array (cf. Peate et al., 2010). Most Icelandic lavas define a tight linear array below the Northern Hemisphere Reference Line (NHRL; Hart, 1984) on a $^{207}Pb/^{204}Pb$ vs. $^{206}Pb/^{204}Pb$ diagram and straddle the NHRL on a $^{208}Pb/^{204}Pb$ vs. $^{206}Pb/^{204}Pb$ diagram (Fig. 5). The H-S samples occupy a relatively restricted area in Pb-Pb space, with $^{206}Pb/^{204}Pb$ =18.9680 to 19.1136, $^{207}Pb/^{204}Pb$ =15.5134 to 15.5271, and $^{208}Pb/^{204}Pb$ =38.5207-38.6783. Sample FlI1201, the lone granophyre, consistently plots toward the non-radiogenic end of the array, while DrE1302 is the most radiogenic. Pb-isotope ratios generally follow those measured from the propagating EVZ (Peate et al., 2010).

4.3. In situ zircon O isotopes

Oxygen isotope ratios ($\delta^{18}O$) for zircon from 8 H-S samples (n=152) are depleted compared to mantle zircon (cf. Valley, 2003), ranging from 1.5 to 4.6‰ with a mean value of 2.8‰ (Table 4; Fig. 6; Appendix D). Sample averages fall between 2.2 ± 0.7 and 3.5 ± 0.8 ‰ (2SD). Most H-S samples have low $\delta^{18}O$ scatter and standard deviations <0.5 ‰. The exceptions to this are samples SvE and ShE, with standard deviations >1 ‰, and sample FlI (SD=0.7 ‰). Larger spread in zircon $\delta^{18}O$ values in single samples may indicate greater variability in petrogenetic process than in the majority of H-S samples.

4.4. In situ zircon U-Pb geochronology

Zircon U-Pb ages from all major silicic units at Hafnarfjall-Skarðsheiði occur in 2 distinct crystallization phases: Individual grain ages from Phase 1 samples FeE1301 (*n*=9), SvE1302 (*n*=12), BrE1201 (*n*=43), and TuE1301 (*n*=10) range from 4.93 ± 0.25 Ma to 5.86 ± 0.45 Ma (1σ standard deviation), and Phase 2 samples ShE1302 (*n*=9), RnE1201 (*n*=7), DrE1302 (*n*=9), FlI1201 (*n*=8) and gabbro HrI1202 (*n*=16) range from 3.57 ± 0.14 Ma to 4.57 ± 0.10 Ma. Weighted mean ages for each sample are presented in Tables 4 and full analytical results are in Appendix E. Weighted mean ages define the two magmatic phases more narrowly than individual grain ages: Phase 1 from 5.33 ± 0.04 Ma to 5.43 ± 0.14 Ma (2σ standard error for weighted mean ages) and Phase 2 from 3.88 ± 0.19 Ma to 4.38 ± 0.11 Ma (Fig. 6). The presence of a 11.34± 0.17 Ma (1σ SD) inherited zircon core in sample BrE1201 indicates potential for incorporation of older material into H-S magmas. The range of values for mean squared weighted deviations (MSWD; weighted by $1/\sigma^2$) for calculated weighted mean ages are within the range expected for a homogeneous population based upon Monte Carlo simulations by Mahon (2006). Our measured MSWD's range from 0.82-2.0 which are interpreted to represent a single population. Tera-Wasserburg plots (Fig. 7) reveal a range in common Pb contamination, from zero (samples ShE1302, TuE1301, and DrE1302) to up to 65% correction for common Pb in sample BrE1201. It should be noted that timing of magmatism as interpreted by zircon crystallization ages is not necessarily correlated with time of eruption or intrusion as established by Franzson (1978) (Table 1). Potential explanations for this include: a) zircon crystallization occurs long before eruption; b) ages provided by Franzson (1978) are incorrect; or c) the samples analyzed here do not correlate with the units analyzed by Franzson (1978). These possibilities are addressed further in the Discussion.

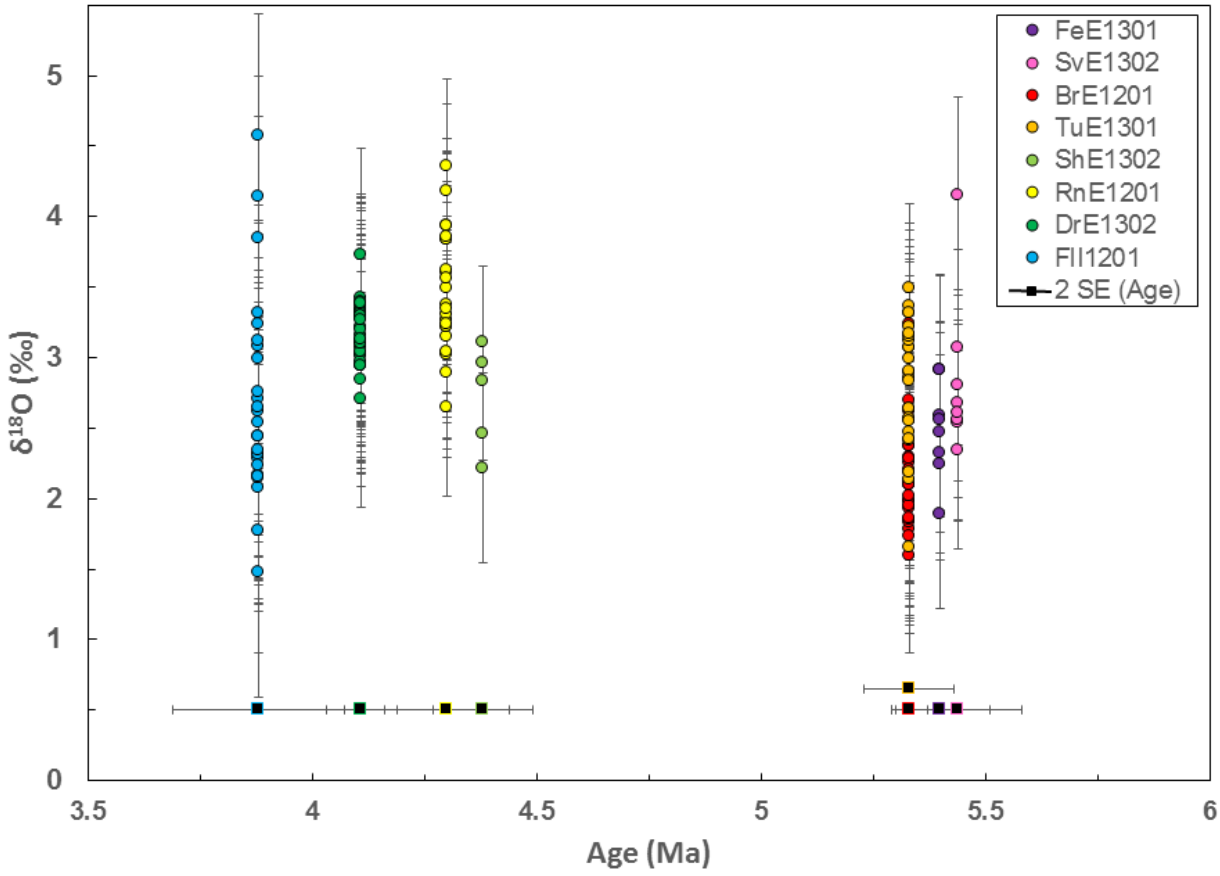

Fig. 6. *In situ* zircon $\delta^{18}O$ analyses vs. weighted mean U-Pb age for H-S samples. Oxygen isotope errors are 2 SD; 2 SE age errors are denoted by horizontal error bars and box color-coded to the sample it represents.

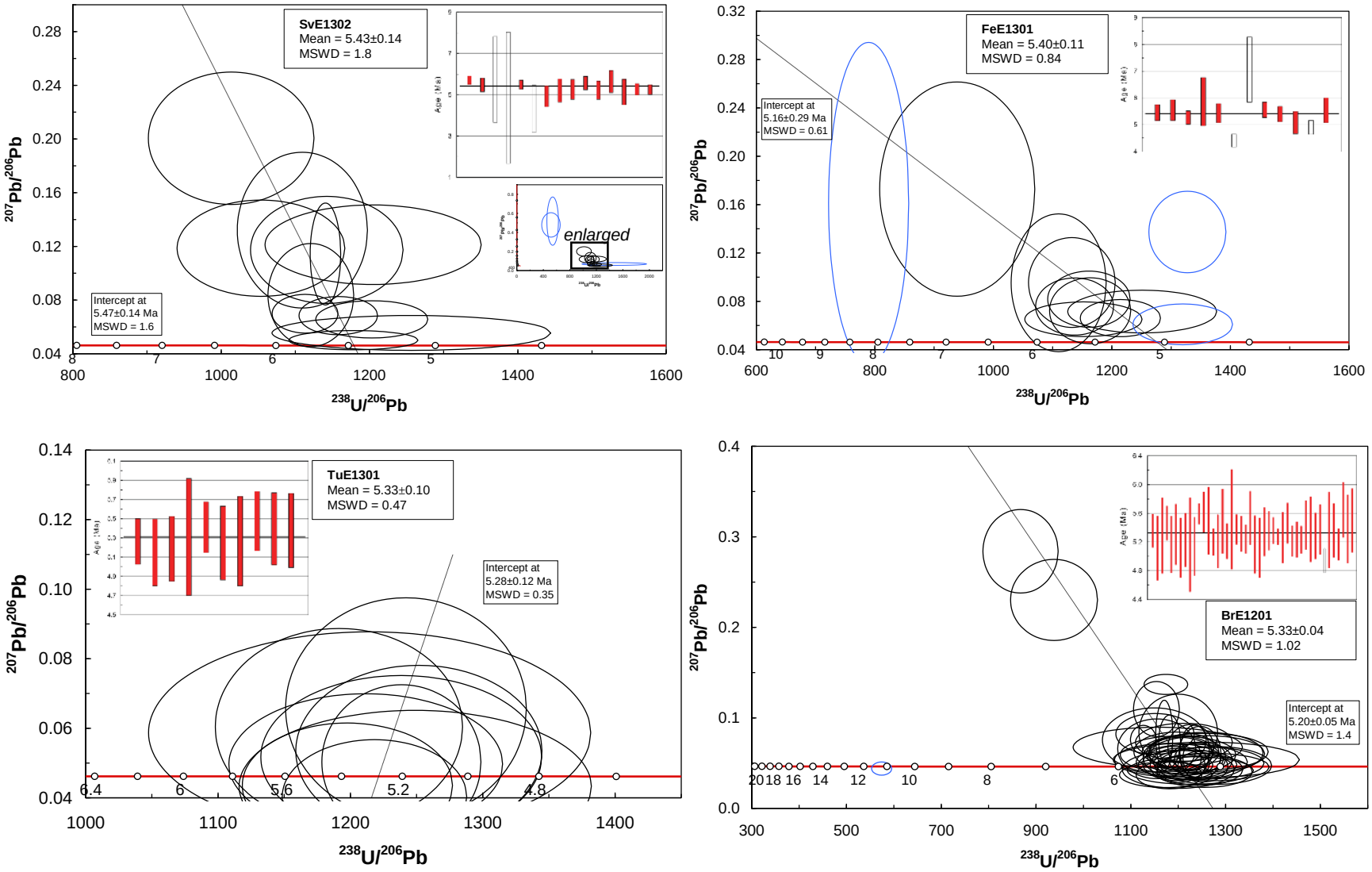

Fig. 7: Tera-Wasserberg diagrams and corresponding zircon weighted average age results (insets). Box heights are 2 SD uncertainties; black bar is sample age in inset. Data point error ellipses are 2 SD. Blue ellipses and unfilled boxes indicate omission of that grain from the weighted mean age calculation.

Fig. 7 cont.: Tera-Wasserberg diagrams and corresponding zircon weighted average age results (insets). Box heights are 2 SD uncertainties; black bar is sample age in inset. Data point error ellipses are 2 SD. Blue ellipses and unfilled boxes indicate omission of that grain from the weighted mean age calculation.

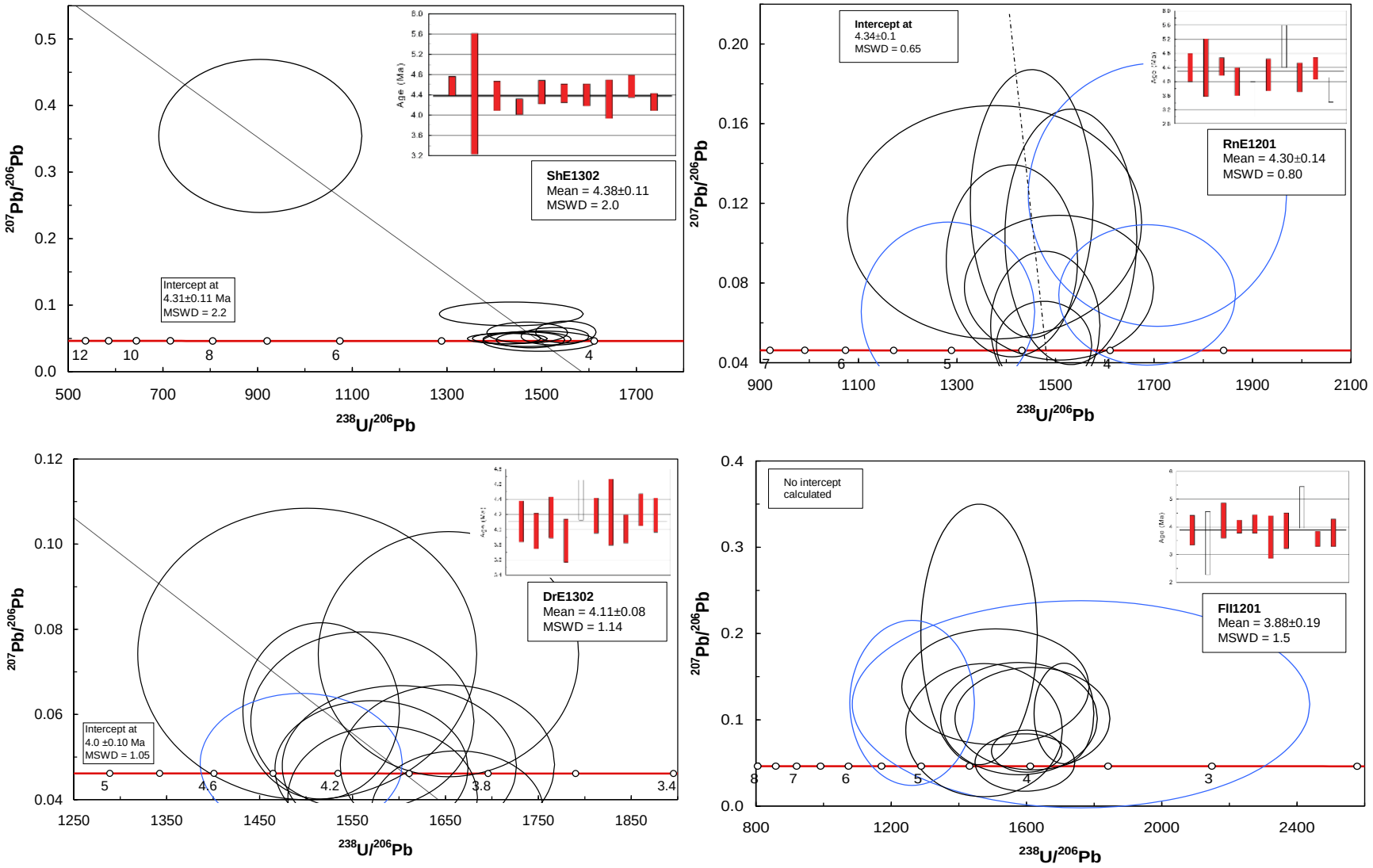

4.5. In situ zircon trace elements

4.5.1. Rare Earth elements (REE)

Zircons from all H-S samples have zircon-normalized (from average of all H-S analyses) REE patterns (Appendix F; Figs. 8, 9) that illustrate the variability in H-S zircon. Positive Ce anomalies and negative Eu anomalies in chondrite-normalized plots are ubiquitous in Fig. 8 (indicative of oxidation fugacity of magma, and zircon growth in magmas from which feldspars have grown, respectively; Hoskin and Schaltegger, 2003) but manifest as small positive or negative anomalies as compared to other H-S zircons in Fig. 9. Heavy REE (HREE) are greatly enriched relative to chondrite, spanning more than an order of magnitude, from ~1,000 to >10,000. Each H-S sample has a distinct REE signature that varies in slope, abundance, and anomaly magnitudes. Several samples (SvE, BrE, and HrI) have patterns that are relatively enriched, probably due to the presence of nanometer-scale LREE-rich inclusions which are commonly found in zircon. At least one sample, ShE, shows evidence of growth from a uniform and strongly fractionated melt based on higher concentrations of REEs and its small spread in REE concentration between grains.

4.5.2. Ti and Hf

The Ti content of H-S zircons ranges from ~5 to ~38 ppm, with a mean concentration of 12.4 ppm (Appendix D; Fig. 10). Hafnium at Hafnarfjall-Skarðsheiði spans a range from ~6,800 ppm to 12,300 ppm. The mean Hf concentration is ~9,500 ppm. The intrusive units (HrI1202 and FlI1201) plot in discernible Ti vs. Hf domains and have high Ti concentrations for corresponding Hf concentrations, averaging ~8000 ppm Hf at ~19 ppm Ti (HrI1202) and ~9000 ppm Hf at ~22 ppm Hf (FlI1201). Several of the volcanic samples—especially ShE1302 and SvE1302—show a wide range of intra-sample variability. Samples BrE1201 and DrE1302 have the most restricted range of Ti and Hf. Overall, these volcanic H-S data form a coherent population within the greater Iceland array (Fig. 10) (cf. Carley, 2014).

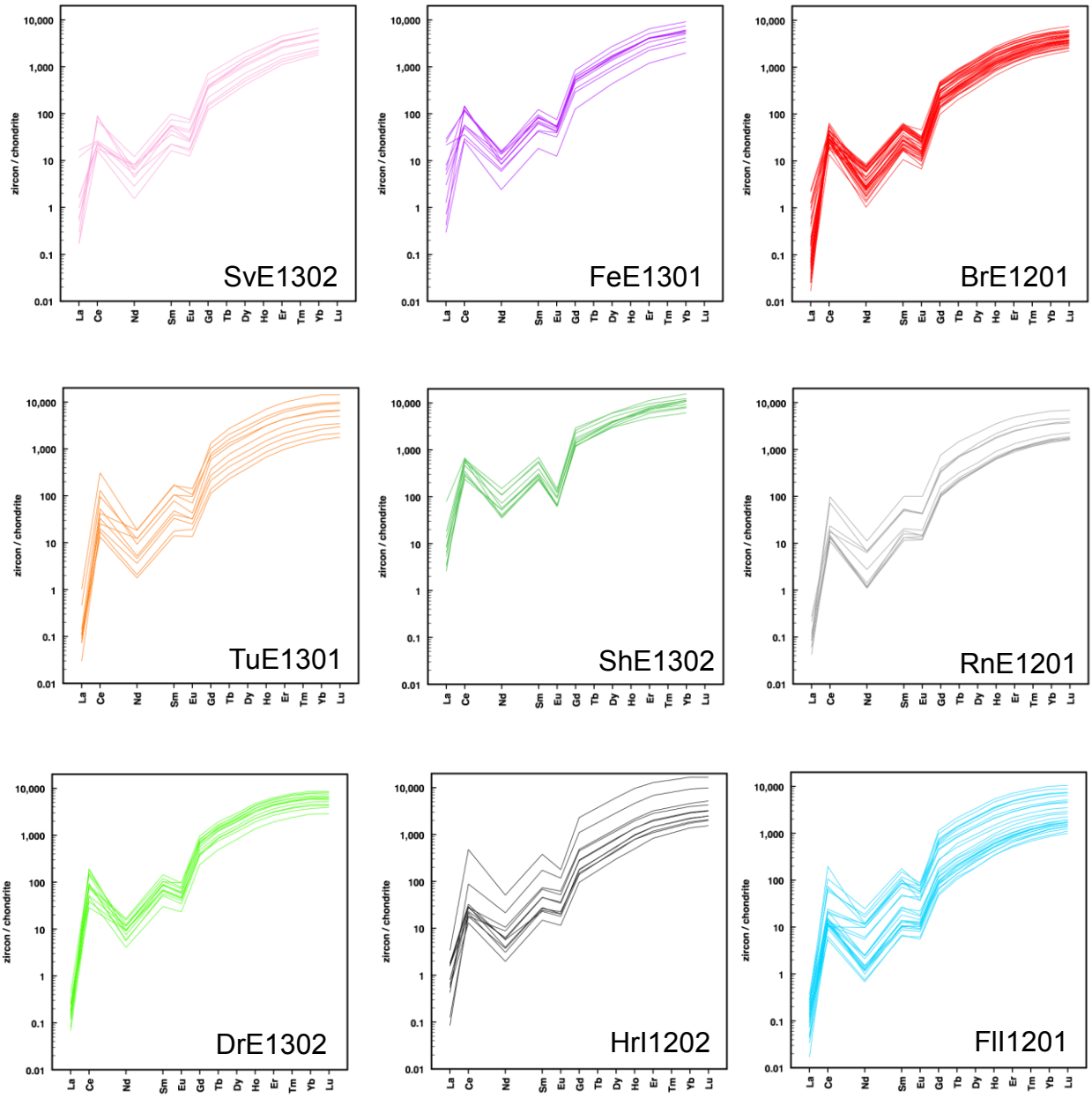

Fig. 8: H-S zircon REE normalized to chondrite (McDonough and Sun, 1995).

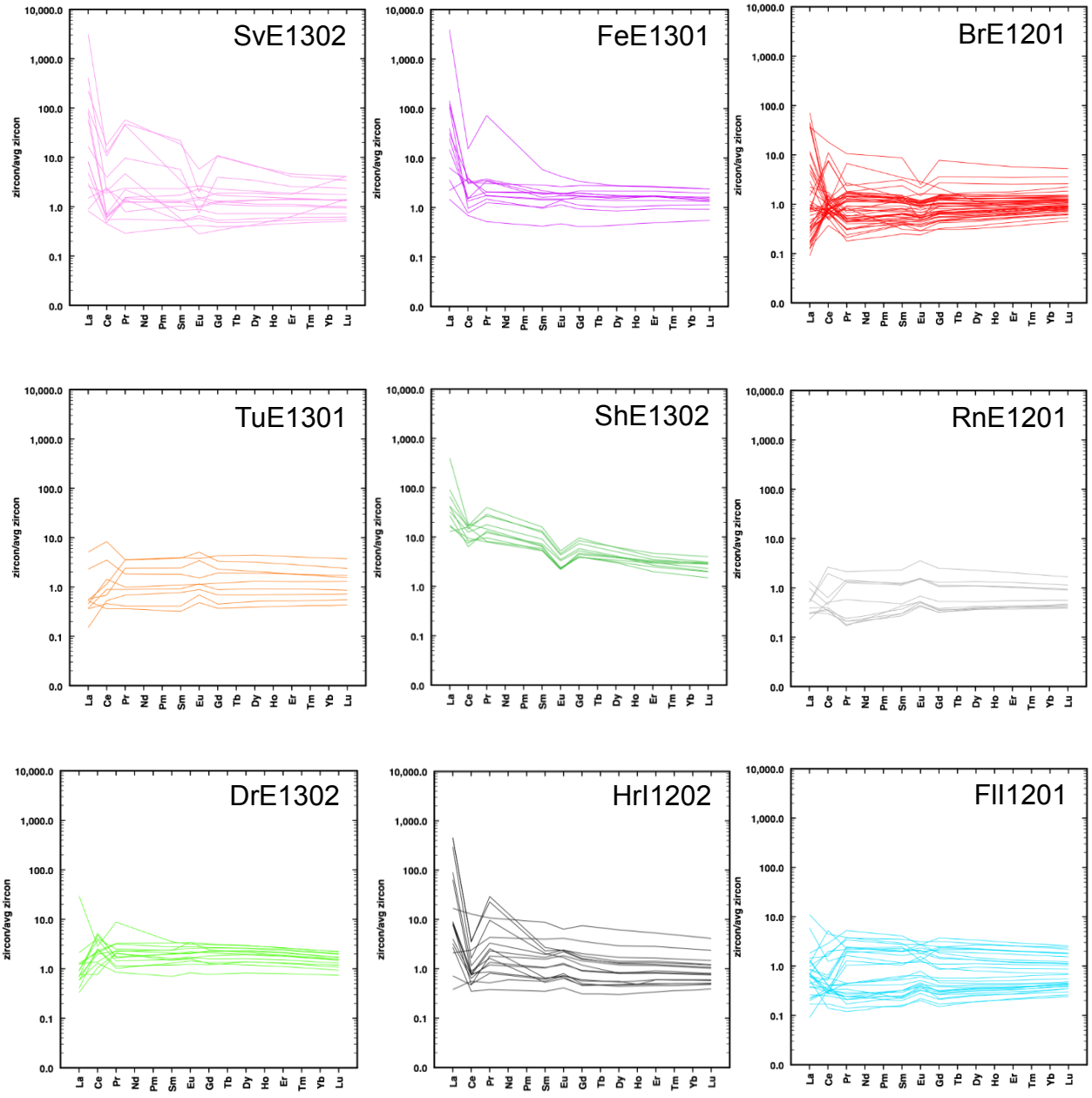

Fig. 9: Zircon-normalized REE plots of H-S zircons.

Fig. 10: Ti vs. Hf concentrations in H-S zircons plotted against the Iceland array from Carley (2014).

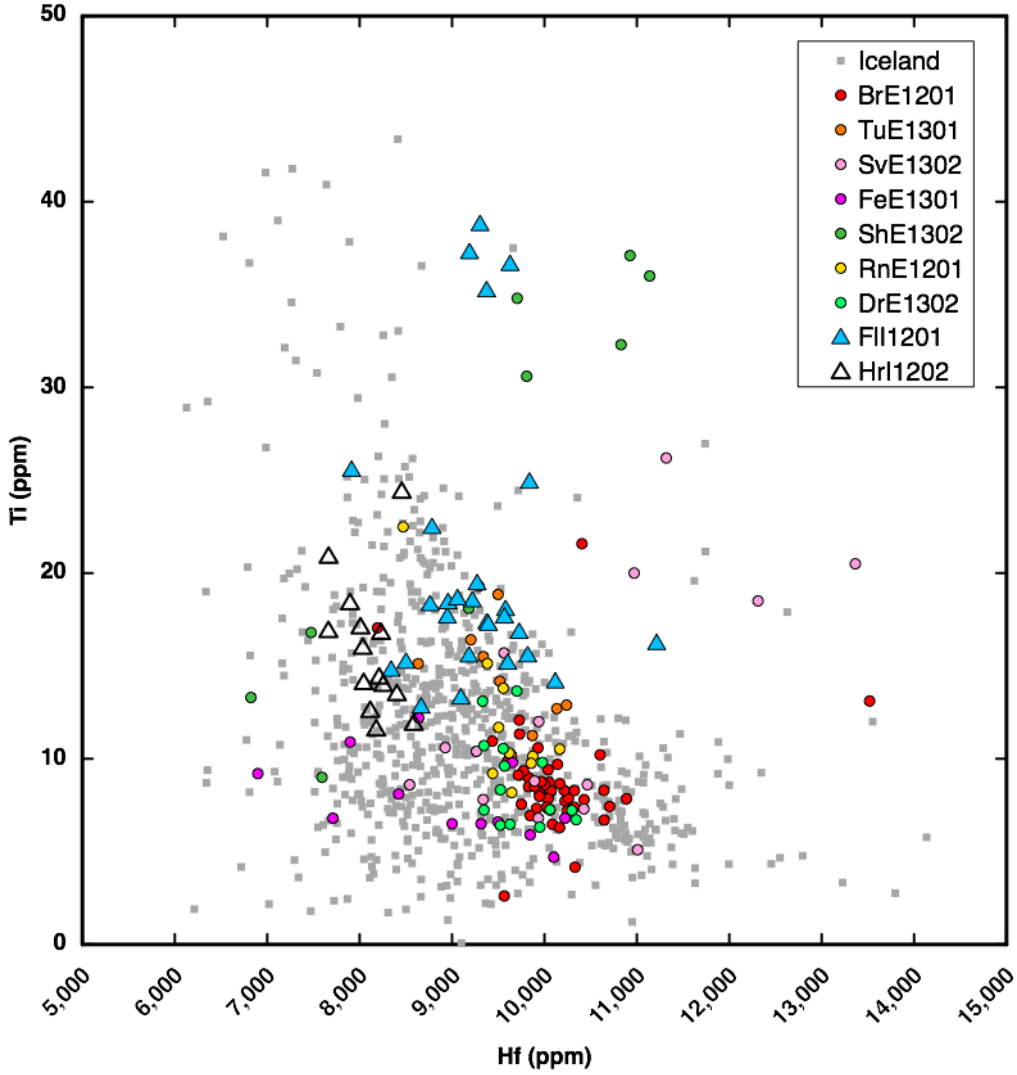

4.5.3. Ti-in-zircon thermometry

We applied the Ferry and Watson (2007) Ti-in-zircon thermometer to our measured *in situ* zircon Ti values using a_{TiO2}=0.7 and a_{SiO2}=1 for all silicic samples (Appendix D). Ferry and Watson (2007) and Watson et al. (2006) note a common a_{TiO2} range of 0.6 to 0.9 in silicic magmas, and Ghiorso and Gualda (2012) suggest that a wider a_{TiO2} range from 0.3 to 0.9 may be possible. While uncertainty surrounding the range of realistic a_{TiO2} values exists, we use a fixed a_{TiO2} value here to facilitate comparison amongst H-S sample. Since it is likely that zircon grows in conditions near silica saturation, and the SiO_2 content of the H-S samples is (with one exception, BrE1201) >70 wt%, an a_{SiO2} value of 1.0 is realistic. Prior application of the Ti-in-zircon thermometer to silicic systems in Iceland (Carley et al., 2014) also suggests these are reasonable activity values. Crystallization temperatures for Hafnarfjall-Skarðsheiði ~725-950°C, with the majority of grains between 750-850°C. There appears to be no correlation between zircon crystallization temperature and age.

4.6. In situ zircon Hf isotopes

The range of ε_{Hf} for the H-S zircon population (n=58) is 8.3 ± 1.9 to 13.2 ± 1.4 (errors are 2SE) (Table 4; Fig. 11; Appendix G), and there is considerable variation among the 5 units that were analyzed. Samples BrE1021 and TuE1301, which have nearly identical U-Pb ages, have average ε_{Hf} of 11.7± 1.6 (2σ SD) and 11.5 ± 1.5, respectively. Average values for samples RnE1201 (ε_{Hf}=10.6 ± 3.2), DrE1302 (ε_{Hf}=11.2 ± 1.1), and FlI1201 (ε_{Hf}=11.6 ± 2.0) are also statistically indistinguishable at the 2σ level. H-S zircon ε_{Hf} values are within the range of typical Icelandic values, but tend to deviate from the corresponding whole rock ε_{Hf} values (Fig. 11). This will be elaborated on in the Discussion.

Table 4. *In situ* zircon analysis summary

	U-Pb geochronology				Oxygen isotopes			Hafnium isotopes			
	Age (Ma)	2 SE[1]	*n*	MSWD	$\delta^{18}O$ (‰)	2 SE[2]	*n*	εHf	2σ[3]	*n*	Outliers
SvE1302	5.43	0.14	12	1.80	2.8	1.14	8	--	--	--	--
FeE1301	5.40	0.11	9	0.82	2.5	0.68	8	--	--	--	--
BrE1201	5.33	0.04	43	1.02	2.2	0.55	27	11.7	1.6	11	4
TuE1301	5.33	0.10	10	0.47	2.8	0.90	24	11.5	1.5	14	0
ShE1302	4.38	0.11	10	2.00	2.8	2.60	5	--	--	--	--
RnE1201	4.30	0.14	7	0.80	3.5	0.85	24	10.6	3.2	9	0
DrE1302	4.11	0.08	9	1.14	3.2	0.42	30	11.2	1.1	15	0
HrI1202	4.00	0.08	16	1.19	--	--	--	--	--	--	--
FlI1201	3.88	0.19	8	1.50	2.7	1.42	26	11.6	2.0	13	0

[1] *Standard error of each sample, not including internal and external uncertainties*

[2] *Standard error, including internal and external uncertainties*

[3] *Standard deviation from the sample average*

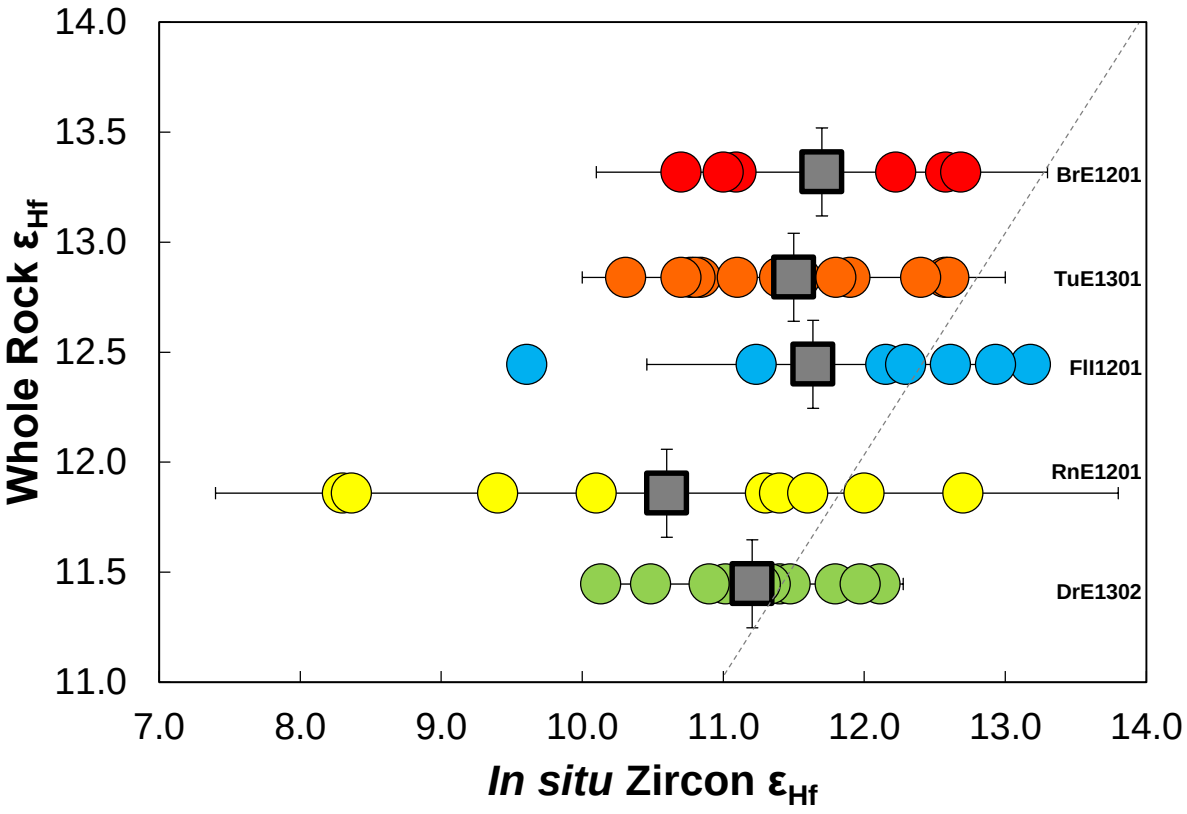

Fig. 11: Whole rock ε_{Hf} vs. *in situ* ε_{Hf} for H-S samples. Dashed line is 1:1. Individual zircon analyses as circles. Grey boxes are sample averages. Uncertainty for whole rock ε_{Hf} values is 2 SE and 2 SD for *in situ* ε_{Hf} sample means.

5. Discussion

5.1. Timing and duration of silicic magmatism

U-Pb zircon crystallization ages from 8 silicic units record two distinct phases of silicic magmatism: Phase 1 from 5.33 ± 0.04 Ma to 5.43 ± 0.14 Ma (2σ standard error for weighted mean ages) and Phase 2 from 3.88 ± 0.19 Ma to 4.38 ± 0.11 Ma, including the intrusive Flyðrur granophyre unit. Phase 2 volcanic samples range from 4.11 ± 0.08 Ma to 4.38 ± 0.11 Ma, indicating zircon crystallization in the Flyðrur unit continued for roughly 200 kyr past cessation of crystallization of zircon from all other silicic units. Based on available sampling, Phase 2 magmatism in total is roughly 5 times longer than Phase 1 magmatism, which may imply a shift in petrogenetic process. The U-Pb zircon ages presented here deviate somewhat from those noted by Franzson (1978) and references therein based on paleomagnetic and K-Ar age constraints. Sample RnE1201, thought to have erupted well before sample ShE1302 (Franzson, 1978), has a U-Pb zircon age ~0.08 Myr younger than ShE1302. SvE1302 has a U-Pb zircon age ~0.85 Ma older than its estimated stratigraphic age based on paleomagnetic correlation (5.43 vs. ~4.6 Ma) (Franzson, 1978). FeE1301 has zircons ~3 Myr younger than its proposed stratigraphic age, although this is an unrealistic expectation for zircon storage duration, indicating that most likely the initial age estimate of the FeE unit was incorrect. These discrepancies between previous estimated ages and our U–Pb zircon ages indicate that magma residence times—as recorded by zircon—are often of longer duration than eruptive frequencies and that long-term magma storage commonly, but not universally, occurred at H-S. All samples show a range of at least a few hundred kyr in zircon crystallization ages, which likely reflects crystallization of zircon for an extended time period. This phenomenon has been described in other locations (e.g. Claiborne et al., 2010a; Schmitt et al., 2010; and many others) and is likely a common occurrence in the volcanic record, but the timescales of residence indicated by our data are over an order of magnitude longer than the 10^3-10^4 years previously suggested for young Icelandic volcanic systems (cf. Carley et al., 2011). More work is

needed to determine if a correlation exists between zircon residence times and magmatic system age on a larger (i.e. Iceland-wide) scale.

Overall, silicic magmatism at H-S lasted for at least 1.5 Myr—one of the longest-lived examples of silicic volcanism on record in Iceland (cf. Carley, 2014). The overall lifespan of central volcanoes is commonly considered to be 300 kyr to >1 Myr (Sæmundsson, 1986), which are predominantly basaltic in composition. When the basalts that precede and follow the silicic units at H-S are considered (Franzson, 1978), the overall lifespan of the Hafnarfjall-Skarðsheiði central volcano is at least 2 Myr.

Hafnarfjall-Skarðsheiði central volcano occupies an interesting niche in Iceland's geodynamic setting because it lies on Tertiary bedrock despite being composed of material erupted from the WRZ, while most other areas with significant silicic magmatism and Tertiary bedrock in western Iceland erupted from the SSRZ. H-S is therefore uniquely situated to record the processes and timescales associated with silicic magma genesis post-dating rift relocation. Rift relocation is likely an incremental process (e.g. Benediktsdóttir et al., 2012; Harðarson et al., 2008; Martin and Sigmarsson, 2010) with both the declining and incipient rifts receiving magma—therefore establishing a timescale for initial silicic magma production after a relocation relies on constraining the point at which enough melt is being diverted to the incipient rift to induce petrogenetic processes that lead to evolved magma compositions. Martin and Sigmarsson (2010) established that SSRZ magmatism transitioned to the WRZ sometime between 6.7 and 5.5 Ma, suggesting there was a ~1.3 Myr hiatus between basaltic magmatism and the initiation of silicic magmatism at H-S. It is also possible that early basaltic magmatism and zircon crystallization in silicic magmas was concurrent.

5.2. Zircon oxygen isotope interpretation

Zircons from H-S silicic units occupy a narrow range (1.5-3.5‰) of oxygen isotope variation, and sample means fall well within 2σ error of each other. Evolved compositions in Icelandic magmas likely result from a combination of inputs from partial melting of hydrothermally altered rocks, primary mantle melts, and AFC processes operating during partial melting. The isotopically depleted zircon $\delta^{18}O$ compositions (1.6–4.4‰; mean 2.8‰) for all H-S zircons analyzed in this study indicates that incorporation of older, hydrothermally altered material—whether basalt or rhyolite—was involved in generating evolved melts, as has been invoked for Iceland petrogenesis on a broad scale (e.g. Bindeman et al., 2012). The presence of a 11.3 Ma inherited zircon core in BrE1201 supports the idea of involvement of older, more altered material. The 11.3 Ma inherited zircon core has $\delta^{18}O$ of 3.2‰, which—while higher than average BrE—is within the overall oxygen isotope range at H-S and is close in $\delta^{18}O$ than what appears to be average (3.0‰) for tertiary Icelandic central volcano silicic magmas (Carley et al., 2014). Therefore, it is reasonable and likely that similar initial petrogenetic processes involving incorporation of previously-altered material were active to varying degrees in producing each silicic unit at H-S.

5.3. Interpretation of Pb, Nd, and Hf isotope data

5.3.1. Pb isotopes

It is well established that the upper mantle beneath Iceland is heterogeneous and composed of at least 3-4 end members (e.g. Peate et al., 2010; Thirlwall et al., 2004). Peate et al. (2010) also established that there is a NE-SW variation in the mantle source across Iceland with the NVZ and EVZ having parallel but offset trends in $^{207}Pb/^{204}Pb$ vs. $^{206}Pb/^{204}Pb$ plots and the EVZ and WVZ intersecting at a common source that is not involved in producing NVZ magmas. Samples from Hafnarfjall-Skarðsheiði fall within a narrow range on all Pb isotope diagrams and are very similar to basalt Pb isotope values from the currently propagating Eastern rift zone, indicating that they share

an isotopically similar source. H-S is more isotopically similar in Pb, Nd, and Hf to the EVZ than it is to the WVZ—the rift it erupted from (Fig. 5). This apparent discrepancy can be explained if either: a) H-S and the EVZ are derived from a geochemically similar mantle source; or b) H-S and the EVZ have a similar contribution from crustal melts whose isotopic signatures reflect those of the basement rocks. If (b) was the case, we would expect that H-S basalts to be produced by near-complete melting of bedrock areas while the more evolved H-S compositions formed from varying degrees of bedrock partial melting displayed a wide range of geochemical variation different from those of the basalts. Since near-complete melting of the Icelandic bedrock is likely impossible due to thermal constraints and the basalt at H-S (sample ÖlE1301) is isotopically identical in Pb, Nd, and Hf to the rhyolites, it is reasonable to conclude that both basalts and rhyolites at Hafnarfjall-Skarðsheiði are geochemically derived—likely to a large degree—by primary melts from the mantle that include a significant enriched plume component. This is the same isotopic signature displayed by modern magmas from a propagating rift, indicating that the geodynamic and petrogenetic environment in which H-S magmas evolved was likely similar to that of the modern EVZ.

5.3.2. Nd isotopes

Whole rock Nd isotope ratios from 6 H-S samples compose a coherent population with little Nd variation ($^{143}Nd/^{144}Nd$=0.51301–0.51303; ε_{Nd}=+7.2 to +7.6) that overlap values from EVZ magmas (Fig. 4). According to the guidelines established by Martin and Sigmarsson (2010) that infer $^{143}Nd/^{144}Nd$ >0.51297 indicates an on-rift petrogenetic environment (as opposed to an off-rift, or flank zone, environment), all H-S magmas formed in an on-rift setting. However, these authors propose that on-rift silicic magmas are generated dominantly through crustal anatexis, which does not seem to play a dominant role in producing H-S magmas based on the Pb isotope data.

5.3.3. Comparison of whole rock and in situ Hf isotopes

Whole rock Hf isotope data from H-S are relatively unradiogenic compared to the bulk of Icelandic rocks (Fig. 4), and also plot with modern EVZ products on an ε_{Hf} vs. ε_{Nd} plot. Statistically

significant variation in ε_{Hf} among the H-S samples indicates either variability within the mantle source, potentially due to evolution of the tectonic regime, or varying degrees of heterogeneity introduced through AFC processes. Silicic samples RnE, DrE, and FlI, all from Phase 2 magmatism, have compositions more similar to that of basalt sample ÖlE, while Phase 1 silicic samples plot on or near the Nd/Hf mantle array and are characterized by higher ε_{Hf} than other samples. Based on their similarity to ÖlE, it appears that the Phase 2 silicic samples have more MORB-influenced Hf and Nd isotopic signature than Phase 1 samples. The Phase 2 samples also overlap the field of Tertiary magmatism and current NVZ/WVZ magmatism, while the Phase 1 samples do not. Therefore, it appears that there is a component of potentially older, isotopically distinct material contributing to the Phase 1 magmas.

An intriguing feature of H-S silicic samples is a slight discrepancy between whole rock ε_{Hf} and *in situ* zircon ε_{Hf} values (Fig. 11). Hf is strongly compatible in zircon but not in other common phenocryst phases. Therefore, Hf in a magmatic system that is not in zircon must primarily be in the melt, and assuming both the zircon and the melt from which it crystallizes are in equilibrium during zircon crystallization, they both should have identical Hf isotopic values. Discrepancies between whole rock and zircon Hf isotopes may indicate that the zircons grew in a magmatic environment that had a different ε_{Hf} value than the magma in which they were finally entrained. While the H-S zircon data all seem to be in good agreement with each other, the most radiogenic whole rock values are more radiogenic than the zircons. At H-S, whole rock ε_{Hf} is higher than the average *in situ* zircon ε_{Hf} value, with the exception of sample DrE1302, which has almost identical values for each. This implies that the mechanisms by which silicic magmas were produced and erupted or emplaced at H-S occurred in discrete batches and were multi-stage. In the case of BrE, which likely had a component of older crustal material based on presence of an inherited, older core, some zircon Hf isotope values suggest they crystallized from a magma (ex. “Melt a” in Fig. 12) with a MORB-like source. Hypothetically, these zircons were then re-mobilized and entrained in a

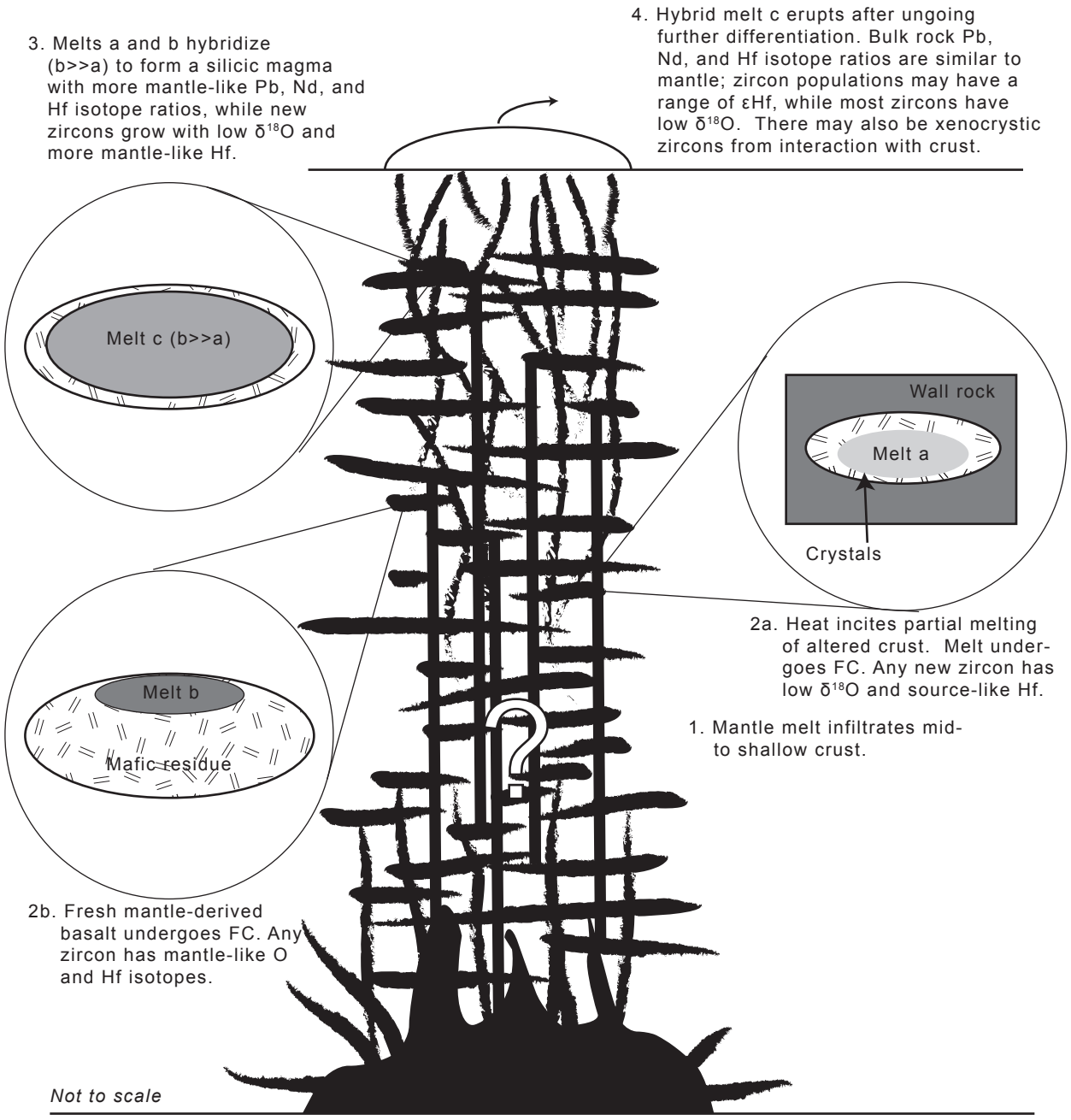

Fig. 12. Potential petrogenetic processes operating at Hafnarfjall-Skarðsheiði central volcano to produce silicic magmas that share whole-rock isotopic characteristics with co-genetic basalts but have zircon with low $\delta^{18}O$ and variable εHf. No arrangement of magmatic plumbing system is implied. Figure is not to scale.

new H-S magma (ex. “Melt b” in Fig. 12), zircon growth continued during differentiation, and the resulting hybrid magma (Ex. “Melt c” in Fig. 12) with a partial bedrock melt component erupted that retained whole rock isotope characteristics of the current geodynamic environment but contained zircons from “Melt a” with an isotopic record of their original bedrock source. Similar situations likely occurred for all silicic units at Hafnarfjall-Skarðsheiði, but with varying degrees of assimilation of bedrock and zircon crystallization. It may be plausible that the trend of decrease in whole rock Hf to less MORB-like values with decreasing age (with the exception of the intrusive FlI unit) may indicate a progressive shift in H-S‘s geodynamic environment and a shift in locus of magmatism and melting. Magmas forming the intrusive unit FlI may be incorporating material previously erupted in the volcano‘s lifetime, and its geographic location far from Phase 2 magmatism and the rift axis indicates that its source magmas were likely more derived from AFC processes than primary mantle melts.

5.4. Petrogenesis of silicic magmas and geodynamics at Hafnarfjall-Skarðsheiði

5.4.1. Petrogenesis of silicic magmas

Hafnarfjall-Skarðsheiði volcano matured in a dynamic tectonic and magmatic setting at the nascent Western rift zone. Whole rock Pb, Nd, and Hf isotope data do not correlate with those from the established Western rift zone, but instead with those from the modern propagating Eastern rift, indicating that the rifting environment in which H-S magmas were produced was likely similar to that of the EVZ—a propagating, dynamic rift. This is supported by our $^{143}Nd/^{144}Nd$ data plotting in the on-rift zone, rather than a flank area, as defined by Martin and Sigmarsson (2010). In addition, these data also suggest that because H-S basalt and silicic samples define coherent, tight groups, they must be from materials with the same small isotopic range. Given the demonstrated variability and geographic correlation of these isotopes in the distribution of Icelandic rocks, it is unreasonable to expect that silicic materials could be produced largely through partial melts of

altered crust and have an isotopic signature nearly identical to that of basalt whose geochemical composition is generated dominantly by mantle melting. Whole rock isotopic signatures in H-S silicic and mafic magmas are derived from melting of enriched mantle, as is currently the case in the EVZ (e.g. Peate et al., 2010).

In order to account for the <5.3 ‰ oxygen isotope signatures observed in H-S zircons, there must be a low-$\delta^{18}O$ component involved in their petrogenesis. The oxygen isotopic composition of the Icelandic mantle is debated (e.g. Eiler et al., 2000; Thirlwall et al., 2006; Peate et al., 2010; Pope et al., 2013; and many others). Since variation in H-S *in situ* zircon $\delta^{18}O$ values does not correlate with increasing differentiation as has proposed to result from lower than normal mantle $\delta^{18}O$ (+5.5 ‰) (Eiler et al., 2000), we invoke a model of assimilation of altered crust to explain the trends observed at H-S. Pope et al. (2013) presented a scenario for Krafla volcano in which a mantle-derived basalt ($\delta^{18}O$=5.5‰) may assimilate ~5% melt from a hydrothermally altered parcel of bedrock ($\delta^{18}O$=-10‰) to produce a magma with a final $\delta^{18}O$=4.8‰. The oxygen isotope fractionation between zircon and rock ($\Delta^{18}O$(zrc-WR)) ranges from ~-0.5‰ for mafic rocks to ~-2‰ for granites (Valley et al., 2005, and references therein). Therefore, we would expect zircons crystallizing from a silicic magma to have $\delta^{18}O$ ~2.8‰ based on the conditions above—which is the same as the mean $\delta^{18}O$ of 2.8‰ of H-S zircons. $\delta^{18}O$ zircon signatures lower than 2.8‰ indicate either: a) a higher proportion of the zircon source magma is derived from partial melting of altered bedrock; or b) the bedrock contribution is more altered than that in other H-S units. Achieving the mean BrE1201 $\delta^{18}O$ value of 2.2‰ requires only a modest increase in the partial melting component to ~8%, assuming crust $\delta^{18}O$=-10‰. However, it seems unlikely that sufficient heat would be available to provide increased melting during Phase 1 magmatism when the WRZ is likely less established than during Phase 2 magmatism. It is more likely that contribution from a more altered source created the lower $\delta^{18}O$ signature of the BrE zircons. In order to leverage a shift to ~2.2‰, a ~6.5% contribution from bedrock with $\delta^{18}O$=-15‰ or a 12% contribution from bedrock

with $\delta^{18}O$=-5.5‰ is required. It should be noted that altered crust with $\delta^{18}O$=-10‰ or -15‰ is unusual for Iceland as a whole (Hattori and Muehlenbachs, 1982), and most altered crustal material within the upper few km falls between 0 and ~5‰. However, the bedrock contribution to H-S magmas appears to be less than that of fresh mantle-derived material based on whole rock isotopic data, and thus cannot be "typical" for Iceland because so much partial melting would have to occur to generate the observed H-S $\delta^{18}O$ values that the mantle-derived signature would be lost. Therefore, highly altered bedrock is likely to play a role in all H-S magma petrogenesis.

Our Hf isotope data suggests that a portion of these partial melts remain isolated from the rest of the mantle melt-dominated magmatic system (which is, in part, undergoing AFC processes itself) for at least a portion of their lifetimes, so that the Hf isotope signature of the zircons records that of their "parent" melts. However, the amount of isolation time required to generate the variation in whole rock and *in situ* εHf seems to vary between units. Zircon crystallization temperatures estimated via the Ti-in-zircon thermometer (Ferry and Watson, 2007) suggest that many samples, including BrE, TuE, DrE, and RnE experienced near-solidus—especially DrE and BrE—crystallization, which would result from crystallization in a magma in relative spatial, chemical, and perhaps thermal isolation. Other samples have protracted (based on U-Pb zircon ages) but higher-T crystallization histories, which likely indicates zircon growth in systems receiving constant magmatic input. At the same time, H-S zircons show uniform and low $\delta^{18}O$ values that must come from a hybrid magma with mantle-derived and altered bedrock-derived components. This is possible within the given constraints if the mantle-derived material is rhyolite resulting from fractional crystallization of mantle-derived basalt. Rhyolites generated in this manner would retain the isotopic characteristics of the mantle-derived component, as we see at H-S, but would be available to mix with the rhyolite produced via partial melting. While both sources of rhyolite are likely to have zircon, their hybridization would likely also lead to additional zircon crystallizing with the hybrid isotopic signature. This model explains the general spread in *in situ* ε_{Hf}

analyses and also the variability among most H-S sample $\delta^{18}O$ analyses. Therefore, we summarize the following petrogenetic model for Hafnarfjall-Skarðsheiði silicic units as follows (Fig. 12):

1. Mantle-derived basalts infiltrate the mid-to-shallow crust.

2a. Heat from fresh basalt intrusions induces partial melting of hydrothermally altered, low $\delta^{18}O$ crust. Melt is chemically isolated for some period of time. Resulting rhyolite melt crystallizes zircon with low $\delta^{18}O$ values and the source rock's ε_{Hf} values.

2b. Concurrently, fresh mantle-derived basalt undergoes fractional crystallization—perhaps undergoing magma replenishment—to produce rhyolite, which also saturates and crystallizes zircon with higher $\delta^{18}O$ values and ε_{Hf} values shared with the fresh mantle source.

3. Rhyolites produced in (2a) and (2b) hybridize and continue to crystallize zircons. Overall, the volume of (2b) is larger than (2a), because the whole rock Pb, Nd, and ε_{Hf} data are consistent between basalt and rhyolite, indicating dominance of mantle end-member input.

4. Eruption or emplacement occurs, with a hybrid magma composed of a large proportion of FC-derived rhyolite and a small proportion of PM-derived rhyolite. Parts of both rhyolite sources must be left behind in the crust.

5.4.2. Geodynamic controls on petrogenesis

We have thus far neglected the significance of the U-Pb zircon ages for the petrogenesis of Hafnafjall-Skarðsheiði volcano, although they play a crucial role in placing processes in the correct spatial context. *In situ* zircon U-Pb ages indicate 2 distinct iterations of silicic magmatism at H-S: Phases 1 and 2, separated from each other by a gap of ~ 1 Myr in which only basalts erupted (Table 1). Phase 1 magmatism had a maximum duration of ~110 kyr, while Phase 2 magmatism lasted ~500 kyr. These ages indicate that the rate or volume of silicic magma production likely increased over the eruptive history of this volcano, which agrees with Franzson (1978)'s conclusion that

roughly 3-4% of Phase 1 magmas were rhyolitic, while later silicic units composed 12-13% of the eruptive sequence. We contend that the magmatic Phases, as well as the geochemical and isotopic characteristics discussed above, can be integrated into a geodynamic model for petrogenesis of silicic units at Hafnarfjall-Skarðsheiði central volcano as follows (Fig. 13):

1. Pre-Phase 1 basalts erupted before the onset of silicic magmatism, as soon as enough melting at the propagating/relocating WRZ allowed for eruption.
2. Onset of silicic magmatism around 5.5 Myr, with a major burst of Phase 1 silicic magmatism that lasted ~100 kyr from ~5.3-5.4 Ma. The geographic center of volcanism is in the north-central portion of the volcano, and the Phase 1 volcanic units (with the exception of FeE, which is north of the volcano) are located within 500 m of this approximate center spot. Silicic magmatism ceased when the volcano drifted too far from the rift axis to partially melt bedrock that was likely still colder than what is normally found in a rift zone.
3. Basalts were the only evident magmatic products from ~5.3 to ~4.4 Ma, which likely indicates a shift in the locus of eruption due to rift drift processes acting on the volcano. While it is possible that rhyolites were produced from fractional crystallization during this time, they were not erupted.
4. Phase 2 silicic magmatism active 4.38-4.11 Ma based on extrusive samples. The locus of Phase 2 volcanism in the central-eastern region of the volcano is ~4 km from the locus of Phase 1 volcanism normal to the rift axis. It's possible that during this time the spreading rate was significantly less than the average spreading rate of 1 cm/yr.
5. Phase 2 extrusive magmatism ended 4.11 Ma, and the distance between the Phase 2 locus of eruption and the modern rift axis is ~40 km—the distance achieved through rift drift in the ~4 Ma since silicic magmatism ceased. Magmatism at H-S ceased shortly thereafter because the plume head was far enough from the volcano that rift-supplied

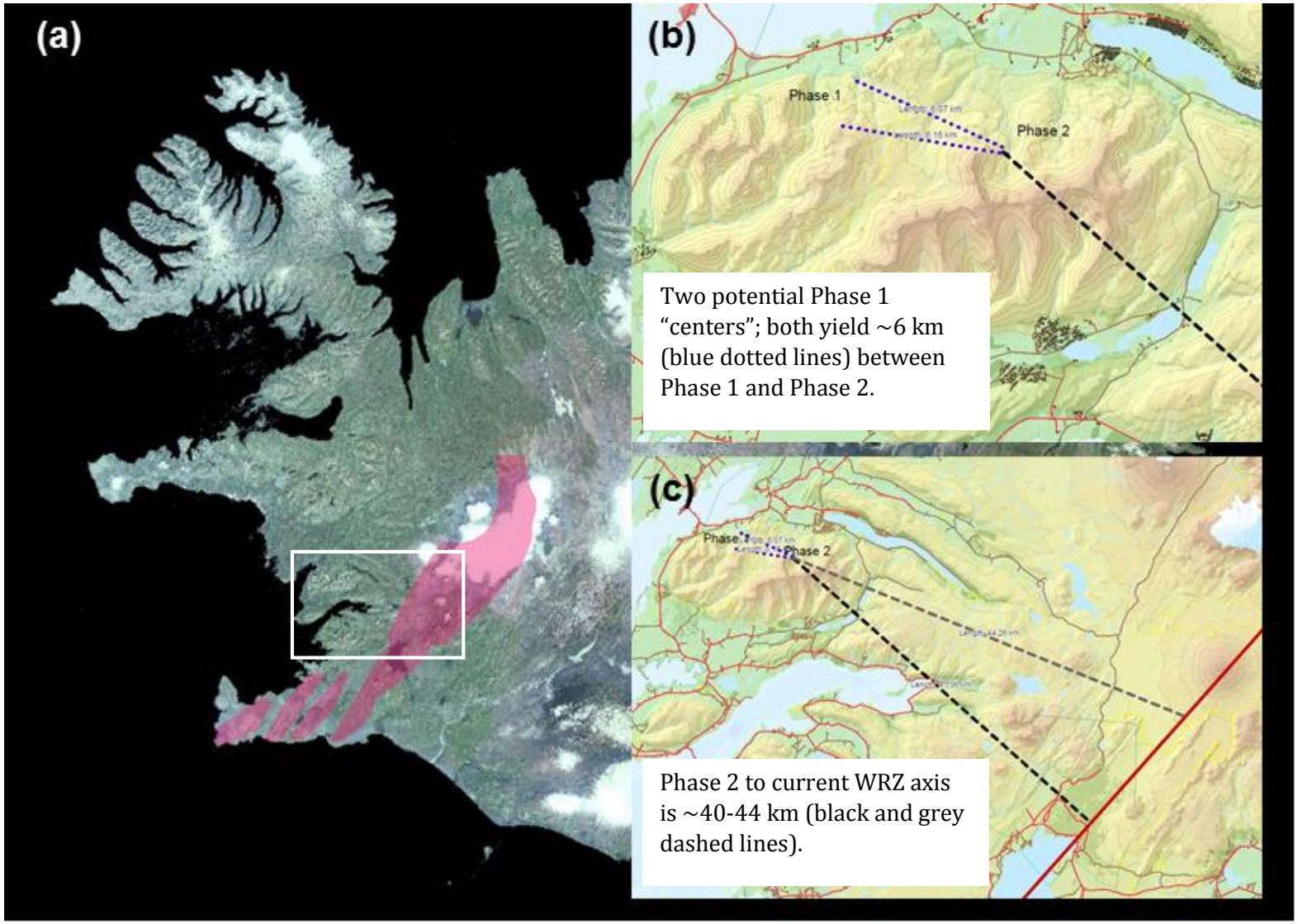

Fig. 13: Map of H-S demonstrating geodynamic evolution through the volcano's lifetime. a) The WRZ. b) Distance between Phase 1 and Phase 2 eruption loci is ~6 km. c) Distance between Phase 2 volcanism and present center of rift axis is ~40 km—the amount of time elapsed since the final silicic H-S eruption.

heat was insufficient to maintain petrogenesis, and the main source of heat and chemical diversity—the mantle-derived enriched basalt from the plume—moved too far from the rift to be tapped. The Flyðrur granophyre is the youngest silicic unit at H-S, but its intrusive nature, isotopic values, and geographical location strongly indicate that its petrogenesis is largely from fractional crystallization processes operating on a remnant of an earlier magmatic unit and therefore it is not a true part of Phase 2 magmatism.

It should be stressed that this general series of events could be duplicated at any central volcano that occupies a relatively uncomplicated tectonic area—that is, there are minimal major faults, no microplate boundaries, and no flank zones to interfere with rift drift's control over the timescales of magma production. In volcanoes formed in mature rift zones, magmatism will likely only occur in one phase, not in multiple phases as seen in H-S.

6. Conclusions

Silicic magmas produced at Hafnarfjall-Skarðsheiði central volcano in western Iceland between ~5.4 and ~3.9 Ma are the product of petrogenetic processes dominated geochemically by fractionates of mantle-derived basalt with a minor component of partially melted altered crust and tectonically controlled by rift drift. This study provides an in-depth, comprehensive view of petrogenesis of a single volcanic system in order to show that: a) ultimate timescales of silicic magma production depend upon tectonism; b) it takes 10s to 100s of kyr to generate silicic magmas after a rift relocation; c) silicic systems may persist for >1.5 Myr, which is longer than many central volcanoes' lifetimes; and d) that zircon isotopic and trace element data, coupled with whole rock isotope data, are critical to unravelling subtleties in source components, residence times, and making inferences regarding magma body dynamics involved in magma-producing processes. Our data indicate that magmas at the long-lived Hafnarfjall-Skarðsheiði volcano are generated largely through fractionation of mantle-derived melts, with volumetrically minor (~15%) amounts of melts

derived from partial melting of hydrothermally altered, low $\delta^{18}O$ crust. This challenges alternate viewpoints invoking large-scale partial melting of altered crust for rhyolite generation in Iceland, and highlights the importance of multi-technique studies to further advance understanding of silicic crust generation processes in this unique geologic environment.

CHAPTER 4

Petrogenesis of evolved magmas and implications for geodynamic evolution in the northern Westfjords, Iceland

Abstract

Icelandic magmatism with a significant silicic component results from the unique coupling of the Mid-Atlantic Ridge and the Iceland hot spot. Despite the relative abundance (~10-15%) of silicic rocks in a dominantly basaltic setting, there is little consensus regarding their origin and evolution and a wide range of explanations for their petrogenesis has been presented. However, few prior studies employed the accessory mineral zircon to aid in deciphering the mechanisms by which silicic Icelandic rocks form. Using *in situ* zircon U-Pb geochronology, oxygen and hafnium isotopes, and trace element compositions, and supplemented by whole rock major and trace element and Pb, Nd, and Hf isotope compositions, we investigate here the roles of partial melting and fractional crystallization in the petrogenesis of two large silicic volcanic centers in the northern Westfjords: Hrafnfjörður and Árnes central volcanoes. We present data confirming Hrafnfjörður as the oldest known central volcano in Iceland, as well as establishing an older age for Árnes (silicic activity 13.4 ± 0.6 to 12.8 ± 0.1 Ma; 2σ SE) than previously suggested based on paleomagnetic data. Our data point to a general petrogenetic model for these two volcanoes in which partial melts of altered crust and fractional crystallization of fresh mantle-derived magma hybridize to varying degrees and undergo further fractional crystallization prior to eruption. In addition, our geochronology data bring into question the current paradigm for geodynamic evolution of the Westfjords and suggest that the interaction of the rift and hot spot may be more complicated than originally thought.

1. Introduction

The petrogenetic mechanisms responsible for producing Iceland's abundant (for an ocean island) silicic rocks in Iceland have been discussed and debated for decades. However, one of the most powerful analytical tools available for deciphering magmatic processes—the accessory mineral zircon—has been largely ignored in this debate. Zircon is a premier geochronometer and trace element repository and is especially useful when dealing with silicic magmatic systems in Iceland, because silicic magmas are invariably associated with central volcano complexes (e.g. Harðarson et al., 2008) that foster active hydrothermal systems. Zircon is highly physically and chemically resistant to alteration processes that may be deleterious to other mineral phases (Hoskin and Schaltegger, 2003), and therefore its original magmatic geochemical composition remains intact. This is critical when trying to assess the nature, timing, and volume of silicic magma petrogenesis in Iceland and globally. In addition to the general paucity of zircon studies contributing to in-depth inquiry into these issues, western Iceland—often assumed to be the oldest part of the island—has been neglected for zircon work. We present the first *in situ* zircon U-Pb ages for the two oldest magmatic systems yet dated in Iceland—Hrafnfjörður and Árnes central volcanoes in western Iceland—as well as *in situ* trace element and Hf and O isotope data and whole rock major and trace element and Nd, Hf, and Pb isotope data, to examine the earliest record of silicic petrogenesis still preserved.

2. Geologic Setting

The Iceland hot spot appeared in what became the North Atlantic at ~60 Ma (e.g. Bjarnason, 2008; Lawver and Müller, 1994). The Mid-Atlantic ridge (MAR) separating the North American and Eurasian plates and the plume were initially completely independent of one another, but because the MAR axis moves northwest at ~1–3 cm/yr, the resulting surface expression of the Iceland plume moved first under the MAR axis and then progressively east of it (Lawver and Müller 1994;

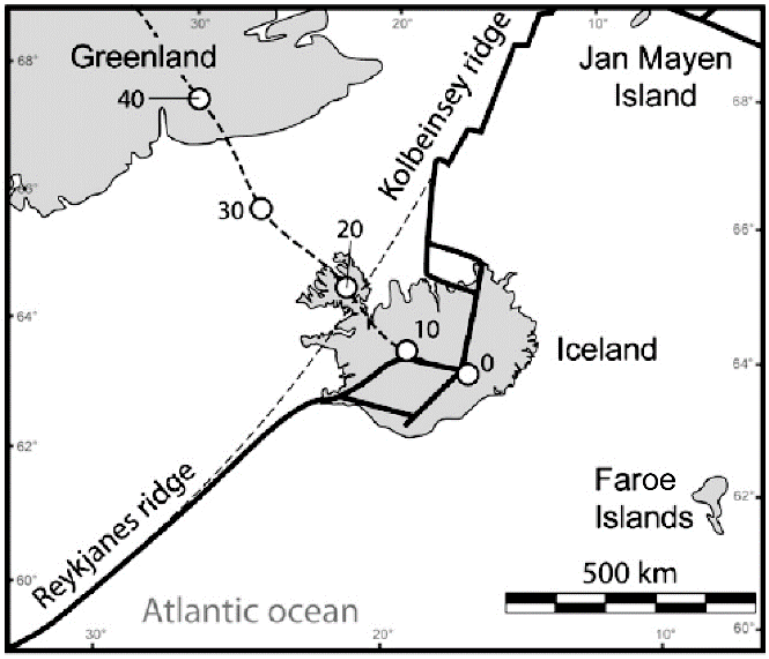

Fig. 1: Geologic setting of Iceland, the mid-Atlantic ridge (MAR), and the Iceland hot spot track (black dashed line). Numbered circles indicate location of plume center in millions of year ago (Mya). Grey dashed line represents hypothetical location of MAR in the absence of the Iceland plume. Modified from Martin et al., 2011.

Fig. 1). The MAR and plume became coupled roughly 25 Myr ago, which led to abnormally high rates of magma production and constructed the plateau that Iceland caps (e.g. Bjarnason, 2008; Brandsdóttir and Menke, 2008). As a result of MAR/plume coupling and northwestern drift of the ridge axis, the MAR around Iceland—exposed on land as a series of rift zones—relocates progressively east of the main MAR axis to remain coupled with the plume. The plume periodically recaptures the rift through a rift relocation, or "rift jump", which effectively moves the rift eastward (Harðarson et al. 2008).

The oldest rocks in the northern Westfjords erupted from the oldest Icelandic rift, the Northwest Rift Zone (NWRZ; Fig. 2a) during the latter stages of the rift's active lifetime (~24-15 Ma) (Hardarson and Fitton, 1997; Hardarson et al., 1997). Martin et al. (2011) suggest that sometime between 20 and 15 Ma, another rift axis, the future Snæfellsnes-Skagi Rift Zone (SSRZ) axis, began to propagate >100 km to the southeast in order to follow the plume center. These authors hypothesized that the NWRZ to SSRZ transition resulted in trapping a portion of older oceanic crust between the two rift axes, which implies the position of the trapped crust—if it exists—is directly under the Westfjords. Magmatism completely shifted from the extinct NWRZ rift axis to the SSRZ around 15 Ma (Harðarson et al., 2008; Martin et al., 2011). Both Hrafnfjörður and Árnes central volcanoes are strongly suspected to have erupted from the SSRZ based on regional dip direction and paleomagmetic ages of coeval rocks (Jordan et al., 2013; Sigmarsson, pers. comm.). However, both volcanoes likely lie unconformably on basalts erupted from the NWRZ toward the middle to end of its active life. Although magmatic activity associated with the SSRZ continued until 6.7-5.5 Ma (Harðarson et al., 2008; Martin et al., 2011), Martin et al. (2011) propose that—contrary to accepted rift relocation timescales (e.g. Harðarson et al., 2008)—the currently active Northern rift zone (NRZ) began propagating ~200 km east of the SSRZ around 13 Ma, and the SSRZ and NRZ simultaneously (but with no net increase in Icelandic magma flux) operated until the

SSRZ's demise. This idea is potentially important in Árnes' petrogenesis, while Hrafnfjörður was likely unaffected (see Discussion).

Hrafnfjörður and Árnes central volcanoes are located in the northern Westfjords of Iceland—Hrafnfjörður near the most northerly peninsula, Árnes on the northeastern coast (Fig. 2a). Both volcanoes are composed largely of basalt, but—uncommonly for Iceland (Jónasson, 2007)—also have volumetrically significant andesite and other intermediate composition rocks. Hrafnfjörður is notable in that the most evolved compositions are dacites (>50% of intermediate/silicic exposure), along with ~15% intermediate composition exposures, while Árnes has ~5% andesite, 1% dacite, and >20% rhyolite in addition to coeval basalt (Jordan and Olin, 2008; Jordan et al., 2013). Icelandic magmatism overall is highly bimodal (e.g. Jónasson, 2007; Sigmarsson et al., 2008; and many others), which means the abundance of intermediate—in addition to silicic—magmas in several Tertiary volcanic centers potentially indicates change in petrogenetic processes over time (Jordan and Olin, 2008).

3. Methods

3.1. Sampling

We collected at least one sample from each major rhyolite unit at Árnes, as well as one shallow silicic intrusive unit (Figs. 2b and 2c; Table 1). Samples of Tr1 rhyolite with "DH" prefix were provided by Brennan Jordan. At Hrafnfjörður, we sampled a dacite dome (unit Tdh) and a previously unsampled and unmapped silicic unit of unknown origin, as well as the Tad andesite as mapped by Jordan et al. (2013). We also incorporate zircon data from sample KK-24 of the main Hrafnfjörður dacite whose *in situ* zircon oxygen and hafnium isotope and trace element data were previously published in Carley et al., (2014) and whose ages were included in Jordan et al., (2013).

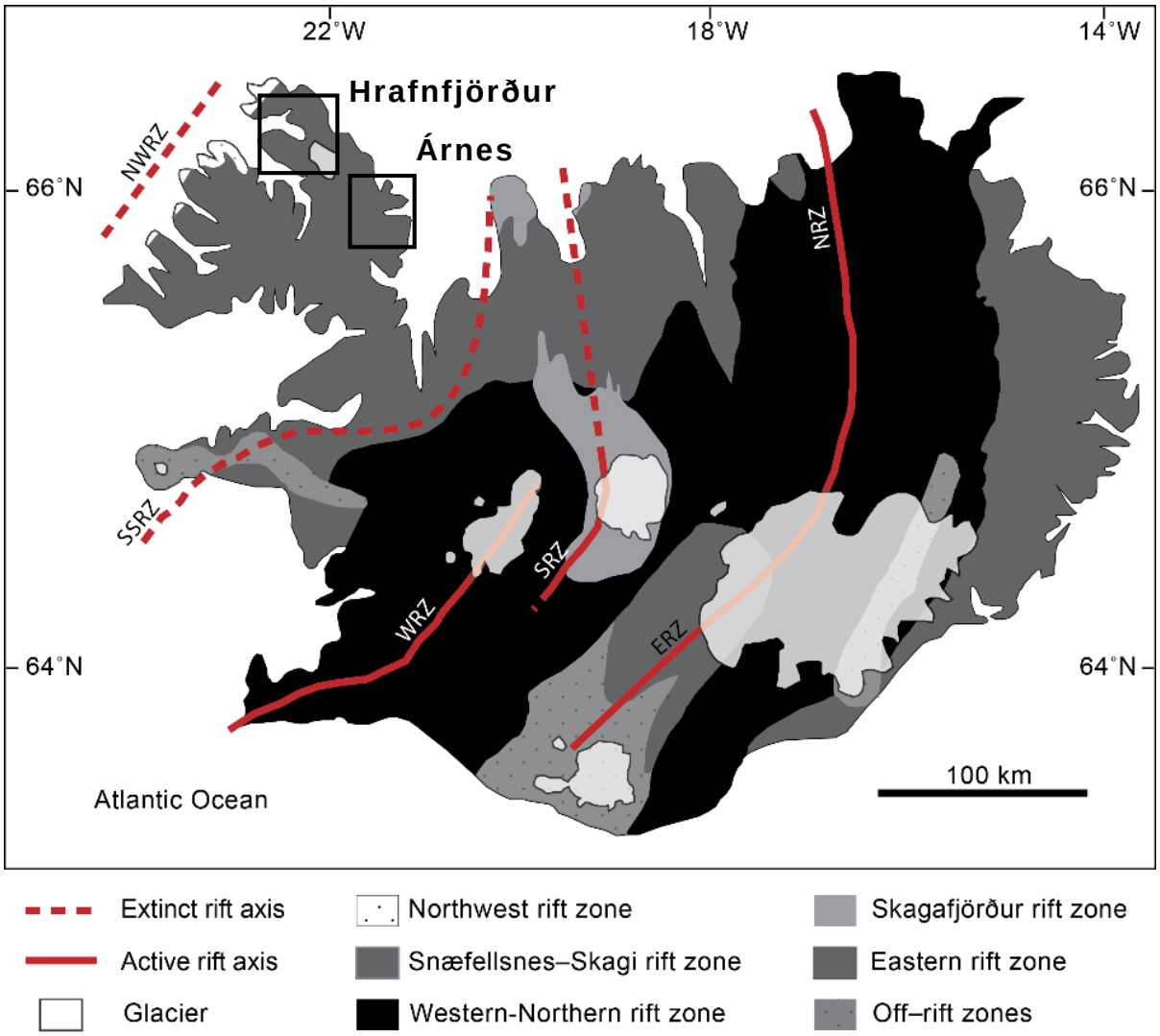

Fig. 2a: Geologic setting of Árnes (2b) and Hrafnfjörður (2c) central volcanoes, northwestern Iceland. Map above shows rift source of bedrock in Iceland and locations of current and extinct rift axes.

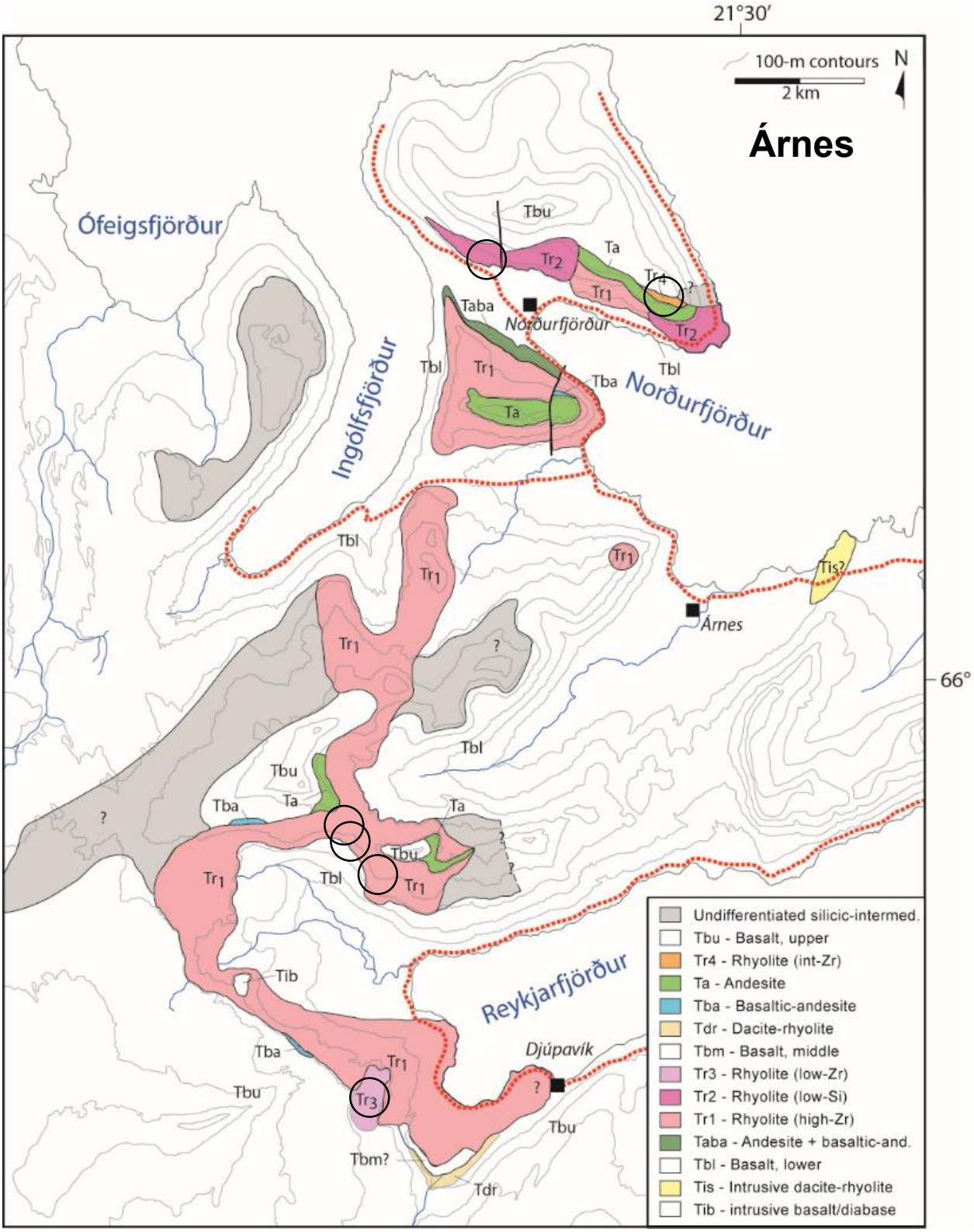

Fig. 2b: Geologic map of Árnes central volcano. Open circles indicate sample locations. Modified from Jordan et al. (2013).

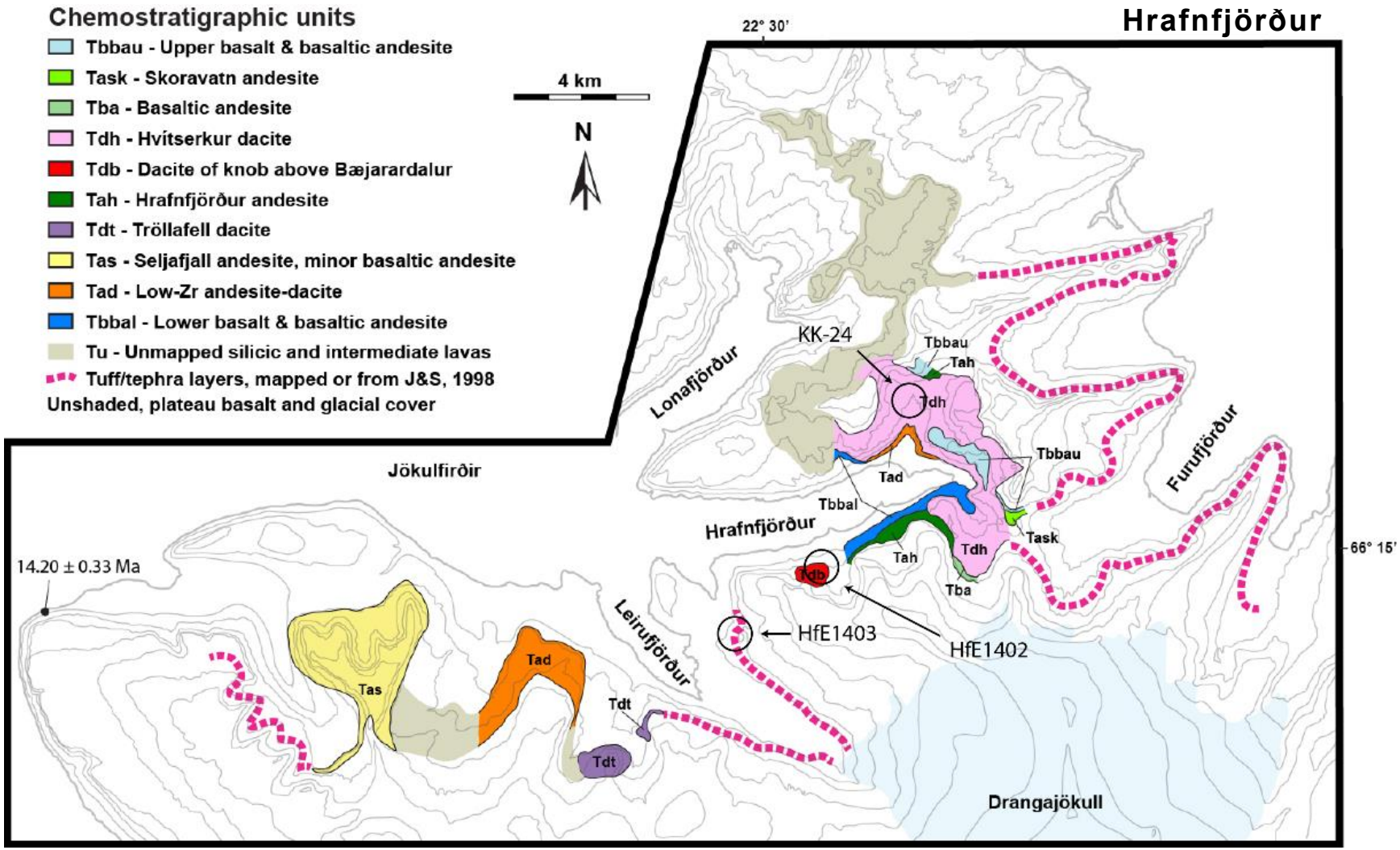

Fig. 2c: Geologic map of Hrafnfjörður central volcano. Open circles indicate sample locations. Modified from Jordan et al. (2013).

Volcano	Sample name	Unit	Latitude*	Longitude*	Elevation (m)	Rock type	Description	Zircon?
Árnes	ÁrE1301	Tr4	N66°03.115'	W21°30.902'	233	Rhyolite	Fresh with minor flow bands	✓
' "	ÁrE1302	Tr1? Ta?	N66°03.133'	W21°31.594'	168	Bas-Andesite	Moderate alteration, platey	✓
' "	ÁrE1303	Tr2	N66°03.591'	W21°34.938'	178	Rhyolite	Major flow bands, platey, pervasive alteration	✓
' "	ÁrE1304	Tr3	N65°56.495'	W21°37.482'	268	Rhyolite	Platey and maybe altered; white dome top	✓
' "	ÁrE1305	Tr3	N65°56.345'	W21°37.196'	200	Rhyolite	Black and vitreous, but altered	
' "	ÁrE1306	Tis	N66°01.002'	W21°27.715'	18	Dacite	Black and vitreous, aphyric, columnar, fresh	
Hrafnfjörður	HfE1401	Tad	N66°17.430'	W22°23.347'	210	Bas-Andesite	Aphanitic, black, fresh with weathering veneer	
' "	HfE1402	Tdb	N66°14.795'	W22°26.953'	225	Dacite	Aphanitic, black, fresh with weathering veneer	✓
' "	HfE1403	--	N66°13.795'	W22°30.269'	141	Dacite	Minor flow bands, weathered surface, grey, aphyric	✓
' "	KK-24	Tdh	N66°15.183'	W22°20.684'	--	And-Dacite		✓

**Datum: WGS84*

Table 1. Summary of samples collected from Árnes and Hrafnfjörður.

3.2. Analytical methods

Hand samples were cut into slabs to provide fresh rock for whole rock analysis and billets for thin sections. Whole rock trace element abundances for Árnes samples and sample KK-24 were determined using both XRF and ICP-MS via standard techniques at WSU. Precision for XRF analyses is better than 1% (2σ) for trace elements and within 2 ppm (2σ) for trace elements. Precision for ICP-MS analyses is typically better than 5% (RSD) for the REEs and 10% for the remaining trace elements. Whole rock major and trace elemental analyses on remaining Hrafnfjörður samples were carried out at ActLabs commercial laboratory. Additional fresh rock chips from a subset of Árnes samples were powdered and dissolved for whole rock Pb, Nd, and Hf isotopic analysis at the Radiogenic Isotope and Geochronology Laboratory (RIGL) at Washington State University using the procedure outlined in McDowell et al. (2014). Determination of isotopic compositions on the WSU Thermo-Finnigan Neptune MC-ICP-MS. Whole rock Hf analyses were corrected for mass fractionation using $^{179}Hf/^{177}Hf = 0.7325$ and normalized using Hf standard JMC475 ($^{176}Hf/^{177}Hf = 0.282160$). Our measured JMC475 $^{176}Hf/^{177}Hf$ value was 0.282132 ± 0.000007 (2σ SD), which resulted in a correction factor of 1.000093. Nd analyses were corrected for mass fractionation using $^{146}Nd/^{144}Nd = 0.7219$ and normalized using a correction factor of 1.000052 based on measurements of Nd standard La Jolla ($^{143}Nd/^{144}Nd = 0.511858$ (Vervoort et al., 2011); our value was 0.511831 ± 0.000014 (2σ SD)). We corrected for mass bias in the Pb analyses using $^{205}Tl/^{203}Tl = 2.388$ and normalized the mass bias corrected values for standard NBS 981 using $^{206}Pb/^{204}Pb = 16.9405$, $^{207}Pb/^{204}Pb = 15.4963$, $^{208}Pb/^{204}Pb = 36.7219$ (Galer and Abouchami, 1998). Our measured NBS 981 values, with 2σ SD, were: $^{206}Pb/^{204}Pb = 16.9361 \pm 0.0010$, $^{207}Pb/^{204}Pb = 15.4924 \pm 0.0008$, and $^{208}Pb/^{204}Pb = 36.7016 \pm 0.0018$.

In situ zircon oxygen and hafnium isotopic analyses, U-Pb age determinations, and trace elements analyses on a subset of Árnes and Hrafnfjörður samples were carried out according to the procedures presented in Chapters 2 and 3.

4. Results

4.1. Petrography

Hrafnfjörður samples HfE1401, 1402, and 1403 are all aphanitic in hand sample. In thin section, all Hrafnfjörður samples appear porphyritic with plagioclase as the dominant phenocryst and a plagioclase-dominated groundmass with trachytic texture (Fig. 3). Detailed petrographic description are listed in Appendix C. Árnes samples share similar mineralogy, with plagioclase the dominant phenocryst and groundmass mineral and minor pyroxene, opaques, and alteration phases (Fig. 3). Detailed petrography listed in Appendix C.

4.2. Whole rock major and trace elements

Major and trace element compositions are presented in Table 2. Our data agree well with those presented by Jordan et al. (2013) (Fig. 4), with the exception of sample ÁrE1302 from the Tr1 rhyolite unit, which has FeO=12.24 wt% and SiO_2=53.39 wt%, which are higher and lower, respectively, than the other rhyolite units at Árnes. It is possible that we sampled an unmapped andesite unit instead of the intended Tr1 rhyolite. Sample HfE1402 is notably depleted in TiO_2, FeO, and MgO and enriched in Zr compared to the other Hrafnfjörður samples.

4.2.1. Zircon saturation temperatures

In the absence of fresh glass analyses which would have yielded the most geologically realistic results, we use whole rock compositions to calculate zircon saturation temperatures for all silicic units using the methods of Watson and Harrison (1983) (Table 2), which range from 727 to 939°C. The lowest saturation temperature is from sample ÁrE1302 and is uncharacteristically low for Árnes and Hrafnfjörður. The three remaining samples from the Tr1 rhyolite unit, DH-04, -08, and -15, yield almost identical results (933-939°C) that are taken to be representative of Tr1 zircon saturation Ts. Overall, samples are phenocryst-poor and therefore likely to represent near-melt compositions. Application of the Boehnke et al. (2013) method of zircon saturation calculation

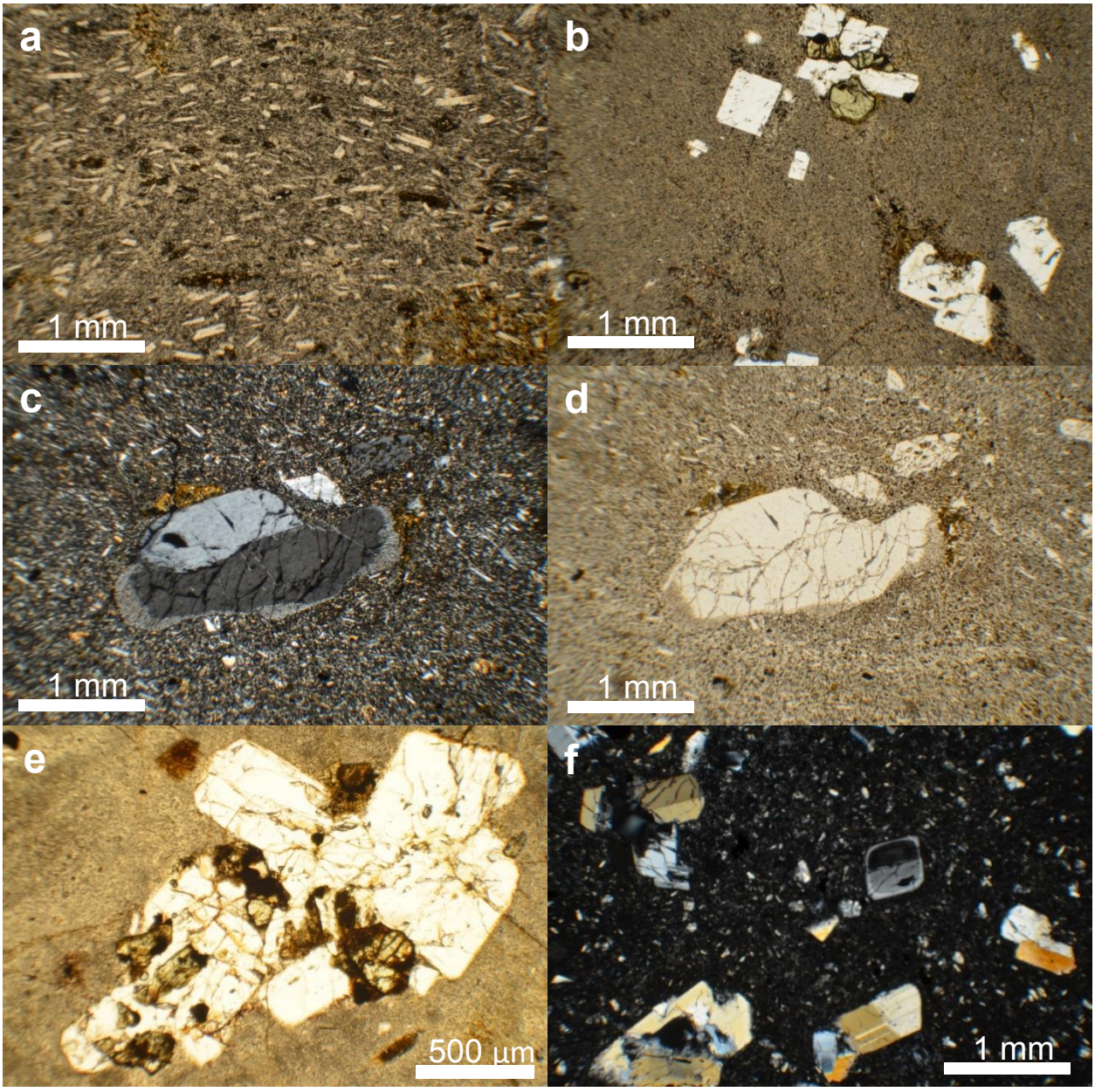

Fig. 3: Photomicrographs of selected units. a) trachytic texture in HfE1402; b) euhedral plagioclase and a plag-cpx glomerocrysts in ÁrE1301; c) and d) Sieve-texture plagioclase is common in HfE1403; e)ÁrE1303 has plag-cpx glomerocrysts; f) ÁrE1304 displays a range of plag textures from euhedral to those with resorbed cores and fresh rims. All photographs are at 2.5x except (e) at 5x. (c) and (f) are under crossed polars.

yields temperatures that are lower by 20 to 30°C and an increase in range of ~20°C, but does not change the relationship between units.

4.3. Whole rock Nd, Hf, and Pb isotopes

Neodymium, hafnium, and lead isotope ratios for 3 silicic whole rock samples from Árnes samples ÁrE1302, 1303, and 1304 fall within established ranges for Icelandic rocks (Table 2) (e.g. Peate et al., 2010; Willbold et al., 2009). $^{143}Nd/^{144}Nd$ values fall in a restricted range (0.513011-0.513031; εNd is 7.3 to 7.7). $^{176}Hf/^{177}Hf$ values occupy a comparatively small range (for Icelandic samples) to corresponding Nd isotope ratios (0.283147-0.283164; εHf is 12.8 to 13.4) (Fig. 5). Sample ÁrE1303 is slightly less radiogenic in Hf and Nd than the other two samples, but all analyzed samples plot on or below the εHf/εNd mantle array previously established for Iceland (cf. Andres et al., 2004). Most Icelandic lavas plot on a tight linear array below the Northern Hemisphere Reference Line (NHRL; Hart, 1984) on a $^{207}Pb/^{204}Pb$ vs. $^{206}Pb/^{204}Pb$ diagram and straddle the NHRL on a $^{208}Pb/^{204}Pb$ vs. $^{206}Pb/^{204}Pb$ diagram (Fig. 6). The Árnes samples occupy a fairly constrained area in Pb-Pb space, with $^{206}Pb/^{204}Pb$ =18.6353 to 18.7812, $^{207}Pb/^{204}Pb$ =15.4786 to 15.4915, and $^{208}Pb/^{204}Pb$ =38.3453 to 38.4787. All samples plot above the NHRL, and ÁrE1302 and 1303 show almost identical values in Pb-Pb space and plot toward the less radiogenic end of the mantle array. Sample ÁrE1303 has higher $^{207}Pb/^{204}Pb$ than the other measured Icelandic samples. Pb-isotope ratios loosely follow those established for young basalts erupted from the currently active NRZ and WRZ (Peate et al., 2010).

4.4. In situ zircon O isotopes

Oxygen isotope ratios ($\delta^{18}O$) in zircons from 6 samples (n=24 from Hrafnfjörður; n=66 from Árnes) are all isotopically light when compared to mantle zircon ($\delta^{18}O$=5.3 ± 0.3 ‰; Valley, 2003), ranging from 2.1±0.4 to 4.2±0.8‰ (2σ SE) at Árnes and 2.8±0.7 to 4.1±0.7‰ at Hrafnfjörður

Table 2. Whole rock major and trace elements and isotopes

	ÁrE1301 Rhyolite	ÁrE1302 Basaltic-Andesite	ÁrE1303 Rhyolite	ÁrE1304 Rhyolite	ÁrE1305 Rhyolite	ÁrE1306 Dacite
SiO_2	72.79	53.39	70.57	75.63	75.85	67.04
TiO_2	0.33	3.01	0.54	0.19	0.19	0.94
Al_2O_3	13.42	14.62	14.45	12.83	13.00	14.32
FeO*	3.99	12.24	3.87	2.30	1.84	5.35
MnO	0.08	0.23	0.15	0.07	0.06	0.11
MgO	0.27	3.96	0.41	0.10	0.08	1.57
CaO	1.79	7.79	1.92	1.11	1.18	3.92
Na_2O	5.21	3.70	5.47	5.34	4.99	4.53
K_2O	2.08	0.65	2.51	2.40	2.81	1.99
P_2O_5	0.05	0.41	0.11	0.03	0.02	0.21
LOI (%)	0.88	0.20	0.81	0.07	3.53	3.47
Total	98.42	99.17	98.78	99.11	95.97	96.33
Ni	1	3	1	1	2	11
Cr	2	<1	3	3	3	17
V	7	274	20	6	2	66
Ga	23	23	27	24	23	21
Cu	10	34	18	8	15	39
Zn	159	177	103	206	167	139
La	62.77	26.75	64.23	58.87	60.44	48.08
Ce	106.72	56.74	133.14	128.86	127.54	95.77
Pr	16.10	7.51	15.46	14.64	14.89	11.36
Nd	64.27	31.89	59.11	56.70	57.82	44.22
Sm	15.36	8.20	13.50	13.19	13.43	9.95
Eu	3.12	2.85	3.20	2.24	2.25	2.38
Gd	15.76	8.93	12.98	13.00	13.45	9.76
Tb	2.78	1.48	2.28	2.34	2.41	1.65
Dy	17.05	8.94	13.89	14.31	14.92	10.01
Ho	3.54	1.80	2.82	2.93	3.08	2.03
Er	9.64	4.74	7.57	8.18	8.50	5.41
Tm	1.43	0.66	1.10	1.22	1.25	0.79
Yb	9.14	3.97	6.87	7.74	7.83	4.89
Lu	1.41	0.61	1.03	1.16	1.19	0.77
Ba	324	135	388	363	353	288
Th	7.23	2.53	9.01	8.37	8.28	6.73
Nb	48.09	28.61	60.19	51.16	49.21	36.78
Y	89.49	44.77	72.32	75.95	79.43	51.97
Hf	14.43	6.31	15.93	11.78	11.38	11.29
Ta	3.27	1.95	4.13	3.64	3.59	2.64
U	2.03	0.67	2.27	1.94	2.19	1.87
Pb	4.58	1.80	5.43	4.86	5.74	4.43
Rb	41.1	8.9	48.0	49.5	51.5	41.1
Cs	0.22	0.06	0.19	0.31	0.53	0.43
Sr	142	300	160	78	77	191
Sc	9.5	28.8	6.0	5.4	4.6	11.2
Zr	568	249	621	390	372	433
$^{143}Nd/^{144}Nd$		0.513031	0.513011	0.513023		
ε_{Nd}		7.7	7.3	7.5		
$^{176}Hf/^{177}Hf$		0.283160	0.283147	0.283164		
ε_{Hf}		13.3	12.8	13.4		
$^{206}Pb/^{204}Pb$		18.6417	18.7812	18.6353		
$^{207}Pb/^{204}Pb$		15.4810	15.4915	15.4786		
$^{208}Pb/^{204}Pb$		38.3556	38.4787	38.3453		
Zircon Sat (°C)	900	727	905	867	864	845

Table 2. Whole rock major and trace elements and isotopes

	DH-04 Rhyolite	DH-08 Rhyolite	DH-15 Rhyolite	HfE1401 Basaltic-Andesite	HfE1402 Dacite	HfE1403 Andesite-Dacite
SiO_2	73.66	74.08	74.13	53.81	63.92	60.05
TiO_2	0.36	0.32	0.34	2.20	0.42	1.64
Al_2O_3	13.66	13.01	13.80	15.01	15.49	14.81
FeO*	2.94	3.67	2.38	13.49	8.86	10.15
MnO	0.04	0.03	0.03	0.21	0.24	0.18
MgO	0.17	0.23	0.10	3.56	0.26	2.43
CaO	0.95	0.62	0.82	7.16	4.47	5.54
Na_2O	5.66	5.49	5.73	3.63	4.91	4.04
K_2O	2.54	2.52	2.62	0.65	1.31	0.91
P_2O_5	0.04	0.03	0.03	0.29	0.11	0.24
LOI (%)	--	--	--	0.35	0.26	1.15
Total	96.56	95.82	95.96	100.20	98.86	100.60
Ni				19	1	10
Cr	2	1	2	12	< 0.5	22
V	7	4	7	248	5	155
Ga				22	27	22
Cu	2	2	2	86	17	42
Zn	177	237	194	130	220	120
La	83.6	111.5	55.0	17.50	50.30	28.30
Ce	126.9	113.2	125.6	40.70	115.00	61.50
Pr				5.60	14.90	8.40
Nd	81.4	102.1	57.4	26.10	64.80	37.00
Sm				7.35	16.10	9.86
Eu				2.62	4.00	2.69
Gd				8.38	16.00	10.80
Tb				1.56	2.94	1.99
Dy				9.74	18.80	12.30
Ho				1.86	3.93	2.50
Er				5.39	11.70	7.22
Tm				0.78	1.75	1.07
Yb				5.02	12.10	7.01
Lu				0.81	1.97	1.12
Ba				140	262	208
Th	9.40	10.10	11.20	1.69	4.22	3.08
Nb	84.80	86.50	86.40	12.70	25.40	14.60
Y				49.00	106.00	71.00
Hf				4.00	17.30	6.90
Ta				0.93	1.76	1.04
U	2	2	2	0.55	1.39	0.95
Pb	5.30	6.80	5.80	< 5	< 5	< 5
Rb	50.2	48.7	50.8	13.0	24.0	20.0
Cs				0.10	0.10	0.20
Sr	162	140	158	185	176	180
Sc	6.5	3.7	6.5	26.7	19.2	19.5
Zr	721	732	736	172	922	291
$^{143}Nd/^{144}Nd$						
ε_{Nd}						
$^{176}Hf/^{177}Hf$						
ε_{Hf}						
$^{206}Pb/^{204}Pb$						
$^{207}Pb/^{204}Pb$						
$^{208}Pb/^{204}Pb$						
Zircon Sat (°C)	933	939	937	794	905	814

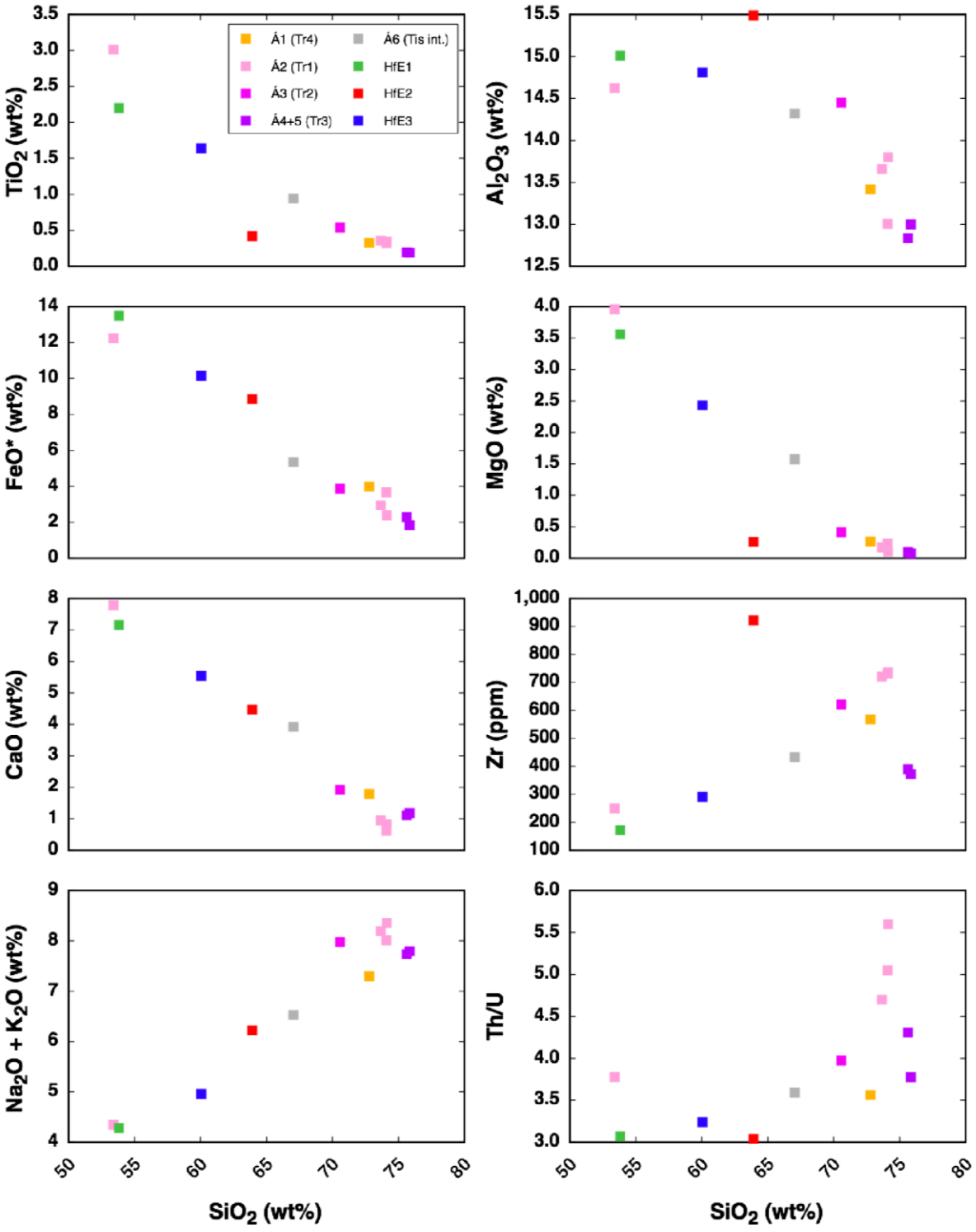

Fig. 4: Major and trace element variation diagrams for Árnes and Hrafnfjörður bulk rock samples. Color distinctions correspond to the unit colors in Figs. 2b and 2c.

Fig. 5: ε_{Hf} vs. ε_{Nd} for Árnes (n=3) and Hrafnfjörður (n=1) whole rock samples. The most depleted sample is from Hrafnfjörður.

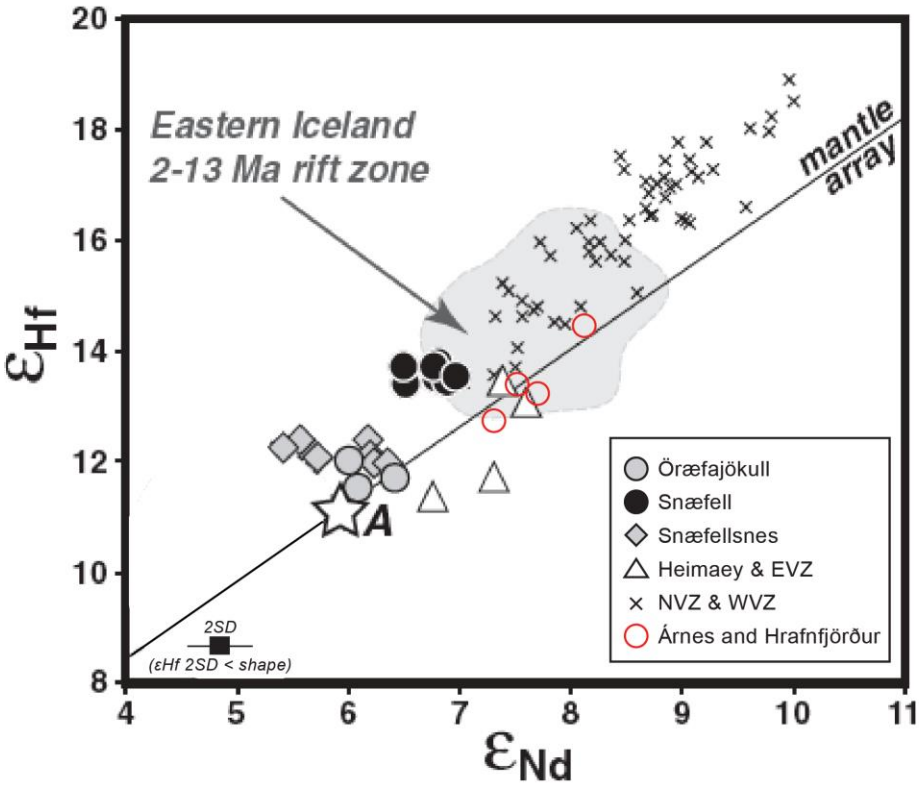

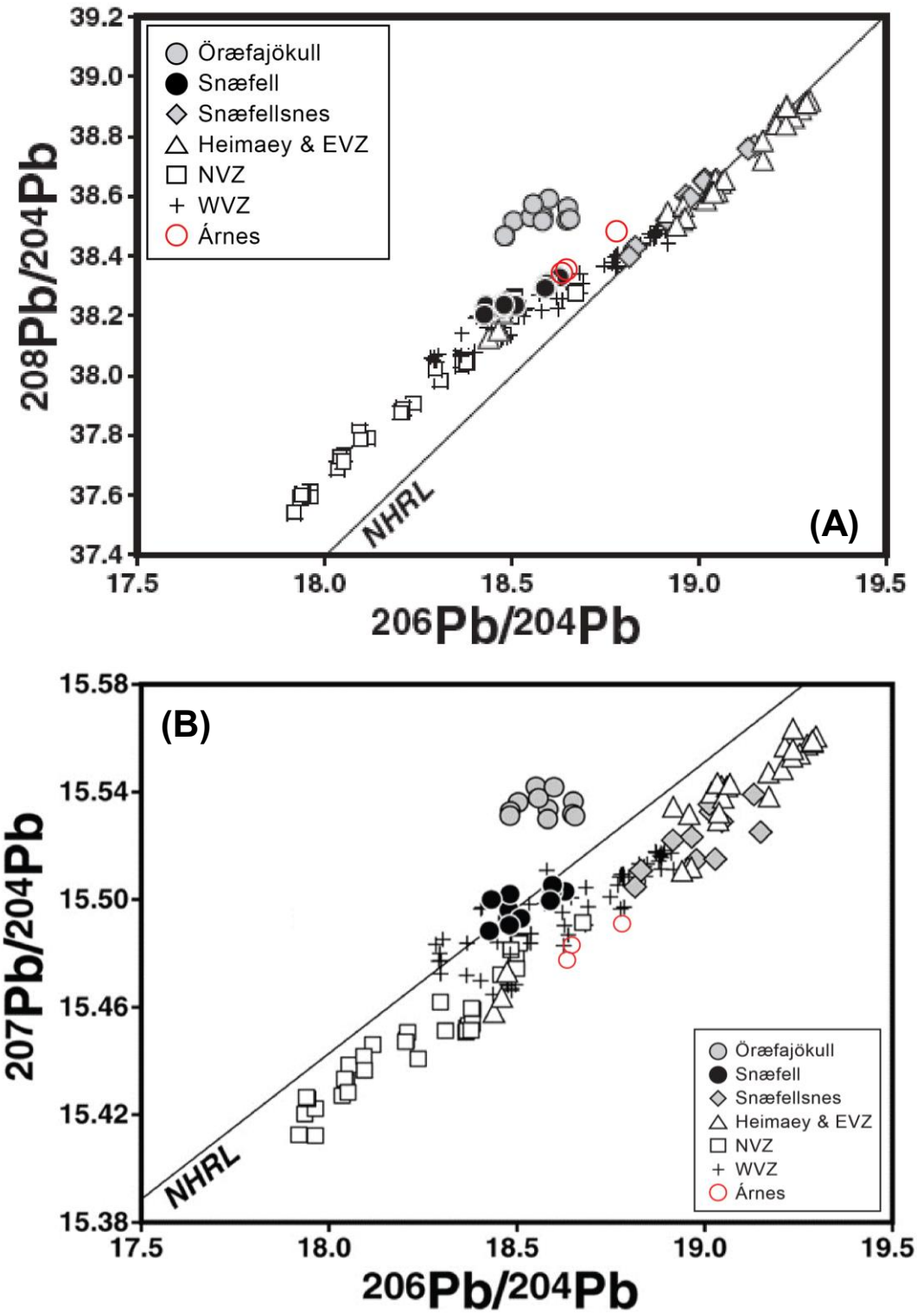

Fig. 6: Lead isotope variation diagrams for Árnes bulk rock samples modified from Peate et al. (2010). A) $^{208}Pb/^{204}Pb$ vs. $^{206}Pb/^{204}Pb$. Árnes samples plot about the Northern Hemisphere Reference Line (NHRL) and overlap domains of several magmatic systems. B) $^{207}Pb/^{204}Pb$ vs. $^{206}Pb/^{204}Pb$. Árnes samples plot below the NHRL and most closely align with samples from the Western Volcanic Zone (WVZ).

(Table 3; Fig. 7; Appendix D). As far as we are aware, these are the first oxygen isotope data—either *in situ* zircon or whole rock—reported from either Hrafnfjörður or Árnes.

4.5. In situ zircon U-Pb geochronology

U-Pb geochronology results are presented in Table 3, Figs. 7 and 8, and Appendix E. Weighted ages for all samples have mean squared weighted deviations (MSWD; calculated using SQUID2 software (Ludwig, 2009)) values within the 95% confidence range established by Mahon (2006). Weighted mean sample ages from Hrafnfjörður and Árnes range from 14.2±0.2 Ma (error is 2σ SE) to 12.8±0.1. KK-24 is the oldest-known zircon-dated unit in Iceland, and Hrafnfjörður is the oldest silicic magmatic system exposed on Iceland (Jordan et al., 2013). Hrafnfjörður samples HfE1402 (13.7±0.2 Ma) and HfE1403 (13.6±0.2 Ma) have zircon ages with probability density plots that are skewed slightly right toward the youngest individual ages (Fig. 8). Sample HfE1403 has a sub-population visible in Fig. 7 from ~14.4 Ma. Analysis of an HfE1403 grain with a potentially inherited core (based on cathodoluminescense imaging) yielded an age of ~16.3 Ma with evidence of common Pb contamination. Similarly, HfE1402 has a few older grains that could be inherited from previous crystallization episodes in the same age range as KK-24.

Weighted mean sample ages from Árnes are younger than those from Hrafnfjörður (Table 3; Figs. 7, 8; Appendix D). Ages for Árnes samples are: 13.4±0.6 Ma (2σ SE) (ÁrE1301); 13.1±0.4 Ma (ÁrE1303); 12.9±0.8 Ma (DH-08/15); and 12.8±0.1 Ma (ÁrE1304). Similar to sample HfE1403, sample DH-08/15 also had a suspected inherited core with an age of ~16.2 Ma, although it also experienced common Pb contamination. Sample ÁrE1303 has a sub-population of grains from ~13.6 Ma.

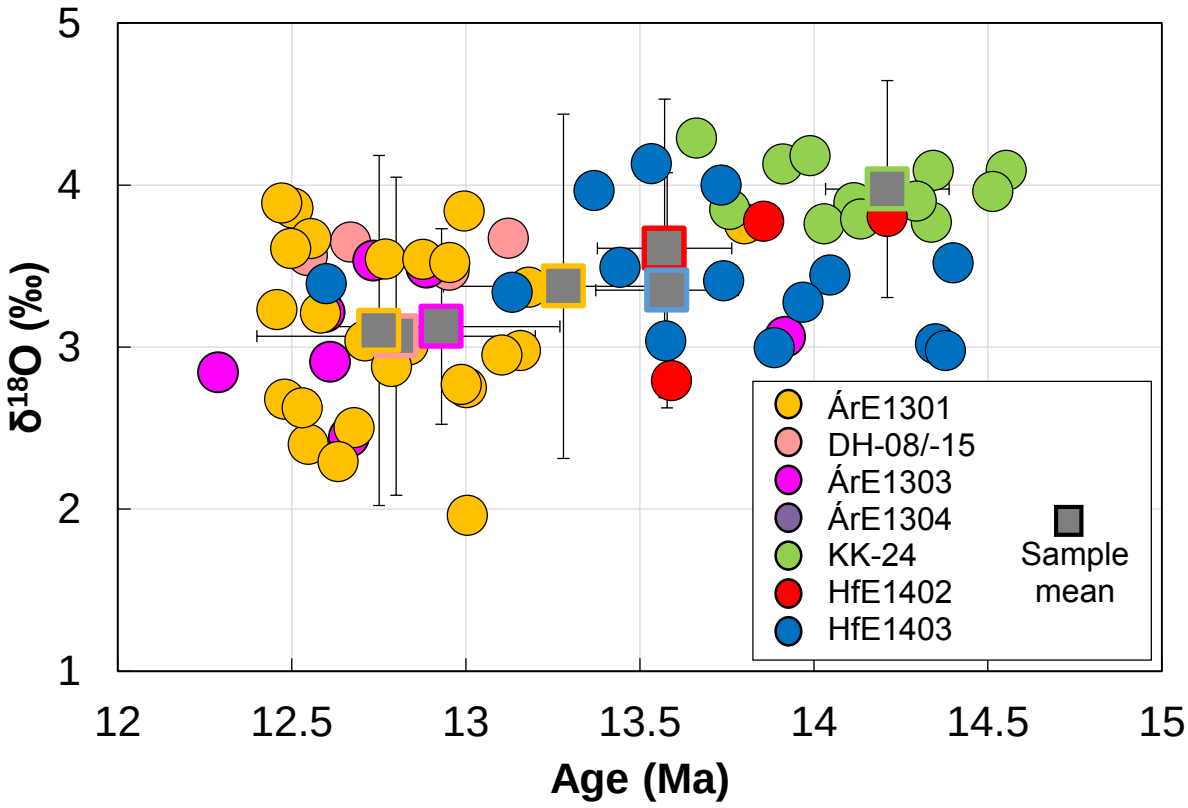

Fig. 7: *In situ* $\delta^{18}O$ vs. U-Pb ages for Hrafnfjörður zircons. One analysis per spot, with sample average as grey square outlined in sample color. Errors are 2σ. Only grains with corresponding $\delta^{18}O$ and U-Pb analyses shown, while sample averages reflect all analyzed grains.

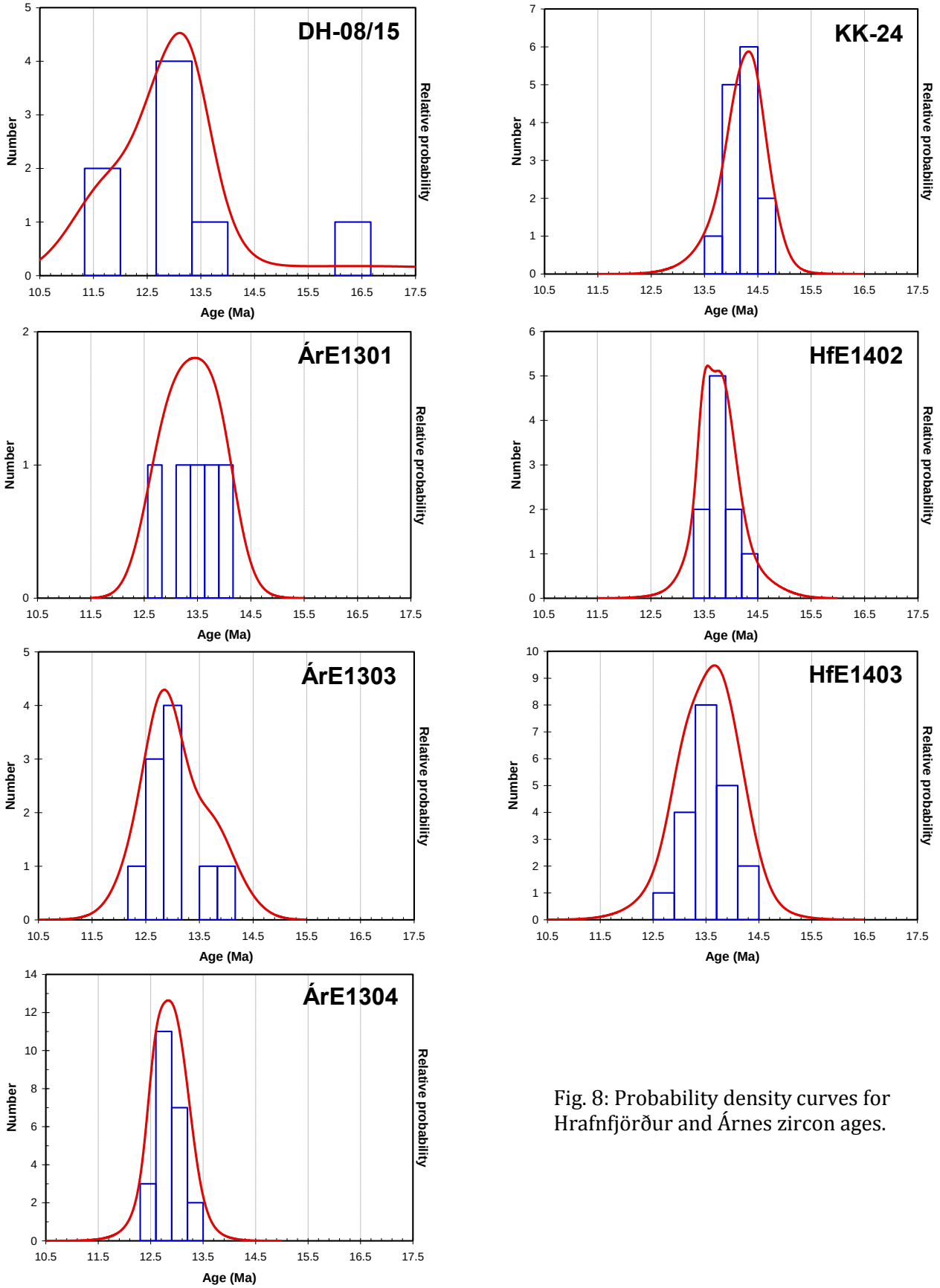

Fig. 8: Probability density curves for Hrafnfjörður and Árnes zircon ages.

4.6. In situ zircon U, Th, and REE

Trace elements in zircon at Árnes and Hrafnfjörður generally occupy a continuum with a large amount of compositional overlap (Fig. 9). The dome units from each location, samples ÁrE1304 and HfE1402, are particularly similar in several ways (U, Yb, Yb/Gd). Hrafnfjörður samples have a more enriched REE signature and have an increased concentration in heavy rare earth elements (HREE) and steeper REE slopes than Árnes samples, indicating they may be derived from a more enriched source (Fig. 10). Th/U ratios range from ~0.25-1.4 in Hrafnfjörður samples and Árnes samples ÁrE1304 and DH-08/15, while Árnes samples ÁrE1301 and ÁrE1302 have more restricted Th/U (~0.3-0.8). Partition coefficients for U and Th into zircon in rhyolite melts ($D_U^{zrc/melt}$=16, $D_{Th}^{zrc/melt}$=4.5) (Colombini et al., 2011) were used to calculate Th/U of zircon in equilibrium with Hrafnfjörður and Árnes samples, using whole rock composition as a proxy for melt composition (Table 2), with results ranging from Th/U =1.0 to 1.6. Árnes DH-08 and -15 have substantially higher whole rock Th/U than other samples. Because mineral/melt partition coefficients generally increase at lower temperatures (Blundy and Wood, 2003) and for more silicic melt compositions (Watson and Green, 1981), enrichment of late-stage residual melts in U and Th by advanced crystallization differentiation may be responsible for the high U and Th concentrations in DH zircon (Bacon et al., 2007).

4.7. In situ zircon Hf isotopes

Árnes zircons range from ε_{Hf}=11.1±1.4 to 14.2±1.8 (2SE) (Tables 3 and S4; Fig. 11), while Hrafnfjörður sample KK-24 (n=14) has a more radiogenic composition with zircon ranging from ε_{Hf}=14.5±1.8 to 17.0 2.1 (sample average ε_{Hf}=15.7±1.6 (2σ SD)) (Carley, 2014). Árnes samples ÁrE1303 and 1304 have sample averages of ε_{Hf}=12.5±1.7 and 12.65±1.9, respectively, with sample DH-04 slightly lower with ε_{Hf}=11.9±1.2. Sample ÁrE1301 is the least radiogenic with ε_{Hf}=11.4±1.0.

	U-Pb geochronology				Oxygen isotopes			Hafnium isotopes			
Sample	*n*	Age (Ma)	2σ SE	MSWD	*n*	$\delta^{18}O$ (‰)	2σ SD	*n*	ε_{Hf}	2σ SD	Outliers
KK-24*	14	14.2	0.2	0.75	12	4.0	0.7	14	15.7	1.6	0
HfE1402	10	13.7	0.2	0.78	6	3.6	0.9	--	--	--	--
HfE1403	20	13.6	0.2	1.20	18	3.3	0.7	--	--	--	--
ÁrE1301	5	13.4	0.6	1.70	3	3.2	1.1	1	12.4	--	0
ÁrE1303	10	13.1	0.4	1.70	24	3.6	0.6	15	12.6	1.3	0
ÁrE1304	23	12.8	0.1	1.08	23	3.3	0.7	15	13.0	2.0	0
DH-04	--	--	--	--	--	--	--	3	11.9	1.2	0
DH-08	8	12.9	0.5	1.40	16	3.1	1.0	--	--	--	--
DH-15								--	--	--	--

**O and Hf isotope data from Carley et al. (2014). Age from Jordan et al. (2013) and unpublished data from T. Carley.*

Table 3. Summary of *in situ* zircon analyses from Árnes and Hrafnfjörður. Age and oxygen isotope data for samples DH-08 and DH-15 are pooled.

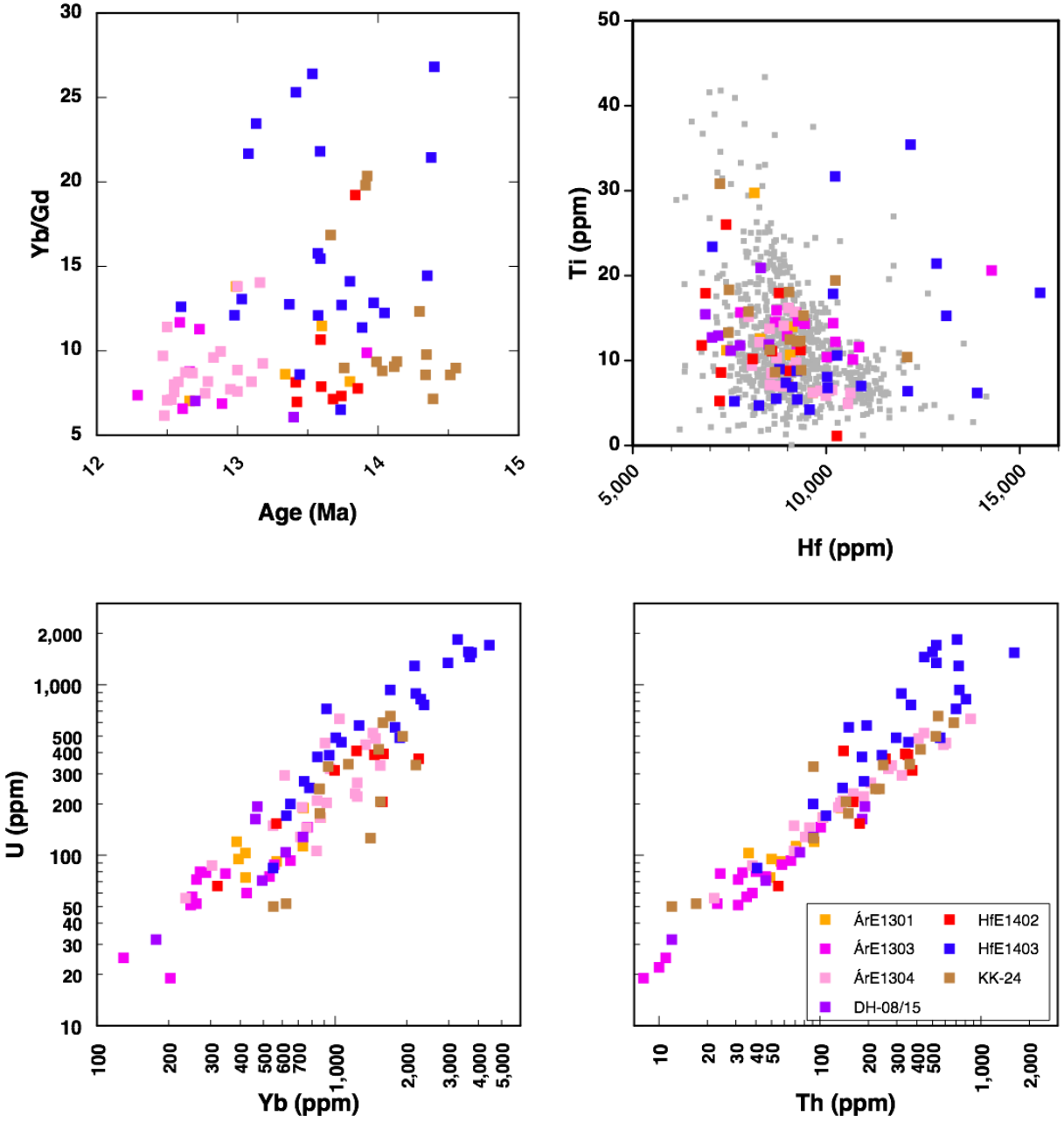

Fig. 9: Trace element variation diagrams for Árnes and Hrafnfjörður zircons. Grey field in Ti vs. Hf plot represents the typical variation amongst Icelandic zircon (Carley, 2014).

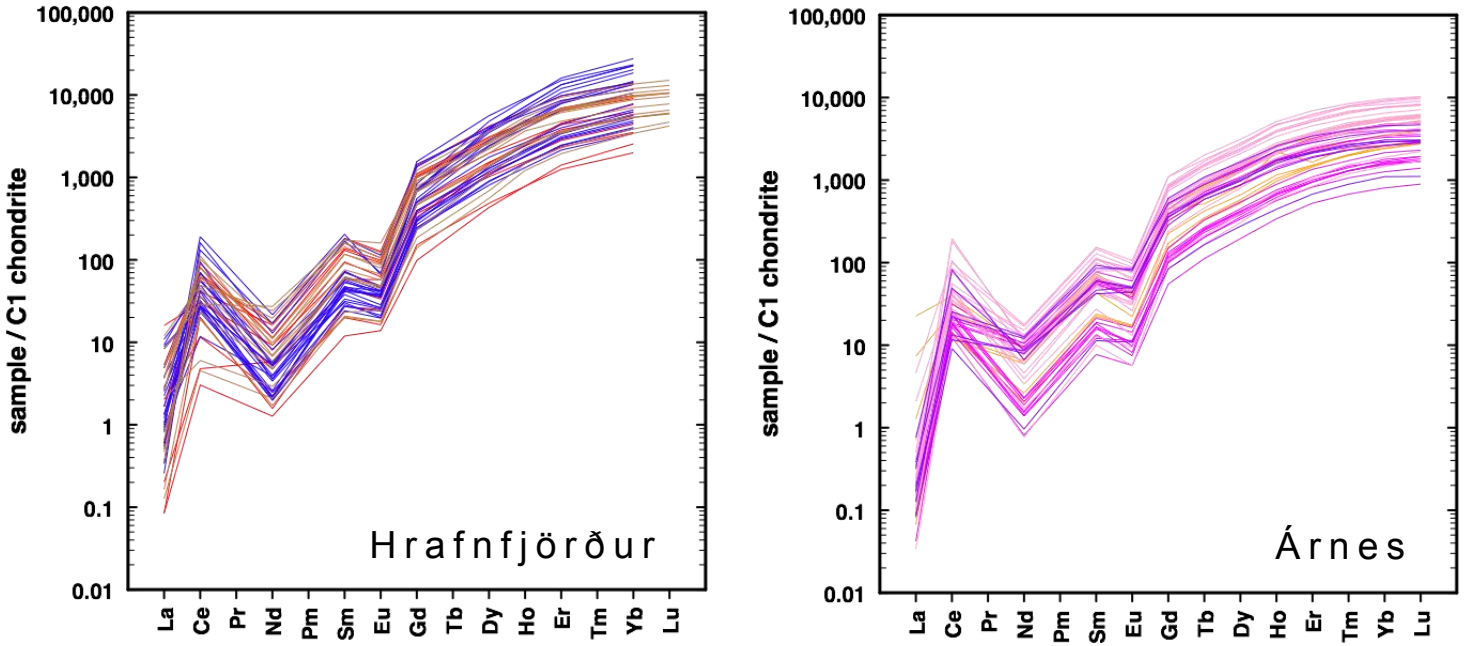

Fig. 10: I*n situ* zircon REE normalized to C1 chondrite (McDonough and Sun, 1995). Hrafnfjörður (left) has a steeper and slightly more elevated pattern than Árnes (right). Colors as in Fig. 9.

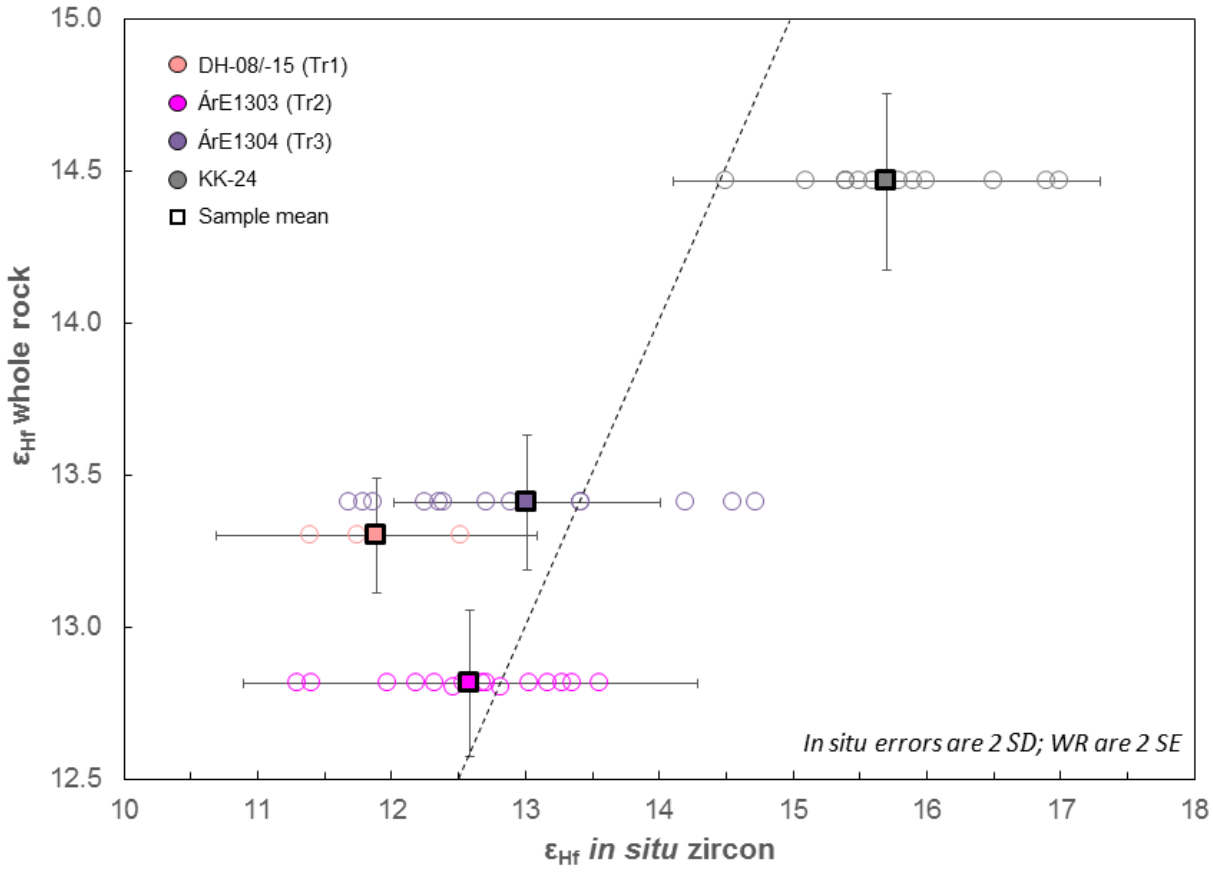

Fig. 11: Whole rock ε_{Hf} vs. *in situ* zircon ε_{Hf} from Árnes and Hrafnfjörður. The Tr1 rhyolite unit is represented here with zircon ε_{Hf} from sample DH-04 and whole rock ε_{Hf} from sample ArE1302, which may instead be the Ta andesite unit. *In situ* zircon ε_{Hf} was also obtained for sample ArE1301 (zircon ε_{Hf} =12.4 ± 1.7 (2 SE)), but we did not measure corresponding whole rock ε_{Hf}. Dashed line is 1:1.

5. Discussion

5.1. Whole rock Nd, Hf, and Pb isotopes

Nd isotopic values suggest that the Árnes and Hrafnfjörður samples were produced in an "on-rift" setting according to the interpretation of Martin and Sigmarsson (2010) (see Chapter 3 for more details). However, Árnes samples overlap compositions of propagating and off-rift magmas when compared with the data of Peate et al. (2010) (Fig. 5), and Hrafnfjörður sample KK-24 has a more depleted composition similar to samples from the currently established WVZ and NVZ.

An intriguing feature of the Árnes and Hrafnfjörður silicic samples is an apparent discrepancy between whole rock ε_{Hf} and *in situ* zircon ε_{Hf} values (Fig.11). Hafnium is strongly compatible in zircon but not in other common phenocryst phases. Therefore, Hf in a magmatic system that is not in zircon must primarily be in the melt, and assuming both the zircon and the melt from which it crystallizes are in equilibrium during zircon crystallization, they both should have identical Hf isotopic compositions. This is not the case for many Árnes zircons. Samples ÁrE1303 and ÁrE1304 have zircon ε_{Hf} that covers ~3 ε_{Hf} units, including the corresponding whole rock ε_{Hf} values, although both have average *in situ* ε_{Hf} values lower than whole rock. The Árnes Tr1 rhyolite unit has whole rock ε_{Hf} from sample ÁrE1302 and *in situ* ε_{Hf} from sample DH-04. Therefore, a direct comparison is impossible. If combined for a general Tr1 comparison, *in situ* εHf values are all lower than the whole rock value but correspond will with zircon analyses from the other Árnes units. Discrepancies between whole rock and zircon Hf isotope composition may indicate the zircons grew in a magmatic environment that had a different ε_{Hf} value than that represented by the samples from which we extracted them. This implies a complex and multi-stage history petrogenetic history. All Árnes samples have a range of zircon Hf isotope values that suggest contributions from depleted and enriched sources during the magma's life, whereas zircons from Hrafnfjörður sample KK-24 have Hf isotope values reminiscent of a depleted, more MORB-like source.

A potential explanation for the wide range of *in situ* zircon Hf values in Árnes samples is that open system processes involving fresh mantle melts and partial melts of pre-existing crust generated the magmas from which zircons grew. These source contributions likely also had zircon from earlier crystallization. We see evidence for older sub-populations in some Árnes silicic units and sub-mantle $\delta^{18}O$ values in Árnes and Hrafnfjörður zircons that may be relics from hybridization. Such a magma hybridization would result in zircons with a potentially wide range of *in situ* ε_{Hf} values inherited from the partial melt and the mantle melt components individually and from crystallization from the hybrid magma itself—which has a whole rock ε_{Hf} value resulting from hybridization.

5.2. In situ zircon U–Pb ages and oxygen isotopes

Assuming the oxygen isotope signature of the sub-Iceland mantle is not inherently isotopically lighter than average mantle (cf. Eiler et al., 2000; Hattori and Muehlenbachs, 1982; Muehlenbachs et al., 1974; Thirlwall et al., 2006), the low $\delta^{18}O$ signatures of zircons from Hrafnfjörður and Árnes can be explained by contribution of hydrothermally altered crust in part or in whole to petrogenesis. Based on our current understanding of tectonic evolution of the northern Westfjords, Hrafnfjörður sits on crust erupted late in the NWRZ's lifetime, meaning it was likely only a few million years old when Hrafnfjörður was active, and was probably never buried by subsequent eruptions before the NWRZ went extinct. Therefore, the rocks under Hrafnfjörður are not likely to be extremely hydrothermally altered. Pope et al. (2013) show that rocks ~0.5-1 km below the surface at Krafla have $\delta^{18}O \sim$ -4 to -5.5‰. Incorporation of ~11-22% of this altered material (or less with a more altered crustal component) with a fresh mantle melt (or partial melt of unaltered rock) is required to generate the oxygen isotope signature measured in our Hrafnfjörður samples. The relationship of the Árnes central volcano and its spatial relationship to its source rift is less well understood than at Hrafnfjörður, which makes estimating the oxygen

isotope composition difficult. Therefore, while a similar scenario as described above for Hrafnfjörður can likely also be applied to Árnes, the range of potential $\delta^{18}O$ crustal contributions precludes a more quantitative approach. An alternative method of generating the observed isotopically light signature in Hrafnfjörður and Árnes zircons is via zircon crystallization in magma derived completely from partial melting of low-$\delta^{18}O$ hydrothermally altered crust.

Regardless of exact provenance, multiple zircon populations in Hrafnfjörður samples indicates open system processes play a noticeable role in silicic petrogenesis, which petrography and major and trace element compositions also suggest. In these samples (Fig. 8), the bins with the largest number of individual ages are likely to represent eruption age, despite both samples recording earlier episodes of zircon crystallization. At Árnes, individual grain age ranges are >1 Myr for all samples except ÁrE1304. While most of the grains define coherent populations, the ones that do not were not considered in determining the overall sample age because they likely do not indicate the age of the dominant population. Rather, they seem to correlate well in age with grains from Hrafnfjörður sample KK-24.

5.3. Summary of petrogenesis

Our findings support diversity in petrogenesis between and within Árnes and Hrafnfjörður silicic units. Oxygen isotope values in zircon from both volcanoes indicate a role for partially-melted, hydrothermally altered crust in their petrogenesis, but the amount of the contribution varies. Similarly, variation in whole rock and *in situ* Hf isotopes from Árnes and Hrafnfjörður samples indicates that many zircons did not end up in the magma in which they crystalized—a finding supported by lack of equilibrium Th/U concentrations in many zircons.

These magmas from these central volcanoes are the products of a complicated and somewhat unclear petrogenetic model resulting from varying inputs of partially melted altered crust, fractionates of fresh mantle melts, and potentially partial melts from unaltered crust. In

general we observe interplay between partial melting and fractional crystallization processes at both locations, although the dominance of one or the other may shift from unit to unit. Overall, the Árnes and Hrafnfjörður silicic rocks share many geochemical features, indicating some similarity in petrogenetic mechanisms. Exceptions to this are the Tr1 rhyolite at Árnes and the HfE1402 dacite from Hrafnfjörður. With one exception (Tr1 rhyolite), Árnes units appear to have formed through fractional crystallization of a melt with a dominant fresh basalt component and a subordinate altered crust component. The Tr1 unit was likely the product of very dominant crustal partial melting. At Hrafnfjörður, these is evidence of continued magmatic input, mixing, and crystallization, leading us to conclude that mixing between a large volume of partially melted mildly altered crust and a minor component of fractional crystallization-derived magma was the dominant method of petrogenesis. In both volcanoes, zircon populations from the hybrid magmas and their partial melt components are retained in the final rock.

5.4. Geodynamic evolution of the Westfjords

U-Pb zircon ages indicate that Árnes (silicic activity ~13.4-12.8 Ma) and Hrafnfjörður (~14.2-13.6 Ma) magmatic systems were actively evolving and erupted from the SSRZ fairly early in its lifetime. Numerous studies (e.g. Benediktsdóttir et al., 2012; Hey et al., 2010; Sæmundsson, 1979; Sigmundsson, 2006) have measured the Icelandic rift zone spreading rate and the spreading rate of the North MAR at 0.9-1 cm/yr on each side of the rift. Based on the established location of the SSRZ (Harðarson et al., 2008; Martin et al., 2011) and refined based on bathymetry of the Icelandic plateau around northern Iceland, and using a 1 cm/yr spreading rate (in one direction), we reconstructed the rift-drift motion of these two volcanoes (Fig. 12). The approximate center of Hrafnfjörður central volcano lies 75 km west of the SSRZ axis if a perpendicular spreading direction is assumed, and ~83 km west of the SSRZ axis if the spreading direction is a 30° offset from perpendicular, as has been suggested for parts of the MAR around Iceland (Benediktsdóttir et al.,

2012). The timing of the SSRZ's extinction is constrained between 6.7 Ma and 5.5 Ma (Martin et al., 2011). Therefore, if we assume that the oldest dated silicic unit at Hrafnfjörður (KK-24) was near the rift axis during petrogenesis and eruption and the spreading rate was 1 cm/yr, a separation distance of between 75 and 87 km should result between Hrafnfjörður and the now-extinct SSRZ axis, which correlates well with the distances we measured even given a range of spreading angles. Therefore, we conclude that the geodynamic setting into which Hrafnfjörður erupted remained roughly unchanged and was dominated by rift drift during the lifetime of the SSRZ.

At Árnes, the approximate center of which lies between ~44 km and ~51 km from the SSRZ axis assuming perpendicular and 30° offset from perpendicular spreading, respectively. Again, assuming an average spreading rate of 1 cm/yr, and assuming the oldest silicic unit at Árnes, sample ÁrE1301, formed near the rift axis, we would expect that Árnes would lie ~64-76 km from the SSRZ axis. This estimation clearly does not match how far from the SSRZ axis Árnes is now, and even small deviations in location of the axis or the placement of the approximate center of magmatism cannot account for the >30% difference in the measured and expected distances. Similarly, given the age difference between Hrafnfjörður and Árnes, we should see an approximate longitudinal difference of 10-15 km, but in reality the difference is ~30 km.

The reason for this apparent discrepancy is not clear. Several authors (e.g. Foulger, 2006; Martin et al., 2011) have suggested that older crust may become trapped between rift axes during rift relocation and subsequently covered by newly-erupted lava. Foulger's (2006) suggestion that a rifted piece of the Jan Mayen microcontinent (JMM) may be trapped is likely not the case in the Westfjords as there are no rocks reported with continental isotopic characteristics as seen in southeastern Iceland where the presence of JMM crust has been implicated (Torsvik et al., 2015). Martin et al. (2011) suggest that a piece of older oceanic crust was trapped during the NWRZ to SSRZ transition. These authors did not specify the exact location or extent of the hypothetical trapped crust, but seismic estimates of crustal thickness indicate an area of slightly thickened crust

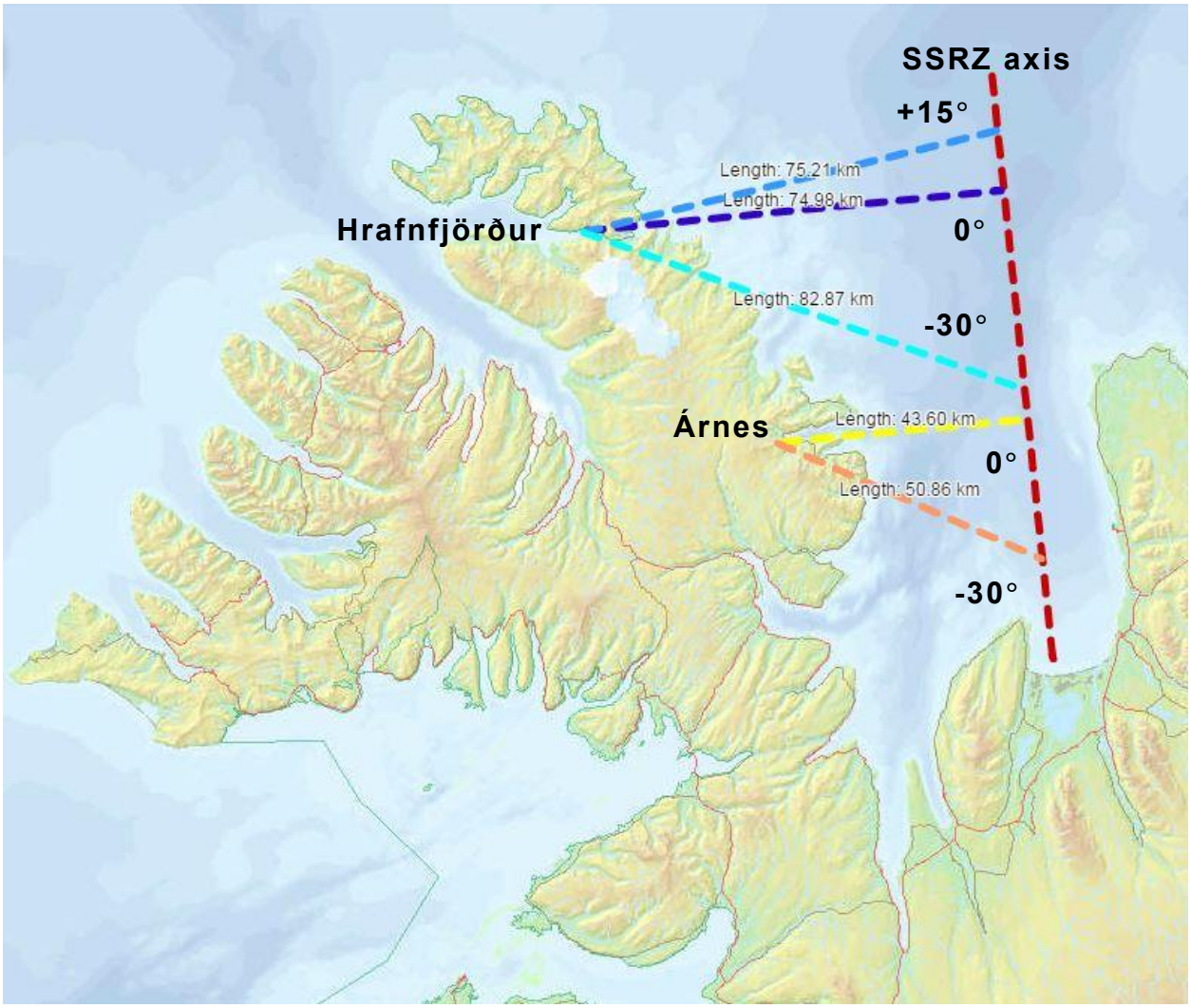

Fig. 12: Distances between extinct Snæfellsnes-Skagi rift axis (red dashed line) and current locations of approximate centers of Árnes and Hrafnfjörður central volcanoes. Distances and map from Landmælingar Íslands' online atlas (lmi.is). Distances measured to simulate varying obliquity of spreading. Distances to Hrafnfjörður are 75.2 km (light blue line), 75 km (dark blue line), or 82.9 km (teal line). Distances to Árnes are 43.6 km (yellow line) or 50.9 km (orange line), based on a maximum obliquity of spreading 30° from perpendicular.

in the Gláma area of the central Westfjords (Darbyshire et al., 2000; Kaban et al., 2002). This area is 10s of km farther south than Árnes and even farther from Hrafnfjörður, but the possibility of trapped crust interfering with petrogenesis along the SSRZ cannot be ruled out. Determining the geochemical influence of such a crust would be challenging based on the chemical and isotopic similarities between oceanic crust and Icelandic rocks that normally result from plume-rift interaction. Another possible explanation for Árnes' distance discrepancy could be drastically increased magmatic production for the ~1 Myr between when Hrafnfjörður and Árnes were active followed by a reduced magmatic output for the remainder of the SSRZ's lifetime. If the Icelandic hot spot—which has been suspected of pulsing rather than maintaining steady heat flux (e.g. Jones et al., 2002; Kitagawa et al., 2008; O'Connor et al., 2000; White and Lovell, 1997)—experienced an increase in heat flux for a sustained period of time leading to increased magma production and an increase in the spreading rate to ~30 cm/yr for ~1 Myr to account for the age difference between Hrafnfjörður and Árnes, a lateral separation distance of ~30 km would result, which accounts for their present-day separation distance. Extreme spreading would then be followed by a period of lower-than-average spreading of <0.5 cm/yr. Martin et al. (2011) proposed that the SSRZ began to share magmatic output with the propagating Northern rift zone (NRZ) around 13 Ma, meaning that overall flux (and potentially spreading rate) at the SSRZ would be diminished. However, it is unreasonable to think a pulsing plume likely can induce over 30 cm/yr of spreading. Even the fastest-spreading ridge in the world, the East Pacific Rise (EPR) between 13°S and 23°S, only manages a spreading rate of ~13 cm/yr (Mahoney et al., 1994). The EPR is not influenced by a hot spot like the rift zones on Iceland, but it is unlikely that the presence of one could more than double the spreading rate. Therefore, we must acknowledge that the current paradigm of geodynamic development of the northern Westfjords is not fully suited to explaining the discrepancies in distances between at least one volcanic center and the rift axis from which it erupted, and suggest

this is an area that would benefit immensely from additional geochronological and geochemical investigation.

6. Conclusions

- Ages from the two oldest as-yet dated silicic volcanoes in Iceland indicate silicic lifespans of ~600 kyr for each system. Árnes rhyolites yield weighted mean ages from 12.8 ± 0.1 to 13.4 ± 0.6 Ma (2σ SE), while Hrafnfjörður samples have weighted mean ages from 13.6 ±0.2 to 14.2 ± 0.2 Ma (2σ SE); these ranges are on the short end of typical Icelandic central volcano lifespans, but do not include associated basalts and therefore these systems were likely longer-lived;
- All silicic magmas sampled from Hrafnfjörður and Árnes have at least a volumetrically minor component of partially melted altered crust based on *in situ* zircon oxygen isotope results; the amount of partial melt component is generally higher in Hrafnfjörður magmas than those from Árnes;
- Open system processes dominate at least early stages of silicic magma petrogenesis at these two volcanic centers based on whole rock Pb, Nd, and Hf isotopic data and *in situ* zircon Hf and O isotope measurements and U–Pb geochronology results;
- Geodynamic evolution of the Westfjords is not as straightforward as previously indicated, as demonstrated by the apparent mis-match in ages of Árnes and Hrafnfjörður and distances between those volcanoes and the SSRZ axis.

CHAPTER 5

Króksfjörður revisited

Abstract

Iceland is the only place on modern Earth where an active mid-ocean ridge and a major mantle plume coincide to produce a plateau and island of appreciable size, resulting in a geologically unique environment with a dynamic history. Amid the dominantly tholeiitic magmatic landscape is one locality, Króksfjörður, with calc-alkaline (CA) silicic rocks. This is unexpected because CA magmas are normally associated with subduction zones. The mechanisms that produce these rare CA magmas are unclear. This study investigates the processes forming CA magmatism in Iceland using whole rock isotopes and in situ zircon analyses, leading to further understanding of complexities of magma production at ocean islands and ways in which CA magmas may be generated. In addition to finding a ~1 Myr range in ages in both CA and coeval silicic tholeiites, we find notable isotopic differences between CA and coeval tholeiitic rocks which imply a deep-seated difference in petrogenetic processes occurring within one volcanic system.

1. Background

Prior chapters in this dissertation have established the abundance of silicic rocks on Iceland and provided a glimpse at the myriad variations in petrogenetic processes and tectonic setting that influence their formation. The presence of calc-alkaline (CA) silicic rocks—in addition to more voluminous basaltic and silicic tholeiites—at the mid-Miocene Króksfjörður central volcano hints at an even more complicated interaction of source materials, heat, and tectonic setting-driven geochemical evolution than is the norm. Previous work at Króksfjörður revealed the CA rocks are far more arc-like (primary amphibole, lack of Eu anomaly, high Mg#, high field strength element

depletion) (Hald et al., 1971; Jónasson et al., 1992; Pedersen et al., 1979) than other Icelandic rocks, which potentially indicates a fundamentally different petrogenetic process at work than elsewhere in Iceland.

In total, the silicic units are a volumetrically minor portion of the Króksfjörður central volcano and comprise no more than 20% of the exposed units. However, their origin—specifically that of the calc-alkaline dacites—is a matter of debate. Jónasson et al. (1992) postulated that the generation of the tholeiitic silicic rocks required a shallow magma chamber and invoked either fractionation of basaltic magma, partial melting of country rock heated by basaltic magma, or a combination of the two, as potential differentiation mechanisms. Willbold et al. (2009) invoked partial melting of basalt followed by fractional crystallization as the generation mechanism for the calc-alkaline silicic units but failed to explain the concurrent tholeiitic silicic magmatism. Both models are problematic in that it is long-established that these are the dominant mechanisms by which *all* silicic rocks in Iceland are postulated to form, and it does not offer an explanation for the uniqueness of the calc-alkaline Króksfjörður rocks.

Most of Earth's continental crust is CA and generally inferred to have been produced by subduction—a tectonic setting that has never occurred in Iceland. Gaining an understanding of how CA magmas may be produced in absence of subduction may provide vital clues to a fuller in understanding of crust-building processes. One of the uncertainties about CA magma petrogenesis revolves around the extent of involvement of amphibole. Amphibole is not thought to be involved in production of typical Iceland tholeiites—the magmas are too hot and dry to crystallize hydrous amphibole, and any amphibole in crustal source regions is thought to break down before or during high-T melting reactions. The presence of primary amphibole—which may result in CA-like HFSE- and HREE-depleted magmas lacking an Eu anomaly—in the CA rocks at Króksfjörður is consistent with the hypothesis that amphibole played a role in their generation. This work integrates new *in situ* zircon data (geochronology, trace elements, O and Hf isotopes) and whole rock isotopic data

from the full suite of silicic CA rocks and tholeiites at Króksfjörður to reassess the petrogenetic conditions under which these magmas were generated.

2. Geologic Background

The central volcanic complex at Króksfjörður in the southern Westfjords (Fig. 1) is one of Iceland's best-studied but most enigmatic Neogene volcanoes. It is presumed to have erupted from the Snæfellsnes-Skagi rift zone (SSRZ) (Fig. 1), which the U-Pb zircon ages presented here (see Section 4) confirm. Thoroddsen first noted the presence of silicic rocks in the area in 1888 (Hald et al., 1971; Jónasson, 1990), but no subsequent studies on the silicic rocks occurred until Hald et al.'s (1971) work, which produced the first geologic map and general descriptions of Króksfjörður. Hald et al. (1971) identified a central volcano comprised of a lower series of tholeiitic basalt and basaltic andesite flows that subsequently collapsed to result in a water-filled caldera. Continued eruptive activity yielded intracaldera breccias, tuffs, lavas, and volcanic plugs, while silicic domes and shallow intrusions formed around the rim of the caldera. The climactic silicic eruption deposited an ignimbrite that is present throughout the northeastern section of the Króksfjörður area. Renewed basalt activity marked the final 'upper' phase of volcanic activity, although both Hald et al. (1971) and Harðarson (1988) emphasized the likelihood that the upper basalt unit resulted from another volcanic system. Hydrothermal alteration is common—particularly in the western portion of the caldera—but not ubiquitous and most of the volcanic plugs are unaltered. Further work by Pedersen et al. (1982) provided a detailed description of the Kambur dacite and noted cummingtonite phenocrysts and amphibole-rich xenoliths. These assemblages and whole-rock elemental compositions indicate a magma type (low T, water-rich; CA) previously unseen in Iceland but similar to those seen in orogenic volcanic systems (Ewart, 1979). Further detailed description of the other major silicic units in the Króksfjörður volcanic complex in Jónasson (1990) and Jónasson et al. (1992) revealed several more CA dacite units (Valshamar, Strýta, Geitafell) and

Jónasson 1990, modified from Hald et al. 1971

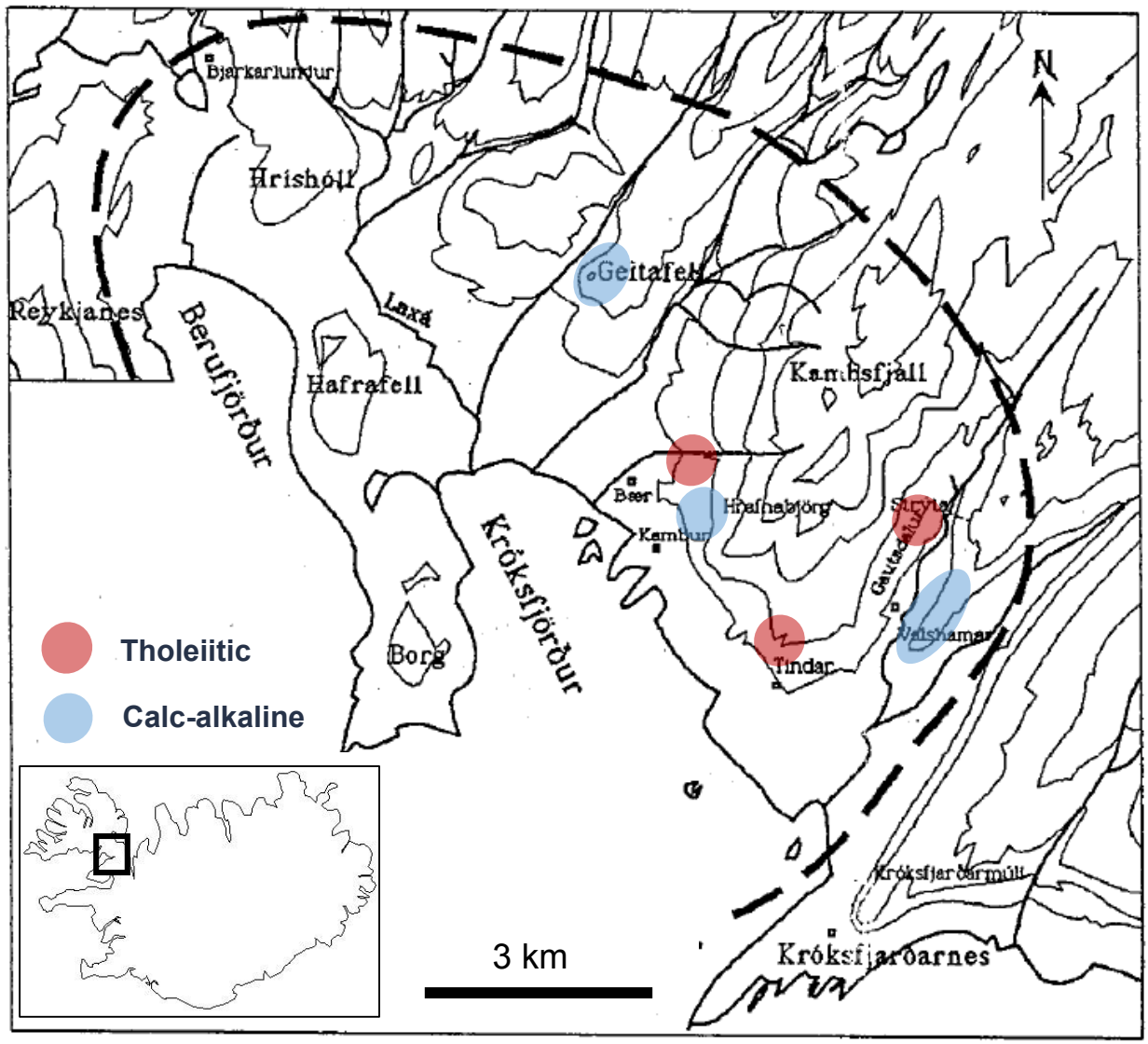

Figure 1. Location of Króksfjörður central volcano and sampled outcrops.

confirmed the more usual tholeiitic trend of dacites and rhyolites at Tindar, Gautsdalur and Bær, and that are typical of silicic units throughout Iceland.

3. Sampling and Methods

Samples were collected from three major silicic CA outcrops as identified by Jónasson (1990)—Kambur, Geitafell, and Valshamar—as well as three tholeiitic silicic units at Bær, Tindar, and Geitafell (Table 1). Zircons were extracted from all samples except Geitafell (no zircon found) using standard physical, density, and magnetic separation techniques prior to hand-picking. Zircons were mounted in epoxy, polished, and imaged via cathodoluminescence and backscatter electrons before being analyzed for O isotopes (UCLA; CAMECA ims-1270), U-Pb geochronology and trace elements (Stanford/USGS SHRIMP-RG), and *in situ* Hf isotopes (WSU Radiogenic Isotope and Geochronology Laboratory (RIGL); ThermoFinnigan Neptune LA-MC-ICPMS). These are the first analyses of their kind reported from Króksfjörður. Fresh rock chips were powdered and analyzed for Nd, Hf, and Pb isotopes at RIGL using the procedure outlined in McDowell et al. (2015). Please refer to Chapters 3 and 4 for detailed methodology. Although whole rock geochemistry was also obtained for these samples, our results are in agreement with those presented more thoroughly in previous studies (Jónasson, 1990; Jónasson et al., 1992; Pedersen et al., 1979) and are not addressed further here. They are listed in Appendix I.

4. Results and Discussion

4.1. In situ U-Pb geochronology

Zircon grains (n=44) from 5 samples at Króksfjörður range in age from 10.3 to 13.5 Ma, with a median of 11.7 Ma and mean of 11.6 Ma. A summary of age results is provided in Table 2 and the full dataset is in Appendix E. Weighted mean average sample ages range from 11.5±0.5 Ma to 12.2±0.2 Ma (Fig. 2). Two of the 5 samples, tholeiitic Bær (IEKBr-1) and CA Kambur (IIKK-1), have

Sample name	Distinction	Latitude*	Longitude*	Elevation (m)	Rock type	Description	Zircon?
IEKBr-1	Th	N65°30.679'	W21°57.212'	210	Dacite	Black pitchstone with dominantly plag phenos + glass	✓
IEKTr-1	Th	N65°29.196'	W21°56.139'	157	Rhyolite	Fresh, grey, vitrophyric with few phenocrysts	✓
IEKGd-1	Th	N65°30.824'	W21°52.404'	160	Rhyolite	Fresh ignimbrite with fiamme, glass, and clasts/phenos	✓
IEKGf-1	CA	N65°31.832'	W21°59.902'	122	Dacite	Black glassy pitchstone, aphyric (<15% phenos)	
IEKVl-1	CA	N65°29.472'	W21°53.676'	83	Dacite	Glassy and light purple; abundant small phenocrysts	✓
IIKK-1	CA	N65°29.858'	W21°57.261'	--	Dacite	Grey/tan and glassy with abundant phenos of amph, plag	✓

*All coordinates are WGS84

Table 1. Location and description of Króksfjörður samples. All samples except Geitafell are zircon-bearing.

	U-Pb geochronology				Oxygen isotopes			Hafnium isotopes			
	n	Age (Ma)	2σ SE	MSWD	*n*	$\delta^{18}O$ (‰)	2σ SE	*n*	ε_{Hf}	2σ SD	Outliers
IEKBr-1	8	11.9	0.5	3.70	8	1.7	1.6	3	12.0	1.9	0
Subset1	*5*	*12.3*	*0.3*	*0.64*	5	1.8	1.9	--	--	--	--
Subset2	*3*	*11.2*	*0.3*	*0.76*	3	1.5	1.2	--	--	--	--
IEKTr-1	11	12.2	0.2	0.55	13	2.8	0.9	3	11.5	2.8	0
IEKGd-1	8	10.9	0.3	1.60	5	2.8	1.0	--	--	--	--
IEKVl-1	9	11.8	0.4	0.35	14	2.1	1.6	5	13.9	2.2	1
IIKK-1*	8	11.5	0.5	5.10	7	2.3	1.4	6	13.9	1.5	0
Subset1	*3*	*12.1*	*0.3*	*0.79*	2	2.0	0.3	--	--	--	--
Subset2	*5*	*11.1*	*0.5*	*1.80*	5	2.4	1.6	--	--	--	--

**O isotope data from Carley et al. (2014); ages and Hf isotope data from Carley (unpublished and 2014, respectively)*

Table 2. Summary of all *in situ* zircon analyses from Króksfjörður.

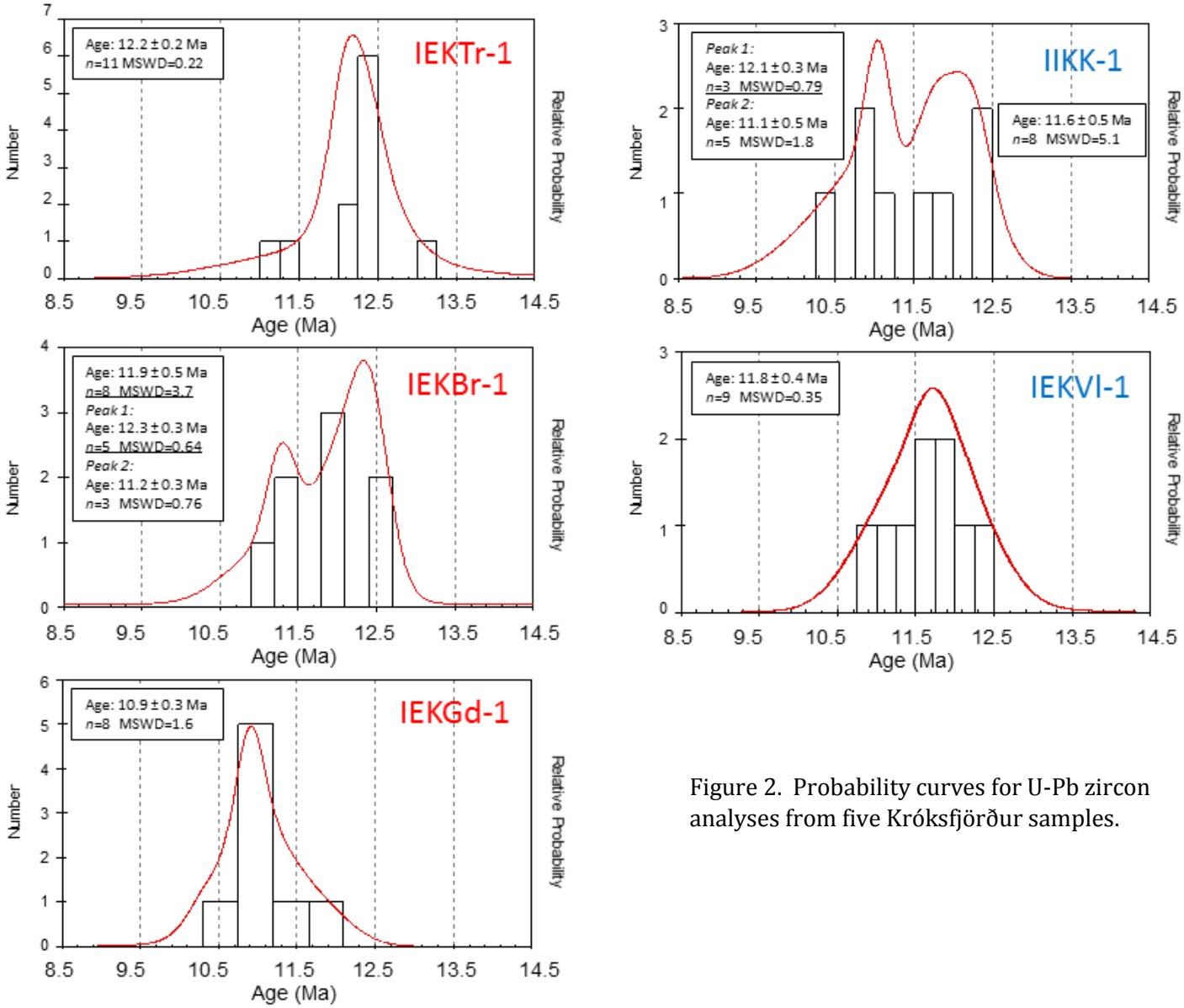

Figure 2. Probability curves for U-Pb zircon analyses from five Króksfjörður samples.

zircon ages that result in a bimodal age distribution with similar ages for both samples—subset 1 of each sample has an age of ~12.2 Ma (IEKBr-1=12.3; IIKK-1=12.1 Ma) and subset 2 has an age of ~11.1 Ma (IIKK-1) to ~11.2 Ma (IEKBr-1). These appear statistically to be legitimate sub-populations, and the remaining Króksfjörður samples (IEKVl-1 excepted) match these general ages well—IEKGd-1 has a sample age of ~11 Ma, while IEKTr-1 has an age of ~12.2 Ma. IEKVl-1 seems to occupy the time between these two age peaks, with an age of ~11.8 Ma. Geographically, the two most westerly zircon-bearing samples—Bær and Kambur—are the ones displaying a bimodal age distribution. Whether this is a coincidence or indicative of significant interaction is undetermined, but *in situ* zircon data point to overlap in trace element characteristics (see Section 4.3; Fig. 3; Appendix F), indicating potential for spatially indistinct petrogenetic processes. Regardless, Króksfjörður appears to have produced silicic magmas with two different bulk compositions for over 1 Myr, with peaks in activity around 12.2 Ma and ~11.2 Ma.

4.2. In situ oxygen isotopes

Forty-nine *in situ* zircon oxygen analyses were acquired over 5 samples. Results are summarized in Table 2, with full results in Appendix D. Not unsurprisingly, Króksfjörður zircons have an isotopically light $\delta^{18}O$ signature that is characteristic of evolved Icelandic rocks. Average sample $\delta^{18}O$ values for Króksfjörður range from 1.7‰ to 2.8‰—significantly below the equilibrium mantle zircon value of 5.3‰ (Valley, 2003). As discussed in Chapters 3 and 4, below-mantle $\delta^{18}O$ in Icelandic silicic magmas is frequently associated with incorporation of crust altered by high-temperature interaction with meteoric water, either through partial melting or wholescale assimilation of crust material (e.g. Bindeman et al., 2012; Hattori and Muehlenbachs, 1982; Óskarsson et al., 1982). However, it cannot be ruled out that inherently low mantle $\delta^{18}O$ (e.g. Muehlenbachs et al., 1974; Thirlwall et al., 2006) or incorporation of regionally metamorphosed, unaltered rocks (Jónasson, 1990) can account for isotopically light magmas. Notable at

Kroksfjorður is the relatively tight range of $\delta^{18}O$ values that show no correlation with host rock composition (tholeiitic vs. CA) or age population (~12.2 Ma vs. ~11.1 Ma). This implies either: a) a common parent magma with low $\delta^{18}O$ that underwent variable differentiation to produce the two geochemical trends at Króksfjörður; or b) each type of magma was produced in a different spatial and/or temporal regime and independently achieved similar end $\delta^{18}O$ compositions. Jónasson et al. (1992) convincingly demonstrated on the basis of whole rock geochemistry and phase stability that the tholeiitic and CA magmas are not cogenetic and cannot be related through simple fractional crystallization, ruling out Scenario (a). Therefore, it must be concluded that these two magma types illustrate a case of convergent evolution in terms of oxygen isotopic composition.

4.3. In situ trace elements

As expected, zircons from tholeiitic and calc-alkaline samples vary markedly in their trace element compositions (Fig. 3; Appendix F). Depletion in high field strength elements is ubiquitous in CA magmas worldwide, and zircons from Króksfjörður CA samples generally follow that trend. CA zircons have lower Yb and Nb (~150-1000 ppm Yb; 1-30 ppm Nb) than tholeiitic zircons (200-~1000 ppm Yb; 5-200 ppm Nb) and zircons from the 2 rock types plot in slightly subparallel trends in log-log space. CA and tholeiites zircons also form two different, slightly subparallel trends on a Th vs. Nb log-scale plot, again demonstrating the general Nb depletion of CA zircons. Zircon data from CA rocks plot in the low-Ti, high-Hf area of a Ti vs. Hf plot (Ti< 20 ppm; ~8000 ppm < Hf < ~13,000 ppm), which is indicative of crystallization from more evolved magmas (Claiborne et al., 2010)—tholeiitic zircons have greater variation in Ti (up to ~40 ppm) and none have Hf>10,000. Since Ti in zircon has been shown to vary with crystallization temperature (e.g. Claiborne et al., 2010; Ferry and Watson, 2007), generally lower Ti in the CA zircons also indicates lower crystallization temperatures than the tholeiitic sample zircons experienced. Zircon from CA rocks are also enriched in HREE compared to tholeiites sample zircons, the CA zircons having Yb/Gd

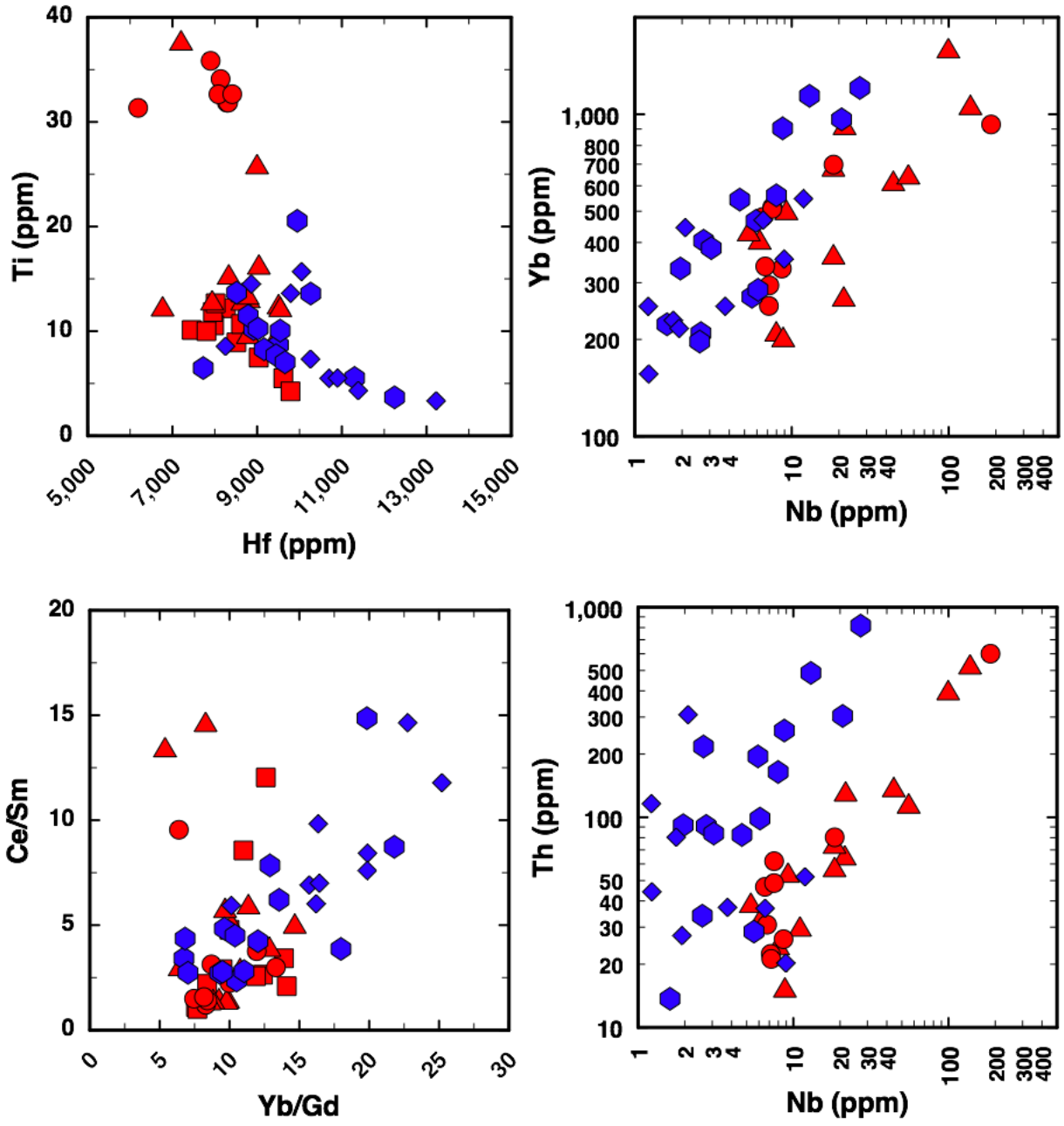

Figure 3. *In situ* trace element concentrations for Króksfjörður zircons. Symbols are the same as in Figure 2. Calc-alkaline sample symbols are blue, tholeiitic sample symbols are red.

ranging from 7-25 ppm, while tholeiites have a more restricted range of 6-15 ppm. When plotted on a chondrite-normalized (values from McDonough and Sun, 1995) REE diagram (Fig. 4), zircon compositions from tholeiitic rocks should have slightly steeper HREE patterns and have higher Yb and Lu concentrations than CA-source zircons, although both groups show strong positive Ce anomalies, negative Eu anomalies, and increasing HREE characteristic of all zircon. However, there appear to be several CA zircons that plot amongst the highest-concentration HREE grains.

All of these trends point to zircon from CA rocks recording different differentiation processes than those recorded by zircon from tholeiitic rocks at Króksfjörður. Curiously, many of the trace element trends described here indicate overlap between the two populations. As previously mentioned, the two most westerly units, Bær and Kambur, appear to have similar bimodal age distributions as well as overlapping to some degree in trace element plots. Similarly, units Valshamar and Gautsdalur appear to have zircons with overlapping trace elements ranges and are also geographically close together. While the surface spatial correlation may not correlate to spatial relationships during subsurface differentiation processes, it cannot be ruled out that there are "tholeiitic" zircons in otherwise CA rocks and vice-versa. Efforts to further resolve the nature of each zircon are ongoing.

4.4. In situ Hf isotopes and whole rock Pb, Nd, and Hf isotopes

In situ Hf isotope values are highly correlated with rock type (Fig. 5) and loosely correlated with age, although not all grains with *in situ* Hf isotope data have corresponding age data so the connection is more tenuous. Tholeiitic sample zircons have ε_{Hf} = +10.0 to +13.0, while CA sample zircons have ε_{Hf} =+12.7 to +15.4 (2SE ~1 for each analysis) (Table 2 and Appendix G). While there may be some overlap between the two rock types, the overall trend is that tholeiitic-sourced zircons have lower, less radiogenic ε_{Hf} than CA-sourced grains. This trend is also seen when considering whole rock ε_{Hf} values (Fig. 5; Appendix H)—tholeiitic samples (*n*=2) have values (ε_{Hf}

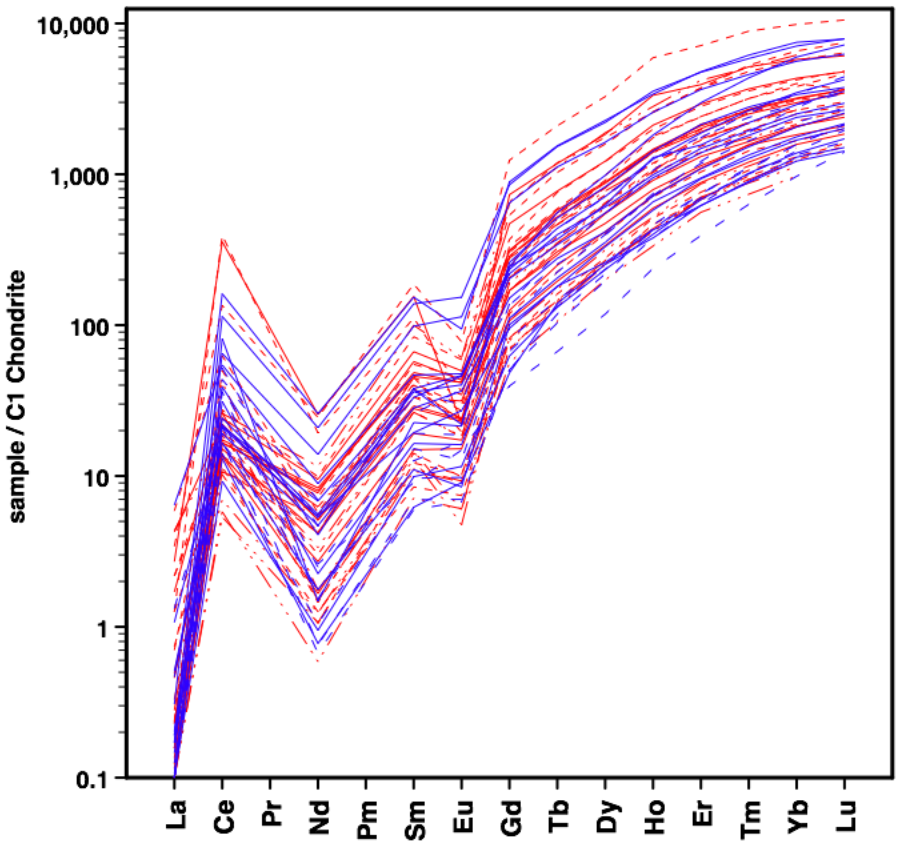

Figure 4. *In situ* rare earth element concentrations for Króksfjörður zircons normalized to C1 chrondrite values of McDonough and Sun (1995). Calc-alkaline sample line are blue, tholeiitic sample lines are red.

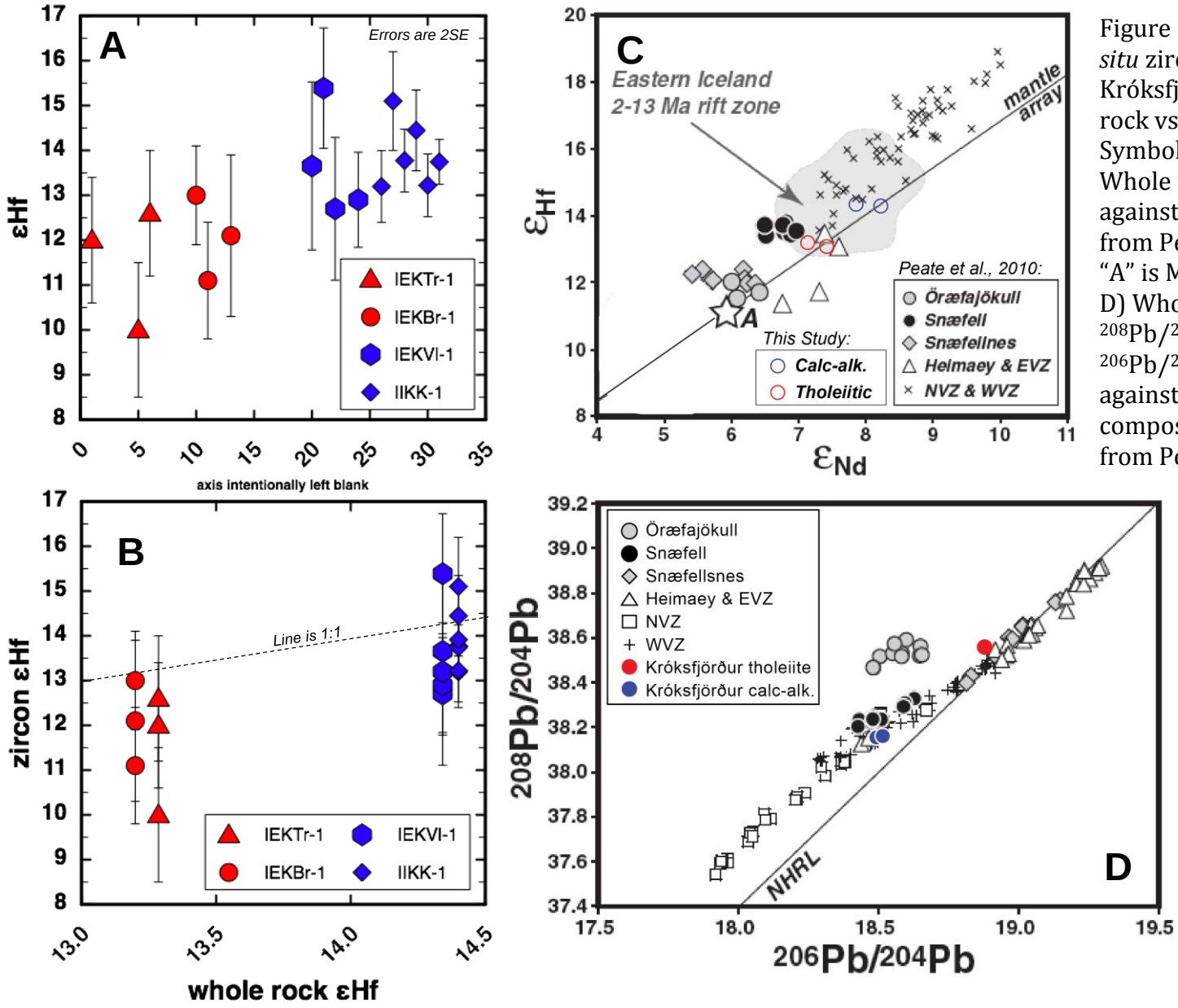

Figure 5. A) Range of *in situ* zircon ε_{Hf} for Króksfjörður. B) Whole rock vs. *in situ* ε_{Hf}. Symbols as in (A). C) Whole rock ε_{Hf} plotted against Icelandic samples from Peate et al. (2010). "A" is MORB composition. D) Whole rock $^{208}Pb/^{204}Pb$ vs. $^{206}Pb/^{204}Pb$ plotted against Icelandic compositions. Modified from Peate et al. (2010).

=13.2 and 13.3; 2SE~0.2) over one ε_{Hf} unit lower than those from CA samples (n=2; ε_{Hf} =14.3 and 14.4), well outside of error. These ε_{Hf} values are in agreement with typical Icelandic values from Tertiary rocks (Carley, 2014; Peate et al., 2010). Individual magmatic centers in Iceland rarely—if ever—display this much variation in whole rock ε_{Hf} (Peate et al., 2010, and references therein), indicating involvement of multiple source materials to an uncommon degree. Similarly, whole rock ε_{Nd} values vary between tholeiitic (ε_{Nd}=7.3 and 7.4; 2SE~0.2) and CA rocks (ε_{Nd}=7.8 and 8.3), occupying a range that is uncharacteristically large for an Icelandic magmatic center.

Whole rock Pb isotopes for tholeiitic Tindar and calc-alkaline Kambur and Valshamar also vary significantly based on rock type (Fig. 5). Tindar has a much more radiogenic composition ($^{208}Pb/^{204}Pb$ = 38.5532 ± 0.0025; $^{206}Pb/^{204}Pb$ = 18.8627 ± 0.0013) than either Kambur ($^{208}Pb/^{204}Pb$ = 38.1338 ± 0.0051; $^{206}Pb/^{204}Pb$ = 18.5112 ± 0.0022) or Valshamar ($^{208}Pb/^{204}Pb$ = 38.1244 ± 0.0025; $^{206}Pb/^{204}Pb$ = 18.4905 ± 0.0012), which have very similar, less radiogenic Pb isotope compositions. While variation in Pb isotope composition is well established in Iceland (e.g. Kitagawa et al., 2008; Peate et al., 2010; Thirlwall et al., 2004; and many others) due to inputs of at least 3 types of mantle (DMM, EM1, and EM2, and likely HIMU), these samples differ in composition by roughly a third of the total variation seen across all Icelandic rocks (Peate et al., 2010). Clearly, the two magmatic composition groups at Króksfjörður result from substantial inputs of material with distinguishably different source materials.

The processes by which magmas that erupt from the same volcano over the same time span can display very different evolutionary trends, isotopic compositions, and likely source materials remain enigmatic. Jónasson (1990) and Jónasson et al. (1992) invoked formation from different depths in the crust and horizontal distances away from the volcano's center, relying on partial melting of rocks with amphibolite characteristics to produce the CA magmas and shallow fractional crystallization, potentially from partial melts of altered rocks, to produce the tholeiites. However, this scenario does not account for the extreme whole rock isotopic differences between the groups,

nor does it offer an explanation for the seemingly bimodal age pattern, relatively invariant low *in situ* zircon oxygen isotope composition, or the apparent overlap in zircon trace element trends. One potential scenario that could explain all these characteristics involves a rift relocation—or, more precisely, the propagation of a new rift (the current Northern rift; NRZ) as described by Martin et al. (2011) and described in Chapter 4. These authors suggest that around 13 Ma, the SSRZ began to share magmatic output with the nascent NRZ and by ~12 Ma magmatism as we know it today was established. However, the ~1 Myr gap between NRZ initiation to apparent stabilization may have been a dynamic time for the SSRZ. There is growing evidence in the bathymetric record around Iceland that in between the major rift zones were smaller, propagating rifts that inevitably failed (Á. Höskuldsson, pers. comm.). If one of these smaller, propagating rifts was operating near Króksfjörður at the same time as the SSRZ, the potential for unique magmatism through partial melting of crust segments of varying ages, depths, compositions, etc. combined with the normal MORB and plume inputs was likely a real possibility. Another possible explanation for the observed differences in co-genetic Króksfjörður rocks invokes the incorporation of a trapped block of old, oceanic crust under that area of the Westfjords, as suggested by Martin et al. (2011). As previously noted, detecting the geochemical signature of melts from an oceanic crust block that—depending on its age and source—could be functionally identical to Icelandic rocks would be very difficult. Therefore, in order for this scenario to be viable, we would need to assume a very discernable geochemical profile for the introduced crust or crustal melt.

5. Conclusions

The investigations presented here involving whole rock isotopic analyses and in situ U-Pb geochronology, trace element, and O and Hf isotopic analyses of zircon from CA and tholeiitic silicic rocks at Króksfjörður—the first of analyses of this kind at this volcano—indicate significant longevity in both CA and tholeiite systems, potential interaction of zircon populations from both

magma types, similar O isotope compositions between the two groups, and Hf, Pb, and Nd isotopic variation that is strongly correlated with magma type. The cogenetic nature of the tholeiitic and CA rocks at Króksfjörður imply a localized environment in which subduction zone-like geochemical signatures are produced in a non-subduction setting. However, the existing models for petrogenesis of these magmas cannot explain the age and isotopic variations presented here. The magmatic history at Króksfjörður remains enigmatic.

CHAPTER 6

Future Directions

Completing this dissertation research has led to many insights and opportunities, and I look forward to expanding and diversifying those in the future. My plans for future research include field-based, geochemistry- and petrology-oriented studies that focus on questions related to silicic magmatism and development of silicic crust in Iceland and other non-subduction zone settings. Topics I intend to pursue further are:

1. Isotopic variation within Icelandic volcanic centers

The research presented in this dissertation draws attention to the geochemical variation present within a single magmatic center. Of particular interest to me is the continuation of comparative isotopic studies between silicic and mafic units from the same volcanic centers. Although young basalts have been extensively isotopically characterized, particularly in Pb, Nd, and Hf isotopes (e.g. Peate et al., 2010, and references therein), any co-existing silicic material is generally overlooked, and Tertiary and older Quaternary volcanic systems are often neglected entirely. The results presented in Chapter 3 based on Pb, Nd, and Hf isotopic analyses of basalt and rhyolite from the Hafnarfjall-Skarðsheiði system indicate that mafic and silicic magmas at H-S had a source with the same isotopic composition, which effectively rules out a partially melted crustal component being the dominant source of silicic material—but does this finding apply to other systems, or is H-S the exception? Comparing coeval mafic and silicic samples from volcanoes with a range of ages will also help to identify systematic changes in silicic petrogenesis throughout Iceland's history.

2. Assessing magma body longevity in spreading centers

Spreading centers produce the largest volume of magma on Earth, but remain largely hidden beneath the oceans—exceptions to this being the terrestrial rifts in Iceland and Eritrea (Alid). These terrestrial ridges are known to produce magmas with evolved chemical compositions in addition to voluminous basaltic magma frequently associated with rifting. Oceanic ridge systems are also capable of producing magmatic compositions more evolved than basalt, as has been discovered in the Reykjanes ridge of the North Atlantic. Silicic magma production is typically understood as a hallmark of continent formation at subduction zones, not at spreading centers. Given the large volumes of magma produced in rift zones, it is important to gain understanding of silicic petrogenesis in these areas and understand the longevities of silicic magmas associated with rift zones. Using zircon from silicic volcanic rocks as a primary research tool, I hope to evaluate the longevity of rift zone silicic magma bodies, which—when coupled with *in situ* Hf isotopic analyses—will help to constrain the petrogenesis of silicic magmas from Iceland, Eritrea, and ideally Reykjanes and address these questions:

- How long are silicic systems active in rift zones?
- Do zircons in silicic magmas continue to crystallize until eruption, or do they remain in a functionally sub-solidus state for long periods of time before eruption?
- Are there systematic differences in silicic magma body longevity and zircon residence habits between Iceland (and Reykjanes) and Eritrea?
- What is the primary mechanism by which silicic magmas are generated? Does it vary between locations?

3. Oxygen isotope priming of the Icelandic crust

As demonstrated throughout this dissertation, Icelandic zircons (and many rocks) have ubiquitously depleted oxygen isotope compositions stemming from incorporation of

hydrothermally altered (at high temperatures) material into the zircons' source magmas. Hydrothermal alteration is widespread in the Icelandic crust due to an abundance of precipitation and the presence of the mantle plume and rift zones, which lead to high crustal temperatures that facilities hydrothermal alteration. The degree of hydrothermal alteration should be largely a function of available heat. The surface expression of the Iceland hot spot moves progressively to the southeast due to northwestern movement of the Eurasian and North American tectonic plates, and the mid-Atlantic ridge follows, relocating every few million years to remain coupled with the hot spot. However, the few million year gap between rift relocations may mean that there is a swath of crust immediately above the plume head that is getting heated by the plume and becoming hydrothermally altered, thereby locally lowering the crustal $\delta^{18}O$. When and if that altered crust ever gets relocated into and the new rift segment starts propagating in that location, crust that is already altered—and likely warm—will melt more easily than pristine, cold basaltic bedrock. Inducing rift propagation might be easier in these areas, and partially melting pre-altered crust may contribute a silicic component to a magmatic system larger and earlier than would otherwise be expected, leading to large, quickly developing magmatic centers. Examining a subset of the myriad drill cores produced during geothermal energy exploration across Iceland and examining oxygen isotope variation within and between them could provide valuable insight into the sub-surface dynamics of high-temperature hydrothermal alteration. Combining those results with zircon ages (if present) would provide an added dimension when assessing the timescales and pervasiveness of oxygen isotope changes in the Icelandic crust.

APPENDIX A: Yerington Rock Descriptions

Table A1. Description of Yerington mine rocks**		
Sample	IUGS Rock Type	Mineralogy and Alteration
Jqmp1	Granite	Porphyry dike with the most intense Cu sulfide mineralization, potassic alteration, secondary magnetite, and abundant quartz veins. Abundant 1-4 mm subhedral plagioclase phenocrysts, less abundant potassium feldspar phenocrysts ≤1 cm diameter, occasional rounded quartz eyes, and 5-10% mafic phehocrysts with hornblende~biotite and a fine to medium-grained (k-spar>plagioclase)>quartz groundmess. Accessory sphene is common.
Jqmp1.5	Granite	Porphyry dike with moderate to intense mineralization, potassic alteration and quartz veins. Abundant 1-4 mm subhedral plagioclase phenocrysts, less abundant potassium feldspar phenocrysts ≤1 cm diameter, occasional rounded quartz eyes, and 5-10% mafic phehocrysts with hornblende~biotite and a fine-grained (k-spar>plagioclase)>quartz groundmess. Accessory sphene is common and magnetite is abundant.
Jqmp2	Granite	Porphyry dike with slight to moderate mineralization, potassic alteration and quartz veins. More phenocrysts than other porphyries. Abundant 1-4 mm subhedral plagioclase phenocrysts, less abundant potassium feldspar phenocrysts ≤1 cm diameter, occasional rounded quartz eyes, and 5-10% mafic phehocrysts with hornblende~biotite and a fine-grained (k-spar>plagioclase)>quartz groundmess. Sphene and magnetite are common accessories. Minor seritization.
Jqmp3	Granite	Late porphyry dike with little to no mineralization or quartz veins. Abundant 1-4 mm subhedral plagioclase phenocrysts, less abundant potassium feldspar phenocrysts ≤1 cm diameter, common rounded quartz eyes, and 5-10% mafic phehocrysts with hornblende >>biotite and a fine-grained (k-spar>plagioclase)>quartz groundmess. Sphene and magnetite are common accessories. Weak seritization, chloritized mafics, and clay-altered feldspars are common.
Jbqm	Granite	Seriate, fine-grained; abundant biotite, hornblende, and graphic quartz and potassium feldspar up to 1 cm. This sample could also be from the main Jqm unit, which is medium-grained. It is a porphyry dike host.
Jpqm	Granite	Porphyritic with equigranular, medium-grained groundmass of quartz, plagioclase, hornblende, biotite, magnetite, sphene, and 7-8% eu-to-subhedral potassium feldspar phenocrysts ≤1 cm diameter; minor sericitic alteration. Largest magmatic source of the porphyry dikes.
Jgd	Quartz monzodiorite	Fine-to-medium grained and seriate, with plagioclase>>potassium feldspar, abundant magnetite and sphene and little quartz. Jgd is a minor porphyry host.

**Source of all descriptions is Dilles and Proffett, 1984; Dilles 1987; and Dilles and Wright, 1988 with minor supplemental imformation from J. Proffett (pers. comm.)

APPENDIX B: Laser Raman Spectrometry Analyses

Table B1. Laser Raman analyses and characterization											
	E_g (tetrahedron rotation, I)		A_{1g} (symmetric bending, υ_2)		B_{1g} (antisymmetric stretching, υ_3)				Extra Peaks?	Corrected FWHM	FWHM measured in Origin
Analysis	**υ (cm^{-1})**	**I (counts)**	**υ (cm^{-1})**	**I (counts)**	**υ (cm^{-1})**	**I (counts)**	**FWHM (cm^{-1})**	**SE FWHM**			
Jqmp1											
qmp1_1.1	354.7	6953	438.7	9927	1005.9	34207	6.4	0.2	No	6.45	6.79
qmp1_3.1	354.8	4834	438.7	6044	1007.8	15761	6.6	0.2	No	6.59	6.92
qmp1_4.1	354.8	9015	438.7	7414	1005.9	19002	6.5	0.2	No	6.51	6.85
qmp1_5.1	355.0	8397	438.7	13970	1005.9	41566	5.9	0.2	No	5.90	6.27
qmp1_6.1	355.0	6221	438.7	10194	1007.8	40292	5.7	0.1	No	5.67	6.05
qmp1_10.1	354.8	4424	438.7	10856	1005.9	45261	6.7	0.2	No	6.65	6.98
qmp1_13.1	354.8	6688	438.7	4666	1005.9	16284	6.5	0.2	No	6.54	6.88
qmp1_14.1	354.7	4624	438.7	8635	1007.8	29273	6.2	0.1	No	6.25	6.60
qmp1_15.1	354.5	4306	438.7	7065	1005.9	24160	5.8	0.2	No	5.80	6.17
qmp1_19.1	354.8	7339	438.7	10325	1007.8	31547	5.9	0.2	No	5.95	6.31
						MEAN	6.2		Jqmp1 (untreated)	6.23	6.58
Jqmp1 (TA/CA)											
qmp1cata_1.1	356.9	9472	438.7	11309	1007.8	42003	5.5	0.1	No	5.54	5.93
qmp1cata_3.1	356.9	2885	438.7	9640	1007.8	27353	5.9	0.1	No	5.85	6.22
qmp1cata_4.1	356.9	10345	438.7	13340	1007.8	16361	6.3	0.2	No	6.29	6.63
qmp1cata_5.1	357.0	3874	438.7	7983	1007.8	27308	6.0	0.2	No	6.04	6.40
qmp1cata_6.1	356.9	6020	438.7	5987	1007.6	3082	19.1	8.1	No	19.15	19.26
qmp1cata_7.1	356.7	6083	438.7	10130	1007.8	31003	5.9	0.1	No	5.89	6.26
qmp1cata_8.1	355.1	4520	438.7	7906	1007.8	21080	5.7	0.1	No	5.67	6.06
qmp1cata_9.1	356.9	11769	439.1	3335	1007.8	11281	5.7	0.1	Yes	5.67	6.06
qmp1cata_10.1	356.4	7483	438.7	10964	1007.8	44515	5.5	0.1	No	5.49	5.88
qmp1cata_12.1	356.9	8742	438.7	6044	1007.8	8974	5.6	0.1	Yes	5.64	6.03
qmp1cata_13.1	356.9	5280	438.7	5059	1007.8	14971	8.0	0.2	No	8.01	8.28
qmp1cata_14.1	356.1	5582	438.7	8417	1007.8	25244	6.0	0.2	No	5.98	6.34
						MEAN	6.0		Jqmp1 (treated)	6.01	6.37
									All Jqmp1	6.11	
Jqmp1.5											
qmp1.5_1.1	354.8	11810	438.7	10822	1007.7	36134	5.8	0.2	No	5.83	6.21
qmp1.5_2.1	353.7	9769	438.7	13122	1005.9	49247	6.0	0.1	No	5.97	6.33
qmp1.5_4.2	354.7	8490	438.7	12384	1007.8	46932	6.0	0.2	No	6.04	6.40
qmp1.5_6.1	354.9	4082	438.7	6893	1007.8	25758	6.2	0.1	No	6.22	6.57
qmp1.5_8.1	354.9	7373	438.7	11850	1005.9	49393	5.8	0.2	No	5.77	6.14
qmp1.5_9.1	354.8	7349	438.7	10908	1005.9	41237	7.3	0.2	No	7.31	7.61
qmp1.5_10.1	354.8	13127	438.7	13022	1005.9	44848	5.8	0.1	No	5.80	6.18
qmp1.5_24.1	354.8	7638	438.7	13092	1007.8	34869	5.8	0.1	Yes	5.85	6.22
qmp1.5_25.1	354.8	11901	438.7	9922	1005.9	19082	6.3	0.2	Yes	6.30	6.65
qmp1.5_26.1	354.7	7873	438.7	12290	1005.9	45383	5.8	0.1	No	5.83	6.20
						MEAN	6.1		Jqmp1.5 (untr.)	6.09	6.45
Jqmp1.5 (TA/CA)											
qmp1.5cata_2.1	356.9	7797	438.7	5673	1007.8	10426	5.8	0.1	No	5.81	6.18
qmp1.5cata_3.1	356.9	5578	438.7	10176	1007.8	33145	5.7	0.2	No	5.72	6.10
qmp1.5cata_3.2	355.0	7047	438.7	13246	1007.8	46451	5.4	0.1	No	5.45	5.85
qmp1.5cata-4.1	354.8	10123	438.7	9916	1007.8	21782	5.7	0.1	No	5.70	6.08
qmp1.5cata-5.1	355.7	7697	438.7	13258	1007.8	47309	5.5	0.1	No	5.49	5.89
qmp1.5cata-6.1	355.0	9937	438.7	16148	1007.8	66492	5.5	0.1	No	5.45	5.85
qmp1.5cata-7.1	354.8	5833	438.7	15186	1007.8	31127	5.4	0.1	No	5.43	5.83
qmp1.5cata-8.1	356.9	15978	438.7	9944	1007.8	19989	5.5	0.1	No	5.55	5.94

Analysis	E_g (tetrahedron rotation, I)		A_{1g} (symmetric bending, υ_2)		B_{1g} (antisymmetric stretching, υ_3)				Extra Peaks?	Corrected FWHM	FWHM measured in Origin
	υ (cm^{-1})	I (counts)	υ (cm^{-1})	I (counts)	υ (cm^{-1})	I (counts)	FWHM (cm^{-1})	SE FWHM			
qmp1.5cata_10.1	356.9	15889	438.7	10972	1007.8	20329	5.8	0.1	No	5.77	6.15
qmp1.5cata_12.1	354.8	13593	438.8	8206	1007.8	40640	5.2	0.1	No	5.17	5.59
qmp1.5cata_15.1	354.8	13151	438.7	5260	1007.8	21279	5.3	0.1	No	5.27	5.68
						MEAN	5.5		Jqmp1.5 (treated)	5.53	5.92
									All Jqmp1.5	5.80	
Jqmp2											
qmp2_1.1	355.0	5701	438.7	10168	1005.9	34630	6.0	0.2	No	6.01	6.37
qmp2_2.1	354.6	5891	438.7	8452	1005.9	29639	6.0	0.1	No	6.04	6.40
qmp2_3.1	354.8	9137	438.7	9937	1005.9	37981	5.5	0.1	No	5.55	5.94
qmp2_4.1	354.8	6243	438.7	9837	1007.8	25154	6.0	0.2	No	5.95	6.32
qmp2_5.1	354.8	6932	438.7	10572	1005.9	20884	5.7	0.1	Yes	5.67	6.06
qmp2_6.1	354.5	7647	438.7	13065	1007.8	42429	6.1	0.2	No	6.08	6.44
qmp2_7.1	355.0	2576	438.7	4214	1005.9	11732	6.3	0.2	No	6.30	6.64
qmp2_9.1	355.0	9789	438.7	18011	1005.9	48734	5.6	0.1	No	5.56	5.95
						MEAN	5.9		Jqmp2 (untr.)	5.90	6.27
Jqmp2 (TA/CA)											
qmp2cata_1.1	354.8	11808	438.7	8494	1007.8	29553	5.4	0.1	No	5.45	5.85
qmp2cata_2.1	355.9	5096	438.7	13708	1007.8	59662	5.3	0.1	No	5.28	5.69
qmp2cata_3.1	354.8	6088	438.7	9676	1007.8	12902	5.9	0.2	Yes	5.89	6.26
qmp2cata_4.1	354.9	6670	438.7	11842	1007.8	46228	5.2	0.1	No	5.20	5.62
qmp2cata_5.1	355.6	8230	438.7	10937	1007.8	41850	5.5	0.1	No	5.54	5.93
qmp2cata_6.1	355.9	6681	438.7	10695	1007.8	42205	5.6	0.1	No	5.55	5.94
qmp2cata_8.1	355.9	6287	438.7	9695	1007.8	36180	5.6	0.1	No	5.60	5.99
qmp2cata_10.1	356.5	4420	438.7	10913	1007.8	37266	5.3	0.1	No	5.28	5.69
						MEAN	5.5		Jqmp2 (treated)	5.47	5.87
									All Jqmp2	5.68	
Jqmp3											
qmp3_5.1	354.8	11948	438.7	4917	1005.9	15240	5.6	0.1	Yes	5.56	5.95
qmp3_6.1	354.8	9628	438.7	13522	1007.8	10893	5.8	0.2	Yes	5.78	6.16
qmp3_7.1	354.8	9914	436.8	4022	1004.0	11718	9.4	0.2	Yes	9.39	9.62
qmp3_8.1	354.8	10826	438.7	7136	1005.9	13093	6.2	0.2	Yes	6.19	6.54
qmp3_17.1	354.8	8762	438.7	10154	1005.9	36075	6.6	0.2	No	6.64	6.97
qmp3_18.1	354.8	9184	438.7	10811	1005.9	29040	6.5	0.2	No	6.49	6.83
qmp3_19.1	354.8	11919	438.7	13203	1005.9	49568	5.6	0.1	No	5.59	5.98
qmp3_20.1	354.9	8085	438.7	13275	1005.9	49312	5.9	0.2	No	5.93	6.30
						MEAN	6.5		Jqmp3 (untr.)	6.45	6.79
Jqmp3 (TA/CA)											
qmp3cata_1.1	354.8	9442	438.7	9089	1007.8	17582	6.1	0.2	Yes	6.07	6.43
qmp3cata_2.1	354.6	9072	438.7	17029	1007.8	53575	5.6	0.1	No	5.62	6.00
qmp3cata_3.1	354.8	11331	438.7	5212	1007.8	22634	5.4	0.1	No	5.45	5.84
qmp3cata_4.1	354.8	13152	438.7	9665	1007.8	7343	5.5	0.2	Yes	5.53	5.92
qmp3cata_6.1	354.8	9613	438.7	8059	1007.5	3878	6.1	0.4	Yes	6.12	6.47
qmp3cata_7.1	356.0	7243	437.6	9732	1007.8	46867	5.1	0.1	No	5.13	5.55
qmp3cata_10.1	356.8	2770	438.7	12385	1007.8	50672	5.3	0.1	No	5.29	5.70
						MEAN	5.6		Jqmp3 (treated)	5.60	5.99
									All Jqmp3	6.05	

Analysis	E_g (tetrahedron rotation, I)		A_{1g} (symmetric bending, υ_2)		B_{1g} (antisymmetric stretching, υ_3)				Extra Peaks?	Corrected FWHM	FWHM measured in Origin
	υ (cm^{-1})	I (counts)	υ (cm^{-1})	I (counts)	υ (cm^{-1})	I (counts)	FWHM (cm^{-1})	SE FWHM			
Jbqm											
bqm_1.1	355.1	7261	438.7	11742	1007.8	48644	5.8	0.1	No	5.79	6.17
bqm_2.1	355.2	8115	438.7	15320	1007.8	65238	5.7	0.1	No	5.68	6.06
bqm_3.1	354.8	10398	438.7	10987	1005.9	40608	6.7	0.2	No	6.71	7.04
bqm_4.1	354.8	9829	438.7	10606	1005.9	38612	7.0	0.2	No	7.04	7.36
bqm_6.1	355.2	7711	438.7	13662	1007.8	57445	5.6	0.1	No	5.61	5.99
bqm_7.1	354.6	7095	438.7	10731	1005.9	43454	6.4	0.2	No	6.39	6.73
bqm_8.1	355.0	8679	438.7	14669	1005.9	63554	6.0	0.2	No	5.95	6.32
bqm_9.1	354.6	6630	438.7	10998	1007.8	41465	5.9	0.1	No	5.93	6.30
						MEAN	6.1		Jbqm (untreated)	6.14	6.50
Jbqm (TA/CA)											
bqmcata_1.1	355.3	11287	438.7	15939	1007.8	58117	5.8	0.1	No	5.81	6.18
bqmcata_9.1	356.2	3452	438.7	6321	1007.8	15551	5.9	0.2	No	5.94	6.30
bqmcata_10.1	354.6	5688	438.7	7701	1007.8	24091	6.8	0.2	No	6.75	7.08
bqmcata_11.1	355.1	6753	438.7	12764	1007.8	36348	5.4	0.1	No	5.35	5.76
bqmcata_12.1	356.9	9810	438.7	8119	1007.8	20578	5.7	0.1	No	5.69	6.07
bqmcata_13.1	354.8	5298	438.7	6530	1007.8	17050	6.6	0.1	No	6.62	6.95
bqmcata_14.1	355.7	4810	438.7	8428	1007.8	34001	5.2	0.1	No	5.22	5.63
bqmcata_15.1	355.5	7884	438.7	14399	1007.8	63856	5.6	0.1	No	5.55	5.94
						MEAN	5.9		Jbqm (treated)	5.87	6.24
									All Jbqm	6.00	
Jpqm											
pqm_2.1	354.6	3271	439.5	4425	1005.9	19353	5.7	0.2	No	5.71	6.09
pqm_5.1	354.8	2817	436.7	4023	1005.9	5276	6.6	0.2	Yes	6.55	6.89
pqm_6.1	354.6	3306	438.7	5283	1005.9	18484	6.3	0.2	No	6.30	6.65
pqm_9.1	354.6	2889	438.7	4184	1005.9	14750	6.7	0.2	No	6.72	7.05
pqm_10.1	353.5	3123	438.7	4246	1005.9	13756	7.9	0.4	No	7.90	8.18
						MEAN	6.3		Jpqm (untreated)	6.32	6.67
Jpqm (TA/CA)											
pqmcata_1.1	354.8	2175	438.7	1868	1005.0	868	3.6	0.2	Yes	3.57	4.15
pqmcata_2.1	354.8	3998	438.7	5317	1007.8	8678	5.7	0.3	Yes	5.67	6.05
pqmcata_3.1	354.8	3817	438.7	4319	1007.8	9953	5.5	0.1	Yes	5.49	5.88
pqmcata_6.1	355.8	2910	438.7	4796	1007.8	19105	4.9	0.1	No	4.93	5.36
pqmcata_8.1	354.8	3316	438.7	4773	1007.8	16556	5.5	0.2	No	5.46	5.86
						MEAN	4.9		Jpqm (treated)	5.03	5.46
									All Jpqm	5.83	

Analysis	E_g (tetrahedron rotation, I)		A_{1g} (symmetric bending, υ_2)		B_{1g} (antisymmetric stretching, υ_3)				Extra Peaks?	Corrected FWHM	FWHM measured in Origin
	υ (cm^{-1})	I (counts)	υ (cm^{-1})	I (counts)	υ (cm^{-1})	I (counts)	FWHM (cm^{-1})	SE FWHM			
Jgd											
gd_1.1	353.5	2497	438.1	4478	1005.9	19662	6.5	0.2	No	6.53	6.86
gd_2.1	352.7	649	436.7	602	1004.0	935	6.8	0.2	Yes	6.81	7.13
gd_3.1	354.8	3885	438.7	2949	1005.9	6952	6.4	0.2	No	6.42	6.76
gd_4.1	354.3	2530	438.7	3347	1004.0	11467	7.0	0.2	No	6.97	7.29
gd_5.1	354.8	1986	438.7	3038	1005.9	3943	7.4	0.2	Yes	7.36	7.66
						MEAN	6.8		Jgd (untreated)	6.82	7.14
Jgd (TA/CA)											
gdcata_2.1	354.8	2972	438.7	5100	1005.9	19468	5.9	0.2	No	5.86	6.24
gdcata_3.1	354.6	2696	436.7	3905	1005.9	13243	7.7	0.2	No	7.66	7.95
gdcata_4.1	354.7	5514	438.7	7496	1005.9	22383	7.9	0.3	No	7.91	8.19
gdcata_7.1	354.8	3788	438.7	3082	1005.9	4077	6.7	0.2	Yes	6.72	7.05
gdcata_11.1	354.8	2973	438.7	3648	1005.9	3910	7.5	0.3	Yes	7.46	7.75
						MEAN	7.1		Jgd (treated)	7.12	7.44
									All gd	6.97	
Mt. Dromedary											
MtD_27.2	352.7	6111	438.7	10792	1005.9	8946	10.0	0.3	Yes	9.82	10.05
MtD_28.1	354.2	2420	438.7	13704	1005.9	39378	6.4	0.2	No	6.05	6.41
MtD_29.1	354.8	13772	438.7	10664	1005.9	27370	6.7	0.2	No	6.31	6.66
MtD_31.2	353.2	6673	438.7	12445	1005.9	52781	6.9	0.2	No	6.59	6.93
						MEAN	7.5		Mt. Drom. (untr.)	7.20	7.51
Mt. Dromedary (TA/CA)											
MtDC_24.1	354.8	6738	438.7	4795	1007.8	6037	6.8	0.2	Yes	6.43	6.77
MtDC_25.1	356.9	12619	438.7	9716	1007.8	32636	6.1	0.1	No	5.69	6.07
MtDC_26.2	355.2	9259	438.7	14470	1007.8	44230	6.3	0.2	No	5.94	6.30
MtDC_27.1	355.0	5293	438.7	9778	1007.8	40306	6.7	0.2	No	6.37	6.71
						MEAN	6.5		Mt. Drom. (treat.)	6.10	6.46
									All Mt. Drom.	6.65	

APPENDIX C: Petrographic Descriptions

Table C1. Petrography of Yerington mine rocks

Jqmp1

Mineralogy	Plagioclase	Orthoclase	Quartz	Hornblende	Biotite	Opaques (mt, il, Cu-S minerals)	Alteration minerals
Mode	5%	10%	70%	<5%	trace	<10%	trace
Textures	anhedral; microlites to ~200x200 µm; surrounded by hbl shreds in veins between qtz	30% as microlites up to 40 µm long; anhedral and ratty edged; >1x1 mm max, avg 500 µm; highly included	60% as patches of anhedral grains ~100-200 x ≤ 500 µm, roughly equant and intergrown; many grains mottled; v.fg. grains in microveins and included in larger xtal portion	Only as small anhedral xtals in vein-like structures	~40 x 100 µm shreds surrounded by minor chl(?) and hbl in veins between qtz; secondary	Highly anhedral and space-filling in clumps and masses; not evenly distributed	Sericite with minor chl; shreddy laths; usually in clumps and filling cracks, or concentrated around qtz grains
Description	There appear to be 3 main textural components: 1) the original (now altered) groundmass w/ Kspar>plag>qtz, ~40%; 2) the results of QSP alteration--large rextal qtz patches, ~40%; and 3) vein-like structures that run through and between 1 + 2 w/ shreddy hbl, ep, v.fg. qtz, and large amounts of opaques.						

Jqmp1.5

Mineralogy	Plagioclase	Orthoclase	Quartz	Muscovite	Biotite	Opaques (mt, il, Cu-S minerals)	Alteration minerals	Accessories
Mode	30%	10%	30%	5%	10%	trace	~5%	trace
Textures	20% as euhedral phenos ~2.5x1.5 mm avg, up to >3 x >2 mm; a few phenos broken and subhedral; 10% as v.fg., anhedral in g'mass	5% as euhedral phenos ~150x200 µm avg; likely in g'mass but masked by overprint	10% in g'mass overprinted by sericite; 20% as v.fg. grains in vein, xtal w/diffuse boundaries	Anhedral shreds; likely from alteration	~50 x 100 µm avg (500x50 µm max) anhedral shreds w/ musc + v.fg. qtz; secondary	Anhedral clusters concentrated in veins w/ v.fg. qtz + bt/musc	Pervasive (>95% overprint) sericite with 5% chl and trace epidote; chl in veins b/w large qtz xtlas; also around feldspar in g'mass; ep anhedral in veins	Zircon 60x20 µm to 50x100 µm
Description	There appear to be 3 main textural components: 1) the original (now altered) groundmass w/ Kspar~plag>qtz, v.fg. and ~20-25% large phenos of plag and Kspar; 2) qtz/mica veins that cut g'mass up to 1 mm thick. Qtz is rextal with 2ndary micas/opaques; and 3) late sericitic alteration added veneer of sericite to everything, rendering ovservation of initial textures difficult.							

Table C1. Petrography of Yerington mine rocks

Jqmp2

Mineralogy	Plagioclase	Orthoclase	Quartz	Trace minerals	Opaques (mt, il, Cu-S minerals)	Alteration minerals
Mode	30%	20%	30%	trace	0.05	0.15
Textures	Transitioning to Kspar; 25% an-to-euhedral phenos; grains 2x1mm avg; equigranular; 5% g'mass	5% as g'mass; 15% as sub-to-anhedral phenos up to 5x3mm; no visible zoning	10% in masses, ~100x100 µm max size ; 20% anhedral, in veins, 150x150 µm to 750 µm x 200 mm and rextal/intergrown; 1-2 eyes 1x1 mm	Zircon in trace amounts	Highly anhedral and space-filling in clumps and masses; not evenly distributed	Sericite with 5% chl in shreddy laths; 10% 2ndary epidote and clinozoisite, anhedral
Description	There appear to be 3 main textural components: 1) primary texture is porphyritic w/ large proportion of phenocrysts ; 2) sericitic and potassic alteration overprints, causing plag-->Kspar+chl; and 3) late silicic alteration in veins --> qtz overprint					

Jqmp3

Mineralogy	Plagioclase	Orthoclase	Quartz	Muscovite	Biotite	Opaques (mt, il, Cu-S minerals)	Alteration minerals	Accessories
Mode	40%	35%	10%	5-8%	trace	1%	trace	~2%
Textures	25% euhedral phenocryst laths >3 x >1 mm max, avg 1x2 mm; 15% g'mass; overprinted w/ sericite and transitioning to Kspar	20% as euhedral phenos ~3x1.5 mm w/ rxn rims and plentiful microlite inclusions; ~5% in g'mass but masked by overprint	5-10 eyes ~1x1 mm; most isolated grains subhedral 200x200 µm avg	Replacing bt books, an-euhedral	Pseudo- morphs of bt	Anhedral interstitial blebs up to 500 µm x 500 µm	Isolated clumps of chl and epidote and sericite overprint	Trace zircon; 2% euhedral titanite 500 x 200 µm avg up to >1mm x 500 µm
Description	Fine-grained groundmass dominated by phenocrysts (~15-20% g'mass, 80-85% phenos) overprinted by sericite. Late qtz alteration formed qtz eyes.							

Table C1. Petrography of Yerington mine rocks

Jbqm

Mineralogy	Plagioclase	Orthoclase	Quartz	Hornblende	Accessories	Opaques (mt, il, Cu-S minerals)	Alteration minerals
Mode	20%	25%	25%	15%	5%	trace	~10%
Textures	Phenos transitioning to Kspar; oscillatory zoning; ~500 x 700 µm avg; highly included	Highly included w/ sericite overprint; 600x700 µm avg size, equigranular	Anhedral and interstitial w/ undulose ext., likely late-stage rextal; ~500x500 µm avg, equigranular	Max 750 x 750 µm, avg 350 x 400 µm; clumped anhedral shreds	Zircon, apatite, allanite/chevkinite, muscovite in trace amounts	Interstitial and in veins	Sericite with trace clinozoisite
Description	Equigranular, medium to fine-grained, with some alteration. Most of original texutre and structure intact. One ~750 µm-wide qtz vein w/ central location surrounded by qtz dominates section.						

Jpqm

Mineralogy	Plagioclase	Orthoclase	Quartz	Accessories	Biotite	Opaques (mt, il, Cu-S minerals)	Alteration minerals
Mode	25%	25%	40%	~3%	~2%	0%	5%
Textures	Highly included phenos >3 x 1.5 mm, eu- to subhedral tabular	Phenos up to 5 x 3 mm, highly included; prominent oscillatory zoning; tabular subhedral	15% as euhedral phenos 3x2 mm max, 1x1 mm avg, anhedral and equant; 25% in g'mass, ~50x100 µm avg, equant and anhedral; all have rextal textures	~2-3% allanite (being replaced by epidote); trace titanite (being replaced by (likely) leucoxene); trace zircon	Subhedral grains with ratty edges; ~1x1 mm max, 500x200 µm most common	None seen	5% epidote/clinozoisite in multiple generations; trace chl associated w/ bt
Description	Overall strongly porphyritic w/ >>50% phenocrysts and only ~25% definite g'mass. Sericitic and silicic alteration minor. No veins or opaques.						

Table C1. Petrography of Yerington mine rocks

Jgd								
Mineralogy	Plagioclase	Orthoclase	Quartz	Hornblende	Biotite	Opaques (mt, il, Cu-S minerals)	Alteration minerals	Muscovite
Mode	30%	30%	20%	2%	10%	trace	~3%	~5%
Textures	Highly sericitzed and converting to Kspar; highly included; eu- to subhedral, 2x2 mm max, 1.5 x 1.75 mm avg, tabular to square	Highly sericitized, eu- to subhedral tabular; 3x2 mm max, avg ~1.5 x 1 mm	Space-filling anhedral w/ undulose ext. and possible suturing; 1x1 mm max, 500 x 500 µm avg, generally ~equant	Anhedral and shreddy grains, ~ 3x3 mm	Shreddy an- to subhedral grains, avg 1 x 0.5 mm	Interstitial and very minor	Epidote interstitial 200x300 µm xtals, roughly equant, subhedral; sericite overprint	Zircon, apatite, allanite/chevkinite, muscovite in trace amounts
Description	Feldspar-dominated original texture w/ minor later qtz alteration and pervasive sericitization.							

Table C2. Petrography of Árnes and Hrafnfjörður rocks

ÁrE1301 (Tr4 rhyolite)

Mineralogy	Plagioclase	Cpx
Mode	15%	5%
Textures	10% as eu- to subhedral tabular phenocrysts; range from 150 x 150 µm to 1.1 x 1.1 mm; oscillatory zoning common; ubiquitous simple twins; 5% as v.f.g. microlites in groundmass glass to yield felty texture	Eu-to subhedral; max size 250 x 400 µm, avg. 200 x 100 µm; occasional embayments and skeletal grains
Description	Porphyritic with glass-dominated groundmass.	

ÁrE1302 (Tr1 rhyolite)

Mineralogy	Plagioclase	(C?)px	Opaques	Alteration Min.
Mode	60%	10%	30%	trace
Textures	V.f.g. microlites and subhedral laths ≤ 30 x 30 µm; lineated to produce trachytic texture; in groundmass with glass	≤20 x 20 µm subhedral to anhedral grains, equant to elongate	≤20 x 20 µm eu- to subhedral grains, equant, evenly distributed; likely Mt based on magnetism of hand sample	Something brown
Description	Equigranular, fine-grained w/ homogeneous mineralogy in plag/px/mt; slight lineation esp. in plag sub-horizontal; rare plag + px phenos (<5 in thin section)			

Table C2. Petrography of Árnes and Hrafnfjörður rocks

ÁrE1303 (Tr2 rhyolite)

Mineralogy	Plagioclase	Cpx	Alteration min.
Mode	18%	12%	10%
Textures	As phenocrysts, avg. ~750 x 700 µm, but glomerocrysts up to 2.5x2.5 mm; elongate to tabular, eu- to subhedral; zoning common	2 populations, each ~50% of cpx total: 1) altered to brown and sometimes completely replaced; 2) relatively unaltered. Both pops have microlite inclusions in xtals, sub- to anhedral. Avg. ~ 350 x 500 µm; max ~1.25 mm x 500 µm. Pop 1 xtals esp. form glomerocrysts w/in and near plag.	Brown and orange
Description	Porphyritic. Groundmass (70%) is vfg and glassy, with dendritic cystallites in some areas.		

ÁrE1304 (Tr3 rhyolite, top)

Mineralogy	Plagioclase	Cpx	Opaques
Mode	55%	<2%	3%
Textures	40% as phenocrysts; max size 1.5x1 mm, avg. ~ 1x1 mm; eu- to subhedral, zoned rims common; many grains with diffuse edges; a few small glomerocrysts <1.5 mm; 15% in g'mass <100 x 100 µm; eu- to anhedral, tabular to elongate; felty texture	Eu- to anhedral phenos ~150x150 µm or smaller; sometimes ratty or embayed	<50x50 µm, equant, square x-section; likely Mt
Description	Porphyritic with 40% glassy groundmass.		

Table C2. Petrography of Árnes and Hrafnfjörður rocks

ÁrE1305 (Tr3 rhyolite, bottom)

Mineralogy	Plagioclase	Cpx
Mode	15%	5%
Textures	Phenocrysts; max size 1.5x1 mm, avg. ~ 1x1 mm; eu- to subhedral, zoned rims common	Phenos ~200 x 200 µm; subhedral
Description	Porphyritic with 80% glassy groundmass.	

HfE1401 (Hrafnfjörður andesite [Tad])

Mineralogy	Plagioclase	Opx	Cpx	Opaques	Alteration min.
Mode	50%	20%	15%	15%	trace
Textures	40% as f.g. g'mass; equigranular 100x20 µm, eu- subhedral; aligned and often distorted around phenos; trachytic texture; 10% phenos 1 mm x 400 µm max; eu-subhedral tabs, zoned with relict rxn rim; some melt inclusions; frequently sub-horizontal w/ lineation	Sub- to anhedral, equigranular, slightly elongate to equant; avg. ~40 x 20 µm, occasional grains up to 100 x 40 µm	Anhedral and elongate to equant; avg. 40 x 30 µm, a few grains up to 100 x 60 µm	Eu- to anhedral; square x-section; 100x100 µm max, avg. 40 x 40 µm	Brown, diffuse
Description	Porphyritic w/ phaneritic g-mass in thin section (hand sample is all aphanitic) w/ plag + px phenos in g'mass displaying hoziontal/sub-horizontal lineation that phenos almost all follow. G'mass roughly equigranular. Plag phenos have relict rxn rims indicating multi-stage histories. Lineation from post-eruption flow???				

Table C2. Petrography of Árnes and Hrafnfjörður rocks

HfE1402 (Hrafnfjörður dacite dome [Tdh])

Mineralogy	Plagioclase	Hbl (?)	Fayalite	Opaques	Alteration min.
Mode	40%	<5%	5%	5%	trace
Textures	30% phenocrysts alined w/ lineation, 10% in g'mass; euhedral laths to subhedral w/shreddy edges; avg. 20 x 5 µm (>90% of phenos) but from 75x15 µm to vfg in g'mass; trachytic texture	Elongate to needle-like; subhedral w/ ratty edges; undergoing replacement?	Sub- and anhedral and patchy/ratty; <100 x 100 µm avg.	<<50 x 50 µm, equant, square x-section, euhedral; likely Mt	Brown alteration min. in g'mass, but not in plag
Description	Aphanitic, equigranular in hand sample and very dark; thin section is porphyritic w/ at least 2 iterations of plag as phenos, along with hbl (?) and fayalite. G'mass is aphanitic trending toward phaneritic, and both g'mass and phenos define a lineation.				

HfE1403 (Hrafnfjörður lava[?])

Mineralogy	Plagioclase	Opx	Cpx	Opaques	Quartz	Alteration min.
Mode	47%	15%	5%	8%	5%	5%
Textures	40% in g'mass; ~equigranular 200x40 µm, eu- subhedral laths; horizontal/sub-horiz lineation wraps around phenos; trachytic; 7% as phenos ranging from 200x500 µm to 2x2 mm; intricate zoning, sieve texture rims, and melt inclusions; many grains have relict resorption forms in interior	Sub- to anhedral, elongate to equant; avg. ~20 x 80 µm with rounded corners common	Sub- to anhedral, elongate to equant; avg. ~60 x 80 µm, max. 100 x 200 µm; 1 grain 360x 360 µm	Eu- to subhedral; evenly dispersed; 80x80 µm max, avg. and majority 15 x 15 µm	Anhedral w/ melt pockets and embayments; 1x1 mm to 400x400 µm	Zeolites, palagonite, and brown mineral
Description	Porphyritic w/ phaneritic g-mass in thin section w/ plag + px phenos in g'mass displaying hoziontal/sub-horizontal lineation that phenos almost all follow. Plag phenos show clear evidence of multi-stage histories.					

APPENDIX D: Zircon Oxygen Isotope Analyses

Table D1. Yerington *in situ* zircon oxygen isotope compositions

Spot Name	Mount	Date	^{16}O Measured	^{16}O Error	^{18}O Measured	^{18}O Error	$\delta^{18}O$ Raw	$\delta^{18}O$ Error	$^{18}O/^{16}O$ Measured	$^{18}O/^{16}O$ Error	Corrected $^{18}O/^{16}O$	Corrected $\delta^{18}O$ (‰)	Total Error (2σ SE)	Internal Error (1σ)
Jqmp1 (untreated)														
q1@3.ais	TJB.12	Dec. 2014	3.51E+09	7.59E+06	7.06E+06	1.47E+04	2.88	1.08E-01	2.0110E-03	2.17E-07	0.00201651	5.64	0.68	0.11
q1@5.ais	TJB.12	Dec. 2014	3.52E+09	6.94E+06	7.09E+06	1.33E+04	3.23	9.05E-02	2.0117E-03	1.82E-07	0.00201722	6.00	0.67	0.09
q1@6.ais	TJB.12	Dec. 2014	3.55E+09	8.04E+06	7.14E+06	1.60E+04	3.05	5.60E-02	2.0113E-03	1.13E-07	0.00201687	5.82	0.65	0.06
q1@7.ais	TJB.12	Dec. 2014	3.71E+09	1.04E+07	7.46E+06	2.05E+04	1.79	6.82E-02	2.0088E-03	1.37E-07	0.00201433	4.55	0.65	0.07
q1@8.ais	TJB.12	Dec. 2014	3.52E+09	6.18E+06	7.08E+06	1.23E+04	3.15	1.05E-01	2.0115E-03	2.11E-07	0.00201708	5.92	0.67	0.10
q1@14.ais	TJB.12	Dec. 2014	3.55E+09	6.08E+06	7.14E+06	1.19E+04	2.86	6.55E-02	2.0109E-03	1.32E-07	0.00201649	5.63	0.65	0.07
q1@15.ais	TJB.12	Dec. 2014	3.52E+09	7.10E+06	7.09E+06	1.42E+04	3.16	3.12E-02	2.0115E-03	6.27E-08	0.00201709	5.93	0.64	0.03
q1@16.ais	TJB.12	Dec. 2014	3.55E+09	6.90E+06	7.14E+06	1.32E+04	2.90	1.05E-01	2.0110E-03	2.12E-07	0.00201657	5.67	0.67	0.11
q1@17.ais	TJB.12	Dec. 2014	3.55E+09	6.80E+06	7.14E+06	1.30E+04	2.85	1.13E-01	2.0109E-03	2.28E-07	0.00201647	5.62	0.68	0.11
q1@19.ais	TJB.12	Dec. 2014	3.55E+09	6.28E+06	7.13E+06	1.20E+04	2.58	1.12E-01	2.0104E-03	2.26E-07	0.00201591	5.34	0.68	0.11
q1@20.ais	TJB.12	Dec. 2014	3.54E+09	7.39E+06	7.11E+06	1.42E+04	2.56	1.30E-01	2.0103E-03	2.62E-07	0.00201588	5.33	0.69	0.13
q1@24.ais	TJB.12	Dec. 2014	3.55E+09	5.96E+06	7.13E+06	1.17E+04	2.47	1.04E-01	2.0101E-03	2.09E-07	0.00201569	5.23	0.67	0.10
q1@30.ais	TJB.12	Dec. 2014	3.56E+09	7.23E+06	7.16E+06	1.43E+04	2.99	4.83E-02	2.0112E-03	9.71E-08	0.00201674	5.75	0.65	0.05
q1@28.ais	TJB.12	Dec. 2014	3.53E+09	7.68E+06	7.11E+06	1.56E+04	3.04	9.67E-02	2.0113E-03	1.95E-07	0.00201684	5.81	0.67	0.10
q1@29.ais	TJB.12	Dec. 2014	3.54E+09	5.94E+06	7.11E+06	1.16E+04	2.63	8.40E-02	2.0105E-03	1.69E-07	0.00201603	5.40	0.66	0.08
Jqmp1 (treated)														
q1cata@14.ais	TJB.12	Dec. 2014	3.45E+09	5.97E+06	6.94E+06	1.20E+04	3.11	3.82E-02	2.0114E-03	7.68E-08	0.00201699	5.88	0.64	0.04
q1cata@13.ais	TJB.12	Dec. 2014	3.55E+09	6.83E+06	7.13E+06	1.34E+04	2.74	6.73E-02	2.0107E-03	1.35E-07	0.00201624	5.51	0.65	0.07
q1cata@3.ais	TJB.12	Dec. 2014	3.52E+09	6.78E+06	7.09E+06	1.35E+04	2.62	6.08E-02	2.0104E-03	1.22E-07	0.00201600	5.38	0.65	0.06
q1cata@9.ais	TJB.12	Dec. 2014	1.70E+09	1.04E+06	3.39E+06	2.00E+03	-5.02	2.19E-01	1.9951E-03	4.37E-07	0.00200064	-2.28	0.78	0.22
q1cata@11.ais	TJB.12	Dec. 2014	3.54E+09	1.18E+07	7.09E+06	2.30E+04	-0.73	1.12E-01	2.0037E-03	2.24E-07	0.00200926	2.02	0.68	0.11
Jqmp1.5 (untreated)														
q15@2.ais	TJB.12	Dec. 2014	3.48E+09	7.44E+06	7.01E+06	1.43E+04	3.23	1.08E-01	2.01E-03	2.17E-07	0.00201723	6.00	0.68	0.11
q15@3.ais	TJB.12	Dec. 2014	3.57E+09	8.33E+06	7.17E+06	1.64E+04	2.21	6.62E-02	2.01E-03	1.33E-07	0.00201517	4.97	0.65	0.07
q15@4.ais	TJB.12	Dec. 2014	3.52E+09	7.08E+06	7.09E+06	1.39E+04	3.01	8.14E-02	2.01E-03	1.64E-07	0.00201678	5.78	0.66	0.08
q15@5.ais	TJB.12	Dec. 2014	3.51E+09	8.88E+06	7.05E+06	1.76E+04	2.07	5.59E-02	2.01E-03	1.12E-07	0.00201491	4.84	0.65	0.06
q15@6.ais	TJB.12	Dec. 2014	3.51E+09	6.78E+06	7.07E+06	1.33E+04	2.97	8.85E-02	2.01E-03	1.78E-07	0.00201670	5.74	0.66	0.09
q15@10.ais	TJB.12	Dec. 2014	3.53E+09	6.40E+06	7.10E+06	1.22E+04	2.57	1.03E-01	2.01E-03	2.07E-07	0.00201591	5.34	0.67	0.10
q15@11.ais	TJB.12	Dec. 2014	3.47E+09	6.53E+06	6.99E+06	1.29E+04	3.08	1.05E-01	2.01E-03	2.11E-07	0.00201693	5.85	0.67	0.10
q15@12.ais	TJB.12	Dec. 2014	3.52E+09	6.98E+06	7.08E+06	1.38E+04	2.86	8.18E-02	2.01E-03	1.65E-07	0.00201648	5.63	0.66	0.08
q15@24.ais	TJB.12	Dec. 2014	3.50E+09	5.54E+06	7.03E+06	1.08E+04	2.71	6.47E-02	2.01E-03	1.30E-07	0.00201619	5.48	0.65	0.06
q15@26.ais	TJB.12	Dec. 2014	3.49E+09	6.68E+06	7.03E+06	1.32E+04	3.05	8.27E-02	2.01E-03	1.66E-07	0.00201686	5.82	0.66	0.08
q15@28.ais	TJB.12	Dec. 2014	3.51E+09	7.89E+06	7.06E+06	1.54E+04	2.37	9.30E-02	2.01E-03	1.87E-07	0.00201549	5.13	0.67	0.09
Jqmp1.5 (treated)														
q15cata@1.ais	TJB.12	Dec. 2014	3.45E+09	4.97E+06	6.92E+06	1.00E+04	0.63	5.33E-02	2.01E-03	1.07E-07	0.00201199	3.39	0.65	0.05
q15cata@2.ais	TJB.12	Dec. 2014	3.46E+09	2.97E+06	6.94E+06	5.64E+03	0.99	7.53E-02	2.01E-03	1.51E-07	0.00201272	3.75	0.66	0.08
q15cata@3.ais	TJB.12	Dec. 2014	3.53E+09	7.05E+06	7.09E+06	1.37E+04	2.06	1.01E-01	2.01E-03	2.03E-07	0.00201487	4.82	0.67	0.10
q15cata@7.ais	TJB.12	Dec. 2014	3.36E+09	1.10E+07	6.72E+06	2.13E+04	-1.03	1.11E-01	2.00E-03	2.21E-07	0.00200866	1.72	0.68	0.11
q15cata@8.ais	TJB.12	Dec. 2014	3.56E+09	2.78E+07	7.14E+06	5.51E+04	0.78	1.11E-01	2.01E-03	2.22E-07	0.00201229	3.54	0.68	0.11
q15cata@9.ais	TJB.12	Dec. 2014	3.50E+09	1.21E+07	7.03E+06	2.36E+04	-0.04	1.03E-01	2.01E-03	2.07E-07	0.00201064	2.71	0.67	0.10
Jqmp2 (untreated)														
q2@2.ais	TJB.12	Dec. 2014	3.50E+09	7.90E+06	7.03E+06	1.57E+04	1.17	5.89E-02	2.01E-03	1.18E-07	0.00201308	3.93	0.65	0.06
q2@5.ais	TJB.12	Dec. 2014	3.48E+09	7.01E+06	7.00E+06	1.38E+04	2.49	9.16E-02	2.01E-03	1.84E-07	0.00201573	5.25	0.67	0.09

RED analysis is partially off the grain or on an inclusion or crack, not included in sample average

Table D1. Yerington *in situ* zircon oxygen isotope compositions

Spot Name	Mount	Date	^{16}O Measured	^{16}O Error	^{18}O Measured	^{18}O Error	$\delta^{18}O$ Raw	$\delta^{18}O$ Error	$^{18}O/^{16}O$ Measured	$^{18}O/^{16}O$ Error	Corrected $^{18}O/^{16}O$	Corrected $\delta^{18}O$ (‰)	Total Error (2σ SE)	Internal Error (1σ)
q2@6.ais	TJB.12	Dec. 2014	3.49E+09	5.72E+06	7.02E+06	1.15E+04	2.49	7.27E-02	2.01E-03	1.46E-07	0.00201574	5.26	0.66	0.07
q2@7.ais	TJB.12	Dec. 2014	3.49E+09	6.46E+06	7.01E+06	1.26E+04	2.60	6.64E-02	2.01E-03	1.33E-07	0.00201597	5.37	0.65	0.07
q2@8.ais	TJB.12	Dec. 2014	3.49E+09	6.37E+06	7.01E+06	1.23E+04	2.44	1.01E-01	2.01E-03	2.02E-07	0.00201564	5.21	0.67	0.10
q2@10.ais	TJB.12	Dec. 2014	3.46E+09	6.17E+06	6.95E+06	1.23E+04	2.46	6.48E-02	2.01E-03	1.30E-07	0.00201569	5.23	0.65	0.06
q2@12.ais	TJB.12	Dec. 2014	3.49E+09	7.33E+06	7.01E+06	1.44E+04	2.28	9.66E-02	2.01E-03	1.94E-07	0.00201533	5.05	0.67	0.10
q2@14.ais	TJB.12	Dec. 2014	3.46E+09	6.80E+06	6.96E+06	1.34E+04	2.86	1.32E-01	2.01E-03	2.66E-07	0.00201648	5.63	0.69	0.13
q2@15.ais	TJB.12	Dec. 2014	3.54E+09	6.70E+06	7.12E+06	1.31E+04	2.37	9.83E-02	2.01E-03	1.98E-07	0.0020155	5.14	0.67	0.10
q2@18.ais	TJB.12	Dec. 2014	3.49E+09	6.51E+06	7.02E+06	1.27E+04	2.38	7.14E-02	2.01E-03	1.43E-07	0.00201552	5.15	0.66	0.07
q2@19.ais	TJB.12	Dec. 2014	3.44E+09	6.43E+06	6.92E+06	1.24E+04	2.95	9.05E-02	2.01E-03	1.82E-07	0.00201667	5.72	0.67	0.09
q2@20.ais	TJB.12	Dec. 2014	3.52E+09	1.05E+07	7.06E+06	2.10E+04	0.94	3.38E-02	2.01E-03	6.78E-08	0.00201262	3.70	0.64	0.03
Jqmp2 (treated)														
q2cata@2.ais	TJB.12	Dec. 2014	3.46E+09	8.01E+06	6.95E+06	1.55E+04	1.30	9.00E-02	2.01E-03	1.81E-07	0.00201335	4.06	0.67	0.09
q2cata@4.ais	TJB.12	Dec. 2014	3.18E+09	1.51E+07	6.37E+06	2.98E+04	-1.47	8.95E-02	2.00E-03	1.79E-07	0.00200778	1.29	0.66	0.09
q2cata@5.ais	TJB.12	Dec. 2014	3.44E+09	5.28E+06	6.92E+06	1.03E+04	1.43	8.23E-02	2.01E-03	1.65E-07	0.00201362	4.20	0.66	0.08
q2cata@9.ais	TJB.12	Dec. 2014	3.46E+09	6.72E+06	6.95E+06	1.34E+04	1.99	5.39E-02	2.01E-03	1.08E-07	0.00201473	4.75	0.65	0.05
q2cata@10.ais	TJB.12	Dec. 2014	3.47E+09	5.36E+06	6.98E+06	1.03E+04	1.99	8.61E-02	2.01E-03	1.73E-07	0.00201474	4.76	0.66	0.09
q2cata@14.ais	TJB.12	Dec. 2014	3.31E+09	1.72E+06	6.64E+06	3.65E+03	-0.50	4.19E-02	2.00E-03	8.39E-08	0.00200973	2.26	0.65	0.04
q2cata@16.ais	TJB.12	Dec. 2014	3.47E+09	5.66E+06	6.97E+06	1.10E+04	2.06	7.68E-02	2.01E-03	1.54E-07	0.00201488	4.83	0.66	0.08
q2cata@17.ais	TJB.12	Dec. 2014	2.97E+09	1.42E+07	5.93E+06	2.83E+04	-4.82	4.12E-02	2.00E-03	8.22E-08	0.00200105	-2.07	0.65	0.04
Jqmp3 (untreated)														
q3@1.ais	TJB.12	Dec. 2014	2.91E+09	1.42E+07	5.83E+06	2.84E+04	-1.38	5.85E-02	2.00E-03	1.17E-07	0.00200796	1.38	0.65	0.06
q3@6.ais	TJB.12	Dec. 2014	3.46E+09	6.02E+06	6.96E+06	1.16E+04	2.28	9.14E-02	2.01E-03	1.84E-07	0.00201533	5.05	0.67	0.09
q3@12.ais	TJB.12	Dec. 2014	3.46E+09	7.39E+06	6.95E+06	1.44E+04	1.67	1.01E-01	2.01E-03	2.03E-07	0.00201409	4.44	0.67	0.10
q3@16.ais	TJB.12	Dec. 2014	3.40E+09	6.69E+06	6.83E+06	1.29E+04	2.27	9.50E-02	2.01E-03	1.91E-07	0.0020153	5.04	0.67	0.09
q3@14.ais	TJB.12	Dec. 2014	3.51E+09	1.05E+07	7.05E+06	2.07E+04	0.29	1.12E-01	2.01E-03	2.24E-07	0.00201131	3.05	0.68	0.11
q3@19.ais	TJB.12	Dec. 2014	3.41E+09	7.22E+06	6.86E+06	1.40E+04	2.37	7.80E-02	2.01E-03	1.57E-07	0.0020155	5.14	0.66	0.08
Jqmp3 (treated)														
q3cata@1.ais	TJB.12	Dec. 2014	3.17E+09	1.29E+07	6.34E+06	2.59E+04	-0.52	9.49E-02	2.00E-03	1.90E-07	0.00200969	2.24	0.67	0.09
q3cata@2.ais	TJB.12	Dec. 2014	3.47E+09	6.53E+06	6.96E+06	1.26E+04	1.98	9.78E-02	2.01E-03	1.97E-07	0.00201471	4.74	0.67	0.10
q3cata@6.ais	TJB.12	Dec. 2014	3.45E+09	5.94E+06	6.92E+06	1.15E+04	1.53	7.46E-02	2.01E-03	1.50E-07	0.00201382	4.30	0.66	0.07
Jbqm (untreated)														
bqm@1.ais	TJB.12	Dec. 2014	3.42E+09	5.56E+06	6.88E+06	1.10E+04	2.92	3.48E-02	2.01E-03	7.00E-08	0.0020166	5.69	0.64	0.03
bqm@2.ais	TJB.12	Dec. 2014	3.39E+09	7.17E+06	6.82E+06	1.41E+04	3.11	9.73E-02	2.01E-03	1.96E-07	0.00201699	5.88	0.67	0.10
bqm@3.ais	TJB.12	Dec. 2014	3.39E+09	1.46E+07	6.79E+06	2.92E+04	-0.28	8.05E-02	2.00E-03	1.61E-07	0.00201018	2.48	0.66	0.08
bqm@5.ais	TJB.12	Dec. 2014	3.46E+09	7.07E+06	6.95E+06	1.41E+04	2.51	8.03E-02	2.01E-03	1.61E-07	0.00201579	5.28	0.66	0.08
bqm@6.ais	TJB.12	Dec. 2014	3.47E+09	6.13E+06	6.99E+06	1.20E+04	2.69	7.73E-02	2.01E-03	1.55E-07	0.00201615	5.46	0.66	0.08
bqm@7.ais	TJB.12	Dec. 2014	3.44E+09	5.14E+06	6.92E+06	1.03E+04	2.81	6.33E-02	2.01E-03	1.27E-07	0.00201638	5.58	0.65	0.06
bqm@9.ais	TJB.12	Dec. 2014	3.45E+09	6.59E+06	6.94E+06	1.27E+04	2.50	1.06E-01	2.01E-03	2.12E-07	0.00201577	5.27	0.67	0.11
bqm@11.ais	TJB.12	Dec. 2014	3.48E+09	6.44E+06	6.99E+06	1.25E+04	2.46	8.73E-02	2.01E-03	1.75E-07	0.00201568	5.23	0.66	0.09
bqm@12.ais	TJB.12	Dec. 2014	3.46E+09	6.52E+06	6.97E+06	1.27E+04	2.93	8.62E-02	2.01E-03	1.73E-07	0.00201662	5.69	0.66	0.09
bqm@10.ais	TJB.12	Dec. 2014	3.51E+09	7.62E+06	7.06E+06	1.47E+04	2.18	1.03E-01	2.01E-03	2.06E-07	0.00201511	4.94	0.67	0.10
bqm@13.ais	TJB.12	Dec. 2014	3.47E+09	7.45E+06	6.97E+06	1.46E+04	2.87	6.61E-02	2.01E-03	1.33E-07	0.00201651	5.64	0.65	0.07
Jbqm (treated)														
bqmcata@1.ais	TJB.12	Dec. 2014	3.73E+09	9.45E+06	7.48E+06	1.87E+04	1.24	7.97E-02	2.01E-03	1.60E-07	0.00201323	4.01	0.66	0.08

RED analysis is partially off the grain or on an inclusion or crack, not included in sample average

Table D1. Yerington *in situ* zircon oxygen isotope compositions

Spot Name	Mount	Date	^{16}O Measured	^{16}O Error	^{18}O Measured	^{18}O Error	$\delta^{18}O$ Raw	$\delta^{18}O$ Error	$^{18}O/^{16}O$ Measured	$^{18}O/^{16}O$ Error	Corrected $^{18}O/^{16}O$	Corrected $\delta^{18}O$ (‰)	Total Error (2σ SE)	Internal Error (1σ)
bqmcata@2.ais	TJB.12	Dec. 2014	3.51E+09	5.99E+06	7.06E+06	1.21E+04	2.17	1.23E-01	2.01E-03	2.47E-07	0.0020151	4.93	0.69	0.12
bqmcata@11.ais	TJB.12	Dec. 2014	3.49E+09	6.82E+06	7.01E+06	1.31E+04	2.92	1.10E-01	2.01E-03	2.21E-07	0.00201661	5.69	0.68	0.11
bqmcata@12.ais	TJB.12	Dec. 2014	3.47E+09	7.81E+06	6.98E+06	1.52E+04	2.48	9.74E-02	2.01E-03	1.96E-07	0.00201571	5.24	0.67	0.10
bqmcata@13.ais	TJB.12	Dec. 2014	3.51E+09	6.95E+06	7.06E+06	1.39E+04	2.22	7.24E-02	2.01E-03	1.46E-07	0.0020152	4.99	0.66	0.07
bqmcata@14.ais	TJB.12	Dec. 2014	3.47E+09	6.07E+06	6.98E+06	1.18E+04	2.75	9.81E-02	2.01E-03	1.97E-07	0.00201627	5.52	0.67	0.10
Jpqm (untreated)														
pqm@5.ais	TJB.12	Dec. 2014	3.80E+09	1.06E+07	7.62E+06	2.11E+04	0.16	8.21E-02	2.01E-03	1.65E-07	0.00201106	2.92	0.66	0.08
pqm@6.ais	TJB.12	Dec. 2014	3.53E+09	6.07E+06	7.10E+06	1.19E+04	2.95	1.04E-01	2.01E-03	2.08E-07	0.00201666	5.72	0.67	0.10
pqm@7.ais	TJB.12	Dec. 2014	3.53E+09	6.37E+06	7.09E+06	1.24E+04	2.17	7.84E-02	2.01E-03	1.57E-07	0.00201509	4.93	0.66	0.08
pqm@8.ais	TJB.12	Dec. 2014	3.54E+09	6.66E+06	7.11E+06	1.31E+04	2.05	1.14E-01	2.01E-03	2.30E-07	0.00201486	4.82	0.68	0.11
pqm@10.ais	TJB.12	Dec. 2014	3.50E+09	6.14E+06	7.05E+06	1.17E+04	3.22	1.36E-01	2.01E-03	2.74E-07	0.0020172	5.99	0.70	0.14
pqm@11.ais	TJB.12	Dec. 2014	3.50E+09	6.61E+06	7.04E+06	1.30E+04	2.75	1.04E-01	2.01E-03	2.10E-07	0.00201627	5.52	0.67	0.10
pqm@12.ais	TJB.12	Dec. 2014	3.50E+09	7.78E+06	7.04E+06	1.54E+04	2.22	9.10E-02	2.01E-03	1.83E-07	0.0020152	4.99	0.67	0.09
pqm@13.ais	TJB.12	Dec. 2014	3.48E+09	6.20E+06	7.00E+06	1.23E+04	2.50	8.57E-02	2.01E-03	1.72E-07	0.00201575	5.26	0.66	0.09
pqm@14.ais	TJB.12	Dec. 2014	3.48E+09	6.36E+06	7.00E+06	1.28E+04	2.70	1.29E-01	2.01E-03	2.60E-07	0.00201615	5.46	0.69	0.13
pqm@20.ais	TJB.12	Dec. 2014	3.47E+09	9.64E+06	6.94E+06	1.93E+04	-1.31	8.95E-02	2.00E-03	1.79E-07	0.0020081	1.45	0.66	0.09
Jpqm (treated)														
pqmcata@1.ais	TJB.12	Dec. 2014	3.62E+09	9.88E+06	7.25E+06	1.90E+04	0.40	1.26E-01	2.01E-03	2.53E-07	0.00201154	3.16	0.69	0.13
pqmcata@2.ais	TJB.12	Dec. 2014	3.52E+09	4.53E+06	7.08E+06	9.06E+03	2.39	4.77E-02	2.01E-03	9.58E-08	0.00201554	5.16	0.65	0.05
pqmcata@4.ais	TJB.12	Dec. 2014	3.39E+09	1.24E+07	6.79E+06	2.47E+04	-0.14	8.47E-02	2.00E-03	1.70E-07	0.00201045	2.62	0.66	0.08
Jgd (untreated)														
gd@1.ais	TJB.12	Dec. 2014	3.44E+09	6.33E+06	6.92E+06	1.19E+04	3.11	1.23E-01	2.01E-03	2.48E-07	0.00201698	5.88	0.69	0.12
gd@5.ais	TJB.12	Dec. 2014	3.53E+09	1.00E+07	7.08E+06	1.96E+04	1.39	7.95E-02	2.01E-03	1.60E-07	0.00201353	4.15	0.66	0.08
gd@8.ais	TJB.12	Dec. 2014	3.01E+09	7.10E+06	6.04E+06	1.36E+04	-1.45	1.46E-01	2.00E-03	2.92E-07	0.00200782	1.31	0.70	0.15
gd@13.ais	TJB.12	Dec. 2014	3.53E+09	7.31E+06	7.08E+06	1.45E+04	0.52	7.86E-02	2.01E-03	1.58E-07	0.00201179	3.29	0.66	0.08
gd@14.ais	TJB.12	Dec. 2014	3.61E+09	1.47E+07	7.23E+06	2.95E+04	-1.46	9.09E-02	2.00E-03	1.82E-07	0.00200781	1.30	0.67	0.09
gd@15.ais	TJB.12	Dec. 2014	3.49E+09	7.03E+06	7.02E+06	1.40E+04	2.79	5.70E-02	2.01E-03	1.15E-07	0.00201634	5.56	0.65	0.06
gd@17.ais	TJB.12	Dec. 2014	3.70E+09	1.24E+07	7.43E+06	2.45E+04	0.65	6.58E-02	2.01E-03	1.32E-07	0.00201205	3.41	0.65	0.07
gd@19.ais	TJB.12	Dec. 2014	3.57E+09	1.01E+07	7.15E+06	1.96E+04	-0.20	9.96E-02	2.00E-03	2.00E-07	0.00201033	2.56	0.67	0.10
gd@22.ais	TJB.12	Dec. 2014	3.50E+09	9.88E+06	7.02E+06	1.99E+04	1.19	8.29E-02	2.01E-03	1.66E-07	0.00201313	3.95	0.66	0.08
Jgd (treated)														
gdcata@2.ais	TJB.12	Dec. 2014	3.41E+09	5.30E+06	6.84E+06	1.03E+04	-0.49	7.40E-02	2.00E-03	1.48E-07	0.00200975	2.27	0.66	0.07
gdcata@4.ais	TJB.12	Dec. 2014	3.45E+09	6.09E+06	6.95E+06	1.17E+04	3.46	1.02E-01	2.01E-03	2.05E-07	0.00201768	6.23	0.67	0.10
gdcata@6.ais	TJB.12	Dec. 2014	3.45E+09	1.42E+07	6.93E+06	2.86E+04	2.47	9.59E-02	2.01E-03	1.93E-07	0.00201551	5.14	0.67	0.10
gdcata@7.ais	TJB.12	Dec. 2014	3.41E+09	3.08E+07	6.84E+06	6.03E+04	0.21	3.16E-01	2.01E-03	6.34E-07	0.00201095	2.87	0.90	0.32
gdcata@8.ais	TJB.12	Dec. 2014	3.53E+09	1.79E+07	7.07E+06	3.53E+04	-0.99	2.02E-01	2.00E-03	4.05E-07	0.00200855	1.67	0.76	0.20
Mt. Dromedary (untreated)														
MtD@27.ais	TJB.12	Dec. 2014	3.52E+09	5.43E+06	7.08E+06	1.06E+04	3.77	9.57E-02	2.01E-03	1.93E-07	0.00201831	6.54	0.67	0.10
MtD@28.ais	TJB.12	Dec. 2014	3.50E+09	6.55E+06	7.05E+06	1.29E+04	4.06	7.44E-02	2.01E-03	1.50E-07	0.0020189	6.83	0.66	0.07
MtD@29.ais	TJB.12	Dec. 2014	3.54E+09	6.27E+06	7.13E+06	1.21E+04	3.70	9.63E-02	2.01E-03	1.94E-07	0.00201818	6.47	0.67	0.10
MtD@31.ais	TJB.12	Dec. 2014	3.51E+09	6.05E+06	7.06E+06	1.14E+04	4.28	1.24E-01	2.01E-03	2.49E-07	0.00201933	7.05	0.69	0.12
Mt. Dromedary (treated)														
MtDcata@24.ais	TJB.12	Dec. 2014	3.53E+09	8.49E+06	7.10E+06	1.64E+04	2.00	1.09E-01	2.01E-03	2.20E-07	0.00201476	4.77	0.68	0.11
MtDcata@25.ais	TJB.12	Dec. 2014	3.47E+09	6.04E+06	6.99E+06	1.17E+04	3.75	7.55E-02	2.01E-03	1.52E-07	0.00201827	6.52	0.66	0.08

RED analysis is partially off the grain or on an inclusion or crack, not included in sample average

Table D1. Yerington *in situ* zircon oxygen isotope compositions

Spot Name	Mount	Date	^{16}O Measured	^{16}O Error	^{18}O Measured	^{18}O Error	$\delta^{18}O$ Raw	$\delta^{18}O$ Error	$^{18}O/^{16}O$ Measured	$^{18}O/^{16}O$ Error	Corrected $^{18}O/^{16}O$	Corrected $\delta^{18}O$ (‰)	Total Error (2σ SE)	Internal Error (1σ)
MtDcata@26.ais	TJB.12	Dec. 2014	3.49E+09	6.10E+06	7.03E+06	1.19E+04	3.58	6.90E-02	2.01E-03	1.39E-07	0.00201794	6.35	0.66	0.07
MtDcata@27.ais	TJB.12	Dec. 2014	3.52E+09	5.70E+06	7.08E+06	1.11E+04	3.51	1.16E-01	2.01E-03	2.34E-07	0.00201779	6.28	0.68	0.12

RED analysis is partially off the grain or on an inclusion or crack, not included in sample average

Table D2. Hafnarfjall-Skarðsheiði *in situ* zircon oxygen isotope compositions

Spot Name	Mount	Date	^{16}O Measured	^{16}O Error	^{18}O Measured	^{18}O Error	$\delta^{18}O$ Raw	$\delta^{18}O$ Error	$^{18}O/^{16}O$ Measured	$^{18}O/^{16}O$ Error	Corrected $^{18}O/^{16}O$	Corrected $\delta^{18}O$ (‰)	Total Error (2σ SE)	Internal Error (1σ)
BrE1201: Brekkufjall rhyolite														
BrE1_TJB03@1.ais	TJB.3	Nov. 2013	2.10E+09		4.21E+06		1.43	1.06E-01	2.0081E-03	2.12E-07	0.00200906	1.93	0.69	0.11
BrE1_TJB03@2.ais	TJB.3	Nov. 2013	2.10E+09		4.22E+06		1.69	8.55E-02	2.0086E-03	1.72E-07	0.00200958	2.19	0.68	0.09
BrE1_TJB03@3.ais	TJB.3	Nov. 2013	2.13E+09		4.27E+06		1.48	6.91E-02	2.0082E-03	1.39E-07	0.00200918	1.98	0.68	0.07
BrE1_TJB03@4.ais	TJB.3	Nov. 2013	2.11E+09		4.24E+06		1.75	8.92E-02	2.0087E-03	1.79E-07	0.00200971	2.25	0.68	0.09
BrE1_TJB03@5.ais	TJB.3	Nov. 2013	2.10E+09		4.22E+06		1.48	1.04E-01	2.0082E-03	2.09E-07	0.00200917	1.98	0.69	0.10
BrE1_TJB03@6.ais	TJB.3	Nov. 2013	2.14E+09		4.30E+06		1.60	1.10E-01	2.0084E-03	2.21E-07	0.00200940	2.10	0.70	0.11
BrE1_TJB03@7.ais	TJB.3	Nov. 2013	1.86E+09		3.74E+06		2.12	7.31E-02	2.0094E-03	1.47E-07	0.00201045	2.62	0.68	0.07
BrE1_TJB03@8.ais	TJB.3	Nov. 2013	1.81E+09		3.63E+06		1.87	5.70E-02	2.0090E-03	1.14E-07	0.00200995	2.37	0.67	0.06
BrE1_TJB03@9.ais	TJB.3	Nov. 2013	1.80E+09		3.61E+06		1.28	6.54E-02	2.0078E-03	1.31E-07	0.00200877	1.78	0.67	0.07
BrE1_TJB03@10.ais	TJB.3	Nov. 2013	1.80E+09		3.61E+06		1.45	1.31E-01	2.0081E-03	2.62E-07	0.00200911	1.95	0.71	0.13
BrE1_TJB03@11.ais	TJB.3	Nov. 2013	1.81E+09		3.62E+06		1.23	1.05E-01	2.0077E-03	2.11E-07	0.00200868	1.73	0.69	0.11
BrE1_TJB03@12.ais	TJB.3	Nov. 2013	1.83E+09		3.67E+06		1.60	1.16E-01	2.0084E-03	2.32E-07	0.00200940	2.09	0.70	0.12
BrE1_TJB03@13.ais	TJB.3	Nov. 2013	1.89E+09		3.80E+06		1.52	1.01E-01	2.0083E-03	2.04E-07	0.00200925	2.02	0.69	0.10
BrE1_TJB03@14.ais	TJB.3	Nov. 2013	1.89E+09		3.80E+06		1.33	1.18E-01	2.0079E-03	2.37E-07	0.00200887	1.83	0.70	0.12
BrE1_TJB03@15.ais	TJB.3	Nov. 2013	1.90E+09		3.81E+06		1.87	1.06E-01	2.0090E-03	2.14E-07	0.00200995	2.37	0.69	0.11
BrE1_TJB03@16.ais	TJB.3	Nov. 2013	1.91E+09		3.83E+06		1.35	1.17E-01	2.0079E-03	2.34E-07	0.00200891	1.85	0.70	0.12
BrE1_TJB03@17.ais	TJB.3	Nov. 2013	1.92E+09		3.86E+06		1.36	7.95E-02	2.0079E-03	1.60E-07	0.00200892	1.86	0.68	0.08
BrE1_TJB03@18.ais	TJB.3	Nov. 2013	1.88E+09		3.78E+06		1.79	9.75E-02	2.0088E-03	1.96E-07	0.00200980	2.29	0.69	0.10
BrE1_TJB03@19.ais	TJB.3	Nov. 2013	1.90E+09		3.81E+06		1.09	8.94E-02	2.0074E-03	1.79E-07	0.00200840	1.59	0.68	0.09
BrE1_TJB03@20.ais	TJB.3	Nov. 2013	1.91E+09		3.84E+06		2.20	7.36E-02	2.0096E-03	1.48E-07	0.00201061	2.70	0.68	0.07
BrE1_TJB03@21.ais	TJB.3	Nov. 2013	1.89E+09		3.80E+06		1.78	1.07E-01	2.0088E-03	2.15E-07	0.00200977	2.28	0.69	0.11
BrE1_TJB03@22.ais	TJB.3	Nov. 2013	1.90E+09		3.82E+06		2.06	1.30E-01	2.0093E-03	2.62E-07	0.00201033	2.56	0.71	0.13
BrE1_TJB03@23.ais	TJB.3	Nov. 2013	1.94E+09		3.90E+06		2.73	7.01E-02	2.0107E-03	1.41E-07	0.00201168	3.23	0.68	0.07
BrE1_TJB03@24.ais	TJB.3	Nov. 2013	1.98E+09		3.97E+06		1.62	1.09E-01	2.0084E-03	2.19E-07	0.00200945	2.12	0.70	0.11
BrE1_TJB03@26.ais	TJB.3	Nov. 2013	1.87E+09		3.76E+06		1.70	8.24E-02	2.0086E-03	1.66E-07	0.00200962	2.20	0.68	0.08
BrE1_TJB03@27.ais	TJB.3	Nov. 2013	1.82E+09		3.66E+06		2.13	1.24E-01	2.0095E-03	2.48E-07	0.00201048	2.63	0.71	0.12
BrE1_TJB03@28.ais	TJB.3	Nov. 2013	1.81E+09		3.64E+06		1.60	9.78E-02	2.0084E-03	1.96E-07	0.00200941	2.10	0.69	0.10
DeE1302: Drageyraröxl ignimbrite														
DrE2_TJB06@1.ais	TJB.6	Nov. 2013	1.77E+09	6.45E+05	3.56E+06	1.52E+03	2.50	9.38E-02	2.0102E-03	1.89E-07	0.00201109	2.94	0.76	0.09
DrE2_TJB06@2.ais	TJB.6	Nov. 2013	1.77E+09	9.82E+05	3.55E+06	1.86E+03	3.29	9.64E-02	2.0118E-03	1.94E-07	0.00201267	3.73	0.76	0.10
DrE2_TJB06@3.ais	TJB.6	Nov. 2013	1.76E+09	1.33E+06	3.54E+06	2.89E+03	2.58	1.14E-01	2.0104E-03	2.30E-07	0.00201126	3.02	0.77	0.11
DrE2_TJB06@4.ais	TJB.6	Nov. 2013	1.76E+09	1.02E+06	3.54E+06	2.05E+03	2.84	1.04E-01	2.0109E-03	2.09E-07	0.00201177	3.28	0.76	0.10
DrE2_TJB06@5.ais	TJB.6	Nov. 2013	1.75E+09	8.81E+05	3.52E+06	1.66E+03	2.92	1.22E-01	2.0111E-03	2.46E-07	0.00201194	3.36	0.77	0.12
DrE2_TJB06@6.ais	TJB.6	Nov. 2013	1.74E+09	8.78E+05	3.50E+06	1.62E+03	2.72	9.59E-02	2.0107E-03	1.93E-07	0.00201153	3.16	0.76	0.10
DrE2_TJB06@7.ais	TJB.6	Nov. 2013	1.72E+09	9.19E+05	3.45E+06	1.81E+03	2.63	1.18E-01	2.0105E-03	2.36E-07	0.00201135	3.07	0.77	0.12
DrE2_TJB06@8.ais	TJB.6	Nov. 2013	1.71E+09	1.26E+06	3.44E+06	2.57E+03	2.57	7.26E-02	2.0103E-03	1.46E-07	0.00201123	3.01	0.75	0.07
DrE2_TJB06@9.ais	TJB.6	Nov. 2013	1.74E+09	1.37E+06	3.49E+06	2.56E+03	2.50	1.14E-01	2.0102E-03	2.29E-07	0.00201109	2.94	0.77	0.11
DrE2_TJB06@10.ais	TJB.6	Nov. 2013	1.71E+09	1.70E+06	3.43E+06	3.50E+03	2.98	6.04E-02	2.0112E-03	1.21E-07	0.00201205	3.42	0.74	0.06
DrE2_TJB06@11.ais	TJB.6	Nov. 2013	1.71E+09	1.19E+06	3.45E+06	2.25E+03	2.95	1.18E-01	2.0111E-03	2.36E-07	0.00201200	3.39	0.77	0.12
DrE2_TJB06@12.ais	TJB.6	Nov. 2013	1.71E+09	5.23E+05	3.44E+06	1.11E+03	2.41	9.80E-02	2.0100E-03	1.97E-07	0.00201091	2.85	0.76	0.10
DrE2_TJB06@13.ais	TJB.6	Nov. 2013	1.71E+09	1.77E+06	3.43E+06	3.62E+03	2.90	9.59E-02	2.0110E-03	1.93E-07	0.00201189	3.34	0.76	0.10
DrE2_TJB06@14.ais	TJB.6	Nov. 2013	1.70E+09	9.26E+05	3.42E+06	1.96E+03	2.53	1.07E-01	2.0103E-03	2.14E-07	0.00201116	2.97	0.76	0.11
DrE2_TJB06@15.ais	TJB.6	Nov. 2013	1.70E+09	1.07E+06	3.41E+06	2.37E+03	2.50	1.01E-01	2.0102E-03	2.03E-07	0.00201110	2.94	0.76	0.10
DrE2_TJB06@16.ais	TJB.6	Nov. 2013	1.70E+09	1.14E+06	3.41E+06	2.25E+03	2.77	9.46E-02	2.0108E-03	1.90E-07	0.00201165	3.21	0.76	0.09
DrE2_TJB06@17.ais	TJB.6	Nov. 2013	1.70E+09	1.24E+06	3.41E+06	2.39E+03	2.89	1.51E-01	2.0110E-03	3.04E-07	0.00201189	3.33	0.79	0.15

Table D2. Hafnarfjall-Skarðsheiði *in situ* zircon oxygen isotope compositions

Spot Name	Mount	Date	^{16}O Measured	^{16}O Error	^{18}O Measured	^{18}O Error	$\delta^{18}O$ Raw	$\delta^{18}O$ Error	$^{18}O/^{16}O$ Measured	$^{18}O/^{16}O$ Error	Corrected $^{18}O/^{16}O$	Corrected $\delta^{18}O$ (‰)	Total Error (2σ SE)	Internal Error (1σ)
DrE2_TJB06@18.ais	TJB.6	Nov. 2013	1.69E+09	1.16E+06	3.39E+06	2.45E+03	2.89	1.29E-01	2.0110E-03	2.60E-07	0.00201187	3.33	0.78	0.13
DrE2_TJB06@19.ais	TJB.6	Nov. 2013	1.68E+09	8.02E+05	3.38E+06	1.75E+03	2.60	1.17E-01	2.0104E-03	2.35E-07	0.00201129	3.04	0.77	0.12
DrE2_TJB06@20.ais	TJB.6	Nov. 2013	1.68E+09	9.98E+05	3.38E+06	2.03E+03	2.88	1.13E-01	2.0110E-03	2.27E-07	0.00201186	3.32	0.77	0.11
DrE2_TJB06@21.ais	TJB.6	Nov. 2013	1.69E+09	1.47E+06	3.39E+06	2.89E+03	2.66	1.12E-01	2.0105E-03	2.25E-07	0.00201142	3.10	0.77	0.11
DrE2_TJB06@22.ais	TJB.6	Nov. 2013	1.67E+09	1.17E+06	3.37E+06	2.46E+03	2.75	8.58E-02	2.0107E-03	1.73E-07	0.00201160	3.19	0.75	0.09
DrE2_TJB06@23.ais	TJB.6	Nov. 2013	1.68E+09	1.48E+06	3.38E+06	3.14E+03	2.85	1.06E-01	2.0109E-03	2.14E-07	0.00201181	3.29	0.76	0.11
DrE2_TJB06@24.ais	TJB.6	Nov. 2013	1.68E+09	1.53E+06	3.38E+06	3.15E+03	2.86	1.44E-01	2.0109E-03	2.90E-07	0.00201181	3.30	0.79	0.14
DrE2_TJB06@25.ais	TJB.6	Nov. 2013	1.67E+09	6.95E+05	3.37E+06	1.52E+03	2.68	6.95E-02	2.0106E-03	1.40E-07	0.00201145	3.12	0.75	0.07
DrE2_TJB06@26.ais	TJB.6	Nov. 2013	1.68E+09	1.34E+06	3.37E+06	2.73E+03	2.94	1.05E-01	2.0111E-03	2.12E-07	0.00201198	3.38	0.76	0.11
DrE2_TJB06@27.ais	TJB.6	Nov. 2013	1.68E+09	1.19E+06	3.37E+06	2.50E+03	2.82	1.27E-01	2.0109E-03	2.55E-07	0.00201174	3.26	0.78	0.13
DrE2_TJB06@28.ais	TJB.6	Nov. 2013	1.67E+09	1.69E+06	3.36E+06	3.30E+03	2.66	1.11E-01	2.0105E-03	2.24E-07	0.00201141	3.10	0.77	0.11
DrE2_TJB06@29.ais	TJB.6	Nov. 2013	1.68E+09	1.56E+06	3.37E+06	3.24E+03	2.26	1.00E-01	2.0097E-03	2.02E-07	0.00201062	2.70	0.76	0.10
DrE2_TJB06@30.ais	TJB.6	Nov. 2013	1.67E+09	1.26E+06	3.36E+06	2.41E+03	2.69	7.04E-02	2.0106E-03	1.42E-07	0.00201148	3.13	0.75	0.07
FlI1201: Flyðrur granophyre														
FlI1_TJB02@1.ais	TJB.2	Nov. 2013	1.59E+09	1.64E+06	3.19E+06	3.27E+03	2.31	8.26E-02	2.01E-03	1.66E-07	0.00201009	2.44	0.85	0.08
FlI1_TJB02@2.ais	TJB.2	Nov. 2013	1.60E+09	7.13E+05	3.21E+06	1.57E+03	2.41	8.35E-02	2.01E-03	1.68E-07	0.00201030	2.54	0.85	0.08
FlI1_TJB02@3.ais	TJB.2	Nov. 2013	1.58E+09	9.76E+05	3.18E+06	1.94E+03	3.72	8.88E-02	2.01E-03	1.79E-07	0.00201292	3.85	0.86	0.09
FlI1_TJB02@4.ais	TJB.2	Nov. 2013	1.58E+09	7.53E+05	3.17E+06	1.52E+03	2.57	1.09E-01	2.01E-03	2.20E-07	0.00201062	2.70	0.87	0.11
FlI1_TJB02@5.ais	TJB.2	Nov. 2013	1.57E+09	1.42E+06	3.16E+06	2.70E+03	2.03	1.65E-01	2.01E-03	3.32E-07	0.00200954	2.16	0.90	0.17
FlI1_TJB02@6.ais	TJB.2	Nov. 2013	1.56E+09	1.09E+06	3.15E+06	2.32E+03	2.95	1.19E-01	2.01E-03	2.40E-07	0.00201138	3.08	0.87	0.12
FlI1_TJB02@7.ais	TJB.2	Nov. 2013	1.55E+09	1.62E+06	3.13E+06	3.23E+03	3.18	7.51E-02	2.01E-03	1.51E-07	0.00201184	3.31	0.85	0.08
FlI1_TJB02@8.ais	TJB.2	Nov. 2013	1.56E+09	8.27E+05	3.14E+06	1.73E+03	2.19	1.31E-01	2.01E-03	2.63E-07	0.00200984	2.32	0.88	0.13
FlI1_TJB02@9.ais	TJB.2	Nov. 2013	1.58E+09	1.32E+06	3.17E+06	2.71E+03	2.86	1.45E-01	2.01E-03	2.92E-07	0.00201119	2.99	0.89	0.15
FlI1_TJB02@10.ais	TJB.2	Nov. 2013	1.57E+09	6.01E+05	3.15E+06	1.30E+03	1.64	1.02E-01	2.01E-03	2.04E-07	0.00200874	1.77	0.86	0.10
FlI1_TJB02@11.ais	TJB.2	Nov. 2013	1.57E+09	1.05E+06	3.15E+06	2.04E+03	2.15	1.02E-01	2.01E-03	2.04E-07	0.00200978	2.28	0.86	0.10
FlI1_TJB02@12.ais	TJB.2	Nov. 2013	1.57E+09	1.03E+06	3.15E+06	2.08E+03	1.95	1.26E-01	2.01E-03	2.53E-07	0.00200936	2.08	0.87	0.13
FlI1_TJB02@13.ais	TJB.2	Nov. 2013	1.56E+09	1.17E+06	3.14E+06	2.30E+03	2.31	8.27E-02	2.01E-03	1.66E-07	0.00201010	2.44	0.85	0.08
FlI1_TJB02@14.ais	TJB.2	Nov. 2013	1.57E+09	1.40E+06	3.15E+06	2.81E+03	2.10	6.01E-02	2.01E-03	1.21E-07	0.00200967	2.23	0.85	0.06
FlI1_TJB02@15.ais	TJB.2	Nov. 2013	1.55E+09	1.46E+06	3.13E+06	3.17E+03	2.48	1.24E-01	2.01E-03	2.50E-07	0.00201044	2.61	0.87	0.12
FlI1_TJB02@16.ais	TJB.2	Nov. 2013	1.56E+09	1.30E+06	3.14E+06	2.60E+03	2.52	1.36E-01	2.01E-03	2.74E-07	0.00201051	2.65	0.88	0.14
FlI1_TJB02@17.ais	TJB.2	Nov. 2013	1.55E+09	8.91E+05	3.11E+06	1.80E+03	2.01	1.54E-01	2.01E-03	3.10E-07	0.00200950	2.14	0.89	0.15
FlI1_TJB02@18.ais	TJB.2	Nov. 2013	1.55E+09	1.08E+06	3.11E+06	2.31E+03	2.18	1.45E-01	2.01E-03	2.91E-07	0.00200983	2.31	0.89	0.14
FlI1_TJB02@19.ais	TJB.2	Nov. 2013	1.55E+09	1.98E+06	3.12E+06	4.07E+03	1.35	1.45E-01	2.01E-03	2.92E-07	0.00200816	1.48	0.89	0.15
FlI1_TJB02@20.ais	TJB.2	Nov. 2013	1.55E+09	1.31E+06	3.11E+06	2.68E+03	2.63	1.06E-01	2.01E-03	2.13E-07	0.00201073	2.76	0.86	0.11
FlI1_TJB02@21.ais	TJB.2	Nov. 2013	1.54E+09	7.10E+05	3.09E+06	1.42E+03	3.11	6.26E-02	2.01E-03	1.26E-07	0.00201169	3.24	0.85	0.06
FlI1_TJB02@22.ais	TJB.2	Nov. 2013	1.48E+09	2.13E+06	2.98E+06	4.31E+03	0.48	1.40E-01	2.01E-03	2.80E-07	0.00200642	0.61	0.88	0.14
FlI1_TJB02@23.ais	TJB.2	Nov. 2013	1.56E+09	1.30E+06	3.13E+06	2.67E+03	2.03	1.07E-01	2.01E-03	2.15E-07	0.00200953	2.16	0.86	0.11
FlI1_TJB02@24.ais	TJB.2	Nov. 2013	1.55E+09	1.72E+06	3.11E+06	3.43E+03	4.01	9.03E-02	2.01E-03	1.82E-07	0.00201350	4.14	0.86	0.09
FlI1_TJB02@25.ais	TJB.2	Nov. 2013	1.55E+09	1.66E+06	3.13E+06	3.39E+03	4.44	1.04E-01	2.01E-03	2.10E-07	0.00201436	4.57	0.86	0.10
FlI1_TJB02@26.ais	TJB.2	Nov. 2013	1.55E+09	1.10E+06	3.13E+06	2.20E+03	2.99	7.84E-02	2.01E-03	1.58E-07	0.00201145	3.12	0.85	0.08
FlI1_TJB02@27.ais	TJB.2	Nov. 2013	1.55E+09	1.23E+06	3.12E+06	2.55E+03	2.21	1.03E-01	2.01E-03	2.07E-07	0.00200989	2.34	0.86	0.10
FlI1_TJB02@28.ais	TJB.2	Nov. 2013	1.52E+09	1.62E+06	3.08E+06	3.21E+03	9.66	1.13E-01	2.02E-03	2.29E-07	0.00202484	9.79	0.87	0.11
RnE1201: Rauðihnúkur rhyolite														
RnE1_TJB05@1.ais	TJB.5	Nov. 2013	1.51E+09	8.85E+05	3.03E+06	1.74E+03	2.42	8.30E-02	2.01E-03	1.67E-07	0.00201100	2.89	0.60	0.08
RnE1_TJB05@2.ais	TJB.5	Nov. 2013	1.51E+09	1.43E+06	3.04E+06	2.90E+03	2.18	1.36E-01	2.01E-03	2.73E-07	0.00201051	2.65	0.63	0.14
RnE1_TJB05@3.ais	TJB.5	Nov. 2013	1.52E+09	1.03E+06	3.05E+06	2.14E+03	2.56	1.16E-01	2.01E-03	2.34E-07	0.00201128	3.03	0.62	0.12

Table D2. Hafnarfjall-Skarðsheiði *in situ* zircon oxygen isotope compositions

Spot Name	Mount	Date	^{16}O Measured	^{16}O Error	^{18}O Measured	^{18}O Error	$\delta^{18}O$ Raw	$\delta^{18}O$ Error	$^{18}O/^{16}O$ Measured	$^{18}O/^{16}O$ Error	Corrected $^{18}O/^{16}O$	Corrected $\delta^{18}O$ (‰)	Total Error (2σ SE)	Internal Error (1σ)
RnE1_TJB05@4.ais	TJB.5	Nov. 2013	1.51E+09	1.25E+06	3.04E+06	2.71E+03	2.55	1.76E-01	2.01E-03	3.54E-07	0.00201126	3.02	0.67	0.18
RnE1_TJB05@5.ais	TJB.5	Nov. 2013	1.50E+09	1.25E+06	3.01E+06	2.52E+03	2.79	1.41E-01	2.01E-03	2.83E-07	0.00201174	3.26	0.64	0.14
RnE1_TJB05@6.ais	TJB.5	Nov. 2013	1.52E+09	1.24E+06	3.05E+06	2.33E+03	3.13	1.11E-01	2.01E-03	2.22E-07	0.00201243	3.60	0.61	0.11
RnE1_TJB05@7.ais	TJB.5	Nov. 2013	1.53E+09	1.13E+06	3.07E+06	2.31E+03	2.91	1.21E-01	2.01E-03	2.44E-07	0.00201197	3.38	0.62	0.12
RnE1_TJB05@8.ais	TJB.5	Nov. 2013	1.54E+09	3.63E+06	3.10E+06	7.31E+03	2.68	1.09E-01	2.01E-03	2.20E-07	0.00201151	3.15	0.61	0.11
RnE1_TJB05@9.ais	TJB.5	Nov. 2013	1.53E+09	1.86E+06	3.08E+06	3.68E+03	3.37	1.21E-01	2.01E-03	2.44E-07	0.00201290	3.84	0.62	0.12
RnE1_TJB05@10.ais	TJB.5	Nov. 2013	1.53E+09	1.88E+06	3.08E+06	3.76E+03	2.74	8.55E-02	2.01E-03	1.72E-07	0.00201165	3.21	0.60	0.09
RnE1_TJB05@11.ais	TJB.5	Nov. 2013	1.54E+09	1.96E+06	3.09E+06	3.79E+03	3.02	9.75E-02	2.01E-03	1.96E-07	0.00201220	3.49	0.61	0.10
RnE1_TJB05@12.ais	TJB.5	Nov. 2013	1.53E+09	1.86E+06	3.07E+06	3.74E+03	2.56	1.05E-01	2.01E-03	2.11E-07	0.00201129	3.04	0.61	0.11
RnE1_TJB05@13.ais	TJB.5	Nov. 2013	1.52E+09	3.41E+05	3.07E+06	7.51E+02	3.36	1.21E-01	2.01E-03	2.44E-07	0.00201289	3.84	0.62	0.12
RnE1_TJB05@14.ais	TJB.5	Nov. 2013	1.52E+09	1.79E+06	3.05E+06	3.40E+03	3.15	1.35E-01	2.01E-03	2.71E-07	0.00201245	3.62	0.63	0.13
RnE1_TJB05@15.ais	TJB.5	Nov. 2013	1.52E+09	9.71E+05	3.05E+06	1.92E+03	2.83	1.54E-01	2.01E-03	3.10E-07	0.00201183	3.31	0.65	0.15
RnE1_TJB05@16.ais	TJB.5	Nov. 2013	1.43E+09	1.83E+06	2.88E+06	3.74E+03	2.87	9.29E-02	2.01E-03	1.87E-07	0.00201191	3.35	0.60	0.09
RnE1_TJB05@17.ais	TJB.5	Nov. 2013	1.53E+09	1.22E+06	3.07E+06	2.49E+03	3.46	1.12E-01	2.01E-03	2.26E-07	0.00201309	3.93	0.62	0.11
RnE1_TJB05@18.ais	TJB.5	Nov. 2013	1.53E+09	1.08E+06	3.07E+06	2.29E+03	3.46	1.24E-01	2.01E-03	2.50E-07	0.00201308	3.93	0.62	0.12
RnE1_TJB05@19.ais	TJB.5	Nov. 2013	1.52E+09	1.32E+06	3.06E+06	2.47E+03	2.75	1.44E-01	2.01E-03	2.90E-07	0.00201166	3.22	0.64	0.14
RnE1_TJB05@20.ais	TJB.5	Nov. 2013	1.52E+09	1.06E+06	3.05E+06	2.11E+03	3.38	6.91E-02	2.01E-03	1.39E-07	0.00201293	3.85	0.59	0.07
RnE1_TJB05@21.ais	TJB.5	Nov. 2013	1.53E+09	1.10E+06	3.07E+06	2.14E+03	3.70	1.18E-01	2.01E-03	2.37E-07	0.00201357	4.18	0.62	0.12
RnE1_TJB05@22.ais	TJB.5	Nov. 2013	1.53E+09	1.47E+06	3.07E+06	2.98E+03	3.09	1.10E-01	2.01E-03	2.21E-07	0.00201235	3.56	0.61	0.11
RnE1_TJB05@23.ais	TJB.5	Nov. 2013	1.52E+09	1.07E+06	3.05E+06	2.24E+03	3.88	1.24E-01	2.01E-03	2.49E-07	0.00201393	4.36	0.62	0.12
RnE1_TJB05@24.ais	TJB.5	Nov. 2013	1.51E+09	4.75E+06	3.04E+06	9.37E+03	2.77	1.65E-01	2.01E-03	3.32E-07	0.00201169	3.24	0.66	0.17
TuE1301: Tungukollur rhyolite														
TuE1_TJB05@1.ais	TJB.5	Nov. 2013	1.52E+09	1.23E+06	3.05E+06	2.50E+03	2.59	1.06E-01	2.01E-03	2.13E-07	0.00201134	3.06	0.61	0.11
TuE1_TJB05@2.ais	TJB.5	Nov. 2013	1.52E+09	1.16E+06	3.05E+06	2.23E+03	2.60	1.31E-01	2.01E-03	2.64E-07	0.00201135	3.07	0.63	0.13
TuE1_TJB05@3.ais	TJB.5	Nov. 2013	1.52E+09	8.06E+05	3.06E+06	1.62E+03	2.64	1.26E-01	2.01E-03	2.52E-07	0.00201145	3.11	0.63	0.13
TuE1_TJB05@4.ais	TJB.5	Nov. 2013	1.60E+09	1.89E+07	3.22E+06	3.82E+04	1.93	1.57E-01	2.01E-03	3.16E-07	0.00201003	2.41	0.65	0.16
TuE1_TJB05@5.ais	TJB.5	Nov. 2013	1.54E+09	1.13E+06	3.09E+06	2.16E+03	2.16	9.93E-02	2.01E-03	1.99E-07	0.00201049	2.64	0.61	0.10
TuE1_TJB05@6.ais	TJB.5	Nov. 2013	1.50E+09	1.17E+06	3.01E+06	2.27E+03	2.42	1.16E-01	2.01E-03	2.33E-07	0.00201100	2.89	0.62	0.12
TuE1_TJB05@7.ais	TJB.5	Nov. 2013	1.52E+09	8.35E+05	3.05E+06	1.74E+03	2.51	8.63E-02	2.01E-03	1.74E-07	0.00201119	2.99	0.60	0.09
TuE1_TJB05@8.ais	TJB.5	Nov. 2013	1.51E+09	7.58E+05	3.04E+06	1.69E+03	2.10	1.21E-01	2.01E-03	2.43E-07	0.00201035	2.57	0.62	0.12
TuE1_TJB05@9.ais	TJB.5	Nov. 2013	1.51E+09	1.22E+06	3.03E+06	2.49E+03	2.84	1.41E-01	2.01E-03	2.84E-07	0.00201184	3.31	0.64	0.14
TuE1_TJB05@10.ais	TJB.5	Nov. 2013	1.51E+09	1.99E+06	3.03E+06	4.18E+03	1.19	1.10E-01	2.01E-03	2.22E-07	0.00200852	1.66	0.61	0.11
TuE1_TJB05@11.ais	TJB.5	Nov. 2013	1.53E+09	2.17E+06	3.07E+06	4.45E+03	2.38	1.39E-01	2.01E-03	2.80E-07	0.00201092	2.85	0.64	0.14
TuE1_TJB05@12.ais	TJB.5	Nov. 2013	1.54E+09	8.68E+05	3.09E+06	1.79E+03	1.67	1.14E-01	2.01E-03	2.29E-07	0.00200949	2.14	0.62	0.11
TuE1_TJB05@13.ais	TJB.5	Nov. 2013	1.53E+09	5.66E+05	3.08E+06	1.32E+03	2.43	1.32E-01	2.01E-03	2.66E-07	0.00201102	2.90	0.63	0.13
TuE1_TJB05@14.ais	TJB.5	Nov. 2013	1.51E+09	5.14E+05	3.03E+06	1.13E+03	3.02	8.49E-02	2.01E-03	1.71E-07	0.00201220	3.49	0.60	0.08
TuE1_TJB05@15.ais	TJB.5	Nov. 2013	1.49E+09	1.98E+06	3.00E+06	4.08E+03	2.36	1.22E-01	2.01E-03	2.46E-07	0.00201089	2.84	0.62	0.12
TuE1_TJB05@16.ais	TJB.5	Nov. 2013	1.52E+09	1.74E+06	3.06E+06	3.52E+03	2.00	1.14E-01	2.01E-03	2.28E-07	0.00201015	2.47	0.62	0.11
TuE1_TJB05@17.ais	TJB.5	Nov. 2013	1.50E+09	2.61E+05	3.02E+06	7.30E+02	2.75	1.16E-01	2.01E-03	2.33E-07	0.00201165	3.22	0.62	0.12
TuE1_TJB05@18.ais	TJB.5	Nov. 2013	1.50E+09	1.69E+06	3.02E+06	3.30E+03	1.95	9.76E-02	2.01E-03	1.96E-07	0.00201005	2.42	0.61	0.10
TuE1_TJB05@19.ais	TJB.5	Nov. 2013	1.38E+09	1.62E+06	2.78E+06	3.23E+03	2.08	9.77E-02	2.01E-03	1.96E-07	0.00201031	2.55	0.61	0.10
TuE1_TJB05@20.ais	TJB.5	Nov. 2013	1.52E+09	1.17E+06	3.06E+06	2.32E+03	2.67	6.79E-02	2.01E-03	1.36E-07	0.00201151	3.15	0.59	0.07
TuE1_TJB05@21.ais	TJB.5	Nov. 2013	1.50E+09	3.60E+05	3.02E+06	8.26E+02	2.89	7.43E-02	2.01E-03	1.49E-07	0.00201194	3.36	0.59	0.07
TuE1_TJB05@22.ais	TJB.5	Nov. 2013	1.48E+09	5.24E+05	2.97E+06	1.11E+03	2.69	1.28E-01	2.01E-03	2.58E-07	0.00201154	3.16	0.63	0.13
TuE1_TJB05@23.ais	TJB.5	Nov. 2013	1.46E+09	7.03E+05	2.94E+06	1.38E+03	2.85	1.38E-01	2.01E-03	2.77E-07	0.00201185	3.32	0.64	0.14
TuE1_TJB05@24.ais	TJB.5	Nov. 2013	1.46E+09	6.99E+05	2.94E+06	1.41E+03	1.71	1.18E-01	2.01E-03	2.36E-07	0.00200958	2.18	0.62	0.12

Table D2. Hafnarfjall-Skarðsheiði *in situ* zircon oxygen isotope compositions

Spot Name	Mount	Date	^{16}O Measured	^{16}O Error	^{18}O Measured	^{18}O Error	$\delta^{18}O$ Raw	$\delta^{18}O$ Error	$^{18}O/^{16}O$ Measured	$^{18}O/^{16}O$ Error	Corrected $^{18}O/^{16}O$	Corrected $\delta^{18}O$ (‰)	Total Error (2σ SE)	Internal Error (1σ)
SvE1302: Svartitindur rhyolite														
SVE1302-10_1.ais	TJB.11	Dec. 2014	3.35E+09	7.95E+06	6.70E+06	1.55E+04	-1.42	7.69E-02	2.00E-03	1.54E-07	0.00200647	0.63	0.68	0.08
SVE1302-11_1.ais	TJB.11	Dec. 2014	3.39E+09	9.29E+06	6.79E+06	1.84E+04	-0.15	9.16E-02	2.00E-03	1.84E-07	0.00200903	1.91	0.69	0.09
SVE1302-12_1.ais	TJB.11	Dec. 2014	3.44E+09	5.19E+06	6.89E+06	9.95E+03	-0.89	1.09E-01	2.00E-03	2.19E-07	0.00200754	1.17	0.70	0.11
SVE1302-14_1.ais	TJB.11	Dec. 2014	3.41E+09	1.07E+07	6.84E+06	2.14E+04	0.48	1.13E-01	2.01E-03	2.26E-07	0.00201028	2.53	0.70	0.11
SVE1302-15_1.ais	TJB.11	Dec. 2014	3.27E+09	8.68E+06	6.57E+06	1.70E+04	2.09	1.20E-01	2.01E-03	2.41E-07	0.00201352	4.15	0.70	0.12
SVE1302-18_1.ais	TJB.11	Dec. 2014	3.47E+09	8.19E+06	6.97E+06	1.65E+04	-0.18	4.08E-02	2.00E-03	8.18E-08	0.00200896	1.88	0.67	0.04
SVE1302-19_1.ais	TJB.11	Dec. 2014	3.33E+09	5.83E+06	6.69E+06	1.15E+04	0.62	1.05E-01	2.01E-03	2.11E-07	0.00201057	2.68	0.69	0.10
SVE1302-2_1.ais	TJB.11	Dec. 2014	3.39E+09	9.54E+06	6.80E+06	1.89E+04	1.01	4.78E-02	2.01E-03	9.59E-08	0.00201136	3.07	0.67	0.05
SVE1302-20_1.ais	TJB.11	Dec. 2014	3.40E+09	8.53E+06	6.82E+06	1.66E+04	0.50	1.08E-01	2.01E-03	2.16E-07	0.00201033	2.56	0.70	0.11
SVE1302-21_1.ais	TJB.11	Dec. 2014	3.40E+09	1.16E+07	6.82E+06	2.26E+04	0.75	1.27E-01	2.01E-03	2.54E-07	0.00201082	2.80	0.71	0.13
SVE1302-5_1.ais	TJB.11	Dec. 2014	3.24E+09	6.77E+06	6.49E+06	1.34E+04	0.29	8.36E-02	2.01E-03	1.68E-07	0.00200990	2.34	0.68	0.08
SVE1302-6_1.ais	TJB.11	Dec. 2014	3.41E+09	9.29E+06	6.83E+06	1.81E+04	0.55	1.22E-01	2.01E-03	2.44E-07	0.00201043	2.61	0.70	0.12
SVE1302-7_1.ais	TJB.11	Dec. 2014	3.47E+09	9.40E+06	6.94E+06	1.84E+04	-2.47	9.45E-02	2.00E-03	1.89E-07	0.00200437	-0.41	0.69	0.09
SVE1302-9_1.ais	TJB.11	Dec. 2014	3.29E+09	4.82E+06	6.59E+06	9.68E+03	0.09	1.16E-01	2.01E-03	2.32E-07	0.00200950	2.14	0.70	0.12
FeE1301: Ferjubakki rhyolite														
FEE1301-2_1.ais	TJB.11	Dec. 2014	3.33E+09	8.57E+06	6.67E+06	1.70E+04	-0.56	4.98E-02	2.00E-03	9.98E-08	0.00200820	1.50	0.67	0.05
FEE1301-3_1.ais	TJB.11	Dec. 2014	3.27E+09	1.05E+07	6.55E+06	2.07E+04	-1.19	6.72E-02	2.00E-03	1.35E-07	0.00200693	0.86	0.67	0.07
FEE1301-4_1.ais	TJB.11	Dec. 2014	3.38E+09	6.54E+06	6.78E+06	1.29E+04	-0.30	6.61E-02	2.00E-03	1.32E-07	0.00200873	1.76	0.67	0.07
FEE1301-8_1.ais	TJB.11	Dec. 2014	3.41E+09	8.55E+06	6.84E+06	1.70E+04	0.53	3.96E-02	2.01E-03	7.95E-08	0.00201039	2.59	0.67	0.04
FEE1301-9_1.ais	TJB.11	Dec. 2014	3.39E+09	6.36E+06	6.81E+06	1.25E+04	0.85	5.72E-02	2.01E-03	1.15E-07	0.00201104	2.91	0.67	0.06
FEE1301-11_1.ais	TJB.11	Dec. 2014	3.39E+09	9.05E+06	6.81E+06	1.77E+04	0.50	8.88E-02	2.01E-03	1.78E-07	0.00201033	2.56	0.68	0.09
FEE1301-12_1.ais	TJB.11	Dec. 2014	3.32E+09	7.97E+06	6.66E+06	1.62E+04	0.85	8.04E-02	2.01E-03	1.61E-07	0.00201103	2.91	0.68	0.08
FEE1301-13_1.ais	TJB.11	Dec. 2014	3.43E+09	9.00E+06	6.88E+06	1.75E+04	0.19	8.41E-02	2.01E-03	1.69E-07	0.00200970	2.25	0.68	0.08
FEE1301-17_1.ais	TJB.11	Dec. 2014	3.42E+09	9.38E+06	6.86E+06	1.82E+04	0.41	1.27E-01	2.01E-03	2.55E-07	0.00201015	2.47	0.71	0.13
FeE1301@18.ais	TJB.11	Dec. 2014	3.47E+09	9.88E+06	6.95E+06	1.96E+04	-0.17	5.78E-02	2.00E-03	1.16E-07	0.00200899	1.89	0.67	0.06
FeE1301@19.ais	TJB.11	Dec. 2014	3.40E+09	1.83E+07	6.83E+06	3.59E+04	0.26	1.26E-01	2.01E-03	2.52E-07	0.00200985	2.32	0.71	0.13
ShE1302: Skessuhorn rhyolite														
ShE2@1.ais	TJB.11	Dec. 2014	3.08E+09	6.57E+06	6.16E+06	1.24E+04	-0.66	1.78E-01	2.00E-03	3.56E-07	0.002008	1.40	0.75	0.18
ShE2@2.ais	TJB.11	Dec. 2014	3.07E+09	2.56E+06	6.16E+06	4.94E+03	0.16	6.22E-02	2.01E-03	1.25E-07	0.00200964	2.22	0.67	0.06
ShE2@5.ais	TJB.11	Dec. 2014	2.67E+09	1.88E+07	5.32E+06	3.83E+04	-7.09	1.84E-01	1.99E-03	3.67E-07	0.00199508	-5.04	0.76	0.18
ShE2@6.ais	TJB.11	Dec. 2014	3.06E+09	4.40E+06	6.14E+06	8.91E+03	0.90	5.81E-02	2.01E-03	1.17E-07	0.00201114	2.96	0.67	0.06
ShE2@7.ais	TJB.11	Dec. 2014	3.19E+09	6.74E+06	6.38E+06	1.30E+04	-1.34	1.10E-01	2.00E-03	2.20E-07	0.00200663	0.71	0.70	0.11
ShE2@8.ais	TJB.11	Dec. 2014	3.01E+09	1.06E+07	6.04E+06	2.09E+04	-1.06	1.07E-01	2.00E-03	2.14E-07	0.0020072	1.00	0.69	0.11
ShE2@9.ais	TJB.11	Dec. 2014	2.81E+09	4.21E+06	5.65E+06	8.31E+03	3.02	1.01E-01	2.01E-03	2.03E-07	0.0020154	5.09	0.69	0.10
ShE2@10.ais	TJB.11	Dec. 2014	3.00E+09	3.56E+06	6.02E+06	7.14E+03	0.40	9.60E-02	2.01E-03	1.93E-07	0.00201012	2.46	0.69	0.10
ShE2@11.ais	TJB.11	Dec. 2014	3.08E+09	6.15E+06	6.17E+06	1.21E+04	-0.80	1.34E-01	2.00E-03	2.68E-07	0.00200771	1.25	0.71	0.13
ShE2@12.ais	TJB.11	Dec. 2014	2.95E+09	1.36E+07	5.92E+06	2.72E+04	0.77	1.03E-01	2.01E-03	2.06E-07	0.00201087	2.83	0.69	0.10
ShE2@13.ais	TJB.11	Dec. 2014	2.84E+09	4.32E+06	5.68E+06	9.25E+03	-0.94	1.33E-01	2.00E-03	2.66E-07	0.00200745	1.12	0.71	0.13
ShE2@14.ais	TJB.11	Dec. 2014	2.43E+09	2.26E+06	4.85E+06	4.22E+03	-3.87	1.68E-01	2.00E-03	3.36E-07	0.00200154	-1.82	0.74	0.17
ShE2@15.ais	TJB.11	Dec. 2014	2.90E+09	5.57E+06	5.81E+06	1.06E+04	-1.32	1.14E-01	2.00E-03	2.28E-07	0.00200668	0.74	0.70	0.11
ShE2@16.ais	TJB.11	Dec. 2014	2.95E+09	3.71E+06	5.90E+06	6.99E+03	-0.96	1.10E-01	2.00E-03	2.20E-07	0.0020074	1.10	0.70	0.11
ShE2@17.ais	TJB.11	Dec. 2014	2.86E+09	5.35E+06	5.75E+06	1.07E+04	1.05	7.81E-02	2.01E-03	1.57E-07	0.00201144	3.11	0.68	0.08

BLUE analysis on portion ofmottled grain, not included in sample average

RED analysis is partially off the grain or on an inclusion or crack, not included in sample average

GREEN analysis had not identifiably wrong with it, but not representative of sample and not included in sample average

Table D3. Árnes and Hrafnfjörður *in situ* zircon oxygen isotope compositions

Spot Name	Mount	Date	^{16}O Measured	^{16}O Error	^{18}O Measured	^{18}O Error	$\delta^{18}O$ Raw	$\delta^{18}O$ Error	$^{18}O/^{16}O$ Measured	$^{18}O/^{16}O$ Error	Corrected $^{18}O/^{16}O$	Corrected $\delta^{18}O$ (‰)	Total Error (2σ SE)	Internal Error (1σ)
ÁrE1303: Tr2 rhyolite														
ArE3_TJB06@1.ais	TJB.6	Nov. 2013	1.67E+09	1.33E+06	3.37E+06	2.61E+03	2.89	1.16E-01	2.0110E-03	2.34E-07	0.00201187	3.33	0.77	0.12
ArE3_TJB06@2.ais	TJB.6	Nov. 2013	1.67E+09	1.13E+06	3.37E+06	2.29E+03	3.06	8.92E-02	2.0113E-03	1.80E-07	0.00201222	3.50	0.75	0.09
ArE3_TJB06@3.ais	TJB.6	Nov. 2013	1.68E+09	9.92E+05	3.37E+06	1.91E+03	3.22	8.62E-02	2.0116E-03	1.73E-07	0.00201253	3.66	0.75	0.09
ArE3_TJB06@4.ais	TJB.6	Nov. 2013	1.67E+09	1.06E+06	3.36E+06	2.29E+03	3.20	1.06E-01	2.0116E-03	2.12E-07	0.00201249	3.64	0.76	0.11
ArE3_TJB06@5.ais	TJB.6	Nov. 2013	1.67E+09	9.66E+05	3.36E+06	2.14E+03	3.20	1.19E-01	2.0116E-03	2.40E-07	0.00201249	3.64	0.77	0.12
ArE3_TJB06@6.ais	TJB.6	Nov. 2013	1.67E+09	1.74E+06	3.37E+06	3.40E+03	3.30	1.15E-01	2.0118E-03	2.31E-07	0.00201271	3.74	0.77	0.11
ArE3_TJB06@7.ais	TJB.6	Nov. 2013	1.67E+09	1.20E+06	3.36E+06	2.54E+03	3.49	1.35E-01	2.0122E-03	2.72E-07	0.00201308	3.93	0.78	0.14
ArE3_TJB06@8.ais	TJB.6	Nov. 2013	1.67E+09	8.13E+05	3.37E+06	1.54E+03	2.84	6.24E-02	2.0109E-03	1.25E-07	0.00201179	3.28	0.74	0.06
ArE3_TJB06@9.ais	TJB.6	Nov. 2013	1.67E+09	9.53E+05	3.35E+06	1.99E+03	2.91	1.21E-01	2.0110E-03	2.44E-07	0.00201192	3.35	0.77	0.12
ArE3_TJB06@10.ais	TJB.6	Nov. 2013	1.69E+09	1.73E+06	3.40E+06	3.59E+03	2.44	1.03E-01	2.0101E-03	2.07E-07	0.00201099	2.89	0.76	0.10
ArE3_TJB06@11.ais	TJB.6	Nov. 2013	1.68E+09	9.90E+05	3.37E+06	1.97E+03	3.39	7.83E-02	2.0120E-03	1.57E-07	0.00201287	3.83	0.75	0.08
ArE3_TJB06@12.ais	TJB.6	Nov. 2013	1.67E+09	6.91E+05	3.36E+06	1.56E+03	3.53	1.24E-01	2.0123E-03	2.50E-07	0.00201317	3.97	0.77	0.12
ArE3_TJB06@13.ais	TJB.6	Nov. 2013	1.67E+09	6.06E+05	3.37E+06	1.22E+03	3.27	1.32E-01	2.0118E-03	2.65E-07	0.00201264	3.71	0.78	0.13
ArE3_TJB06@14.ais	TJB.6	Nov. 2013	1.68E+09	1.01E+06	3.37E+06	2.00E+03	2.91	7.56E-02	2.0110E-03	1.52E-07	0.00201192	3.35	0.75	0.08
ArE3_TJB06@15.ais	TJB.6	Nov. 2013	1.67E+09	1.19E+06	3.37E+06	2.33E+03	3.40	1.44E-01	2.0120E-03	2.90E-07	0.00201291	3.84	0.79	0.14
ArE3_TJB06@16.ais	TJB.6	Nov. 2013	1.67E+09	2.22E+06	3.37E+06	4.44E+03	3.14	1.12E-01	2.0115E-03	2.26E-07	0.00201238	3.58	0.77	0.11
ArE3_TJB06@17.ais	TJB.6	Nov. 2013	1.68E+09	8.30E+05	3.38E+06	1.69E+03	2.65	8.92E-02	2.0105E-03	1.79E-07	0.00201140	3.09	0.75	0.09
ArE3_TJB06@18.ais	TJB.6	Nov. 2013	1.67E+09	1.28E+06	3.36E+06	2.68E+03	3.77	1.01E-01	2.0128E-03	2.03E-07	0.00201364	4.21	0.76	0.10
ArE3_TJB06@19.ais	TJB.6	Nov. 2013	1.67E+09	8.15E+05	3.36E+06	1.51E+03	3.09	6.16E-02	2.0114E-03	1.24E-07	0.00201227	3.53	0.74	0.06
ArE3_TJB06@20.ais	TJB.6	Nov. 2013	1.67E+09	8.16E+05	3.36E+06	1.64E+03	3.21	1.29E-01	2.0116E-03	2.59E-07	0.00201252	3.65	0.78	0.13
ArE3_TJB06@21.ais	TJB.6	Nov. 2013	1.66E+09	1.44E+06	3.34E+06	3.00E+03	2.91	9.35E-02	2.0110E-03	1.88E-07	0.00201192	3.35	0.76	0.09
ArE3_TJB06@22.ais	TJB.6	Nov. 2013	1.66E+09	1.40E+06	3.34E+06	2.83E+03	2.96	9.50E-02	2.0111E-03	1.91E-07	0.00201202	3.40	0.76	0.09
ArE3_TJB06@23.ais	TJB.6	Nov. 2013	1.67E+09	1.17E+06	3.36E+06	2.29E+03	3.41	9.13E-02	2.0120E-03	1.84E-07	0.00201292	3.85	0.76	0.09
ArE3_TJB06@24.ais	TJB.6	Nov. 2013	1.67E+09	8.31E+05	3.36E+06	1.63E+03	2.86	1.06E-01	2.0109E-03	2.14E-07	0.00201181	3.30	0.76	0.11
ÁrE1304: Tr3 rhyolite														
ArE4_TJB08@1.ais	TJB.8	Nov. 2013	2.25E+09		4.53E+06		2.50	7.98E-02	2.0102E-03	1.61E-07	0.00201181	3.30	0.51	0.08
ArE4_TJB08@2.ais	TJB.8	Nov. 2013	2.28E+09		4.59E+06		2.68	9.62E-02	2.0106E-03	1.93E-07	0.00201217	3.48	0.52	0.10
ArE4_TJB08@3.ais	TJB.8	Nov. 2013	2.26E+09		4.55E+06		2.40	9.57E-02	2.0100E-03	1.92E-07	0.00201161	3.20	0.52	0.10
ArE4_TJB08@4.ais	TJB.8	Nov. 2013	2.21E+09		4.44E+06		2.29	8.12E-02	2.0098E-03	1.63E-07	0.00201139	3.09	0.51	0.08
ArE4_TJB08@5.ais	TJB.8	Nov. 2013	2.17E+09		4.35E+06		2.63	8.95E-02	2.0105E-03	1.80E-07	0.00201206	3.42	0.52	0.09
ArE4_TJB08@6.ais	TJB.8	Nov. 2013	2.14E+09		4.30E+06		2.88	7.42E-02	2.0110E-03	1.49E-07	0.00201257	3.68	0.51	0.07
ArE4_TJB08@7.ais	TJB.8	Nov. 2013	2.14E+09		4.30E+06		1.96	9.99E-02	2.0091E-03	2.01E-07	0.00201073	2.76	0.52	0.10
ArE4_TJB07@1.ais	TJB.7	Nov. 2013	1.61E+09	9.79E+05	3.23E+06	2.06E+03	2.75	1.06E-01	2.0107E-03	2.13E-07	0.00201044	2.61	0.73	0.11
ArE4_TJB07@2.ais	TJB.7	Nov. 2013	1.59E+09	1.87E+06	3.20E+06	3.76E+03	3.54	1.02E-01	2.0123E-03	2.05E-07	0.00201203	3.41	0.72	0.10
ArE4_TJB07@3.ais	TJB.7	Nov. 2013	1.58E+09	1.69E+06	3.18E+06	3.46E+03	3.86	9.98E-02	2.0129E-03	2.01E-07	0.00201266	3.72	0.72	0.10
ArE4_TJB07@4.ais	TJB.7	Nov. 2013	1.57E+09	2.19E+06	3.16E+06	4.53E+03	3.54	1.07E-01	2.0123E-03	2.16E-07	0.00201203	3.41	0.73	0.11
ArE4_TJB07@5.ais	TJB.7	Nov. 2013	1.58E+09	1.04E+06	3.17E+06	2.18E+03	3.21	1.26E-01	2.0116E-03	2.53E-07	0.00201136	3.07	0.74	0.13
ArE4_TJB07@6.ais	TJB.7	Nov. 2013	1.56E+09	7.10E+06	3.14E+06	1.42E+04	3.23	1.46E-01	2.0117E-03	2.93E-07	0.00201140	3.09	0.75	0.15
ArE4_TJB07@7.ais	TJB.7	Nov. 2013	1.60E+09	1.65E+06	3.21E+06	3.42E+03	3.04	8.34E-02	2.0113E-03	1.68E-07	0.00201102	2.90	0.71	0.08
ArE4_TJB07@8.ais	TJB.7	Nov. 2013	1.58E+09	1.54E+06	3.17E+06	2.90E+03	3.89	1.35E-01	2.0130E-03	2.71E-07	0.00201272	3.75	0.74	0.13
ArE4_TJB07@9.ais	TJB.7	Nov. 2013	1.59E+09	1.45E+06	3.20E+06	2.96E+03	3.37	1.36E-01	2.0120E-03	2.74E-07	0.00201168	3.23	0.75	0.14
ArE4_TJB07@10.ais	TJB.7	Nov. 2013	1.58E+09	1.36E+06	3.18E+06	2.87E+03	3.01	1.29E-01	2.0112E-03	2.59E-07	0.00201097	2.88	0.74	0.13
ArE4_TJB07@11.ais	TJB.7	Nov. 2013	1.58E+09	1.89E+06	3.19E+06	3.99E+03	3.67	1.14E-01	2.0126E-03	2.29E-07	0.00201228	3.53	0.73	0.11
ArE4_TJB07@12.ais	TJB.7	Nov. 2013	1.58E+09	1.28E+06	3.19E+06	2.55E+03	3.52	9.62E-02	2.0123E-03	1.94E-07	0.00201199	3.38	0.72	0.10
ArE4_TJB07@13.ais	TJB.7	Nov. 2013	1.60E+09	1.56E+06	3.22E+06	3.20E+03	2.98	7.74E-02	2.0112E-03	1.56E-07	0.00201090	2.84	0.71	0.08

Table D3. Árnes and Hrafnfjörður *in situ* zircon oxygen isotope compositions

Spot Name	Mount	Date	^{16}O Measured	^{16}O Error	^{18}O Measured	^{18}O Error	$\delta^{18}O$ Raw	$\delta^{18}O$ Error	$^{18}O/^{16}O$ Measured	$^{18}O/^{16}O$ Error	Corrected $^{18}O/^{16}O$	Corrected $\delta^{18}O$ (‰)	Total Error (2σ SE)	Internal Error (1σ)
ArE4_TJB07@14.ais	TJB.7	Nov. 2013	1.60E+09	1.66E+06	3.21E+06	3.31E+03	3.61	9.56E-02	2.0124E-03	1.92E-07	0.00201216	3.47	0.72	0.10
ArE4_TJB07@15.ais	TJB.7	Nov. 2013	1.55E+09	8.85E+05	3.12E+06	1.64E+03	3.84	8.82E-02	2.0129E-03	1.78E-07	0.00201263	3.70	0.72	0.09
ArE4_TJB07@16.ais	TJB.7	Nov. 2013	1.60E+09	1.39E+06	3.21E+06	2.69E+03	2.95	8.20E-02	2.0111E-03	1.65E-07	0.00201084	2.81	0.71	0.08
ÁrE1301: Tr4 rhyolite														
ArE1_TJB07@1.ais	TJB.7	Nov. 2013	1.58E+09	1.33E+06	3.19E+06	2.62E+03	3.60	1.08E-01	2.01E-03	2.17E-07	0.00201214	3.46	0.73	0.11
ArE1_TJB07@2.ais	TJB.7	Nov. 2013	1.59E+09	7.29E+06	3.19E+06	1.47E+04	2.77	1.14E-01	2.01E-03	2.30E-07	0.00201048	2.63	0.73	0.11
ArE1_TJB@3.ais	TJB.7	Nov. 2013	1.58E+09	4.50E+05	3.17E+06	1.20E+03	3.76	1.62E-01	2.01E-03	3.26E-07	0.00201247	3.62	0.77	0.16
DH-08: Tr1 rhyolite														
DH-08@1.ais	TJB.9	Apr. 2014	4.51E+09	4.75E+06	9.07E+06	9.55E+03	0.00	1.00E-07	2.01E-03	2.01E-13	0.00201251	3.65	0.37	0.00
DH-08@2.ais	TJB.9	Apr. 2014	4.54E+09	5.95E+06	9.13E+06	1.18E+04	0.00	7.92E-08	2.01E-03	1.59E-13	0.00201235	3.57	0.37	0.00
DH-08@3.ais	TJB.9	Apr. 2014	4.47E+09	2.31E+06	8.99E+06	4.59E+03	0.00	8.81E-08	2.01E-03	1.77E-13	0.00201217	3.47	0.37	0.00
DH-08@4.ais	TJB.9	Apr. 2014	4.42E+09	3.10E+06	8.89E+06	6.25E+03	0.00	8.21E-08	2.01E-03	1.65E-13	0.00201256	3.67	0.37	0.00
DH-08@5.ais	TJB.9	Apr. 2014	4.38E+09	3.19E+06	8.80E+06	6.48E+03	0.00	8.25E-08	2.01E-03	1.66E-13	0.00201140	3.09	0.37	0.00
DH-08@6.ais	TJB.9	Apr. 2014	4.39E+09	1.04E+07	8.82E+06	2.13E+04	0.00	1.10E-07	2.01E-03	2.22E-13	0.00201140	3.09	0.37	0.00
DH-08@7.ais	TJB.9	Apr. 2014	4.48E+09	1.27E+07	9.01E+06	2.50E+04	0.00	1.33E-07	2.01E-03	2.68E-13	0.00201159	3.18	0.37	0.00
DH-15: Tr1 rhyolite														
DH-15@1.ais	TJB.9	Apr. 2014	3.75E+09	3.82E+06	7.53E+06	7.26E+03	0.00	1.29E-07	2.01E-03	2.59E-13	0.00200998	2.38	0.37	0.00
DH-15@2.ais	TJB.9	Apr. 2014	4.51E+09	1.11E+07	9.06E+06	2.23E+04	0.00	7.38E-08	2.01E-03	1.48E-13	0.00201116	2.97	0.37	0.00
DH-15@3.ais	TJB.9	Apr. 2014	4.33E+09	7.46E+06	8.71E+06	1.50E+04	0.00	9.53E-08	2.01E-03	1.91E-13	0.00201089	2.84	0.37	0.00
DH-15@4.ais	TJB.9	Apr. 2014	4.39E+09	1.02E+07	8.82E+06	2.05E+04	0.00	9.56E-08	2.01E-03	1.92E-13	0.00201067	2.73	0.37	0.00
DH-15@5.ais	TJB.9	Apr. 2014	4.36E+09	1.11E+07	8.76E+06	2.21E+04	0.00	1.02E-07	2.01E-03	2.04E-13	0.00201109	2.94	0.37	0.00
DH-15@6.ais	TJB.9	Apr. 2014	4.44E+09	8.54E+06	8.92E+06	1.75E+04	0.00	1.37E-07	2.01E-03	2.76E-13	0.00201299	3.89	0.37	0.00
DH-15@7.ais	TJB.9	Apr. 2014	4.31E+09	2.02E+07	8.66E+06	4.05E+04	0.00	1.10E-07	2.01E-03	2.21E-13	0.00201073	2.76	0.37	0.00
DH-15@8.ais	TJB.9	Apr. 2014	4.05E+09	8.23E+06	8.13E+06	1.61E+04	0.00	1.12E-07	2.00E-03	2.25E-13	0.00200665	0.73	0.37	0.00
DH-15@9.ais	TJB.9	Apr. 2014	4.11E+09	2.06E+07	8.27E+06	4.18E+04	0.00	1.35E-07	2.01E-03	2.72E-13	0.00201076	2.77	0.37	0.00
DH-15@10.ais	TJB.9	Apr. 2014	3.17E+09	3.34E+06	6.36E+06	6.50E+03	0.00	1.37E-07	2.01E-03	2.74E-13	0.00200937	2.08	0.37	0.00
HfE1402: Tdb dacite (mapped)														
HfE2@3.ais	TJB.11	Dec. 2014	3.27E+09	8.07E+06	6.58E+06	1.59E+04	1.69	7.63E-02	2.01E-03	1.53E-07	0.00201272	3.75	0.68	0.08
HfE2@4.ais	TJB.11	Dec. 2014	3.35E+09	1.13E+07	6.72E+06	2.23E+04	0.71	7.62E-02	2.01E-03	1.53E-07	0.00201075	2.77	0.68	0.08
HfE2@6.ais	TJB.11	Dec. 2014	3.32E+09	6.56E+06	6.66E+06	1.26E+04	1.33	1.35E-01	2.01E-03	2.72E-07	0.00201201	3.39	0.72	0.14
HfE2@8.ais	TJB.11	Dec. 2014	3.28E+09	8.79E+06	6.59E+06	1.70E+04	1.72	1.29E-01	2.01E-03	2.59E-07	0.00201277	3.78	0.71	0.13
HfE2@10.ais	TJB.11	Dec. 2014	3.31E+09	8.08E+06	6.64E+06	1.58E+04	1.63	8.84E-02	2.01E-03	1.77E-07	0.00201261	3.69	0.69	0.09
HfE2@12.ais	TJB.11	Dec. 2014	3.04E+09	8.51E+06	6.11E+06	1.67E+04	2.05	9.98E-02	2.01E-03	2.01E-07	0.00201344	4.11	0.69	0.10
HfE1403: dacite flow (?)														
HfE3@3.ais	TJB.11	Dec. 2014	3.10E+09	8.63E+06	6.22E+06	1.73E+04	1.91	3.84E-02	2.01E-03	7.72E-08	0.00201316	3.97	0.67	0.04
HfE3@4.ais	TJB.11	Dec. 2014	3.13E+09	4.87E+06	6.29E+06	9.59E+03	1.25	6.54E-02	2.01E-03	1.31E-07	0.00201184	3.31	0.68	0.07
HfE3@5.ais	TJB.11	Dec. 2014	3.18E+09	3.92E+06	6.38E+06	6.91E+03	0.95	1.75E-01	2.01E-03	3.52E-07	0.00201123	3.01	0.75	0.18
HfE3@6.ais	TJB.11	Dec. 2014	3.05E+09	1.91E+06	6.13E+06	3.39E+03	1.19	1.39E-01	2.01E-03	2.79E-07	0.00201172	3.25	0.72	0.14
HfE3@7.ais	TJB.11	Dec. 2014	3.03E+09	4.76E+06	6.10E+06	9.72E+03	2.04	1.05E-01	2.01E-03	2.11E-07	0.00201343	4.11	0.70	0.10
HfE3@8.ais	TJB.11	Dec. 2014	3.14E+09	5.47E+06	6.30E+06	1.07E+04	1.01	7.17E-02	2.01E-03	1.44E-07	0.00201135	3.07	0.68	0.07
HfE3@9.ais	TJB.11	Dec. 2014	3.07E+09	4.36E+06	6.17E+06	8.28E+03	0.95	8.37E-02	2.01E-03	1.68E-07	0.00201122	3.00	0.68	0.08
HfE3@10.ais	TJB.11	Dec. 2014	3.04E+09	5.58E+06	6.11E+06	1.08E+04	1.40	1.12E-01	2.01E-03	2.25E-07	0.00201215	3.46	0.70	0.11
HfE3@11.ais	TJB.11	Dec. 2014	3.11E+09	6.02E+06	6.25E+06	1.15E+04	1.36	1.15E-01	2.01E-03	2.31E-07	0.00201205	3.42	0.70	0.11
HfE3@12.ais	TJB.11	Dec. 2014	3.07E+09	4.76E+06	6.16E+06	9.41E+03	1.88	6.71E-02	2.01E-03	1.35E-07	0.00201310	3.94	0.68	0.07

RED analysis is partially off the grain or on an inclusion or crack, not included in sample average

Table D3. Árnes and Hrafnfjörður *in situ* zircon oxygen isotope compositions

Spot Name	Mount	Date	^{16}O Measured	^{16}O Error	^{18}O Measured	^{18}O Error	$\delta^{18}O$ Raw	$\delta^{18}O$ Error	$^{18}O/^{16}O$ Measured	$^{18}O/^{16}O$ Error	Corrected $^{18}O/^{16}O$	Corrected $\delta^{18}O$ (‰)	Total Error (2σ SE)	Internal Error (1σ)
HfE3@21.ais	TJB.11	Dec. 2014	3.13E+09	6.14E+06	6.28E+06	1.19E+04	0.89	8.78E-02	2.01E-03	1.76E-07	0.00201112	2.95	0.69	0.09
HfE3@22.ais	TJB.11	Dec. 2014	3.09E+09	3.89E+06	6.21E+06	7.29E+03	1.43	1.02E-01	2.01E-03	2.05E-07	0.00201220	3.49	0.69	0.10
HfE3@23.ais	TJB.11	Dec. 2014	3.19E+09	8.75E+06	6.39E+06	1.73E+04	0.91	1.13E-01	2.01E-03	2.28E-07	0.00201115	2.97	0.70	0.11
HfE3@24.ais	TJB.11	Dec. 2014	3.20E+09	6.98E+06	6.43E+06	1.39E+04	1.30	8.32E-02	2.01E-03	1.67E-07	0.00201195	3.36	0.68	0.08
HfE3@15.ais	TJB.11	Dec. 2014	3.26E+09	6.71E+06	6.55E+06	1.29E+04	0.93	1.03E-01	2.01E-03	2.08E-07	0.00201120	2.99	0.70	0.10
HfE3@17.ais	TJB.11	Dec. 2014	3.26E+09	6.24E+06	6.54E+06	1.19E+04	1.32	1.17E-01	2.01E-03	2.35E-07	0.00201198	3.38	0.70	0.12
HfE3@18.ais	TJB.11	Dec. 2014	3.43E+09	1.10E+07	6.87E+06	2.18E+04	-1.37	7.31E-02	2.00E-03	1.46E-07	0.00200658	0.69	0.68	0.07
HfE3@19.ais	TJB.11	Dec. 2014	3.35E+09	9.83E+06	6.72E+06	1.92E+04	1.05	8.57E-02	2.01E-03	1.72E-07	0.00201143	3.10	0.69	0.09
HfE3@20.ais	TJB.11	Dec. 2014	3.37E+09	8.57E+06	6.76E+06	1.72E+04	0.98	9.49E-02	2.01E-03	1.90E-07	0.00201129	3.04	0.69	0.09

RED analysis is partially off the grain or on an inclusion or crack, not included in sample average

Table D4. Króksfjörður *in situ* zircon oxygen isotope compositions

Spot Name	Mount	Date	^{16}O Measured	^{16}O Error	^{18}O Measured	^{18}O Error	$\delta^{18}O$ Raw	$\delta^{18}O$ Error	$^{18}O/^{16}O$ Measured	$^{18}O/^{16}O$ Error	Corrected $^{18}O/^{16}O$	Corrected $\delta^{18}O$ (‰)	Total Error (2σ SE)	Internal Error (1σ)
IEKBr-1: Bær rhyolite														
Br1_TJB07@1.ais	TJB.7	Nov. 2013	1.56E+09		3.15E+06		3.41	9.43E-02	2.0120E-03	1.90E-07	0.00201177	3.28	0.72	0.09
Br1_TJB07@2.ais	TJB.7	Nov. 2013	1.62E+09		3.24E+06		1.21	1.05E-01	2.0076E-03	2.11E-07	0.00200735	1.07	0.73	0.10
Br1_TJB07@3.ais	TJB.7	Nov. 2013	1.58E+09		3.18E+06		2.20	7.37E-02	2.0096E-03	1.48E-07	0.00200933	2.06	0.71	0.07
Br1_TJB07@4.ais	TJB.7	Nov. 2013	1.60E+09		3.22E+06		1.32	6.99E-02	2.0078E-03	1.40E-07	0.00200757	1.18	0.71	0.07
Br1_TJB07@5.ais	TJB.7	Nov. 2013	1.61E+09		3.23E+06		1.87	9.91E-02	2.0089E-03	1.99E-07	0.00200867	1.73	0.72	0.10
Br_TJB08@1.ais	TJB.8	Nov. 2013	2.17E+09		4.35E+06		1.00	7.34E-02	2.0072E-03	1.47E-07	0.00200694	0.87	0.51	0.07
Br_TJB08@2.ais	TJB.8	Nov. 2013	2.16E+09		4.34E+06		0.97	6.80E-02	2.0071E-03	1.37E-07	0.00200687	0.83	0.50	0.07
Br_TJB08@3.ais	TJB.8	Nov. 2013	2.11E+09		4.23E+06		0.98	6.35E-02	2.0072E-03	1.27E-07	0.00200690	0.85	0.50	0.06
IEKTr-1: Tindar rhyolite														
Tr1_TJB07_redo@1.ais	TJB.7	Nov. 2013	1.65E+09		3.31E+06		2.71	1.22E-01	2.0106E-03	2.45E-07	0.00201036	2.57	0.74	0.12
Tr1_TJB07_redo@2.ais	TJB.7	Nov. 2013	1.62E+09		3.26E+06		2.99	1.59E-01	2.0112E-03	3.20E-07	0.00201093	2.86	0.76	0.16
Tr1_TJB07_redo@3.ais	TJB.7	Nov. 2013	1.63E+09		3.28E+06		2.63	1.03E-01	2.0105E-03	2.07E-07	0.00201019	2.49	0.72	0.10
Tr1_TJB07@4.ais	TJB.7	Nov. 2013	1.62E+09		3.26E+06		3.01	8.64E-02	2.0112E-03	1.74E-07	0.00201096	2.87	0.72	0.09
Tr1_TJB07@5.ais	TJB.7	Nov. 2013	1.62E+09		3.27E+06		2.86	1.25E-01	2.0109E-03	2.52E-07	0.00201067	2.73	0.74	0.13
Tr1_TJB07@6.ais	TJB.7	Nov. 2013	1.63E+09		3.28E+06		3.53	9.53E-02	2.0123E-03	1.92E-07	0.00201199	3.39	0.72	0.10
Tr1_TJB07@7.ais	TJB.7	Nov. 2013	1.62E+09		3.26E+06		2.81	1.15E-01	2.0108E-03	2.32E-07	0.00201056	2.67	0.73	0.12
Tr1_TJB07@8.ais	TJB.7	Nov. 2013	1.61E+09		3.24E+06		2.64	1.15E-01	2.0105E-03	2.31E-07	0.00201022	2.50	0.73	0.11
Tr1_TJB07@9.ais	TJB.7	Nov. 2013	1.64E+09		3.30E+06		3.00	1.42E-01	2.0112E-03	2.85E-07	0.00201094	2.86	0.75	0.14
Tr1_TJB07@10.ais	TJB.7	Nov. 2013	1.61E+09		3.25E+06		3.61	1.44E-01	2.0124E-03	2.90E-07	0.00201216	3.47	0.75	0.14
Tr1_TJB08@1.ais	TJB.8	Nov. 2013	2.14E+09		4.30E+06		2.33	9.85E-02	2.0099E-03	1.98E-07	0.00200961	2.20	0.52	0.10
Tr1_TJB08@2.ais	TJB.8	Nov. 2013	2.15E+09		4.31E+06		2.47	7.42E-02	2.0102E-03	1.49E-07	0.00200988	2.33	0.51	0.07
Tr1_TJB08@3.ais	TJB.8	Nov. 2013	2.17E+09		4.35E+06		0.74	8.37E-02	2.0067E-03	1.68E-07	0.00200641	0.60	0.51	0.08
Tr1_TJB08@4.ais	TJB.8	Nov. 2013	2.15E+09		4.32E+06		1.92	9.96E-02	2.0090E-03	2.00E-07	0.00200877	1.78	0.52	0.10
IEKVl-1: Valshamar dacite														
IEKVl-1@1.ais	TJB.9	Apr. 2014	4.34E+09	7.98E+06	8.71E+06	1.60E+04	2.06	4.11E-02	2.01E-03	8.22E-08	0.00200840	1.60	0.38	0.04
IEKVl-1@2.ais	TJB.9	Apr. 2014	4.37E+09	1.03E+07	8.77E+06	2.04E+04	1.44	5.06E-02	2.01E-03	1.01E-07	0.00200715	0.97	0.38	0.05
IEKVl-1@3.ais	TJB.9	Apr. 2014	4.54E+09	1.41E+07	9.10E+06	2.86E+04	1.10	3.92E-02	2.00E-03	7.84E-08	0.00200647	0.64	0.38	0.04
IEKVl-1@4.ais	TJB.9	Apr. 2014	3.97E+09	2.64E+06	7.98E+06	5.34E+03	2.72	4.47E-02	2.01E-03	8.95E-08	0.00200972	2.25	0.38	0.04
IEKVl-1@5.ais	TJB.9	Apr. 2014	4.43E+09	1.13E+07	8.88E+06	2.28E+04	1.98	3.75E-02	2.01E-03	7.51E-08	0.00200823	1.51	0.38	0.04
IEKVl-1@6.ais	TJB.9	Apr. 2014	4.71E+09	1.48E+07	9.41E+06	2.89E+04	-1.92	9.82E-02	2.00E-03	1.97E-07	0.00200042	-2.38	0.42	0.10
IEKVl-1@7.ais	TJB.9	Apr. 2014	4.53E+09	3.69E+06	9.10E+06	7.21E+03	2.81	5.41E-02	2.01E-03	1.08E-07	0.00200990	2.34	0.39	0.05
IEKVl-1@8.ais	TJB.9	Apr. 2014	4.51E+09	3.99E+06	9.06E+06	7.96E+03	3.14	6.83E-02	2.01E-03	1.37E-07	0.00201056	2.67	0.40	0.07
IEKVl-1@9.ais	TJB.9	Apr. 2014	4.62E+09	6.13E+06	9.27E+06	1.22E+04	2.27	6.04E-01	2.01E-03	1.21E-06	0.00200882	1.80	1.26	0.60
IEKVl-1@10.ais	TJB.9	Apr. 2014	4.67E+09	8.79E+06	9.38E+06	1.74E+04	2.60	4.77E-02	2.01E-03	9.56E-08	0.00200949	2.14	0.38	0.05
IEKVl-1@11.ais	TJB.9	Apr. 2014	4.53E+09	1.04E+07	9.10E+06	2.09E+04	2.72	3.14E-02	2.01E-03	6.28E-08	0.00200972	2.26	0.38	0.03
IEKVl-1@12.ais	TJB.9	Apr. 2014	4.68E+09	5.87E+06	9.41E+06	1.15E+04	3.88	4.42E-02	2.01E-03	8.84E-08	0.00201206	3.42	0.38	0.04
IEKVl-1@13.ais	TJB.9	Apr. 2014	4.65E+09	5.41E+06	9.33E+06	1.07E+04	1.99	4.57E-02	2.01E-03	9.14E-08	0.00200826	1.52	0.38	0.05
IEKVl-1@14.ais	TJB.9	Apr. 2014	4.61E+09	5.52E+06	9.27E+06	1.11E+04	3.64	6.61E-02	2.01E-03	1.32E-07	0.00201156	3.17	0.39	0.07
IEKVl-1@15.ais	TJB.9	Apr. 2014	4.58E+09	5.62E+06	9.20E+06	1.11E+04	3.22	5.37E-02	2.01E-03	1.08E-07	0.00201072	2.75	0.39	0.05

RED analysis is partially off the grain or on an inclusion or crack, not included in sample average

APPENDIX E: Zircon U–Pb Geochronology Analyses

Table E1. Yerington i*n situ* zircon U-Pb geochronology

Analysis	Mount	Date	^{207}Pb-corr. ^{206}Pb/^{238}U Age (Ma)	1σ err	Th (ppm)	U (ppm)	^{204}Pb / ^{206}Pb	% err	^{207}Pb / ^{206}Pb	% err	^{208}Pb / ^{206}Pb	% err	^{207}Pb-corrected ^{204}Pb / ^{206}Pb	^{207}Pb-corrected % com ^{206}Pb	^{232}Th/^{238}U	% err	Total ^{238}U/ ^{206}Pb	% err	Total ^{207}Pb/ ^{206}Pb	% err	^{204}Pb-corrected ^{207}Pb*/^{235}U	% err	^{206}Pb/^{238}U	% err	err corr
Yerington: Jqmp1 (untreated)																									
qmp1_1.1	TJB.12	Oct-14	168	4	90	179	3.57E-04	71	0.0462	5.0	0.152	5.0	-2.19E-04	-0.40	0.523	0.41	37.92	2.5	0.0462	5.0	0.1479	11.1	2.62E-02	2.5	0.23
qmp1_3.1	TJB.12	Oct-14	165	3	98	199	1.49E-04	100	0.0504	4.0	0.177	4.4	6.61E-05	0.12	0.506	2.06	38.53	1.5	0.0504	4.0	0.1719	6.4	2.59E-02	1.6	0.25
qmp1_4.1	TJB.12	Oct-14	168	2	174	299	8.79E-05	100	0.0492	3.1	0.202	3.1	-1.98E-05	-0.04	0.602	0.59	37.88	1.4	0.0492	3.1	0.1739	4.4	2.64E-02	1.4	0.31
qmp1_5.1	TJB.12	Oct-14	170	3	98	142	-1.89E-04	100	0.0448	4.9	0.212	8.1	-3.20E-04	-0.59	0.715	0.89	37.66	1.7	0.0448	4.9	0.1748	7.6	2.66E-02	1.8	0.23
qmp1_6.1	TJB.12	Oct-14	169	2	93	149	2.27E-04	100	0.0495	5.2	0.210	5.1	-1.54E-07	0.00	0.646	4.02	37.57	1.1	0.0495	5.2	0.1685	9.3	2.65E-02	1.2	0.13
qmp1_10.1	TJB.12	Oct-14	173	2	631	863	1.00E-32	100	0.0493	1.9	0.244	1.7	-1.68E-05	-0.03	0.756	0.97	36.88	1.0	0.0493	1.9	0.1843	2.1	2.71E-02	1.0	0.46
qmp1_13.1	TJB.12	Oct-14	171	1	303	475	1.00E-32	100	0.0477	2.7	0.201	2.6	-1.20E-04	-0.22	0.659	1.03	37.38	0.9	0.0477	2.7	0.1761	2.8	2.67E-02	0.9	0.30
qmp1_14.1	TJB.12	Oct-14	168	2	147	190	1.62E-04	100	0.0501	4.3	0.229	4.1	4.06E-05	0.07	0.796	2.52	37.76	1.0	0.0501	4.3	0.1735	6.9	2.64E-02	1.1	0.15
qmp1_15.1	TJB.12	Oct-14	168	2	291	315	2.95E-04	58	0.0478	3.5	0.300	2.8	-1.14E-04	-0.21	0.954	4.86	38.00	0.9	0.0478	3.5	0.1566	7.1	2.62E-02	1.0	0.14
qmp1_19.1	TJB.12	Oct-14	167	8	95	157	1.61E-03	35	0.1065	18.9	0.297	10.6	3.88E-03	7.16	0.623	0.41	35.33	4.3	0.1065	18.9	0.3175	27.0	2.75E-02	4.4	0.16
Weighted mean age (N=10):					**169.3**		**Probability**							**0.46**											
Age error (95% conf., with error in Std)					**1.5**		**Age error (95% conf., without error in Std)**							**1.3**											
MSWD					**0.97**																				
Yerington: Jqmp1 (treated)																									
qmp1cata_1.1	TJB.12	Oct-14	166	3	120	216	5.50E-04	50	0.048	4.0	0.182	4.1	-9.86E-05	-0.18	0.58	0.56	38.43	1.7	0.048	4.0	0.1412	11.6	2.58E-02	2	0.15
qmp1cata_3.1	TJB.12	Oct-14	170	2	129	284	1.91E-04	71	0.047	3.4	0.144	3.8	-1.93E-04	-0.36	0.47	1.05	37.49	1.4	0.047	3.4	0.1606	6.0	2.66E-02	1	0.24
qmp1cata_6.1	TJB.12	Oct-14	169	3	1943	1197	2.25E-05	100	0.050	1.6	0.559	11.6	2.66E-06	0.00	1.68	10.00	37.69	1.7	0.050	1.6	0.1798	2.5	2.65E-02	2	0.70
qmp1cata_7.1	TJB.12	Oct-14	174	2	430	375	8.42E-05	100	0.046	3.2	0.368	2.3	-2.34E-04	-0.43	1.18	1.95	36.77	0.9	0.046	3.2	0.1680	4.4	2.72E-02	1	0.21
qmp1cata_8.1	TJB.12	Oct-14	165	2	285	384	3.28E-04	50	0.050	3.0	0.232	2.8	5.98E-05	0.11	0.77	1.32	38.55	0.9	0.050	3.0	0.1615	6.4	2.58E-02	1	0.15
qmp1cata_9.1	TJB.12	Oct-14	166	3	95	158	3.86E-04	71	0.051	4.6	0.192	4.7	1.09E-04	0.20	0.62	0.72	38.20	1.5	0.051	4.6	0.1624	10.5	2.60E-02	2	0.16
qmp1cata_10.1	TJB.12	Oct-14	170	4	121	224	-1.40E-04	100	0.049	4.0	0.153	4.5	-4.24E-05	-0.08	0.56	0.36	37.52	2.5	0.049	4.0	0.1876	6.1	2.67E-02	3	0.41
qmp1cata_12.1	TJB.12	Oct-14	167	3	138	168	2.15E-12	9999	0.049	4.6	0.255	7.2	-4.61E-05	-0.09	0.85	0.34	38.20	1.7	0.049	4.6	0.1759	4.9	2.62E-02	2	0.35
qmp1cata_13.1	TJB.12	Oct-14	170	4	965	974	1.00E-32	100	0.050	1.7	0.342	1.3	8.79E-06	0.02	1.02	4.61	37.31	2.7	0.050	1.7	0.1834	3.1	2.68E-02	3	0.85
qmp1cata_14.1	TJB.12	Oct-14	169	6	46	94	3.18E-04	100	0.046	6.3	0.163	6.5	-2.15E-04	-0.40	0.50	1.72	37.85	3.4	0.046	6.3	0.1506	13.8	2.63E-02	3	0.25
Weighted mean age (N=9):					**167.0**		**Probability**							**0.71**											
Age error (95% conf., with error in Std)					**1.9**		**Age error (95% conf., without error in Std)**							**1.8**											
MSWD					**0.7**																				
	Mean age of coherent group (N=20*)					**169.0**		**Probability**							**0.08**										
All Jqmp1:	**Age error (95% conf., with error in Std)**					**1.2**		**Age error (95% conf., without error in Std)**							**1.0**										
	MSWD					**1.5**		**Includes qmp1cata_7.1*																	
Yerington: Jqmp1.5 (untreated)																									
qmp1.5_1.1	TJB.12	Oct-14	173	2	79	173	3.47E-04	71	0.046	4.6	0.150	5.1	-2.52E-04	-0.46	0.47	0.42	37.00	1.0	0.046	4.6	0.1507	10.5	2.69E-02	1	0.11
qmp1.5_2.1	TJB.12	Oct-14	164	3	61	155	1.00E-32	100	0.051	4.7	0.134	5.9	1.29E-04	0.24	0.40	0.48	38.70	1.7	0.051	4.7	0.1827	5.0	2.58E-02	2	0.34
qmp1.5_4.2	TJB.12	Oct-14	168	3	65	151	2.16E-04	100	0.054	8.0	0.139	5.9	3.25E-04	0.60	0.45	1.07	37.68	1.6	0.054	8.0	0.1860	10.7	2.64E-02	2	0.16
qmp1.5_6.1	TJB.12	Oct-14	165	3	73	187	1.71E-04	100	0.049	4.4	0.132	5.5	-1.48E-05	-0.03	0.40	0.50	38.64	2.0	0.049	4.4	0.1659	7.4	2.58E-02	2	0.27
qmp1.5_8.1	TJB.12	Oct-14	169	2	64	149	-1.44E-12	9999	0.046	5.3	0.133	6.2	-2.03E-04	-0.37	0.44	1.01	37.87	1.1	0.046	5.3	0.1692	5.5	2.64E-02	1	0.20
qmp1.5_9.1	TJB.12	Oct-14	169	2	836	717	4.28E-05	100	0.047	2.2	0.385	1.6	-1.53E-04	-0.28	1.21	0.26	37.85	1.0	0.047	2.2	0.1695	2.9	2.64E-02	1	0.37
qmp1.5_10.1	TJB.12	Oct-14	167	3	110	220	2.69E-04	71	0.050	4.1	0.168	4.3	1.26E-05	0.02	0.51	3.88	38.07	1.5	0.050	4.1	0.1644	7.8	2.61E-02	2	0.20
qmp1.5_24.1	TJB.12	Oct-14	172	2	150	326	1.00E-32	100	0.047	3.3	0.148	3.7	-1.53E-04	-0.28	0.48	0.31	37.19	0.9	0.047	3.3	0.1753	3.4	2.69E-02	1	0.27
qmp1.5_25.1	TJB.12	Oct-14	167	1	263	397	8.67E-05	100	0.051	3.2	0.214	6.1	1.19E-04	0.22	0.68	1.80	38.09	0.9	0.051	3.2	0.1803	4.2	2.62E-02	1	0.21
qmp1.5_26.1	TJB.12	Oct-14	165	3	145	305	1.04E-04	100	0.052	3.4	0.169	3.8	1.51E-04	0.28	0.49	0.36	38.57	1.8	0.052	3.4	0.1786	5.0	2.59E-02	2	0.37
Weighted mean age (N=10):					**168.6**		**Probability**							**0.06**											
Age error (95% conf., with error in Std)					**1.5**		**Age error (95% conf., without error in Std)**							**1.3**											
MSWD					**1.8**																				
Yerington: Jqmp1.5 (treated)																									
qmp1.5cata_2.1	TJB.12	Oct-14	170	2	103	225	1.25E-04	100	0.048	3.8	0.155	4.2	-1.28E-04	-0.24	0.48	1.45	37.51	1.0	0.048	3.8	0.1678	5.7	2.66E-02	1	0.17
qmp1.5cata_3.2	TJB.12	Oct-14	169	2	172	308	1.05E-04	100	0.049	3.4	0.192	3.5	-3.93E-06	-0.01	0.58	1.53	37.54	0.9	0.049	3.4	0.1755	4.9	2.66E-02	1	0.19
qmp1.5cata-4.1	TJB.12	Oct-14	166	4	150	278	1.00E-32	100	0.048	3.7	0.170	3.9	-9.15E-05	-0.17	0.56	0.76	38.43	2.4	0.048	3.7	0.1724	4.4	2.60E-02	2	0.54

RED not included in sample average

Table E1 cont. Yerington *in situ* zircon U-Pb geochronology

Analysis	Mount	Date	^{207}Pb-corr. ^{206}Pb/^{238}U Age (Ma)	1σ err	Th (ppm)	U (ppm)	^{204}Pb / ^{206}Pb	% err	^{207}Pb / ^{206}Pb	% err	^{208}Pb / ^{206}Pb	% err	^{207}Pb-corrected ^{204}Pb / ^{206}Pb	^{207}Pb-corrected % com ^{206}Pb	^{232}Th / ^{238}U	% err	Total ^{238}U/ ^{206}Pb	% err	Total ^{207}Pb/ ^{206}Pb	% err	^{204}Pb-corrected ^{207}Pb*/^{235}U	% err	^{206}Pb/^{238}U	% err	err corr
qmp1.5cata-5.1	TJB.12	Oct-14	172	2	285	429	8.15E-05	100	0.046	3.3	0.220	3.0	-2.17E-04	-0.40	0.69	0.91	37.14	0.9	0.046	3.3	0.1673	4.4	2.69E-02	1	0.20
qmp1.5cata-6.1	TJB.12	Oct-14	170	3	167	298	6.89E-13	9999	0.052	3.4	0.177	3.7	1.68E-04	0.31	0.58	0.31	37.41	2.0	0.052	3.4	0.1915	3.9	2.67E-02	2	0.50
qmp1.5cata-7.1	TJB.12	Oct-14	172	3	144	257	1.00E-32	100	0.049	3.7	0.185	3.8	-3.64E-05	-0.07	0.58	0.32	37.05	2.0	0.049	3.7	0.1823	4.2	2.70E-02	2	0.47
qmp1.5cata-8.1	TJB.12	Oct-14	166	2	146	214	1.00E-32	100	0.051	3.6	0.220	4.0	1.30E-04	0.24	0.70	0.34	38.17	1.0	0.051	3.6	0.1854	3.8	2.62E-02	1	0.27
qmp1.5cata_10.1	TJB.12	Oct-14	162	3	67	134	-2.74E-21	9999	0.054	4.4	0.151	6.0	2.99E-04	0.55	0.52	0.82	38.98	2.0	0.054	4.4	0.1900	4.9	2.57E-02	2	0.42
qmp1.5cata_12.1	TJB.12	Oct-14	168	3	278	381	1.00E-32	100	0.049	2.8	0.240	2.6	-3.93E-05	-0.07	0.75	0.23	37.97	1.7	0.049	2.8	0.1774	3.3	2.63E-02	2	0.51
qmp1.5cata_15.1	TJB.12	Oct-14	167	2	385	469	-5.79E-05	100	0.048	2.5	0.266	2.5	-8.02E-05	-0.15	0.85	0.39	38.21	1.3	0.048	2.5	0.1773	3.3	2.62E-02	1	0.39
Mean age of coherent group (N=10)					**168.9**		**Probability**						**0.15**												
Age error (95% conf., with error in Std)					**1.5**		**Age error (95% conf., without error in Std)**						**1.3**												
MSWD					**1.5**																				
	Weighted mean age (N=20):					**168.7**	**Probability**							**0.05**											
All Jqmp1.5:	**Age error (95% conf., with error in Std)**					**1.1**	**Age error (95% conf., without error in Std)**							**0.9**											
	MSWD					**1.6**																			
Yerington: Jqmp2 (untreated)																									
qmp2_1.1	TJB.12	Oct-14	164	2	106	244	1.17E-04	100	0.051	3.5	0.142	4.3	1.28E-04	0.24	0.447	0.78	38.73	0.9	0.051	3.5	0.1759	5.1	2.58E-02	0.9	0.18
qmp2_2.1	TJB.12	Oct-14	171	2	204	344	-1.55E-04	71	0.046	3.1	0.183	3.1	-2.30E-04	-0.42	0.612	0.57	37.40	1.1	0.046	3.1	0.1790	4.6	2.68E-02	1.1	0.24
qmp2_3.1	TJB.12	Oct-14	170	2	49	131	1.00E-32	100	0.049	4.6	0.112	6.5	-1.06E-05	-0.02	0.382	3.25	37.36	1.0	0.049	4.6	0.1821	4.7	2.68E-02	1.0	0.22
qmp2_4.1	TJB.12	Oct-14	173	4	86	179	1.00E-32	100	0.048	3.9	0.156	7.2	-7.37E-05	-0.14	0.495	0.37	36.89	2.2	0.048	3.9	0.1811	4.5	2.71E-02	2.2	0.49
qmp2_5.1	TJB.12	Oct-14	172	5	269	421	5.22E-05	100	0.049	2.4	0.204	5.9	-4.71E-05	-0.09	0.661	3.42	36.95	3.0	0.049	2.4	0.1792	4.2	2.70E-02	3.0	0.71
qmp2_6.1	TJB.12	Oct-14	170	1	252	398	1.00E-32	100	0.051	2.6	0.212	2.6	7.25E-05	0.13	0.653	0.80	37.39	0.8	0.051	2.6	0.1864	2.7	2.67E-02	0.8	0.31
qmp2_7.1	TJB.12	Oct-14	164	3	137	290	1.65E-04	71	0.054	3.2	0.158	3.5	2.92E-04	0.54	0.487	0.33	38.62	1.6	0.054	3.2	0.1824	5.0	2.58E-02	1.6	0.33
qmp2_9.1	TJB.12	Oct-14	168	1	247	408	1.08E-04	71	0.048	2.6	0.192	2.6	-1.01E-04	-0.19	0.626	0.22	37.94	0.9	0.048	2.6	0.1682	3.8	2.63E-02	0.9	0.23
Weighted mean age (N=7):					**169.3**		**Probability**						**0.31**												
Age error (95% conf., with error in Std)					**1.6**		**Age error (95% conf., without error in Std)**						**1.5**												
MSWD					**1.2**																				
Yerington: Jqmp2 (treated)																									
qmp2cata_1.1	TJB.12	Oct-14	169	2	174	341	1.68E-04	71	0.052	3.0	0.170	3.3	1.45E-04	0.27	0.53	0.61	37.48	1	0.0516	3.0	0.1802	4.9	2.66E-02	0.9	0.19
qmp2cata_2.1	TJB.12	Oct-14	165	3	255	415	1.00E-32	100	0.051	5.6	0.192	2.9	8.37E-05	0.15	0.63	0.23	38.62	2	0.0506	5.6	0.1807	5.9	2.59E-02	1.9	0.32
qmp2cata_3.1	TJB.12	Oct-14	171	2	121	259	-2.99E-04	58	0.052	3.3	0.149	6.5	1.35E-04	0.25	0.48	1.21	37.03	1	0.0515	3.3	0.2092	5.6	2.72E-02	1.4	0.24
qmp2cata_4.1	TJB.12	Oct-14	173	2	156	265	-9.55E-05	100	0.047	3.3	0.209	3.2	-1.99E-04	-0.37	0.61	1.18	36.96	1	0.0466	3.3	0.1795	4.5	2.71E-02	1.3	0.28
qmp2cata_5.1	TJB.12	Oct-14	168	3	234	360	6.96E-05	100	0.047	2.9	0.220	2.7	-1.61E-04	-0.30	0.67	0.25	38.07	2	0.0471	2.9	0.1665	4.1	2.62E-02	1.8	0.43
qmp2cata_6.1	TJB.12	Oct-14	168	3	105	209	7.11E-13	9999	0.047	6.1	0.158	4.0	-1.53E-04	-0.28	0.52	0.83	37.88	2	0.0472	6.1	0.1718	6.3	2.64E-02	1.6	0.25
qmp2cata_8.1	TJB.12	Oct-14	169	2	136	262	1.89E-04	71	0.050	3.2	0.166	3.5	2.47E-05	0.05	0.54	0.81	37.61	1	0.0498	3.2	0.1719	5.6	2.65E-02	1.2	0.22
qmp2cata_10.1	TJB.12	Oct-14	166	4	49	128	1.71E-04	100	0.047	4.5	0.121	5.7	-1.65E-04	-0.30	0.39	1.64	38.34	2	0.0470	4.5	0.1593	7.7	2.60E-02	2.1	0.28
Weighted mean age (N=8):					**169.3**		**Probability**						**0.47**												
Age error (95% conf., with error in Std)					**1.8**		**Age error (95% conf., without error in Std)**						**1.6**												
MSWD					**0.9**																				
	Weighted mean age (N=16*):					**168.7**	**Probability**							**0.06**											
All Jqmp2:	**Age error (95% conf., with error in Std)**					**1.2**	**Age error (95% conf., without error in Std)**							**1.0**											
	MSWD					**1.6**	**Includes qmp2_1.1*																		
Yerington: Jqmp3 (untreated)																									
qmp3_5.1	TJB.12	Oct-14	168	3	98	224	1.00E-32	100	0.050	3.5	0.147	4.1	1.72E-04	0.32	0.45	0.34	37.84	1.8	0.050	3.5	0.1815	3.9	2.64E-02	1.8	0.45
qmp3_6.1	TJB.12	Oct-14	170	3	159	301	-9.16E-05	100	0.050	3.2	0.164	3.6	-4.34E-05	-0.08	0.55	0.90	37.37	1.9	0.050	3.2	0.1884	4.5	2.68E-02	1.9	0.42
qmp3_7.1	TJB.12	Oct-14	171	1	1137	1142	1.00E-32	100	0.050	1.6	0.324	1.3	-1.81E-05	-0.03	1.03	0.44	37.17	0.8	0.050	1.6	0.1844	1.8	2.69E-02	0.8	0.43
qmp3_8.1	TJB.12	Oct-14	169	1	272	435	-5.68E-05	100	0.052	2.5	0.199	5.1	-2.13E-04	-0.39	0.65	1.90	37.59	0.8	0.052	2.5	0.1945	3.0	2.66E-02	0.8	0.27
qmp3_17.1	TJB.12	Oct-14	168	2	119	256	4.21E-04	50	0.052	5.6	0.154	3.9	2.49E-05	0.05	0.48	0.32	37.78	0.9	0.052	5.6	0.1657	9.4	2.63E-02	1.0	0.11
qmp3_18.1	TJB.12	Oct-14	171	3	168	256	-1.83E-04	71	0.049	3.2	0.208	6.6	8.59E-06	0.02	0.68	0.27	37.29	1.5	0.049	3.2	0.1913	5.0	2.69E-02	1.5	0.30

RED not included in sample average

Table E1 cont. Yerington *in situ* zircon U-Pb geochronology

Analysis	Mount	Date	^{207}Pb-corr. ^{206}Pb/^{238}U Age (Ma)	1σ err	Th (ppm)	U (ppm)	^{204}Pb / ^{206}Pb	% err	^{207}Pb / ^{206}Pb	% err	^{208}Pb / ^{206}Pb	% err	^{207}Pb-corrected ^{204}Pb / ^{206}Pb	^{207}Pb-corrected % com ^{206}Pb	^{232}Th / ^{238}U	% err	Total ^{238}U/ ^{206}Pb	% err	Total ^{207}Pb/ ^{206}Pb	% err	^{204}Pb-corrected ^{207}Pb*/^{235}U	% err	^{206}Pb/^{238}U	% err	err corr
qmp3_19.1	TJB.12	Oct-14	167	3	280	407	1.00E-32	100	0.049	2.6	0.231	4.0	1.33E-05	0.02	0.71	1.83	38.10	1.9	0.049	2.6	0.1779	3.2	2.62E-02	1.9	0.58
qmp3_20.1	TJB.13	Nov-14	173	1	410	517	1.00E-32	100	0.046	2.2	0.258	1.9	1.83E-04	0.34	0.82	1.06	36.93	0.8	0.046	2.2	0.1733	2.4	2.71E-02	0.8	0.33
Weighted mean age (N=8):					**170.1**		**Probability**						**0.25**												
Age error (95% conf., with error in Std)					**1.4**		**Age error (95% conf., without error in Std)**						**1.3**												
MSWD					**1.3**																				
Yerington: Jqmp3 (treated)																									
qmp3cata-7.1	TJB.12	Oct-14	167	2	149	305	1.00E-32	100	0.051	3.0	0.162	3.4	1.11E-04	0.20	0.50	0.49	38.13	0.9	0.051	3.0	0.1846	3.1	2.62E-02	0.9	0.29
qmp3cata-6.1	TJB.12	Oct-14	168	1	212	350	-6.29E-05	100	0.049	2.7	0.194	4.4	-3.35E-05	-0.06	0.63	2.71	37.94	0.9	0.049	2.7	0.1814	3.4	2.64E-02	0.9	0.26
qmp3cata-4.1	TJB.12	Oct-14	168	3	44	126	6.01E-04	58	0.053	4.6	0.112	6.3	2.30E-04	0.42	0.36	2.79	37.71	2.1	0.053	4.6	0.1589	13.3	2.62E-02	2.2	0.16
qmp3cata-10.1	TJB.12	Oct-14	170	2	108	245	1.73E-04	71	0.048	3.1	0.147	3.6	-7.22E-05	-0.13	0.46	1.04	37.53	1.3	0.048	3.1	0.1680	5.3	2.66E-02	1.3	0.25
qmp3cata-2.1	TJB.12	Oct-14	171	2	462	530	4.95E-05	100	0.048	2.4	0.271	2.0	-7.35E-05	-0.14	0.90	0.98	37.29	1.0	0.048	2.4	0.1762	3.0	2.68E-02	1.0	0.32
qmp3cata-1.1	TJB.12	Oct-14	171	1	160	342	7.42E-05	100	0.052	2.8	0.160	3.2	1.47E-04	0.27	0.48	0.27	37.03	0.9	0.052	2.8	0.1881	3.7	2.70E-02	0.9	0.23
qmp3cata-3.1	TJB.12	Oct-14	173	2	575	684	9.43E-05	58	0.050	1.9	0.277	1.6	2.82E-05	0.05	0.87	0.35	36.84	1.4	0.050	1.9	0.1814	2.9	2.71E-02	1.4	0.48
Weighted mean age (N=7):					**169.4**		**Probability**						**0.18**												
Age error (95% conf., with error in Std)					**1.5**		**Age error (95% conf., without error in Std)**						**1.4**												
MSWD					**1.5**																				
	Weighted mean age (N=15):					**169.8**		**Probability**						**0.18**											
All Jqmp3:	**Age error (95% conf., with error in Std)**					**1.1**		**Age error (95% conf., without error in Std)**						**0.9**											
	MSWD					**1.3**																			
Yerington: Jbqm (untreated)																									
bqm_1.1	TJB.12	Oct-14	167	3	120	168	---	100	0.047	4.6	0.26	3.9	-1.38E-04	-0.25	0.74	0.93	38.23	1.6	0.047	4.6	0.171	4.8	2.6E-2	1.6	0.32
bqm_2.1	TJB.12	Oct-14	170	2	107	178	-1.5E-4	100	0.046	5.1	0.19	7.6	-2.52E-04	-0.46	0.62	5.38	37.62	1.0	0.046	5.1	0.177	6.8	2.7E-2	1.1	0.16
bqm_3.1	TJB.12	Oct-14	168	2	64	104	9.8E-4	50	0.049	5.3	0.18	5.4	-7.15E-06	-0.01	0.64	0.91	37.80	1.2	0.049	5.3	0.124	23.0	2.6E-2	1.5	0.06
bqm_4.1	TJB.12	Oct-14	166	1	241	315	9.2E-5	100	0.052	3.1	0.24	2.9	1.84E-04	0.34	0.79	0.25	38.14	0.9	0.052	3.1	0.183	4.3	2.6E-2	0.9	0.21
bqm_6.1	TJB.12	Oct-14	168	2	183	263	1.0E-4	100	0.050	3.4	0.22	3.3	4.50E-06	0.01	0.72	0.59	37.85	0.9	0.050	3.4	0.174	4.9	2.6E-2	0.9	0.19
bqm_7.1	TJB.12	Oct-14	171	3	119	434	---	---	0.052	2.5	0.09	3.7	1.45E-04	0.27	0.28	0.62	37.06	1.6	0.052	2.5	0.192	3.0	2.7E-2	1.6	0.54
bqm_8.1	TJB.12	Oct-14	171	2	67	227	---	100	0.047	3.7	0.10	5.2	-1.46E-04	-0.27	0.31	0.41	37.38	0.9	0.047	3.7	0.175	3.8	2.7E-2	0.9	0.24
bqm_9.1	TJB.12	Oct-14	172	2	219	364	1.6E-4	71	0.048	3.1	0.20	6.6	-7.57E-05	-0.14	0.62	0.26	37.04	1.3	0.048	3.1	0.171	5.1	2.7E-2	1.4	0.26
Weighted mean age (N=8):					**168.9**		**Probability**						**0.34**												
Age error (95% conf., with error in Std)					**1.5**		**Age error (95% conf., without error in Std)**						**1.3**												
MSWD					**1.1**																				
Yerington: Jbqm (treated)																									
bqmcata_1.1	TJB.12	Oct-14	229	3	87	313	7.0E-5	100	0.051	2.8	0.09	7.5	5.14E-06	0.01	0.29	0.69	27.67	1.2	0.051	2.8	0.248	3.7	3.6E-2	1.2	0.33
bqmcata_9.1	TJB.12	Oct-14	231	4	66	210	2.1E-4	71	0.050	3.4	0.09	4.9	-4.73E-05	-0.09	0.32	0.43	27.45	1.9	0.050	3.4	0.235	6.2	3.6E-2	1.9	0.31
bqmcata_10.1	TJB.12	Oct-14	174	3	70	967	---	100	0.049	1.8	0.02	5.4	-1.12E-05	-0.02	0.07	0.39	36.58	1.5	0.049	1.8	0.186	2.4	2.7E-2	1.5	0.63
bqmcata_11.1	TJB.12	Oct-14	167	2	51	92	---	100	0.048	6.1	0.19	6.1	-8.03E-05	-0.15	0.57	0.52	38.20	1.3	0.048	6.1	0.174	6.2	2.6E-2	1.3	0.21
bqmcata_12.1	TJB.12	Oct-14	169	2	113	222	-1.3E-4	100	0.048	3.9	0.15	5.0	-7.11E-05	-0.13	0.53	1.27	37.63	1.5	0.048	3.9	0.185	5.6	2.7E-2	1.5	0.26
bqmcata_13.1	TJB.12	Oct-14	171	1	383	516	-5.7E-5	---	0.048	2.6	0.24	2.3	-1.29E-04	-0.24	0.77	1.14	37.35	0.8	0.048	2.6	0.179	3.2	2.7E-2	0.8	0.26
bqmcata_14.1	TJB.12	Oct-14	173	4	55	108	2.7E-4	100	0.047	5.6	0.16	6.2	-1.78E-04	-0.33	0.53	0.49	36.93	2.1	0.047	5.6	0.160	11.4	2.7E-2	2.2	0.19
bqmcata_15.1	TJB.12	Oct-14	173	2	66	118	4.3E-4	71	0.054	9.7	0.18	5.1	3.01E-04	0.55	0.57	0.91	36.49	1.1	0.054	9.7	0.178	14.7	2.7E-2	1.3	0.09
Weighted mean age (N=6):					**170.9**		**Probability**						**0.27**												
Age error (95% conf., with error in Std)					**1.9**		**Age error (95% conf., without error in Std)**						**1.8**												
MSWD					**1.3**																				
	Weighted mean age (N=14):					**169.6**		**Probability**						**0.17**											
All Jbqm:	**Age error (95% conf., with error in Std)**					**1.3**		**Age error (95% conf., without error in Std)**						**1.1**											
	MSWD					**1.4**																			
Yerington: Jpqm (untreated)																									
pqm_2.1	TJB.12	Oct-14	169	2	171	353	3.2E-4	50	0.048	3.0	0.16	3.3	-1.32E-04	-0.24	0.50	1.35	37.64	1.3	0.0475	3.0	0.156	6.6	2.6E-2	1.4	0.21
pqm_5.1	TJB.12	Oct-14	170	1	390	1293	2.4E-5	100	0.048	2.9	0.10	2.3	-7.79E-05	-0.14	0.31	0.45	37.50	0.9	0.0483	2.9	0.176	3.2	2.7E-2	0.9	0.27

RED not included in sample average

Table E1 cont. Yerington *in situ* zircon U-Pb geochronology

Analysis	Mount	Date	^{207}Pb-corr. ^{206}Pb/^{238}U Age (Ma)	1σ err	Th (ppm)	U (ppm)	^{204}Pb / ^{206}Pb	% err	^{207}Pb / ^{206}Pb	% err	^{208}Pb / ^{206}Pb	% err	^{207}Pb-corrected ^{204}Pb / ^{206}Pb	^{207}Pb-corrected % com ^{206}Pb	^{232}Th / ^{238}U	% err	Total ^{238}U/ ^{206}Pb	% err	Total ^{207}Pb/ ^{206}Pb	% err	^{204}Pb-corrected ^{207}Pb*/^{235}U	% err	^{206}Pb/^{238}U	% err	err corr
pqm_6.1	TJB.12	Oct-14	167	2	262	423	-6.6E-5	100	0.049	2.7	0.20	2.7	-2.45E-05	-0.05	0.64	0.49	38.02	1.1	0.0491	2.7	0.182	3.5	2.6E-2	1.1	0.31
pqm_9.1	TJB.12	Oct-14	171	2	312	503	---	100	0.048	2.3	0.20	2.2	-1.14E-04	-0.21	0.64	0.20	37.32	1.1	0.0478	2.3	0.177	2.5	2.7E-2	1.1	0.44
pqm_10.1	TJB.12	Oct-14	452	7	81	138	-1.4E-4	100	0.054	2.6	0.19	2.8	-1.69E-04	-0.30	0.61	0.38	13.78	1.7	0.054	2.6	0.558	4.8	7.3E-2	1.7	0.35
Weighted mean age (N=4):					**169.4**		**Probability**							**0.61**											
Age error (95% conf., with error in Std)					**1.9**		**Age error (95% conf., without error in Std)**							**1.8**											
MSWD					**0.6**																				
Yerington: Jpqm (treated)																									
pqmcata_1.1	TJB.12	Oct-14	171	2	115	250	1.0E-4	100	0.050	3.3	0.16	3.7	5.65E-05	0.10	0.47	0.31	37.16	0.9	0.050	3.3	0.181	4.6	2.7E-2	0.9	0.20
pqmcata_2.1	TJB.12	Oct-14	168	6	45	132	2.1E-4	100	0.048	4.9	0.12	6.4	-8.94E-05	-0.16	0.35	0.52	37.88	3.6	0.048	4.9	0.163	9.5	2.6E-2	3.6	0.38
pqmcata_3.1	TJB.12	Oct-14	163	2	107	212	---	100	0.050	3.7	0.16	4.2	6.73E-05	0.12	0.52	0.35	39.00	1.0	0.050	3.7	0.178	3.9	2.6E-2	1.0	0.26
pqmcata_6.1	TJB.12	Oct-14	167	2	71	171	3.7E-4	71	0.051	9.0	0.13	5.5	7.73E-05	0.14	0.43	3.28	38.01	1.0	0.051	9.0	0.162	13.4	2.6E-2	1.1	0.08
pqmcata_8.1	TJB.12	Oct-14	169	2	219	379	1.6E-4	71	0.047	5.3	0.21	3.2	-1.35E-04	-0.25	0.60	2.22	37.67	0.9	0.047	5.3	0.165	6.7	2.6E-2	0.9	0.13
Weighted mean age (N=4):					**169.4**		**Probability**							**0.49**											
Age error (95% conf., with error in Std)					**2.0**		**Age error (95% conf., without error in Std)**							**1.9**											
MSWD					**0.8**																				
	Weighted mean age (N=8):					**169.4**		**Probability**						**0.75**											
All Jpqm:	**Age error (95% conf., with error in Std)**					**1.5**		**Age error (95% conf., without error in Std)**						**1.3**											
	MSWD					**0.6**																			
Yerington: Jgd (untreated)																									
gd_1.1	TJB.12	Oct-14	168	1	1450	886	---	100	0.049	1.9	0.55	2.7	-4.78E-05	-0.09	1.69	2.34	37.85	0.8	0.049	1.9	0.178	2.1	2.6E-2	0.8	0.38
gd_2.1	TJB.12	Oct-14	163	4	88	230	7.8E-4	38	0.050	6.4	0.13	4.4	7.73E-05	0.14	0.40	1.54	38.95	2.2	0.050	6.4	0.135	14.4	2.5E-2	2.3	0.16
gd_3.1	TJB.12	Oct-14	171	2	351	389	-7.4E-5	100	0.050	3.1	0.32	2.6	4.85E-05	0.09	0.93	5.10	37.24	0.9	0.050	3.1	0.190	3.8	2.7E-2	0.9	0.24
gd_4.1	TJB.12	Oct-14	171	1	709	716	-3.8E-5	100	0.049	2.1	0.32	2.9	-2.69E-05	-0.05	1.02	2.80	37.21	0.8	0.049	2.1	0.184	2.5	2.7E-2	0.8	0.33
gd_5.1	TJB.12	Oct-14	170	1	547	594	3.4E-4	35	0.048	2.2	0.30	1.8	-1.16E-04	-0.21	0.95	0.17	37.60	0.8	0.048	2.2	0.155	5.0	2.6E-2	0.8	0.17
Weighted mean age (N=5):					**169.6**		**Probability**							**0.22**											
Age error (95% conf., with error in Std)					**1.5**		**Age error (95% conf., without error in Std)**							**1.4**											
MSWD					**1.4**																				
Yerington: Jgd (treated)																									
gdcata_2.1	TJB.12	Oct-14	172	3	227	459	-8.9E-5	71	0.050	5.1	0.15	4.8	2.31E-05	0.04	0.51	3.09	37.06	1.9	0.050	5.1	0.191	5.6	2.7E-2	1.9	0.34
gdcata_3.1	TJB.12	Oct-14	104	1	1466	2189	-1.9E-5	100	0.049	2.7	0.22	1.4	8.28E-05	0.15	0.69	1.69	61.31	1.3	0.049	2.7	0.112	3.0	1.6E-2	1.3	0.42
gdcata_4.1	TJB.12	Oct-14	101	1	1717	1702	---	100	0.047	3.2	0.33	1.3	-6.71E-05	-0.12	1.04	0.38	63.68	0.7	0.047	3.2	0.102	3.3	1.6E-2	0.7	0.22
gdcata_7.1	TJB.12	Oct-14	173	2	875	737	----	9999	0.049	2.0	0.38	2.8	-7.68E-06	-0.01	1.23	1.10	36.83	1.1	0.049	2.0	0.185	2.3	2.7E-2	1.1	0.46
gdcata_11.1	TJB.12	Oct-14	175	2	1860	1100	---	100	0.050	1.6	0.55	2.7	-2.56E-06	0.00	1.75	1.89	36.30	1.1	0.050	1.6	0.188	1.9	2.8E-2	1.1	0.55
Weighted mean age (N=3):					**173.6**		**Probability**							**0.51**											
Age error (95% conf., with error in Std)					**2.5**		**Age error (95% conf., without error in Std)**							**2.4**											
MSWD					**0.7**																				
	Weighted mean age (N=7*):					**170.0**		**Probability**						**0.20**											
All Jgd:	**Age error (95% conf., with error in Std)**					**1.4**		**Age error (95% conf., without error in Std)**						**1.3**											
	MSWD					**1.4**		**Does not include gdcata_11.1*																	
Mt. Dromedary (untreated)																									
MtD_27.2	TJB.12	Oct-14	103	2	1375	1535	-3.0E-6	100	0.044	2.0	0.30	1.6	-2.58E-04	-0.48	0.93	0.59	62.46	1.8	0.0443	2.0	0.0979	2.7	1.60E-02	1.8	0.66
MtD_28.1	TJB.12	Oct-14	97.1	1	125	360	1.4E-4	---	0.053	6.6	0.12	5.3	3.44E-04	0.64	0.36	0.33	65.48	1.2	0.0530	6.6	0.1072	7.5	1.52E-02	1.2	0.16
MtD_29.1	TJB.12	Oct-14	101	1	372	505	-1.1E-4	100	0.045	3.6	0.24	6.7	-1.75E-04	-0.32	0.76	0.87	63.33	1.4	0.0455	3.6	0.1028	5.1	1.58E-02	1.4	0.28
MtD_31.2	TJB.12	Oct-14	95.9	1	224	348	-1.7E-4	9999	0.053	3.5	0.23	3.9	3.34E-04	0.62	0.67	0.27	66.28	1.2	0.0529	3.5	0.1155	###	1.51E-02	31.4	0.07
Weighted mean age (N=4):					**98.4**		**Probability**							**0.00**											
Age error (95% conf., with error in Std)					**4.9**		**Age error (95% conf., without error in Std)**							**4.9**											
MSWD					**5.22**																				

RED not included in sample average

Table E1 cont. Yerington i*n situ* zircon U-Pb geochronology

Analysis	Mount	Date	^{207}Pb-corr. ^{206}Pb/^{238}U Age (Ma)	1σ err	Th (ppm)	U (ppm)	^{204}Pb / ^{206}Pb	% err	^{207}Pb / ^{206}Pb	% err	^{208}Pb / ^{206}Pb	% err	^{207}Pb-corrected ^{204}Pb / ^{206}Pb	^{207}Pb-corrected % com ^{206}Pb	^{232}Th / ^{238}U	% err	Total ^{238}U/ ^{206}Pb	% err	Total ^{207}Pb/ ^{206}Pb	% err	^{204}Pb-corrected ^{207}Pb*/^{235}U	% err	^{204}Pb-corrected ^{206}Pb/^{238}U	% err	err corr
Mt. Dromedary (treated)																									
MtDC_24.1	TJB.12	Oct-14	100	1	68	184	-5.8E-4	91	0.044	10.3	0.12	7.3	-2.50E-04	-0.46	0.38	0.44	64.18	1.3	0.0444	10.3	0.1149	17.0	1.57E-02	1.6	0.09
MtDC_25.1	TJB.12	Oct-14	99.2	2	112	358	-1.3E-5	---	0.049	4.1	0.10	5.7	4.51E-05	0.08	0.32	0.34	64.40	1.8	0.0487	4.1	0.1047	9.4	1.55E-02	1.9	0.20
MtDC_26.2	TJB.12	Oct-14	100	2	279	442	-1.3E-4	73	0.049	3.7	0.21	3.6	3.32E-05	0.06	0.65	0.24	63.87	1.8	0.0485	3.7	0.1092	4.9	1.57E-02	1.8	0.37
MtDC_27.1	TJB.12	Oct-14	100	1	254	653	-2.6E-5	390	0.049	2.8	0.12	4.0	6.93E-05	0.13	0.40	0.25	63.70	1.5	0.0491	2.8	0.1071	4.4	1.57E-02	1.5	0.34
Weighted mean age (N=4):					**100.0**		**Probability**						**0.97**												
Age error (95% conf., with error in Std)					**1.7**		**Age error (95% conf., without error in Std)**						**1.6**												
MSWD					**0.08**																				
	Weighted mean age (N=8):					**99.1**			**Probability**					**0.01**												
All Mt. Drom.:	**Age error (95% conf., with error in Std)**					**2.0**			**Age error (95% conf., without error in Std)**					**2.0**												
	MSWD					**2.61**																			

Table E2. Hafnarfjall-Skarðsheiði *in situ* zircon U-Pb geochronology

Analysis	Mount	Date	^{207}Pb-corr. ^{206}Pb/^{238}U Age (Ma)	1σ err	Th (ppm)	U (ppm)	^{204}Pb/ ^{206}Pb	% err	^{207}Pb-corrected ^{207}Pb ^{206}Pb	% err	^{208}Pb/^{206} Pb	% err	^{207}Pb-corrected ^{204}Pb/^{206}Pb	^{207}Pb-corrected % com ^{206}Pb	UO/U	% err	^{232}Th/^{23} ^{8}U	% err	Total ^{238}U/ ^{206}Pb	% err	Total ^{207}Pb/ ^{206}Pb	% err	^{204}Pb-corrected ^{207}Pb*/^{235} U	% err	^{204}Pb-corrected ^{206}Pb/ ^{238}U	% err	err corr
Hafnarfjall-Skarðsheiði: DrE1302																											
DrE1302-4.1	TJB.6	Apr-14	4.19	0.12	563	642	-2.2E-3	129	0.0473	14	0.153	27	7.6E-5	0.14	5.67	2.5	0.667	0.78	1570	2.7	0.0473	14	0.0072	50	6.6E-4	6	0.1
DrE1302-5.1	TJB.6	Apr-14	4.23	0.22	70	123	5.2E-3	158	0.0742	19	0.224	42	1.9E-3	3.55	5.69	2.7	0.532	0.58	1501	5.0	0.0742	19	0.0006	1673	6.0E-4	18	0.0
DrE1302-6.1	TJB.6	Apr-14	4.01	0.09	376	522	6.3E-3	75	0.0373	16	0.228	22	-6.0E-4	-1.12	5.69	2.4	0.629	1.07	1663	2.3	0.0373	16	0.0051	42	5.3E-4	10	0.2
DrE1302-7.1	TJB.6	Apr-14	4.26	0.11	236	368	3.8E-3	112	0.0608	14	0.310	22	9.9E-4	1.86	5.69	2.4	0.583	0.17	1516	2.3	0.0608	14	0.0001	6117	6.1E-4	9	0.0
DrE1302-8.1	TJB.6	Apr-14	4.19	0.11	230	371	3.6E-3	112	0.0405	17	0.295	22	-3.8E-4	-0.71	5.61	2.6	0.556	0.66	1582	2.6	0.0405	17	0.0014	162	5.9E-4	9	0.1
DrE1302-10.1	TJB.6	Apr-14	4.11	0.14	296	404	-9.9E-4	224	0.0479	16	0.306	22	1.2E-4	0.23	5.62	2.4	0.602	1.60	1600	3.2	0.0479	16	0.0055	52	6.4E-4	5	0.1
DrE1302-12.1	TJB.6	Apr-14	3.98	0.12	233	381	-3.9E-3	112	0.0482	16	0.258	24	1.4E-4	0.26	5.77	2.3	0.534	0.72	1652	2.9	0.0482	16	0.0091	56	6.5E-4	8	0.1
DrE1302-13.1	TJB.6	Apr-14	4.16	0.14	201	350	-6.0E-3	91	0.0584	15	0.145	32	8.3E-4	1.55	5.54	2.7	0.437	0.53	1561	3.1	0.0584	15	0.0135	48	7.1E-4	10	0.2
DrE1302-14.1	TJB.6	Apr-14	3.85	0.14	124	234	-3.3E-3	158	0.0742	16	0.272	30	1.9E-3	3.55	5.43	2.0	0.474	0.64	1653	3.5	0.0742	16	0.0105	58	6.4E-4	10	0.2
DrE1302-15.1	TJB.6	Apr-14	4.39	0.13	400	590	6.4E-3	79	0.0485	14	0.154	28	1.6E-4	0.30	6.06	3.4	0.503	0.92	1495	3.0	0.0485	14	0.0047	23	5.9E-4	11	0.5
Weighted mean age (N=9)				4.11			**Probability**		0.33																		
Age error (95% conf., w/error in Std)				0.08			**MSWD**		1.14																		
Hafnarfjall-Skarðsheiði: RnE1201																											
RnE1201-11.1	TJB.5	Apr-14	4.40	0.20	74	148	-8.3E-3	158	0.091	22	0.364	41	3.0E-3	5.69	5.46	1.62	0.52	0.94	1412	3.9	0.0911	22	0.0215	75	8.2E-4	22	0.3
RnE1201-13.1	TJB.5	Apr-14	4.39	0.41	55	118	4.5E-2	75	0.110	22	0.296	51	4.4E-3	8.15	5.55	1.79	0.48	0.69	1376	8.9	0.1105	22	0.0597	621	1.1E-4	407	0.7
RnE1201-14.1	TJB.5	Apr-14	4.43	0.13	480	486	-1.3E-3	224	0.049	19	0.302	26	1.7E-4	0.32	5.59	1.82	1.02	0.66	1477	2.7	0.0487	19	0.0065	64	6.9E-4	6	0.1
RnE1201-16.1	TJB.5	Apr-14	4.00	0.20	36	92	2.6E-2	112	0.103	25	0.477	45	3.9E-3	7.22	5.76	1.17	0.40	0.51	1531	3.6	0.1032	25	0.0270	206	3.4E-4	104	0.5
RnE1201-18.1	TJB.5	Apr-14	3.50	0.25	51	112	1.0E-32	100	0.124	22	0.085	100	5.3E-3	9.90	5.84	1.68	0.47	0.43	1707	6.3	0.1243	22	0.0100	23	5.9E-4	6	0.3
RnE1201-20.1	TJB.5	Apr-14	4.19	0.23	136	208	5.5E-3	158	0.078	19	0.075	75	2.1E-3	3.99	5.79	1.70	0.67	1.23	1507	5.2	0.0777	19	0.0008	1194	5.9E-4	19	0.0
RnE1201-21.1	TJB.5	Apr-14	5.00	0.30	43	104	-5.0E-3	224	0.066	28	0.071	104	1.3E-3	2.46	5.64	2.02	0.43	0.78	1282	5.6	0.0656	28	0.0155	106	8.5E-4	20	0.2
RnE1201-22.1	TJB.5	Apr-14	4.12	0.21	35	90	-1.2E-2	158	0.120	23	0.353	51	5.0E-3	9.33	5.68	1.90	0.40	0.51	1452	3.5	0.1198	23	0.0295	74	8.5E-4	30	0.4
RnE1201-23.1	TJB.5	Apr-14	4.38	0.16	74	144	7.8E-3	158	0.059	26	0.105	75	8.4E-4	1.58	5.71	1.73	0.53	0.36	1479	3.1	0.0586	26	0.0059	54	5.8E-4	27	0.5
RnE1201-24.1	TJB.5	Apr-14	3.77	0.17	156	213	1.4E-2	100	0.074	19	0.329	35	1.9E-3	3.53	5.42	2.09	0.75	0.69	1686	4.3	0.0740	19	0.0115	89	4.4E-4	35	0.4
Weighted mean age (N=7)				4.30			**Probability**		0.57																		
Age error (95% conf., w/error in Std)				0.14			**MSWD**		0.8																		
Hafnarfjall-Skarðsheiði: TuE1301																											
TuE1301-13.1	TJB.5	Apr-14	5.26	0.12	190	292	7.5E-3	100	0.050	18	0.337	26	2.8E-4	0.52	5.86	1.54	0.67	0.22	1239	2.0	0.0503	18	0.0074	46	6.9E-4	16	0.4
TuE1301-15.1	TJB.5	Apr-14	5.15	0.17	112	189	1.0E-2	112	0.066	20	0.225	41	1.3E-3	2.47	5.60	1.91	0.61	1.12	1242	3.0	0.0657	20	0.0102	65	6.5E-4	26	0.4
TuE1301-16.1	TJB.5	Apr-14	5.19	0.17	199	306	7.9E-3	100	0.053	19	0.261	30	5.0E-4	0.93	5.54	1.63	0.67	1.10	1252	3.0	0.0535	19	0.0077	47	6.8E-4	18	0.4
TuE1301-17.1	TJB.5	Apr-14	5.31	0.30	99	171	1.0E-32	100	0.059	20	0.282	35	8.5E-4	1.59	5.94	1.32	0.60	1.07	1215	5.6	0.0587	20	0.0067	21	8.2E-4	6	0.3
TuE1301-18.1	TJB.5	Apr-14	5.41	0.13	346	437	3.8E-3	112	0.040	17	0.257	24	-4.0E-4	-0.74	5.88	1.21	0.82	0.17	1218	2.3	0.0403	17	0.0022	116	7.6E-4	9	0.1
TuE1301-20.1	TJB.5	Apr-14	5.25	0.19	283	333	-2.8E-3	158	0.052	19	0.351	24	3.8E-4	0.70	5.55	1.74	0.88	0.52	1238	3.5	0.0517	19	0.0106	66	8.5E-4	9	0.1
TuE1301-21.1	TJB.5	Apr-14	5.27	0.23	146	245	1.6E-2	75	0.043	21	0.244	34	-2.0E-4	-0.37	5.74	1.48	0.62	0.25	1249	4.4	0.0433	21	0.0235	98	5.6E-4	33	0.3
TuE1301-22.1	TJB.5	Apr-14	5.48	0.15	406	436	3.0E-3	129	0.044	17	0.329	21	-1.8E-4	-0.33	5.67	1.62	0.96	0.94	1198	2.7	0.0436	17	0.0004	1498	7.9E-4	8	0.0
TuE1301-23.1	TJB.5	Apr-14	5.40	0.19	184	252	5.3E-3	129	0.060	19	0.184	38	9.7E-4	1.81	5.58	1.90	0.75	0.88	1191	3.2	0.0604	19	0.0027	201	7.6E-4	15	0.1
TuE1301-24.1	TJB.5	Apr-14	5.38	0.19	322	423	5.6E-3	100	0.050	17	0.284	24	2.4E-4	0.45	5.59	2.05	0.79	0.62	1212	3.5	0.0497	17	0.0043	33	7.4E-4	12	0.4
Weighted mean age (N=10)				5.32			**Probability**		0.93																		
Age error (95% conf., w/error in Std)				0.10			**MSWD**		0.42																		
Hafnarfjall-Skarðsheiði: FlI1201																											
FlI1201-3.1	TJB.2	Apr-14	3.86	0.32	53	90	8.5E-3	158	0.138	20	0.307	46	6.2E-3	11.66	5.48	1.32	0.61	0.35	1508	7.5	0.1383	20	0.0005	4081	5.6E-4	31	0.0
FlI1201-4.1	TJB.2	Apr-14	3.57	0.14	44	88	1.5E-2	129	0.107	22	0.143	73	4.1E-3	7.75	5.40	1.79	0.51	0.38	1711	2.1	0.1073	22	0.0107	94	4.2E-4	52	0.6
FlI1201-5.1	TJB.2	Apr-14	3.79	0.25	52	71	1.0E-1	53	0.101	24	0.327	51	3.7E-3	7.00	5.53	1.27	0.76	0.35	1618	5.8	0.1014	24	-0.1264	125	-5.5E-4	112	0.9
FlI1201-11.1	TJB.2	Apr-14	3.88	0.27	58	81	-1.4E-2	158	0.101	26	-0.014	274	3.7E-3	7.00	5.66	1.91	0.73	1.88	1578	6.0	0.1014	26	0.0273	82	7.9E-4	32	0.4
FlI1201-12.1	TJB.2	Apr-14	3.42	0.57	18	30	-2.0E-2	224	0.118	42	0.275	104	4.9E-3	9.10	5.60	1.64	0.60	0.71	1761	15.7	0.1180	42	0.0333	120	7.8E-4	62	0.5
FlI1201-13.1	TJB.2	Apr-14	4.23	0.32	33	60	-3.3E-2	129	0.088	36	1.287	36	2.8E-3	5.30	5.08	1.33	0.56	0.55	1475	6.4	0.0880	36	0.0565	79	1.1E-3	50	0.6
FlI1201-14.1	TJB.2	Apr-14	4.01	0.12	376	385	7.3E-3	100	0.064	16	0.544	20	1.2E-3	2.22	5.73	1.71	1.01	0.85	1601	2.7	0.0636	16	0.0043	28	5.4E-4	16	0.6
FlI1201-15.1	TJB.2	Apr-14	4.11	0.17	80	140	-3.6E-3	224	0.050	27	0.375	38	2.9E-4	0.55	5.90	1.23	0.59	0.53	1595	3.8	0.0505	27	0.0092	106	6.7E-4	15	0.1
FlI1201-29.1	TJB.2	Apr-14	3.63	0.39	881	816	1.1E-2	53	0.199	31	0.625	21	1.0E-2	19.35	5.47	2.18	1.11	1.84	1460	4.8	0.1990	31	0.0032	307	5.5E-4	14	0.0
FlI1201-30.1	TJB.2	Apr-14	4.70	0.37	1306	1139	5.4E-2	34	0.120	33	0.446	20	5.0E-3	9.30	5.60	1.13	1.18	0.29	1262	6.0	0.1196	33	-0.0795	3658	-1.0E-5	2606	0.7
Weighted mean age (N=8)				3.88			**Probability**		0.18																		
Age error (95% conf., with error in Std)				0.19			**MSWD**		1.50																		

RED not included in sample average

Table E2 cont. Hafnarfjall-Skarðsheiði *in situ* zircon U-Pb geochronology

Analysis	Mount	Date	^{207}Pb-corr. ^{206}Pb/^{238}U Age (Ma)	1σ err	Th (ppm)	U (ppm)	^{204}Pb/ ^{206}Pb	% err	^{207}Pb ^{206}Pb	% err	^{208}Pb/^{206} Pb	% err	^{207}Pb-corrected ^{204}Pb/^{206}Pb	^{207}Pb-corrected % com ^{206}Pb	UO/U	% err	^{232}Th/^{23} ^{8}U	% err	Total ^{238}U/ ^{206}Pb	% err	Total ^{207}Pb/ ^{206}Pb	% err	^{204}Pb-corrected ^{207}Pb*/^{235} U	% err	^{204}Pb-corrected ^{206}Pb/ ^{238}U	% err	err corr
Hafnarfjall-Skarðsheiði: BrE1201																											
BrE1-1.1	TJB.3	Jan-14	5.36	0.12	106	169	7.5E-3	120	0.081	20	0.203	29	2.3E-3	4.37	5.34	1.38	0.65	0.74	1171	0.6	0.0807	20	0.0042	139	7.4E-4	19	0.1
BrE1-10.1	TJB.3	Jan-14	5.12	0.22	71	144	7.6E-3	158	0.063	13	0.109	46	1.1E-3	2.09	5.24	1.05	0.51	0.27	1257	4.3	0.0627	13	0.0062	32	6.8E-4	27	0.8
BrE1-11.1	TJB.3	Jan-14	5.29	0.26	39	88	2.0E-2	75	0.284	7	0.779	18	1.6E-2	30.11	5.36	0.62	0.45	0.35	867	3.7	0.2840	7	0.0040	731	7.3E-4	44	0.1
BrE1-12.1	TJB.3	Jan-14	5.46	0.12	57	117	1.7E-2	85	0.048	16	0.370	26	9.1E-5	0.17	5.43	0.35	0.50	0.29	1199	2.0	0.0475	16	0.0246	111	5.7E-4	39	0.3
BrE1-13.1	TJB.3	Jan-14	5.17	0.20	87	152	4.2E-3	100	0.050	14	0.168	35	2.6E-4	0.48	5.45	0.76	0.59	0.24	1265	3.8	0.0500	14	0.0018	201	7.3E-4	9	0.0
BrE1-14.1	TJB.3	Jan-14	5.31	0.21	58	120	1.7E-2	85	0.051	16	0.245	32	3.4E-4	0.64	5.63	0.58	0.50	0.30	1229	3.9	0.0512	16	0.0236	110	5.6E-4	39	0.4
BrE1-15.1	TJB.3	Jan-14	5.12	0.21	67	129	8.6E-3	158	0.061	15	0.276	31	1.0E-3	1.90	5.44	0.67	0.54	0.28	1258	3.9	0.0612	15	0.0080	65	6.7E-4	31	0.5
BrE1-16.1	TJB.3	Jan-14	5.23	0.19	93	158	2.0E-3	183	0.073	12	0.236	29	1.8E-3	3.41	5.53	0.31	0.61	0.24	1212	3.5	0.0731	12	0.0047	135	7.9E-4	8	0.1
BrE1-17.1	TJB.3	Jan-14	5.17	0.33	59	121	1.5E-2	100	0.054	15	0.165	41	5.1E-4	0.96	5.44	0.32	0.50	0.48	1259	6.4	0.0537	15	0.0194	115	5.7E-4	39	0.3
BrE1-18.1	TJB.3	Jan-14	5.14	0.20	49	111	2.5E-2	77	0.047	18	0.418	28	8.5E-5	0.16	5.36	0.60	0.45	0.56	1277	3.9	0.0474	18	0.0370	149	4.2E-4	67	0.5
BrE1-19.1	TJB.3	Jan-14	5.59	0.07	1047	1139	2.1E-3	75	0.076	9	0.343	9	2.0E-3	3.76	5.60	0.31	0.95	0.29	1126	1.0	0.0759	9	0.0052	57	8.5E-4	3	0.1
BrE1-2.1	TJB.3	Jan-14	5.62	0.14	69	133	-2.0E-3	105	0.037	17	0.198	32	-6.2E-4	-1.16	5.52	0.78	0.54	0.26	1181	2.4	0.0370	17	0.0079	46	8.8E-4	4	0.1
BrE1-20.1	TJB.3	Jan-14	5.49	0.23	65	135	8.4E-5	129	0.076	19	0.339	31	2.0E-3	3.72	4.89	1.29	0.49	0.32	1150	3.9	0.0756	19	0.0089	20	8.7E-4	4	0.2
BrE1-21.1	TJB.3	Jan-14	5.20	0.09	65	127	2.0E-2	77	0.063	19	0.130	45	1.2E-3	2.16	5.60	0.56	0.53	0.30	1235	1.0	0.0632	19	0.0286	116	5.0E-4	48	0.4
BrE1-22.1	TJB.3	Jan-14	5.21	0.19	39	88	3.8E-2	65	0.084	20	0.256	38	2.6E-3	4.82	5.48	0.39	0.46	0.38	1200	2.8	0.0842	20	0.0581	260	2.5E-4	155	0.6
BrE1-23.1	TJB.3	Jan-14	11.34	0.17	423	444	1.9E-3	100	0.044	7	0.317	12	-1.5E-4	-0.29	5.51	0.70	0.98	0.41	574	1.5	0.0440	7	0.0033	217	1.7E-3	4	0.0
BrE1-24.1	TJB.3	Jan-14	5.49	0.22	58	119	2.8E-3	183	0.043	20	0.268	32	-2.1E-4	-0.39	5.55	0.76	0.50	0.31	1200	4.0	0.0431	20	0.0000	18965	7.9E-4	11	0.0
BrE1-25.1	TJB.3	Jan-14	5.21	0.12	99	167	-2.0E-3	105	0.054	15	0.246	29	5.0E-4	0.93	5.44	0.63	0.61	0.58	1247	2.2	0.0535	15	0.0094	37	8.3E-4	4	0.1
BrE1-26.1	TJB.3	Jan-14	5.52	0.35	65	131	-2.3E-3	105	0.068	13	0.277	29	1.5E-3	2.71	5.54	0.32	0.51	0.29	1157	6.3	0.0676	13	0.0123	34	9.0E-4	8	0.2
BrE1-27.1	TJB.3	Jan-14	5.38	0.10	260	353	7.0E-3	77	0.048	9	0.290	18	1.1E-4	0.21	5.44	1.13	0.76	0.65	1217	1.9	0.0478	9	0.0070	32	7.1E-4	12	0.4
BrE1-29.1	TJB.3	Jan-14	5.32	0.12	136	333	6.7E-3	77	0.065	9	0.165	23	1.3E-3	2.44	5.41	1.08	0.42	0.58	1205	2.2	0.0655	9	0.0045	43	7.3E-4	11	0.3
BrE1-3.1	TJB.3	Jan-14	5.24	0.10	84	151	6.8E-3	158	0.046	15	0.260	28	1.5E-5	0.03	5.34	1.13	0.57	0.24	1252	1.7	0.0464	15	0.0066	65	7.0E-4	23	0.4
BrE1-30.1	TJB.3	Jan-14	5.54	0.19	83	143	1.0E-2	100	0.066	20	0.268	27	1.3E-3	2.50	5.37	0.73	0.60	0.24	1155	2.9	0.0659	20	0.0112	61	7.0E-4	24	0.4
BrE1-31.1	TJB.3	Jan-14	5.17	0.20	96	164	3.7E-3	100	0.046	14	0.293	25	-3.5E-5	-0.06	5.48	0.88	0.61	0.23	1271	3.9	0.0457	14	0.0013	267	7.3E-4	8	0.0
BrE1-32.1	TJB.3	Jan-14	5.12	0.21	58	124	4.8E-3	100	0.060	14	0.236	32	9.6E-4	1.80	5.52	0.70	0.48	0.29	1260	4.0	0.0604	14	0.0016	314	7.2E-4	11	0.0
BrE1-33.1	TJB.3	Jan-14	5.34	0.17	39	93	1.1E-2	158	0.056	17	0.220	38	6.9E-4	1.29	5.51	0.68	0.44	0.36	1213	2.9	0.0564	17	0.0129	127	6.6E-4	40	0.3
BrE1-34.1	TJB.3	Jan-14	5.36	0.13	99	166	4.0E-3	100	0.060	12	0.318	25	9.5E-4	1.78	5.31	0.47	0.62	0.23	1203	2.4	0.0602	12	0.0003	2107	7.7E-4	8	0.0
BrE1-35.1	TJB.3	Jan-14	5.36	0.09	26	74	8.0E-3	100	0.074	16	0.078	71	1.9E-3	3.58	5.41	0.40	0.36	0.42	1182	0.8	0.0744	16	0.0058	43	7.2E-4	17	0.4
BrE1-36.1	TJB.3	Jan-14	5.27	0.06	106	176	7.5E-3	120	0.056	12	0.273	25	6.5E-4	1.21	5.34	0.77	0.62	0.43	1229	0.6	0.0557	12	0.0069	38	7.0E-4	20	0.5
BrE1-37.1	TJB.3	Jan-14	5.26	0.17	58	113	5.5E-3	100	0.041	17	0.137	45	-3.7E-4	-0.70	5.48	1.03	0.53	0.50	1256	3.3	0.0407	17	0.0051	30	7.1E-4	12	0.4
BrE1-38.1	TJB.3	Jan-14	5.46	0.14	62	129	1.1E-2	120	0.050	16	0.123	45	2.4E-4	0.44	5.43	0.31	0.50	0.29	1196	2.4	0.0497	16	0.0140	106	6.6E-4	31	0.3
BrE1-39.1	TJB.3	Jan-14	5.21	0.11	48	107	1.7E-2	100	0.067	15	0.320	32	1.4E-3	2.67	5.40	0.76	0.46	0.34	1227	1.6	0.0672	15	0.0225	123	5.5E-4	47	0.4
BrE1-4.1	TJB.3	Jan-14	5.23	0.12	38	94	3.1E-3	183	0.110	11	0.296	32	4.3E-3	8.05	5.31	0.77	0.42	0.59	1154	1.7	0.1097	11	0.0074	133	8.2E-4	11	0.1
BrE1-40.1	TJB.3	Jan-14	5.23	0.09	125	192	4.4E-5	129	0.055	13	0.163	32	5.9E-4	1.10	5.56	0.66	0.67	0.56	1241	1.6	0.0548	13	0.0060	13	8.1E-4	2	0.1
BrE1-41.1	TJB.3	Jan-14	5.44	0.17	80	134	4.7E-3	100	0.082	11	0.438	23	2.4E-3	4.57	5.41	0.55	0.61	0.26	1151	2.9	0.0823	11	0.0011	783	7.9E-4	10	0.0
BrE1-42.1	TJB.3	Jan-14	5.38	0.23	74	142	4.6E-3	100	0.059	14	0.293	28	8.9E-4	1.67	5.38	0.57	0.54	0.66	1200	4.2	0.0593	14	0.0014	385	7.6E-4	10	0.0
BrE1-43.1	TJB.3	Jan-14	5.29	0.16	74	140	2.3E-3	183	0.043	17	0.226	32	-2.2E-4	-0.40	5.46	0.70	0.55	0.26	1247	2.9	0.0430	17	0.0007	1057	7.7E-4	9	0.0
BrE1-44.1	TJB.3	Jan-14	5.37	0.17	54	113	1.5E-2	100	0.063	14	0.193	38	1.1E-3	2.07	5.42	0.64	0.49	0.31	1196	3.1	0.0625	14	0.0194	108	6.0E-4	38	0.4
BrE1-45.1	TJB.3	Jan-14	4.94	0.08	1102	976	5.6E-3	46	0.137	3	0.516	8	6.1E-3	11.50	5.23	1.08	1.17	0.07	1174	1.6	0.1370	3	0.0058	78	7.6E-4	6	0.1
BrE1-46.1	TJB.3	Jan-14	5.36	0.26	49	82	3.8E-2	54	0.230	8	0.700	20	1.2E-2	23.30	5.42	0.37	0.63	2.85	938	4.0	0.2302	8	0.0528	198	3.1E-4	130	0.7
BrE1-5.1	TJB.3	Jan-14	5.36	0.19	92	155	3.7E-3	100	0.048	14	0.314	24	1.5E-4	0.28	5.47	0.54	0.61	0.23	1220	3.5	0.0484	14	0.0011	379	7.6E-4	8	0.0
BrE1-6.1	TJB.3	Jan-14	5.17	0.11	96	157	1.5E-2	77	0.061	20	0.309	25	1.0E-3	1.89	5.41	1.21	0.63	0.23	1246	1.5	0.0611	20	0.0191	85	5.8E-4	30	0.4
BrE1-7.1	TJB.3	Jan-14	5.65	0.19	78	142	4.1E-3	100	0.037	15	0.261	28	-6.2E-4	-1.15	5.57	0.69	0.57	0.25	1174	3.4	0.0371	15	0.0031	39	7.9E-4	9	0.2
BrE1-8.1	TJB.3	Jan-14	5.38	0.24	103	180	1.8E-3	183	0.042	15	0.220	28	-2.9E-4	-0.55	5.33	1.02	0.59	0.22	1226	4.4	0.0418	15	0.0016	344	7.9E-4	8	0.0
BrE1-9.1	TJB.3	Jan-14	5.50	0.22	74	129	4.8E-3	100	0.054	14	0.190	35	5.0E-4	0.94	5.40	0.73	0.60	0.74	1181	4.0	0.0536	14	0.0025	144	7.7E-4	11	0.1
Weighted mean age (N=43)				5.33		**Probability**			0.43																		
Age error (95% conf., with error in Std)				0.04		**MSWD**			1.02																		
Hafnarfjall-Skarðsheiði: SvE1302																											
SvE1302-1.1	TJB.11	Oct-14	5.71	0.10	275	480	3.3E-3	50	0.070	8	0.267	8	1.6E-3	3.00	5.16	1.95	0.59	1.23	1113	1.6	0.0698	8	0.0023	138	8.4E-4	4	0.0
SvE1302-2.1	TJB.11	Oct-14	5.21	0.28	45	109	1.5E-2	45	0.201	10	0.609	11	1.0E-2	19.55	5.12	1.66	0.43	0.79	1014	4.5	0.2006	10	0.0056	162	7.0E-4	19	0.1
SvE1302-3.1	TJB.11	Oct-14	5.27	0.24	102	179	1.3E-2	41	0.132	18	0.477	10	5.8E-3	10.88	5.15	1.88	0.59	0.28	1110	3.2	0.1321	18	0.0082	48	6.9E-4	13	0.3
SvE1302-4.1	TJB.11	Oct-14	5.57	0.16	37	97	3.7E-3	100	0.084	19	0.372	16	2.5E-3	4.75	5.29	2.28	0.40	2.08	1121	2.1	0.0837	19	0.0031	230	8.3E-4	8	0.0

RED not included in sample average

Table E2 cont. Hafnarfjall-Skarðsheiði *in situ* zircon U-Pb geochronology

Analysis	Mount	Date	^{207}Pb-corr. ^{206}Pb/^{238}U Age (Ma)	1σ err	Th (ppm)	U (ppm)	^{204}Pb/ ^{206}Pb	% err	^{207}Pb ^{206}Pb	% err	^{208}Pb/^{206} Pb	% err	^{207}Pb-corrected ^{204}Pb/^{206}Pb	^{207}Pb-corrected % com ^{206}Pb	UO/U	% err	^{232}Th/^{23} ^{8}U	% err	Total ^{238}U/ ^{206}Pb	% err	Total ^{207}Pb/ ^{206}Pb	% err	^{204}Pb-corrected ^{207}Pb*/^{235} U	% err	^{204}Pb-corrected ^{206}Pb/ ^{238}U	% err	err corr
SvE1302-5.1	TJB.11	Oct-14	5.23	0.22	54	117	3.3E-2	32	0.117	14	0.473	13	4.8E-3	9.01	5.15	1.31	0.48	0.59	1142	3.7	0.1173	14	0.0478	89	3.4E-4	51	0.6
SvE1302-6.1	TJB.11	Oct-14	5.65	0.27	56	121	1.2E-2	50	0.119	12	0.519	12	4.9E-3	9.17	5.20	1.98	0.47	0.96	1054	4.4	0.1186	12	0.0092	33	7.3E-4	15	0.5
SvE1302-7.1	TJB.11	Oct-14	5.14	0.31	2150	1611	2.9E-3	30	0.056	10	0.491	3	6.3E-4	1.19	5.33	1.27	1.38	4.98	1257	6.1	0.0555	10	0.0012	130	7.5E-4	6	0.0
SvE1302-8.1	TJB.11	Oct-14	5.27	0.14	1385	686	6.6E-3	33	0.066	9	0.771	5	1.3E-3	2.47	4.89	2.37	2.09	1.46	1203	2.6	0.0657	9	0.0043	26	7.3E-4	5	0.2
SvE1302-9.1	TJB.11	Oct-14	5.26	0.12	72	135	2.6E-2	33	0.114	14	0.232	17	4.6E-3	8.63	5.23	1.79	0.55	0.68	1141	0.7	0.1143	14	0.0347	60	4.6E-4	31	0.5
SvE1302-10.1	TJB.11	Oct-14	5.48	0.17	3108	1350	2.2E-3	35	0.050	6	0.809	3	2.7E-4	0.50	5.38	2.00	2.38	0.79	1178	3.0	0.0501	6	0.0018	84	8.1E-4	3	0.0
SvE1302-11.1	TJB.11	Oct-14	5.75	1.04	858	2119	3.3E-2	14	0.479	11	1.200	10	2.9E-2	54.79	4.96	3.51	0.42	7.18	515	11.1	0.4789	11	0.0086	243	7.5E-4	25	0.1
SvE1302-12.1	TJB.11	Oct-14	4.86	1.59	922	881	2.4E-2	11	0.519	20	1.401	19	3.2E-2	59.83	4.56	5.79	1.08	5.18	541	6.6	0.5187	20	0.0372	74	1.0E-3	11	0.1
SvE1302-13.1	TJB.11	Oct-14	5.50	0.11	253	396	3.4E-3	50	0.068	9	0.374	7	1.5E-3	2.82	5.28	2.45	0.66	1.28	1158	1.9	0.0684	9	0.0019	167	8.1E-4	4	0.0
SvE1302-14.1	TJB.11	Oct-14	4.33	0.58	493	409	4.8E-3	41	0.069	9	0.546	6	1.5E-3	2.88	5.91	12.8	1.25	1.32	1471	13.6	0.0689	9	0.0006	402	6.2E-4	14	0.0
SvE1302-15.1	TJB.11	Oct-14	4.93	0.25	88	154	2.4E-2	29	0.121	10	0.503	10	5.1E-3	9.51	5.17	2.27	0.59	0.24	1205	4.9	0.1212	10	0.0284	45	4.6E-4	23	0.5
Weighted mean age (N=12)				5.43		**Probability**			0.05																		
Age error (95% conf., with error in Std)				0.14		**MSWD**			1.80																		
Hafnarfjall-Skarðsheiði: ShE1302																											
ShE1302-1.1	TJB.11	Oct-14	4.57	0.10	1870	1745	7.4E-4	71	0.050	7	0.38	5	2.6E-4	0.50	5.20	1.82	1.11	0.56	1426	2.1	0.0501	7	0.004	22	6.9E-4	2	0.1
ShE1302-2.1	TJB.11	Oct-14	4.38	0.14	803	591	1.1E-3	100	0.046	14	0.43	8	-1.2E-5	-0.02	5.44	1.29	1.40	3.04	1496	3.3	0.0460	14	0.003	61	6.6E-4	4	0.1
ShE1302-3.1	TJB.11	Oct-14	4.17	0.08	509	564	2.4E-3	71	0.060	11	0.32	9	9.0E-4	1.69	5.30	0.86	0.93	1.08	1551	1.7	0.0595	11	0.002	122	6.2E-4	4	0.0
ShE1302-4.1	TJB.11	Oct-14	4.45	0.12	678	740	2.8E-3	50	0.049	9	0.32	7	1.9E-4	0.36	5.20	1.47	0.95	1.99	1469	2.6	0.0490	9	0.000	482	6.4E-4	4	0.0
ShE1302-5.1	TJB.11	Oct-14	4.43	0.09	1054	923	2.9E-3	50	0.048	10	0.38	7	1.1E-4	0.20	5.24	1.26	1.18	0.94	1477	2.0	0.0477	10	0.000	923	6.4E-4	3	0.0
ShE1302-6.1	TJB.11	Oct-14	4.40	0.11	435	528	2.4E-3	---	0.059	11	0.29	10	8.5E-4	1.60	5.30	1.19	0.85	0.16	1470	2.4	0.0588	11	0.002	122	6.5E-4	4	0.0
ShE1302-7.1	TJB.11	Oct-14	4.32	0.19	1056	649	7.0E-3	38	0.087	8	0.59	16	2.8E-3	5.15	5.05	1.72	1.68	0.68	1436	4.3	0.0868	8	0.002	111	6.1E-4	7	0.1
ShE1302-8.1	TJB.11	Oct-14	4.57	0.11	2040	1813	1.0E-3	58	0.050	6	0.39	4	2.4E-4	0.46	5.33	1.51	1.16	0.49	1428	2.4	0.0498	6	0.003	28	6.9E-4	3	0.1
ShE1302-9.1	TJB.11	Oct-14	4.26	0.08	934	933	1.7E-3	71	0.053	10	0.35	7	4.8E-4	0.90	5.10	1.51	1.03	0.82	1528	1.9	0.0533	10	0.002	74	6.3E-4	3	0.0
ShE1302-10.1	TJB.11	Oct-14	4.42	0.60	680	796	1.9E-2	36	0.354	13	0.98	9	2.1E-2	39.01	5.36	0.85	0.88	0.42	906	9.7	0.3543	13	0.008	195	7.1E-4	22	0.1
Weighted mean age (N=10)				4.38		**Probability**			0.04																		
Age error (95% conf., with error in Std)				0.11		**MSWD**			2.00																		
Hafnarfjall-Skarðsheiði: FeE1301																											
FeE1301-1.1	TJB.11	Oct-14	5.44	0.15	458	452	3.4E-3	50	0.072	15	0.54	6	1.8E-3	3.29	5.32	4.50	1.05	1.79	1163	2.4	0.0722	15	0.0022	150	8.0E-4	4	0.0
FeE1301-2.1	TJB.12	Oct-14	5.43	0.18	85	118	-3.3E-3	100	0.096	16	0.60	11	3.3E-3	6.26	5.32	1.95	0.74	5.43	1132	2.6	0.0956	16	0.0178	31	9.4E-4	6	0.2
FeE1301-3.1	TJB.11	Oct-14	4.39	0.12	97	160	2.0E-3	100	0.137	10	0.53	9	6.2E-3	11.55	6.24	6.40	0.63	4.55	1327	2.0	0.1374	10	0.0111	28	7.3E-4	4	0.2
FeE1301-4.1	TJB.11	Oct-14	7.06	0.61	359	406	1.8E-2	27	0.161	34	0.57	20	7.8E-3	14.53	4.14	3.92	0.91	1.15	790	3.5	0.1610	34	0.0221	46	8.3E-4	14	0.3
FeE1301-5.1	TJB.11	Oct-14	5.55	0.15	153	215	2.2E-2	30	0.076	13	0.30	12	2.0E-3	3.74	5.18	1.87	0.73	0.24	1137	2.4	0.0757	13	0.0319	47	5.2E-4	21	0.4
FeE1301-6.1	TJB.11	Oct-14	5.39	0.15	168	236	1.2E-2	38	0.082	12	0.22	14	2.4E-3	4.51	5.30	2.63	0.74	0.76	1161	2.5	0.0818	12	0.0125	24	6.7E-4	11	0.5
FeE1301-7.1	TJB.11	Oct-14	5.07	0.21	394	404	1.2E-3	100	0.072	10	0.34	9	1.7E-3	3.21	5.30	1.68	1.01	0.42	1251	4.1	0.0715	10	0.0059	35	7.8E-4	5	0.1
FeE1301-8.1	TJB.11	Oct-14	4.89	0.13	251	393	2.5E-3	71	0.061	11	0.24	11	1.0E-3	1.87	5.32	3.23	0.66	1.26	1320	2.6	0.0609	11	0.0024	121	7.2E-4	4	0.0
FeE1301-9.1	TJB.11	Oct-14	5.54	0.23	90	134	9.5E-3	58	0.095	24	0.42	14	3.3E-3	6.22	5.05	4.56	0.69	3.85	1110	2.9	0.0953	24	0.0066	57	7.4E-4	13	0.2
FeE1301-10.1	TJB.11	Oct-14	5.54	0.20	616	578	-1.6E-3	71	0.065	9	0.37	7	1.3E-3	2.40	5.01	3.45	1.10	4.58	1152	3.5	0.0651	9	0.0108	19	8.9E-4	4	0.2
FeE1301-11.1	TJB.11	Oct-14	5.26	0.12	387	417	2.9E-3	58	0.066	9	0.35	8	1.4E-3	2.52	5.44	1.98	0.96	0.75	1214	2.3	0.0661	9	0.0024	125	7.8E-4	4	0.0
FeE1301-12.1	TJB.11	Oct-14	5.86	0.45	33	72	5.1E-2	29	0.173	21	0.55	14	8.6E-3	16.03	5.43	1.82	0.47	0.43	939	5.7	0.1728	21	0.0910	762	5.5E-5	528	0.7
Weighted mean age (N=9)				5.40		**Probability**			0.57																		
Age error (95% conf., with error in Std)				0.11		**MSWD**			0.84																		
Hafnarfjall-Skarðsheiði: HrI1202																											
BURI_2.2_L	TJB.1	May-13	4.04	0.08	346	399	8.6E-3	41	0.070	16	0.28	17	1.6E-3	3.04	5.41	0.91	0.89	1.27	1579	1.3	0.0701	16	0.006	20	5.3E-4	7.9	0.4
BURI_2.2_M	TJB.1	May-13	4.24	0.28	83	138	----	---	0.083	17	0.30	29	2.5E-3	4.64	4.85	1.12	0.62	0.32	1479	6.5	0.0828	17	0.008	18	6.8E-4	6.5	0.4
BURI_2.2_R	TJB.1	May-13	4.45	0.29	58	102	1.2E-2	58	0.127	25	0.34	25	5.5E-3	10.20	5.53	0.89	0.59	0.63	1328	5.0	0.1267	25	0.007	61	5.8E-4	18.2	0.3
BURI_2.3	TJB.1	May-13	4.35	0.22	95	143	7.0E-3	71	0.073	15	0.36	22	1.8E-3	3.37	5.45	1.49	0.69	0.43	1461	5.0	0.0728	15	0.003	69	6.0E-4	11.7	0.2
BURI_2.4	TJB.1	May-13	4.00	0.05	1289	850	2.9E-3	45	0.046	7	0.55	15	1.1E-6	0.00	5.59	2.30	1.57	0.83	1633	1.2	0.0462	7	0.000	7550	5.8E-4	2.8	0.0
BURI_3.3_L	TJB.1	May-13	4.12	0.20	61	110	4.6E-3	100	0.075	31	0.25	31	2.0E-3	3.65	5.61	0.46	0.57	1.13	1540	4.0	0.0749	31	0.000	2514	5.9E-4	10.2	0.0
BURI_3.3_R	TJB.1	May-13	3.98	0.28	73	132	9.1E-3	71	0.064	17	0.34	26	1.2E-3	2.23	5.44	0.77	0.57	0.32	1620	7.1	0.0638	17	0.007	36	5.1E-4	16.3	0.5
BURI_3.5	TJB.1	May-13	3.95	0.16	130	202	5.1E-3	71	0.052	27	0.32	20	4.1E-4	0.76	5.64	0.35	0.67	0.25	1655	3.6	0.0521	27	0.002	79	5.5E-4	8.2	0.1
BURI_3.6_L	TJB.1	May-13	4.38	0.31	40	93	2.8E-2	45	0.237	12	0.55	23	1.3E-2	24.21	4.84	3.20	0.45	1.05	1139	5.6	0.2374	12	0.025	70	4.1E-4	51.5	0.7
BURI_3.6_M	TJB.1	May-13	4.13	0.25	127	162	3.5E-2	32	0.182	9	0.55	18	9.2E-3	17.14	4.92	2.62	0.81	0.50	1321	5.7	0.1815	9	0.039	100	2.6E-4	62.4	0.6
BURI_3.7_L	TJB.1	May-13	3.58	0.19	55	102	7.7E-2	26	0.129	14	0.38	26	5.6E-3	10.43	5.34	2.36	0.56	0.73	1654	4.7	0.1285	14	-0.090	101	-2.7E-4	84.6	0.8
BURI_3.7_M	TJB.1	May-13	3.91	0.12	25	65	2.9E-2	58	0.101	19	0.48	32	3.7E-3	6.88	5.27	0.62	0.40	0.54	1573	1.9	0.1005	19	0.031	131	2.9E-4	69	0.5

RED not included in sample average

Table E2 cont. Hafnarfjall-Skarðsheiði *in situ* zircon U-Pb geochronology

													^{207}Pb-corrected										^{204}Pb-corrected				
Analysis	**Mount**	**Date**	**^{207}Pb-corr. ^{206}Pb/^{238}U Age (Ma)**	**1σ err**	**Th (ppm)**	**U (ppm)**	**^{204}Pb/ ^{206}Pb**	**% err**	**^{207}Pb ^{206}Pb**	**% err**	**^{208}Pb/^{206} Pb**	**% err**	**^{204}Pb/^{206}Pb**	**% com ^{206}Pb**	**UO/U**	**% err**	**^{232}Th/^{23} ^{8}U**	**% err**	**Total ^{238}U/ ^{206}Pb**	**% err**	**Total ^{207}Pb/ ^{206}Pb**	**% err**	**^{207}Pb*/^{235} U**	**% err**	**^{206}Pb/ ^{238}U**	**% err**	**err corr**
BURI_3.7_r	TJB.1	May-13	4.03	0.13	43	91	1.8E-2	58	0.103	16	0.27	34	3.9E-3	7.21	5.33	1.64	0.49	0.45	1520	2.5	0.1031	16	0.016	63	4.3E-4	30	0.5
BURI2.11	TJB.1	May-13	3.37	0.41	54	93	7.8E-3	100	0.249	28	0.61	26	1.4E-2	25.66	5.79	0.66	0.60	0.47	1459	3.4	0.2488	28	0.012	97	5.9E-4	17	0.2
BURI2.13	TJB.1	May-13	3.68	0.26	92	149	6.0E-3	71	0.224	18	0.76	29	1.2E-2	22.54	5.44	1.53	0.64	3.74	1388	2.5	0.2241	18	0.013	54	6.4E-4	9	0.2
BURI2_MID	TJB.1	May-13	3.83	0.36	160	224	3.0E-2	19	0.563	3	1.32	15	3.5E-2	65.42	5.22	2.19	0.74	1.92	594	6.7	0.5628	3	0.023	73	7.5E-4	24	0.3
Weighted mean age (N=16)				4.00		**Probability**			0.27																		
Age error (95% conf., with error in Std)				0.08		**MSWD**			1.19																		

Table E3. Árnes and Hrafnfjörður *in situ* zircon U-Pb geochronology

Analysis	Mount	Date	^{207}Pb-corr. ^{206}Pb/^{238}U Age (Ma)	1σ err	Th (ppm)	U (ppm)	^{204}Pb/ ^{206}Pb	% err	^{207}Pb ^{206}Pb	% err	^{208}Pb/^{206} Pb	% err	^{207}Pb-corrected ^{204}Pb/^{206}Pb	^{207}Pb-corrected % com ^{206}Pb	UO/U	% err	^{232}Th/^{23} ^{8}U	% err	Total ^{238}U/ ^{206}Pb	% err	Total ^{207}Pb/ ^{206}Pb	% err	^{204}Pb-corrected ^{207}Pb*/^{235} U	% err	^{204}Pb-corrected ^{206}Pb/ ^{238}U	% err	err corr
Árnes: ÁrE1301 (Tr4 rhyolite)																											
ArE1301-1.1	TJB.07	Apr-14	11.6	0.4	70	118	8.7E-3	77	0.0671	11	0.382	18	1.4E-3	2.63	4.99	0.8	0.612	0.26	545	2.9	0.0671	11	0.0173	25	1.5E-3	15	0.6
ArE1301-2.1	TJB.07	Apr-14	13.1	0.4	39	73	1.7E-3	183	0.0778	15	0.297	26	2.1E-3	3.98	5.05	1.3	0.554	0.42	475	2.5	0.0778	15	0.0150	89	2.0E-3	6	0.1
ArE1301-3.1	TJB.07	Apr-14	13.9	0.3	69	122	-1.9E-3	105	0.0950	12	0.441	19	3.3E-3	6.16	4.59	2.1	0.582	1.00	437	1.8	0.0950	12	0.0391	23	2.4E-3	4	0.2
ArE1301-4.1	TJB.07	Apr-14	12.8	0.4	91	152	1.5E-2	54	0.0703	11	0.248	21	1.6E-3	3.03	4.84	2.2	0.620	2.23	493	2.7	0.0703	11	0.0459	56	1.5E-3	21	0.4
ArE1301-5.1	TJB.07	Apr-14	12.0	0.5	101	172	4.1E-3	100	0.0686	9	0.274	19	1.5E-3	2.82	5.06	1.3	0.605	0.64	526	3.9	0.0686	9	0.0011	1477	1.8E-3	9	0.0
ArE1301-6.1	TJB.07	Apr-14	13.7	0.5	66	114	2.4E-2	54	0.0894	13	0.407	21	2.9E-3	5.45	4.53	2.2	0.593	1.69	447	3.1	0.0894	13	0.0859	90	1.3E-3	43	0.5
ArE1301-7.1	TJB.07	Apr-14	13.4	0.4	117	155	9.3E-4	183	0.0575	19	0.211	23	7.6E-4	1.41	4.80	2.1	0.776	0.24	475	2.3	0.0575	19	0.0125	64	2.1E-3	4	0.1
Mean age of coherent group (N=9)				13.4		**Probability**			0.16																		
Age error (95% conf., with error in Std)				0.6		**MSWD**			1.70																		
Árnes: ÁrE1303 (Tr2 rhyolite)																											
ArE1303-10.1	TJB.06	Apr-14	12.8	0.5	60	110	4.5E-3	112	0.056	16	0.179	31	6.3E-4	1.17	5.78	2.07	0.57	0.32	500	3.8	0.0556	16	0.0041	306	1.8E-3	11	0.0
ArE1303-12.1	TJB.06	Apr-14	12.9	0.3	58	94	-9.1E-3	91	0.042	19	0.444	23	-2.7E-4	-0.51	5.82	1.93	0.64	0.35	506	2.3	0.0423	19	0.0501	59	2.3E-3	13	0.2
ArE1303-2.1	TJB.06	Apr-14	14.1	0.4	65	99	8.5E-3	91	0.049	20	0.208	32	1.7E-4	0.31	5.92	1.74	0.68	0.36	459	2.6	0.0488	20	0.0255	60	1.8E-3	18	0.3
ArE1303-25.1	TJB.06	Apr-14	13.1	0.5	54	88	1.4E-2	75	0.046	19	0.357	26	-6.0E-6	-0.01	5.72	2.10	0.63	0.37	494	3.6	0.0462	19	0.0497	87	1.5E-3	28	0.3
ArE1303-26.1	TJB.06	Apr-14	13.0	0.4	115	173	-3.3E-3	112	0.030	20	0.179	26	-1.1E-3	-2.06	5.80	1.77	0.69	0.51	508	2.7	0.0301	20	0.0222	65	2.1E-3	7	0.1
ArE1303-27.1	TJB.06	Apr-14	13.7	0.3	679	711	-6.9E-4	129	0.051	7	0.254	12	3.0E-4	0.57	5.97	1.94	0.99	0.60	469	2.3	0.0508	7	0.0181	22	2.2E-3	3	0.1
ArE1303-3.1	TJB.06	Apr-14	12.7	0.5	62	94	9.0E-3	100	0.071	17	0.188	38	1.7E-3	3.11	5.72	1.83	0.68	0.38	493	3.7	0.0709	17	0.0194	32	1.7E-3	20	0.6
ArE1303-7.1	TJB.06	Apr-14	13.0	0.8	50	85	1.8E-3	224	0.061	19	0.101	52	9.9E-4	1.85	5.90	1.87	0.60	0.41	488	5.8	0.0609	19	0.0093	188	2.0E-3	10	0.1
ArE1303-8.1	TJB.06	Apr-14	12.4	0.4	172	215	1.5E-3	158	0.044	14	0.167	26	-1.4E-4	-0.26	5.88	2.27	0.83	1.05	523	3.1	0.0442	14	0.0055	177	1.9E-3	6	0.0
ArE1303-9.1	TJB.06	Apr-14	12.8	0.3	54	96	3.2E-3	158	0.050	18	0.189	36	2.3E-4	0.42	5.93	2.19	0.58	0.40	506	2.1	0.0497	18	0.0003	8085	1.9E-3	10	0.0
Mean age of coherent group (N=10)				13.1		**Probability**			0.09																		
Age error (95% conf., with error in Std)				0.4		**MSWD**			1.70																		
Árnes: ÁrE1304 (Tr3 rhyolite)																											
ArE1304-1.1	TJB.07	Apr-14	13.1	0.2	111	183	4.4E-3	120	0.040	12	0.161	21	-4.4E-4	-0.80	5.51	0.73	0.63	0.23	499	1.3	0.0398	12	0.0036	244	1.9E-3	4	0.0
ArE1304-10.1	TJB.07	Apr-14	12.9	0.4	86	147	1.4E-2	50	0.080	17	0.280	19	2.3E-3	4.16	5.50	0.90	0.60	0.96	483	2.6	0.0803	17	0.0266	28	1.7E-3	13	0.5
ArE1304-11.1	TJB.07	Apr-14	12.6	0.2	74	114	1.2E-2	71	0.065	12	0.241	22	1.3E-3	2.28	5.42	0.63	0.67	0.82	503	1.0	0.0649	12	0.0166	19	1.7E-3	12	0.6
ArE1304-12.1	TJB.07	Apr-14	13.0	0.2	182	256	5.0E-3	77	0.041	10	0.246	16	-3.7E-4	-0.66	5.53	0.52	0.73	0.18	503	1.4	0.0409	10	0.0017	433	1.9E-3	5	0.0
ArE1304-13.1	TJB.07	Apr-14	12.7	0.2	154	192	3.0E-3	100	0.049	11	0.325	17	1.7E-4	0.31	5.35	0.46	0.83	3.11	510	1.4	0.0489	11	0.0132	11	2.0E-3	1	0.1
ArE1304-14.1	TJB.07	Apr-14	12.6	0.4	48	100	2.3E-3	129	0.046	16	0.082	42	-3.7E-5	-0.07	5.55	0.76	0.50	0.66	517	3.4	0.0458	16	0.0240	58	2.0E-3	7	0.1
ArE1304-15.1	TJB.07	Apr-14	12.8	0.3	79	141	7.0E-3	100	0.045	14	0.199	22	-1.1E-4	-0.20	5.54	0.95	0.58	0.27	508	2.5	0.0447	14	0.0019	531	1.9E-3	7	0.0
ArE1304-16.1	TJB.07	Apr-14	12.6	0.2	83	143	6.5E-3	100	0.046	12	0.187	22	-3.8E-5	-0.07	5.69	0.30	0.60	0.63	517	1.8	0.0457	12	0.0007	1589	1.8E-3	6	0.0
ArE1304-2.1	TJB.07	Apr-14	13.3	0.2	155	239	1.6E-3	183	0.044	10	0.201	18	-1.5E-4	-0.28	5.34	0.53	0.67	1.32	490	1.5	0.044	10	0.0150	31	2.1E-3	2	0.1
ArE1304-3.1	TJB.07	Apr-14	12.9	0.1	284	367	1.5E-3	316	0.055	7	0.261	13	6.1E-4	1.11	5.55	0.89	0.80	0.75	496	1.1	0.055	7	0.0148	13	2.0E-3	1	0.1
ArE1304-4.1	TJB.07	Apr-14	12.6	0.4	105	179	2.9E-3	100	0.046	11	0.342	17	-8.6E-6	-0.02	5.48	0.85	0.60	1.51	513	2.9	0.046	11	0.0124	12	1.9E-3	3	0.3
ArE1304-5.1	TJB.07	Apr-14	13.0	0.2	140	192	4.5E-3	100	0.045	10	0.270	18	-6.4E-5	-0.12	4.87	1.23	0.75	0.32	498	1.5	0.045	10	0.0032	292	1.9E-3	4	0.0
ArE1304-6.1	TJB.07	Apr-14	13.3	0.4	40	74	1.1E-2	120	0.046	17	0.140	36	-5.5E-6	-0.01	5.55	0.84	0.56	0.61	490	3.2	0.046	17	0.0051	182	1.9E-3	10	0.1
ArE1304-7.1	TJB.07	Apr-14	12.6	0.6	27	79	1.3E-2	100	0.050	17	0.111	41	2.6E-4	0.46	5.24	1.02	0.36	0.43	513	4.6	0.050	17	0.0123	23	1.7E-3	13	0.6
ArE1304-8.1	TJB.07	Apr-14	13.1	0.2	100	162	5.6E-3	100	0.038	12	0.183	21	-5.8E-4	-1.04	5.63	0.76	0.64	0.64	501	1.3	0.038	12	0.0010	971	1.9E-3	5	0.0
ArE1304-9.1	TJB.07	Apr-14	13.2	0.3	194	281	3.3E-3	100	0.044	9	0.201	16	-1.5E-4	-0.27	5.58	0.67	0.71	0.78	493	2.3	0.044	9	0.0054	128	2.0E-3	4	0.0
ArE1304F-1.1	TJB.08	Apr-14	12.8	0.2	633	701	2.1E-3	75	0.049	6	0.300	9	2.1E-4	0.39	5.41	1.87	0.93	0.81	506	1.4	0.049	6	0.0043	156	1.9E-3	3	0.0
ArE1304F-2.1	TJB.08	Apr-14	12.6	0.1	354	340	6.8E-4	129	0.042	18	0.330	12	-3.0E-4	-0.57	5.66	1.54	1.07	0.86	519	0.6	0.042	18	0.0083	49	1.9E-3	2	0.0
ArE1304F-3.1	TJB.08	Apr-14	12.6	0.3	219	280	3.0E-3	120	0.049	9	0.281	15	2.0E-4	0.37	5.34	1.17	0.81	0.34	511	2.0	0.049	9	0.0007	2147	1.8E-3	7	0.0
ArE1304F-4.1	TJB.08	Apr-14	12.7	0.2	311	374	2.6E-3	120	0.041	9	0.172	17	-3.6E-4	-0.67	5.26	1.58	0.86	1.35	513	1.4	0.041	9	0.0002	6433	1.9E-3	6	0.0
ArE1304F-5.1	TJB.08	Apr-14	12.6	0.3	355	375	6.2E-3	50	0.043	8	0.263	12	-2.4E-4	-0.45	5.59	1.52	0.98	0.51	516	2.1	0.043	8	0.0146	20	1.7E-3	7	0.4
ArE1304F-6.1	TJB.08	Apr-14	12.9	0.2	550	565	3.7E-4	129	0.043	6	0.264	10	-2.1E-4	-0.40	5.72	1.08	1.01	1.57	506	1.7	0.043	6	0.0102	20	2.0E-3	2	0.1
ArE1304F-7.1	TJB.08	Apr-14	13.1	0.3	167	268	1.8E-3	100	0.052	18	0.239	15	4.1E-4	0.76	5.38	1.88	0.64	1.78	491	1.6	0.052	18	0.0068	120	2.0E-3	4	0.0
Mean age of coherent group (N=23)				12.9		**Probability**			0.29																		
Age error (95% conf., with error in Std)				0.1		**MSWD**			1.14																		
Árnes: DH-08 and -15 (Tr1 rhyolite)																											
DH08-1.1	TJB.09	41730	12.8	0.9	45	80	-1.2E-2	100	0.035	26	0.166	46.4	-7.8E-4	-1.46	6.02	2.04	0.58	0.49	513	7.07	0.034788	26	0.0591	69	2.4E-3	19	0.3
DH08-2.1	TJB.09	41730	12.7	0.4	102	128	-1.8E-3	224	0.057	18	0.236	34.2	7.1E-4	1.32	4.708	2.18	0.82	0.31	504	2.9	0.056749	18	0.0233	69	2.1E-3	8	0.1

RED not included in sample average

Table E3 cont. Árnes and Hrafnfjörður *in situ* zircon U-Pb geochronology

Analysis	Mount	Date	^{207}Pb-corr. ^{206}Pb/^{238}U Age (Ma)	1σ err	Th (ppm)	U (ppm)	^{204}Pb/ ^{206}Pb	% err	^{207}Pb ^{206}Pb	% err	^{208}Pb/^{206} Pb	% err	^{207}Pb-corrected ^{204}Pb/^{206}Pb	^{207}Pb-corrected % com ^{206}Pb	UO/U	% err	^{232}Th/^{23} ^{8}U	% err	Total ^{238}U/ ^{206}Pb	% err	Total ^{207}Pb/ ^{206}Pb	% err	^{204}Pb-corrected ^{207}Pb*/^{235} U	% err	^{204}Pb-corrected ^{206}Pb/ ^{238}U	% err	err corr
DH08-4.1	TJB.09	Apr-14	11.6	0.7	16	39	5.1E-3	224	0.082	25	0.362	46	2.4E-3	4.47	5.74	2.46	0.42	0.78	533	5.4	0.082	25	0.0005	9466	1.7E-3	24	0.0
DH08-5.1	TJB.09	Apr-14	13.4	0.5	73	119	-1.4E-3	224	0.069	16	0.391	23	1.6E-3	2.91	5.77	1.22	0.64	0.35	468	3.4	0.069	16	0.0266	49	2.2E-3	7	0.1
DH08-7.1	TJB.09	Apr-14	13.1	0.5	139	192	5.0E-3	91	0.164	8	0.537	16	7.9E-3	14.84	5.20	2.59	0.75	0.78	421	3.4	0.164	8	0.0281	76	2.2E-3	10	0.1
DH15-13.1	TJB.09	Apr-14	16.4	2.8	620	618	5.8E-3	53	0.237	21	0.713	16	1.3E-2	24.07	3.98	3.24	1.04	0.84	300	15.1	0.237	21	0.0670	46	3.0E-3	16	0.4
DH15-12.1	TJB.09	Apr-14	11.9	0.6	68	101	3.3E-3	158	0.074	17	0.314	28	1.9E-3	3.49	5.45	0.97	0.69	0.99	527	5.1	0.074	17	0.0059	349	1.8E-3	11	0.0
DH15-3.1	TJB.09	Apr-14	13.3	0.4	89	126	2.6E-2	51	0.082	14	0.472	21	2.4E-3	4.54	5.01	2.31	0.73	0.31	466	2.3	0.082	14	0.0980	102	1.1E-3	50	0.5
Mean age of coherent group (N=8)				12.9		**Probability**			0.18																		
Age error (95% conf., with error in Std)				0.5		**MSWD**			1.40																		
Hrafnfjörður: HfE1402 (Tdb dacite)																											
HfE1402-1.1	TJB.11	Oct-14	13.8	0.2	161	206	1.6E-3	71	0.049	10	0.294	8	2.1E-4	0.39	5.11	0.98	0.81	0.63	469	1.4	0.049	10	0.0073	71	2.1E-3	3	0.0
HfE1402-10.1	TJB.11	Oct-14	13.7	0.3	29	55	1.0E-32	100	0.083	16	0.282	15	2.5E-3	4.65	5.10	1.74	0.54	0.47	451	1.0	0.083	16	0.0254	16	2.2E-3	1	0.1
HfE1402-10.1	TJB.11	Oct-14	13.7	0.3	176	153	-4.4E-3	50	0.061	11	0.380	9	9.8E-4	1.83	5.11	1.83	1.19	0.22	464	2.3	0.061	11	0.0384	24	2.3E-3	4	0.2
HfE1402-2.1	TJB.11	Oct-14	13.9	0.3	140	409	1.0E-32	100	0.054	7	0.109	9	5.2E-4	0.97	5.17	1.95	0.35	0.20	461	2.2	0.054	7	0.0161	7	2.2E-3	2	0.3
HfE1402-3.1	TJB.11	Oct-14	13.9	0.2	339	393	2.4E-3	41	0.056	7	0.322	5	6.7E-4	1.24	5.06	1.17	0.89	2.80	460	1.6	0.056	7	0.0056	84	2.1E-3	3	0.0
HfE1402-4.1	TJB.11	Oct-14	13.7	0.7	55	66	-2.3E-3	100	0.059	16	0.382	12	8.6E-4	1.61	5.10	0.95	0.86	1.50	465	4.6	0.059	16	0.0281	36	2.2E-3	6	0.2
HfE1402-5.1	TJB.11	Oct-14	13.5	0.3	255	368	9.2E-4	71	0.049	8	0.264	6	1.5E-4	0.28	5.11	1.54	0.72	0.16	479	2.4	0.049	8	0.0098	31	2.1E-3	3	0.1
HfE1402-6.1	TJB.11	Oct-14	12.0	0.8	86	150	5.2E-3	45	0.068	9	0.275	9	1.5E-3	2.76	4.93	2.66	0.59	7.02	527	7.1	0.068	9	0.0035	183	1.7E-3	9	0.0
HfE1402-7.1	TJB.11	Oct-14	13.8	0.3	352	388	2.8E-3	45	0.093	11	0.350	6	3.2E-3	5.93	4.59	2.70	0.94	0.18	441	2.0	0.093	11	0.0155	43	2.1E-3	3	0.1
HfE1402-8.1	TJB.11	Oct-14	14.3	0.5	10	35	8.5E-3	71	0.086	17	0.356	17	2.7E-3	5.01	5.10	1.41	0.29	0.71	429	2.8	0.086	17	0.0148	59	2.0E-3	14	0.2
HfE1402-9.1	TJB.11	Oct-14	13.5	0.1	374	315	-5.6E-4	100	0.053	8	0.396	6	4.7E-4	0.88	5.15	1.48	1.23	0.15	476	0.6	0.053	8	0.0180	15	2.1E-3	1	0.1
Mean age of coherent group (N=10)				13.7		**Probability**			0.63																		
Age error (95% conf., with error in Std)				0.2		**MSWD**			0.78																		
Hrafnfjörður: HfE1403																											
HfE1403-1.1	TJB.11	Oct-14	13.6	0.3	195	577	3.4E-3	30	0.059	12	0.138	7	8.8E-4	1.64	4.62	1.64	0.35	0.36	467	2.3	0.059	12	0.0019	279	2.0E-3	3	0.0
HfE1403-10.1	TJB.11	Oct-14	13.4	0.5	807	824	1.1E-3	41	0.051	5	0.338	4	3.0E-4	0.57	5.13	1.65	1.01	0.76	479	3.5	0.051	5	0.0095	23	2.0E-3	4	0.2
HfE1403-11.1	TJB.11	Oct-14	14.1	0.2	701	722	-2.6E-4	100	0.053	5	0.334	4	4.2E-4	0.78	5.03	1.05	1.00	0.12	456	1.5	0.053	5	0.0171	8	2.2E-3	2	0.2
HfE1403-12.1	TJB.11	Oct-14	13.5	0.4	109	171	2.3E-3	71	0.055	19	0.222	11	6.1E-4	1.14	4.95	0.38	0.66	0.26	476	3.1	0.055	19	0.0058	134	2.0E-3	4	0.0
HfE1403-13.1	TJB.11	Oct-14	13.1	0.5	138	248	9.6E-3	25	0.091	7	0.272	13	3.0E-3	5.64	4.78	1.81	0.57	4.50	466	3.6	0.091	7	0.0175	15	1.8E-3	7	0.4
HfE1403-14.1	TJB.11	Oct-14	13.1	0.3	188	271	1.3E-3	71	0.063	8	0.266	7	1.1E-3	2.13	4.97	1.20	0.71	0.55	486	2.2	0.063	8	0.0123	33	2.0E-3	3	0.1
HfE1403-15.1	TJB.11	Oct-14	13.4	0.5	500	1559	2.2E-4	71	0.047	4	0.111	5	4.3E-5	0.08	5.14	1.67	0.33	2.05	485	3.6	0.047	4	0.0124	7	2.1E-3	4	0.5
HfE1403-16.1	TJB.11	Oct-14	13.6	0.5	182	377	-4.1E-4	100	0.057	7	0.197	7	7.3E-4	1.37	4.98	1.81	0.50	0.85	469	3.3	0.057	7	0.0187	12	2.2E-3	3	0.3
HfE1403-17.1	TJB.11	Oct-14	13.9	0.5	91	200	2.7E-3	58	0.052	11	0.164	12	3.7E-4	0.70	4.90	2.02	0.47	0.87	463	3.5	0.052	11	0.0028	269	2.0E-3	5	0.0
HfE1403-18.1	TJB.11	Oct-14	14.4	0.1	243	386	1.8E-3	45	0.057	6	0.232	6	7.5E-4	1.40	5.09	2.95	0.65	1.34	443	0.6	0.057	6	0.0092	43	2.2E-3	2	0.0
HfE1403-19.1	TJB.11	Oct-14	13.1	0.3	321	888	1.0E-3	41	0.059	4	0.141	11	8.6E-4	1.60	5.52	2.24	0.37	1.24	488	2.2	0.059	4	0.0123	15	2.0E-3	2	0.2
HfE1403-2.1	TJB.11	Oct-14	13.5	0.4	727	1290	3.3E-4	58	0.058	3	0.194	4	7.6E-4	1.42	5.12	1.48	0.58	2.63	472	3.2	0.058	3	0.0153	7	2.1E-3	3	0.4
HfE1403-20.1	TJB.11	Oct-14	13.7	0.2	735	933	1.1E-3	35	0.051	4	0.300	3	3.2E-4	0.60	5.54	2.72	0.81	1.30	470	1.8	0.051	4	0.0101	17	2.1E-3	2	0.1
HfE1403-21.1	TJB.11	Oct-14	16.4	1.9	354	460	3.7E-3	30	0.062	6	0.332	5	1.0E-3	1.94	4.74	7.96	0.79	16	387	11.6	0.062	6	0.0016	403	2.4E-3	12	0.0
HfE1403-22.1	TJB.11	Oct-14	10.1	1.5	367	762	2.1E-3	25	0.054	4	0.196	4	5.5E-4	1.04	5.63	20.6	0.50	0.80	639	15.3	0.054	4	0.0046	42	1.5E-3	15	0.4
HfE1403-23.1	TJB.11	Oct-14	14.3	0.3	528	1344	4.8E-4	45	0.044	4	0.136	6	-1.3E-4	-0.24	5.39	2.67	0.41	0.20	454	2.1	0.044	4	0.0112	10	2.2E-3	2	0.2
HfE1403-24.1	TJB.11	Oct-14	14.3	0.6	528	1707	8.1E-4	32	0.050	3	0.117	4	2.7E-4	0.51	5.19	2.11	0.32	1.68	451	4.4	0.050	3	0.0115	12	2.2E-3	4	0.4
HfE1403-3.1	TJB.11	Oct-14	14.0	0.3	41	84	4.0E-19	--	0.097	11	0.349	11	3.4E-3	6.37	4.90	0.45	0.50	2.47	433	1.9	0.097	11	0.0307	11	2.3E-3	2	0.2
HfE1403-4.1	TJB.11	Oct-14	12.6	0.6	151	563	1.0E-3	50	0.056	5	0.130	7	6.3E-4	1.18	4.96	1.30	0.28	0.33	507	5.1	0.056	5	0.0108	21	1.9E-3	5	0.2
HfE1403-5.1	TJB.11	Oct-14	13.8	0.4	558	489	2.1E-3	38	0.046	6	0.361	4	1.0E-6	0.00	5.24	1.39	1.18	4.32	470	2.7	0.046	6	0.0040	92	2.0E-3	3	0.0
HfE1403-6.1	TJB.11	Oct-14	13.0	0.6	711	1842	7.5E-4	33	0.052	3	0.142	4	3.8E-4	0.71	5.03	1.87	0.40	0.96	495	4.3	0.052	3	0.0112	11	2.0E-3	4	0.4
HfE1403-7.1	TJB.11	Oct-14	13.4	0.6	1611	1542	4.8E-4	41	0.048	3	0.354	2	8.7E-5	0.16	5.28	0.68	1.08	0.70	481	4.6	0.048	3	0.0115	10	2.1E-3	5	0.5
HfE1403-8.1	TJB.11	Oct-14	14.0	0.3	297	489	2.9E-3	33	0.052	6	0.219	6	4.0E-4	0.75	4.74	1.80	0.63	1.49	459	2.0	0.052	6	0.0021	216	2.1E-3	3	0.0
HfE1403-9.1	TJB.11	Oct-14	13.5	0.4	445	1454	4.2E-4	50	0.049	4	0.115	5	2.0E-4	0.38	5.17	1.63	0.32	0.10	480	2.9	0.049	4	0.0123	9	2.1E-3	3	0.3
Mean age of coherent group (N=20)				13.6		**Probability**			0.25																		
Age error (95% conf., with error in Std)				0.2		**MSWD**			1.20																		

RED not included in sample average

Table E4. Króksfjörður *in situ* zircon U-Pb geochronology

Analysis	Mount	Date	^{207}Pb-corr. ^{206}Pb/^{238}U Age (Ma)	1σ err	Th (ppm)	U (ppm)	^{204}Pb/ ^{206}Pb	% err	^{207}Pb ^{206}Pb	% err	^{208}Pb/^{206} Pb	% err	^{207}Pb-corrected ^{204}Pb/^{206}Pb	^{207}Pb-corrected % com ^{206}Pb	UO/U	% err	^{232}Th/^{23} ^{8}U	% err	Total ^{238}U/ ^{206}Pb	% err	Total ^{207}Pb/ ^{206}Pb	% err	^{204}Pb-corrected ^{207}Pb*/^{235} U	% err	^{204}Pb-corrected ^{206}Pb/ ^{238}U	% err	err corr
Króksfjörður: IEKBr-1																											
IEKBr-1-2.1	TJB.7	Apr-14	12.4	0.3	59	76	8.5E-3	100	0.0713	13	0.313	23	1.7E-3	3.16	5.48	1.0	0.795	0.30	506	1.7	0.0713	13	0.0168	24	1.7E-3	19	0.8
IEKBr-1-3.1	TJB.7	Apr-14	11.3	0.2	37	52	-3.5E-3	105	0.0487	20	0.468	25	1.6E-4	0.31	5.51	0.5	0.734	0.40	573	1.1	0.0487	20	0.0248	51	1.9E-3	7	0.1
IEKBr-1-4.1	TJB.7	Apr-14	11.8	0.4	23	50	5.8E-3	100	0.0679	19	0.064	71	1.5E-3	2.73	5.28	1.2	0.477	0.49	534	3.2	0.0679	19	0.0060	187	1.7E-3	13	0.1
IEKBr-1-5.1	TJB.7	Apr-14	12.4	0.2	37	52	1.2E-2	120	0.0398	22	0.085	59	-4.4E-4	-0.82	5.44	0.9	0.732	0.40	526	1.5	0.0398	22	0.0393	128	1.5E-3	35	0.3
IEKBr-1-6.1	TJB.7	Apr-14	12.1	0.4	32	56	1.4E-2	100	0.0614	19	0.387	27	1.0E-3	1.91	5.09	1.5	0.578	0.42	528	3.3	0.0614	19	0.0422	105	1.4E-3	37	0.3
IEKBr-1-1.1	TJB.8	Apr-14	11.3	4.4	61	58	5.1E-2	20	0.5018	17	1.101	25	3.1E-2	57.65	5.64	0.5	1.090	1.78	243	29.2	0.5018	17	0.1688	594	1.8E-4	427	0.7
IEKBr-1-2.1	TJB.8	Apr-14	12.1	0.3	30	55	4.6E-3	129	0.0608	20	0.216	36	9.8E-4	1.83	5.45	0.5	0.571	0.43	527	2.1	0.0608	20	0.0028	593	1.7E-3	12	0.0
IEKBr-1-3.1	TJB.8	Apr-14	10.9	0.4	39	62	9.7E-3	100	0.0788	16	0.478	24	2.2E-3	4.12	5.48	0.8	0.638	0.39	569	3.6	0.0788	16	0.0177	32	1.4E-3	22	0.7
Weighted mean age (N=8)				11.9		**Probability**			---		**All grains**																
Age error (95% conf., with error in Std)				0.5		**MSWD**			3.70																		
Weighted mean age (N=5)				12.3		**Probability**			0.63		**Subset 1**																
Age error (95% conf., with error in Std)				0.3		**MSWD**			0.64																		
Weighted mean age (N=3)				11.2		**Probability**			0.76		**Subset 2**																
Age error (95% conf., with error in Std)				0.3		**MSWD**			0.28																		
Króksfjörður: IEKTr-1																											
IEKTr-1-1.1	TJB.7	Apr-14	12.3	0.3	84	129	7.9E-3	77	0.041	14	0.157	26	-3.3E-4	-0.61	5.44	1.03	0.67	0.40	533	2.1	0.0415	14	0.0212	53	1.6E-3	13	0.3
IEKTr-1-10.1	TJB.7	Apr-14	12.1	0.2	579	565	-4.2E-5	129	0.056	6	0.273	10	6.9E-4	1.29	5.59	1.04	1.06	0.35	531	1.3	0.0565	6	0.0148	6	1.9E-3	1	0.2
IEKTr-1-2.1	TJB.7	Apr-14	12.1	0.3	26	58	-4.5E-4	129	0.064	19	0.315	29	1.2E-3	2.29	5.31	1.11	0.46	0.46	526	1.5	0.0644	19	0.0187	21	1.9E-3	2	0.1
IEKTr-1-3.1	TJB.7	Apr-14	12.3	0.5	34	64	1.2E-2	100	0.054	19	0.167	38	5.1E-4	0.95	5.41	0.46	0.55	1.19	524	4.0	0.0538	19	0.0366	96	1.5E-3	30	0.3
IEKTr-1-5.1	TJB.7	Apr-14	13.1	1.0	22	48	2.2E-2	52	0.470	6	0.836	15	2.9E-2	53.56	5.07	1.62	0.48	0.52	230	2.7	0.4696	6	0.0711	124	2.5E-3	38	0.3
IEKTr-1-6.1	TJB.7	Apr-14	12.4	0.3	150	185	6.1E-4	183	0.043	12	0.234	18	-1.9E-4	-0.36	5.65	0.44	0.84	0.20	524	2.0	0.0435	12	0.0089	51	1.9E-3	3	0.1
IEKTr-1-7.1	TJB.7	Apr-14	11.4	0.8	14	35	6.9E-3	100	0.123	16	0.339	33	5.2E-3	9.69	5.44	0.61	0.42	0.60	512	6.4	0.1229	16	0.0040	717	1.7E-3	16	0.0
IEKTr-1-9.1	TJB.7	Apr-14	12.5	0.5	71	116	1.0E-3	183	0.045	15	0.243	22	-7.9E-5	-0.15	5.55	0.34	0.64	0.54	521	3.6	0.0451	15	0.0077	99	1.9E-3	5	0.1
IEKTr-1-1.1	TJB.8	Apr-14	11.1	1.0	12	35	1.0E-2	183	0.120	30	0.458	29	5.0E-3	9.38	5.78	1.44	0.36	0.64	528	7.2	0.1204	30	0.0103	344	1.5E-3	44	0.1
IEKTr-1-2.1	TJB.8	Apr-14	12.4	0.5	25	59	3.8E-3	129	0.063	18	0.226	32	1.1E-3	2.09	5.47	0.46	0.44	0.77	510	3.7	0.0628	18	0.0008	2586	1.8E-3	11	0.0
IEKTr-1-3.1	TJB.8	Apr-14	12.3	0.2	1213	762	2.0E-3	71	0.082	4	0.556	6	2.4E-3	4.49	5.40	1.77	1.64	0.56	503	1.6	0.0818	4	0.0138	42	1.9E-3	3	0.1
Weighted mean age (N=11)				12.2		**Probability**			0.85																		
Age error (95% conf., with error in Std)				0.2		**MSWD**			0.55																		
Króksfjörður: IEKGd-1																											
IEKGd1-1.1	TJB.11	Oct-14	10.9	0.2	171	218	3.5E-3	58	0.062	11	0.242	10	1.1E-3	2.02	5.37	0.89	0.81	0.45	584	1.6	0.0623	11	0.0019	388	1.6E-3	4	0.0
IEKGd1-10.1	TJB.11	Oct-14	1554	70.5	81	177	2.0E-4	19	0.108	1	0.152	3	8.4E-4	1.35	5.02	1.65	0.47	0.27	4	4.7	0.1080	1	3.9956	5	2.8E-1	5	0.9
IEKGd1-11.1	TJB.11	Oct-14	10.4	0.3	24	54	8.9E-3	71	0.108	16	0.325	18	4.2E-3	7.80	5.12	1.65	0.46	1.11	576	1.1	0.1079	16	0.0075	169	1.4E-3	14	0.1
IEKGd1-2.1	TJB.11	Oct-14	10.9	0.2	111	146	1.0E-32	100	0.055	13	0.276	11	6.2E-4	1.17	5.51	0.89	0.78	11	589	1.3	0.0555	13	0.0130	13	1.7E-3	1	0.1
IEKGd1-3.1	TJB.11	Oct-14	11.1	0.4	81	150	1.7E-3	100	0.048	15	0.206	14	1.1E-4	0.21	5.11	0.96	0.56	0.30	582	3.1	0.0479	15	0.0052	121	1.7E-3	4	0.0
IEKGd1-4.1	TJB.11	Oct-14	11.8	0.4	15	41	1.0E-32	100	0.061	21	0.247	20	9.8E-4	1.82	5.23	0.71	0.39	0.61	539	2.8	0.0607	21	0.0155	21	1.9E-3	3	0.1
IEKGd1-5.1	TJB.11	Oct-14	11.2	0.4	95	174	2.9E-3	71	0.053	13	0.273	11	4.4E-4	0.82	4.88	1.69	0.56	0.31	573	3.3	0.0528	13	0.0018	440	1.7E-3	5	0.0
IEKGd1-6.1	TJB.11	Oct-14	1585	33.1	188	265	5.0E-6	100	0.104	1	0.225	4	4.1E-4	0.66	5.25	1.16	0.73	1.90	4	2.2	0.1036	1	4.0049	2	2.8E-1	2	1.0
IEKGd1-7.1	TJB.11	Oct-14	10.9	0.7	33	54	8.4E-3	71	0.073	18	0.359	16	1.8E-3	3.40	5.06	1.72	0.63	1.56	575	6.1	0.0731	18	0.0138	28	1.5E-3	14	0.5
IEKGd1-8.1	TJB.11	Oct-14	12.4	0.5	15	43	9.8E-3	71	0.067	20	0.410	17	1.4E-3	2.66	5.11	1.38	0.37	0.64	511	3.5	0.0673	20	0.0233	39	1.6E-3	16	0.4
IEKGd1-9.1	TJB.11	Oct-14	11.0	0.4	58	87	-1.0E-2	58	0.053	19	0.312	17	4.4E-4	0.83	4.82	0.54	0.69	1.19	584	3.0	0.0528	19	0.0512	36	2.0E-3	10	0.3
Weighted mean age (N=8)				10.9		**Probability**			0.13																		
Age error (95% conf., with error in Std)				0.3		**MSWD**			1.6																		
Króksfjörður: IEKVl-1																											
IEKVl1-1.1	TJB.9	Apr-14	11.6	0.3	103	201	6.3E-3	129	0.048	15	0.122	34	1.2E-4	0.23	5.82	1.21	0.53	1.11	556	2.6	0.048	15	0.0013	1079	1.7E-3	7	0.0
IEKVl1-10.1	TJB.9	Apr-14	11.8	0.9	174	327	4.0E-2	29	0.073	10	0.229	20	1.8E-3	3.43	5.12	0.68	0.55	1.59	531	7.4	0.073	10	0.1318	112	5.8E-4	66	0.6
IEKVl1-12.1	TJB.9	Apr-14	10.9	0.4	87	112	2.0E-2	75	0.072	17	0.219	32	1.8E-3	3.29	5.50	1.75	0.80	0.30	577	3.4	0.072	17	0.0339	68	1.3E-3	26	0.4
IEKVl1-16.1	TJB.9	Apr-14	11.7	0.2	252	383	4.9E-3	85	0.050	10	0.168	20	2.3E-4	0.43	5.27	2.19	0.68	1.50	550	1.9	0.050	10	0.0001	18732	1.7E-3	6	0.0
IEKVl1-17.1	TJB.9	Apr-14	12.1	0.3	117	241	1.8E-3	158	0.045	17	0.301	22	-7.8E-5	-0.15	4.84	3.60	0.50	0.28	536	1.9	0.045	17	0.0191	58	1.9E-3	6	0.1
IEKVl1-19.1	TJB.9	Apr-14	11.8	0.3	107	317	4.9E-3	129	0.047	14	0.134	28	7.4E-5	0.14	5.48	2.02	0.35	0.30	548	2.8	0.047	14	0.0035	306	1.8E-3	6	0.0
IEKVl1-22.1	TJB.9	Apr-14	11.4	0.3	816	931	7.3E-3	40	0.058	6	0.250	21	8.2E-4	1.54	4.31	1.11	0.91	2.61	561	2.9	0.058	6	0.0106	13	1.6E-3	6	0.5
IEKVl1-23.1	TJB.9	Apr-14	13.6	2.3	76	210	4.8E-2	25	0.403	15	0.867	21	2.4E-2	45.16	5.56	4.50	0.37	1.27	261	10.4	0.403	15	0.1652	208	5.5E-4	150	0.7
IEKVl1-5.1	TJB.9	Apr-14	12.5	0.3	749	1378	6.2E-4	224	0.042	6	0.185	12	-3.1E-4	-0.58	5.82	1.45	0.56	0.50	522	2.6	0.042	6	0.0105	13	1.9E-3	3	0.2

RED not included in sample average

Table E4 cont. Króksfjörður *in situ* zircon U-Pb geochronology

Analysis	Mount	Date	^{207}Pb-corr. $^{206}Pb/^{238}U$ Age (Ma)	1σ err	Th (ppm)	U (ppm)	$^{204}Pb/^{206}Pb$	% err	$^{207}Pb/^{206}Pb$	% err	$^{208}Pb/^{206}Pb$	% err	^{207}Pb-corrected $^{204}Pb/^{206}Pb$	^{207}Pb-corrected % com ^{206}Pb	UO/U	% err	$^{232}Th/^{238}U$	% err	Total $^{238}U/^{206}Pb$	% err	Total $^{207}Pb/^{206}Pb$	% err	^{204}Pb-corrected $^{207}Pb^*/^{235}U$	% err	$^{206}Pb/^{238}U$	% err	err corr
IEKVl1-7.1	TJB.9	Apr-14	11.2	0.4	185	295	2.5E-3	224	0.046	11	0.223	19	1.1E-5	0.02	5.49	1.36	0.65	0.21	581	3.5	0.046	11	0.0091	47	1.7E-3	4	0.1
Weighted mean age (N=10)				11.8		**Probability**			0.95																		
Age error (95% conf., with error in Std)				0.4		**MSWD**			0.35																		
Króksfjörður: IIKK-1 (from Carley 2014, with ^{230}Th correction applied)																											
IIKKU-1.1C	jw529	Aug-11	10.33	0.56			1.7E-2	50	0.039	21	0.514	14.6	-4.9E-4	-0.92	4.89	1.13	0.64	0.44	635	5.4	0.039	21	0.0504	70	1.1E-3	24.7	0.4
IIKKU-1.3E	jw529	Aug-11	10.85	0.63			8.1E-3	50	0.037	17	0.189	16.4	-6.2E-4	-1.15	5.44	0.45	0.44	0.84	606	5.8	0.037	17	0.0203	40	1.4E-3	10.7	0.3
IIKKU-2.1E	jw529	Aug-11	12.26	0.22			-1.1E-19	--	0.047	7	0.296	6.3	4.1E-5	0.08	5.51	0.48	0.85	0.94	528	1.8	0.047	7	0.0122	7	1.9E-3	1.8	0.2
IIKKU-2.2I	jw529	Aug-11	11.90	0.24			2.4E-3	45	0.042	7	0.317	5.8	-3.2E-4	-0.60	5.60	0.23	0.87	2.48	548	2.0	0.042	7	0.0012	345	1.7E-3	2.9	0.0
IIKKU-3.1E	jw529	Aug-11	11.05	0.16			2.9E-3	41	0.057	6	0.350	5.7	7.6E-4	1.41	5.67	0.58	0.89	0.43	579	1.4	0.057	6	0.0030	146	1.6E-3	2.7	0.0
IIKKU-3.2I	jw529	Aug-11	11.65	0.25			2.3E-3	71	0.045	12	0.260	10.7	-1.1E-4	-0.21	5.27	0.77	0.67	0.42	558	2.1	0.045	12	0.0021	302	1.7E-3	3.8	0.0
IIKKU-3.3E	jw529	Aug-11	12.34	0.36			-1.1E-11	--	0.038	11	0.198	10.4	-5.6E-4	-1.04	5.40	1.00	0.70	0.22	531	2.9	0.038	11	0.0099	12	1.9E-3	2.9	0.2
IIKKU-4.2E	jw529	Aug-11	10.95	0.38			5.9E-3	58	0.053	14	0.334	12.3	4.7E-4	0.88	4.99	0.41	0.42	0.36	589	3.4	0.053	14	0.0090	26	1.5E-3	7.9	0.3
Weighted mean age (N=8)				11.5		**Probability**			0.00		**All grains**																
Age error (95% conf., with error in Std)				0.5		**MSWD**			5.10																		
Weighted mean age (N=5)				12.1		**Probability**			0.46		**Subset 1**																
Age error (95% conf., with error in Std)				0.3		**MSWD**			0.79																		
Weighted mean age (N=3)				11.1		**Probability**			0.13		**Subset 2**																
Age error (95% conf., with error in Std)				0.5		**MSWD**			1.80																		

APPENDIX F: Zircon Trace Element Analyses

Table F1a. Hafnarfjall-Skarðsheiði *in situ* zircon trace element (ppm) concentrations (Atomic number ≤ 41)

Mount	Analysis	Date	TE notes	Li	Be	B	F	Na	Al	P	K	Ca	Sc	48Ti	49Ti	Fe	Y	Nb
BrE1201																		
TJB.3	BrE1-1.1	Jan. 2014		0.00	14.31	0.11	53.10	3.11	5.68	414.84	2.12	4.44	22.74	7.55	7.99	2.60	2943	24.28
TJB.3	BrE1-2.1	Jan. 2014		0.01	11.54	0.10	33.80	2.83	4.68	251.12	1.77	3.95	17.71	7.34	8.07	2.49	1981	14.94
TJB.3	BrE1-3.1	Jan. 2014		0.32	4.70	1.16	429.67	472.92	198.44	411.45	450.23	48.48	20.29	11.33	13.27	2.95	2545	35.96
TJB.3	BrE1-4.1	Jan. 2014	Same zone, opposite end as U/Pb	0.00	1.25	0.10	27.44	2.32	4.95	346.47	1.40	2.91	18.99	7.43	7.11	2.58	1234	34.04
TJB.3	BrE1-5.1	Jan. 2014		0.01	1.53	0.05	20.12	6.30	3.91	380.10	20.71	3.69	28.67	7.72	8.41	2.43	1305	27.46
TJB.3	BrE1-6.1	Jan. 2014		0.02	21.21	0.24	55.26	3.17	4.14	321.59	1.86	4.33	20.13	7.21	7.36	2.54	2509	20.14
TJB.3	BrE1-7.1	Jan. 2014		0.00	20.43	0.41	92.58	8.57	5.03	533.67	4.06	3.26	31.57	9.42	9.83	2.51	3063	41.03
TJB.3	BrE1-8.1	Jan. 2014		0.00	2.72	0.09	22.28	6.64	4.20	458.80	1.78	5.99	25.68	7.88	8.18	2.44	1725	50.63
TJB.3	BrE1-9.1	Jan. 2014	U/O in core; TE rim	0.00	6.96	0.09	22.21	4.87	4.57	255.83	1.65	4.72	20.00	7.80	8.14	2.38	1160	12.21
TJB.3	BrE1-10.1	Jan. 2014		0.40	9.92	0.10	11.21	3.10	4.88	553.90	1.48	4.37	30.58	8.30	8.64	2.47	2069	55.77
TJB.3	BrE1-11.1	Jan. 2014	Matches U/O/Hf	0.02	1.08	0.13	12.00	2.91	5.17	356.85	1.42	3.64	24.38	7.91	8.07	2.69	1149	23.52
TJB.3	BrE1-11.2	Jan. 2014	Inher. Core	0.65	80.58	0.04	124.13	6.27	8.74	1534.93	22.73	3.70	73.74	2.61	2.22	2.42	7677	461.20
TJB.3	BrE1-12.1	Jan. 2014		0.02	2.60	0.13	12.89	3.40	4.91	501.64	1.33	4.17	32.71	9.00	9.19	2.45	1704	37.97
TJB.3	BrE1-13.1	Jan. 2014		0.02	1.80	0.19	12.98	3.57	4.72	425.26	1.28	3.62	29.53	8.16	8.32	2.48	1460	31.32
TJB.3	BrE1-14.1	Jan. 2014		0.00	4.54	0.19	43.80	2.16	4.67	369.89	1.00	3.24	21.69	7.24	7.15	2.53	2393	24.25
TJB.3	BrE1-15.1	Jan. 2014		0.00	5.29	0.09	19.98	3.17	4.66	379.34	1.08	3.68	25.40	9.35	10.31	2.48	1351	32.26
TJB.3	BrE1-16.1	Jan. 2014		0.00	2.38	0.13	29.14	3.79	4.10	456.21	1.52	3.51	28.32	8.73	8.50	2.55	1746	43.56
TJB.3	BrE1-17.1	Jan. 2014		0.00	7.20	0.10	14.00	9.08	4.26	369.27	9.01	5.21	31.22	9.89	9.22	2.39	1507	35.31
TJB.3	BrE1-18.1	Jan. 2014		0.00	6.35	0.15	70.25	6.19	4.63	328.49	6.39	3.80	17.83	8.27	8.24	2.51	2229	19.27
TJB.3	BrE1-19.1	Jan. 2014		4.72	157.36	11.06	4549.75	1414.26	769.65	486.48	1150.05	4.78	52.76	127.50	128.94	4.32	15116	550.14
TJB.3	BrE1-20.1	Jan. 2014	U+TE at opp end as O, same zone	0.01	73.45	0.53	148.26	7.70	8.96	407.07	13.63	8.24	20.66	10.58	11.38	2.43	2988	26.79
TJB.3	BrE1-21.1	Jan. 2014		0.00	14.11	0.38	89.64	11.22	10.18	458.37	14.78	8.44	26.05	17.05	18.35	2.50	3013	64.17
TJB.3	BrE1-22.1	Jan. 2014		6.12	3.99	0.53	207.53	4831.80	3225.07	198.54	9420.58	10.63	15.09	10.21	10.71	2.93	788	22.71
TJB.3	BrE1-23.1	Jan. 2014	Matches U/O/Hf	0.00	9.24	0.06	23.77	6.38	8.12	942.81	23.20	7.84	61.81	8.50	9.31	2.40	3211	46.86
TJB.3	BrE1-23.2	Jan. 2014	At far end, young	0.01	0.86	0.04	5.34	7.21	7.67	307.50	4.27	6.83	17.70	8.30	8.42	2.63	1170	31.74
TJB.3	BrE1-24.1	Jan. 2014		0.00	7.02	0.05	11.07	8.65	5.43	437.21	2.09	4.95	27.67	9.12	8.52	2.44	1587	37.67
TJB.3	BrE1-25.1	Jan. 2014		0.00	6.40	0.05	18.63	120.68	99.37	370.43	268.99	5.01	21.12	7.39	7.66	2.50	1649	16.52
TJB.3	BrE1-26.1	Jan. 2014		0.00	9.04	0.11	5.96	2.75	4.30	445.17	1.23	3.07	29.41	8.61	9.22	2.47	1664	36.86
TJB.3	BrE1-27.1	Jan. 2014	TE+O opp end as UPb	0.00	0.56	0.05	4.34	3.49	13.55	303.03	1.07	62.02	21.99	7.85	8.13	2.52	1366	36.61
TJB.3	BrE1-29.1	Jan. 2014	In hil area; fairly unzoned	0.00	49.25	0.12	67.47	2.16	4.04	451.18	1.05	2.43	22.22	13.11	13.14	2.66	3878	616.51
TJB.3	BrE1-30.1	Jan. 2014		0.01	12.67	0.16	113.24	46.00	29.04	356.00	24.40	11.80	21.99	21.58	15.43	2.47	2435	23.96
TJB.3	BrE1-31.1	Jan. 2014		0.01	19.90	0.21	50.17	15.48	3.95	383.90	56.78	3.89	22.09	7.33	7.74	2.49	2882	21.05
TJB.3	BrE1-32.1	Jan. 2014		0.03	7.26	0.05	22.62	6.11	5.23	554.79	5.04	4.61	29.32	8.29	8.05	2.53	2197	67.52
TJB.3	BrE1-33.1	Jan. 2014		0.00	1.24	0.05	23.10	15.18	9.32	288.37	12.69	4.57	19.19	7.85	8.75	2.55	1061	28.40
TJB.3	BrE1-34.1	Jan. 2014		0.00	1.99	0.07	16.63	2.40	3.86	429.93	1.25	2.96	28.10	8.66	8.64	2.48	1568	36.80
TJB.3	BrE1-35.1	Jan. 2014		0.00	8.38	0.21	66.54	37.24	10.38	289.51	12.43	17.09	25.15	10.95	10.61	2.59	1783	19.53
TJB.3	BrE1-36.1	Jan. 2014	Diff sector	0.00	6.89	0.19	40.84	3.11	5.39	385.53	1.83	3.14	21.74	6.47	7.17	2.48	2892	23.27
TJB.3	BrE1-37.1	Jan. 2014		0.00	19.75	0.08	72.90	5.98	5.04	417.48	1.36	4.70	23.23	6.29	6.68	2.56	2998	23.99
TJB.3	BrE1-38.1	Jan. 2014		0.00	3.37	0.10	27.88	5.08	4.20	308.51	5.48	3.41	20.42	6.94	6.45	2.42	2330	15.92
TJB.3	BrE1-39.1	Jan. 2014		0.00	5.52	0.12	33.10	3.15	4.27	388.30	1.67	4.10	25.17	7.98	7.86	2.47	1787	35.84
TJB.3	BrE1-40.1	Jan. 2014		0.00	18.69	0.26	116.60	4.01	5.02	453.39	1.94	43.83	23.97	7.40	7.03	2.43	3269	26.99
TJB.3	BrE1-41.1	Jan. 2014		0.00	5.03	0.06	29.66	3.18	4.43	455.78	1.51	4.55	31.94	8.51	8.19	2.44	1625	32.92
TJB.3	BrE1-42.1	Jan. 2014		0.05	11.83	0.52	205.44	49.15	40.52	512.33	123.76	8.89	24.77	12.08	13.02	2.46	2499	46.29
TJB.3	BrE1-43.1	Jan. 2014		0.00	5.33	0.16	19.03	14.93	14.27	393.84	2.68	2.59	25.67	8.77	8.79	2.56	2436	24.73
TJB.3	BrE1-44.1	Jan. 2014		0.00	0.05	0.05	31.65	256.89	197.99	272.89	545.24	9.72	22.07	6.70	7.24	2.60	862	25.64
TJB.3	BrE1-45.1	Jan. 2014	U/O in core; TE rim	0.03	37.15	0.27	75.55	3.05	5.14	1199.56	1.37	3.83	60.27	4.16	4.60	2.45	5538	246.99
TJB.3	BrE1-46.1	Jan. 2014		0.02	0.47	0.10	79.01	9.22	33.05	266.36	6.04	26.27	19.50	9.70	12.73	2.43	2224	41.58
RnE1201																		
TJB.5	RnE1201-13.1	Apr, 2014	core	0.01	66.03	0.30	0.00	233.51	98.50	222.87	315.09	70.16	3.20	13.80	14.17	49.01	2349	27.73
TJB.5	RnE1201-13.2	Apr, 2014	rim	0.00	12.06	0.08	0.00	3.26	3.23	149.76	1.85	1.13	2.72	10.31	9.57	0.14	809	15.74
TJB.5	RnE1201-14.1	Apr, 2014	core	0.10	138.55	0.16	2.78	4.20	4.42	571.50	2.43	4.92	14.03	22.49	22.13	0.12	4393	138.82
TJB.5	RnE1201-14.2	Apr, 2014	rim	0.00	9.15	0.03	0.00	2.99	4.36	157.97	2.06	1.27	2.61	10.14	10.91	0.11	865	16.35
TJB.5	RnE1201-18.1	Apr, 2014	rim	0.00	0.48	0.03	0.00	3.78	4.17	141.67	2.73	3.08	2.64	9.76	10.44	0.11	850	17.08

Table F1a. Hafnarfjall-Skarðsheiði *in situ* zircon trace element (ppm) concentrations (Atomic number ≤ 41)

Mount	Analysis	Date	TE notes	Li	Be	B	F	Na	Al	P	K	Ca	Sc	48Ti	49Ti	Fe	Y	Nb
TJB.5	RnE1201-18.1	Apr, 2014	rim	0.00	0.48	0.03	0.00	3.78	4.17	141.67	2.73	3.08	2.64	9.76	10.44	0.11	850	17.08
TJB.5	RnE1201-19.1	Apr, 2014	core	0.01	5.24	0.05	2.64	3.74	4.15	186.40	2.10	2.09	2.18	8.18	7.70	0.31	2215	16.51
TJB.5	RnE1201-20.1	Apr, 2014	core	0.00	10.43	0.02	0.00	3.63	3.38	482.37	2.01	1.46	3.85	15.13	15.48	0.19	2820	100.79
TJB.5	RnE1201-20.2	Apr, 2014	rim	0.03	2.23	0.10	0.00	2.77	3.65	227.83	1.90	0.86	3.19	11.69	11.32	0.15	1200	25.34
TJB.5	RnE1201-22.1	Apr, 2014	core	0.04	8.30	0.07	2.87	3.55	3.52	160.51	4.38	1.55	2.56	10.52	11.15	0.34	834	20.48
TJB.5	RnE1201-22.2	Apr, 2014	rim	0.00	13.14	0.47	14.32	6.53	3.36	182.41	14.68	10.25	2.77	9.21	9.65	0.15	913	18.95
TuE1301																		
TJB.5	TuE1301-18.1	Apr, 2014	core	0.00	15.15	0.12	13.20	2.78	3.49	678.75	1.70	1.81	10.65	10.18	10.94	0.32	5469	148.42
TJB.5	TuE1301-18.2	Apr, 2014	rim	0.00	0.68	0.05	2.65	2.90	28.91	209.82	2.05	5.18	1.84	12.70	12.97	0.51	883	28.86
TJB.5	TuE1301-20.1	Apr, 2014		0.00	2.73	0.00	0.00	2.25	3.02	237.09	1.49	1.04	1.71	15.50	16.67	0.19	1138	34.27
TJB.5	TuE1301-21.1	Apr, 2014		0.00	50.17	0.00	0.00	5.31	7.81	322.96	3.09	4.47	1.76	14.17	13.87	0.21	3802	38.09
TJB.5	TuE1301-22.1	Apr, 2014	core	0.00	118.39	1.22	14.48	4.65	21.70	505.88	2.97	4.08	2.19	15.12	14.85	6.34	6128	75.90
TJB.5	TuE1301-22.2	Apr, 2014	rim	0.00	1.72	0.15	0.00	3.13	5.04	352.93	2.30	1.25	2.47	16.41	16.79	0.12	1946	57.87
TJB.5	TuE1301-24.2	Apr, 2014	core	0.00	29.11	0.03	0.00	8.97	17.08	509.15	41.84	2.26	12.43	11.25	10.52	6.16	2800	87.32
TJB.5	TuE1301-24.1	Apr, 2014	rim	0.00	8.26	0.00	0.00	3.01	5.79	323.12	2.46	2.14	3.84	18.85	20.37	1.53	1540	36.49
TJB.5	TuE1301-25.1	Apr, 2014	dark core	0.00	10.29	0.03	2.52	99.36	64.15	673.58	215.63	31.90	11.27	12.89	12.95	88.84	4027	191.74
TJB.5	TuE1301-26.1	Apr, 2014	dark core	0.06	212.54	0.64	6.23	8849.99	5558.90	1225.13	59492.78	912.02	11.70	44.61	48.96	1268.17	8592	429.90
DrE1302																		
TJB.6	DrE1302-4.1	Apr, 2014		0.00	5.65	0.59	12.57	2.36	5.23	551.34	5.55	3.70	3.62	10.55	10.40	0.22	4574	345.08
TJB.6	DrE1302-5.1	Apr, 2014		0.00	17.21	0.21	14.72	2.11	4.65	208.25	3.87	4.00	5.47	8.33	8.86	0.21	2507	25.72
TJB.6	DrE1302-6.1	Apr, 2014		0.00	1.80	0.15	10.22	2.02	4.76	511.65	4.09	4.05	3.09	9.61	10.52	0.35	3926	254.62
TJB.6	DrE1302-7.1	Apr, 2014		0.00	22.86	0.78	14.00	2.13	5.50	354.65	4.30	3.28	2.26	7.24	7.23	0.25	5932	111.99
TJB.6	DrE1302-8.1	Apr, 2014	matches	0.00	17.45	0.52	5.82	2.50	5.06	377.06	9.81	2.31	1.86	6.42	5.87	0.29	5553	106.36
TJB.6	DrE1302-8.2	Apr, 2014	Rim	0.00	8.77	0.15	0.00	2.74	4.53	454.49	6.55	7.05	2.85	13.10	14.04	6.16	4185	231.31
TJB.6	DrE1302-9.1	Apr, 2014		0.00	105.96	0.14	12.01	1.94	4.53	332.13	4.36	3.16	2.42	7.26	7.24	0.14	2875	164.90
TJB.6	DrE1302-10.1	Apr, 2014		0.00	2.39	0.11	1.96	1.84	3.75	408.45	3.90	2.54	2.48	9.80	9.72	0.16	2869	176.77
TJB.6	DrE1302-11.1	Apr, 2014		0.00	34.83	0.37	3.90	2.89	4.47	309.97	7.64	4.14	1.69	7.22	7.20	3.17	4363	74.48
TJB.6	DrE1302-12.1	Apr, 2014	Matches	0.00	15.09	0.63	13.21	2.13	4.71	442.90	2.78	2.85	2.22	13.65	17.02	158.48	6352	139.49
TJB.6	DrE1302-12.2	Apr, 2014	rim	0.00	0.51	0.08	1.92	2.84	3.03	292.91	4.01	24.23	1.70	6.72	6.34	0.18	1732	89.99
TJB.6	DrE1302-13.1	Apr, 2014		0.00	10.46	0.54	9.00	1.53	4.48	346.96	3.24	2.47	2.00	6.47	5.50	0.49	5349	96.65
TJB.6	DrE1302-14.1	Apr, 2014		0.00	1.82	0.04	0.00	1.64	4.05	216.91	3.34	2.64	1.52	6.32	6.35	0.19	3042	44.70
TJB.6	DrE1302-15.1	Apr, 2014		0.08	8.56	0.54	3.52	2.45	5.10	545.76	6.30	5.40	3.57	10.71	11.07	0.37	4727	321.11
FlI1201																		
TJB.2	FlI1201-21.1	Apr, 2014	same grain; matches O spot 211	0.00	0.07	0.03	4.06	1.68	5.33	269.49	14.32	2.43	15.84	18.53	19.23	1.14	808	14.39
TJB.2	FlI1201-21.2	Apr, 2014		0.00	0.98	0.01	6.78	1.60	4.65	526.35	2.80	3.49	17.19	17.66	18.23	0.36	3733	31.92
TJB.2	FlI1201-3	Apr, 2014		0.00	0.15	0.05	2.05	1.82	4.50	297.24	2.03	4.21	22.17	25.56	25.01	0.26	2944	11.44
TJB.2	FlI1201-4.1	Apr, 2014	end	0.04	0.03	0.16	11.44	7.75	21.17	182.57	4.18	7.99	13.38	15.56	15.25	9.66	556	11.11
TJB.2	FlI1201-4.2	Apr, 2014	side sector	0.00	3.95	0.00	45.89	1.85	4.40	523.69	2.32	3.09	17.81	18.43	18.44	0.29	2714	17.78
TJB.2	FlI1201-6.1	Apr, 2014	Light zone @ end	0.00	0.02	0.00	10.56	2.00	5.22	175.28	2.92	3.92	11.59	16.23	16.60	0.38	394	7.19
TJB.2	FlI1201-6.2	Apr, 2014	Dark side zone	0.00	1.69	0.02	3.26	1.77	5.68	412.83	2.04	4.12	19.40	18.64	15.72	0.37	2730	15.27
TJB.2	FlI1201-7.2	Apr, 2014	Inher core w/O	0.00	1.46	0.03	25.25	2.91	4.46	580.44	3.04	196.79	23.91	22.48	22.48	0.81	2467	62.28
TJB.2	FlI1201-7.1	Apr, 2014	End	0.00	0.02	0.00	8.31	2.25	6.66	153.27	18.89	4.09	12.91	17.35	18.13	0.36	475	8.19
TJB.2	FlI1201-8.2	Apr, 2014	Inher core w/O	0.01	7.15	0.08	32.59	15.50	12.81	855.70	7.55	12.97	15.85	15.17	15.59	0.48	4691	279.09
TJB.2	FlI1201-8.1	Apr, 2014	End	0.00	0.01	0.03	9.49	2.61	4.53	196.60	2.38	2.82	15.50	19.45	20.40	0.41	651	9.48
TJB.2	FlI1201-9.2	Apr, 2014	Inher core w/O	0.00	32.84	0.02	38.79	2.33	4.62	991.03	4.42	2.57	12.38	12.81	14.08	0.27	6652	99.71
TJB.2	FlI1201-9.1	Apr, 2014	End	0.00	0.04	0.01	6.31	2.44	4.28	243.74	3.21	3.92	12.85	15.57	16.80	0.38	688	13.78
TJB.2	FlI1201-10.2	Apr, 2014	Side with others	0.00	3.18	0.03	6.62	4.35	5.03	282.71	3.67	49.18	15.21	13.30	16.17	0.35	1891	11.17
TJB.2	FlI1201-10.1	Apr, 2014	End	0.00	1.53	0.00	9.40	2.12	4.01	359.69	2.52	2.23	16.64	18.32	18.04	0.28	1278	21.17
TJB.2	FlI1201-11.1	Apr, 2014		0.00	3.73	0.05	9.87	2.76	4.49	415.92	5.41	7.07	24.53	38.79	40.68	0.38	1580	7.37
TJB.2	FlI1201-12.2	Apr, 2014	End	0.00	0.02	0.07	1.08	2.31	7.65	273.49	2.81	3.94	18.86	35.23	38.45	0.31	549	5.34
TJB.2	FlI1201-12.1	Apr, 2014	With U/O	0.00	0.02	0.03	11.86	2.55	7.24	385.78	3.46	6.05	24.24	37.28	37.51	0.35	756	8.49
TJB.2	FlI1201-13.1	Apr, 2014		0.00	0.22	0.05	11.08	3.30	6.13	263.41	5.60	12.58	16.22	18.06	19.43	0.29	823	11.90
TJB.2	FlI1201-14.2	Apr, 2014	Core with others	0.01	0.15	0.02	3.40	5.11	7.61	1008.86	6.29	9.29	24.11	17.26	17.43	0.66	4248	102.09

Table F1a. Hafnarfjall-Skarðsheiði *in situ* zircon trace element (ppm) concentrations (Atomic number ≤ 41)

Mount	Analysis	Date	TE notes	Li	Be	B	F	Na	Al	P	K	Ca	Sc	48Ti	49Ti	Fe	Y	Nb
TJB.2	FII1201-14.1	Apr, 2014	End	0.00	0.01	0.04	1.14	3.77	8.58	230.19	46.20	5.16	12.65	16.83	17.14	0.29	707	16.94
TJB.2	FII1201-17.2	Apr, 2014	Core with others	0.17	26.07	0.15	53.11	217.87	195.77	773.55	4377.30	202.29	7.10	57.36	62.42	967.76	5394	518.69
TJB.2	FII1201-17.1	Apr, 2014	End	0.00	0.08	0.04	2.79	2.73	6.88	220.76	4.14	8.33	15.83	14.16	7.48	0.53	599	11.05
TJB.2	FII1201-18.1	Apr, 2014		0.00	0.59	0.01	6.02	2.06	6.00	315.66	2.13	1.80	21.94	36.64	36.31	0.21	994	7.27
TJB.2	FII1201-19.1	Apr, 2014		0.00	0.04	0.01	3.87	1.54	4.54	473.16	2.83	3.25	18.30	24.92	24.62	0.33	1143	18.82
TJB.2	FII1201-20.1	Apr, 2014		0.00	14.74	0.08	11.53	1.92	4.14	884.87	3.18	10.00	17.40	15.22	15.63	0.33	4567	78.11
SvE1302														22.19				
TJB.11	SvE1302-1.1	Oct. 2014												5.06	5.26	1.60	3253	
TJB.11	SvE1302-2.1	Oct. 2014												8.56	8.64	0.89	1154	
TJB.11	SvE1302-3.1	Oct. 2014	Core											10.58	10.62	22.86	3507	
TJB.11	SvE1302-4.1	Oct. 2014	Mantle											7.30	7.44	0.80	991	
TJB.11	SvE1302-5.1	Oct. 2014												7.82	7.95	1.86	1621	
TJB.11	SvE1302-6.1	Oct. 2014												8.79	9.30	1.43	1308	
TJB.11	SvE1302-7.1	Oct. 2014												18.52	19.01	9.45	4721	
TJB.11	SvE1302-8.1	Oct. 2014												26.22	26.57	3.74	15760	
TJB.11	SvE1302-9.1	Oct. 2014												10.37	10.46	9.03	2329	
TJB.11	SvE1302-10.1	Oct. 2014												20.54	19.76	0.81	12482	
TJB.11	SvE1302-11.1	Oct. 2014	On CL-mottled area											12.01	11.42	762.73	7329	
TJB.11	SvE1302-12.1	Oct. 2014	On CL-mottled area											20.03	20.76	648.32	1349	
TJB.11	SvE1302-13.1	Oct. 2014	Core											6.79	6.68	0.12	3254	
TJB.11	SvE1302-14.1	Oct. 2014	Core											15.67	15.71	0.52	4878	
TJB.11	SvE1302-15.1	Oct. 2014	Core											8.63	8.48	8.65	2519	
ShE1301																		
TJB.11	ShE1302-1.1	Oct. 2014												32.33	32.29	1.31	9243	
TJB.11	ShE1302-2.1	Oct. 2014	Core; O on rim											18.06	18.06	16.87	12176	
TJB.11	ShE1302-3.1	Oct. 2014	Core											9.02	9.08	0.17	8396	
TJB.11	ShE1302-4.1	Oct. 2014												16.77	16.96	3.93	6921	
TJB.11	ShE1302-5.1	Oct. 2014	On end											36.03	36.06	87.98	15676	
TJB.11	ShE1302-6.1	Oct. 2014												13.35	13.25	0.45	6280	
TJB.11	ShE1302-7.1	Oct. 2014												34.84	35.01	79.62	14335	
TJB.11	ShE1302-8.1	Oct. 2014	Mantle; adjacent to O spot											37.09	37.64	3.00	9757	
TJB.11	ShE1302-9.1	Oct. 2014	Core; adjacent to O spot											19.32	19.31	0.59	8970	
TJB.11	ShE1302-10.1	Oct. 2014												30.60	30.43	1558.66	8045	
FeE1301																		
TJB.11	FeE1301-1.1	Oct. 2014												6.50	6.57	22.12	6322	
TJB.11	FeE1301-2.1	Oct. 2014	Adjacent to O spot											12.20	12.46	6.08	2021	
TJB.11	FeE1301-3.1	Oct. 2014	Adjacent to O spot											6.82	6.96	1.19	4103	
TJB.11	FeE1301-4.1	Oct. 2014	Core; O on rim											9.16	9.83	9.39	4060	
TJB.11	FeE1301-5.1	Oct. 2014												6.76	6.64	0.15	3382	
TJB.11	FeE1301-6.1	Oct. 2014												8.11	8.23	0.76	4160	
TJB.11	FeE1301-7.1	Oct. 2014												10.92	10.96	0.40	4534	
TJB.11	FeE1301-8.1	Oct. 2014												4.73	4.79	0.21	3660	
TJB.11	FeE1301-9.1	Oct. 2014												9.75	9.79	0.34	2563	
TJB.11	FeE1301-10.1	Oct. 2014												6.47	6.50	0.23	5149	
TJB.11	FeE1301-11.1	Oct. 2014	Core											5.86	5.55	0.12	6511	
TJB.11	FeE1301-12.1	Oct. 2014	Rim											6.58	6.60	3.86	1088	
Hrl1202																		
TJB.1	BURI_2.4	May 2013											17.32	64.23	60.57	223.85	13611	315.64
TJB.1	BURI2.13	May 2013	Core										12.25	24.44	24.20	384.50	2762	32.58
TJB.1	BURI2.11	May 2013	Rim										9.34	12.64	12.04	28.09	1046	23.13
TJB.1	BURI2_MID	May 2013											9.62	106.54	106.26	1822.33	3322	45.77
TJB.1	BURI_2.3	May 2013											19.83	17.10	16.66	14.93	3013	25.13
TJB.1	BURI_2.2_M	May 2013											12.39	13.95	14.35	6198.37	1369	32.72

Table F1a. Hafnarfjall-Skarðsheiði *in situ* zircon trace element (ppm) concentrations (Atomic number ≤ 41)

Mount	Analysis	Date	TE notes	Li	Be	B	F	Na	Al	P	K	Ca	Sc	48Ti	49Ti	Fe	Y	Nb
TJB.1	BURI_3.7_r	May 2013											10.31	14.08	14.93	2.18	1098	22.65
TJB.1	BURI_3.7_M	May 2013											9.45	13.53	12.82	0.56	787	16.91
TJB.1	BURI_3.7_L	May 2013											12.70	16.78	15.13	6.54	1818	26.84
TJB.1	BURI_3.6_M	May 2013											13.83	16.90	16.12	71.58	1910	37.85
TJB.1	BURI_3.6_L	May 2013											9.92	16.03	15.42	14.82	1053	23.33
TJB.1	BURI_3.5	May 2013											12.71	11.91	11.43	11.63	3752	40.10
TJB.1	BURI_3.3_R	May 2013											8.84	11.62	11.15		2757	17.50
TJB.1	BURI_3.3_L	May 2013											10.30	14.42	14.31		1287	23.89

Table F1b. Hafnarfjall-Skarðsheiði *in situ* zircon trace element (ppm) concentrations (Atomic number > 41)

Analysis	La	Ce	Nd	Sm	Eu	Gd	Tb	Dy	Ho	Er	Tm	Yb	Lu	Hf	Pb	Th	U	Eu/Eu*	T (°C)[1]
BrE1201																			
BrE1-1.1	0.03	18.70	3.57	8.17	1.70	77.13	26.99	321	123	519	105	827	141	9750	0	97	175	0.21	753
BrE1-2.1	0.02	12.80	2.11	5.88	1.21	57.20	19.42	217	82	345	71	544	94	10032	0	55	104	0.20	750
BrE1-3.1	1.74	23.88	3.65	7.76	1.63	71.83	24.61	283	110	458	93	736	129	9730	0	103	160	0.21	793
BrE1-4.1	0.01	18.03	0.94	2.67	0.55	28.34	10.75	134	51	231	49	397	70	10705	0	56	127	0.19	752
BrE1-5.1	0.01	17.15	1.05	2.83	0.72	33.03	12.11	145	56	256	55	451	82	10223	0	61	128	0.23	755
BrE1-6.1	0.02	17.25	2.72	8.23	1.55	77.18	24.54	281	107	443	90	690	119	10246	0	91	145	0.19	749
BrE1-7.1	0.30	26.40	3.23	8.57	1.86	88.22	30.84	354	136	577	115	902	153	10039	0	124	209	0.21	775
BrE1-8.1	0.01	27.47	1.24	4.09	0.82	41.46	14.69	181	71	312	65	524	90	10260	0	123	206	0.19	757
BrE1-9.1	0.01	8.43	0.60	2.44	0.63	29.15	11.42	136	50	239	49	421	74	10429	0	43	91	0.23	756
BrE1-10.1	0.01	32.97	1.49	5.18	0.92	54.23	19.24	228	87	387	82	636	112	10214	0	160	248	0.17	762
BrE1-11.1	0.01	14.88	0.80	2.58	0.55	27.71	9.44	117	47	209	44	359	65	10037	0	46	100	0.20	758
BrE1-11.2	0.03	253.00	6.05	20.02	3.37	222.08	75.64	871	319	1340	275	2130	351	9565	1	1685	1250	0.15	661
BrE1-12.1	0.02	23.82	1.17	3.97	0.85	41.16	14.87	181	71	309	66	517	90	9825	0	111	170	0.20	770
BrE1-13.1	0.01	18.68	1.05	3.20	0.76	37.66	12.85	147	61	260	56	446	80	9948	0	61	115	0.21	761
BrE1-14.1	0.21	17.09	3.06	7.30	1.50	65.60	22.81	254	104	427	88	691	117	10058	0	78	141	0.21	749
BrE1-15.1	0.01	16.11	0.85	3.28	0.78	34.03	12.67	144	57	252	54	455	78	9773	0	80	146	0.22	774
BrE1-16.1	0.02	23.03	1.30	3.96	0.84	40.53	15.07	176	72	309	65	531	94	10052	0	89	163	0.20	767
BrE1-17.1	0.01	15.08	1.35	3.55	0.86	40.12	13.54	161	64	282	61	491	87	9604	0	56	124	0.22	779
BrE1-18.1	0.04	15.00	2.60	6.75	1.47	63.70	20.59	232	93	377	78	600	103	10073	0	66	129	0.22	762
BrE1-19.1	1.74	412.44	23.04	55.70	3.93	474.70	153.69	1624	568	2200	421	3240	490	8929	1	869	1009	0.07	1118
BrE1-20.1	3.34	28.02	5.02	8.86	1.82	82.82	27.85	313	120	509	101	765	132	9929	0	109	174	0.20	786
BrE1-21.1	0.23	25.58	3.59	8.81	2.57	98.05	33.45	377	134	562	113	856	143	8194	0	239	268	0.27	837
BrE1-22.1	2.16	14.57	1.38	1.96	0.46	19.11	6.43	77	33	138	31	249	44	10602	0	20	61	0.23	783
BrE1-23.1	0.11	39.33	2.02	7.67	1.75	90.46	31.87	379	150	629	133	1056	182	9828	1	256	335	0.20	765
BrE1-23.2	0.05	15.68	0.78	2.77	0.60	28.22	9.72	119	47	211	46	365	65	10644	0	50	116	0.21	762
BrE1-24.1	0.09	22.38	1.30	4.07	0.87	38.01	13.96	169	67	282	60	485	83	9717	0	122	177	0.21	771
BrE1-25.1	0.05	12.09	1.81	4.30	0.95	44.59	16.84	209	77	357	74	606	108	10324	0	123	189	0.21	751
BrE1-26.1	0.00	23.19	1.17	4.12	0.92	42.59	14.35	173	69	299	62	504	89	10002	0	85	138	0.21	766
BrE1-27.1	0.04	17.36	1.13	2.92	0.68	33.83	11.78	134	56	244	52	420	74	10038	0	61	120	0.21	757
BrE1-29.1	0.07	174.04	3.94	9.81	0.74	94.93	36.35	421	157	690	151	1237	195	13519	2	2054	1945	0.07	808
BrE1-30.1	0.30	18.05	2.63	6.96	1.41	59.90	23.24	272	104	451	92	715	123	10406	0	80	144	0.21	864
BrE1-31.1	0.04	16.92	3.43	7.75	1.67	82.05	26.55	311	120	508	102	802	136	9914	0	96	168	0.20	750
BrE1-32.1	0.02	35.36	1.68	5.26	1.06	55.37	19.37	234	93	396	81	642	109	10324	0	156	251	0.19	762
BrE1-33.1	0.02	15.59	0.66	2.47	0.45	25.82	9.34	109	45	201	44	348	62	10888	0	45	109	0.17	757
BrE1-34.1	0.01	22.05	1.11	3.40	0.77	39.01	13.17	158	62	275	58	470	82	10166	0	69	134	0.20	766
BrE1-35.1	0.14	10.88	2.05	5.07	1.32	49.65	16.33	195	72	312	66	531	91	9436	0	51	98	0.25	790
BrE1-36.1	0.03	16.76	3.27	8.67	1.73	80.04	27.53	323	121	515	105	827	140	10086	0	104	171	0.20	739
BrE1-37.1	0.04	22.42	3.37	8.79	1.89	85.41	27.98	319	127	503	101	756	134	10164	0	112	181	0.21	736
BrE1-38.1	0.02	14.31	2.84	7.36	1.47	63.62	21.73	253	97	414	80	657	113	9846	0	78	141	0.21	745
BrE1-39.1	0.01	19.24	1.73	4.68	1.09	44.22	16.26	198	77	332	70	561	95	9946	0	77	137	0.23	758
BrE1-40.1	0.51	21.67	3.88	9.46	1.85	92.90	30.48	342	136	557	115	886	152	10025	0	110	188	0.19	751
BrE1-41.1	0.01	21.47	1.23	3.98	0.85	41.78	13.91	173	67	292	61	509	89	9892	0	73	132	0.20	765
BrE1-42.1	0.56	28.23	2.85	6.77	1.38	62.96	21.83	247	97	413	83	648	114	9727	0	146	206	0.20	800
BrE1-43.1	0.05	17.50	2.81	7.28	1.65	76.62	25.92	285	107	445	88	699	121	9966	0	90	151	0.21	768
BrE1-44.1	0.04	11.86	0.47	1.58	0.38	19.55	7.43	89	36	166	37	301	54	10647	0	38	78	0.21	742
BrE1-45.1	0.04	168.86	4.58	15.20	2.36	166.85	57.08	634	233	983	199	1542	251	10331	1	887	836	0.14	699
BrE1-46.1	1.99	22.46	12.50	22.16	4.55	129.44	29.52	280	100	323	61	448	71	10141	0	95	87	0.26	777
RnE1201																			
RnE1201-13.1	0.06	14.34	3.16	7.67	2.49	68.67	26.28	271	100	406	76	585	97	9555	0	66	113	0.33	814
RnE1201-13.2	0.01	6.73	0.52	1.70	0.67	19.69	7.40	89	34	142	29	229	39	9618	0	18	46	0.35	784
RnE1201-14.1	0.02	60.01	5.09	14.80	5.62	152.47	53.85	560	193	781	141	1064	168	8471	0	733	512	0.36	869
RnE1201-14.2	0.01	8.03	0.50	1.94	0.79	21.08	8.20	94	36	159	32	258	42	9874	0	23	61	0.38	782

[1]Calculated using the method of Ferry and Watson (2007) using *a* SiO_2=1.0 and *a* TiO_2=0.7.

Table F1b. Hafnarfjall-Skarðsheiði *in situ* zircon trace element (ppm) concentrations (Atomic number > 41)

Analysis	La	Ce	Nd	Sm	Eu	Gd	Tb	Dy	Ho	Er	Tm	Yb	Lu	Hf	Pb	Th	U	Eu/Eu*	T (°C)[1]
RnE1201-18.1	0.03	7.87	0.64	2.36	0.84	21.84	7.89	95	36	155	31	252	43	9856	0	21	60	0.36	778
RnE1201-19.1	0.05	10.57	2.87	7.30	2.39	64.55	25.13	266	95	393	76	561	91	9646	0	46	90	0.34	761
RnE1201-20.1	0.02	44.30	3.07	7.97	2.38	78.87	26.61	328	119	499	96	711	112	9382	0	217	242	0.29	824
RnE1201-20.2	0.01	11.65	1.26	3.04	1.07	32.65	11.61	128	50	213	42	332	56	9504	0	48	97	0.33	796
RnE1201-22.1	0.02	9.07	0.55	1.95	0.70	19.66	8.08	91	34	153	29	240	41	10165	0	23	57	0.34	786
RnE1201-22.2	0.01	8.40	0.54	2.73	0.82	23.41	9.09	102	39	164	33	270	46	9440	0	34	77	0.31	772
TuE1301																			
TuE1301-18.1	0.03	58.67	5.53	15.56	3.95	157.68	58.24	644	233	980	189	1412	227	9643	1	412	479	0.24	782
TuE1301-18.2	0.02	8.14	0.81	2.07	0.76	22.57	8.34	96	37	157	32	252	44	10134	0	24	64	0.34	805
TuE1301-20.1	0.02	10.51	0.95	2.62	1.09	27.65	10.62	124	47	202	40	322	53	9338	0	33	75	0.39	826
TuE1301-21.1	0.03	15.51	5.59	15.46	5.42	139.74	48.22	504	172	706	130	976	161	9517	0	97	163	0.36	817
TuE1301-22.1	0.03	25.90	8.40	24.55	8.01	204.17	74.29	777	270	1102	207	1508	242	8634	0	201	285	0.34	824
TuE1301-22.2	0.02	20.25	2.10	5.89	1.82	53.78	19.95	223	82	352	69	525	85	9204	0	100	165	0.31	833
TuE1301-24.2	0.02	32.53	2.38	7.06	1.79	73.02	27.96	316	115	494	98	767	122	9869	0	248	303	0.24	793
TuE1301-24.1	0.01	12.17	1.65	4.90	1.40	42.28	15.23	169	63	271	53	425	73	9498	0	67	114	0.30	848
TuE1301-25.1	0.11	79.93	4.23	11.57	2.40	117.43	41.44	463	171	701	134	1043	164	10239	0	564	553	0.20	807
TuE1301-26.1	0.24	189.23	8.56	25.14	5.95	262.63	98.97	1080	386	1586	300	2299	352	11154	1	593	897	0.22	956
DrE1302																			
DrE1302-4.1	0.03	118.77	4.11	12.90	3.19	136.90	54.03	569	205	825	151	1097	165	9554	0.23	563	642	0.23	786
DrE1302-5.1	0.04	17.49	4.29	9.49	2.52	77.52	27.36	290	105	427	81	594	97	9524	0.08	70	123	0.28	762
DrE1302-6.1	0.04	87.21	3.43	9.85	2.57	111.77	43.78	469	168	688	128	943	141	9568	0.39	376	522	0.24	777
DrE1302-7.1	0.06	51.98	7.61	21.26	5.38	193.76	69.47	722	259	1014	189	1401	210	9346	0.24	236	368	0.26	749
DrE1302-8.1	0.03	45.24	5.33	15.28	4.11	161.20	59.13	642	237	954	179	1285	203	9522	0.21	230	371	0.25	738
DrE1302-8.2	0.10	92.81	5.70	15.02	5.42	147.56	49.27	520	181	725	135	1005	154	9330	0.21	495	507	0.35	808
DrE1302-9.1	0.03	57.01	2.68	7.58	1.94	73.07	30.67	336	124	506	96	730	111	10060	0.19	121	273	0.25	749
DrE1302-10.1	0.02	56.14	2.57	8.30	2.29	81.57	31.42	340	125	494	93	681	106	9977	0.47	296	404	0.27	778
DrE1302-11.1	0.06	31.51	5.23	13.27	3.49	127.48	45.86	480	181	705	133	960	149	10296	0.09	118	239	0.26	749
DrE1302-12.1	1.41	64.76	15.03	22.57	4.97	186.32	69.39	714	265	1029	192	1395	209	9701	0.18	233	381	0.23	813
DrE1302-12.2	0.03	29.55	1.85	4.47	1.31	47.22	17.68	201	75	308	59	455	70	10343	0.12	74	179	0.27	742
DrE1302-13.1	0.06	48.32	7.04	17.69	4.37	164.88	59.82	631	229	905	170	1247	186	9628	0.17	201	350	0.25	739
DrE1302-14.1	0.02	23.78	4.42	10.33	2.72	96.68	35.42	387	144	586	111	818	129	9950	0.17	124	234	0.26	736
DrE1302-15.1	0.04	109.57	4.22	12.54	3.34	138.29	51.43	551	202	806	150	1082	165	9345	0.25	400	590	0.24	788
Fll1201																			
Fll1201-21.1	0.02	8.44	0.56	2.06	0.60	19.48	7.38	87	34	139	29	237	41	9220	0.00	17	42	0.18	846
Fll1201-21.2	0.04	14.79	5.13	12.48	3.68	119.20	42.27	455	164	668	123	956	160	8949	0.08	96	146	0.15	841
Fll1201-3	0.03	6.18	4.49	12.85	4.30	112.60	34.20	360	131	509	98	750	127	7913	0.11	45	75	0.10	884
Fll1201-4.1	0.03	6.48	0.53	1.30	0.45	12.83	4.90	60	23	103	21	174	31	9184	0.00	10	26	0.15	827
Fll1201-4.2	0.04	13.17	4.41	10.51	2.90	87.09	29.60	326	112	461	90	698	117	8956	0.06	55	90	0.13	846
Fll1201-6.1	0.02	3.30	0.31	1.00	0.31	9.43	3.79	46	18	86	18	148	27	11214	0.03	6	22	0.15	832
Fll1201-6.2	0.03	11.81	5.35	12.90	3.29	93.04	30.43	325	115	455	89	674	110	9059	0.03	47	85	0.13	847
Fll1201-7.2	0.28	28.22	3.39	7.44	1.91	66.79	24.70	272	97	415	80	623	105	8783	0.24	121	158	0.25	869
Fll1201-7.1	0.01	3.88	0.34	0.94	0.35	10.44	4.23	46	19	81	17	137	25	9377	0.00	7	21	0.15	839
Fll1201-8.2	0.05	119.81	5.44	15.72	2.05	140.01	50.03	543	196	785	152	1134	181	9602	0.50	514	554	0.49	824
Fll1201-8.1	0.01	5.61	0.52	1.60	0.52	16.06	5.73	69	27	115	23	198	35	9271	0.03	12	30	0.15	852
Fll1201-9.2	0.09	65.51	11.20	26.15	4.23	226.89	77.09	824	290	1145	213	1620	258	8665	0.09	260	335	0.21	806
Fll1201-9.1	0.03	9.44	0.45	1.50	0.57	17.52	6.05	75	28	127	26	218	38	9819	0.00	14	34	0.15	827
Fll1201-10.2	0.01	6.77	2.49	7.28	2.09	51.90	21.85	231	81	344	68	525	87	9095	0.00	30	60	0.11	810
Fll1201-10.1	0.06	9.23	1.15	4.04	1.02	34.80	12.25	138	53	237	49	393	65	8763	0.03	29	68	0.17	845
Fll1201-11.1	0.01	7.97	2.78	6.68	2.46	54.79	18.13	196	68	284	56	425	72	9303	0.00	24	40	0.09	937
Fll1201-12.2	0.03	7.19	0.57	1.55	0.62	13.58	4.83	64	23	104	22	193	34	9374	0.03	8	16	0.08	924
Fll1201-12.1	0.02	6.93	0.60	2.02	0.73	18.51	7.39	84	32	138	29	238	43	9189	0.00	10	24	0.10	932
Fll1201-13.1	0.00	7.60	0.66	2.04	0.68	23.14	7.76	90	34	149	31	241	43	9579	0.03	16	41	0.17	843
Fll1201-14.2	0.03	45.35	5.10	14.44	3.13	128.67	47.21	526	183	771	146	1120	183	9393	0.09	341	334	0.30	838

[1]Calculated using the method of Ferry and Watson (2007) using *a* SiO_2=1.0 and *a* TiO_2=0.7.

Table F1b. Hafnarfjall-Skarðsheiði *in situ* zircon trace element (ppm) concentrations (Atomic number > 41)

Analysis	La	Ce	Nd	Sm	Eu	Gd	Tb	Dy	Ho	Er	Tm	Yb	Lu	Hf	Pb	Th	U	Eu/Eu*	T (°C)[1]
FlI1201-14.1	0.02	7.52	0.69	1.44	0.50	16.31	6.84	77	28	130	26	222	38	9727	0.03	16	37	0.17	836
FlI1201-17.2	0.52	101.33	8.06	18.53	2.82	147.00	57.83	660	249	983	198	1470	237	11746	0.35	580	447	0.30	991
FlI1201-17.1	0.03	7.39	0.67	1.89	0.66	18.79	7.36	85	33	143	30	248	42	10117	0.00	13	34	0.14	817
FlI1201-18.1	0.01	7.04	1.13	3.72	1.24	28.15	10.32	108	40	168	35	265	48	9628	0.00	11	23	0.09	929
FlI1201-19.1	0.02	13.29	1.10	3.38	0.95	30.69	10.85	120	47	198	40	321	56	9838	0.00	27	54	0.17	881
FlI1201-20.1	0.05	40.15	7.35	17.44	4.34	150.87	50.19	552	193	775	147	1106	180	8502	0.11	319	279	0.25	824
SvE1302														9395					
SvE1302-1.1	0.04	55.08	2.02	6.69	1.54	73.16		328		553		825		11009		275	480	0.21	749
SvE1302-2.1	2.77	15.19	2.33	3.34	0.92	29.14		120		205		330		10464		45	109	0.28	801
SvE1302-3.1	0.14	10.58	3.70	10.95	3.65	104.70		388		576		824		8926		102	179	0.33	824
SvE1302-4.1	0.04	10.23	0.74	2.45	0.66	23.87		101		177		293		10427		37	97	0.27	785
SvE1302-5.1	3.94	16.26	3.72	5.34	1.40	43.90		179		280		429		9336		54	117	0.28	792
SvE1302-6.1	0.39	12.53	1.27	3.33	1.04	32.34		139		232		365		9892		56	121	0.30	804
SvE1302-7.1	0.78	89.03	18.83	36.47	1.17	241.58		834		988		1455		12311		2150	1611	0.04	888
SvE1302-8.1	10.64	402.54	91.55	118.17	9.10	650.11		1618		1772		2544		11318		1385	686	0.10	932
SvE1302-9.1	0.23	13.59	2.90	7.75	2.21	68.41		255		396		581		9264		72	135	0.29	821
SvE1302-10.1	4.47	242.36	85.49	139.59	3.17	661.90		1661		1578		2168		13364		3108	1350	0.03	901
SvE1302-11.1	149.93	286.08	44.33	21.95	2.28	114.59		458		686		1864		9939		858	2119	0.14	838
SvE1302-12.1	19.65	46.46	5.39	3.65	0.44	20.07		105		243		648		10971		922	881	0.16	898
SvE1302-13.1	0.07	52.49	2.88	8.06	1.62	79.06		335		538		826		9934		253	396	0.20	777
SvE1302-14.1	0.12	42.68	5.47	14.72	4.18	140.75		503		722		1076		9562		493	409	0.28	868
SvE1302-15.1	0.38	13.87	3.27	8.41	2.46	77.45		279		427		614		8541		88	154	0.29	802
ShE1301																			
ShE1302-1.1	0.61	362.37	17.01	37.48	3.50	269.88		931		1215		1746		10829		1870	1745	0.11	960
ShE1302-2.1	3.16	332.25	50.73	78.90	6.80	450.53		1234		1357		1836		9181		803	591	0.11	885
ShE1302-3.1	0.84	170.69	23.84	46.36	5.21	319.55		962		1171		1508		7593		509	564	0.13	806
ShE1302-4.1	0.77	216.13	16.11	33.84	3.47	243.15		767		958		1274		7475		678	740	0.12	876
ShE1302-5.1	2.02	375.34	49.33	84.63	7.31	516.98		1522		1810		2523		11139		1054	923	0.11	975
ShE1302-6.1	1.29	144.73	24.18	41.16	3.80	242.35		738		770		988		6824		435	528	0.12	849
ShE1302-7.1	4.33	386.11	68.10	102.19	8.29	586.08		1495		1542		2007		9705		1056	649	0.10	971
ShE1302-8.1	18.80	413.86	26.18	42.67	3.57	287.29		968		1272		1862		10926		2040	1813	0.10	979
ShE1302-9.1	1.54	284.51	33.10	58.24	5.56	356.45		1013		1043		1331		9291		934	933	0.12	893
ShE1302-10.1	1.96	188.11	18.52	34.63	3.72	235.49		834		1144		1741		9808		680	796	0.13	953
FeE1301																			
FeE1301-1.1	185.36	346.49	72.78	37.41	6.74	205.82		670		994		1455		9001		458	452	0.23	773
FeE1301-2.1	5.06	21.75	2.98	6.19	1.80	56.71		207		357		552		8640		85	118	0.29	839
FeE1301-3.1	1.89	34.66	6.21	10.26	2.73	105.26		367		647		903		10223		97	160	0.25	778
FeE1301-4.1	5.86	73.91	7.30	14.11	3.05	120.14		414		641		858		6899		359	406	0.23	808
FeE1301-5.1	1.19	30.77	3.86	9.60	2.38	90.52		340		541		806		7711		153	215	0.25	777
FeE1301-6.1	0.71	34.54	4.68	12.30	3.04	118.16		426		648		977		8422		168	236	0.24	795
FeE1301-7.1	6.82	68.65	6.63	11.90	3.05	104.15		397		644		978		7898		394	404	0.26	827
FeE1301-8.1	1.48	90.76	3.76	9.08	2.26	100.26		392		667		949		10101		251	393	0.23	742
FeE1301-9.1	0.17	17.56	2.71	6.48	2.18	67.95		246		421		670		9654		90	134	0.32	815
FeE1301-10.1	0.10	85.52	4.78	12.92	2.94	132.03		523		823		1201		9314		616	578	0.22	772
FeE1301-11.1	0.30	74.21	6.94	18.18	4.20	169.71		670		1032		1477		9846		387	417	0.23	763
FeE1301-12.1	0.07	15.71	1.12	2.69	0.74	24.88		107		191		318		9498		33	72	0.28	774
Hrl1202																			
BURI_2.4	0.80	292.95	23.28	56.04	10.05	457.71		1500	525	2048		2687	409	8019		1289	850	0.19	1008
BURI2.13	21.50	79.27	30.75	17.42	3.67	99.17		313	115	469		666	111	8456		92	149	0.27	879
BURI2.11	0.43	20.45	2.61	3.39	1.01	28.48		114	43	189		299	51	8115		54	93	0.31	805
BURI2_MID	4.27	26.09	6.49	12.54	3.82	110.38		346	126	550		764	127	6708		160	224	0.31	1087
BURI_2.3	0.41	16.97	4.84	10.87	3.51	96.22		323	118	512		739	128	8009		95	143	0.33	837

[1]Calculated using the method of Ferry and Watson (2007) using *a* SiO_2=1.0 and *a* TiO_2=0.7.

Table F1b. Hafnarfjall-Skarðsheiði *in situ* zircon trace element (ppm) concentrations (Atomic number > 41)

Analysis	La	Ce	Nd	Sm	Eu	Gd	Tb	Dy	Ho	Er	Tm	Yb	Lu	Hf	Pb	Th	U	Eu/Eu*	T (°C)[1]
BURI_2.2_M	0.37	18.28	1.82	4.07	1.15	36.38		133	54	231		352	61	8254		83	138	0.29	815
BURI_3.7_r	3.05	18.22	3.77	4.16	1.08	28.20		117	46	194		300	52	8044		43	91	0.30	816
BURI_3.7_M	0.13	7.93	0.86	2.24	0.65	18.77		74	27	133		223	38	8403		25	65	0.31	812
BURI_3.7_L	0.15	14.46	2.89	6.75	1.92	56.70		204	74	324		479	80	8231		55	102	0.30	835
BURI_3.6_M	0.19	16.84	2.66	6.67	2.04	54.71		195	75	311		461	78	7662		127	162	0.33	836
BURI_3.6_L	0.38	11.22	1.71	3.88	1.27	30.44		107	43	175		281	49	8034		40	93	0.36	830
BURI_3.5	21.50	83.87	24.67	14.81	3.77	124.81		415	146	634		915	150	8586		130	202	0.27	798
BURI_3.3_R	0.03	10.63	4.02	10.07	2.92	88.60		292	107	450		637	105	8179		73	132	0.30	796
BURI_3.3_L	0.02	12.75	1.40	3.56	1.14	34.71		136	52	231		360	61	8211		61	110	0.31	819

[1]Calculated using the method of Ferry and Watson (2007) using *a* SiO_2=1.0 and *a* TiO_2=0.7.

Table F1c. Hafnarfjall-Skarðsheiði *in situ* zircon REE for zircon-normalized plots

Analysis	La	Ce	Pr	Nd	Pm	Sm	Eu	Gd	Tb	Dy	Ho	Er	Tm	Yb	Lu
BrE1201															
BrE1-1.1	0.03	18.70	0.75	3.57	5.40	8.17	1.70	77.13	26.99	321.44	123.37	518.85	105.19	827.19	140.53
BrE1-2.1	0.02	12.80	0.42	2.11	3.52	5.88	1.21	57.20	19.42	217.49	81.65	344.90	70.86	544.04	93.76
BrE1-3.1	1.74	23.88	2.85	3.65	5.32	7.76	1.63	71.83	24.61	282.99	110.48	457.64	93.27	735.99	128.53
BrE1-4.1	0.01	18.03	0.18	0.94	1.59	2.67	0.55	28.34	10.75	134.10	51.32	231.13	48.64	396.74	70.29
BrE1-5.1	0.01	17.15	0.23	1.05	1.73	2.83	0.72	33.03	12.11	144.59	56.00	256.10	55.41	450.90	82.47
BrE1-6.1	0.02	17.25	0.50	2.72	4.74	8.23	1.55	77.18	24.54	281.48	107.24	443.18	89.52	689.73	118.96
BrE1-7.1	0.30	26.40	1.47	3.23	5.26	8.57	1.86	88.22	30.84	353.86	135.53	576.77	114.95	902.47	153.08
BrE1-8.1	0.01	27.47	0.21	1.24	2.25	4.09	0.82	41.46	14.69	180.65	71.34	312.48	65.15	523.71	90.26
BrE1-9.1	0.01	8.43	0.13	0.60	1.21	2.44	0.63	29.15	11.42	136.22	49.86	238.77	49.17	421.26	73.89
BrE1-10.1	0.01	32.97	0.30	1.49	2.77	5.18	0.92	54.23	19.24	227.84	87.36	386.51	81.91	636.44	111.75
BrE1-11.1	0.01	14.88	0.21	0.80	1.44	2.58	0.55	27.71	9.44	116.94	47.42	208.86	44.32	358.56	64.96
BrE1-11.2	0.03	253.00	1.06	6.05	11.01	20.02	3.37	222.08	75.64	870.59	319.13	1340.06	274.84	2129.56	350.96
BrE1-12.1	0.02	23.82	0.30	1.17	2.15	3.97	0.85	41.16	14.87	181.20	71.50	308.75	66.23	517.15	90.48
BrE1-13.1	0.01	18.68	0.20	1.05	1.83	3.20	0.76	37.66	12.85	146.78	60.98	260.09	55.65	445.73	80.10
BrE1-14.1	0.21	17.09	1.24	3.06	4.73	7.30	1.50	65.60	22.81	253.58	104.25	427.18	87.75	691.37	117.43
BrE1-15.1	0.01	16.11	0.18	0.85	1.67	3.28	0.78	34.03	12.67	143.72	56.68	251.70	54.28	454.78	77.79
BrE1-16.1	0.02	23.03	0.32	1.30	2.27	3.96	0.84	40.53	15.07	176.20	72.48	308.69	64.89	531.07	93.93
BrE1-17.1	0.01	15.08	0.29	1.35	2.19	3.55	0.86	40.12	13.54	161.22	63.95	282.10	61.08	491.18	86.93
BrE1-18.1	0.04	15.00	0.64	2.60	4.19	6.75	1.47	63.70	20.59	232.35	93.13	376.72	78.21	599.60	102.65
BrE1-19.1	1.74	412.44	9.73	23.04	35.82	55.70	3.93	474.70	153.69	1623.74	567.91	2199.66	421.00	3239.64	490.31
BrE1-20.1	3.34	28.02	4.38	5.02	6.67	8.86	1.82	82.82	27.85	313.42	120.45	508.61	100.95	764.64	132.22
BrE1-21.1	0.23	25.58	1.45	3.59	5.63	8.81	2.57	98.05	33.45	377.28	133.90	562.46	112.65	856.26	143.24
BrE1-22.1	2.16	14.57	1.60	1.38	1.64	1.96	0.46	19.11	6.43	77.16	32.54	138.40	30.56	248.57	43.54
BrE1-23.1	0.11	39.33	0.76	2.02	3.94	7.67	1.75	90.46	31.87	378.95	149.89	629.01	133.17	1055.71	181.79
BrE1-23.2	0.05	15.68	0.32	0.78	1.47	2.77	0.60	28.22	9.72	119.44	47.48	211.22	45.61	364.59	65.13
BrE1-24.1	0.09	22.38	0.54	1.30	2.30	4.07	0.87	38.01	13.96	169.41	66.85	282.35	59.98	485.35	83.02
BrE1-25.1	0.05	12.09	0.53	1.81	2.79	4.30	0.95	44.59	16.84	208.78	77.47	356.95	73.62	606.42	108.18
BrE1-26.1	0.00	23.19	0.18	1.17	2.20	4.12	0.92	42.59	14.35	173.39	69.43	299.19	62.35	503.74	88.96
BrE1-27.1	0.04	17.36	0.37	1.13	1.82	2.92	0.68	33.83	11.78	133.74	56.11	244.11	52.09	419.99	74.46
BrE1-29.1	0.07	174.04	1.03	3.94	6.22	9.81	0.74	94.93	36.35	420.97	156.79	690.41	150.81	1237.24	195.25
BrE1-30.1	0.30	18.05	1.27	2.63	4.28	6.96	1.41	59.90	23.24	272.31	104.38	451.09	91.74	715.16	123.31
BrE1-31.1	0.04	16.92	0.78	3.43	5.16	7.75	1.67	82.05	26.55	310.89	119.62	508.21	102.49	801.80	135.58
BrE1-32.1	0.02	35.36	0.36	1.68	2.97	5.26	1.06	55.37	19.37	233.60	92.87	396.10	81.22	642.41	109.40
BrE1-33.1	0.02	15.59	0.21	0.66	1.28	2.47	0.45	25.82	9.34	109.03	44.52	200.72	43.86	347.54	61.74
BrE1-34.1	0.01	22.05	0.21	1.11	1.95	3.40	0.77	39.01	13.17	157.63	62.14	275.49	58.22	470.09	81.95
BrE1-35.1	0.14	10.88	0.84	2.05	3.22	5.07	1.32	49.65	16.33	195.21	72.04	312.45	66.06	531.00	90.71
BrE1-36.1	0.03	16.76	0.67	3.27	5.33	8.67	1.73	80.04	27.53	322.75	120.83	514.91	105.34	827.47	139.66
BrE1-37.1	0.04	22.42	0.75	3.37	5.44	8.79	1.89	85.41	27.98	319.44	127.23	503.16	100.88	755.88	134.19
BrE1-38.1	0.02	14.31	0.50	2.84	4.58	7.36	1.47	63.62	21.73	253.06	96.59	413.94	79.94	657.01	113.01
BrE1-39.1	0.01	19.24	0.29	1.73	2.85	4.68	1.09	44.22	16.26	198.09	76.51	332.24	69.80	560.72	95.33
BrE1-40.1	0.51	21.67	1.97	3.88	6.06	9.46	1.85	92.90	30.48	342.29	135.71	557.09	115.26	885.56	151.95
BrE1-41.1	0.01	21.47	0.28	1.23	2.22	3.98	0.85	41.78	13.91	172.73	66.63	291.93	60.81	508.84	89.32
BrE1-42.1	0.56	28.23	1.66	2.85	4.40	6.77	1.38	62.96	21.83	246.98	96.99	412.87	82.74	648.46	114.05
BrE1-43.1	0.05	17.50	0.71	2.81	4.52	7.28	1.65	76.62	25.92	284.69	106.76	445.02	87.76	699.01	121.19
BrE1-44.1	0.04	11.86	0.21	0.47	0.86	1.58	0.38	19.55	7.43	89.05	36.14	166.42	36.87	301.07	54.47
BrE1-45.1	0.04	168.86	0.93	4.58	8.34	15.20	2.36	166.85	57.08	633.62	232.57	983.45	199.15	1542.42	251.13
BrE1-46.1	1.99	22.46	6.77	12.50	16.64	22.16	4.55	129.44	29.52	279.85	100.28	323.02	61.31	448.42	71.37
RnE1201															
RnE1201-13.1	0.06	14.34	0.86	3.16	4.92	7.67	2.49	68.67	26.28	271.47	100.29	406.14	75.90	584.53	96.86
RnE1201-13.2	0.01	6.73	0.16	0.52	0.94	1.70	0.67	19.69	7.40	88.91	33.90	142.00	28.90	228.78	39.39
RnE1201-14.1	0.02	60.01	0.86	5.09	8.68	14.80	5.62	152.47	53.85	559.82	193.10	780.95	141.36	1063.70	168.10
RnE1201-14.2	0.01	8.03	0.15	0.50	0.98	1.94	0.79	21.08	8.20	93.92	35.55	158.78	31.89	258.14	41.90
RnE1201-18.1	0.03	7.87	0.23	0.64	1.23	2.36	0.84	21.84	7.89	94.66	35.87	155.45	31.16	251.93	43.34
RnE1201-19.1	0.05	10.57	0.73	2.87	4.58	7.30	2.39	64.55	25.13	265.51	95.42	393.37	75.59	560.66	90.82
RnE1201-20.1	0.02	44.30	0.61	3.07	4.94	7.97	2.38	78.87	26.61	328.46	119.25	498.54	96.21	710.80	111.53
RnE1201-20.2	0.01	11.65	0.26	1.26	1.95	3.04	1.07	32.65	11.61	127.62	49.87	212.51	41.88	331.83	56.14
RnE1201-22.1	0.02	9.07	0.18	0.55	1.03	1.95	0.70	19.66	8.08	90.91	34.23	152.85	29.48	239.52	41.31
RnE1201-22.2	0.01	8.40	0.16	0.54	1.21	2.73	0.82	23.41	9.09	102.06	38.65	164.18	33.03	270.06	46.22
TuE1301															
TuE1301-18.1	0.02	8.14	0.25	0.81	1.29	2.07	0.76	22.57	8.34	95.60	36.61	157.49	32.22	252.17	43.63
TuE1301-19.1	0.03	58.67	1.00	5.53	9.27	15.56	3.95	157.68	58.24	643.97	233.13	980.21	188.69	1411.59	227.00
TuE1301-20.1	0.02	10.51	0.25	0.95	1.57	2.62	1.09	27.65	10.62	123.97	46.93	201.92	39.85	321.51	53.03
TuE1301-21.1	0.03	15.51	0.95	5.59	9.30	15.46	5.42	139.74	48.22	503.66	172.00	706.45	130.02	976.37	161.14
TuE1301-22.1	0.03	25.90	1.22	8.40	14.36	24.55	8.01	204.17	74.29	776.85	270.10	1102.35	206.52	1508.34	242.48
TuE1301-22.2	0.02	20.25	0.43	2.10	3.52	5.89	1.82	53.78	19.95	223.48	81.61	351.98	69.38	524.95	85.02
TuE1301-24.1	0.01	12.17	0.27	1.65	2.84	4.90	1.40	42.28	15.23	169.22	63.48	270.90	53.42	424.77	73.16
TuE1301-24.2	0.02	32.53	0.49	2.38	4.10	7.06	1.79	73.02	27.96	316.10	115.04	493.62	98.39	767.12	121.91
TuE1301-25.1	0.11	79.93	1.25	4.23	7.00	11.57	2.40	117.43	41.44	462.96	170.93	700.82	133.78	1043.39	163.76
TuE1301-26.1	0.24	189.23	2.61	8.56	14.67	25.14	5.95	262.63	98.97	1080.40	385.87	1586.25	300.18	2299.46	351.89

[1]Calculated using the method of Ferry and Watson (2007) using $a\,SiO_2$=1.0 and $a\,TiO_2$=0.7.

Table F1c. Hafnarfjall-Skarðsheiði *in situ* zircon REE for zircon-normalized plots

Analysis	La	Ce	Pr	Nd	Pm	Sm	Eu	Gd	Tb	Dy	Ho	Er	Tm	Yb	Lu
DrE1302															
DrE1302-4.1	0.03	118.77	0.82	4.11	7.29	12.90	3.19	136.90	54.03	569.02	205.12	824.63	151.45	1096.57	164.61
DrE1302-5.1	0.04	17.49	0.87	4.29	6.38	9.49	2.52	77.52	27.36	289.79	105.05	427.43	80.82	594.24	97.17
DrE1302-6.1	0.04	87.21	0.80	3.43	5.81	9.85	2.57	111.77	43.78	469.36	167.95	687.76	127.92	943.25	140.92
DrE1302-7.1	0.06	51.98	1.49	7.61	12.72	21.26	5.38	193.76	69.47	721.96	258.76	1014.02	189.31	1401.34	210.12
DrE1302-8.1	0.03	45.24	0.98	5.33	9.02	15.28	4.11	161.20	59.13	642.40	237.18	954.50	179.31	1284.72	202.73
DrE1302-8.2	0.10	92.81	1.48	5.70	9.25	15.02	5.42	147.56	49.27	520.24	180.81	725.05	135.40	1005.39	153.82
DrE1302-9.1	0.03	57.01	0.58	2.68	4.51	7.58	1.94	73.07	30.67	336.36	124.01	506.12	96.40	729.96	110.65
DrE1302-10.1	0.02	56.14	0.50	2.57	4.62	8.30	2.29	81.57	31.42	339.75	124.82	494.44	92.64	681.35	106.06
DrE1302-11.1	0.06	31.51	1.18	5.23	8.33	13.27	3.49	127.48	45.86	479.95	181.33	704.91	132.97	959.58	148.83
DrE1302-12.1	1.41	64.76	6.83	15.03	18.42	22.57	4.97	186.32	69.39	713.93	264.98	1029.49	192.22	1395.49	209.35
DrE1302-12.2	0.03	29.55	0.46	1.85	2.88	4.47	1.31	47.22	17.68	200.84	75.19	307.72	58.97	455.17	70.43
DrE1302-13.1	0.06	48.32	1.45	7.04	11.16	17.69	4.37	164.88	59.82	630.62	228.99	905.42	170.29	1246.50	186.37
DrE1302-14.1	0.02	23.78	0.67	4.42	6.76	10.33	2.72	96.68	35.42	387.10	143.59	585.96	110.51	818.33	128.78
DrE1302-15.1	0.04	109.57	0.91	4.22	7.27	12.54	3.34	138.29	51.43	550.50	202.33	805.53	150.06	1082.04	164.94
FlI1201															
FlI1201-21.1	0.02	8.44	0.18	0.56	1.08	2.06	0.60	19.48	7.38	86.75	33.75	139.29	29.23	237.09	41.41
FlI1201-21.2	0.04	14.79	1.03	5.13	8.00	12.48	3.68	119.20	42.27	454.51	164.22	668.33	123.35	955.64	160.17
FlI1201-3	0.03	6.18	0.88	4.49	7.59	12.85	4.30	112.60	34.20	360.10	131.10	508.77	98.12	750.07	127.32
FlI1201-4.1	0.03	6.48	0.21	0.53	0.83	1.30	0.45	12.83	4.90	60.27	22.93	103.34	21.28	174.17	30.95
FlI1201-4.2	0.04	13.17	0.92	4.41	6.81	10.51	2.90	87.09	29.60	326.12	112.42	461.33	89.68	697.78	116.66
FlI1201-6.1	0.02	3.30	0.13	0.31	0.56	1.00	0.31	9.43	3.79	45.66	18.35	85.89	18.36	147.90	27.49
FlI1201-6.2	0.03	11.81	0.94	5.35	8.31	12.90	3.29	93.04	30.43	324.88	114.79	455.13	89.04	673.59	110.05
FlI1201-7.2	0.28	28.22	1.48	3.39	5.02	7.44	1.91	66.79	24.70	272.20	96.74	415.06	80.03	622.64	104.63
FlI1201-7.1	0.01	3.88	0.10	0.34	0.56	0.94	0.35	10.44	4.23	45.60	18.59	81.12	16.80	137.34	24.60
FlI1201-8.2	0.05	119.81	1.16	5.44	9.25	15.72	2.05	140.01	50.03	542.72	196.29	785.49	152.31	1133.78	180.95
FlI1201-8.1	0.01	5.61	0.15	0.52	0.91	1.60	0.52	16.06	5.73	69.08	27.21	114.66	23.33	197.69	34.89
FlI1201-9.2	0.09	65.51	2.21	11.20	17.12	26.15	4.23	226.89	77.09	823.91	290.13	1145.31	212.94	1619.71	258.04
FlI1201-9.1	0.03	9.44	0.18	0.45	0.82	1.50	0.57	17.52	6.05	75.25	27.92	127.45	26.48	218.19	38.05
FlI1201-10.2	0.01	6.77	0.40	2.49	4.26	7.28	2.09	51.90	21.85	231.01	80.60	344.03	67.64	524.56	86.71
FlI1201-10.1	0.06	9.23	0.43	1.15	2.16	4.04	1.02	34.80	12.25	138.41	52.86	236.85	48.62	393.47	64.89
FlI1201-11.1	0.01	7.97	0.43	2.78	4.31	6.68	2.46	54.79	18.13	196.06	67.89	283.58	55.82	424.79	72.32
FlI1201-12.2	0.03	7.19	0.22	0.57	0.94	1.55	0.62	13.58	4.83	64.30	22.51	104.47	22.41	192.90	34.27
FlI1201-12.1	0.02	6.93	0.19	0.60	1.10	2.02	0.73	18.51	7.39	84.15	31.65	137.94	29.02	238.21	42.70
FlI1201-13.1	0.00	7.60	0.12	0.66	1.16	2.04	0.68	23.14	7.76	89.93	33.55	148.53	30.66	241.48	42.87
FlI1201-14.2	0.03	45.35	0.95	5.10	8.58	14.44	3.13	128.67	47.21	526.10	183.43	770.54	146.49	1120.44	183.41
FlI1201-14.1	0.02	7.52	0.22	0.69	0.99	1.44	0.50	16.31	6.84	77.07	28.33	130.22	26.31	222.39	37.66
FlI1201-15.1	0.07	36.19	1.70	8.44	13.73	22.32	4.92	192.47	64.90	693.80	251.77	1002.60	187.72	1381.47	218.75
FlI1201-16.1	0.06	9.01	0.39	0.96	1.60	2.68	0.81	24.38	8.84	99.00	37.60	162.76	33.77	275.04	46.95
FlI1201-17.2	0.52	101.33	3.24	8.06	12.22	18.53	2.82	147.00	57.83	660.16	249.03	982.88	197.71	1469.96	236.73
FlI1201-17.1	0.03	7.39	0.25	0.67	1.13	1.89	0.66	18.79	7.36	85.33	33.14	142.69	30.33	247.93	42.33
FlI1201-18.1	0.01	7.04	0.23	1.13	2.05	3.72	1.24	28.15	10.32	107.94	40.44	167.61	34.52	264.82	47.86
FlI1201-19.1	0.02	13.29	0.29	1.10	1.93	3.38	0.95	30.69	10.85	119.73	46.74	198.30	39.87	320.59	55.60
FlI1201-20.1	0.05	40.15	1.36	7.35	11.32	17.44	4.34	150.87	50.19	551.72	192.87	774.57	147.02	1106.05	179.57
SvE1302															
SvE1302-1.1	0.04	55.08	0.56	2.02	3.68	6.69	1.54	73.16	154.90	327.96	425.75	552.69	675.12	824.68	1007.37
SvE1302-2.1	2.77	15.19	2.47	2.33	2.79	3.34	0.92	29.14	59.02	119.53	156.51	204.92	259.89	329.59	417.99
SvE1302-3.1	0.14	10.58	1.24	3.70	6.37	10.95	3.65	104.70	201.51	387.82	472.67	576.08	688.88	823.76	985.05
SvE1302-4.1	0.04	10.23	0.28	0.74	1.34	2.45	0.66	23.87	49.05	100.82	133.67	177.24	227.98	293.24	377.19
SvE1302-5.1	3.94	16.26	3.79	3.72	4.46	5.34	1.40	43.90	88.59	178.79	223.74	279.98	346.77	429.49	531.94
SvE1302-6.1	0.39	12.53	0.86	1.27	2.06	3.33	1.04	32.34	67.00	138.82	179.59	232.33	291.24	365.08	457.65
SvE1302-7.1	0.78	89.03	6.52	18.83	26.20	36.47	1.17	241.58	448.75	833.59	907.34	987.62	1198.71	1454.93	1765.91
SvE1302-8.1	10.64	402.54	44.68	91.55	104.01	118.17	9.10	650.11	1025.46	1617.52	1692.79	1771.57	2123.08	2544.33	3049.16
SvE1302-9.1	0.23	13.59	1.24	2.90	4.74	7.75	2.21	68.41	132.19	255.43	317.89	395.63	479.63	581.47	704.94
SvE1302-10.1	4.47	242.36	31.97	85.49	109.24	139.59	3.17	661.90	1048.43	1660.68	1618.59	1577.57	1849.25	2167.73	2541.04
SvE1302-11.1	149.93	286.08	66.54	44.33	31.19	21.95	2.28	114.59	228.97	457.53	560.33	686.22	1131.07	1864.31	3072.88
SvE1302-12.1	19.65	46.46	8.30	5.39	4.44	3.65	0.44	20.07	45.99	105.40	160.16	243.37	397.22	648.32	1058.18
SvE1302-13.1	0.07	52.49	0.84	2.88	4.82	8.06	1.62	79.06	162.75	335.03	424.74	538.47	667.09	826.42	1023.80
SvE1302-14.1	0.12	42.68	1.54	5.47	8.97	14.72	4.18	140.75	266.15	503.26	602.75	721.90	881.48	1076.32	1314.24
SvE1302-15.1	0.38	13.87	1.60	3.27	5.25	8.41	2.46	77.45	146.90	278.63	344.79	426.65	511.68	613.66	735.97
ShE1301															
ShE1302-1.1	0.61	362.37	5.61	17.01	25.25	37.48	3.50	269.88	501.29	931.13	1063.69	1215.13	1456.37	1745.50	2092.04
ShE1302-2.1	3.16	332.25	20.11	50.73	63.26	78.90	6.80	450.53	745.60	1233.91	1293.83	1356.65	1578.11	1835.71	2135.37
ShE1302-3.1	0.84	170.69	7.80	23.84	33.25	46.36	5.21	319.55	554.33	961.61	1060.95	1170.56	1328.80	1508.43	1712.34
ShE1302-4.1	0.77	216.13	5.85	16.11	23.35	33.84	3.47	243.15	431.77	766.71	856.84	957.56	1104.37	1273.70	1469.00
ShE1302-5.1	2.02	375.34	17.00	49.33	64.62	84.63	7.31	516.98	886.94	1521.65	1659.62	1810.10	2137.16	2523.31	2979.24
ShE1302-6.1	1.29	144.73	9.09	24.18	31.54	41.16	3.80	242.35	423.03	738.44	754.00	769.90	872.13	987.93	1119.12
ShE1302-7.1	4.33	386.11	27.17	68.10	83.42	102.19	8.29	586.08	935.90	1494.53	1518.32	1542.50	1759.27	2006.52	2288.51
ShE1302-8.1	18.80	413.86	23.45	26.18	33.43	42.67	3.57	287.29	527.47	968.46	1109.96	1272.12	1539.10	1862.10	2252.90
ShE1302-9.1	1.54	284.51	11.92	33.10	43.91	58.24	5.56	356.45	600.88	1012.91	1028.07	1043.47	1178.56	1331.14	1503.47
ShE1302-10.1	1.96	188.11	8.76	18.52	25.32	34.63	3.72	235.49	443.06	833.60	976.43	1143.74	1411.04	1740.80	2147.62

[1]Calculated using the method of Ferry and Watson (2007) using $a\,SiO_2$=1.0 and $a\,TiO_2$=0.7.

Table F1c. Hafnarfjall-Skarðsheiði *in situ* zircon REE for zircon-normalized plots

Analysis	La	Ce	Pr	Nd	Pm	Sm	Eu	Gd	Tb	Dy	Ho	Er	Tm	Yb	Lu
FeE1301															
FeE1301-1.1	185.36	346.49	99.39	72.78	52.18	37.41	6.74	205.82	371.34	669.96	816.04	993.98	1202.55	1454.88	1760.16
FeE1301-2.1	5.06	21.75	3.56	2.98	4.29	6.19	1.80	56.71	108.43	207.33	272.01	356.88	443.74	551.74	686.03
FeE1301-3.1	1.89	34.66	4.18	6.21	7.98	10.26	2.73	105.26	196.52	366.90	487.23	647.02	764.30	902.85	1066.52
FeE1301-4.1	5.86	73.91	6.79	7.30	10.15	14.11	3.05	120.14	222.95	413.75	515.05	641.16	741.85	858.35	993.14
FeE1301-5.1	1.19	30.77	2.61	3.86	6.09	9.60	2.38	90.52	175.52	340.36	429.13	541.06	660.55	806.44	984.55
FeE1301-6.1	0.71	34.54	2.50	4.68	7.58	12.30	3.04	118.16	224.46	426.40	525.80	648.39	795.80	976.73	1198.79
FeE1301-7.1	6.82	68.65	6.70	6.63	8.89	11.90	3.05	104.15	203.40	397.22	505.73	643.88	793.72	978.43	1206.13
FeE1301-8.1	1.48	90.76	2.76	3.76	5.85	9.08	2.26	100.26	198.22	391.90	511.09	666.52	795.22	948.77	1131.96
FeE1301-9.1	0.17	17.56	1.08	2.71	4.19	6.48	2.18	67.95	129.37	246.29	321.87	420.63	530.99	670.30	846.16
FeE1301-10.1	0.10	85.52	1.34	4.78	7.86	12.92	2.94	132.03	262.85	523.28	656.08	822.56	993.81	1200.70	1450.67
FeE1301-11.1	0.30	74.21	2.44	6.94	11.23	18.18	4.20	169.71	337.19	669.95	831.35	1031.64	1234.60	1477.49	1768.16
FeE1301-12.1	0.07	15.71	0.44	1.12	1.74	2.69	0.74	24.88	51.69	107.42	143.10	190.63	246.15	317.85	410.44
Hrl1202															
BURI_2.4	0.80	292.95	7.56	23.28	36.12	56.04	10.05	457.71	828.65	1500.22	525.31	2048.29	2345.90	2686.76	408.51
BURI2.13	21.50	79.27	27.30	30.75	23.14	17.42	3.67	99.17	176.32	313.49	114.83	468.54	558.54	665.83	110.54
BURI2.11	0.43	20.45	1.43	2.61	2.97	3.39	1.01	28.48	56.91	113.69	43.21	189.38	238.15	299.49	51.29
BURI2_MID	4.27	26.09	5.64	6.49	9.02	12.54	3.82	110.38	195.33	345.65	126.25	550.16	648.52	764.45	126.89
BURI_2.3	0.41	16.97	2.12	4.84	7.25	10.87	3.51	96.22	176.32	323.10	117.91	512.38	615.14	738.51	127.65
BURI_2.2_M	0.37	18.28	1.07	1.82	2.72	4.07	1.15	36.38	69.53	132.87	53.78	231.22	285.16	351.68	61.12
BURI_2.2_L	0.10	54.46	2.12	9.81	15.85	25.61	6.60	219.70	395.62	712.38	252.00	1089.92	1279.01	1500.90	243.97
BURI_2.2_R	14.13	37.38	13.62	13.37	13.25	13.13	2.68	72.68	120.24	198.92	64.00	350.09	420.18	504.29	83.00
BURI_3.7_r	3.05	18.22	3.51	3.77	3.96	4.16	1.08	28.20	57.38	116.73	45.92	193.60	241.03	300.08	52.20
BURI_3.7_M	0.13	7.93	0.46	0.86	1.39	2.24	0.65	18.77	37.25	73.93	27.24	132.70	171.91	222.71	38.02
BURI_3.7_L	0.15	14.46	1.09	2.89	4.42	6.75	1.92	56.70	107.53	203.94	74.36	324.34	394.13	478.94	80.41
BURI_3.6_M	0.19	16.84	1.11	2.66	4.21	6.67	2.04	54.71	103.38	195.33	74.78	311.19	378.72	460.90	78.03
BURI_3.6_L	0.38	11.22	1.03	1.71	2.58	3.88	1.27	30.44	57.12	107.21	43.29	175.44	222.14	281.26	48.80
BURI_3.5	21.50	83.87	23.56	24.67	19.11	14.81	3.77	124.81	227.62	415.11	146.43	634.12	761.75	915.06	149.60
BURI_3.3_R	0.03	10.63	0.82	4.02	6.36	10.07	2.92	88.60	160.80	291.82	106.51	450.00	535.53	637.31	105.01
BURI_3.3_L	0.02	12.75	0.33	1.40	2.23	3.56	1.14	34.71	68.72	136.09	52.14	231.47	288.76	360.23	60.86
Mean concentration															
All	3.23	60.15	3.94	7.47	9.83	13.63	2.37	106.72	114.33	377.59	245.55	544.20	337.74	809.61	412.01
Mean conc. Normal La															
	0.05	22.75	0.64	2.32	3.86	6.40	1.58	61.11	31.76	243.99	107.68	385.22	114.83	597.25	131.42

[1]Calculated using the method of Ferry and Watson (2007) using $a\ SiO_2$=1.0 and $a\ TiO_2$=0.7.

Table F2a. Árnes and Hrafnfjörður *in situ* zircon trace element (ppm) concentrations (Atomic number ≤ 41)

Mount	Analysis	Date	TE notes	Li	Be	B	F	Na	Al	P	K	Ca	Sc	48Ti	49Ti	Fe	Y	Nb
ÁrE1301																		
TJB.7	ArE1301-1.1	Jan. 2014		0.78	3.32	0.24	89.85	2156.10	1153.11	279.29	184.44	49.52	37.50	12.44	12.78	4.78	3080	21.65
TJB.7	ArE1301-1.2	Jan. 2014		0.00	1.40	0.07	11.57	2.53	10.43	290.67	1.91	1.02	65.66	13.98	15.21	2.40	1334	13.04
TJB.7	ArE1301-2.1	Jan. 2014		0.01	2.92	0.03	23.95	1.94	11.09	296.15	1.61	1.19	43.61	12.58	12.85	2.52	2727	10.55
TJB.7	ArE1301-3.1	Jan. 2014		0.59	37.19	0.14	96.89	4.13	32.50	326.21	32.93	15.59	30.16	29.74	29.16	3.21	3222	21.57
TJB.7	ArE1301-4.1	Jan. 2014		0.39	155.35	1.57	32.66	2.09	4.01	408.49	1.61	1.12	19.68	6.22	6.53	2.61	3677	23.11
TJB.7	ArE1301-5.1	Jan. 2014		0.05	7.46	0.06	28.87	15.61	6.85	251.32	6.17	2.44	50.43	10.67	11.23	2.60	1535	15.59
TJB.7	ArE1301-6.1	Jan. 2014		4.64	22.75	0.10	69.37	4.16	12.95	276.58	8.71	11.09	45.07	7.07	7.46	2.47	1430	18.01
TJB.7	ArE1301-7.1	Jan. 2014		1.68	1.03	0.03	18.12	1.74	6.76	282.66	1.48	2.53	42.31	11.22	11.83	2.52	2429	9.47
ÁrE1303																		
TJB.6	ArE1303-2.1	Jan. 2014		0.11	3.21	0.14	0.00	3.47	6.59	210.29	5.79	5.43	8.51	15.65	15.50	0.48	731	12.25
TJB.6	ArE1303-3.1	Jan. 2014		0.00	1.43	0.02	3.85	4.60	9.21	380.21	9.42	7.58	12.53	20.61	19.60	1.33	1234	22.72
TJB.6	ArE1303-4.1	Jan. 2014	Same grain! Core	0.12	9.97	0.10	2.42	3.20	5.51	253.26	6.53	5.21	7.19	15.91	16.37	1.22	906	15.33
TJB.6	ArE1303-5.1	Jan. 2014	Same grain! Rim	0.12	14.99	0.07	7.44	3.36	6.67	252.40	6.17	5.25	9.65	10.13	10.71	2.81	975	21.25
TJB.6	ArE1303-6.1	Jan. 2014		0.01	3.15	0.13	2.52	3.65	7.42	287.74	6.43	5.95	8.77	12.21	11.46	0.34	1012	24.03
TJB.6	ArE1303-7.1	Jan. 2014		0.00	38.93	0.91	12.24	3.20	6.21	286.71	6.86	6.10	8.02	14.53	13.57	105.41	2290	13.25
TJB.6	ArE1303-8.1	Jan. 2014		0.02	69.98	0.44	2.42	3.22	5.50	282.44	6.14	4.62	8.95	14.63	14.62	0.25	2316	12.56
TJB.6	ArE1303-9.1	Jan. 2014		0.01	63.63	0.49	4.76	3.27	7.12	247.63	7.57	2.99	9.79	12.91	13.56	0.52	1914	10.40
TJB.6	ArE1303-10.2	Jan. 2014	Spot location matches U-Pb	0.06	11.56	1.04	0.00	3.61	8.94	386.40	7.48	5.53	11.33	10.41	10.32	158.44	2850	23.52
TJB.6	ArE1303-10.1	Jan. 2014	Low-U rim	0.12	1.10	0.54	0.00	30.35	35.41	264.93	96.12	213.91	14.87	11.17	11.56	20.28	873	14.85
TJB.6	ArE1303-11.1	Jan. 2014		0.00	2.18	0.16	2.28	2.46	4.18	133.76	4.58	3.13	4.73	11.95	12.23	0.25	463	10.77
TJB.6	ArE1303-12.1	Jan. 2014		0.00	4.88	0.32	0.00	2.23	4.89	253.37	5.11	4.46	8.63	14.35	13.75	1.13	861	18.54
TJB.6	ArE1303-13.1	Jan. 2014	Spot location matches U-Pb	0.02	76.61	0.11	3.89	2.56	5.47	296.26	5.98	4.47	7.92	15.67	17.69	38.85	2678	16.50
TJB.6	ArE1303-13.2	Jan. 2014	On rim of same grain	0.00	1.84	0.10	2.13	1.88	4.55	230.64	3.66	2.15	13.72	11.58	11.18	2.61	833	13.99
TJB.6	ArE1303-14.1	Jan. 2014		0.00	2.73	0.16	0.00	3.69	7.45	236.20	7.04	6.35	9.08	14.41	14.34	14.78	585	14.26
TJB.6	ArE1303-15.1	Jan. 2014	Very odd! Maybe beam issues?	0.00	1.42	0.24	0.00	3.28	5.10	227.09	5.26	2.68	9.27	15.47	15.65	0.28	795	14.43
ÁrE1304																		
TJB.7	ArE1304-1.1	Jan. 2014		0.39	155.35	1.57	32.66	2.09	4.01	408.49	1.61	1.12	19.68	6.22	6.53	2.61	3677	23.11
TJB.7	ArE1304-2.1	Jan. 2014		0.19	185.42	1.35	38.88	1.96	4.06	393.77	1.90	1.01	17.86	7.00	7.18	2.58	4295	32.64
TJB.7	ArE1304-3.1	Jan. 2014		0.91	411.53	4.19	92.67	2.87	5.06	435.41	1.94	1.30	30.35	6.98	6.97	2.63	6180	46.76
TJB.7	ArE1304-4.1	Jan. 2014		0.28	138.66	1.36	50.69	11.23	4.94	294.76	1.82	1.65	17.35	6.55	6.68	2.53	2698	19.36
TJB.7	ArE1304-5.1	Jan. 2014		0.33	191.58	1.43	36.96	798.37	691.73	528.50	1828.43	57.67	64.66	16.21	17.15	2.67	3772	80.91
TJB.7	ArE1304-6.1	Jan. 2014		0.39	98.60	0.55	13.43	3.50	5.82	182.43	2.64	1.37	45.21	9.71	9.26	2.52	1998	5.87
TJB.7	ArE1304-7.1	Jan. 2014		0.05	100.59	1.14	32.03	3.17	7.22	245.81	3.65	3.95	20.68	5.89	7.34	2.48	1116	15.93
TJB.7	ArE1304-8.1	Jan. 2014		0.19	165.96	2.79	29.53	2.71	4.76	369.67	2.66	1.44	38.59	9.13	9.56	2.39	2607	32.60
TJB.7	ArE1304-9.1	Jan. 2014		0.31	193.03	1.26	17.69	2.32	4.15	237.33	2.42	1.63	43.92	9.77	10.22	2.47	2388	10.68
TJB.7	ArE1304-10.1	Jan. 2014		0.25	167.73	2.24	47.98	2.68	4.71	359.27	2.72	1.05	26.42	5.87	5.55	2.47	2834	19.42
TJB.7	ArE1304-11.1	Jan. 2014		0.08	80.94	0.47	14.22	3.21	8.48	279.32	1.87	1.29	55.21	9.41	9.63	2.60	3055	9.60
TJB.7	ArE1304-12.1	Jan. 2014		2.19	372.66	2.24	57.50	2.56	4.83	388.62	1.87	1.02	32.28	8.51	8.04	2.50	4900	30.51
TJB.7	ArE1304-13.1	Jan. 2014		0.00	21.08	0.10	3.73	3.63	4.35	189.83	2.23	1.35	25.12	6.18	6.55	2.63	834	19.38
TJB.7	ArE1304-14.1	Jan. 2014		0.01	155.73	1.00	56.13	2.40	4.37	326.41	1.98	1.19	24.24	4.91	4.72	2.52	2071	41.11
TJB.7	ArE1304-15.1	Jan. 2014		0.84	253.57	6.93	84.96	112.08	48.75	338.76	72.11	8.86	55.13	13.74	18.14	2.59	4579	29.54
TJB.7	ArE1304-16.1	Jan. 2014		1.47	106.61	0.47	22.75	3.72	4.40	237.43	2.47	1.98	36.47	7.13	6.07	2.33	2666	14.18
TJB.8	ArE1304-1.1	Jan. 2014		0.29	305.93	4.02	24.34	2.30	4.54	1010.85	1.03	2.05	85.49	8.51	8.54	2.42	6037	101.07
TJB.8	ArE1304-2.1	Jan. 2014		1.93	370.20	2.15	25.36	6.05	5.39	619.42	4.10	100.49	100.18	15.17	15.94	2.17	5626	81.36
TJB.8	ArE1304-3.1	Jan. 2014		0.04	143.98	1.14	6.77	2.14	5.34	545.07	0.98	5.08	72.89	15.73	16.56	2.63	3537	72.19
TJB.8	ArE1304-4.1	Jan. 2014		0.11	74.56	1.31	46.36	6.39	7.82	380.18	2.74	4.15	52.32	14.09	14.47	2.52	2334	34.48
TJB.8	ArE1304-5.1	Jan. 2014		3.09	112.84	0.81	18.50	5.14	13.11	592.56	1.93	2.79	58.50	12.18	12.36	2.43	3722	110.36
TJB.8	ArE1304-6.1	Jan. 2014		1.750475	299.32	2.03	16.02	2.63	3.93	684.84	3.74	2.45	81.91	10.33	11.57	2.48	5755	187.43
TJB.8	ArE1304-7.1	Jan. 2014		0.01	19.93	0.23	10.92	26.35	12.72	261.32	2.19	1.60	26.93	6.46	6.93	2.46	1001	16.40

Table F2a. Árnes and Hrafnfjörður *in situ* zircon trace element (ppm) concentrations (Atomic number ≤ 41)

Mount	Analysis	Date	TE notes	Li	Be	B	F	Na	Al	P	K	Ca	Sc	48Ti	49Ti	Fe	Y	Nb
DH-08 and DH-15																		
TJB.9	DH08-1.1	Apr. 2014		0.26	12.84	0.29	2.46	5.59	5.66	153.58	5.92	3.25	6.49	11.78	11.44	1.95	2054	10.12
TJB.9	DH08-3.1	Apr. 2014		0.00	0.03	0.25	2.45	6.70	7.85	129.04	7.51	53.78	5.94	12.94	13.12	0.71	590	9.94
TJB.9	DH08-4.1	Apr. 2014		0.01	1.64	0.07	6.38	31.07	38.33	152.58	66.03	72.14	6.80	11.89	13.66	2.49	1619	6.75
TJB.9	DH08-5.1	Apr. 2014		69.16	242.16	0.84	41.35	35.66	21.10	453.51	32.77	235.35	9.06	15.45	14.34	0.77	2836	82.01
TJB.9	DH08-6.1	Apr. 2014		3.22	9.63	0.13	3.08	3.43	8.58	243.20	5.34	4.89	7.62	14.76	14.53	3.39	1588	31.71
TJB.9	DH08-9.1	Apr. 2014		38.91	78.23	0.34	11.80	11.40	6.97	235.84	12.45	66.40	4.39	11.17	10.70	1.36	3398	25.07
TJB.9	DH15-1.1	Apr. 2014		0.23	35.65	1.24	70.34	53.17	30.63	156.32	30.34	133.23	9.78	12.72	13.63	3.46	2548	15.34
TJB.9	DH15-11.1	Apr. 2014		0.33	34.74	1.05	8.10	76.44	68.89	334.17	28.91	72.21	16.43	20.91	22.88	30.74	2257	42.82
HfE1402																		
TJB.11	HfE1402-1.1	Oct. 2014												18.60	18.94	145.57	7351	
TJB.11	HfE1402-10.1	Oct. 2014												8.91	8.92	14.47	2683	
TJB.11	HfE1402-11.1	Oct. 2014												10.56	10.65	16.58	2266	
TJB.11	HfE1402-2.1	Oct. 2014												1.17	1.10	8.46	4275	
TJB.11	HfE1402-3.1	Oct. 2014												9.11	9.20	104.50	7273	
TJB.11	HfE1402-4.1	Oct. 2014												5.43	5.32	2.26	1148	
TJB.11	HfE1402-5.1	Oct. 2014												11.64	11.58	250.43	10844	
TJB.11	HfE1402-6.1	Oct. 2014												18.58	18.27	53.63	3707	
TJB.11	HfE1402-7.1	Oct. 2014												26.94	26.92	811.68	6986	
TJB.11	HfE1402-8.1	Oct. 2014												12.21	12.11	3.72	1229	
TJB.11	HfE1402-9.1	Oct. 2014												11.51	11.65	32.29	4350	
HfE1403																		
TJB.11	HfE1403-1.1	Oct. 2014												18.50	18.07	57.44	4622	
TJB.11	HfE1403-10.1	Oct. 2014												5.71	5.69	255.61	11116	
TJB.11	HfE1403-11.1	Oct. 2014												7.02	6.93	21.93	3403	
TJB.11	HfE1403-12.1	Oct. 2014												7.14	7.16	4.21	2323	
TJB.11	HfE1403-13.1	Oct. 2014												24.24	24.09	325.72	3046	
TJB.11	HfE1403-14.1	Oct. 2014												4.38	4.18	4.97	2852	
TJB.11	HfE1403-15.1	Oct. 2014												22.18	22.08	181.06	15361	
TJB.11	HfE1403-16.1	Oct. 2014												8.36	8.23	50.34	2926	
TJB.11	HfE1403-17.1	Oct. 2014												7.65	7.50	10.35	2335	
TJB.11	HfE1403-18.1	Oct. 2014												9.09	9.11	31.18	3393	
TJB.11	HfE1403-19.1	Oct. 2014												15.82	15.00	243.45	8150	
TJB.11	HfE1403-2.1	Oct. 2014												7.26	8.03	180.80	9218	
TJB.11	HfE1403-20.1	Oct. 2014												6.63	6.63	58.24	6558	
TJB.11	HfE1403-21.1	Oct. 2014												10.98	10.64	93.58	4714	
TJB.11	HfE1403-22.1	Oct. 2014												55.72	56.87	166.99	8127	
TJB.11	HfE1403-23.1	Oct. 2014												6.41	6.47	231.77	11111	
TJB.11	HfE1403-24.1	Oct. 2014												18.63	18.66	166.22	18967	
TJB.11	HfE1403-3.1	Oct. 2014												5.63	5.76	48.97	2033	
TJB.11	HfE1403-4.1	Oct. 2014												32.81	33.10	138.90	8261	
TJB.11	HfE1403-5.1	Oct. 2014												9.31	9.34	186.89	9234	
TJB.11	HfE1403-6.1	Oct. 2014												36.69	37.32	257.51	13844	
TJB.11	HfE1403-7.1	Oct. 2014												4.89	4.90	314.35	18395	
TJB.11	HfE1403-8.1	Oct. 2014												5.40	5.39	45.84	3761	
TJB.11	HfE1403-9.1	Oct. 2014												66.82	66.34	173.89	15478	

Table F2b. Árnes and Hrafnfjörður *in situ* zircon trace element (ppm) concentrations (Atomic number > 41)

Analysis	La	Ce	Nd	Sm	Eu	Gd	Tb	Dy	Ho	Er	Tm	Yb	Lu	Hf	Pb	Th	U	Eu/Eu*	T (°C)[1]
ÁrE1301																			
ArE1301-1.1	5.33	24.18	4.22	9.60	2.41	89.89	18.58	211	120	264	62	421	71	4194	0	49	74	0.25	803
ArE1301-1.2	0.02	8.52	0.93	3.33	0.95	30.43	11.77	129	53	232	50	420	74	9121	0	36	103	0.29	815
ArE1301-2.1	0.04	7.83	2.96	8.84	2.72	89.51	30.11	319	118	469	94	732	123	8293	0	71	113	0.29	804
ArE1301-3.1	0.30	19.27	4.18	10.77	2.35	104.78	31.46	346	143	517	101	737	129	8143	0	135	189	0.21	903
ArE1301-4.1	0.02	21.59	3.59	9.18	2.47	97.86	33.02	381	145	588	115	867	147	9651	0	104	166	0.25	735
ArE1301-5.1	0.02	8.17	1.20	3.53	0.98	34.26	12.63	142	57	241	49	393	68	9070	0	50	95	0.27	787
ArE1301-6.1	1.74	15.60	4.40	6.39	1.25	44.81	15.18	163	63	242	50	386	68	8995	0	92	120	0.22	747
ArE1301-7.1	0.04	7.23	2.72	8.05	2.26	62.68	22.76	244	91	363	72	568	98	7422	0	57	92	0.31	792
ÁrE1303																			
ArE1303-2.1	0.02	8.81	0.63	1.79	0.64	20.59	7.34	83	31	131	26	203	34	9211	0	8	19	0.32	828
ArE1303-3.1	0.02	15.97	1.06	3.15	0.92	29.65	11.97	134	48	216	42	346	57	14273	0	24	78	0.29	859
ArE1303-4.1	0.03	10.82	0.86	2.81	0.81	23.24	9.31	104	37	162	32	247	42	8718	0	31	51	0.30	829
ArE1303-5.1	0.02	14.13	0.95	2.44	0.46	25.02	9.11	103	38	175	35	287	48	10688	0	33	79	0.18	782
ArE1303-6.1	0.03	14.70	1.03	2.70	0.55	26.51	9.67	110	41	175	36	271	47	10235	0	40	80	0.20	801
ArE1303-7.1	0.08	12.62	4.79	7.92	2.42	77.20	25.98	268	95	380	73	530	84	8679	0	46	75	0.30	819
ArE1303-8.1	0.05	11.50	4.41	8.40	2.51	75.37	25.62	270	97	390	74	556	88	9270	0	58	88	0.30	820
ArE1303-9.1	0.04	10.93	4.34	8.19	2.14	64.67	21.15	217	78	308	58	425	71	8988	0	38	60	0.28	807
ArE1303-10.2	0.03	19.61	4.04	9.60	2.02	87.43	33.16	343	123	511	100	767	121	10017	0	101	146	0.21	785
ArE1303-10.1	0.03	13.28	0.53	1.97	0.42	20.15	8.29	93	33	159	31	268	44	10475	0	40	81	0.21	792
ArE1303-11.1	0.02	7.66	0.37	1.14	0.32	10.92	4.04	48	19	84	17	129	22	9242	0	11	25	0.27	799
ArE1303-12.1	0.03	11.65	0.70	2.47	0.61	22.26	8.84	99	36	152	32	251	41	9441	0	35	57	0.25	818
ArE1303-13.1	0.04	13.66	4.82	11.47	3.35	103.63	34.19	348	124	485	91	649	99	7783	0	66	93	0.30	828
ArE1303-13.2	0.01	11.25	0.65	1.99	0.42	19.80	7.29	88	34	151	32	262	44	10848	0	31	72	0.20	796
ArE1303-14.1	0.02	10.14	0.72	2.31	0.61	21.97	8.38	94	36	153	32	261	42	10178	0	23	52	0.26	819
ArE1303-15.1	0.03	9.74	0.79	2.59	0.72	20.05	7.84	24	34	47	10	85	15	3996	0	10	22	0.30	826
ÁrE1304																			
ArE1304-1.1	0.02	21.59	3.59	9.18	2.47	97.86	33.02	381	145	588	115	867	147	9651	0	104	166	0.25	735
ArE1304-2.1	0.06	34.24	6.05	16.02	4.71	165.60	56.09	592	218	870	169	1238	206	8775	0	207	266	0.28	746
ArE1304-3.1	0.08	52.22	7.71	21.72	5.47	218.90	72.27	768	280	1107	210	1547	253	8944	1	279	336	0.24	746
ArE1304-4.1	0.17	25.01	2.68	8.20	1.46	84.36	33.72	365	136	558	112	840	138	10150	0	139	209	0.17	740
ArE1304-5.1	11.77	366.69	13.92	14.45	3.09	116.91	41.13	446	165	654	126	953	159	9021	0	266	321	0.23	831
ArE1304-6.1	0.03	6.50	2.97	7.97	2.82	71.37	23.30	250	89	365	77	579	100	8099	0	41	72	0.36	778
ArE1304-7.1	1.92	42.80	2.50	3.00	0.60	24.95	7.38	88	36	145	30	243	41	9649	0	21	46	0.21	730
ArE1304-8.1	0.02	24.82	2.10	6.41	1.90	75.01	26.66	306	112	474	93	728	126	9170	0	130	191	0.26	771
ArE1304-9.1	0.02	15.28	3.48	9.79	2.61	99.67	35.11	384	138	585	117	922	154	9219	0	134	203	0.25	778
ArE1304-10.1	0.03	17.06	2.69	7.56	1.79	78.98	27.66	315	121	497	99	759	127	9990	0	86	145	0.22	730
ArE1304-11.1	0.03	7.67	3.94	11.70	4.57	110.57	37.19	393	139	552	108	836	142	8077	0	69	106	0.39	775
ArE1304-12.1	0.05	27.05	5.61	16.55	4.67	157.03	53.08	555	207	816	159	1213	197	8617	0	161	230	0.28	765
ArE1304-13.1	0.01	7.81	0.35	1.48	0.32	16.78	6.04	75	32	134	29	235	42	10625	0	22	56	0.20	734
ArE1304-14.1	0.06	26.11	1.54	4.06	0.74	48.06	16.56	197	80	343	69	549	95	10558	0	69	149	0.16	714
ArE1304-15.1	0.49	28.46	6.91	19.00	4.94	163.25	55.17	581	211	830	164	1239	201	8535	0	187	221	0.27	813
ArE1304-16.1	0.06	14.46	3.70	9.95	2.62	87.49	28.84	305	117	471	93	715	123	8546	0	81	128	0.27	748
ArE1304-1.1	0.12	110.96	5.35	16.83	3.44	170.20	55.70	644	256	997	198	1478	250	8581	1	409	484	0.20	765
ArE1304-2.1	1.09	61.45	8.08	22.76	5.97	218.09	64.38	679	260	941	190	1343	223	7992	1	585	445	0.26	824
ArE1304-3.1	0.10	48.22	3.09	10.17	2.81	113.38	37.71	420	154	608	123	907	153	9189	1	606	455	0.25	828
ArE1304-4.1	0.08	29.53	1.79	6.33	1.73	70.41	24.03	266	101	410	80	614	105	8902	0	323	294	0.25	816
ArE1304-5.1	0.03	64.89	4.06	14.68	3.68	146.55	48.45	516	186	728	139	1043	175	8276	1	863	631	0.24	801
ArE1304-6.1	0.04	120.43	4.98	16.68	4.23	176.31	60.76	688	252	1004	195	1442	240	8717	1	443	521	0.24	784
ArE1304-7.1	0.08	12.57	0.78	1.90	0.53	22.02	7.67	97	39	175	38	304	55	9848	0	38	87	0.25	738

[1]Calculated using the method of Ferry and Watson (2007) using *a* SiO_2=1.0 and *a* TiO_2=0.7.

Table F2b. Árnes and Hrafnfjörður *in situ* zircon trace element (ppm) concentrations (Atomic number > 41)

Analysis	La	Ce	Nd	Sm	Eu	Gd	Tb	Dy	Ho	Er	Tm	Yb	Lu	Hf	Pb	Th	U	Eu/Eu*	T (°C)[1]
DH-08 and DH-15																			
DH08-1.1	0.04	8.22	3.62	6.85	2.83	70.28	24.17	245	87	348	65	494	75	7770	0	46	71	0.39	797
DH08-3.1	0.02	5.58	0.44	1.68	0.61	16.71	5.95	68	24	108	22	177	27	7213	0	12	32	0.35	807
DH08-4.1	0.05	7.11	3.91	6.22	2.48	56.79	21.17	214	74	299	57	419	70	8518	0	28	1	0.40	798
DH08-5.1	0.07	50.40	3.03	8.95	2.86	77.66	23.75	258	96	355	67	471	72	6876	0	190	193	0.33	826
DH08-6.1	0.06	1.46	1.86	5.08	1.99	49.45	15.60	180	73	274	52	385	61	7480	0	56	88	0.38	821
DH08-9.1	0.03	15.56	5.81	13.74	4.49	119.87	39.32	407	141	549	99	733	115	7529	0	91	128	0.34	792
DH15-1.1	0.09	13.39	5.50	12.62	4.75	103.52	31.96	330	125	454	85	620	98	7048	0	75	104	0.40	805
DH15-11.1	0.18	30.15	4.00	8.75	2.75	71.60	23.24	239	93	340	62	463	75	8304	1	183	163	0.34	860
HfE1402																			
HfE1402-1.1	0.14	25.87	7.63	24.59	6.02	227.99		786		1143		1627		9007		161	206	0.24	847
HfE1402-10.1	0.05	3.00	2.75	9.00	3.27	81.51		289		461		733		7470		29	55	0	769
HfE1402-11.1	0.37	22.74	2.25	7.10	1.91	74.13		259		386		584		8308		176	153	0.25	786
HfE1402-2.1	0.02	12.62	0.74	4.19	1.42	65.95		377		747		1267		10539		140	409	0.26	602
HfE1402-3.1	0.07	57.18	5.38	20.14	5.18	211.70		762		1131		1645		9282		339	393	0.24	771
HfE1402-4.1	0.45	7.29	1.18	3.06	0.93	30.97		123		206		330		7431		55	66	0.29	723
HfE1402-5.1	0.11	38.35	8.12	28.12	7.23	284.28		1060		1605		2311		9579		255	368	0.25	796
HfE1402-6.1	3.60	19.08	4.35	10.99	2.68	102.96		387		622		931		7058		86	150	0.24	847
HfE1402-7.1	1.20	42.63	6.53	21.12	5.63	205.66		719		1061		1506		7603		352	388	0.26	890
HfE1402-8.1	0.02	1.90	0.60	1.84	0.79	20.15		109		232		423		6956		10	35	0.40	801
HfE1402-9.1	0.82	51.48	3.78	14.61	3.54	147.09		496		717		1025		8821		374	315	0.23	795
HfE1403																			
HfE1403-1.1	1.87	17.23	2.45	4.65	1.14	59.59		343		724		1299		10440		195	577	0.21	846
HfE1403-10.1	0.08	82.70	7.98	28.03	6.48	274.37		1037		1613		2358		8934		807	824	0.23	727
HfE1403-11.1	0.37	44.42	1.68	6.69	2.13	77.46		324		567		948		10296		701	722	0.29	746
HfE1403-12.1	0.18	14.57	1.17	4.18	1.36	50.43		229		400		643		9358		109	171	0.29	748
HfE1403-13.1	2.00	17.27	2.49	5.83	1.47	61.57		275		492		804		7237		138	248	0	878
HfE1403-14.1	0.27	22.86	1.60	5.16	1.51	63.11		275		479		764		9816		188	271	0.26	704
HfE1403-15.1	0.30	16.60	1.04	6.97	2.02	147.68		994		2190		3737		13183		500	1559	0.19	867
HfE1403-16.1	0.12	17.44	0.95	4.38	1.21	55.08		272		511		868		10282		182	377	0.24	763
HfE1403-17.1	0.64	15.82	0.93	3.73	1.12	47.38		224		405		668		9188		91	200	0.26	754
HfE1403-18.1	1.09	35.10	2.75	6.51	1.62	67.40		302		555		973		9476		243	386	0.24	771
HfE1403-19.1	2.45	26.92	1.89	7.32	2.05	103.78		607		1288		2249		13443		321	888	0.23	829
HfE1403-2.1	0.22	44.37	2.53	10.82	2.76	143.70		717		1314		2221		11185		727	1290	0.21	749
HfE1403-20.1	0.13	59.58	2.42	11.23	2.59	138.12		616		1076		1755		12419		735	933	0.20	741
HfE1403-21.1	0.58	36.08	2.65	9.51	2.42	102.34		446		657		1095		10547		354	460	0.24	790
HfE1403-22.1	0.24	20.22	1.02	6.32	2.19	113.13		697		1367		2435		11612		367	762	0.25	987
HfE1403-23.1	0.60	31.21	1.71	8.82	2.28	143.04		885		1754		3067		14260		528	1344	0.20	738
HfE1403-24.1	0.51	18.64	1.22	8.17	2.40	170.76		1210		2638		4578		15929		528	1707	0.20	847
HfE1403-3.1	0.21	7.39	1.83	4.83	1.44	49.72		204		352		565		9491		41	84	0.28	726
HfE1403-4.1	25.47	85.01	24.76	22.13	3.36	145.94		582		1096		1839		10494		151	563	0.18	915
HfE1403-5.1	0.19	120.01	10.21	31.52	3.76	295.66		977		1415		1925		9019		558	489	0.12	773
HfE1403-6.1	0.30	25.77	0.97	7.20	2.38	143.61		939		1963		3368		12494		711	1842	0.23	930
HfE1403-7.1	0.06	101.40	6.09	26.20	3.96	319.03		1419		2463		3857		8474		1611	1542	0.13	713
HfE1403-8.1	2.09	34.68	3.87	8.41	2.16	80.81		325		590		1037		7824		297	489	0.25	722
HfE1403-9.1	0.87	16.72	1.05	6.75	2.00	143.56		996		2189		3789		13418		445	1454	0.20	1013

[1]Calculated using the method of Ferry and Watson (2007) using *a* SiO_2=1.0 and *a* TiO_2=0.7.

Table F3a. Króksfjörður *in situ* zircon trace element (ppm) concentrations (Atomic number ≤ 41)

Mount	Analysis	Date	TE notes	Li	Be	B	F	Na	Al	P	K	Ca	Sc	48Ti	49Ti	Fe	Y	Nb
IEKBr-1																		
TJB.8	IEKBr-1.1	Apr. 2014		0.02	4.36	0.33	788.70	170.19	179.47	420.00	901.15	15.29	31.48	73.19	74.86	2.50	5359	186.42
TJB.8	IEKBr-2.1	Apr. 2014		0.00	0.01	0.08	19.23	4.10	5.88	368.88	3.25	5.20	29.76	31.84	35.18	2.57	778	7.15
TJB.8	IEKBr-3.1	Apr. 2014		0.00	0.40	0.00	16.38	8.82	4.43	364.57	3.36	7.40	26.66	31.84	36.28	2.56	1847	7.52
TJB.7	IEKBr-1	Apr. 2014		0.00	0.01	0.01	13.18	2.57	5.07	452.04	1.73	1.96	33.68	35.84	38.73	2.40	960	8.65
TJB.7	IEKBr-2.1	Apr. 2014		0.02	3.25	0.13	89.44	162.81	143.03	744.00	93.50	32.25	18.91	31.34	33.47	2.50	3124	18.47
TJB.7	IEKBr-3.1	Apr. 2014		0.00	0.62	0.03	40.95	1.28	4.87	407.93	1.01	0.52	32.65	34.10	34.42	2.53	1225	6.78
TJB.7	IEKBr-4.1	Apr. 2014		0.00	1.31	0.04	46.75	2.42	4.56	368.56	1.55	1.13	27.80	32.65	34.58	2.51	1807	6.56
TJB.7	IEKBr-5.1	Apr. 2014		1.89	1.26	0.02	73.36	71.55	1024.72	275.78	282.30	398.63	24.03	81.04	110.95	12.92	997	7.20
TJB.7	IEKBr-6.1	Apr. 2014		0.00	2.11	0.06	42.28	2.30	4.40	397.87	1.37	0.68	28.38	32.66	34.59	2.54	1913	7.51
IEKTr-1																		
TJB.8	IEKTr-1.1	Apr. 2014		0.04	0.02	0.01	6.26	6.54	5.45	208.91	2.86	6.05	13.77	9.36	11.33	2.40	894	21.45
TJB.8	IEKTr-2.1	Apr. 2014		0.00	0.00	0.02	13.37	2.56	4.97	239.77	2.96	2.96	21.25	13.03	15.00	2.46	652	7.97
TJB.8	IEKTr-3.1	Apr. 2014		0.16	0.73	0.07	151.52	7.80	10.45	567.87	14.39	5.02	47.24	12.43	13.10	2.62	4351	137.60
TJB.8	IEKTr1-4.1	Apr. 2014		0.00	0.45	0.03	32.03	5.28	5.47	423.11	13.90	5.50	39.81	15.28	17.57	2.50	2337	44.38
TJB.7	IEKTr-1.1	Apr. 2014		0.03	0.12	0.04	43.17	10.20	7.44	208.03	5.67	2.35	17.29	13.58	13.69	2.49	2310	18.43
TJB.7	IEKTr-10.1	Apr. 2014		0.05	0.97	0.12	127.92	3.99	23.27	821.15	7.33	10.14	23.98	9.60	9.87	3.13	6862	99.51
TJB.7	IEKTr-2.1	Apr. 2014		0.00	0.09	0.00	23.21	2.68	4.13	183.60	2.19	1.20	17.21	12.17	12.19	2.54	1441	9.25
TJB.7	IEKTr-3.1	Apr. 2014		0.00	0.18	0.06	22.09	2.46	4.35	186.15	1.41	1.59	22.32	12.79	12.98	2.51	1339	6.25
TJB.7	IEKTr-4.1	Apr. 2014		0.00	0.31	0.09	134.02	6.44	10.15	261.80	24.27	38.78	22.99	13.36	13.18	2.51	1423	5.32
TJB.7	IEKTr-5.1	Apr. 2014		5.05	0.18	0.08	101.95	494.60	371.51	356.79	1520.30	46.57	13.61	25.82	24.23	2.58	2186	55.36
TJB.7	IEKTr-6.1	Apr. 2014		0.01	0.16	0.04	34.11	3.44	6.43	381.46	3.65	5.36	25.72	12.80	12.86	2.39	3450	21.72
TJB.7	IEKTr-7.1	Apr. 2014		0.01	0.00	0.09	22.14	2.90	5.55	201.15	2.05	3.29	19.98	16.22	20.26	2.52	603	8.83
TJB.7	IEKTr-8.1	Apr. 2014		0.02	0.55	0.09	24.57	5.16	6.46	271.60	3.27	2.34	24.44	12.22	12.97	2.66	1343	18.44
TJB.7	IEKTr-9.1	Apr. 2014		4.11	1.11	0.18	467.82	35.66	97.50	1464.61	23.44	5063.16	24.25	37.66	41.76	91.04	1065	11.03
IEKGd-1																		
TJB.11	IEKGd1-1.1	Oct. 2014												12.19	12.22	19.51	3922	
TJB.11	IEKGd1-10.1	Oct. 2014												10.11	9.99	137.50	606	
TJB.11	IEKGd1-11.1	Oct. 2014												10.55	10.69	7.30	635	
TJB.11	IEKGd1-2.1	Oct. 2014												5.49	5.68	3.89	1821	
TJB.11	IEKGd1-3.1	Oct. 2014												8.92	8.97	0.53	1526	
TJB.11	IEKGd1-4.1	Oct. 2014												10.68	10.55	0.07	493	
TJB.11	IEKGd1-5.1	Oct. 2014												4.24	4.26	4.73	1722	
TJB.11	IEKGd1-6.1	Oct. 2014												7.47	7.51	23.36	780	
TJB.11	IEKGd1-7.1	Oct. 2014												9.99	9.79	9.17	1305	
TJB.11	IEKGd1-8.1	Oct. 2014												11.83	11.86	0.62	621	
TJB.11	IEKGd1-9.1	Oct. 2014												12.66	12.80	0.07	1693	
IIKK-1 (from Carley, 2014)																		
jw529	IIKKU-1.1C	Aug. 2011		0.00	0.30	0.04	10.64	1.24	9.23	505.35	0.94	1.22	42.08	13.62	14.57	0.34	1737	6.58
jw529	IIKKU-1.2	Aug. 2011		0.01	0.36	0.02	6.90	1.90	14.75	482.48	1.08	1.42	51.74	15.69	16.14	2.42	1052	8.95
jw529	IIKKU-1.3E	Aug. 2011		0.00	0.02	0.03	9.93	1.17	8.24	477.73	0.86	1.00	79.83	14.50	15.47	0.29	1527	11.89
jw529	IIKKU-2.1E	Aug. 2011		0.00	1.81	0.04	9.42	1.04	9.03	157.83	1.02	1.19	24.89	3.33	3.34	0.28	575	1.76
jw529	IIKKU-2.2I	Aug. 2011		0.00	1.13	0.05	7.29	2.01	9.12	145.65	1.07	1.93	29.96	4.31	4.52	0.29	690	1.22
jw529	IIKKU-3.1E	Aug. 2011		0.00	7.21	0.06	7.39	1.97	14.72	196.48	1.31	1.83	36.89	5.49	5.60	0.22	1125	2.10
jw529	IIKKU-3.2I	Aug. 2011		0.00	0.16	0.04	7.13	2.04	28.15	141.96	1.39	1.92	23.59	8.54	8.54	3.57	433	1.23
jw529	IIKKU-4.1	Aug. 2011		0.00	3.67	0.02	7.88	1.93	9.90	164.75	1.41	1.80	30.84	7.33	7.12	0.34	687	1.92
jw529	IIKKU-4.2E	Aug. 2011		0.00	1.55	0.04	5.76	2.15	10.26	245.19	2.03	2.08	37.19	5.51	5.90	0.30	626	3.77

Table F3a. Króksfjörður *in situ* zircon trace element (ppm) concentrations (Atomic number ≤ 41)

Mount	Analysis	Date	TE notes	Li	Be	B	F	Na	Al	P	K	Ca	Sc	48Ti	49Ti	Fe	Y	Nb
IEKVl-1																		
TJB.9	IEKVl1-1.1	Apr. 2014		2.69	51.72	0.70	125.46	14.56	11.03	287.77	9.24	40.64	65.03	10.20	9.82	2.93	1422	2.74
TJB.9	IEKVl1-10.1	Apr. 2014		12.97	76.27	1.02	18.06	45.91	27.12	349.01	39.73	70.04	50.28	6.47	5.86	3.92	1994	5.92
TJB.9	IEKV1l-11.1	Apr. 2014		0.75	0.84	0.26	5.27	11.24	9.10	269.35	8.30	37.57	30.68	8.67	8.65	1.50	617	1.60
TJB.9	IEKVl1-12.1	Apr. 2014		0.20	35.26	0.20	11.11	11.39	8.48	336.97	8.19	7.09	23.47	13.59	13.55	33.34	1938	4.66
TJB.9	IEKVl1-14	Apr. 2014		0.04	8.07	0.75	5.38	11.31	7.16	332.15	14.57	35.10	24.33	20.55	21.72	13.46	807	5.58
TJB.9	IEKVl1-16.1	Apr. 2014		6.88	154.30	0.45	7.51	42.49	115.09	598.86	432.56	35.42	167.85	11.47	10.50	30.69	4439	12.97
TJB.9	IEKVl1-17.1	Apr. 2014		15.27	9.54	0.55	15.03	29.14	47.15	294.86	478.13	52.15	65.06	8.27	8.77	123.33	1332	3.07
TJB.9	IEKVl1-18	Apr. 2014		3.17	83.62	0.29	5.30	12.00	5.40	362.92	9.45	28.18	61.09	10.25	10.68	2.60	1974	7.98
TJB.9	IEKVl1-19.1	Apr. 2014		0.08	10.15	0.39	12.60	21.86	53.44	318.92	322.97	48.04	41.40	3.67	3.20	42.27	988	6.10
TJB.9	IEKVl1-20	Apr. 2014		1.94	36.98	1.53	29.44	26.78	20.95	199.17	27.17	103.69	24.03	7.70	8.49	1.49	1092	1.95
TJB.9	IEKVl1-21	Apr. 2014		9.55	2.51	0.27	0.00	818.05	283.93	283.55	481.13	34.74	63.00	10.05	9.75	5.47	497	2.64
TJB.9	IEKVl1-3	Apr. 2014		7.87	190.37	2.58	389.98	21.26	24.89	863.36	17.71	27.14	104.10	5.52	5.33	45.41	5329	27.16
TJB.9	IEKVl1-5.1	Apr. 2014		6.87	84.47	0.31	40.15	13.25	8.50	699.34	11.06	29.20	47.06	2.40	2.54	14.08	2796	20.79
TJB.9	IEKVl1-7.1	Apr. 2014		23.15	4.18	1.75	28.85	15.47	25.02	607.23	11.07	38.86	202.35	13.68	13.25	98.43	3519	8.75
TJB.9	IEKVl1-8	Apr. 2014		2.32	0.53	0.84	21.10	38.36	43.97	221.76	95.82	182.94	17.58	7.02	6.49	58.35	683	2.59

Table F3b. Króksfjörður *in situ* zircon trace element (ppm) concentrations (Atomic number > 41)

Analysis	La	Ce	Nd	Sm	Eu	Gd	Tb	Dy	Ho	Er	Tm	Yb	Lu	Hf	Pb	Th	U	Eu/Eu*	T (°C)[1]
IEKBr-1																			
IEKBr-1.1	0.64	218.66	11.67	22.91	1.25	145.79	42.60	453	182	629	128	930	150	8721	1	601	345	0.07	1027
IEKBr-2.1	0.01	8.30	0.76	2.21	0.85	21.27	7.06	83	33	141	30	254	45	8285	0	22	39	0.38	911
IEKBr-3.1	0.05	10.20	3.53	8.48	2.44	62.06	20.11	215	79	321	67	515	89	8315	0	62	64	0.32	911
IEKBr-1	0.12	8.47	1.24	2.83	0.97	24.91	9.01	102	40	176	39	332	62	7902	0	26	56	0.35	926
IEKBr-2.1	0.40	14.76	4.34	9.87	2.80	93.57	27.94	300	116	468	91	698	118	6191	0	80	93	0.28	909
IEKBr-3.1	0.03	9.27	1.91	4.14	1.30	33.72	10.53	135	50	210	41	337	59	8137	0	31	48	0.33	920
IEKBr-4.1	0.06	10.13	3.65	7.18	2.34	57.04	18.85	200	76	306	62	480	85	8085	0	47	59	0.35	914
IEKBr-5.1	1.01	13.50	2.34	4.31	1.33	33.83	11.09	116	43	182	39	294	51	8437	0	21	34	0.34	1043
IEKBr-6.1	0.05	10.66	3.81	6.77	2.35	62.21	20.94	219	80	335	65	508	89	8412	0	49	63	0.35	914
IEKTr-1																			
IEKTr-1.1	0.01	12.41	0.66	2.09	0.56	23.69	8.13	99	39	166	35	269	49	9448	0	65	110	0.24	774
IEKTr-2.1	0.08	7.05	0.48	1.81	0.57	16.30	5.82	68	28	122	26	210	39	8799	0	24	48	0.32	808
IEKTr-3.1	0.30	241.66	8.82	16.54	2.04	127.64	43.06	431	140	597	131	1058	183	9507	1	526	349	0.14	803
IEKTr1-4.1	0.06	30.59	2.32	6.09	1.65	60.60	19.38	224	95	385	79	615	114	8329	0	137	167	0.26	825
IEKTr-1.1	0.11	11.76	3.29	8.13	2.54	73.65	27.35	299	108	452	88	681	119	8662	0	74	110	0.32	812
IEKTr-10.1	0.81	82.83	11.15	27.76	4.36	246.58	75.78	805	323	1141	219	1587	259	8782	0	396	392	0.16	776
IEKTr-2.1	0.03	8.08	1.92	5.61	1.34	50.47	17.66	200	78	317	63	499	85	9546	0	54	93	0.24	801
IEKTr-3.1	0.18	6.84	1.93	4.94	1.36	41.27	13.85	159	59	246	49	404	70	8650	0	33	56	0.29	806
IEKTr-4.1	0.52	8.30	2.51	5.93	1.53	48.60	16.78	179	65	269	55	429	74	8772	0	39	65	0.27	810
IEKTr-5.1	1.39	38.48	2.61	6.69	1.10	66.49	21.35	242	98	387	78	644	90	8997	1	114	200	0.16	885
IEKTr-6.1	0.17	16.77	4.52	12.40	3.33	106.79	37.20	390	142	598	119	917	157	7937	0	131	175	0.28	806
IEKTr-7.1	0.30	6.26	0.58	1.25	0.42	13.72	5.11	62	25	109	24	201	38	9041	0	15	35	0.31	831
IEKTr-8.1	0.52	11.39	1.38	3.95	1.02	33.80	11.66	135	56	223	47	364	64	6768	0	57	86	0.27	801
IEKTr-9.1	108.15	297.58	71.06	22.19	2.68	50.08	12.20	119	48	175	35	270	49	7203	0	30	55	0.25	933
IEKGd-1																			
IEKGd1-1.1	0.24	15.93	5.29	14.77	3.44	131.26		463		672		995		8262		171	218	0.24	839
IEKGd1-10.1	0.04	16.18	0.68	1.92	0.27	16.45		63		109		181		7454		81	177	0.15	819
IEKGd1-11.1	0.11	4.27	0.56	1.65	0.52	15.72		66		113		195		7984		24	54	0.31	823
IEKGd1-2.1	0.07	16.05	1.93	5.64	1.32	56.54		218		343		538		9618		111	146	0.23	757
IEKGd1-3.1	0.04	9.88	1.54	3.91	1.03	37.85		157		275		452		8509		81	150	0.26	805
IEKGd1-4.1	0.01	3.55	0.27	1.06	0.34	11.24		49		90		156		8619		15	41	0.30	825
IEKGd1-5.1	10.02	29.59	6.87	6.31	1.13	47.48		179		296		474		9786		95	174	0.20	732
IEKGd1-6.1	0.03	25.75	0.80	2.18	0.33	19.04		77		138		240		9036		188	265	0.16	787
IEKGd1-7.1	1.03	10.59	2.85	4.91	1.77	41.11		147		228		345		7802		33	54	0.38	817
IEKGd1-8.1	0.02	3.28	0.49	1.60	0.51	13.99		62		111		197		7956		15	43	0.33	836
IEKGd1-9.1	0.04	6.54	2.46	6.62	1.95	55.46		191		284		430		8019		58	87	0.31	843
IIKK-1 (from Carley, 2014)																			
IIKKU-1.1C	0.02	31.72	2.12	5.34	1.67	46.34	15.65	175	67	285	59	469	85	9792	0	37	54	0.32	805
IIKKU-1.2	0.01	22.09	0.70	2.25	0.72	21.73	8.12	98	41	189	41	355	68	10049	0	20	46	0.31	815
IIKKU-1.3E	0.01	23.92	1.14	2.84	1.05	27.52	10.88	134	58	280	63	547	109	8863	0	52	131	0.36	811
IIKKU-2.1E	0.01	15.06	0.35	1.03	0.39	10.07	3.73	48	21	102	25	229	48	13227	0	80	176	0.37	676
IIKKU-2.2I	0.02	12.91	0.79	1.87	0.95	16.13	5.31	61	25	119	27	253	52	11387	0	116	199	0.53	700
IIKKU-3.1E	0.05	26.79	3.16	3.83	2.11	27.07	9.16	97	39	195	47	445	93	10699	0	308	426	0.63	718
IIKKU-3.2I	0.31	10.17	1.20	1.34	0.84	7.86	2.41	29	13	63	16	156	35	8252	0	44	80	0.78	755
IIKKU-4.1	0.01	8.61	0.48	1.43	0.55	13.35	4.81	58	24	112	25	216	40	10260	0	27	62	0.38	738
IIKKU-4.2E	0.01	10.42	0.31	0.88	0.38	10.06	4.28	54	24	120	27	253	53	10899	0	37	96	0.39	722

[1]Calculated using the method of Ferry and Watson (2007) using $a\ SiO_2$=1.0 and $a\ TiO_2$=0.7.

Table F3b. Króksfjörður *in situ* zircon trace element (ppm) concentrations (Atomic number > 41)

Analysis	La	Ce	Nd	Sm	Eu	Gd	Tb	Dy	Ho	Er	Tm	Yb	Lu	Hf	Pb	Th	U	Eu/Eu*	T (°C)[1]
IEKVl-1																			
IEKVl1-1.1	0.03	13.39	2.42	4.91	2.58	43.56	14.36	149	54	237	48	405	73	8917	0	91	163	0.54	783
IEKVl1-10.1	1.52	33.38	4.07	6.91	2.68	48.49	13.38	154	70	250	54	467	87	7726	0	195	307	0.45	739
IEKVl1-11.1	0.02	5.67	0.43	1.47	0.65	12.40	4.75	57	22	109	25	223	42	9502	0	14	36	0.47	766
IEKVl1-12.1	0.04	13.11	3.12	5.55	1.24	51.74	18.52	203	78	342	69	543	93	10264	0	82	121	0.22	812
IEKVl1-14.1	0.12	10.13	0.81	1.63	0.48	20.03	6.48	81	32	149	31	271	50	9947	0	29	58	0.25	858
IEKVl1-16.1	0.05	70.01	9.53	20.48	8.63	169.50	55.16	543	194	760	145	1141	195	8787	1	487	595	0.45	795
IEKVl1-17.1	0.11	14.84	2.55	5.35	2.26	40.46	12.33	136	52	222	45	384	66	9164	0	84	170	0.47	762
IEKVl1-18.1	0.03	23.82	1.86	5.62	2.61	46.57	15.81	175	69	300	65	560	104	9021	1	164	332	0	783
IEKVl1-19.1	0.05	19.10	1.03	2.43	0.91	22.12	7.42	87	36	151	33	285	53	12245	0.26	99	258	0.38	689
IEKVl1-20.1	0.04	11.73	2.15	4.18	2.06	30.07	9.99	102	39	174	38	332	63	9445	0.28	92	181	0.56	755
IEKVl1-21.1	0.03	8.02	0.35	0.92	0.51	9.60	5.02	62	21	99	22	209	37	9543	0.68	217	330	0.52	781
IEKVl1-3.1	0.07	98.91	11.83	22.68	5.31	177.07	55.80	560	186	766	152	1208	194	11300	2.64	817	1089	0.26	724
IEKVl1-5.1	0.02	49.72	0.68	3.35	1.21	48.64	20.12	242	99	477	108	965	177	16665	1.24	304	765	0.29	654
IEKVl1-7.1	0.04	39.77	6.35	14.56	6.40	128.72	40.38	401	141	583	113	905	154	8515	0.57	259	361	0.45	813
IEKVl1-8.1	0.25	12.92	2.46	2.87	1.53	18.95	6.54	64	23	99	22	197	35	9658	0.15	34	86	0.63	746

[1]Calculated using the method of Ferry and Watson (2007) using *a* SiO_2=1.0 and *a* TiO_2=0.7.

APPENDIX G: Zircon Hafnium Isotope Analyses

Table G1. ***In situ*** **hafnium isotope compositions for Hafnarfjall-Skarðsheiði zircon**

	$^{176}Hf/^{177}Hf$	2SE	$^{176}Lu/^{177}Hf$	2SE	$^{176}Yb/^{177}Hf$	2SE	$^{178}Hf/^{177}Hf$	2SE	$^{180}Hf/^{177}Hf$	2SE	TotalHf Beam	εHf	2 SE	Average εHf	2SD	n	# of outliers
Hafnarfjall-Skarðsheiði: Brekkufjall Rhyolite														**11.7**	**1.6**	**7**	**4**
BrE1201_29.1_	0.283172	0.000050	0.0023	0.00008	0.0693	0.0018	1.467163	0.000042	1.886970	0.000210	21.4	13.7	1.8				X
BrE1201_48.1_	0.283043	0.000064	0.0020	0.00008	0.0557	0.0016	1.467103	0.000054	1.887240	0.000190	13.6	9.1	2.3				X
BrE1201_5.1_	0.283131	0.000044	0.0019	0.00006	0.0542	0.0012	1.467149	0.000038	1.887080	0.000140	14.6	12.2	1.6				
BrE1201_6.1_	0.283141	0.000032	0.0018	0.00004	0.0547	0.0012	1.467172	0.000045	1.886957	0.000074	16.4	12.6	1.1				
BrE1201_9.1_	0.283144	0.000032	0.0019	0.00002	0.0558	0.0004	1.467121	0.000048	1.886985	0.000097	16.3	12.7	1.1				
BrE1201_37.1_	0.283099	0.000035	0.0022	0.00009	0.0643	0.0029	1.467138	0.000032	1.887038	0.000089	15.1	11.1	1.2				
BrE1201_13.1_	0.283110	0.000046	0.0019	0.00010	0.0539	0.0022	1.467122	0.000061	1.887000	0.000110	17.6	11.5	1.6				
BrE1201_40.1_	0.283095	0.000044	0.0025	0.00011	0.0754	0.0035	1.467199	0.000033	1.887080	0.000180	18.7	11.0	1.6				
BrE1201_23.1_	0.283044	0.000073	0.0022	0.00007	0.0638	0.0024	1.467129	0.000061	1.887320	0.000180	14.4	9.1	2.6				X
BrE1201_22.1_	0.283085	0.000073	0.0016	0.00012	0.0472	0.0029	1.467111	0.000051	1.887210	0.000220	17.2	10.6	2.6				X
BrE1201_25.1_	0.283089	0.000053	0.0020	0.00004	0.0587	0.0012	1.467202	0.000052	1.887090	0.000140	18.4	10.7	1.9				
Hafnarfjall-Skarðsheiði: Tungukollur Rhyolite														**11.5**	**1.5**	**14**	**0**
TuE1301_1.1_	0.283141	0.000034	0.00163	0.00004	0.04640	0.00110	1.467149	0.000046	1.886980	0.000100	12.34	12.6	1.2				
TuE1301_2.1_	0.283077	0.000037	0.00281	0.00007	0.08040	0.00200	1.467155	0.000040	1.886950	0.000110	12.15	10.3	1.3				
TuE1301_4.1_	0.283122	0.000029	0.00147	0.00002	0.04096	0.00060	1.467140	0.000046	1.887020	0.000099	12.03	11.9	1.0				
TuE1301_7.1_	0.283109	0.000032	0.00210	0.00009	0.05840	0.00240	1.467149	0.000048	1.887040	0.000081	11.03	11.4	1.1				
TuE1301_15.1_	0.283090	0.000042	0.00213	0.00012	0.05900	0.00330	1.467182	0.000058	1.886950	0.000170	14.12	10.8	1.5				
TuE1301_13.1_	0.283141	0.000035	0.00240	0.00007	0.06790	0.00240	1.467177	0.000053	1.887080	0.000110	13.57	12.6	1.2				
TuE1301_16.1_	0.283092	0.000032	0.00225	0.00006	0.06310	0.00180	1.467189	0.000045	1.886970	0.000150	14.49	10.8	1.1				
TuE1301_17.1_	0.283112	0.000050	0.00283	0.00012	0.08140	0.00330	1.467177	0.000045	1.887110	0.000170	13.58	11.5	1.8				
TuE1301_25.1_	0.283088	0.000032	0.00338	0.00003	0.09710	0.00110	1.467149	0.000049	1.887084	0.000093	10.89	10.7	1.1				
TuE1301_20.1_	0.283100	0.000034	0.00311	0.00005	0.08800	0.00140	1.467180	0.000042	1.886880	0.000110	10.96	11.1	1.2				
TuE1301_18.1_	0.283111	0.000035	0.00276	0.00018	0.07850	0.00510	1.467180	0.000057	1.887090	0.000110	13.57	11.5	1.2				
TuE1301_21.1_	0.283091	0.000036	0.00170	0.00004	0.04750	0.00110	1.467171	0.000044	1.887120	0.000110	11.78	10.8	1.3				
TuE1301_24.1_	0.283137	0.000034	0.00279	0.00015	0.08000	0.00450	1.467118	0.000040	1.886970	0.000140	15.49	12.4	1.2				
TuE1301_22.1_	0.283119	0.000049	0.00336	0.00007	0.09630	0.00200	1.467148	0.000060	1.887080	0.000150	13.47	11.8	1.7				
Hafnarfjall-Skarðsheiði: Rauðihnúkur Rhyolite														**10.6**	**3.2**	**9**	**0**
RnE1201_2.1_	0.283104	0.000034	0.00194	0.00005	0.05630	0.00160	1.467124	0.000040	1.886890	0.000120	10.77	11.3	1.2				
RnE1201_10.1_	0.283146	0.000037	0.00128	0.00002	0.03672	0.00031	1.467184	0.000064	1.886950	0.000170	13.63	12.7	1.3				
RnE1201_13.1_	0.283125	0.000034	0.00125	0.00003	0.03569	0.00061	1.467187	0.000039	1.886910	0.000140	13.19	12.0	1.2				
RnE1201_16.1_	0.283107	0.000046	0.00151	0.00002	0.04307	0.00062	1.467102	0.000062	1.887020	0.000200	13.95	11.4	1.6				
RnE1201_20.1_	0.283114	0.000048	0.00214	0.00005	0.06350	0.00170	1.467199	0.000056	1.887070	0.000130	13.09	11.6	1.7				
RnE1201_21.1_	0.283071	0.000045	0.00127	0.00009	0.03660	0.00280	1.467182	0.000045	1.887140	0.000120	11.76	10.1	1.6				
RnE1201_22.1_	0.283019	0.000053	0.00127	0.00006	0.03630	0.00180	1.467146	0.000050	1.887100	0.000170	12.85	8.3	1.9				
RnE1201_23.1_	0.283023	0.000041	0.00141	0.00004	0.04040	0.00130	1.467125	0.000047	1.887160	0.000140	12.30	8.4	1.4				
RnE1201_25.1_	0.283052	0.000044	0.00224	0.00017	0.06390	0.00470	1.467113	0.000059	1.887090	0.000140	11.95	9.4	1.6				

Table G1. ***In situ*** **hafnium isotope compositions for Hafnarfjall-Skarðsheiði zircon**

	$^{176}Hf/^{177}Hf$	2SE	$^{176}Lu/^{177}Hf$	2SE	$^{176}Yb/^{177}Hf$	2SE	$^{178}Hf/^{177}Hf$	2SE	$^{180}Hf/^{177}Hf$	2SE	TotalHf Beam	εHf	2 SE	Average εHf	2SD	n	# of outliers
Hafnarfjall-Skarðsheiði: Drageyraröxl Ignimbrite														**11.2**	**1.1**	**15**	**0**
DrE1302_4.1_	0.283129	0.000028	0.00275	0.00005	0.08290	0.00190	1.467180	0.000036	1.886968	0.000071	13.75	12.1	0.9				
DrE1302_2.1_	0.283119	0.000033	0.00248	0.00008	0.07380	0.00220	1.467175	0.000028	1.886991	0.000087	13.89	11.4	1.1				
DrE1302_5.1_	0.283110	0.000032	0.00112	0.00003	0.03108	0.00099	1.467135	0.000046	1.886950	0.000100	13.49	11.2	1.1				
DrE1302_6.1_	0.283093	0.000023	0.00213	0.00001	0.06358	0.00068	1.467132	0.000038	1.886944	0.000080	14.08	10.5	0.8				
DrE1302_7.1_	0.283148	0.000033	0.00319	0.00012	0.09760	0.00420	1.467139	0.000036	1.886980	0.000110	12.93	11.8	1.1				
DrE1302_9.1_	0.283128	0.000029	0.00192	0.00002	0.05817	0.00079	1.467161	0.000034	1.886980	0.000100	13.46	11.5	1.0				
DrE1302_8.1_	0.283139	0.000035	0.00361	0.00002	0.10970	0.00120	1.467135	0.000034	1.886830	0.000100	13.01	12.0	1.2				
DrE1302_10.1_	0.283090	0.000034	0.00136	0.00005	0.04040	0.00180	1.467151	0.000037	1.886937	0.000091	13.84	10.1	1.2				
DrE1302_11.1_	0.283125	0.000031	0.00288	0.00006	0.08450	0.00200	1.467157	0.000033	1.886973	0.000081	13.28	11.3	1.1				
DrE1302_12.1_	0.283126	0.000042	0.00364	0.00005	0.11090	0.00180	1.467148	0.000044	1.886890	0.000120	13.85	11.3	1.2				
DrE1302_13.1_	0.283112	0.000031	0.00266	0.00014	0.08030	0.00460	1.467129	0.000032	1.886910	0.000110	13.95	11.0	1.2				
DrE1302_15.1_	0.283111	0.000030	0.00260	0.00004	0.07880	0.00160	1.467161	0.000034	1.886931	0.000091	13.04	10.9	1.1				
DrE1302_17.1_	0.283126	0.000033	0.00330	0.00002	0.09822	0.00053	1.467126	0.000039	1.886990	0.000087	12.61	11.5	1.2				
DrE1302_18.1_	0.283110	0.000029	0.00163	0.00004	0.04850	0.00150	1.467156	0.000036	1.886903	0.000069	13.14	10.9	1.0				
DrE1302_19.1_	0.283090	0.000030	0.00231	0.00001	0.06931	0.00018	1.467096	0.000029	1.886861	0.000089	12.54	10.5	1.1				
Hafnarfjall-Skarðsheiði: Flyðrur Granophyre														**11.6**	**2.0**	**13**	**0**
FlI1201_18.1_	0.283151	0.000035	0.00131	0.00006	0.03810	0.00180	1.467159	0.000037	1.886870	0.000120	18.06	12.9	1.2				
FlI1201_20.1_	0.283133	0.000035	0.00275	0.00006	0.08600	0.00160	1.467183	0.000046	1.886950	0.000120	15.12	12.3	1.2				
FlI1201_12.1_	0.283129	0.000023	0.00099	0.00002	0.02939	0.00033	1.467180	0.000031	1.886966	0.000086	14.25	12.2	0.8				
FlI1201_14.1_	0.283103	0.000039	0.00365	0.00014	0.11090	0.00380	1.467155	0.000038	1.887010	0.000120	12.72	11.2	1.2				
FlI1201_29.1_	0.283103	0.000057	0.00552	0.00045	0.19200	0.01500	1.467161	0.000049	1.887000	0.000170	18.68	11.2	2.0				
FlI1201_30.1_	0.283112	0.000048	0.00126	0.00003	0.03849	0.00051	1.467155	0.000032	1.887090	0.000180	15.94	11.6	1.7				
FlI1201_31.1_	0.283079	0.000054	0.00191	0.00005	0.05760	0.00150	1.467124	0.000042	1.887050	0.000150	14.34	10.4	1.0				
FlI1201_33.1_	0.283103	0.000043	0.00212	0.00010	0.06630	0.00220	1.467166	0.000045	1.887000	0.000150	15.55	11.2	1.0				
FlI1201_3.1_	0.283142	0.000036	0.00246	0.00010	0.07520	0.00260	1.467176	0.000041	1.886910	0.000110	12.42	12.6	1.0				
FlI1201_10.1_	0.283158	0.000039	0.00141	0.00006	0.03990	0.00160	1.467173	0.000045	1.886910	0.000160	18.89	13.2	1.4				
FlI1201_9.1_	0.283057	0.000072	0.00357	0.00019	0.10520	0.00560	1.467134	0.000055	1.887090	0.000210	17.56	9.6	1.8				
FlI1201_34.1_	0.283095	0.000035	0.00162	0.00006	0.04870	0.00150	1.467131	0.000035	1.887000	0.000110	13.41	11.0	1.2				
FlI1201_35.1_	0.283121	0.000024	0.00197	0.00004	0.06130	0.00120	1.467143	0.000036	1.886943	0.000066	14.69	11.9	0.8				

Table G2. *In situ* hafnium isotope compositions for Árnes and Hrafnfjörður zircon

	$^{176}Hf/^{177}Hf$	2SE	$^{176}Lu/^{177}Hf$	2SE	$^{176}Yb/^{177}Hf$	2SE	$^{178}Hf/^{177}Hf$	2SE	$^{180}Hf/^{177}Hf$	2SE	TotalHf Beam	εHf	2 SE	Average εHf	2SD	n	# of outliers
Árnes: Tr1 Rhyolite (ÁrE1302)														**11.9**	**1.2**	**3**	**0**
DH-04-1	0.283107	0.000040	0.00138	0.00003	0.03682	0.00084	1.467148	0.000060	1.887060	0.000160	7.34	11.4	1.4				
DH-04-3	0.283117	0.000043	0.00233	0.00018	0.06520	0.00500	1.467140	0.000063	1.886860	0.000130	7.39	11.7	1.5				
DH-04-4	0.283139	0.000049	0.00287	0.00013	0.08030	0.00390	1.467152	0.000055	1.887100	0.000130	7.28	12.5	1.7				
Árnes: Tr2 Rhyolite (ÁrE1303)														**12.6**	**1.3**	**15**	**0**
ArE1303_10.1_	0.283108	0.000042	0.00141	0.00005	0.04020	0.00150	1.467137	0.000060	1.887090	0.000180	14.89	11.4	1.5				
ArE1303_11.1_	0.283134	0.000029	0.00062	0.00001	0.01699	0.00017	1.467155	0.000037	1.886987	0.000098	11.77	12.3	1.0				
ArE1303_12.1_	0.283161	0.000027	0.00123	0.00001	0.03398	0.00040	1.467149	0.000043	1.886980	0.000095	10.59	13.3	1.0				
ArE1303_12.2_	0.283169	0.000022	0.00080	0.00001	0.02190	0.00014	1.467188	0.000037	1.886937	0.000081	13.51	13.6	0.8				
ArE1303_13.1_	0.283124	0.000035	0.00169	0.00003	0.04890	0.00100	1.467149	0.000053	1.887020	0.000100	11.25	12.0	1.2				
ArE1303_14.1_	0.283144	0.000032	0.00211	0.00016	0.06220	0.00490	1.467194	0.000042	1.886930	0.000110	13.05	12.7	1.1				
ArE1303_15.1_	0.283140	0.000027	0.00077	0.00003	0.02160	0.00100	1.467166	0.000035	1.886950	0.000100	12.71	12.5	1.0				
ArE1303_2.1_	0.283145	0.000024	0.00114	0.00002	0.03125	0.00049	1.467133	0.000021	1.886940	0.000110	13.67	12.7	0.8				
ArE1303_26.1_	0.283138	0.000042	0.00148	0.00016	0.04300	0.00510	1.467124	0.000045	1.886840	0.000120	13.20	12.5	1.5				
ArE1303_27.1_	0.283148	0.000037	0.00294	0.00032	0.08500	0.00970	1.467142	0.000040	1.886940	0.000110	16.44	12.8	1.3				
ArE1303_3.1_	0.283105	0.000032	0.00070	0.00001	0.01875	0.00042	1.467148	0.000035	1.887010	0.000110	12.36	11.3	1.1				
ArE1303_4.1_	0.283154	0.000030	0.00120	0.00002	0.03372	0.00067	1.467139	0.000040	1.886929	0.000099	12.11	13.0	1.1				
ArE1303_6.1_	0.283130	0.000028	0.00081	0.00001	0.02224	0.00038	1.467099	0.000044	1.886860	0.000100	14.26	12.2	1.0				
ArE1303_8.1_	0.283163	0.000032	0.00217	0.00008	0.06340	0.00270	1.467180	0.000036	1.887015	0.000098	12.22	13.4	1.1				
ArE1303_9.1_	0.283158	0.000037	0.00232	0.00010	0.06690	0.00300	1.467162	0.000042	1.886900	0.000120	12.51	13.2	1.3				
Árnes: Tr3 Rhyolite (ÁrE1304)														**13.0**	**2.0**	**15**	**0**
ArE1304_7_1.1_	0.283121	0.000044	0.00282	0.00014	0.08020	0.00350	1.467174	0.000045	1.887080	0.000180	13.57	11.9	1.6				
ArE1304_7_10.1_	0.283202	0.000046	0.00238	0.00003	0.06762	0.00076	1.467131	0.000049	1.886780	0.000160	15.70	14.7	1.6				
ArE1304_7_11.1_	0.283165	0.000031	0.00296	0.00010	0.08680	0.00280	1.467127	0.000032	1.886840	0.000140	12.05	13.4	1.1				
ArE1304_7_12.1_	0.283165	0.000043	0.00443	0.00008	0.12900	0.00280	1.467179	0.000049	1.886890	0.000140	11.91	13.4	1.5				
ArE1304_7_13.1_	0.283145	0.000029	0.00236	0.00011	0.06730	0.00300	1.467124	0.000042	1.886910	0.000130	11.66	12.7	1.0				
ArE1304_7_15.1_	0.283163	0.000043	0.00304	0.00003	0.08760	0.00150	1.467100	0.000043	1.886950	0.000120	10.96	13.4	1.5				
ArE1304_7_16.1_	0.283169	0.000033	0.00349	0.00019	0.10120	0.00670	1.467180	0.000036	1.886965	0.000093	10.86	13.6	1.2				
ArE1304_7_2.1_	0.283187	0.000043	0.00535	0.00013	0.14980	0.00390	1.467160	0.000046	1.886926	0.000094	12.85	14.2	1.5				
ArE1304_7_3.1_	0.283135	0.000043	0.00494	0.00010	0.13900	0.00280	1.467163	0.000043	1.887040	0.000130	12.63	12.4	1.5				
ArE1304_7_4.1_	0.283136	0.000030	0.00373	0.00009	0.10300	0.00240	1.467170	0.000041	1.886956	0.000097	12.48	12.4	1.1				
ArE1304_7_5.1_	0.283119	0.000057	0.00484	0.00008	0.13960	0.00280	1.467170	0.000044	1.887110	0.000130	11.32	11.8	2.0				
ArE1304_7_6.1_	0.283150	0.000036	0.00334	0.00012	0.09160	0.00360	1.467124	0.000041	1.887070	0.000110	10.87	12.9	1.3				
ArE1304_7_7.1_	0.283116	0.000048	0.00197	0.00007	0.05890	0.00210	1.467121	0.000047	1.887120	0.000140	14.03	11.7	1.7				
ArE1304_7_8.1_	0.283197	0.000045	0.00421	0.00032	0.11850	0.00920	1.467149	0.000028	1.886990	0.000130	12.93	14.6	1.6				
ArE1304_7_9.1_	0.283132	0.000048	0.00201	0.00009	0.05590	0.00200	1.467156	0.000067	1.887030	0.000140	11.38	12.3	1.7				

Table G2. *In situ* hafnium isotope compositions for Árnes and Hrafnfjörður zircon

	$^{176}Hf/^{177}Hf$	2SE	$^{176}Lu/^{177}Hf$	2SE	$^{176}Yb/^{177}Hf$	2SE	$^{178}Hf/^{177}Hf$	2SE	$^{180}Hf/^{177}Hf$	2SE	TotalHf Beam	εHf	2 SE	Average εHf	2SD	n	# of outliers
Árnes: Tr4 Rhyolite (ÁrE1301)														**12.4**	**--**	**1**	**0**
ArE1301_3.1_	0.283136	0.000049	0.00276	0.00004	0.07710	0.00150	1.467151	0.000049	1.886970	0.000160	15.35	12.4	1.7				
Hrafnsfjörður: KK-24 Dacite														**15.7**	**1.6**	**14**	**0**
kk24_3	0.283192	0.000032	0.002832	0.00007	0.073792	0.00200	1.467253	0.000049	--	--	4.70	14.4					
kk24_4	0.283238	0.000038	0.005540	0.00021	0.154466	0.00659	1.467276	0.000071	--	--	5.41	16.0					
kk24_4b	0.283194	0.000052	0.004215	0.00010	0.117026	0.00313	1.467210	0.000073	--	--	5.54	14.5					
kk24_5	0.283220	0.000022	0.004604	0.00004	0.126084	0.00134	1.467217	0.000050	--	--	7.02	15.4					
kk24_6	0.283264	0.000042	0.002669	0.00008	0.072009	0.00262	1.467215	0.000060	--	--	5.42	16.9					
kk24_7	0.283213	0.000054	0.004732	0.00020	0.130152	0.00586	1.467203	0.000050	--	--	6.89	15.1					
kk24_8	0.283232	0.000033	0.003966	0.00007	0.108907	0.00206	1.467234	0.000042	--	--	6.47	15.8					
kk24_8b	0.283223	0.000033	0.002498	0.00008	0.067850	0.00267	1.467212	0.000042	--	--	6.31	15.5					
kk24_9	0.283219	0.000046	0.005607	0.00010	0.155701	0.00286	1.467241	0.000033	--	--	6.63	15.4					
kk24_9b	0.283253	0.000033	0.004368	0.00023	0.125151	0.00784	1.467221	0.000042	--	--	6.24	16.5					
kk24_10	0.283225	0.000061	0.005950	0.00007	0.170196	0.00177	1.467266	0.000045	--	--	6.81	15.6					
kk24_11	0.283236	0.000039	0.004564	0.00023	0.129999	0.00633	1.467241	0.000052	--	--	6.13	15.9					
kk24_11b	0.283219	0.000029	0.003469	0.00015	0.096956	0.00407	1.467250	0.000057	--	--	6.13	15.4					
kk24_12	0.283266	0.000059	0.005559	0.00033	0.161310	0.00982	1.467190	0.000050	--	--	5.98	17.0					

Table G3. ***In situ*** **hafnium isotope compositions for Króksfjörður zircon**

	$^{176}Hf/^{177}Hf$	2SE	$^{176}Lu/^{177}Hf$	2SE	$^{176}Yb/^{177}Hf$	2SE	$^{178}Hf/^{177}Hf$	2SE	$^{180}Hf/^{177}Hf$	2SE	TotalHf Beam	εHf	2 SE	Average εHf	2SD	n	# of outliers
Króksfjörður: Bær Dacite														**12.0**	**1.9**	**3**	**0**
IEKBr1_7_1.1_	0.283152	0.000032	0.00184	0.00006	0.04960	0.00160	1.467112	0.000048	1.886820	0.000140	14.9	13.0	1.1				
IEKBr1_7_3.1_	0.283099	0.000037	0.00121	0.00004	0.03160	0.00110	1.467173	0.000040	1.887050	0.000100	12.3	11.1	1.3				
IEKBr1_7_5.1_	0.283127	0.000051	0.00112	0.00002	0.02987	0.00056	1.467174	0.000054	1.887050	0.000140	14.9	12.1	1.8				
Króksfjörður: Tindar Rhyolite														**11.5**	**2.8**	**3**	**0**
IEKTr1_7_1.1_	0.283126	0.000041	0.00278	0.00002	0.07798	0.00078	1.467186	0.000046	1.887080	0.000130	12.1	12.0	1.4				
IEKTr1_7_5.1_	0.283068	0.000043	0.00130	0.00006	0.03540	0.00200	1.467142	0.000041	1.887120	0.000150	11.3	10.0	1.5				
IEKTr1_7_6.1_	0.283142	0.000039	0.00283	0.00008	0.08040	0.00170	1.467149	0.000062	1.886980	0.000140	12.3	12.6	1.4				
Króksfjörður: Valshamar Dacite														**13.2**	**3.6**	**5**	**1**
IKEV1-1	0.283171	0.000053	0.00263	0.00011	0.06780	0.00300	1.467141	0.000076	1.886940	0.000150	14.5	13.7	1.9				
IKEV1-2	0.283220	0.000038	0.00291	0.00025	0.07620	0.00700	1.467203	0.000058	1.886957	0.000096	13.3	15.4	1.3				
IKEV1-3	0.283144	0.000045	0.00543	0.00020	0.14670	0.00570	1.467122	0.000046	1.887100	0.000140	14.5	12.7	1.6				
IKEV1-4	0.283083	0.000062	0.00496	0.00017	0.13360	0.00470	1.467148	0.000058	1.887100	0.000190	13.9	10.5	2.2				X
IKEV1-5	0.283174	0.000030	0.00258	0.00016	0.06810	0.00450	1.467163	0.000046	1.887050	0.000120	12.9	13.8	1.1				
Króksfjörður: Kambur Dacite														**13.9**	**1.5**	**6**	**0**
IIKK_1.2	0.283212	0.000030	0.00099	0.00004	0.02440	0.00097	1.467271	0.000063	--	--	15.8	15.1	1.1				
IIKK_3.1	0.283194	0.000026	0.00156	0.00008	0.03273	0.00172	1.467252	0.000037	--	--	13.7	14.4	0.9				
IIKK_1.1	0.283158	0.000023	0.00162	0.00009	0.03989	0.00249	1.467252	0.000043	--	--	13.8	13.2	0.8				
IIKK_2.1	0.283175	0.000021	0.00222	0.00022	0.04934	0.00519	1.467255	0.000031	--	--	15.5	13.8	0.7				
IIKK_4.1	0.283159	0.000019	0.00103	0.00003	0.02398	0.00063	1.467242	0.000032	--	--	15.1	13.2	0.7				
IIKK_4.2	0.283174	0.000015	0.00067	0.00002	0.01566	0.00038	1.467242	0.000035	--	--	16.8	13.7	0.5				

APPENDIX H: Whole Rock Nd, Hf, and Pb Isotope Analyses

Table H1. Whole rock Hf, Nd, and Pb isotopes

Sample	Date	ε_{Hf}	2σ	ε_{Nd}	2σ	$^{176}Hf/^{177}Hf$	2σ	$^{143}Nd/^{144}Nd$	2σ	$^{206}Pb/^{204}Pb$	2σ	$^{207}Pb/^{204}Pb$	2σ	$^{208}Pb/^{204}Pb$	2σ	$^{207}Pb/^{206}Pb$	2σ	$^{208}Pb/^{206}Pb$	2σ
Árnes																			
ÁrE1302	Feb. 2014	13.3	0.2	7.8	0.2	0.283160	5	0.513031	10	18.6417	0.0007	15.4810	0.0006	38.3556	0.0017	0.8305	0.00001	2.0575	0.00003
ÁrE1303	Feb. 2014	12.8	0.2	7.4	0.2	0.283147	7	0.513011	10	18.7812	0.0008	15.4915	0.0006	38.4787	0.0018	0.8248	0.00001	2.0488	0.00003
ÁrE1304	Feb. 2014	13.4	0.2	7.7	0.2	0.283164	6	0.513023	9	18.6353	0.0007	15.4786	0.0007	38.3453	0.0016	0.8306	0.00001	2.0577	0.00003
Hrafnfjörður																			
KK24	Sept. 2014	14.5	0.3	8.1	0.2	0.283194	8	0.513055	0	--	--	--	--	--	--	--	--	--	--
Króksfjörður																			
IEKBr-1	Sept. 2014	13.2	0.3	7.4	0.2	0.283157	8	0.5130158	8	--	--	--	--	--	--	--	--	--	--
IEKTr-1	Feb. 2014	13.3	0.2	7.3	0.2	0.283161	7	0.513003	9	18.8627	0.0008	15.5159	0.0006	38.5532	0.0018	0.8226	0.00001	2.0439	0.00003
IEKVl-1	Feb. 2014	14.3	0.2	8.3	0.2	0.283191	6	0.513058	9	18.4905	0.0006	15.4808	0.0006	38.1244	0.0017	0.8372	0.00001	2.0618	0.00004
IIKK-1a	Sept. 2014	14.4	0.1	7.8	0.2	0.283192	0	0.513039	0	--	--	--	--	--	--	--	--	--	--
Hafnarfjall-Skarðsheiði																			
ÖlE1301	Feb. 2014	11.9	0.3	7.8	0.2	0.283120	7	0.513028	11	19.0402	0.0007	15.5244	0.0006	38.6081	0.0017	0.8153	0.00001	2.0277	0.00003
RnE1201	Feb. 2014	11.9	0.2	7.4	0.2	0.283120	6	0.513010	8	18.9680	0.0006	15.5140	0.0005	38.5462	0.0016	0.8179	0.00001	2.0322	0.00003
TuE1301	Feb. 2014	12.8	0.3	7.4	0.2	0.283148	7	0.513010	10	19.0369	0.0007	15.5271	0.0005	38.6236	0.0015	0.8157	0.00001	2.0289	0.00003
BrE1201	Feb. 2014	13.3	0.2	7.5	0.2	0.283162	7	0.513015	12	18.9724	0.0006	15.5238	0.0005	38.5641	0.0015	0.8182	0.00001	2.0327	0.00003
DrE1302	Feb. 2014	11.4	0.2	7.4	0.2	0.283109	5	0.513012	9	19.1136	0.0007	15.5232	0.0006	38.6783	0.0014	0.8122	0.00001	2.0236	0.00002
FLI 1201	Sept. 2014	12.4	0.2	7.8	0.2	0.283137	6	0.513029	9	18.9466	0.0006	15.5134	0.0005	38.5207	0.0015	0.8188	0.00001	2.0331	0.00003

APPENDIX I: Króksfjörður Whole Rock Major and Trace Element Analyses

Table I. Króksfjörður whole rock major and trace elements[1]

	units	IEKBr-1	IEKTr-1	IEKGd-1	IIKGf-1	IEKVI-1	IIKK-1a[2]	Normalized to 100
SiO_2	wt%	68.28	75.79	69.90	69.10	70.88	70.07	
TiO_2	wt%	1.16	0.29	13.18	0.61	0.46	0.41	
Al_2O_3	wt%	14.30	12.79	6.27	14.52	14.48	14.62	
FeO*	wt%	5.84	2.96	0.16	4.37	3.52	3.67	
MnO	wt%	0.12	0.08	0.71	0.07	0.05	0.06	
MgO	wt%	0.59	0.14	2.46	1.47	1.04	1.34	
CaO	wt%	2.54	1.64	3.32	4.44	3.75	4.11	
Na_2O	wt%	4.51	4.38	3.45	3.50	3.80	3.86	
K_2O	wt%	2.43	1.91	0.48	1.80	1.95	1.75	
P_2O_5	wt%	0.22	0.03	0.06	0.12	0.08	0.10	
LOI	wt%	3.41	5.16	5.32	4.86	1.67	1.21	
Total[3]	wt%	100.10	98.46	98.69	98.54	98.83	99.89	
Au	ppb	1	< 1	< 1	< 1	< 1	< 1	
Ag	ppm	0.7	1.1	1.9	0.7	< 0.5	< 0.5	
As	ppm	< 1	< 1	2	< 1	< 1	< 1	
Ba	ppm	383	428	407	385	415	340	
Be	ppm	4	4	5	2	2	2	
Bi	ppm	< 0.1	< 0.1	< 0.1	< 0.1	< 0.1	0.2	
Br	ppm	< 0.5	2.4	< 0.5	< 0.5	< 0.5	1	
Cd	ppm	1.1	< 0.5	< 0.5	< 0.5	< 0.5	< 0.5	
Co	ppm	9.3	< 0.1	5.9	10.7	11.8	9.4	
Cr	ppm	21.8	18.3	< 0.5	29.5	33.8	23.7	
Cs	ppm	0.3	1.1	0.8	0.9	0.4	0.2	
Cu	ppm	28	16	18	64	51	43	
Ga	ppm	23	24	25	19	18	18	
Ge	ppm	2.1	2.1	1.9	1.6	1.6	1.6	
Hf	ppm	12.9	12.8	14.7	4.6	4.4	4.6	
Hg	ppm	< 1	< 1	< 1	< 1	< 1	< 1	
In	ppm	< 0.1	< 0.1	0.2	< 0.1	< 0.1	< 0.1	
Ir	ppb	< 1	< 1	< 1	< 1	< 1	< 1	
Mo	ppm	< 2	3	4	< 2	< 2	3	
Nb	ppm	66.8	70.3	72.6	12.5	11.2	10.2	
Ni	ppm	5	2	5	14	16	26	
Pb	ppm	10	< 5	5	5	< 5	< 5	
Rb	ppm	45	126	58	88	67	42	
S	%	0.067	0.012	0.032	0.026	0.019	0.004	
Sb	ppm	< 0.1	< 0.1	0.4	0.3	< 0.1	0.2	
Sc	ppm	10.6	4.59	8.99	8.1	7.03	5.99	
Se	ppm	< 0.5	< 0.5	< 0.5	< 0.5	< 0.5	< 0.5	
Sn	ppm	4	5	7	1	1	2	
Sr	ppm	170	99	121	296	250	284	
Ta	ppm	4.26	4.67	5.41	1.11	1.08	1.08	
Th	ppm	8.16	10.6	8.9	6.32	5.89	7.67	
U	ppm	2.4	3.12	2.41	2.16	2.22	2.02	
V	ppm	51	5	20	72	49	56	
W	ppm	< 1	< 1	< 1	< 1	< 1	< 1	
Y	ppm	64	69	121	14	16	15	
Zn	ppm	276	159	186	106	54	53	
Zr	ppm	605	533	688	189	176	180	
La	ppm	59.5	72.7	81.6	29	27.7	48.3	
Ce	ppm	117	136	170	49.9	46	71.6	
Pr	ppm	14	15.5	21.3	5.29	5.01	7.04	
Nd	ppm	54.4	59.1	85.3	19.1	17.8	23.4	
Sm	ppm	11.5	12.8	19.5	3.82	3.54	3.92	
Eu	ppm	2.98	2.33	4.33	1.1	0.939	1.06	
Gd	ppm	10.9	11.5	18.1	3.22	3.06	2.97	
Tb	ppm	1.93	2.04	3.29	0.48	0.49	0.47	
Dy	ppm	11.5	12.6	20.8	2.6	2.77	2.54	
Ho	ppm	2.33	2.55	4.18	0.51	0.55	0.47	
Er	ppm	6.67	7.54	12.7	1.41	1.53	1.38	
Tl	ppm	< 0.05	0.14	0.09	0.07	0.07	0.15	
Tm	ppm	0.995	1.12	1.9	0.191	0.226	0.199	
Yb	ppm	6.72	7.81	12.4	1.21	1.55	1.3	
Lu	ppm	1.02	1.22	1.92	0.2	0.252	0.205	

[1] *Data from ActLabs Ltd. via FUS-ICP* [2] *From Carley, 2014*

[3] *Pre-normaliztion total, including LOI*

REFERENCES

Andres, M., Blichert-Toft, J., Schilling, J.-G., 2004. Nature of the depleted upper mantle beneath the Atlantic: evidence from Hf isotopes in normal mid-ocean ridge basalts from 79°N to 55°S. Earth Planet Sci Lett 225, 89–103.

Bacon, C.R., Sisson, T.W., Mazdab, F.K., 2007. Young cumulate complex beneath Veniaminof caldera, Aleutian arc, dated by zircon in erupted plutonic blocks. Geology 35, 491.

Baertschi, P., 1976. Absolute ^{18}O content of standard mean ocean water. Earth Planet Sci Lett 31, 341–344.

Ballard, J.R., Palin, M.J., Campbell, I.H., 2002. Relative oxidation states of magmas inferred from Ce(IV)/Ce(III) in zircon: application to porphyry copper deposits of northern Chile. Contrib Mineral Petrol 144, 347–364.

Barth, A.P., Wooden, J.L., 2010. Coupled elemental and isotopic analyses of polygenetic zircons from granitic rocks by ion microprobe, with implications for melt evolution and the sources of granitic magmas. Chem Geol 277, 149–159.

Benediktsdóttir, Á., Hey, R., Martinez, F., Höskuldsson, Á., 2012. Detailed tectonic evolution of the Reykjanes Ridge during the past 15 Ma. Geochemistry, Geophysics, Geosystems 13.

Bindeman, I., Gurenko, A., Carley, T., Miller, C., Martin, E., Sigmarsson, O., 2012. Silicic magma petrogenesis in Iceland by remelting of hydrothermally altered crust based on oxygen isotope diversity and disequilibria between zircon and magma with implications for MORB. Terra Nova 24, 227–232.

Bjarnason, I., 2008. An Iceland Hotspot Saga. Jökull 58, 1–16.

Black, L.P., Kamo, S.L., Allen, C.M., Davis, D.W., Aleinikoff, J.N., Valley, J.W., 2004. Improved $^{206}Pb/^{238}U$ microprobe geochronology by the monitoring of a trace-element-related matrix effect; SHRIMP, ID–TIMS, ELA–ICP–MS and oxygen isotope documentation for a series of zircon standards. Chem Geol 205, 115–140.

Boehnke, P., Watson, E.B., Trail, D., Harrison, T.M., Schmitt, A.K., 2013. Zircon saturation re-revisited. Chem Geol 351, 324–334.

Bouvier, A., Vervoort, J.D., Patchett, P.J., 2008. The Lu–Hf and Sm–Nd isotopic composition of CHUR: Constraints from unequilibrated chondrites and implications for the bulk composition of terrestrial planets. Earth Planet Sci Lett 273, 48–57.

Brandsdóttir, B., Menke, W.H., 2008. The seismic structure of Iceland. Jökull 58, 17–34.

Browning, J., Gudmundsson, A., 2015. Caldera faults capture and deflect inclined sheets: an alternative mechanism of ring dike formation. Bull Volcanol 77, 4.

Carley, T. L, 2014. The generation and evolution of silicic magma and juvenile crust: Insight from the Icelandic zircon record. Dissertation. Vanderbilt University.

Carley, T.L., Miller, C.F., Wooden, J.L., Padilla, A.J., Schmitt, A.K., Economos, R.C., Bindeman, I.N., Jordan, B.T., 2014. Iceland is not a magmatic analog for the Hadean: Evidence from the zircon record. Earth Planet Sci Lett 405, 85–97.

Carley, T.L., Miller, C.F., Wooden, J.L., Bindeman, I.N., Barth, A.P., 2011. Zircon from historic eruptions in Iceland: reconstructing storage and evolution of silicic magmas. Mineral Petrol 102, 135–161.

Carmichael, I.S.E., 1964. The petrology of Thingmuli, a Tertiary volcano in eastern Iceland. J Petrol 5, 435–460.

Claiborne, L.L., Miller, C.F., Flanagan, D.M., Clynne, M.A., Wooden, J.L., 2010a. Zircon reveals protracted magma storage and recycling beneath Mount St. Helens. Geology 38, 1011–1014.

Claiborne, L.L., Miller, C.F., Wooden, J.L., 2010b. Trace element composition of igneous zircon: a thermal and compositional record of the accumulation and evolution of a large silicic batholith, Spirit Mountain, Nevada. Contrib to Mineral Petrol 160, 511–531.

Cline, J.S., Bodnar, R.J., 1991. Can Economic Porphyry Copper Mineralization Be Generated by a Typical Calc-Alkaline Melt? J Geophys Res 96, 8113–8126.

Colombini, L.L., Miller, C.F., Gualda, G.A.R., Wooden, J.L., Miller, J.S., 2011. Sphene and zircon in the Highland Range volcanic sequence (Miocene, southern Nevada, USA): elemental partitioning, phase relations, and influence on evolution of silicic magma. Mineral Petrol 102, 29–50.

Darbyshire, F.A., White, R.S., Priestley, K.F., 2000., Structure of the crust and uppermost mantle of Iceland from a combined seismic and gravity study. Earth Planet Sci Lett 181, 409–428.

Dilles, J. H. 1987., Petrology of the Yerington Batholith, Nevada; Evidence for Evolution of Porphyry Copper Ore Fluids. Econ Geol 82, 1750–1789.

Dilles, J. H., Gans, P.B., 1995. The Chronology of Cenozoic Volcanism and Deformation in the Yerington Area, Western Basin and Range and Walker Lane. GSA Bull 107, 474–486.

Dilles, J.H., Kent, A.J.R., Wooden, J.L., Tosdal, R.M., Koleszar, A., Lee, R.G., Farmer, L.P., 2015. Zircon Compositional Evidence for Sulfur-Degassing from Ore-Bearing Arc Magmas. Econ Geol 110, 241–251.

Dilles, J.H., Wright, J.E., 1988. The Chronology of Early Mesozoic Arc Magmatism in the Yerington District of Western Nevada and Its Regional Implications. GSA Bull 100, 644–652.

Dilles, J.H., Einaudi, M.T., Proffett, J.M., Barton, M.D., 2000. Overview of the Yerington Porphyry Copper District: Magmatic to Nonmagmatic Sources of Hydrothermal Fluids, Their Flow Paths, Alteration Affects on Rocks, and Cu-Mo-Fe-Au Ores. In Contrasting Styles of Intrusion Associated with Hydrothermal Systems, eds. J.H. Dilles et al., 55–66.

Eiler, J.M., Grönvold, K., Kitchen, N., 2000. Oxygen isotope evidence for the origin of chemical variations in lavas from Theistareykir volcano in Iceland's northern volcanic zone. Earth Planet Sci Lett 184, 269–286.

Ewart, A., 1979. A review of the mineralogy and chemistry of Tertiary-Recent dacite, latite, rhyolite and related salic volcanic rocks, in: Barker, F. (Ed.), Trondhjemites, Dacites and Related Rocks (Developments in Petrology 6). Elsevier, New York, pp. 13–121.

Ferry, J.M., Watson, E.B., 2007. New thermodynamic models and revised calibrations for the Ti-in-zircon and Zr-in-rutile thermometers. Contrib to Mineral Petrol 154, 429–437.

Finch, R.J., Hanchar, J., 2003. Structure and Chemistry of Zircon and Zircon-Group Minerals. Rev Mineral Geochem 53, 1–25.

Fisher, C.M., Vervoort, J.D., DuFrane, S.A., 2014. Accurate Hf isotope determinations of complex zircons using the laser ablation split stream method. Geochemistry, Geophysics, Geosystems 15, 121–139.

Fohey-Breting, N.K., Barth, A.P., Wooden, J.L., Mazdab, F.K., Carter, C.A., Schermer, E.R., 2010. Relationship of voluminous ignimbrites to continental arc plutons: Petrology of Jurassic ignimbrites and contemporaneous plutons in southern California. J Volcanol Geotherm Res 189, 1–11.

Foulger, G.R., 2006. Older crust underlies Iceland. Geophys J Int 165, 672–676.

Franzson, H., 1972. The Brekkufjall caldera formation, W. Iceland. University of St. Andrews.

Franzson, H., 1978. Structure and petrochemistry of the Hafnarfjall-Skarðsheiði central volcano and the surrounding basalt succession, W-Iceland. University of Edinburgh.

Franzson, H., Zierenberg, R., Schiffman, P., 2008. Chemical transport in geothermal systems in Iceland. J Volcanol Geotherm Res 173, 217–229.

Furman, T., Frey, F.A., Meyer, P.S., 1992. Petrogenesis of Evolved Basalts and Rhyolites at Austurhorn, Southeastern Iceland: the Role of Fractional Crystallization. J Petrol 33, 1405–1445.

Galer, S., Abouchami, W., 1998. Practical application of lead triple spiking for correction of instrumental mass discrimination. Mineral Mag 62A, 491–492.

Gao, Y.-Y., Li, X.-H., Griffin, W.L., O'Reilly, S.Y., Wang, Y.-F. 2014. Screening criteria for reliable U–Pb geochronology and oxygen isotope analysis in uranium-rich zircons: a case study from the suzhou A-type granites, SE China. Lithos 192-195, 180–191.

Ghiorso, M.S., Gualda, G.A.R., 2012. A method for estimating the activity of titania in magmatic liquids from the compositions of coexisting rhombohedral and cubic iron–titanium oxides. Contrib to Mineral Petrol 165, 73–81.

Gunnarsson, B., Marsh, B.D., Taylor, H.P., 1998. Generation of Icelandic rhyolites: silicic lavas from the Torfajökull central volcano. J Volcanol Geotherm Res 83, 1–45.

Hald, N., Noe-Nygaard, A., Pedersen, A.K., 1971. The Króksfjörður central volcano in north-west Iceland. Acta Nat Islandica II, 1–29.

Harðarson, B.S., 1988. Gangasvelmur Króksfjarðareldstöðvar. Háskóli Íslands (University of Iceland).

Hardarson, B.S., Fitton, J.G., 1997. Mechanisms of crustal accretion in Iceland. Geology 25, 1043-1046.

Hardarson, B.S., Fitton, J.G., Ellam, R.M., Pringle, M.S., 1997. Rift relocation — A geochemical and geochronological investigation of a palaeo-rift in northwest Iceland. Earth Planet Sci Lett 153, 181–196.

Harðarson, B.S., Fitton, J.G., Hjartarson, Á., 2008. Tertiary volcanism in Iceland. Jökull 58, 161–178.

Hart, S.R., 1984. A large-scale isotope anomaly in the Southern Hemisphere mantle. Nature 309, 753–757.

Hattori, K., Muehlenbachs, K., 1982. Oxygen Isotope Ratios of the Icelandic Crust 87, 6559–6565.

Hey, R., Martinez, F., Höskuldsson, Á., Benediktsdóttir, Á., 2010. Propagating rift model for the V-shaped ridges south of Iceland. Geochemistry, Geophysics, Geosystems 11.

Hoskin, P.W.O., Schaltegger, U., 2003. The Composition of Zircon and Igneous and Metamorphic Petrogenesis. Rev Mineral Geochemistry 53, 27–62.

Irmer, G., 1985. On the Influence of the Apparatus Function on the Determination of Scattering Cross Sections and Lifetime from Optical Phonon Spectra. Experimentalle Technik der Physik 33, 501–506 (in German).

Jóhannesson, H., 1980. Evolution of rift zones in western Iceland. Náttúrufræðingurinn 50, 13–31.

Johnson, D., Hooper, P., Conrey, R., 1999. XRF Analysis of Rocks and Minerals for Major and Trace Elements on a Single Low Dilution Li-tetraborate Fused Bead. Adv X-ray Anal 41, 843–867.

Jónasson, K., 1990. Petrology of silicic rocks from the Króksfjörður central volcano in NW-Iceland. Dissertation. University of Copenhagen, Denmark.

Jónasson, K., Holm, P., Pederson, K., 1992. Petrogenesis of Silicic Rocks from the Króksfjörður Central Volcano, NW Iceland. J Geophys Res 33, 1345–1369.

Jónasson, K., 1994. Rhyolite volcanism in the Krafla central volcano, north-east Iceland. Bull Volcanol 56, 516–528.

Jónasson, K., 2007. Silicic volcanism in Iceland: Composition and distribution within the active volcanic zones. J Geodyn 43, 101–117.

Jones, S.M., White, N., Maclennan, J., 2002. V-shaped ridges around Iceland: Implications for spatial and temporal patterns of mantle convection. Geochemistry Geophys Geosystems 3, 1–23.

Jordan, B.T., Duncan, R.A., Carley, T.L., 2013. A transect of Tertiary central volcanoes across northwest Iceland, in: American Geophysical Union Fall Meeting 2013, abstract #V41B-2804.

Jordan, B.T., Olin, P.H., 2008. Voluminous intermediates at three Tertiary central volcanoes in northwestern Iceland: Implications for crustal magmatic processes during tectonic evolution of Iceland, in: American Geophysical Union, Fall Meeting 2008, abstract #V41D-2127.

Kaban, M.K., Flóvenz, Ó.G., Pálmason, G., 2002. Nature of the crust-mantle transition zone and the thermal state of the upper mantle beneath Iceland from gravity modelling. Geophys J Int 149, 281–299.

Kinney, P., Maas, R., 2003. Lu-Hf and Sm-Nd isotope systems in zircon, in: Hanchar, J., Hoskin, P.W.O. (Eds.), Reviews in Mineralogy and Geochemistry, Vol. 53, Zircon. Mineralogical Society of America, pp. 327–385.

Kitagawa, H., Kobayashi, K., Makishima, A., Nakamura, E., 2008. Multiple Pulses of the Mantle Plume: Evidence from Tertiary Icelandic Lavas. J Petrol 49, 1365–1396.

Kryza, R., Crowley, Q.G., Larionov, A., Pin, C., Oberc-Dziedzic, T., Mochnacka, K., 2012. Chemical Abrasion Applied to SHRIMP Zircon Geochronology: An Example from the Variscan Karkonosze Granite (Sudetes, SW Poland). Gondwana Res 21, 757–67.

Lawver, L.A., Müller, R.D., 1994. Iceland hotspot track. Geology 22, 311–314.

Liang, H., Campbell, IH., Allen, C., Sun, W., Liu, C., Yu, H., Xie, Y., Zhang, Y., 2006. Zircon Ce4+/Ce3+ Ratios and Ages for Yulong Ore-Bearing Porphyries in Eastern Tibet. Mineral Deposita 41, 152–59.

Ludwig, K.R., 2009. SQUID 2, A User's Manual. Berkeley Geochronology Center Spec Pub 100.

———., 2012. Isoplot 3.75, A Geochronological Toolkit for Excel. Berkeley Geochronology Center Spec Pub 75.

Macdonald, R., Sparks, R.S.J., Sigurdsson, H., Mattey, D.P., McGarvie, D.W., Smith, R.L., 1987. The 1875 eruption of Askja volcano, Iceland: combined fractional crystallization and selective contamination in the generation of rhyolitic magma. Mineral Mag 51, 183–202.

Mahon, K.I., 2006. The New York Regression: Application of an Improved Statistical Method to Geochemistry. Int Geol Rev 38, 293–303.

Mahoney, J.J., Sinton, J.M., Kurz, M.D., Macdougall, J.D., Spencer, K.J., Lugmair, G.W., 1994. Isotope and trace element characteristics of a super-fast spreading ridge: East Pacific rise, 13–23°S. Earth Planet Sci Lett 121, 173–193.

Marsh, B.D., Gunnarsson, B., Congdon, R., Carmody, R., 1991. Hawaiian basalt and Icelandic rhyolite: Indicators of differentiation and partial melting. Geol Rundschau 80, 481–510.

Martin, E., Paquette, J.L., Bosse, V., Ruffet, G., Tiepolo, M., Sigmarsson, O., 2011. Geodynamics of rift–plume interaction in Iceland as constrained by new $^{40}Ar/^{39}Ar$ and in situ U–Pb zircon ages. Earth Planet Sci Lett 311, 28–38.

Martin, E., Sigmarsson, O., 2010. Thirteen million years of silicic magma production in Iceland: Links between petrogenesis and tectonic settings. Lithos 116, 129–144.

Mattinson, J.M., 2005. Zircon U–Pb Chemical Abrasion ('CA-TIMS') Method: Combined Annealing and Multi-Step Partial Dissolution Analysis for Improved Precision and Accuracy of Zircon Ages. Chem Geology 220, 47–66.

McDonough, W.F., Sun, S.-s., 1995. The composition of the Earth. Chem Geol 120, 223–253.

McDowell, S., Overton, S., Frazier, W., Fisher, C., Miller, C.F., Miller, J., Economos, R.C., 2015. Whole rock and zircon isotopic insights into the magmatic evolution of the supereruptive southern Black Mountains volcanic center, western Arizona, USA. American Mineralogist.

Muehlenbachs, K., Anderson, A.T., Sigvaldason, G.E., 1974. Low-O^{18} basalts from Iceland. Geochim Cosmochim Acta 38, 577–588.

Moorbath, S., Sigurdsson, H., Goodwin, R., 1968. K-Ar ages of the oldest exposed rocks in Iceland. Earth Planet Sci Lett 4, 197–205.

Morel, M.L.A., Nebel, O., Nebel-Jacobsen, Y.J., Miller, J.S., Vroon, P.Z., 2008. Hafnium isotope characterization of the GJ-1 zircon reference material by solution and laser-ablation MC-ICPMS. Chem Geol 255, 231–235.

Mundil, R., Ludwig, K.L., Metcalfe, I., Renne, P.R., 2004. Age and Timing of the Permian Mass Extinctions: U/Pb Dating of Closed-System Zircons. Science 305, 1760–1763.

Nasdala, L., Irmer, G., Wolf, D., 1995. The degree of metamictization in zircon: a Raman spectroscopic study. Eur J of Mineral 7, 471–478.

Nasdala, L., Pidgeon, R.T., Wolf, D., Irmer, G., 1998. Metamictization and U-Pb isotopic discordance in single zircons: a combined Raman microprobe and SHRIMP ion probe study. Mineral Petrol 62, 1–27.

Nasdala, L., Pidgeon, R.T., Wolf, D., 1996. Heterogeneous metamictization of zircon on a microscale. Geochim Cosmochim Acta 60, 1091–1097.

O'Connor, J.M., Stoffers, P., Wijbrans, J.R., Shannon, P.M., Morrissey, T., 2000. Evidence from episodic seamount volcanism for pulsing of the Iceland plume in the past 70 Myr. Nature 408, 954–958.

Óskarsson, N., Sigvaldason, G.E., Steinthorsson, S., 1982. A dynamic model of rift zone petrogenesis and the regional petrology of Iceland. J Geophys Res 23, 28–74.

Oskarsson, N., Steinthorsson, S., Sigvaldason, G.E., 1985. Iceland Geochemical Anomaly: Origin , Volcanotectonics, Chemical Fractionation and Isotope Evolution of the Crust 90, 10,011–10,025.

Pasteris, J.D., 1996. Mount Pinatubo volcano and 'negative' porphyry copper deposits. Geology 24, 1075–78.

Peate, D.W., Breddam, K., Baker, J. A., Kurz, M.D., Barker, A. K., Prestvik, T., Grassineau, N., Skovgaard, A. C., 2010. Compositional Characteristics and Spatial Distribution of Enriched Icelandic Mantle Components. J Petrol 51, 1447–1475.

Pedersen, A.K., Hald, N., Museum, G., 1979. A cummingtonite-porphyrific dacite with amphibole-rich xenoliths from the Tertiary central volcano at Króksfjörður, NW Iceland.

Pope, E.C., Bird, D.K., Arnórsson, S., 2013. Evolution of low-^{18}O Icelandic crust. Earth Planet Sci Lett 374, 47–59.

Prestvik, T., Goldberg, S., Karlsson, H., Grönvold, K., 2001. Anomalous strontium and lead isotope signatures in the off-rift Öræfajökull central volcano in south-east Iceland. Earth Planet Sci Lett 190, 211–220.

Proffett, J. M., 2009. High Cu Grades in Porphyry Cu Deposits and Their Relationship to Emplacement Depth of Magmatic Sources. Geology 37, 675–678.

Proffett, J.M., 1977. Cenozoic Geology of the Yerington District, Nevada, and Implications for the Nature and Origin of Basin and Range Faulting. GSA Bull 88, 247–266.

Sæmundsson, K., 1967. An outline of the structure of SW-Iceland, in: Björnsson, S. (Ed.), Iceland and Mid-Ocean Ridges. Soc. Sci. Islandica, Rit 38, Reykjavík, Iceland.

Sæmundsson, K., 1974. Evolution of the Axial Rifting Zone in Northern Iceland and the Tjörnes Fracture Zone. GSA Bull 85, 465–504.

Sæmundsson, K., 1979. Outline of geology of Iceland. Jökull 29, 7–28.

Sæmundsson, K., 1986. Subaerial volcanism in the western North Atlantic, in: Vogt, P.R., Tucholke, B.E. (Eds.), The Geology of North America, Vol. M, The Western North Atlantic Region. Geological Society of America, Boulder, CO, pp. 69–86.

Schmitt, A.K., Stockli, D.F., Lindsay, J.M., Robertson, R., Lovera, O.M., Kislitsyn, R., 2010. Episodic growth and homogenization of plutonic roots in arc volcanoes from combined U–Th and (U–Th)/He zircon dating. Earth Planet Sci Lett 295, 91–103.

Schoene, B., Crowley, J.L., Condon, D.J., Schmitz, M.D., Bowring, S.A., 2006. Reassessing the Uranium Decay Constants for Geochronology Using ID-TIMS U–Pb Data. Geochim Cosmochim Acta 70, 426–445.

Sigmarsson, O., Condomines, M., Fourcade, S., 1992. A detailed Th, Sr and O isotope study of Hekla: differentiation processes in an Icelandic Volcano. Contrib Mineral Petrol 112, 20–34.

Sigmarsson, O., Hemond, C., Condomines, M., Fourcade, S., Oskarsson, N., 1991. Origin of silicic magma in Iceland revealed by Th isotopes. Geology 19, 621–624.

Sigmarsson, O., Maclennan, J., Carpentier, M., 2008. Geochemistry of igenous rocks in Iceland: a review. Jökull 58, 139–160.

Sigmundsson, F., 2006. Iceland Geodynamics: Crustal Deformation and Divergent Plate Tectonics. Springer Science & Business Media.

Stacey, J.S., Kramers, J.D., 1975. Approximation of terrestrial lead isotope evolution by a two-stage model. Earth Planet Sci Lett 26, 207–221.

Sun, S.-s., McDonough, W.F., 1989. Chemical and isotopic systematics of oceanic basalts: implications for mantle composition and processes. Geol Soc London, Spec Publ 42, 313–345.

Sun, W., Arculus, R.J., Kamenetsky, V.S., Binns, R.A. 2004., Release of Gold-Bearing Fluids in Convergent Margin Magmas Prompted by Magnetite Crystallization. Nature 431, 975–978.

Sun, W., Liang, H., Ling, M., Zhan, M., Ding, X., Zhang, H., Yang, X., Li, Y., Ireland, T.R., Wei, Q., Fan, W., 2013. The link between reduced porphyry copper deposits and oxidized magmas. Geochim Cosmochim Acta 103, 263–275.

Thirlwall, M.F., Gee, M.A.M., Lowry, D., Mattey, D.P., Murton, B.J., Taylor, R.N., 2006. Low $\delta^{18}O$ in the Icelandic mantle and its origins: Evidence from Reykjanes Ridge and Icelandic lavas. Geochim Cosmochim Acta 70, 993–1019.

Thirlwall, M.F., Gee, M.A.M., Taylor, R.N., Murton, B.J., 2004. Mantle components in Iceland and adjacent ridges investigated using double-spike Pb isotope ratios. Geochim Cosmochim Acta 68, 361–386.

Thorarinsson, S., 1967. Hekla and Katla: The share of acid and intermediate lava and tephra in the volcanic products through the geological history of Iceland. Vís fél Ís 38, 190–199.

Torsvik, T.H., Amundsen, H.E.F., Tronnes, R.G., Doubrovine, P. V., Gaina, C., Kusznir, N.J., Steinberger, B., Corfu, F., Ashwal, L.D., Griffin, W.L., Werner, S.C., Jamtveit, B., 2015. Continental crust beneath southeast Iceland. PNAS 1423099112.

Trail, D., Mojzsis, S.J., Harrison, T.M., Schmitt, A.K., Watson, E.B., Young, E.D., 2007. Constraints on Hadean zircon protoliths from oxygen isotopes, Ti-thermometry, and rare earth elements. Geochemistry, Geophysics, Geosystems 8.

Urich, T., Gunther, D., Heinrich, C.A., 1999. Gold Concentrations of Magmatic Brines and the Metal Budget of Porphyry Copper Deposits. 399, 676–79.

Valley, J.W., 2003. Oxygen Isotopes in Zircon. Rev Mineral Geochemistry 53, 343–385.

Valley, J.W., Chiarenzelli, J.R., McLelland, J.M., 1994. Oxygen Isotope Geochemistry of Zircon. Earth Planet Sci Lett 126, 187–206.

Valley, J.W., Lackey, J.S., Cavosie, A.J., Clechenko, C.C., Spicuzza, M.J., Basei, M.A.S., Bindeman, I.N., Ferreira, V.P., Sial, A.N., King, E.M., Peck, W.H., Sinha, A.K., Wei, C.S., 2005. 4.4 Billion Years of Crustal Maturation: Oxygen Isotope Ratios of Magmatic Zircon. Contrib to Mineral Petrol 150, 561–580.

Vervoort, J.D., Plank, T., Prytulak, J., 2011. The Hf–Nd isotopic composition of marine sediments. Geochim Cosmochim Acta 75, 5903–5926.

Vink, G.E., 1984. A hotspot model for Iceland and the Vøring Plateau. J Geophys Res 89, 9949–9959.

von Quadt, A., Gallhofer, D., Guillong, M., Peytcheva, I., Waelle, M., Sakata, S. 2014. U–Pb Dating of CA/non-CA Treated Zircons Obtained by LA-ICP-MS and CA-TIMS Techniques: Impact for Their Geological Interpretation. J Analytical Atom Spect 29, 1618.

Walker, B.A., Miller, C.F., Lowery Claiborne, L., Wooden, J.L., Miller, J.S., 2007. Geology and geochronology of the Spirit Mountain batholith, southern Nevada: Implications for timescales and physical processes of batholith construction. J Volcanol Geotherm Res 167, 239–262.

Walker, G.P.L., 1966. Acid rocks in Iceland. Bull Volcanol 29, 375–402.

Wang, F., Liu, S., Li, S., He, Y., 2013. Contrasting Zircon Hf–O Isotopes and Trace Elements between Ore-Bearing and Ore-Barren Adakitic Rocks in Central-Eastern China: Implications for Genetic Relation to Cu–Au Mineralization. Lithos 156-159, 97–111.

Wang, X., Coble, M.A., Valley, J.W., Shu, X.-J., Kitajima, K., Spicuzza, M.J., Sun, T., 2014. Influence of Radiation Damage on Late Jurassic Zircon from Southern China: Evidence from in Situ Measurements of Oxygen Isotopes, Laser Raman, U-Pb Ages, and Trace Elements. Chem Geol 389, 122–36.

Watson, E.B., Green, T.H., 1981. Apatite/liquid partition coefficients for the rare earth elements and strontium. Earth Planet Sci Lett 56, 405–421.

Watson, E.B., Harrison, T.M., 1983. Zircon saturation revisited: temperature and composition effects in a variety of crustal magma types. Earth Planet Sci Lett 64, 295–304.

Watson, E.B., Wark, D.A., Thomas, J.B., 2006. Crystallization thermometers for zircon and rutile. Contrib to Mineral Petrol 151, 413–433.

White, L.T., Ireland, T.R., 2012. High-Uranium Matrix Effect in Zircon and Its Implications for SHRIMP U–Pb Age Determinations. Chem Geol 306-307, 78–91.

White, N., Lovell, B., 1997. Measuring the pulse of a plume with the sedimentary record 387, 888–891.

Willbold, M., Hegner, E., Stracke, A., Rocholl, A., 2009. Continental geochemical signatures in dacites from Iceland and implications for models of early Archaean crust formation. Earth Planet Sci Lett 279, 44–52.

Woodhead, J.D., Hergt, J.M., 2005. A Preliminary Appraisal of Seven Natural Zircon Reference Materials for In Situ Hf Isotope Determination. Geostand Geoanalytical Res 29, 183–195.